

Dissertation zur Erlangung des Doktorgrades  
Der Fakultät für Chemie und Pharmazie  
Der Ludwig-Maximilians-Universität München

# **Reactivity Parameters for Understanding Nucleophilic Organocatalysis**

**Biplab Maji**

aus  
Howrah, India

2012



## **Erklärung**

Diese Dissertation wurde im Sinne von § 7 der Promotionsordnung vom 28. November 2011 von Herrn Prof. Dr. Herbert Mayr betreut.

## **Ehrenwörtliche Versicherung**

Diese Dissertation wurde eigenständig und ohne unerlaubte Hilfe erarbeitet

München, am 16.07.12

.....  
Biplab Maji

Dissertation eingereicht am 20.07.2012

1. Gutachter: Prof. Dr. Herbert Mayr
2. Gutachter: Prof. Dr. Hendrik Zipse

Mündliche Prüfung am 31.08.2012



...dedicated to my family



## Acknowledgements

It is a great achievement in my life to be a part of Ludwig-Maximilians-Universität München. I started my journey on July 2009. Apart from the efforts of me, the success of this thesis depends largely on the encouragement and guidelines of many others. I would like to take this opportunity to express my gratitude to the people who have been instrumental in the successful completion of this thesis.

First and foremost, I would like to express my sincere gratitude to my supervisor, Professor Dr. Herbert Mayr for giving me the opportunity to work with his group and allowing me the large degree of independence in my work. His motivational discussion, endless support and accessibility results my research life smooth and rewarding.

Furthermore, I am grateful to Professor Dr. Hendrik Zipse for reviewing this thesis and the board of examiners for their participation in my defense examination.

I am also thankful to my past and present group mates specially, Brigitte Janker, Dr. Armin R. Ofial, Hans Laub, Dr. Nicolas Streidl, Konstantin Troshin, Tobias Nigst, Dr. Christoph Nolte, Johannes Ammer, Dr. Tanja Kanzian, Dr. Wei Han, Dominik Allgäuer, Dr. Roland Appel, Dr. Sami Lakhdar, Dr. Saloua Chelli, Dr. Martin Breugst, Dr. Xi Chen, Dr. Guillaume Berionni, Dr. Mahiuddin Baidya, Francisco Corral, Anna Antipova, Dr. Julia Fleckenstein, Ivo Zenz, Katharina Böck, Alexander Wagner, Elija Wiedemann, Dr. Markus Horn, Dr. Xi. Chen, Dr. Haruyasu Asahara, Elsa Follet, Xingwei Guo, Prof. Dr. Shinjiro Kobayashi, Dr. Jörg Bartl, Dr. Xin-Hua Duan. I spend three years in Munich but seems like I spent more than a decade. That's why I want to thank all my colleagues for their love and efforts that made me feel more at home.

I would like to show my greatest appreciation to Dr. Mahiuddin Baidya, and Dr. Sami Lakhdar for numerous stimulating discussions, help with experimental setup and general advice.

I thank Nathalie Hampel for synthesizing our reference electrophiles, Brigitte Janker for ordering chemicals. I am grateful to Dr. Armin R. Ofial for his critical and valuable suggestions for improvement of manuscripts.

My life in this city perhaps would not be so easy without Frau H. Lipfert. She always stands by me during each and every academic and non academic need.

I would also like to thank Frau Claudia Dubler and Dr. David Stephenson for the measurement of NMR spectra and Dr. Peter Mayer for solving crystal structures.

Furthermore, I express my greatest appreciation to Dr. Caroline Joannesse, Prof. Dr. Andrew D. Smith, Ramesh C. Samanta, and Prof. Dr. Armido Studer for their scientific collaboration. I would like to acknowledge my entire friends in Munich for their help and especially for their companionship which always kept my spirits high during the exhausting daily routine of chemistry. I also like to thank my entire friends living in the rest of the world for their valuable scientific and non-scientific discussions.

Last but not least, I wish to take this opportunity to express a sense of gratitude and love to my beloved parents, brother, and fiancée for their support, motivation, and help for everything.

## Publications

### **N-Heterocyclic Carbenes: Organocatalysts with Moderate Nucleophilicity but extraordinarily High Lewis Basicity**

B. Maji, M. Breugst, H. Mayr, *Angew. Chem.* **2011**, *123*, 7047–7052; *Angew. Chem. Int. Ed.* **2011**, *50*, 6915–6919.

### **Nucleophilicities and Lewis Basicities of Isothiourea Derivatives**

B. Maji, C. Joannesse, T. A. Nigst, A. D. Smith, H. Mayr, *J. Org. Chem.* **2011**, *76*, 5104–5112.

### **Characterization of the nucleophilic reactivities of thiocarboxylate, dithiocarbonate and dithiocarbamate anions**

X.-H. Duan, B. Maji, H. Mayr, *Org. Biomol. Chem.* **2011**, *9*, 8046–8050.

### **Nucleophilicity parameters for designing transition metal-free C-C bond forming reactions of organoboron compounds**

G. Berionni, B. Maji, P. Knochel, H. Mayr, *Chem. Sci.* **2012**, *3*, 878–882.

### **Nucleophilicity Parameters of Enamides and their Implications for Organocatalytic Transformations**

B. Maji, S. Lakhdar, H. Mayr, *Chem. Eur. J.* **2012**, *18*, 5732–5740.

### **Nucleophilic Addition of Enols and Enamines to $\alpha,\beta$ -Unsaturated Acyl Azoliums: Mechanistic Studies**

R. C. Samanta, B. Maji, S. De Sarkar, K. Bergander, R. Fröhlich, C. Mück-Lichtenfeld, H. Mayr, A. Studer, *Angew. Chem.* **2012**, *124*, 5325–5329; *Angew. Chem. Int. Ed.* **2012**, *51*, 5234–5238.

### **Imidazolidinone-Derived Enamines: Nucleophiles with Low Reactivity**

S. Lakhdar, B. Maji, H. Mayr, *Angew. Chem.* **2012**, *124*, 5837–5840; *Angew. Chem. Int. Ed.* **2012**, *51*, 5739–5742.

### **Guanidines: Highly Nucleophilic Organocatalysts**

B. Maji, D. S. Stephenson, H. Mayr, *ChemCatChem* **2012**, *4*, 993–999.

### **Nucleophilic Reactivity of Deoxy-Breslow-Intermediates: How Does Aromaticity Affect the Catalytic Activity of N-Heterocyclic Carbenes?**

B. Maji, M. Horn, H. Mayr, *Angew. Chem.* **2012**, *124*, 6335–6339; *Angew. Chem. Int. Ed.* **2012**, *51*, 6231–6235.

### **Structures and Reactivities of O-Methylated Breslow Intermediates**

B. Maji, H. Mayr, *Angew. Chem.* **2012**, DOI: 10.1002/ange.201204524; *Angew. Chem. Int. Ed.* **2012**, DOI: 10.1002/anie.201204524.

### **A quantitative approach to nucleophilic organocatalysis**

H. Mayr, S. Lakhdar, B. Maji, A. R. Ofial, *Beilstein J. Org. Chem.* **2012**, *8*, 1458–1478.

### **Nucleophilic Reactivities of 2-Imidazoline, Thiazoline, and Oxazoline**

B. Maji, M. Baidya, S. Kobayashi, J. Ammer, P. Mayer, A. R. Ofial, H. Mayr, *Eur. J. Org. Chem.* **2012**, *in preparation*.

## **Conference Contributions**

- 14-17 July, 2010. International Symposium on Organocatalysis (ISO $\mu$  2010), Mülheim an der Ruhr, Germany, poster presentation: **General base catalysis in the reactions of enamides with iminium ions.**
- 11-16 Sept., 2011. European Symposium on Organic Reactivity (ESOR 2011), Tartu, Estonia, oral presentation: **Reactivity Parameters for NHC Organocatalysts**
- 29-30 March, 2012. COST Action on Organocatalysis, ORCA summit, Aix-Marseille University, France, oral presentation: **Reactivity Parameters of the Intermediates in NHC Catalyzed Reactions**

## Table of Contents

<b>Chapter 0:</b>	Summary	<b>1</b>
<b>Chapter 1:</b>	Introduction	<b>17</b>
<b>Chapter 2:</b>	Nucleophilicities and Lewis Basicities of Isothiourea Derivatives	<b>35</b>
<b>Chapter 3:</b>	Guanidines: Highly Nucleophilic Organocatalysts	<b>85</b>
<b>Chapter 4:</b>	Nucleophilic Reactivities of 2-Imidazoline, Thiazoline, and Oxazoline	<b>129</b>
<b>Chapter 5:</b>	What Makes N-Heterocyclic Carbenes Special in Organocatalysis?	<b>183</b>
<b>Chapter 6:</b>	Nucleophilic Reactivity of Deoxy-Breslow-Intermediates: How Does Aromaticity Affect the Catalytic Activity of N-Heterocyclic Carbenes?	<b>213</b>
<b>Chapter 7:</b>	Structures and Reactivities of O-Methylated Breslow Intermediates	<b>245</b>
<b>Chapter 8:</b>	Nucleophilic Addition of Enols and Enamines to $\alpha,\beta$ -Unsaturated Acyl Azoliums: Mechanistic Studies	<b>283</b>
<b>Chapter 9:</b>	Nucleophilicity Parameters of Enamides and their Implications for Organocatalytic Transformations	<b>301</b>
<b>Chapter 10:</b>	Imidazolidinone-Derived Enamines: Nucleophiles with Low Reactivity	<b>355</b>

## List of Abbreviations

abs.	absolute	Me	methyl
aq.	aqueous	mg	milligram(s)
Bu	butyl	MHz	megahertz
calc	calculated	min	minute(s)
DMSO	dimethyl sulfoxide	mL	mililiter(s)
d	doublet	Mp	melting point
<i>E</i>	electrophilicity parameter	NMR	nuclear magnetic resonance
ee	enantiomeric excess	ppm	parts per million
EI	electron impact ionization	<i>N</i>	nucleophilicity parameter
ESI	electron spray ionization	NHC	N-heterocyclic carbene
exp.	experimental	Ph	phenyl
eq.	equation	q	quartet
Et	ethyl	ref.	reference
EtOAc	ethyl acetate	r.t.	room temperature
g	gram(s)	<i>S<sub>N</sub></i>	nucleophile specific sensitivity parameter
GP	general procedure	s	singlet
h	hour(s)	t	triplet
HMBC	heteronuclear multiple bond correlation	T	temperature
HRMS	High resolution mass spectrometry	tert	tertiary
Hz	hertz	THF	tetrahydrofuran
i.e.	id est	tol	tolyl
<i>J</i>	coupling constant	UV	ultra violet
<i>k</i>	rate constant	Vis	visible
<i>K</i>	equilibrium constant	vs.	versus
M	mol L <sup>-1</sup>		

## Chapter 0

# Summary

### 1 General

The key steps of most organocatalytic reactions are combinations of electrophiles with nucleophiles. Their rates can be described by the linear-free-energy relationship (1), where  $k_{(20\text{ }^\circ\text{C})}$  is the second-order rate constant at 20 °C,  $N$  is the nucleophilicity parameter,  $s_N$  is the nucleophile-specific sensitivity parameter, and  $E$  is the electrophilicity parameter  $E$ .

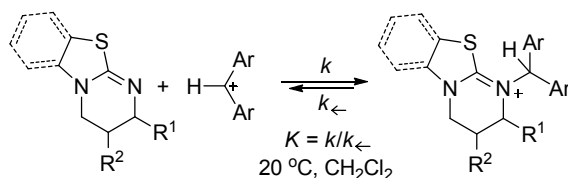
$$\log k_{(20\text{ }^\circ\text{C})} = s_N(N + E) \quad (1)$$

Benzhydrylium ions and structurally related quinone methides have previously been used as reference electrophiles to construct the most comprehensive nucleophilicity and electrophilicity scale presently available based on eq. (1) and the reactivity parameters  $E$  and  $N$  (and  $s_N$ ) can be used for predicting rates and selectivities of polar organic reactions.

This thesis was designed to derive reactivity parameters of several nucleophilic organocatalysts as well as substrates used in organocatalysis. Studies of the structures and reactivities of several reactive intermediates in the organocatalytic cycle will help to understand mechanistic courses of these reactions.

### 2 Nucleophilicities and Lewis Basicities of Isothiourea Derivatives

Rate and equilibrium constants ( $k$  and  $K$ ) for the reactions of a series of isothioureas with benzhydrylium ions have been measured photometrically in  $\text{CH}_2\text{Cl}_2$  at 20 °C (Scheme 1).



**Scheme 1:** Reactions of isothiourea derivatives with benzhydrylium ions.

The data were employed to determine the nucleophilicities, Lewis basicities, and nucleofugalities of isothioureas and compare them with those of other nucleophilic organocatalysts (Figure 1).

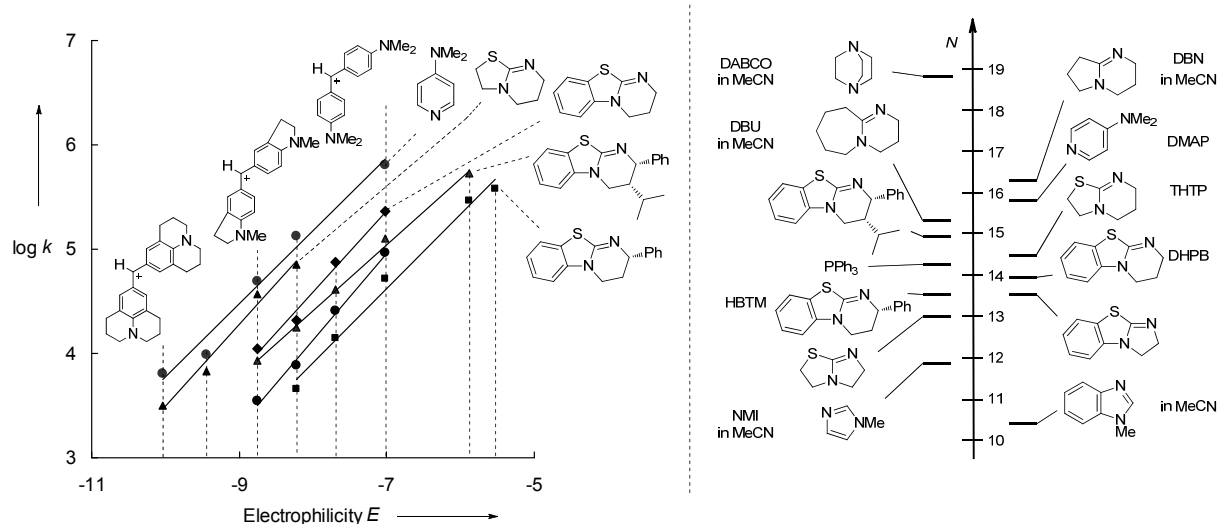


**Figure 1.** Determination of the nucleophilicity parameters  $N$  and  $s_N$  of isothioureas and comparison of with other nucleophilic organocatalysts (solvent is  $\text{CH}_2\text{Cl}_2$  unless otherwise stated).

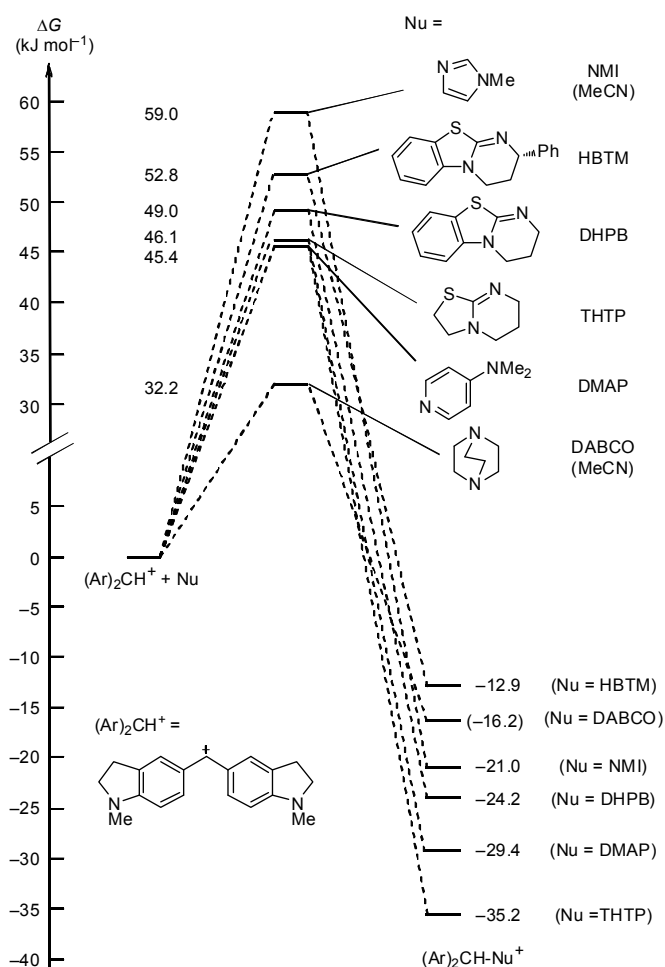


**Figure 2.** Gibbs energy profiles for the reactions of various nucleophilic organocatalysts with a benzhydrylium ion in  $\text{CH}_2\text{Cl}_2$  at 20 °C.

The measured rate and equilibrium constants allowed us to construct quantitative energy profiles for these reactions (Figure 2). While imidazoles are less nucleophilic as well as less Lewis basic than most of the isothioureas, nucleophilicities and Lewis basicities of most isothioureas investigated are comparable to those of 4-(dimethylamino)pyridine (DMAP). 1,4-diazabicyclo[2.2.2]octane (DABCO) is a stronger nucleophile than all isothioureas investigated, but its Lewis basicity (with respect to  $\text{Ar}_2\text{CH}^+$ ) is comparable to those of the least basic isothioureas.

### 3 Guanidines: Highly Nucleophilic Organocatalysts

The rates of the reactions of eight guanidines with diarylcarbenium tetrafluoroborates were measured photometrically in  $\text{CH}_2\text{Cl}_2$  at 20 °C. The second-order rate constants ( $\log k$ ) of the investigated reactions correlate linearly with the empirical electrophilicity parameters  $E$  of benzhydrylium ions as required by eq. (1), which allowed us to calculate the nucleophilicity parameters  $N$  (and  $s_N$ ) for guanidines (Figure 3).

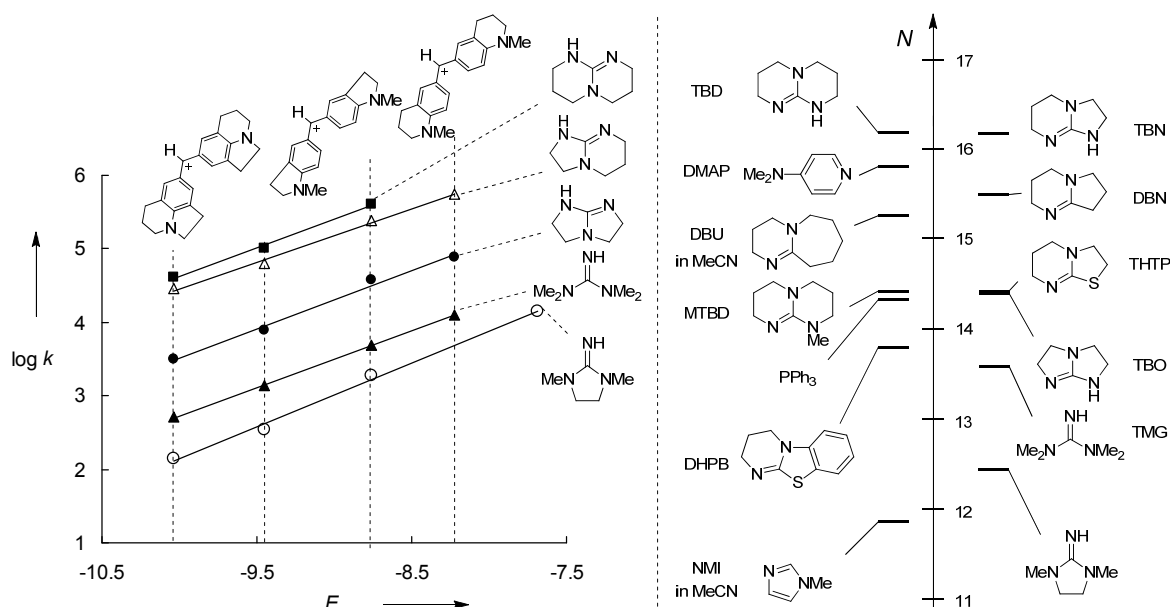


**Figure 3.** Determination of the nucleophilicity parameters  $N$  and  $s_N$  of guanidines and comparison of the nucleophilicities  $N$  of guanidines with other nucleophilic organocatalysts (solvent is  $\text{CH}_2\text{Cl}_2$  unless otherwise stated).

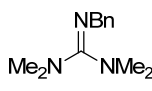
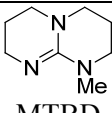
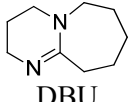
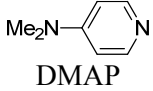
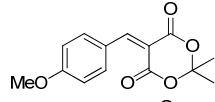
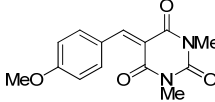
A comparison with other organocatalysts shows that 1,5,7-triazabicyclo[4.4.0]dec-5-ene (TBD), the strongest nucleophile of the guanidine series exceeds the nucleophilicity of 1,8-diazabicyclo[5.4.0]undec-7-ene (DBU) and 1,5-diazabicyclo[4.3.0]non-5-ene (DBN) by one order of magnitude (Figure 3).

The rates of the reactions of guanidines with ordinary Michael acceptors were measured analogously and a comparison of the experimental rate constants with the calculated rate constants (eq. (1) with  $N$ ,  $s_N$ , and  $E$  parameters), shows an agreement between 3–32 demonstrating applicability of these parameters for predicting rate constants of the reactions of guanidines with other kind of electrophiles.

The equilibrium constants for the reactions of guanidines with  $\text{Ar}_2\text{CH}^+$  and Michael acceptors have also been determined photometrically and a comparison shows that the bicyclic guanidine 1-methyl-2,3,4,6,7,8-hexahydro-1H-pyrimido[1,2-a]pyrimidine (MTBD) has a

similar Lewis basicity as DMAP, while the acyclic guanidine 2-benzyl-1,1,3,3-tetramethylguanidine is a much weaker Lewis base (Table 1).

**Table 1.** Comparison of the equilibrium constants  $K$  ( $M^{-1}$ ) of several organocatalysts.

					
	$< 10^2$	$(2.9 \times 10^2)$	$(1-7) \times 10^4$ [a]	large	$1.96 \times 10^2$ [a]
	$< 10^2$	$(2.8 \times 10^2)$	$(2-8) \times 10^4$ [a]	large	$2.41 \times 10^2$ [a]

[a] In MeCN.

#### 4 Nucleophilic Reactivities of 2-Imidazoline, Thiazoline, and Oxazoline

The kinetics of the reactions of 2-methyl imidazolines, thiazolines and oxazolines, and tetrahydropyrimidines with benzhydrylium ions were measured photometrically in  $CH_2Cl_2$ ,  $CH_3CN$ , and DMSO at 20 °C. The obtained second-order rate constants allowed us to determine the nucleophilicity parameters  $N$  and  $s_N$  of these N-heterocycles according to eq. (1) (Figure 4).

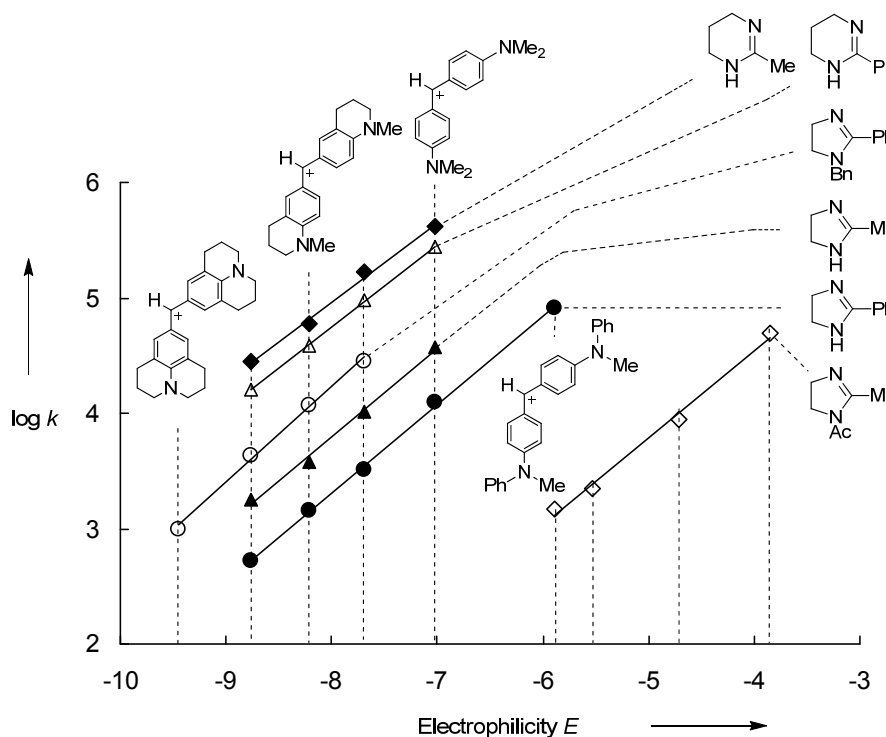
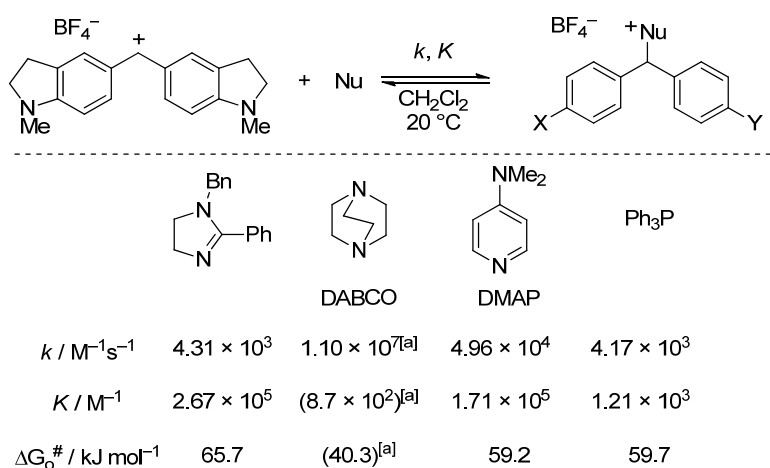


**Figure 4.** Plots of  $\log k$  for the reactions of the N-heterocyclic compounds with benzhydrylium ions versus their electrophilicity parameters  $E$  in  $CH_2Cl_2$  at 20 °C.

The applicability of these parameters for predicting rate constants of the reactions of 2-methyl-imidazoline and 2-methyl-tetrahydropyrimidine with ordinary Michael acceptors have been demonstrated by comparison of the experimentally measured rate constants with the calculated rate constants by using eq. (1).

The equilibrium constants ( $K$ ) for their reactions with benzhydrylium ions have also been measured photometrically. Substitution of the rate ( $k$ ) and equilibrium constants ( $K$ ) into the Marcus equation (2) showed that the reactions of the benzhydrylium ions with imidazoline derivatives proceed via higher intrinsic barriers ( $\Delta G_0^\ddagger$ ) than those with PPh<sub>3</sub>, DMAP, or DABCO. As a consequence 1-benzyl-2-phenyl-4,5-dihydro-1H-imidazole is less nucleophilic than the similarly strong Lewis base DMAP and more Lewis basic than PPh<sub>3</sub> which has a comparable nucleophilicity (Scheme 2).

$$\Delta G^\ddagger = \Delta G_0^\ddagger + 0.5 \Delta G^0 + ((\Delta G^0)^2 / 16 \Delta G_0^\ddagger) \quad (2)$$

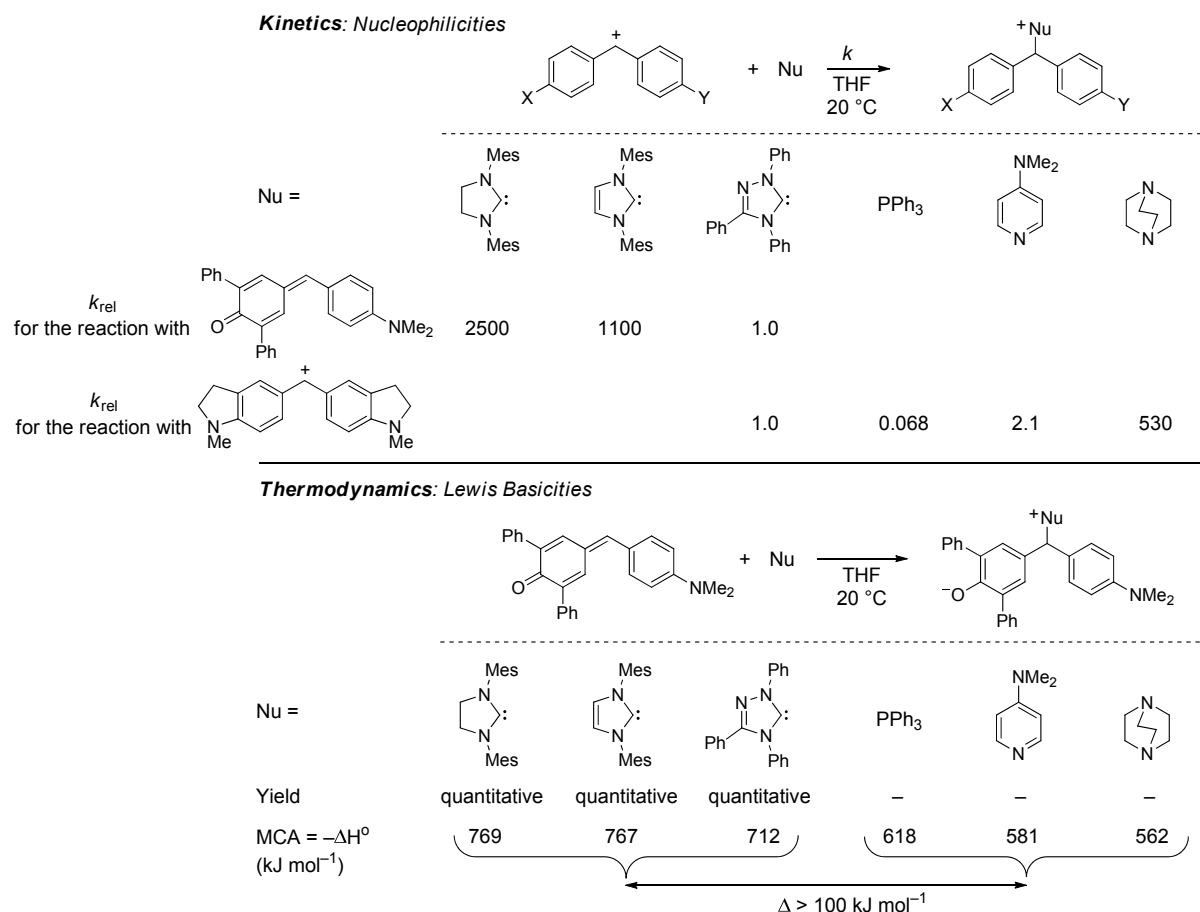


**Scheme 2:** Comparison of rate and equilibrium constants for the reactions of benzhydrylium ion with 1-benzyl-2-phenyl-4,5-dihydro-1H-imidazole, DABCO, DMAP, and PPh<sub>3</sub>. Solvent: CH<sub>2</sub>Cl<sub>2</sub>. [a] In MeCN.

## 5 What Makes N-Heterocyclic Carbenes Special in Organocatalysis?

The second-order-rate constants ( $k_2$ ) for the reactions of three N-heterocyclic carbenes (NHCs) with benzhydrylium ions and structurally related quinone methides were measured photometrically in THF at 20 °C. The linear correlation of the second-order-rate constants ( $\log k$ ) with  $E$  parameters allowed us to calculate the nucleophilicity parameters  $N$  and  $s_N$  of NHCs (Scheme 3).

Comparison of the NHCs with other nucleophilic organocatalysts shows that 1,2,4-triphenyltriazol-5-ylidene (Enders' carbene) has comparable nucleophilicity as DMAP, whereas the nucleophilicity of 1,3-dimesitylimidazol-2-ylidene and 1,3-dimesitylimidazol-2-ylidene (Arduengo carbenes) is comparable to that of DABCO (Scheme 3).

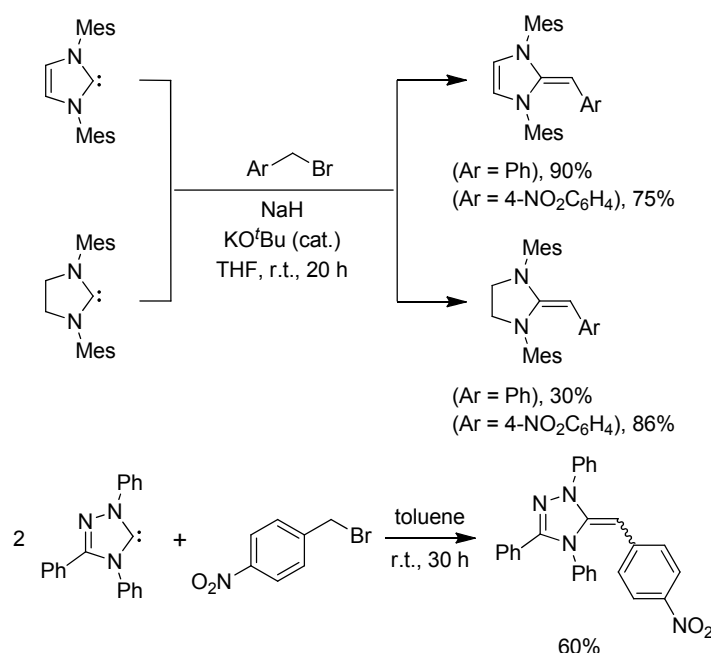


**Scheme 3:** Comparison of the nucleophilicities and Lewis basicities of NHCs with PPh<sub>3</sub>, DMAP and DABCO. Methyl cation affinities (MCAs) were calculated for the reaction  $\text{CH}_3^+ + \text{Nu} \rightarrow \text{CH}_3\text{-Nu}^+$  on MP2/6-31+G(d,p)//B98/6-31G(d) level of theory.

However, the relative nucleophilicities of these compounds differ significantly from the ordering of the Lewis basicities. While all three NHCs react quantitatively with a reference quinone methide, none of the other Lewis bases, despite their similar nucleophilicities, give an adduct. This led to the conclusion that the three NHCs depicted in Scheme 3 are significantly stronger Lewis bases than PPh<sub>3</sub>, DMAP, and DABCO. Since direct measurements of the equilibrium constants were unsuccessful, quantum chemical calculations of the methyl cation affinities (MCAs) were performed to determine the Lewis basicities of these nucleophiles. A comparison shows that the MCAs of the three carbenes are 100–200 kJ mol<sup>-1</sup> higher than those of the other Lewis bases in Scheme 3.

## 6 Nucleophilic Reactivity of Deoxy-Breslow-Intermediates: How Does Aromaticity Affect the Catalytic Activity of N-Heterocyclic Carbenes?

Through the saturated and unsaturated Arduengo carbenes have almost identical nucleophilicities and Lewis basicities, imidazolidin-2-ylidenes have rarely been used as organocatalysts in contrast to their unsaturated analogues. To explain whether the different organocatalytic activities of saturated and unsaturated NHCs are due to different reactivities of the corresponding Breslow intermediates, deoxy-Breslow intermediates were synthesized by the reactions of the NHCs with benzyl bromides and subsequent deprotonation of the resulting amidinium ions (Scheme 4).



**Scheme 4.** Synthesis of deoxy-Breslow intermediates.

The second-order-rate constants of the reactions of deoxy-Breslow intermediates with benzhydrylium ions and quinone methides were measured in DMSO and THF at 20 °C and nucleophilicity parameters  $N$  and  $s_N$  were derived from the linear plots of  $\log k$  vs  $E$  (Figure 5).

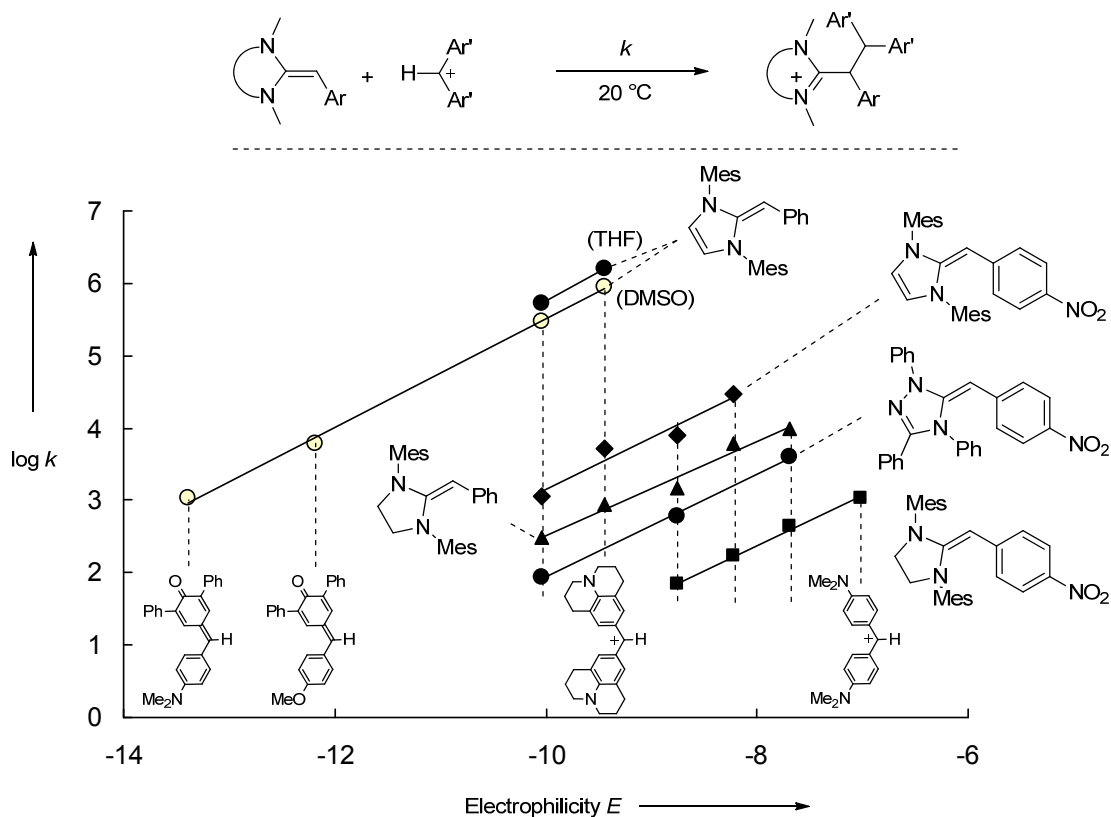


**Figure 5.** Plot of  $\log k$  for the reactions of deoxy Breslow intermediates with reference electrophiles versus their electrophilicity parameters  $E$  in THF at 20 °C.

In contrast to the relative nucleophilic reactivities of the corresponding NHCs, benzylidene-imidazolines are found to be  $10^3$  times more nucleophilic than the corresponding benzylidene-imidazolidines (Figure 6).

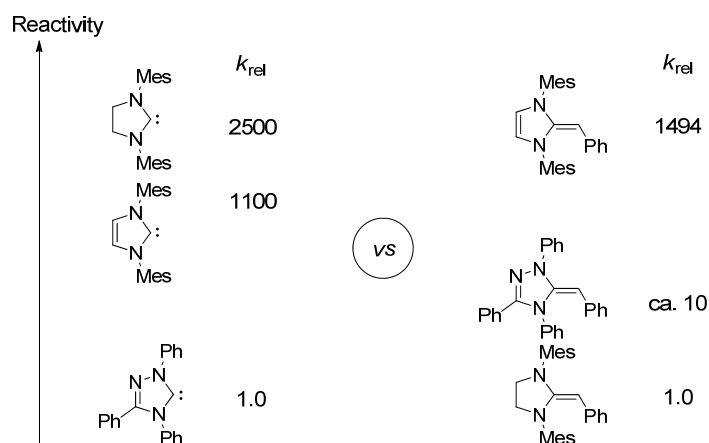


**Figure 6:** Nucleophilic reactivities of free NHCs and the corresponding deoxy-Breslow intermediates.

Quantum chemically calculated proton affinities (PAs) of the deoxy-Breslow intermediates run parallel to their nucleophilicities, and in the same way the Lewis basicities (methyl cation affinities, MCAs) of NHCs parallel their nucleophilicities (Figure 7).

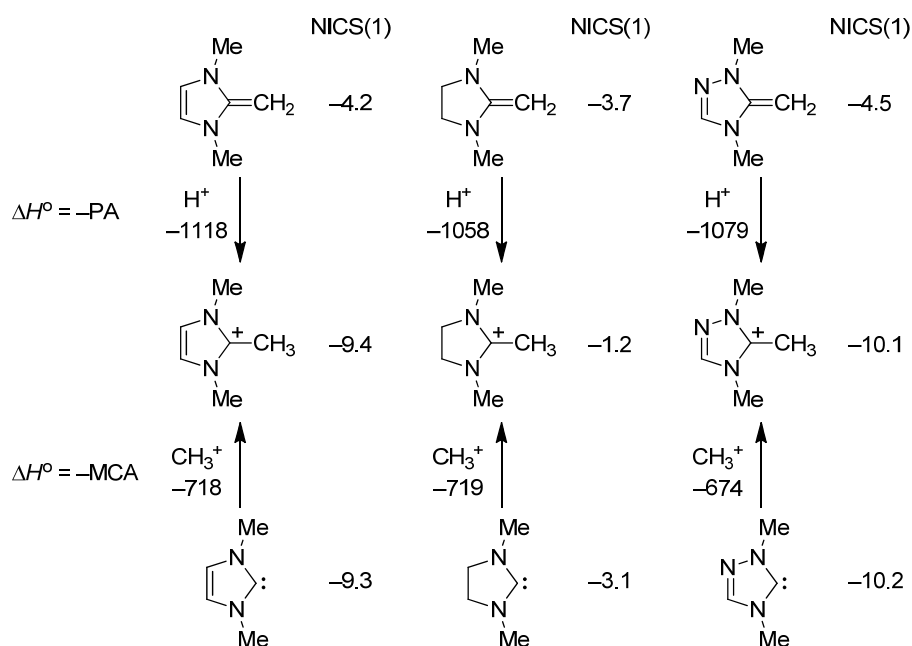
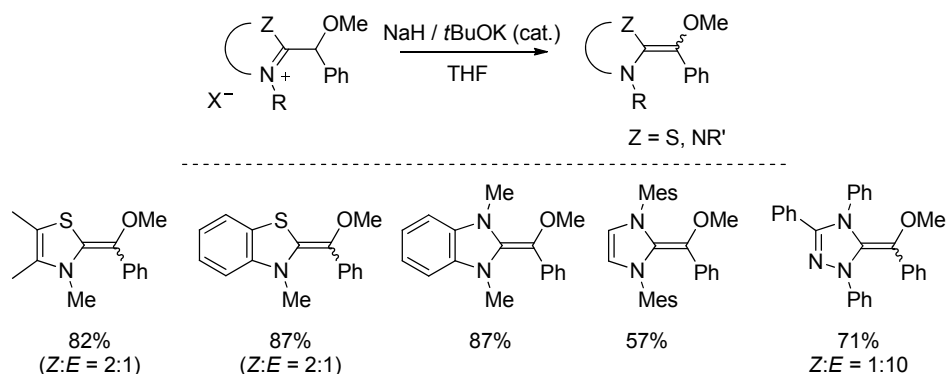


**Figure 7:** Comparison of the proton affinities (PAs) of the diaminoethylenes with the methyl cation affinities (MCAs) of the corresponding NHCs (in  $\text{kJ mol}^{-1}$ , MP2/6-31+G(2d,p)/B98/6-31G(d)), and the NICS(1) values of Breslow intermediates (B3LYP/6-311+G(d)).

As the NHCs are attacked by electrophiles at the nonbonding lone pair in the plane of the heterocyclic ring, the  $\pi$ -system is not affected and the different reactivities of the NHCs can be explained by inductive effects. In contrast, electrophilic additions to Breslow intermediates occur at the conjugated  $\pi$ -system, and resonance effects become important. A rationalization for this different behavior in the two series can be derived from the nucleus independent chemical shifts (NICS), which can be considered as a measure of aromaticity (Figure 7). As aromaticity increases during protonation of 2-methyleneimidazole and 3-methylene-1,2,4-triazoline but not during protonation of 2-methyleneimidazolidine or methyl cation addition to any of the carbenes, the exceptionally high nucleophilicity of the deoxy-Breslow intermediates, derived from the unsaturated carbenes, can be explained.

## 7 Structures and Reactivities of O-Methylated Breslow Intermediates

Since the Breslow intermediates are known to exist in their keto-form, their O-protected forms might be considered as their closest isolable relatives. O-methylated Breslow intermediates were synthesized by deprotonation of the corresponding azolium salts by NaH in the presence of catalytic amounts of potassium *tert*-butoxide in THF (Scheme 5).



**Scheme 5.** Synthesis of O-methylated Breslow intermediates.

X-ray crystallographic analyses of O-methylated Breslow intermediates show that the exocyclic double bonds adopt a planar geometry with CC-bond lengths (135-136 pm) similar to those in the corresponding deoxy-Breslow intermediates ( $\approx 136$  pm) and aza-analogue (136 pm) (Figure 8).

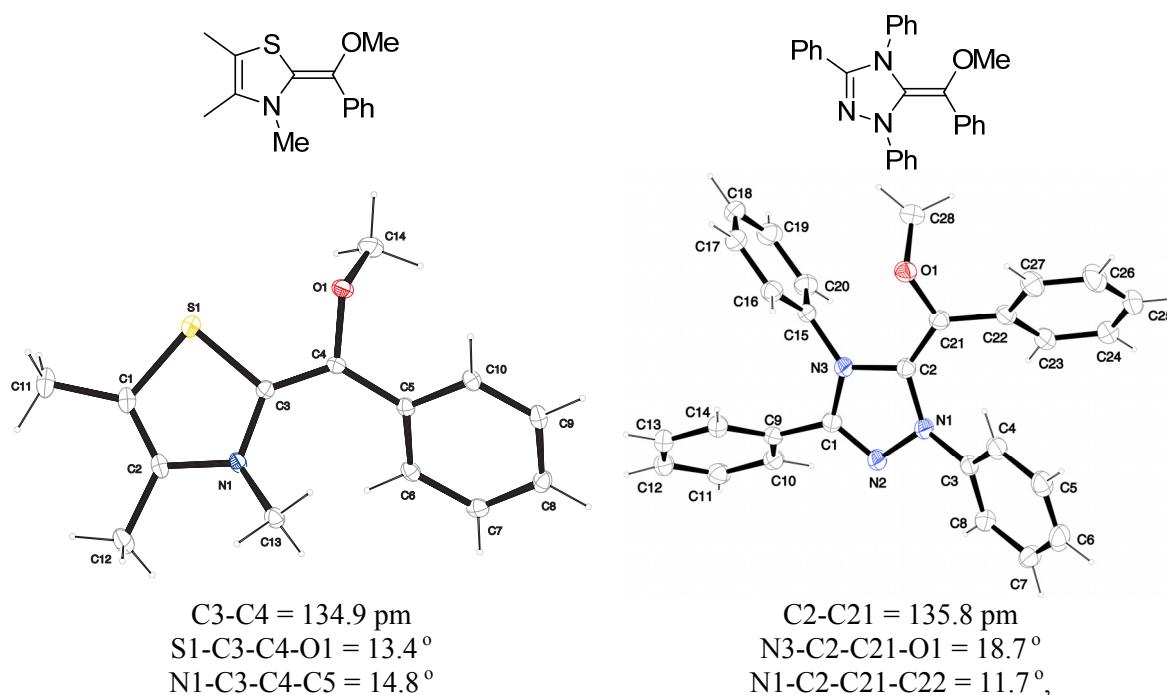
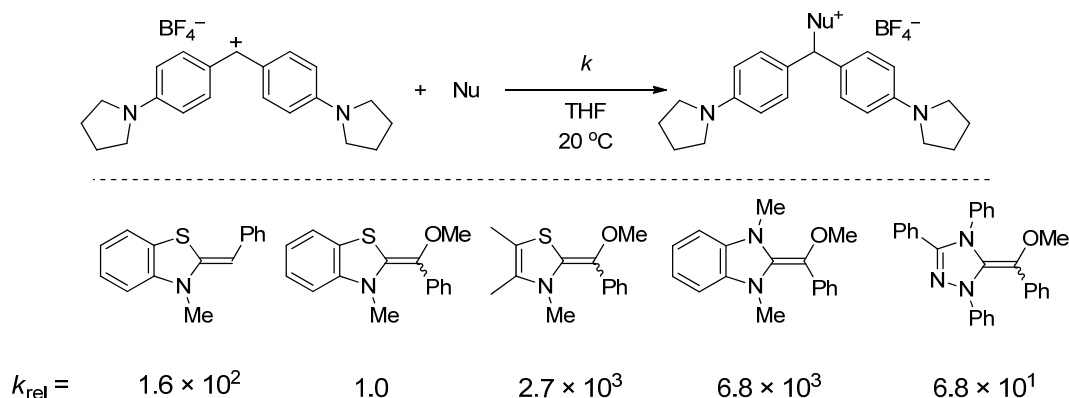


**Figure 8.** Crystal structures of O-methylated Breslow intermediates. Ellipsoids are shown at the 50% probability level.

The kinetics of the reactions of O-methylated Breslow intermediates with stabilized benzhydrylium ions were followed photometrically in THF at 20 °C and the nucleophilicity parameters  $N$  and  $s_N$  were derived from the linear plots of  $\log k$  vs  $E$  according to eq. (1). A comparison of the nucleophilic reactivities shows that O-methylated Breslow intermediates are  $10^2$  times less nucleophilic than the corresponding deoxy-Breslow intermediates and that Breslow intermediates derived from thiazoles are  $10^3$ - $10^4$  times less reactive than those derived from structurally analogous N-methyl imidazoles (Scheme 6).



**Scheme 6.** Relative reactivities of the O-methylated Breslow intermediates and comparison with deoxy-Breslow intermediate.

## 8 Nucleophilic Addition of Enols and Enamines to $\alpha,\beta$ -Unsaturated Acyl Azoliums: Mechanistic Studies

The electrophilic reactivity of the  $\alpha,\beta$ -unsaturated acyl imidazolium ion shown in Figure 9 was investigated towards a variety of nucleophiles (deprotonated  $\beta$ -diketones, and malonodinitrile, enamines, and enol ethers) by NMR and UV/vis-spectroscopy.

The electrophilicity parameter  $E$  of an  $\alpha,\beta$ -unsaturated acyl imidazolium ion ( $E = -11.52$ ) was determined from the linear plot of  $(\log k)/s_N$  vs  $N$ . A comparison of the  $E$  parameters with various electron-poor olefins shows that the strong electron withdrawing nature of the imidazolium ring makes  $\alpha,\beta$ -unsaturated acyl azolium ion  $10^7$  fold more electrophilic than a structurally analogous chalcone. However, its electrophilicity is  $10^3$  times lower than that of the structurally related iminium ion derived from the Hayashi-Jørgensen catalysts and  $10^4$  to  $10^6$  lower than the iminium ions derived from MacMillan's imidazolidinones (Figure 9).

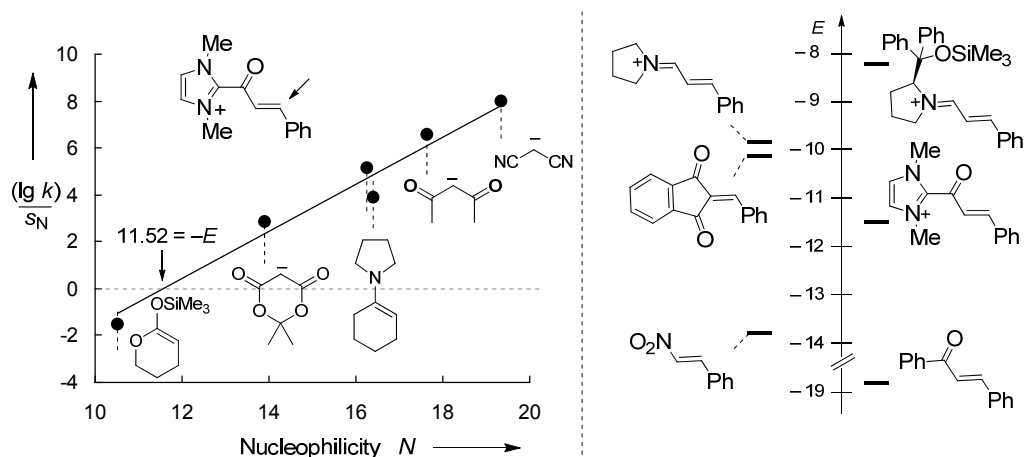
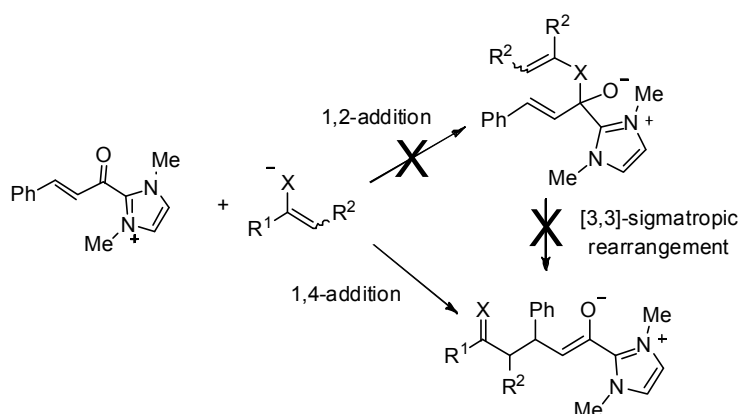


**Figure 9.** Determination of the  $E$  parameter of  $\alpha,\beta$ -unsaturated acyl imidazolium ion and comparison with other electrophilities.

The kinetic data indicate that the CC-bond for the isolated products are formed by a Michael-type 1,4-addition and not by 1,2-addition and subsequent [3,3]-sigmatropic rearrangement (Scheme 7), in line with high level DFT calculations.



**Scheme 7.** Mechanisms of the reactions of enolates or enamines with acyl azolium ion.

## 9 Nucleophilicity Parameters of Enamides and their Implications for Organocatalytic Transformations

The kinetics of the reactions of eleven substituted enamides with benzhydrylium ions were determined in acetonitrile solution at 20 °C. The second-order rate constants ( $\log k_2$ ) follow the correlation eq. (1) allowing us to derive the corresponding nucleophilicity parameters  $N$  and  $s_N$ . With  $4.6 < N < 7.1$ , enamides have similar nucleophilicities as enol ethers and non- or weakly activated indoles and pyrroles (Figure 10).

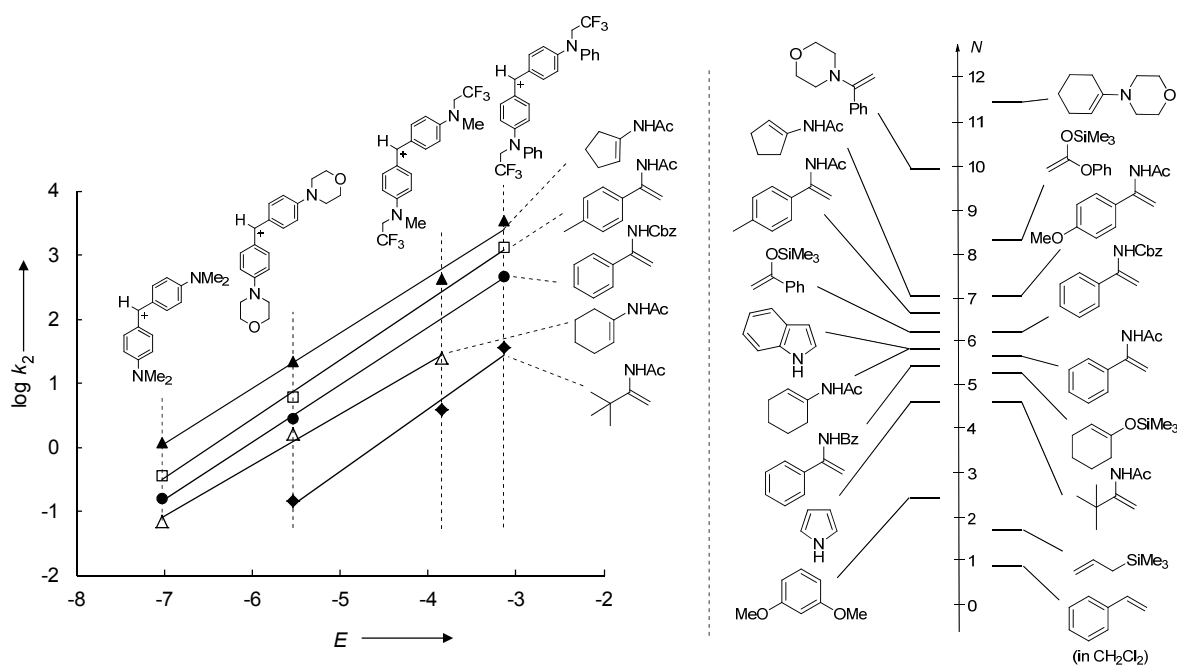


**Figure 10.** Determination of the nucleophilicity parameters  $N$  and  $s_N$  of enamides and comparison of with those of several other C nucleophiles (solvent is  $\text{CH}_3\text{CN}$  unless otherwise mentioned).

The experimental rate constants of the reactions of enamides with typical Michael acceptor 5-benzylidene-2,2-dimethyl-1,3-dioxane-4,6-dione and the chlorinating agent hexachlorocyclohexa-2,4-dienone were reliably reproduced by the  $N$  and  $s_N$  parameters of enamides and the previously reported  $E$  parameters the corresponding electrophiles.

Substitution of the  $N$  and  $s_N$  parameters of enamides and the  $E$  parameters of  $\alpha,\beta$ -unsaturated iminium ions into eq. (1) yields second-order rate constants of  $10^{-2}$  to  $10^1 \text{ M}^{-1} \text{ s}^{-1}$  which corresponds to readily occurring reactions at room temperature. However, the reactions of enamides with  $\alpha,\beta$ -unsaturated iminium ions only proceeded in the presence of bases (e.g., 2,6-lutidine), which was explained by the reversibility of the first step of the reaction sequence depicted in Figure 11. By studying the kinetics of the reactions of enamides with

$\alpha,\beta$ -unsaturated iminium ions in the presence of variable concentrations of lutidine or collidine, we were able to determine the second-order-rate constants for the CC-bond-forming steps which agree within factors of 1-3 with those calculated by eq. (1) (Figure 11).

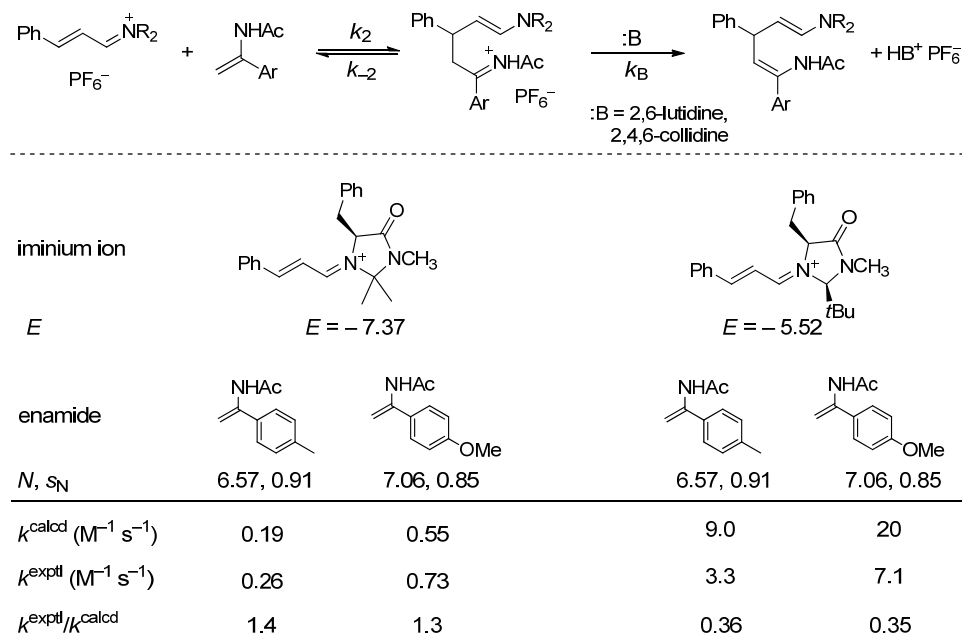
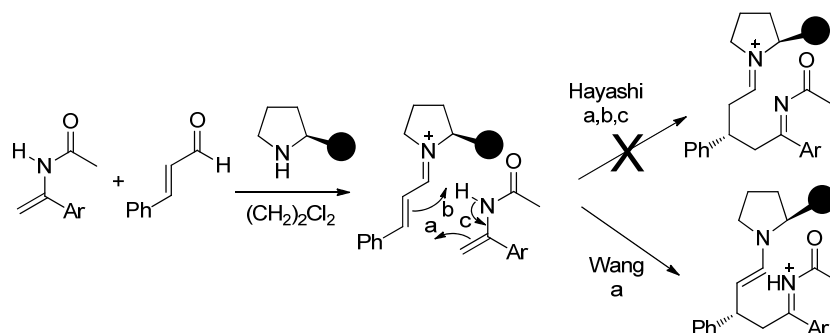


**Figure 11.** Experimental and calculated rate constants  $k_2$  for the reactions of enamides with  $\alpha,\beta$ -unsaturated iminium ions.

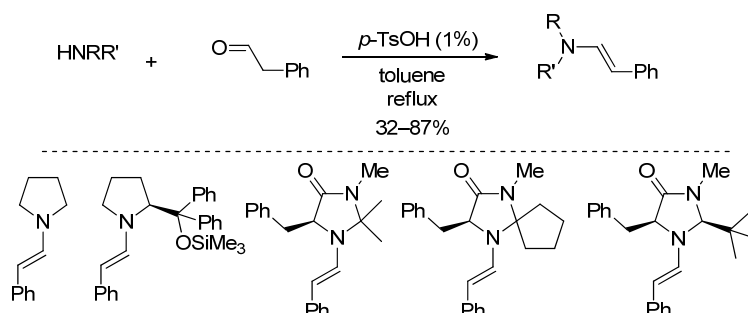
This observation explains why strong acids, e.g. TsOH, are not good cocatalysts for iminium activated reactions of  $\alpha,\beta$ -unsaturated aldehydes with enamides. In line with this argument,  $\text{CF}_3\text{CO}_2\text{H}$  was found to catalyze this reaction although with moderate enantioselectivity. This observation rules out Hayashi's mechanistic proposal of a concerted ene reaction (a,b,c in Scheme 8) for the formation of tetrahydropyrimidines and support Wang's proposal of a stepwise mechanism (a in Scheme 8), because Hayashi's pericyclic process would not require general base catalysis.



**Scheme 8.** Mechanisms for the chiral secondary amine catalyzed reactions of  $\alpha,\beta$ -unsaturated aldehydes and enamides.

## 10 Imidazolidinone-Derived Enamines: Nucleophiles with Low Reactivity

Imidazolidinone-derived enamines were synthesized by the TsOH-catalyzed condensation of the corresponding imidazolidinone and phenyl acetaldehyde and followed by column chromatographic separation on silica-gel using *n*-pentane/EtOAc/ $\text{NEt}_3$  as eluent (Scheme 9).



**Scheme 9:** Synthesis of enamines derived from phenyl acetaldehyde and various secondary amines.

Kinetics of the reactions of these enamines with benzhydrylium ions were studied photometrically in acetonitrile solution at 20 °C, and the obtained second-order-rate constants were used to derive their nucleophilicity parameters  $N$  and  $s_N$  (Figure 12).

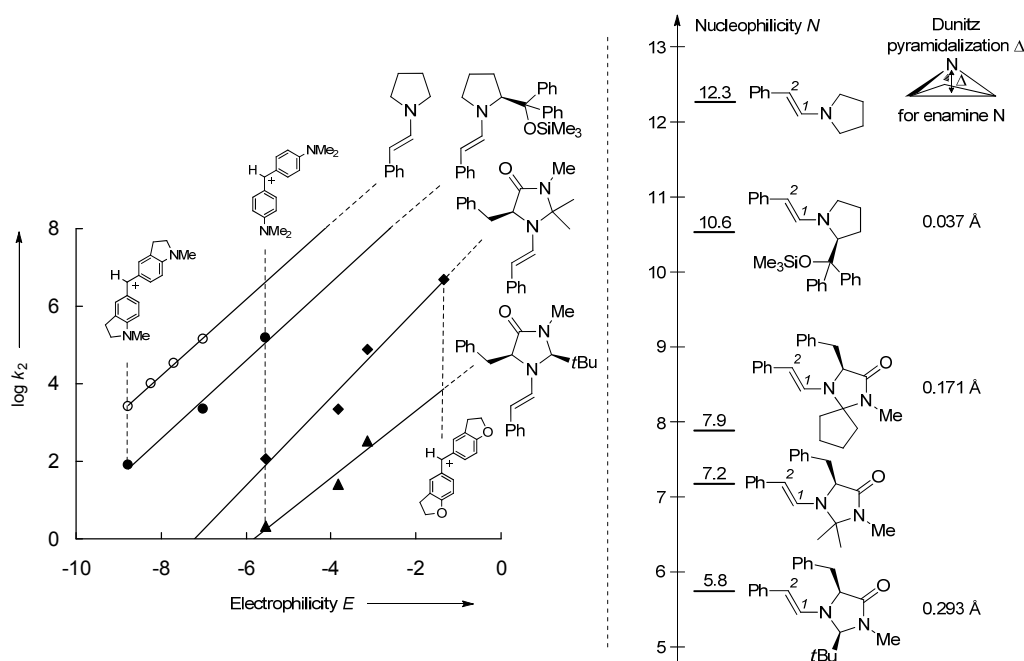


**Figure 12.** Determination of the nucleophilicity parameters of chiral enamines.

A comparison of the nucleophilic reactivities of enamines show that the enamine, derived from the Hayashi-Jørgensen catalyst, is almost two orders of magnitude less reactive than *N*-( $\beta$ -styryl)pyrrolidine which can be explained by the inductive effect of  $(\text{Me}_3\text{SiO})\text{Ph}_2\text{C}$ -group

in 2-position. Imidazolidinone derived enamines are even  $10^3$  to  $10^5$ -times less nucleophilic than the enamine derived from the Hayashi-Jørgensen catalyst. The low nucleophilicities of the imidazolidinone derived enamines, which are in line with the down-field  $^{13}\text{C}$  NMR chemical shifts of C-2, can be realized by extent of pyramidalization of the enamine nitrogen, which reduces the overlap between the nitrogen lone-pair and the  $\pi_{\text{CC}}$ -bond (Figure 12).

## Chapter 1

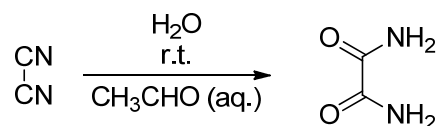
# Introduction

## 1 Organocatalysis

The use of small organic molecules as catalysts in the absence of metal atoms is one of the most important tools for making C–C and C–X bond (X = halogen, ‘O’, ‘N’, ‘S’ etc.) and has emerged as one of most competitive branches of asymmetric catalysis in the last two decades.<sup>[1]</sup> The term organocatalysis was introduced by MacMillan in 2000 and it is defined as *the acceleration of a chemical transformation through addition of a substoichiometric amount of an organic compound which does not contain a metal atom.*<sup>[2]</sup> The operational simplicity, robustness, low cost, availability from renewable sources, and relative nontoxicity makes organocatalysis advantageous over metal- and enzyme catalysis which played the central role in homogeneous catalysis over the last century.<sup>[1]</sup>

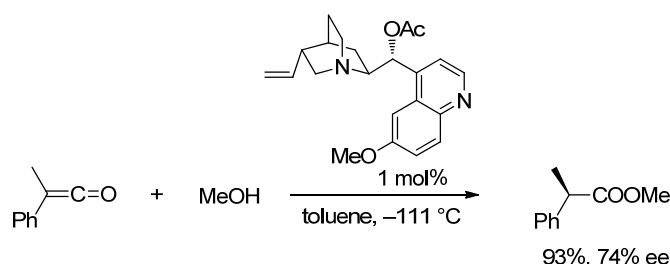
### 1.1 History and development

The transformation of dicyan to oxamide in the presence of an aqueous solution of acetaldehyde by Justus von Liebig in 1860 was considered to be the first report of organocatalysis (Scheme 1).<sup>[3]</sup> The first asymmetric organocatalyzed transformation was reported in 1912 by Bredig and Fiske, who found that cinchona alkaloids catalyzed the addition of HCN to benzaldehyde.<sup>[4]</sup> Few years later, Langenbeck coined the term “Organische Katalysatoren” when publishing a series of papers describing the use of small organic molecules as a mimic of enzyme catalysts.<sup>[5]</sup> In 1943 Ukai et al. found that thiamine can catalyze benzoin condensation reactions.<sup>[6]</sup> Breslow, in 1958 proposed the currently accepted mechanism for these reactions.<sup>[7]</sup>

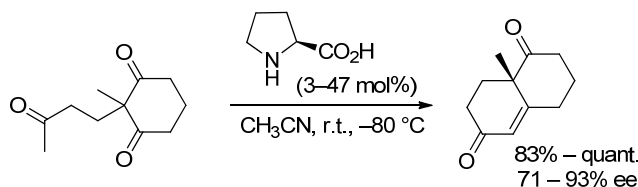


**Scheme 1.** Liebig's oxamide synthesis.<sup>[3]</sup>

The first synthetically useful asymmetric organocatalyzed transformation, however, was achieved in 1960 by Pracejus who found O-acetylquinine to be an excellent catalyst (93% yield and 74% ee with 1 mol% catalyst loading) for the methanolysis of phenylmethylketene (Scheme 2).<sup>[8]</sup> The 1970s witness another breakthrough in organocatalysis, namely the discovery of L-proline as catalysts for an intramolecular aldol reaction (Hajos-Parrish-Eder-Sauer-Wiechert reaction, Scheme 3).<sup>[9]</sup> In the 1980s Inoue reported enantioselective hydrocyanations of benzaldehydes using cyclic peptides as organocatalysts, and it was considered as one of the pioneering works of peptide catalysis.<sup>[10]</sup> Later, poly-amino acid catalyzed epoxidation of chalcones was established by Juliá and Colonna et al.<sup>[11]</sup> At the same time O'Donnell et al. systematically established asymmetric phase transfer catalysis.<sup>[12]</sup>



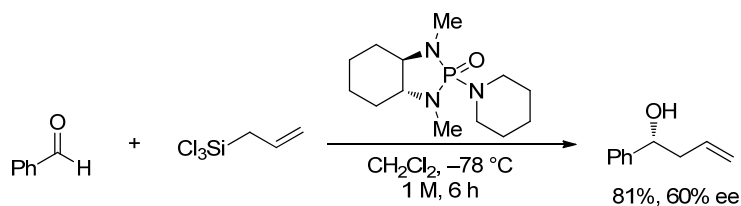
**Scheme 2.** Enantioselective addition of methanol to phenyl methyl ketene as reported by Pracejus.<sup>[8]</sup>



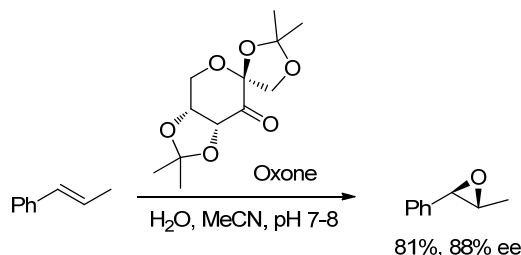
**Scheme 3.** L-Proline-catalyzed Hajos-Parrish-Sauer-Wiechert reaction.<sup>[9]</sup>

The requirement for greener, economical, and general synthetic methods led to the development of organocatalysis in the 1990s. In 1994 Denmark utilized chiral Lewis bases for asymmetric allylations of aldehydes (Scheme 4).<sup>[13]</sup> Two years later, the group of Yang and Shi independently published chiral ketone catalyzed-enantioselective epoxidation of olefins (Scheme 5).<sup>[14]</sup> Asymmetric alkylations of protected glycines, catalyzed by a cinchona alkaloid derived phase transfer catalysts, were disclosed in 1997 by Corey et al. and Lygo et al. (Scheme 6).<sup>[15]</sup> At the same time, Fu introduced a planar chiral DMAP derivative for the kinetic resolution of secondary alcohols.<sup>[16]</sup> In 1998, Jacobsen introduced chiral thioureas to catalyze enantioselective HCN additions to imines (Scheme 7).<sup>[17]</sup> One year later, chiral binaphthalene-based-phase transfer catalysts were developed by Maruoka et al.<sup>[18]</sup> and at the

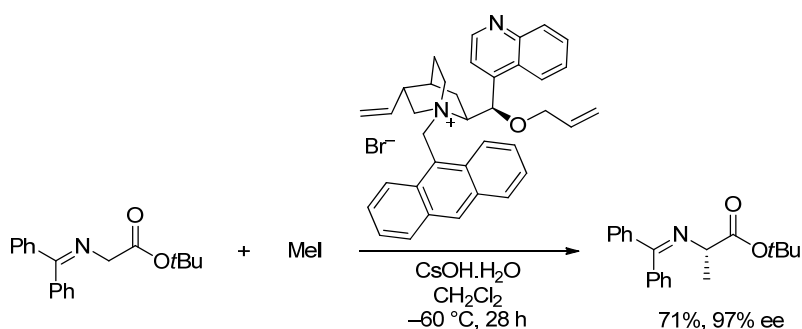
same time, Corey and coworkers utilized chiral guanidines to catalyze hydrocyanations of benzaldehydes (Scheme 8).<sup>[19]</sup>



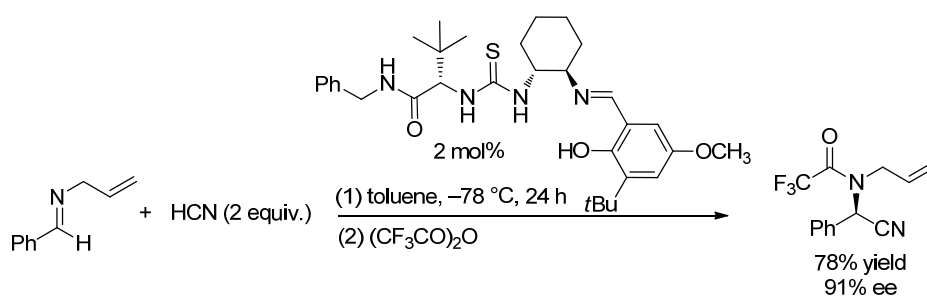
**Scheme 4.** Chiral phosphoramidate-catalyzed asymmetric allylation of benzaldehyde.<sup>[13]</sup>



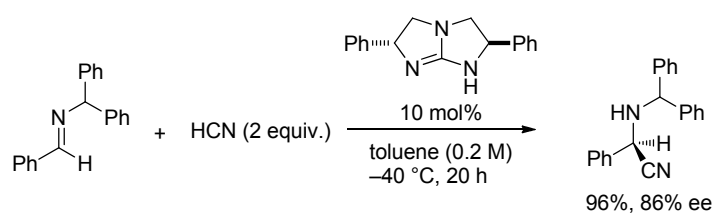
**Scheme 5.** Asymmetric epoxidation of alkenes.<sup>[14]</sup>



**Scheme 6.** Cinchona alkaloid derived phase transfer catalyzed asymmetric methylation of protected glycine.<sup>[15]</sup>

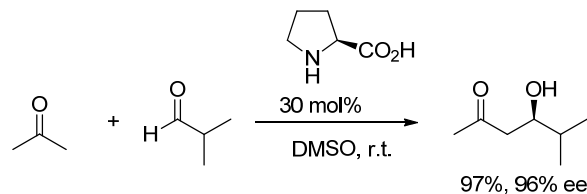


**Scheme 7.** Chiral thiourea-catalyzed enantioselective addition of HCN to an imine.<sup>[17]</sup>

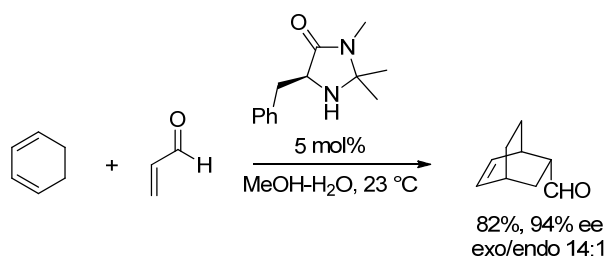


**Scheme 8.** Chiral guanidine catalyzed asymmetric hydrocyanation of an imine.<sup>[19]</sup>

Finally, in the year 2000, pioneering work by List, Lerner, and Barbas on proline-catalyzed intermolecular aldol reactions (Scheme 9)<sup>[20]</sup> and by MacMillan and coworkers on imidazolidinone-catalyzed Diels-Alder reactions (Scheme 10)<sup>[2]</sup> triggered the modern age of organocatalysis and inducing a “gold rush.”<sup>[21]</sup>



**Scheme 9.** L-Proline-catalyzed intermolecular aldol condensation reaction reported by List, Lerner, and Barbas.<sup>[20]</sup>



**Scheme 10.** Imidazolidinone catalyzed Diels-Alder reaction reported by MacMillan.<sup>[2]</sup>

## 1.2 Modes of activation

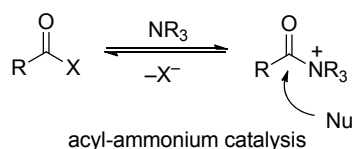
As several criteria may be applicable, the classification of general modes of activation in organocatalytic reactions is difficult. Rough distinctions can be made between catalysts, which form covalent reactive intermediates (e.g., proline, cinchona alkaloids, or N-heterocyclic carbenes), and those which stabilize the transition states via non-covalent interactions (such as thiourea). Another way of differentiation of the organocatalyst can be derived on the basis how they activate the substrate: HOMO activation (e.g., enamine catalysis, N-heterocyclic carbene catalysis) and LUMO activation (e.g., iminium catalysis, thiourea catalysis). Seayad and List classified organocatalytic processes by four categories: Lewis base, Lewis acid, Brønsted base, and Brønsted acid catalysis.<sup>[22]</sup> A phase transfer catalysts (PTC) may work by any of the previously mentioned activation modes providing a chiral “shuttle” for reaction partners located in different phases.<sup>[23]</sup> Sometimes a single organocatalyst promotes reactions by several modes of activation. Mechanistically they can be assigned as multifunctional catalysts.<sup>[24]</sup>

Since most of the work in this thesis concentrates on tertiary amines, secondary amines, and N-heterocyclic carbenes catalyzed reactions, the following discussion will give a brief

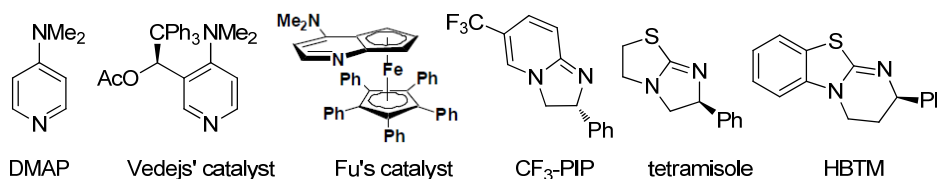
introduction on the tertiary amine, secondary amine, and N-heterocyclic carbene catalyzed reactions.<sup>[25,26]</sup>

### 1.3 Tertiary amine-catalyzed reactions

#### 1.3.1 Acyl-ammonium catalysis

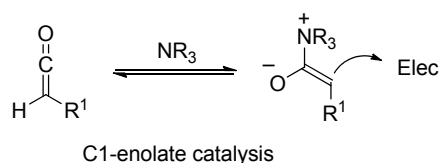


Acyl ammonium catalysis is initiated by the attack of the catalysts (tertiary amine) at an acyl substrate to form an electrophilic acyl-ammonium ion, which then reacts with a nucleophile (generally an alcohol). Well-known organocatalysts developed for trans-esterifications, kinetic resolutions of alcohols, Steglich rearrangements etc., are DMAP based catalysts<sup>[27]</sup> including Fu's planar chiral ferrocenyl catalysts,<sup>[16]</sup> and Vedejs' catalysts,<sup>[28]</sup> Birman's dihydroimidazole-based catalysts CF<sub>3</sub>-PIP,<sup>[29]</sup> and the isothiourea based catalysts like tetramisole and its derivative HBTM (Scheme 11).<sup>[30]</sup>

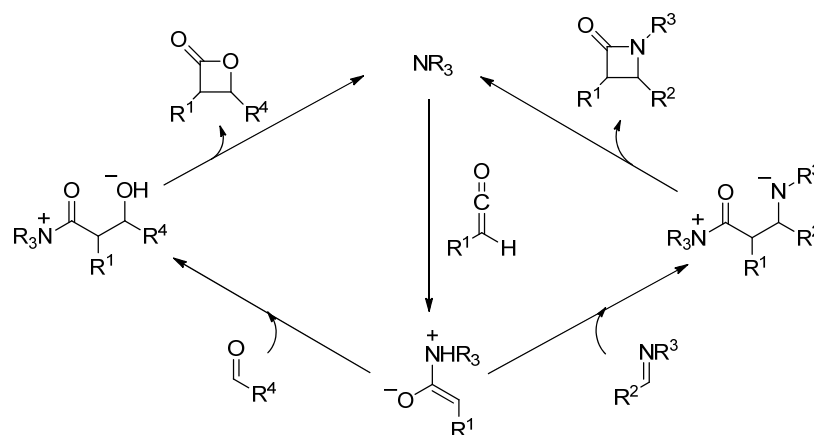


**Scheme 11.** Some common tertiary amine catalysts used for acylation reactions.

#### 1.3.2 C1-enolate catalysis

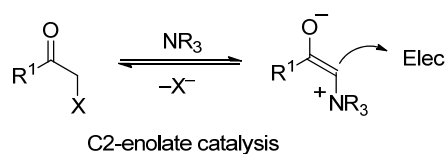


The reaction of a ketene with nucleophilic tertiary amine or phosphane catalysts leads to the formation of a C1-enolate, which subsequently reacts with aldehydes or imines leading to the formation of  $\beta$ -lactones or  $\beta$ -lactams (Scheme 12).<sup>[31,32]</sup> This methodology was also successfully used for the  $\alpha$ -halogenations, and aminations of carboxylic acids, and [4+2]-cycloaddition reactions.<sup>[33]</sup>

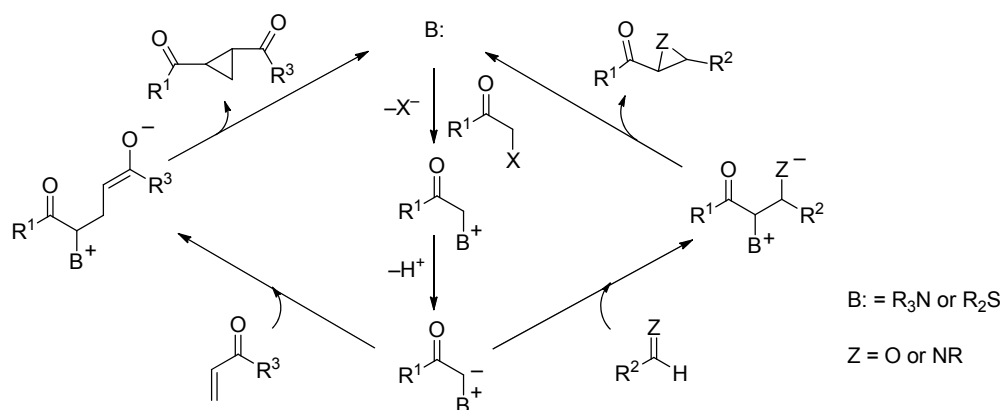


**Scheme 12.** Tertiary amine catalyzed  $\beta$ -lactones or  $\beta$ -lactams formation via C1-enolate.

### 1.3.3 C2- enolate catalysis

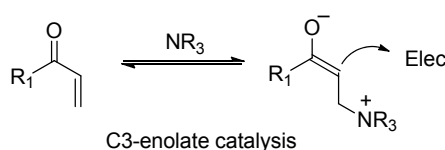


C2-enolate catalysis proceeds with an  $S_N2$  type reaction of a sulfide or tertiary amine (B:) to form a tertiary sulfonium or ammonium salt, which undergoes deprotonation with a base to form a C2-enolate (or an ylide). The ylide then reacts with an aldehyde, imine or electron-deficient CC-double bond to give an epoxide, aziridine, or cyclopropane (Scheme 13).<sup>[31,34]</sup>

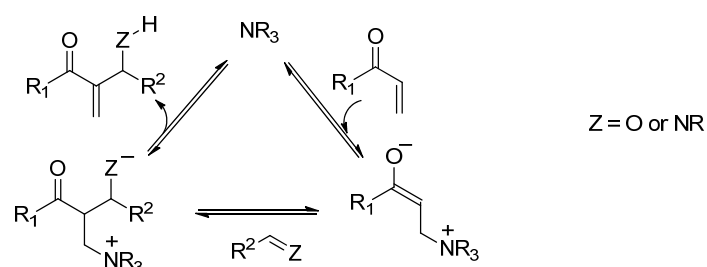


**Scheme 13.** Sulfide and tertiary amine-catalyzed epoxidation, aziridination, and cyclopropanation reactions.

### 1.3.4 C3- enolate catalysis



The Morita-Baylis-Hillman reaction or its aza-counterpart are among the most used Lewis base catalyzed reactions via intermediate C3-enolates.<sup>[35]</sup> Atom economy and generation of highly functionalized compounds makes this reaction a highly important CC-bond forming reaction. A simplified catalytic cycle starts with the 1,4-addition of a nucleophilic tertiary amine to an activated olefin which leads to the formation of the C3-enolate. The reaction of the zwitterionic C3-enolate with a carbonyl compound or an imine followed by proton migration and then elimination of the catalyst provides  $\alpha$ -functionalized product (Scheme 14).<sup>[35]</sup>

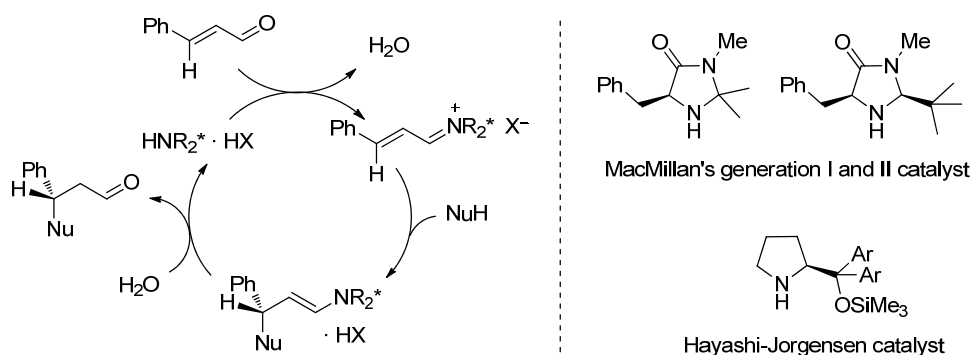


**Scheme 14.** Simplified catalytic cycle for a tertiary amine catalyzed MBH reaction.

## 1.4 Secondary amine-catalyzed reactions

### 1.4.1 Iminium activation

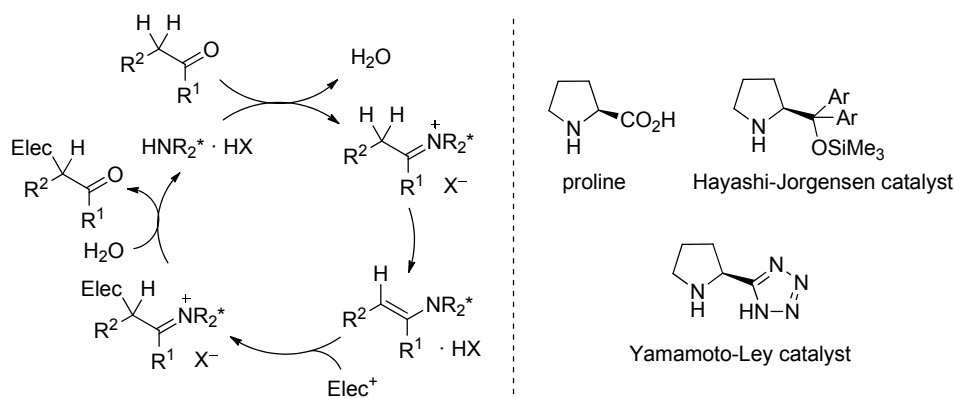
The LUMO-lowering effect is the underlying strategy of the iminium catalysis.<sup>[36]</sup> This mode of activation utilizes the ability of a secondary amine ( $\text{HNR}_2^*$ ) to undergo reversible condensation with an  $\alpha,\beta$ -unsaturated aldehyde to give an iminium ion which undergoes conjugate additions to give the product (Scheme 15). Using the LUMO-lowering strategy, excellent results have been obtained in cycloaddition,<sup>[37]</sup> Diels-Alder,<sup>[2,38]</sup> Friedel-Crafts alkylation,<sup>[39]</sup> Mukaiyama-Michael reactions,<sup>[40]</sup> etc.



**Scheme 15.** Simplified catalytic cycle for iminium-activated reactions and typical secondary amine catalysts used for these reactions.

### 1.4.2 Enamine activation

In enamine activation strategy, enolizable carbonyl compounds are activated by the formation of an enamine intermediate, which then reacts with a variety of electrophiles (Scheme 16).<sup>[41]</sup> This HOMO-raising methodology has successfully been utilized in aldol, Mannich, Michael, Baylis-Hilman reactions, and  $\alpha$ -functionalizations of aldehydes and ketones such as aminations, hydroxylations, alkylations, halogenations etc.<sup>[41]</sup>

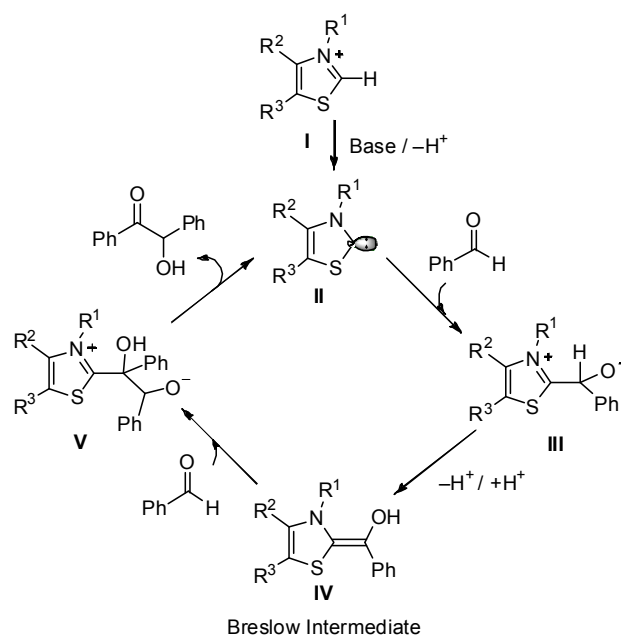


**Scheme 16.** Simplified catalytic cycle for enamine catalysis and typical amine catalysts used for these reactions.

Applying this strategy to enolizable  $\alpha,\beta$ -unsaturated carbonyls or poly-conjugated carbonyls, dienamine or trienamine activations were achieved. Thus  $\gamma$ - and  $\epsilon$ -functionalizations of the unsaturated carbonyl compounds were achieved.<sup>[42]</sup>

### 1.5 Organocatalysis by N-heterocyclic carbenes

The use of N-heterocyclic carbenes (NHCs) as organocatalysts started in 1943, when Ukai and co-workers found that thiazolium salts can be used as catalysts for the benzoin condensation.<sup>[6]</sup> The mechanism nowadays accepted for these reactions was proposed by Breslow in 1958, when he described that the thiazolium ring **I** first undergoes deprotonation at the most acidic position to give an ylide or carbene **II**. The subsequent nucleophilic addition of **II** to an aldehyde generates the zwitterion **III** which undergoes a carbon to oxygen proton shift to give a resonance stabilized enaminal, nowadays called the Breslow intermediate **IV**, a nucleophilic acyl anion equivalent. Its reaction with a second molecule of aldehyde followed by a proton shift and release of **II** generates the benzoin (Scheme 17).<sup>[7]</sup> According to Seebach's terminology, this phenomenon is called "Umpolung" and the umpoled aldehyde reacts as a d<sub>1</sub>-synthon.<sup>[43]</sup>

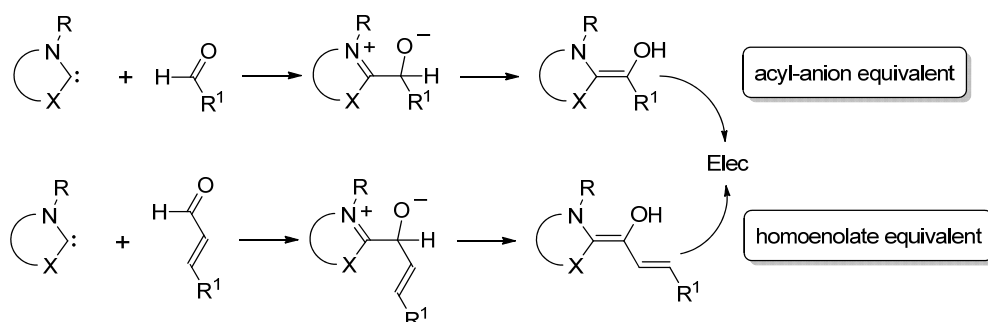


**Scheme 17.** Breslow's mechanistic proposal for thiazole-ylidene catalyzed benzoin condensation reactions.

The application of Breslow intermediates as acyl anion equivalents was further extended by using electron-poor olefins as electrophiles. That reaction is well known as Stetter reaction.<sup>[44]</sup> The last few decades have witnessed a huge application of these methodologies in racemic as well as asymmetric versions of the benzoin condensation and Stetter reaction using various N-heterocyclic carbenes.<sup>[26]</sup>

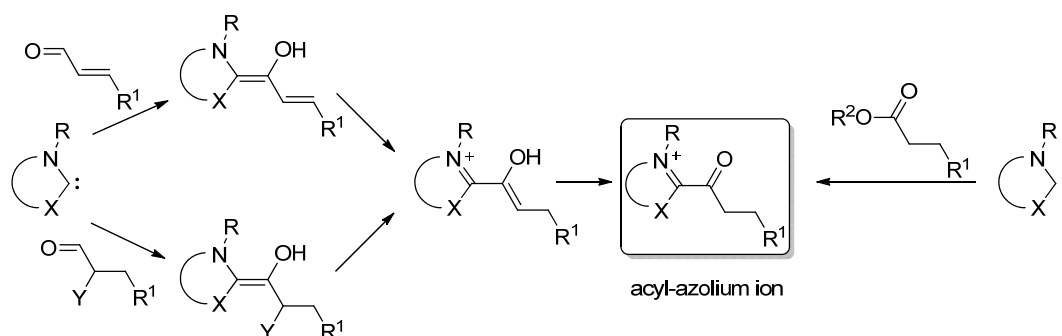
Two independent reports by Glorius and Bode extended umpolung activity of aldehydes to  $\alpha,\beta$ -unsaturated aldehydes to yield a conjugated enaminol intermediate, called homoenolate (Scheme 18). Disubstituted  $\gamma$ -butyrolactones were formed by the addition of this homoenolate to an aliphatic aldehyde.<sup>[45]</sup>

After these initial reports, additions of homoenolates to several other electrophiles including electron deficient ketones, 1,2-dicarbonyls, *N*-sulfonylimines, azomethine imines, cyclic ketimines, 1-acyl-2-aryldiazenes, and nitrosobenzene have been investigated.<sup>[46]</sup>



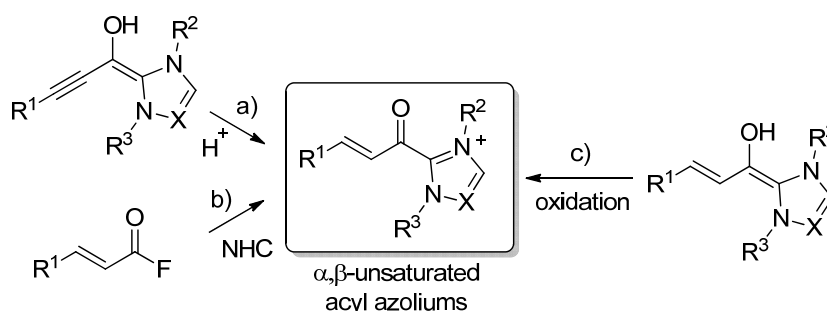
**Scheme 18.** Acyl-anion (top) and Homoenolate (bottom) reactivity.





**Scheme 21.** Different routes for generation of acyl azolium ion.

Along this line, the chemistry of  $\alpha,\beta$ -unsaturated acyl azolium ions have recently gained great attention. These reactive intermediates can be generated by three different routes: a) Protonation of the Breslow intermediate formed in the reaction of an enal with an NHC; b) reaction of an  $\alpha,\beta$ -unsaturated acyl fluoride with an NHC; and c) oxidation of the Breslow intermediate formed in the reaction of an enal with an NHC (Scheme 22). The reactions of  $\alpha,\beta$ -unsaturated acyl azoliums with  $\alpha$ -ketoenols,  $\beta$ -diketones, and enamines led to the formation of dihydropyranones and dihydropyridinones.<sup>[51]</sup>



**Scheme 22.** Different routes for generation of  $\alpha,\beta$ -unsaturated acyl azoliums.

## 2 The benzhydrylium based scale of nucleophilicity

In 1930s, Ingold defined electron-deficient and electron-rich species as ‘electrophiles’ and ‘nucleophiles’, respectively.<sup>[52]</sup> Since most organic reactions are polar in nature, i.e. combinations of electrophilic compounds with nucleophilic compounds quantification of electrophilicities and nucleophilicities on a single basis will be the key to derive a general concept for the description and prediction of polar organic reactivity. In this line the first systematic approach was made by Swain and Scott. By studying the rates of  $S_N2$  reactions, a nucleophilicity scale was developed on the basis of equation (1), where  $n$  represents the nucleophilicity of a certain nucleophile,  $s$  characterizes the sensitivity of an electrophile towards the variation of the nucleophile, and  $\log k_0$  is the rate constant of the reaction of a

particular electrophile with water. As a reference system, they initially chose methyl bromide ( $s = 1.00$ ) in water ( $n = 0.00$ ).<sup>[53]</sup>

$$\log (k/k_0) = sn \quad (1)$$

In 1972, Ritchie discovered that the rates of the reactions various  $n$ -nucleophiles with diazonium ions and stabilized carbocations follow constant selectivity relationships, which can be described by equation (2), where  $k$  is the rate constant for the reaction of a given cation in a given solvent,  $k_0$  is the rate constant for reaction of same cation with water, and  $N_+$  is the electrophile dependent nucleophilicity parameter. Although Ritchie's nucleophilicity scale covers a range of about 13 orders of magnitude, it was shown later, that better correlations were obtained when different families of electrophiles were treated separately.<sup>[54]</sup>

$$\log (k/k_0) = N_+ \quad (2)$$

In 1994, based on the rates of the reactions of carbocations, cationic metal- $\pi$ -complexes, and diazonium ions with  $n$ -,  $\pi$ -, and  $\sigma$ -nucleophiles, Mayr and Patz introduced the three-parameter equation (3), where  $k_{(20\text{ }^\circ\text{C})}$  is the second-order rate constant at 20 °C,  $N$  is the nucleophilicity parameter,  $s_N$  is the nucleophile-specific sensitivity parameter, and  $E$  is the electrophilicity parameter.<sup>[55]</sup>

$$\log k_{(20\text{ }^\circ\text{C})} = s_N(N+E) \quad (3)$$

Benzhydrylium ions and structurally related quinone methides were chosen as reference electrophiles, as the steric surroundings at the reaction centers can be kept constant while the reactivity can widely be varied by introducing different substituents in meta and para position of the aromatic rings.<sup>[56]</sup> Using equation (3) it was possible to construct the most comprehensive nucleophilicity and electrophilicity scale presently available, presently including 720 nucleophiles and 218 electrophiles.<sup>[57]</sup>

Determinations of nucleophilicity ( $N$  and  $s_N$ ), and electrophilicity ( $E$ ) parameters have established a rough ordering principle of polar organic reactivity. The rules of thumb that nucleophile electrophile combinations only occur at room temperature when  $E + N > -5$ , and diffusion controlled reactions will take place when  $E + N > 9$  enable a rational design of organic synthesis with a better understanding of reactivities and selectivities.<sup>[58]</sup>

### 3 Objectives

In the rapidly growing field of organocatalysis the knowledge of structures and reactivities of the organocatalysts and reactive intermediates will not only help to understand the mechanisms of these reactions but also this will be a key to the rational design of new organocatalysts with improved reactivity and selectivity.

The mechanistic considerations in Section 2 show that the efficiency of a nucleophilic organocatalyst will depend on three parameters; 1) nucleophilicity (i.e. how fast organocatalysts will enter into a cycle), 2) Lewis basicity (i.e. how long they are going to stay in the cycle which determines the active concentration of the reactive intermediates), and 3) nucleofugality (i.e. how fast they will exit from the cycle). While characterizations of nucleophilicities and Lewis basicities of several classes of N-centered organocatalysts were possible using the benzhydrylium methodology,<sup>[57]</sup> three important classes of amidine organocatalysts, isothioureas,<sup>[30]</sup> guanidines,<sup>[59]</sup> and azolidines<sup>[60]</sup> are not so far integrated. This was the goal of the first part of this work to characterize their nucleophilicities and Lewis basicities and combine these values to derive the nucleofugalities.

Structure-reactivity relationships for the intermediates of N-heterocyclic carbene catalyzed reactions were the focus of the second part of this thesis. This problem was pending for several years since most NHCs react with most of the solvents we have been using for our investigations.<sup>[61]</sup> Therefore, kinetics of the reactions of the NHCs with reference electrophiles should be determined in a suitable inert solvent. The resulting  $N$  and  $s_N$  parameters will then be compared with other commonly used nucleophilic organocatalysts.

In further experiments, structural, kinetic, and quantum chemical investigations of deoxy-Breslow intermediates should allow one to answer why unsaturated NHCs are more suitable organocatalysts than their saturated analogues, while both classes are equally useful as metal ligands.<sup>[26,49]</sup>

Since Breslow intermediates usually exist in their keto form,<sup>[62]</sup> their O-protected forms may be considered as their closest isolable relatives. They should be synthesized by deprotonation of the corresponding azolium salts and characterized spectroscopically and by X-ray analysis. Their nucleophilic reactivities shall then be derived from the kinetics of their reactions with benzhydrylium ions.

The last part of this work deals with structure-reactivity relationships of secondary amine activated reactions of carbonyl compounds namely 1) iminium activation and 2) enamine activation.<sup>[36,41]</sup> Kinetic and synthetic investigations of these reactions should not only help to

understand their mechanisms but also help to define conditions required for successful organocatalytic conversions.

As parts of this thesis have already been published, accepted or prepared for publication, individual introductions will be given at the beginning of each chapter. In order to identify my contributions to the multiauthor publications, only the kinetic and synthetic experiments, which were performed by me, are described within the corresponding Experimental Section.

## 4 References

- [1] a) P. I. Dalko, *Enantioselective organocatalysis*, Wiley-VCH, Weinheim, **2007**. b) A. Berkessel, H. Gröger, *Asymmetric Organocatalysis*, Wiley-VCH, Weinheim, **2005**.
- [2] K. A. Ahrendt, C. J. Borths, D. W. C. MacMillan, *J. Am. Chem. Soc.* **2000**, *122*, 4243–4244.
- [3] J. Liebig, *Annalen der Chemie und Pharmacie* **1860**, *13*, 246–247.
- [4] G. Bredig, W. S. Fiske, *Biochem. Z.* **1912**, *7*.
- [5] a) W. Langenbeck, *Angew. Chem.* **1928**, *41*, 740–745; b) W. Langenbeck, *Angew. Chem.* **1932**, *45*, 97–99.
- [6] T. Ukai, R. Tanaka, T. Dokawa, *J. Pharm. Soc. Jpn.* **1943**, *63*, 296–300.
- [7] R. Breslow, *J. Am. Chem. Soc.* **1958**, *80*, 3719–3726.
- [8] H. Prajecus, *Justus Liebigs Ann. Chem.* **1960**, *634*, 9–22.
- [9] a) Z. G. Hajos, D. R. J. Parrish, *J. Org. Chem.* **1974**, *39*, 1615–1621; b) U. Eder, G. Sauer, R. Wiechert, *Angew. Chem. Int. Ed.* **1971**, *10*, 496–497.
- [10] J. Oku, S. Inoue, *J. Chem. Soc., Chem. Commun.* **1981**, 229–230.
- [11] a) S. Juliá, J. Masana, J. C. Vega, *Angew. Chem. Int. Ed.* **1980**, *19*, 929–931; b) S. Juliá, J. Guixer, J. Masana, J. Rocas, S. Colonna, R. Annuziata, H. Molinari, *J. Chem. Soc., Perkin. Trans. I* **1982**, 1317–1324.
- [12] a) M. J. O'Donnell, T. M. Eckrich, *Tetrahedron Lett.* **1978**, *19*, 4625–4628; b) M. J. O'Donnell, W. D. Bennett, S. Wu, *J. Am. Chem. Soc.* **1989**, *111*, 2353–2355.
- [13] S. E. Denmark, D. M. Coe, N. E. Pratt, B. D. Griedel, *J. Org. Chem.* **1994**, *59*, 6161–6163.
- [14] a) D. Yang, Y.-C. Yip, M.-W. Tang, M.-K. Wong, J.-H. Zheng, K.-K. Cheung, *J. Am. Chem. Soc.* **1996**, *118*, 491–492; b) Y. Tu, Z.-X. Wang, Y. Shi, *J. Am. Chem. Soc.* **1996**, *118*, 9806–9807.
- [15] a) E. J. Corey, F. Xu, M. C. Noe, *J. Am. Chem. Soc.* **1997**, *119*, 12414–12415; b) B. Lygo, P. G. Wainwright, *Tetrahedron Lett.* **1997**, *38*, 8595–8598.

- [16] a) J. C. Ruble, G. C. Fu, *J. Org. Chem.* **1996**, *61*, 7230–7231; b) J. C. Ruble, H. A. Latham, G. C. Fu, *J. Am. Chem. Soc.* **1997**, *119*, 1492–1493; c) G. C. Fu, *Acc. Chem. Res.* **2004**, *37*, 542–547.
- [17] M. S. Sigman, E. N. Jacobsen, *J. Am. Chem. Soc.* **1998**, *120*, 4901–4902.
- [18] T. Ooi, M. Kameda, K. Maruoka, *J. Am. Chem. Soc.* **1999**, *121*, 6519–6520.
- [19] E. J. Corey, M. J. Grogan, *Org. Lett.* **1999**, *1*, 157–160.
- [20] B. List, R. A. Lerner, C. F. Barbas III, *J. Am. Chem. Soc.* **2000**, *122*, 2395–2396.
- [21] a) P. I. Dalko, L. Moisan, *Angew. Chem. Int. Ed.* **2004**, *43*, 5138–5175; b) P. Melchiorre, M. Marigo, A. Carlone, G. Bartoli, *Angew. Chem. Int. Ed.* **2008**, *47*, 6138–6171; c) S. Bertelsen, K. A. Jørgensen, *Chem. Soc. Rev.* **2009**, *38*, 2178–2189; d) D. W. C. MacMillan, *Nature* **2008**, *455*, 304–308.
- [22] J. Seayad, B. List, *Org. Biomol. Chem.* **2005**, *3*, 719–724.
- [23] T. Hashimoto, K. Maruoka, *Chem. Rev.* **2007**, *107*, 5656–5682.
- [24] a) T. Okino, Y. Hoashi, Y. Takemoto, *J. Am. Chem. Soc.* **2003**, *125*, 12672–12673; b) A. G. Doyle, E. N. Jacobsen, *Chem. Rev.* **2007**, *107*, 5713–5743.
- [25] S. E. Denmark, G. L. Beutner, *Angew. Chem. Int. Ed.* **2008**, *47*, 1560–1638.
- [26] a) D. Enders, O. Niemeier, A. Henseler, *Chem. Rev.* **2007**, *107*, 5606–5655; b) N. Marion, S. Díez-González, S. P. Nolan, *Angew. Chem. Int. Ed.* **2007**, *46*, 2988–3000; c) P.-C. Chiang, J. W. Bode in *N-Heterocyclic Carbenes: From Laboratory Curiosities to Efficient Synthetic Tools* (Ed.: S. S. Díez-González), Royal Society of Chemistry: Cambridge, **2010**, pp. 399–435; d) K. Zeitler, *Angew. Chem. Int. Ed.* **2005**, *44*, 7506–7510; e) J. L. Moore, T. Rovis, *Top. Curr. Chem.* **2010**, *291*, 77–144; f) V. Nair, R. S. Menon, A. T. Biju, C. R. Sinu, R. R. Paul, A. Jose, V. Sreekumar, *Chem. Soc. Rev.* **2011**, *40*, 5336–5346; g) A. T. Biju, N. Kuhl, F. Glorius, *Acc. Chem. Res.* **2011**, *44*, 1182–1195.
- [27] a) E. F. V. Scriven, *Chem. Soc. Rev.* **1983**, *12*, 129–161; b) G. Höfle, W. Steglich, H. Vorbrüggen, *Angew. Chem. Int. Ed.* **1978**, *17*, 569–583; c) G. Höfle, W. Steglich, *Synthesis* **1972**, 619–621; d) W. Steglich, G. Höfle, *Angew. Chem. Int. Ed.* **1969**, *8*, 981.
- [28] S. A. Shaw, P. Aleman, E. Vedejs, *J. Am. Chem. Soc.* **2003**, *125*, 13368–13369.
- [29] V. B. Birman, E. W. Uffman, H. Jiang, X. Li, C. J. Kilbane, *J. Am. Chem. Soc.* **2003**, *126*, 12226–12227.
- [30] a) M. Kobayashi, S. Okamoto, *Tetrahedron Lett.* **2006**, *47*, 4347–4350; b) V. B. Birman, X. Li, *Org. Lett.* **2006**, *8*, 1351–1354; c) V. B. Birman, H. Jiang, X. Li, L.

- Guo, E. W. Uffman, *J. Am. Chem. Soc.* **2008**, *128*, 6536–6537; c) C. Joannesse, C. P. Johnston, C. Concellón, C. Simal, D. Philp, A. D. Smith, *Angew. Chem. Int. Ed.* **2009**, *48*, 8914–8918.
- [31] M. J. Gaunt, C. C. C. Johansson, *Chem. Rev.* **2007**, *107*, 5596–5605.
- [32] a) M. A. Calter, R. K. Orr, W. Song, *Org. Lett.*, **2003**, *5*, 4745–4748; b) H. Wynberg, E. G. J. Staring, *J. Am. Chem. Soc.* **1982**, *104*, 166–168; c) H. Wynberg, E. G. J. Staring, *J. Org. Chem.* **1985**, *50*, 1977–1979; d) A. E. Taggi, A. M. Hafez, H. Wack, B. Young, W. J. Drury III, T. Lectka, *J. Am. Chem. Soc.* **2000**, *124*, 7831–783; e) M. H. Shah, S. France, T. Lectka, *Synlett*, **2003**, 1937–1939; f) S. France, A. Weatherwax, A. E. Taggi, T. Lectka, *Acc. Chem. Res.*, **2004**, *37*, 592–600; g) J. E. Wilson, G. C. Fu, *Angew. Chem. Int. Ed.* **2004**, *43*, 6358–6360.
- [33] a) H. Wack, A. E. Taggi, A. M. Hafez, W. J. Drury III, T. Lectka, *J. Am. Chem. Soc.* **2001**, *123*, 1531–1532; b) T. Bekele, M. H. Shah, J. Wolfer, C. J. Abraham, A. Weatherwax, T. Lectka, *J. Am. Chem. Soc.* **2006**, *128*, 1810–1811.
- [34] E. M. McGarrigle, E. L. Myers, O. Illa, M. A. Shaw, S. L. Riches, V. K. Aggarwal, *Chem. Rev.* **2007**, *107*, 5841–5883.
- [35] a) D. Basavaiah, A. J. Rao, T. Satayanarayana, *Chem. Rev.* **2003**, *103*, 811–891 and references cited therein. (b) D. Basavaiah, K. V. Rao, R. J. Reddy, *Chem. Soc. Rev.* **2007**, *36*, 1518–1588 (c) S. E. Drewes, G. H. P. Roos, *Tetrahedron* **1998**, *44*, 4653–4670.
- [36] A. Erkkilä, I. Majander, P. M. Pihko, *Chem. Rev.* **2007**, *107*, 5416–5470.
- [37] a) W. S. Jen, J. J. M. Wiener, D. W. C. MacMillan, *J. Am. Chem. Soc.* **2000**, *122*, 9874–9875; b) S. Karlsson, H. –E. Högberg, *Tetrahedron Asymmetry* **2002**, *13*, 923–926.
- [38] A. B. Northrup, D. W. C. MacMillan, *J. Am. Chem. Soc.* **2002**, *124*, 2458–2460.
- [39] N. A. Parras, D. W. C. MacMillan, *J. Am. Chem. Soc.* **2002**, *124*, 7894–7895.
- [40] a) S. P. Brown, N. C. Goodwin, D. W. C. MacMillan, *J. Am. Chem. Soc.* **2003**, *125*, 1192–1194; b) W. Wang, H. Li, J. Wang, *Org. Lett.* **2005**, *7*, 1637–1639.
- [41] a) S. Mukherjee, J. W. Yang, S. Hoffmann, B. List, *Chem. Rev.* **2007**, *107*, 5471–5569; b) M. J. Gaunt, C. C.C. Johansson, A. McNally, N. T. Vo, *Drug Discovery Today*, **2007**, *12*, 8–27; c) E. Arceo, P. Melchiorre, *Angew. Chem. Int. Ed.* **2012**, *51*, 5290–5292.
- [42] K. L. Jensen, G. Dickmeiss, H. Jiang, L. Albrecht, K. A. Jorgensen, *Acc. Chem. Res.* **2012**, *45*, 248–264.

- [43] D. Seebach, *Angew. Chem. Int. Ed. Engl.* **1979**, *18*, 239–258.
- [44] H. Stetter, *Angew. Chem. Int. Ed. Engl.* **1976**, *15*, 639–647.
- [45] a) S. S. Sohn, E. L. Rosen, J. W. Bode, *J. Am. Chem. Soc.* **2004**, *126*, 14370–14371; b) C. Burstein, F. Glorius, *Angew. Chem. Int. Ed.* **2004**, *43*, 6205–6208.
- [46] V. Nair, S. Vellalath, B. P. Babu, *Chem. Soc. Rev.* **2008**, *37*, 2691–2698.
- [47] a) C. Burstein, S. Tschan, X. Xie, F. Glorius, *Synthesis* **2006**, 2418–2439; b) M. He, J. R. Struble, J. W. Bode, *J. Am. Chem. Soc.* **2006**, *128*, 8418–8420; c) E. M. Phillips, M. Wadamoto, A. Chan, K. A. Scheidt, *Angew. Chem. Int. Ed.* **2007**, *46*, 3107–3110; d) Y. Kawanaka, E. M. Phillips, K. A. Scheidt, *J. Am. Chem. Soc.* **2009**, *131*, 18028–18029.
- [48] a) C. Fischer, S. W. Smith, D. A. Powell, G. C. Fu, *J. Am. Chem. Soc.* **2006**, *128*, 1472–1473; b) S. Matsuoka, Y. Ota, A. Washio, A. Katada, K. Ichioka, K. Takagi, M. Suzuki, *Org. Lett.* **2011**, *13*, 3722–3725; c) A. T. Biju, M. Padmanaban, N. E. Wurcz, F. Glorius, *Angew. Chem. Int. Ed.* **2011**, *50*, 8412–8415.
- [49] C. E. I. Knappke, A. J. Arduengo, III, H. Jiao, J.-M. Neudörfl, A. J. von Wangelin, *Synthesis* **2011**, 3784–3795.
- [50] a) A. Chan, K. A. Scheidt, *Org. Lett.* **2005**, *7*, 905–908; b) S. S. Sohn, J. W. Bode, *Org. Lett.* **2005**, *7*, 3873–3876; c) K. Zeitler, *Org. Lett.* **2006**, *8*, 637–640; d) N. T. Reynolds, J. Read de Alaniz, T. Rovis, *J. Am. Chem. Soc.* **2004**, *126*, 9518–9519; e) N. T. Reynolds, T. Rovis, *J. Am. Chem. Soc.* **2005**, *127*, 16406–16407; f) H. U. Vora, T. Rovis, *J. Am. Chem. Soc.* *132*, 2860–2861; g) K. Y.-K. Chow, J. W. Bode, *J. Am. Chem. Soc.* **2004**, *126*, 8126–8127; h) S. De Sarkar, S. Grimme, A. Studer, *J. Am. Chem. Soc.* **2010**, *132*, 1190–1191.
- [51] Ref [50c]; a) S. J. Ryan, L. Candish, D. W. Lupton, *J. Am. Chem. Soc.* **2009**, *131*, 14176–14177; b) S. J. Ryan, L. Candish, D. W. Lupton, *J. Am. Chem. Soc.* **2011**, *133*, 4694–4697; c) B. E. Maki, A. Chan, E. M. Phillips, K. A. Scheidt, *Org. Lett.* **2007**, *9*, 371–374; d) J. Kaebamrung, J. Mahatthananchai, P. Zheng, J. W. Bode, *J. Am. Chem. Soc.* **2010**, *132*, 8810–8812; e) J. Mahatthananchai, P. Zheng, J. W. Bode, *Angew. Chem. Int. Ed.* **2011**, *50*, 1673–1677; f) S. De Sarkar, A. Studer, *Angew. Chem. Int. Ed.* **2010**, *49*, 9266–9269; g) Z.-Q. Zhu, J.-C. Xiao, *Adv. Synth. Catal.* **2010**, *352*, 2455–2458; h) Z.-Q. Zhu, X.-L. Zheng, N.-F. Jiang, X. Wan, J.-C. Xiao, *Chem. Commun.* **2011**, *47*, 8670–8672; i) Z.-Q. Rong, M.-Q. Jia, S.-L. You, *Org. Lett.* **2011**, *13*, 4080–4183; j) B. Wanner, J. Mahatthananchai, J. W. Bode, *Org. Lett.* **2011**, *13*, 5378–5381.

- [52] a) C. K. Ingold, *Recl. Trav. Chim. Pays-Bas* **1929**, *42*, 797–812. (b) C. K. Ingold, *J. Chem. Soc.* 1933, 1120–1127. (c) C. K. Ingold, *Chem. Rev.* **1934**, *15*, 225–274.
- [53] C. G. Swain, C. B. Scott, *J. Am. Chem. Soc.* **1953**, *75*, 141–147.
- [54] a) C. D. Ritchie, *Acc. Chem. Res.* **1972**, *5*, 348–354. (b) C. D. Ritchie, J. E. van Verth, P. O. I. Virtanen, *J. Am. Chem. Soc.* **1982**, *104*, 3491–3497. (c) C. D. Ritchie, *J. Am. Chem. Soc.* **1984**, *106*, 7187–7194. (d) C. D. Ritchie, *Can. J. Chem.* **1986**, *64*, 2239–2250.
- [55] H. Mayr, M. Patz, *Angew. Chem. Int. Ed.* **1994**, *33*, 938–957.
- [56] a) H. Mayr, T. Bug, M. F. Gotta, N. Hering, B. Irrgang, B. Janker, B. Kempf, R. Loos, A. R. Ofial, G. Remennikov, H. Schimmel, *J. Am. Chem. Soc.* **2001**, *123*, 9500–9512; c) R. Lucius, R. Loos, H. Mayr, *Angew. Chem. Int. Ed.* **2002**, *41*, 91–95.
- [57] For a comprehensive listing of nucleophilicity parameters  $N$  and electrophilicity parameters  $E$ , see <http://www.cup.uni-muenchen.de/oc/mayr/DBintro.html>.
- [58] H. Mayr, A. R. Ofial, *Angew. Chem. Int. Ed.* **2006**, *45*, 1844–1854.
- [59] a) D. Leow, C.-H. Tan, *Synlett* **2010**, 1589–1605; j) X. Fu, C.-H. Tan, *Chem. Commun.* **2011**, *47*, 8210–8222; b) N. De Rycke, F. Couty, O. R. P. David, *Chem. Eur. J.* **2011**, *17*, 12852–12871; c) J. E. Taylor, S. D. Bull, J. M. J. Williams, *Chem. Soc. Rev.* **2012**, *41*, 2109–2121; d) T. Ishikawa, T. Isobe, *Chem. Eur. J.* **2002**, *8*, 552–557; e) K. Nagasawa, Y. Hashimoto, *Chem. Rec.* **2003**, *3*, 201–211; f) T. Ishikawa, T. Kumamoto, *Synthesis* **2006**, 737–752; g) M. P. Coles, *Chem. Commun.* **2009**, 3659–3676; h) D. Leow, C.-H. Tan, *Chem. Asian J.* **2009**, *4*, 488–507.
- [60] a) S. B. Tsogoeva, G. Dürner, M. Bolte, M.W. Göbel, *Eur. J. Org. Chem.* **2003**, 1661–1664; b) D. Akalay, G. Dürner, J. W. Bats, M. Bolte, M.W. Göbel, *J. Org. Chem.* **2007**, *72*, 5618–5624; c) K. Murai, S. Fukushima, S. Hayashi, Y. Takahara, H. Fujioka, *Org. Lett.* **2010**, *12*, 964–966; d) A. Weatherwax, C. J. Abraham, T. Lectka, *Org. Lett.* **2005**, *7*, 3461–3463; e) J. Xu, Y. Guan, S. Yang, Y. Ng, G. Peh, C.-H. Tan, *Chem. Asian J.* **2006**, *1*, 724–729.
- [61] A. J. Arduengo III, J. C. Calabrese, F. Davidson, H. V. R. Dias, J. R. Goerlich, R. Krafczyk, W. J. Marshall, M. Tamm, R. Schmutzler, *Helv. Chim. Acta* **1999**, *82*, 2348–2364.
- [62] A. Berkessel, S. Elfert, K. Etzenbach-Effers, J. H. Teles, *Angew. Chem. Int. Ed.* **2010**, *49*, 7120–7124.

## Chapter 2

# Nucleophilicities and Lewis Basicities of Isothiourea Derivatives

B. Maji, C. Joannesse, T. A. Nigst, A. D. Smith, H. Mayr, *J. Org. Chem.* **2011**, *76*, 5104–5112.

### 1 Introduction

Lewis bases (e.g. **1–17**) have the ability to promote the acylation of alcohols and amines.<sup>[1]</sup> 4-(Dimethylamino)pyridine<sup>[2]</sup> (DMAP, **1**) and *N*-methylimidazole<sup>[3]</sup> (NMI, **2**) as well as the amidines 1,8-diazabicyclo[5.4.0]undec-7-ene (DBU, **3**)<sup>[4]</sup> or 1,5-diazabicyclo[4.3.0]non-5-ene (DBN, **4**)<sup>[4]</sup> are among the most common achiral catalysts used for these reactions. Birman has shown that chiral amidines act as enantioselective catalysts for the kinetic resolution of alcohols.<sup>[5]</sup> Recent independent work by the Okamoto and Birman groups has demonstrated that isothioureas are highly active *O*-acylation catalysts.<sup>[6,7]</sup> Okamoto found 3,4-dihydro-2*H*-pyrimido[2,1-*b*]benzothiazole (DHPB, **10**) to be remarkably active for catalyzing the acylation of 1-phenylethanol, even more active than the “benchmark” catalyst DMAP (**1**).<sup>[6]</sup> Birman’s concurrent investigations of the acylations of primary and secondary alcohols with a series of amidines and isothioureas revealed a significant variation in catalytic activity with ring size. Notably, tetrahydropyrimidine-based isothioureas THTP **9** and DHPB **10** showed similar or slightly higher catalytic activity in chloroform than DMAP, depending on their concentrations.<sup>[7]</sup> Subsequent related studies probed the ability of a variety of amidines and isothioureas to catalyze the *O*- to *C*-carboxyl transfer rearrangement of oxazolyl and related heterocyclic carbonates, and the *C*-acylation of silyl ketene acetals, and showed that tetrahydropyrimidine-based DHPB **10** was also the optimal achiral catalyst in Figure 1.<sup>[8]</sup> Given their promising reactivity profiles, a series of chiral isothioureas have been prepared and utilized in asymmetric catalysis. Pioneering studies by Birman and Li showed that tetramisole **11** and its benzannulated analogue BTM **12** can catalyze the kinetic resolution of alcohols with exquisite selectivity.<sup>[9]</sup> Since the demonstration of this methodology, a range of

chiral isothioureas (of which **12–17** are representative) have been successfully utilized in a variety of asymmetric processes including kinetic resolutions,<sup>[10]</sup> desymmetrizations,<sup>[11,12]</sup> dynamic kinetic resolutions,<sup>[13]</sup> the generation of ammonium enolates from carboxylic acids,<sup>[14]</sup> as well as enantioselective carboxy and acyl group transfer reactions<sup>[15]</sup>. The commercial availability of tetramisole **11**, and the ease of synthesis of chiral isothioureas such as **12–17** from enantiopure amino alcohols, arguably make these derivatives more readily accessible than many common chiral DMAP derivatives.<sup>[16]</sup> Notably, in many of these processes the catalytic activity and enantioselectivity varies significantly with ring size and stereodirecting unit. For example, Birman has shown that the incorporation of an additional *syn*-C(3)-methyl group within the HBTM-skeleton (**14**, Me instead of *i*Pr) has a dramatic effect upon both catalytic activity and stereoselectivity in kinetic resolutions of aryl-cycloalkanols,<sup>[17]</sup> a similar effect has been noted on the kinetic resolution of aryl alkyl alcohols when introducing a *syn*-C(3)-*iso*-propyl unit (**14**).<sup>[18]</sup>

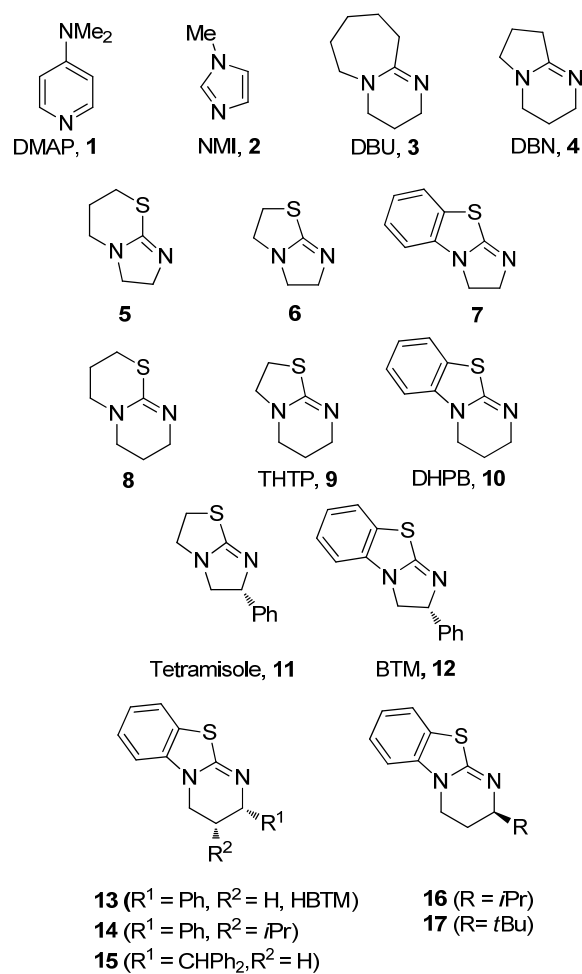


**Figure 1.** Selected nitrogen-containing heterocycles commonly used as acyl transfer catalysts.

While it may be expected that the organocatalytic activities of these heterocycles will depend on their relative nucleophilicities and Lewis basicities, to date a quantitative comparison of these properties has not been reported. To gain insight into some of the factors that may affect their catalytic activities, we have determined rate and equilibrium constants of the reactions of the isothiourea derivatives **5–10** and **13–17** with stabilized benzhydrylium ions (Table 1) and compare these data with those of other nucleophilic organocatalysts such as DMAP (**1**), NMI (**2**), DBU (**3**) and DBN (**4**).<sup>[19,20]</sup>

**Table 1.** Abbreviations and Electrophilicity Parameters for the Benzhydrylium Ions Used for this Work.

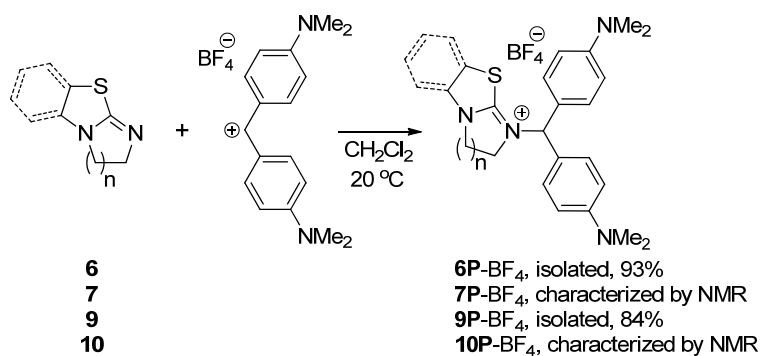
X	Abbreviations	$E$ <sup>[a]</sup>
$N(CH_3)CH_2CF_3$	$(mfa)_2CH^+$	-3.85
$NPh_2$	$(dpa)_2CH^+$	-4.72
$N(CH_2CH_2)_2O$	$(mor)_2CH^+$	-5.53
$N(Ph)CH_3$	$(mpa)_2CH^+$	-5.89
$N(CH_3)_2$	$(dma)_2CH^+$	-7.02
$N(CH_2)_4$	$(pyr)_2CH^+$	-7.69
	$n = 2$ $(thq)_2CH^+$	-8.22
	$n = 1$ $(ind)_2CH^+$	-8.76
	$n = 2$ $(jul)_2CH^+$	-9.45
	$n = 1$ $(lil)_2CH^+$	-10.04

<sup>[a]</sup> Electrophilicity parameters  $E$  for benzhydrylium ions from ref. 19a.

## 2 Results and Discussion

### 2.1 Product Studies

When  $\text{CH}_2\text{Cl}_2$  solutions of the isothioureas **6** or **9** were added to  $\text{CH}_2\text{Cl}_2$  solutions of  $(\text{dma})_2\text{CH}^+\text{BF}_4^-$  at room temperature, the thiuronium tetrafluoroborates **6P-BF<sub>4</sub>** and **9P-BF<sub>4</sub>** formed, which were isolated and characterized (Scheme 1). The  $^{13}\text{C}$  NMR spectra show that the benzhydryl carbon, which absorbs at  $\delta \approx 160$  ppm in  $(\text{dma})_2\text{CH}^+$ , is shifted to  $\delta \approx 70$  ppm due to the change in hybridization from  $\text{sp}^2$  to  $\text{sp}^3$ . Since the reactions of the benzo-annulated isothioureas **7** and **10** with  $(\text{dma})_2\text{CH}^+\text{BF}_4^-$  are highly reversible, the corresponding adducts were not isolated but identified by NMR after mixing the isothioureas **7** and **10** with equimolar amounts of  $(\text{dma})_2\text{CH}^+\text{BF}_4^-$  in deuterated dimethyl sulfoxide.



**Scheme 1.** Products from the Reactions of Isothioureas with  $(\text{dma})_2\text{CH}^+\text{BF}_4^-$ .

### 2.2 Kinetics

Using this information, the rates of the reactions of the isothioureas **5-10** and **13-17** with the benzhydrylium ions shown in Table 1 were measured photometrically by monitoring the decay of the absorbances of the benzhydrylium ions; conventional or stopped-flow techniques were used as previously described.<sup>[19]</sup> By employing the isothioureas in high excess over the benzhydrylium ions, first-order conditions were achieved. The first-order rate constants  $k_{\text{obs}}$  ( $\text{s}^{-1}$ ), obtained by fitting the decay of the absorbances of the benzhydrylium ions to the mono-exponential function  $A = A_0 e^{-k_{\text{obs}} t} + C$  correlated linearly with the nucleophile concentrations (Figure 2). The slopes of these correlation lines yielded the second-order rate constants  $k$  ( $\text{M}^{-1} \text{s}^{-1}$ ) which are collected in Table 2. The kinetic profiles of the reactions of  $(\text{ind})_2\text{CH}^+$  with **7**, **9** and **10** were also studied at variable temperature to determine the Eyring activation parameters which are collected in the footnotes of Table 2. The negative activation entropies ( $-57$  to  $-68 \text{ J mol}^{-1} \text{ K}^{-1}$ ) are similar to those reported for the reactions of other  $n$ -nucleophiles with benzhydrylium ions in  $\text{CH}_2\text{Cl}_2$ .<sup>[20]</sup>

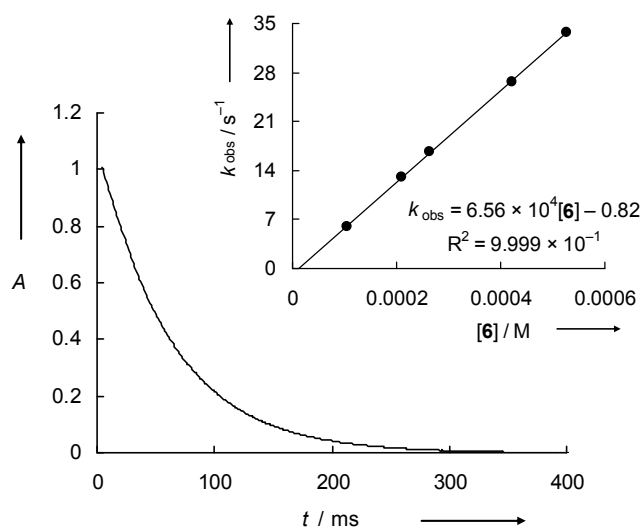


**Figure 2.** Exponential decay of the absorbance at 613 nm during the reaction of **6** ( $2.11 \times 10^{-4}$  M) with  $(\text{dma})_2\text{CH}^+\text{BF}_4^-$  ( $1.41 \times 10^{-5}$  M) at 20 °C in  $\text{CH}_2\text{Cl}_2$  ( $k_{\text{obs}} = 13.0 \text{ s}^{-1}$ ). Insert: Determination of the second-order rate constant  $k = 6.56 \times 10^4 \text{ M}^{-1}\text{s}^{-1}$  from the dependence of  $k_{\text{obs}}$  on the concentration of **6**.

**Table 2.** Second-Order Rate Constants  $k$  for the Reactions of the Isothiourea Derivatives **5**–**10** and **13**–**17** with the Benzhydrylium Ions ( $\text{Ar}_2\text{CH}^+$ , Table 1) in  $\text{CH}_2\text{Cl}_2$  at 20 °C.

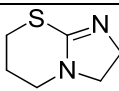
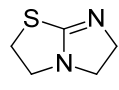
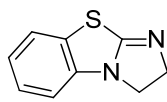
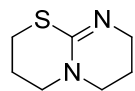
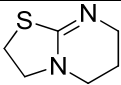
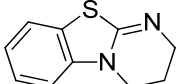
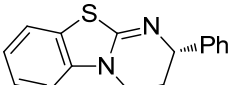
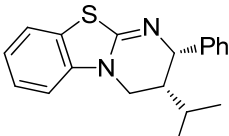
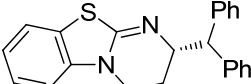
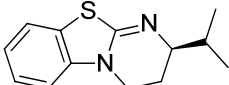
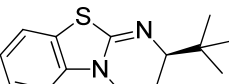
Isothiourea	$N, s_N$ <sup>[a]</sup>	$\text{Ar}_2\text{CH}^+$	$k$ ( $\text{M}^{-1}\text{s}^{-1}$ )
 <b>5</b>	13.00, 0.83	$(\text{dma})_2\text{CH}^+$	$9.16 \times 10^4$
		$(\text{pyr})_2\text{CH}^+$	$2.55 \times 10^4$
		$(\text{thq})_2\text{CH}^+$	$7.72 \times 10^3$
		$(\text{ind})_2\text{CH}^+$	$3.54 \times 10^3$
 <b>6</b>	12.98, 0.81	$(\text{dma})_2\text{CH}^+$	$6.56 \times 10^4$
		$(\text{pyr})_2\text{CH}^+$	$1.93 \times 10^4$
		$(\text{thq})_2\text{CH}^+$	$5.86 \times 10^3$
		$(\text{ind})_2\text{CH}^+$	$2.79 \times 10^3$
 <b>7</b>	13.42, 0.73	$(\text{dma})_2\text{CH}^+$	$4.76 \times 10^4$
		$(\text{pyr})_2\text{CH}^+$	$1.46 \times 10^4$
		$(\text{thq})_2\text{CH}^+$	$5.83 \times 10^3$
		$(\text{ind})_2\text{CH}^+$	$2.60 \times 10^3$ <sup>[b]</sup>
 <b>8</b>	14.10, 0.82	$(\text{thq})_2\text{CH}^+$	$5.88 \times 10^4$
		$(\text{ind})_2\text{CH}^+$	$2.76 \times 10^4$
		$(\text{jul})_2\text{CH}^+$	$4.85 \times 10^3$
		$(\text{lil})_2\text{CH}^+$	$2.27 \times 10^3$

Table 2. continued

Isothiourea	$N, s_N$ <sup>[a]</sup>	$Ar_2CH^+$	$k$ ( $M^{-1}s^{-1}$ )
 <b>THTP, 9</b>	14.45, 0.78	(thq) <sub>2</sub> CH <sup>+</sup>	$7.09 \times 10^4$
		(ind) <sub>2</sub> CH <sup>+</sup>	$3.68 \times 10^4$ <sup>[c]</sup>
		(jul) <sub>2</sub> CH <sup>+</sup>	$6.69 \times 10^3$
		(lil) <sub>2</sub> CH <sup>+</sup>	$3.15 \times 10^3$
 <b>DHPB, 10</b>	13.86, 0.78	(dma) <sub>2</sub> CH <sup>+</sup>	$2.29 \times 10^5$
		(pyr) <sub>2</sub> CH <sup>+</sup>	$7.49 \times 10^4$
		(thq) <sub>2</sub> CH <sup>+</sup>	$2.07 \times 10^4$
		(ind) <sub>2</sub> CH <sup>+</sup>	$1.11 \times 10^4$ <sup>[d]</sup>
 <b>13</b>	13.45, 0.72	(mor) <sub>2</sub> CH <sup>+</sup>	$3.80 \times 10^5$
		(mpa) <sub>2</sub> CH <sup>+</sup>	$2.91 \times 10^5$
		(dma) <sub>2</sub> CH <sup>+</sup>	$5.15 \times 10^4$
		(pyr) <sub>2</sub> CH <sup>+</sup>	$1.40 \times 10^4$
		(thq) <sub>2</sub> CH <sup>+</sup>	$4.60 \times 10^3$
		(ind) <sub>2</sub> CH <sup>+</sup>	$8.59 \times 10^3$
 <b>14</b>	14.96, 0.64	(mpa) <sub>2</sub> CH <sup>+</sup>	$5.28 \times 10^5$
		(dma) <sub>2</sub> CH <sup>+</sup>	$1.26 \times 10^5$
		(pyr) <sub>2</sub> CH <sup>+</sup>	$4.06 \times 10^4$
		(thq) <sub>2</sub> CH <sup>+</sup>	$1.76 \times 10^4$
		(ind) <sub>2</sub> CH <sup>+</sup>	$8.59 \times 10^3$
		(mor) <sub>2</sub> CH <sup>+</sup>	$2.22 \times 10^5$
 <b>15</b>	15.30, 0.55	(dpa) <sub>2</sub> CH <sup>+</sup>	$6.09 \times 10^5$
		(mor) <sub>2</sub> CH <sup>+</sup>	$2.22 \times 10^5$
		(mpa) <sub>2</sub> CH <sup>+</sup>	$1.37 \times 10^5$
		(dma) <sub>2</sub> CH <sup>+</sup>	$3.38 \times 10^4$
 <b>16</b>	16.50, 0.48	(dpa) <sub>2</sub> CH <sup>+</sup>	$4.48 \times 10^5$
		(mor) <sub>2</sub> CH <sup>+</sup>	$1.57 \times 10^5$
		(mpa) <sub>2</sub> CH <sup>+</sup>	$1.05 \times 10^5$
		(dma) <sub>2</sub> CH <sup>+</sup>	$3.73 \times 10^5$
		(pyr) <sub>2</sub> CH <sup>+</sup>	$1.53 \times 10^5$
		(ind) <sub>2</sub> CH <sup>+</sup>	$8.59 \times 10^3$
 <b>17</b>	12.95, 0.58	(mfa) <sub>2</sub> CH <sup>+</sup>	$2.51 \times 10^5$
		(dpa) <sub>2</sub> CH <sup>+</sup>	$4.57 \times 10^4$
		(mor) <sub>2</sub> CH <sup>+</sup>	$2.06 \times 10^4$
		(mpa) <sub>2</sub> CH <sup>+</sup>	$1.58 \times 10^4$

<sup>[a]</sup> Parameters as defined by Equation (1). <sup>[b]</sup> Eyring activation parameters:  $\Delta H^\ddagger = 32.6 \pm 1.3$  kJ mol<sup>-1</sup>,  $\Delta S^\ddagger = -68.0 \pm 4.7$  J mol<sup>-1</sup> K<sup>-1</sup>. <sup>[c]</sup> Eyring activation parameters:  $\Delta H^\ddagger = 29.3 \pm 0.7$  kJ mol<sup>-1</sup>,  $\Delta S^\ddagger = -57.3 \pm 2.5$  J mol<sup>-1</sup> K<sup>-1</sup>. <sup>[d]</sup> Eyring activation parameters:  $\Delta H^\ddagger = 30.6 \pm 1.8$  kJ mol<sup>-1</sup>,  $\Delta S^\ddagger = -63.0 \pm 6.3$  J mol<sup>-1</sup> K<sup>-1</sup>.

### 2.3 Correlation analysis

In previous publications, we have shown that the rates of the reactions of carbocations and Michael acceptors with  $n$ ,  $\pi$ , and  $\sigma$ -nucleophiles can be described by the linear-free-energy relationship (1), where electrophiles are characterized by the electrophilicity parameter  $E$ , nucleophiles are characterized by the nucleophilicity parameters  $N$  and the nucleophile-dependent sensitivity parameter  $s_N$  (previously termed  $s$ ). On the basis of Eq. (1) it was possible to develop the most comprehensive nucleophilicity scale presently available.<sup>[19]</sup>

$$\log k_{20^\circ\text{C}} = s_N(N + E) \quad (1)$$

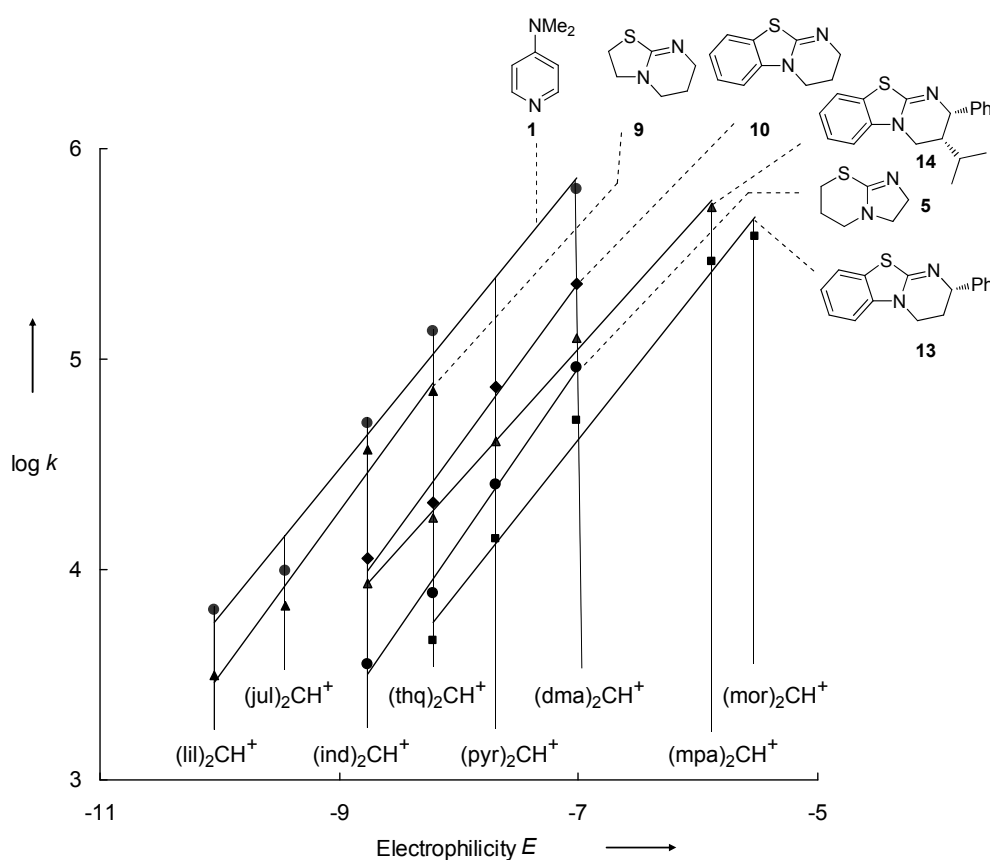


**Figure 3.** Plots of  $\log k$  for the reactions of some isothiureas with benzhydrylium ions versus their electrophilicity parameters  $E$  in  $\text{CH}_2\text{Cl}_2$  at  $20^\circ\text{C}$ . Rate constants for DMAP were taken from ref. [20a].

Figure 3 shows linear correlations between the second-order rate constants  $k$  and the previously published electrophilicity parameters  $E$ , as required by Equation (1). The slopes of

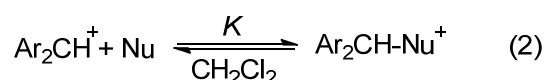
the correlation lines yield the nucleophile-specific sensitivity parameters  $s_N$  and the intercepts on the abscissa give the nucleophilicity parameters  $N$  which are tabulated in Table 2.

The almost equal slopes ( $0.73 < s_N < 0.83$ ) of the correlation lines for the isothioureas **5–10** (unsubstituted at C-2) indicate that their relative nucleophilicities are almost independent of the reactivity of the electrophilic reaction partner. In contrast, the chiral derivatives **13–17** have somewhat lower, variable,  $s_N$  parameters reflecting the dependence of their relative nucleophilicities on the reaction partner.

## 2.4 Lewis basicities and intrinsic reactivities of isothioureas

Brønsted basicities, which have often been used for a first screening of potential nucleophilic organocatalysts, have only been reported for few isothioureas.<sup>[21]</sup> As Lewis basicities are more relevant for their reactions with carbon electrophiles, we have now studied the equilibrium constants of the reactions of several isothioureas with benzhydrylium ions.

The reactions of **7**, **9**, and **10**, and of the C(2)-substituted chiral isothioureas **13–17** with several colored amino-substituted benzhydrylium ions proceed incompletely, allowing the measurement of the equilibrium constants for these reactions by UV-vis spectroscopy. Assuming proportionality between the absorbances and the concentrations of the benzhydrylium ions (as for the evaluation of the kinetic experiments), the equilibrium constants for the reactions (Equation 2) can be determined from the initial absorbances ( $A_0$ ) of the benzhydrylium ions and the absorbances at equilibrium ( $A$ ) according to Equation (3) and are listed in Table 3.



$$K = \frac{[\text{Ar}_2\text{CH-Nu}^+]}{[\text{Ar}_2\text{CH}^+][\text{Nu}]} = \frac{A_0 - A}{A[\text{Nu}]} \quad (3)$$

Substitution of the activation free energies  $\Delta G^\ddagger$  and Gibbs free energies  $\Delta G^0$  into the Marcus equation (4)<sup>[22]</sup> yields the intrinsic barriers  $\Delta G_0^\ddagger$  (i.e., the barriers of the corresponding reactions with  $\Delta G^0 = 0$ ) which are also listed in Table 3.

$$\Delta G^\ddagger = \Delta G_0^\ddagger + 0.5 \Delta G^0 + ((\Delta G^0)^2 / 16 \Delta G_0^\ddagger) \quad (4)$$

**Table 3.** Equilibrium Constants  $K$  ( $M^{-1}$ ), Activation Free Energies  $\Delta G^\ddagger$  ( $\text{kJ mol}^{-1}$ ), Reaction Free Energies  $\Delta G^0$  ( $\text{kJ mol}^{-1}$ ), Intrinsic Barriers  $\Delta G_0^\ddagger$  ( $\text{kJ mol}^{-1}$ ) and the Reverse Rate Constants  $k_{\leftarrow}$  ( $s^{-1}$ ) for the Reactions of Isothioureas with Benzhydrylium Ions ( $\text{Ar}_2\text{CH}^+$ ) in  $\text{CH}_2\text{Cl}_2$  at 20 °C.

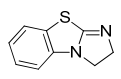
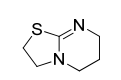
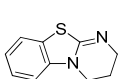
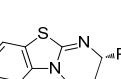
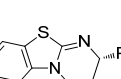
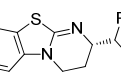
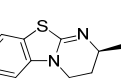
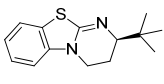
Isothioureas	$\text{Ar}_2\text{CH}^+$	$K$	$\Delta G^\ddagger$ <sup>[a]</sup>	$\Delta G^0$ <sup>[b]</sup>	$\Delta G_0^\ddagger$ <sup>[c]</sup>	$k_{\leftarrow}$ <sup>[d]</sup>	$N_f$ <sup>[e]</sup>
 <b>7</b>	$(\text{thq})_2\text{CH}^+$	$2.56 \times 10^4$	50.6	-24.7	62.3	$2.28 \times 10^{-1}$	-5.79
	$(\text{ind})_2\text{CH}^+$	$2.00 \times 10^4$ <sup>[f]</sup>	52.6	-24.1 <sup>[f]</sup>	64.1	$1.30 \times 10^{-1}$	
 <b>THTP 9</b>	$(\text{ind})_2\text{CH}^+$	$1.90 \times 10^6$ <sup>[g]</sup>	46.1	-35.2 <sup>[g]</sup>	62.5	$1.94 \times 10^{-2}$	-6.49
	$(\text{jul})_2\text{CH}^+$	$6.16 \times 10^4$	50.3	-26.9	63.0	$1.09 \times 10^{-1}$	
	$(\text{lil})_2\text{CH}^+$	$6.27 \times 10^4$	52.1	-26.9	64.9	$5.02 \times 10^{-2}$	
 <b>DHPB 10</b>	$(\text{pyr})_2\text{CH}^+$	$7.73 \times 10^4$	44.4	-27.4	57.3	$9.69 \times 10^{-1}$	-5.26
	$(\text{thq})_2\text{CH}^+$	$2.75 \times 10^4$	47.5	-24.9	59.3	$7.53 \times 10^{-1}$	
	$(\text{ind})_2\text{CH}^+$	$2.02 \times 10^4$ <sup>[h]</sup>	49.0	-24.2 <sup>[h]</sup>	60.5	$5.50 \times 10^{-1}$	
 <b>HBTM 13</b>	$(\text{mpa})_2\text{CH}^+$	$5.95 \times 10^5$	41.1	-32.4	56.1	$4.89 \times 10^{-1}$	-3.98
	$(\text{dma})_2\text{CH}^+$	$1.07 \times 10^4$	45.3	-22.6	56.0	$4.81 \times 10^0$	
	$(\text{pyr})_2\text{CH}^+$	$8.96 \times 10^2$	48.5	-16.6	56.5	$1.56 \times 10^1$	
	$(\text{thq})_2\text{CH}^+$	$3.32 \times 10^2$	51.2	-14.1	58.0	$1.39 \times 10^1$	
	$(\text{ind})_2\text{CH}^+$	$1.98 \times 10^2$ <sup>[i]</sup>	52.8 <sup>[i]</sup>	-12.9 <sup>[i]</sup>	59.1	$1.20 \times 10^1$	
 <b>14</b>	$(\text{dma})_2\text{CH}^+$	$5.54 \times 10^4$	43.1	-26.6	55.6	$2.27 \times 10^0$	-4.24
	$(\text{pyr})_2\text{CH}^+$	$3.88 \times 10^3$	45.9	-20.1	55.5	$1.05 \times 10^1$	
	$(\text{thq})_2\text{CH}^+$	$1.67 \times 10^3$	47.9	-18.1	56.6	$1.05 \times 10^1$	
	$(\text{ind})_2\text{CH}^+$	$1.17 \times 10^3$	49.7	-17.2	58.0	$7.34 \times 10^0$	
 <b>15</b>	$(\text{mpa})_2\text{CH}^+$	$4.66 \times 10^4$	42.9	-26.2	55.2	$2.94 \times 10^0$	-3.15
	$(\text{dma})_2\text{CH}^+$	$9.95 \times 10^2$	46.3	-16.8	54.4	$3.40 \times 10^1$	
 <b>16</b>	$(\text{mpa})_2\text{CH}^+$	$1.01 \times 10^5$	43.6	-28.1	56.8	$1.04 \times 10^0$	-3.57
	$(\text{dma})_2\text{CH}^+$	$2.70 \times 10^3$	46.1	-19.3	55.3	$1.38 \times 10^1$	

Table 3. continued

Isothioureas	Ar <sub>2</sub> CH <sup>+</sup>	<i>K</i>	$\Delta G^\ddagger$ <sup>[a]</sup>	$\Delta G^0$ <sup>[b]</sup>	$\Delta G_0^\ddagger$ <sup>[c]</sup>	<i>k<sub>←</sub></i> <sup>[d]</sup>	<i>N<sub>f</sub></i> <sup>[e]</sup>
 <b>17</b>	(mor) <sub>2</sub> CH <sup>+</sup>	1.36 × 10 <sup>4</sup>	47.5	-23.2	58.5	1.51 × 10 <sup>0</sup>	-2.75
	(mpa) <sub>2</sub> CH <sup>+</sup>	2.45 × 10 <sup>3</sup>	48.2	-19.0	57.3	6.45 × 10 <sup>0</sup>	
DMAP, <b>1</b> <sup>[k]</sup>	(thq) <sub>2</sub> CH <sup>+</sup>	2.81 × 10 <sup>5</sup>	42.9	-30.6	57.2	4.80 × 10 <sup>-1</sup>	-5.32 <sup>[l]</sup>
	(ind) <sub>2</sub> CH <sup>+</sup>	1.71 × 10 <sup>5</sup>	45.4	-29.4	59.2	2.90 × 10 <sup>-1</sup>	

<sup>[a]</sup> From rate constants in Table 2 using the Eyring equation. <sup>[b]</sup> From equilibrium constants *K* in this table ( $-RT \ln K$ ). <sup>[c]</sup> From Eq. (4). <sup>[d]</sup>  $k_{\leftarrow} = k/K$ . <sup>[e]</sup> From eq. (5) assuming *s<sub>f</sub>* = 1. <sup>[f]</sup>  $\Delta H^0 = -49.8 \text{ kJ mol}^{-1}$ ,  $\Delta S^0 = -87.7 \text{ J mol}^{-1} \text{ K}^{-1}$ . <sup>[g]</sup>  $\Delta H^0 = -63.9 \text{ kJ mol}^{-1}$ ,  $\Delta S^0 = -97.9 \text{ J mol}^{-1} \text{ K}^{-1}$ . <sup>[h]</sup>  $\Delta H^0 = -50.2 \text{ kJ mol}^{-1}$ ,  $\Delta S^0 = -88.7 \text{ J mol}^{-1} \text{ K}^{-1}$ . <sup>[i]</sup> Equilibrium constant extrapolated from a van't Hoff plot from measurements at lower temperatures (see the Experimental Section).  $\Delta H^0 = -44.2 \text{ kJ mol}^{-1}$ ,  $\Delta S^0 = -106.9 \text{ J mol}^{-1} \text{ K}^{-1}$ . <sup>[j]</sup> Calculated using Equation (1) and reactivity parameters from Table 1 and 3. <sup>[k]</sup> Data for DMAP was taken from reference [20a]. <sup>[l]</sup> From ref. [24].

With  $\Delta G_0^\ddagger$  between 54 and 65 kJ mol<sup>-1</sup>, the intrinsic barriers are of similar magnitude as previously reported for the reactions of benzhydrylium ions with pyridines<sup>[20a,b]</sup> and azoles.<sup>[20c]</sup> Table 3 shows that also the dependence of the intrinsic barriers  $\Delta G_0^\ddagger$  on the structures of the benzhydrylium ions mirrors previously observed patterns. In particular, the intrinsic barriers for the reactions of the five-membered ring compounds (ind)<sub>2</sub>CH<sup>+</sup> and (lil)<sub>2</sub>CH<sup>+</sup> are always 1–2 kJ mol<sup>-1</sup> higher than those of the corresponding six-membered ring-analogues (thq)<sub>2</sub>CH<sup>+</sup> and (jul)<sub>2</sub>CH<sup>+</sup>, respectively, resulting in a breakdown of rate-equilibrium relationships.<sup>[23,24]</sup>

## 2.5 Structure reactivity relationships

From the observation that the isothioureas **5**, **6**, and **8**, (like the amidines DBU **3** and DBN **4**) react quantitatively with all benzhydrylium tetrafluoroborates investigated, it can be derived that they have higher Lewis basicities than the isothioureas listed in Table 3.

As Figure 3 shows that the relative reactivities of isothioureas are somewhat dependent on the reactivity of the benzhydrylium ion used as the reaction partner, we will first consider the rate and equilibrium constants for the reactions with (ind)<sub>2</sub>CH<sup>+</sup>, for which directly measured rate and equilibrium constants are available for most isothioureas (Figure 4).

Comparison of the imidazoline derivatives **5–7** shows that their nucleophilic reactivities are only slightly affected by the nature of the annelated sulfur-containing heterocycle. The

benzannulation in compound **7** accelerates the reverse reaction  $k_{\leftarrow}$ , however, with the consequence that the equilibrium constant for adduct formation becomes measurable for the reaction of  $(\text{ind})_2\text{CH}^+$  with **7**.

A comparable trend was observed for the tetrahydropyrimidine series **8–10** (line 2 of Figure 4) which are approximately one order of magnitude more nucleophilic than their lower homologs **5–7** ( $k(\mathbf{8})/k(\mathbf{5}) \approx 8$ ;  $k(\mathbf{9})/k(\mathbf{6}) \approx 13$ ;  $k(\mathbf{10})/k(\mathbf{7}) \approx 4$ ). Also in this series, variation of the annelated sulfur heterocycle had a relatively small effect ( $k(\mathbf{9})/k(\mathbf{10}) \approx 3$ ) on the nucleophilic reactivity but a large effect on Lewis basicity ( $K(\mathbf{9})/K(\mathbf{10}) \approx 10^2$ ). Thus lines 1 and 2 of Figure 4 show the same trend that benzannulation has a much larger effect on Lewis basicity than on nucleophilicity.

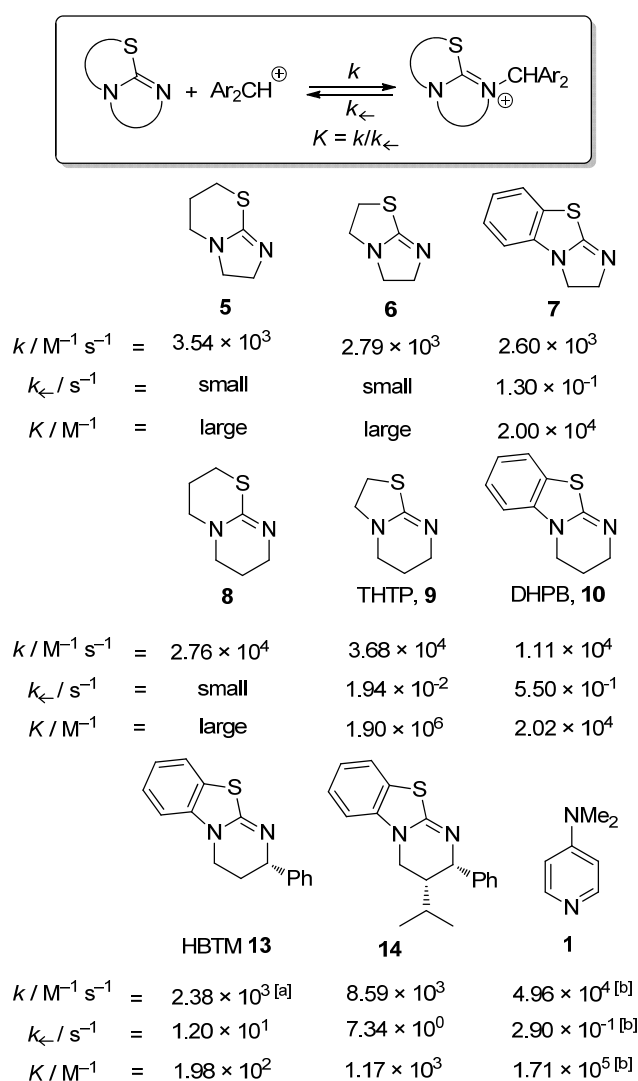


**Figure 4.** Second-order rate constants  $k$ , reverse rate constants  $k_{\leftarrow}$ , and equilibrium constants  $K$  for the reactions of the isothiourea derivatives **5–10** with  $(\text{ind})_2\text{CH}^+\text{BF}_4^-$  in  $\text{CH}_2\text{Cl}_2$  at  $20^\circ\text{C}$ . <sup>[a]</sup> Rate constant calculated by using Eq. (1) from the  $E$  value of  $(\text{ind})_2\text{CH}^+$  (Table 1), and the  $N$  and  $s_N$  value of **13** from Table 2. <sup>[b]</sup> Data for **1** was taken from ref. [20a].

Introduction of the phenyl group in the 2-position of **10** ( $\rightarrow$  **13**) reduces the nucleophilic reactivity by a factor of 4.5 but the Lewis basicity by a factor of 100. Remarkably, an additional *syn*-C(3)-isopropyl group in **14** (relative to HBTM **13**) increases its Lewis basicity (by factor of 6) and nucleophilicity (by factor of 3.6). Though there is no direct correlation between these data, it is notable that this trend corresponds with the experimentally observed beneficial effect of an additional *syn*-3-substituent to **13** ( $\rightarrow$  **14**) in kinetic resolution reactions in terms of catalytic activity and enantioselectivity.<sup>[17,18]</sup> The last entry of Figure 4 shows that both, nucleophilicities and Lewis basicities of the tetrahydropyrimidine derivatives **9-10**, are comparable to those of DMAP (**1**).

The influence of the substituent at C-2 can be derived from the rate and equilibrium constants of its reactions with  $(\text{dma})_2\text{CH}^+$  (Table 4). As in the comparisons of Figure 4, variation of the substituents affects the equilibrium constants much more than the rate constants. While the change from phenyl to *tert*-butyl reduces nucleophilicity by approximately one order of magnitude, the equilibrium constant decreases by more than two orders of magnitude.

**Table 4.** Second-Order Rate constants  $k$ , Reverse Rate Constants  $k_{\leftarrow}$ , and Equilibrium Constants  $K$  for the Reactions of the Isothiourea Derivatives **13**, **15–17** with  $(\text{dma})_2\text{CH}^+\text{BF}_4^-$  in  $\text{CH}_2\text{Cl}_2$ .

R	$k / \text{M}^{-1} \text{s}^{-1}$	$k_{\leftarrow} / \text{s}^{-1}$	$K / \text{M}^{-1}$
Ph ( <b>13</b> )	$5.15 \times 10^4$	$4.81 \times 10^0$	$1.07 \times 10^4$
CHPh <sub>2</sub> ( <b>15</b> )	$3.38 \times 10^4$	$3.40 \times 10^1$	$9.95 \times 10^2$
<i>i</i> Pr ( <b>16</b> )	$3.73 \times 10^4$	$1.38 \times 10^1$	$2.70 \times 10^3$
<i>t</i> Bu ( <b>17</b> )	$2.8 \times 10^3$ <sup>[a]</sup>	$\approx 5 \times 10^1$	$\approx 6 \times 10^1$ <sup>[b]</sup>

<sup>[a]</sup> Rate constant calculated by using Equation (1) as in Figure 4, the  $E$  value of  $(\text{dma})_2\text{CH}^+$ , and the  $N/S_N$  values of **17**. <sup>[b]</sup> Estimated by dividing  $K[(\text{mpa})_2\text{CH}^+]$  by 40, the ratio derived from equilibrium constants of **15** and **16** with  $(\text{mpa})_2\text{CH}^+$  and  $(\text{dma})_2\text{CH}^+$ .

## 2.6 Nucleofugalities of Isothioureas

In analogy to Equation (1),<sup>[19]</sup> which has been used to construct a comprehensive nucleophilicity scale, Equation (5)<sup>[24]</sup> has recently been suggested as the basis for a comprehensive nucleofugality scale. Benzhydrylium ions of variable electrofugality

(characterized by  $E_f$ ) have been employed as reference electrofuges for characterizing the nucleofugalities of leaving groups in different solvents.

$$\log k_{\leftarrow}(25\text{ }^{\circ}\text{C}) = s_f(E_f + N_f) \quad (5)$$

In general, the nucleofugality parameters  $N_f$  and the nucleofuge-specific sensitivity parameters  $s_f$  are obtained from the linear plots of  $\log k_{\leftarrow}(25\text{ }^{\circ}\text{C})$  vs. the previously reported<sup>[24]</sup> electrofugality parameters  $E_f$  of the benzhydrylium ions analogous to the procedure used in Figure 3 for determining the nucleophile-specific parameters  $N$  and  $s_N$ . It has been suggested, however, to assume  $s_f = 1.0$  if only heterolysis rate constants of low precision and/or referring to benzhydrylium ions of similar electrofugality are known. This is the case for the  $k_{\leftarrow}$  values given in Table 3, which are obtained indirectly as the ratios of  $k/K$  and furthermore refer to 20 °C. Neglecting the small difference in temperature, we have therefore calculated the  $N_f$  parameters of isothioureas (listed in Table 3) from Equation (5) setting the  $s_f$  parameter to 1.0 (see also Tables 24).

Due to the high Lewis basicities of DBU **3**, DBN **4**, and the isothioureas **5**, **6**, and **8** equilibrium constants could not be measured, indicating that they are poor nucleofuges. The trends in  $N_f$  shown in Table 3 are equivalent to the trends in  $k_{\leftarrow}$  discussed for Figure 4 and Table 4.

It is the benefit of the  $N_f$  values in Table 3 that they allow a comparison of the leaving group abilities in  $\text{CH}_2\text{Cl}_2$  of isothioureas with those of other nucleofuges. Thus, comparison with  $N_f$  values listed in ref. [24] shows that the nucleofugalities of **7**, **9** and **10** are comparable to those of DMAP (**1**) ( $N_f = -5.32$ ), or N-methyl-imidazole (**2**) ( $N_f = -6.29$  in  $\text{CH}_3\text{CN}$ ) and N-phenyl-imidazole ( $N_f = -5.59$  in  $\text{CH}_3\text{CN}$ ), or tris(*p*-tolyl)phosphane ( $N_f = -5.20$ ) and tris(*p*-anisyl)phosphane ( $N_f = -5.91$ ). The nucleofugalities of **13** and **14** are comparable to that of triphenylphosphane ( $N_f = -4.44$ ) and  $N_f$  of the *tert*-butyl substituted compound **17** is similar to that of 4-methoxypyridines ( $N_f = -2.80$ ) and isoquinoline ( $N_f = -3.04$  in  $\text{CH}_3\text{CN}$ ).

### 3 Conclusion

In a systematic study Birman et al. observed that the relative catalytic activities of DMAP (**1**) and THTP (**9**) in the acylation of alcohols with  $\text{Ac}_2\text{O} / ^i\text{Pr}_2\text{NEt}$  in chloroform vary dramatically and can be reversed when the concentration of the catalyst and the nature of the alcohols is altered.<sup>[7]</sup> One must, therefore, conclude that there is not a single, best acylation

catalyst. Thus the nucleophilicities and Lewis basicities of isothioureas reported in this work are two important but not the only factors controlling catalytic activities.

As the reactions of isothioureas with benzhydrylium ions have been found to follow the linear-free energy relationship (1) it was possible to determine the nucleophilicity parameters for the isothioureas **5–10** and **13–17** and to include these compounds into our comprehensive nucleophilicity scale. Figure 5 shows that the nucleophilicities  $N$  of the investigated isothioureas are in between those of the classical organocatalysts DMAP (**1**) and NMI (**2**).

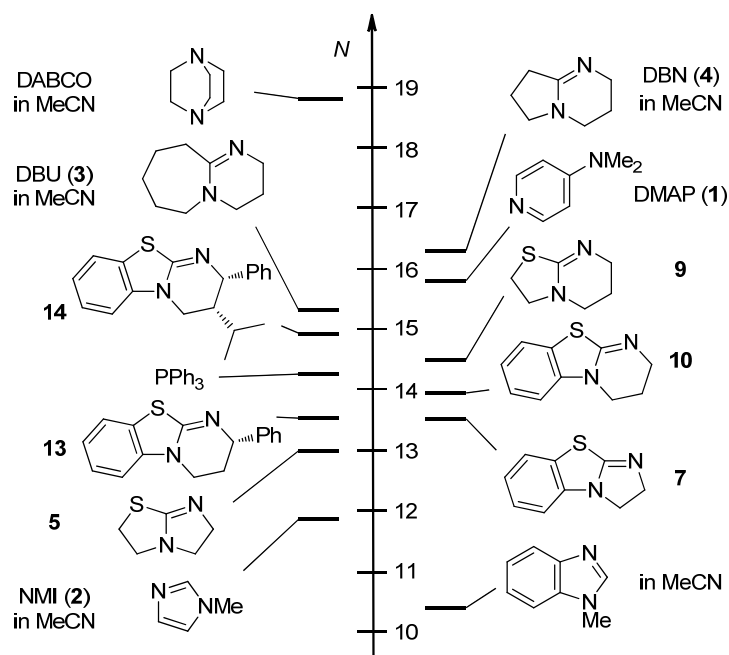


**Figure 5.** Comparison of the nucleophilicities  $N$  of isothioureas with other nucleophilic organocatalysts (solvent is  $\text{CH}_2\text{Cl}_2$  unless otherwise stated,  $N$  from ref. [20]).

The availability of rate and equilibrium constants for the reactions of these nucleophiles with the benzhydrylium ion  $(\text{ind})_2\text{CH}^+$  furthermore allows us to construct the quantitative energy profile diagrams as depicted for some reactions in Figure 6. It is thus found that imidazoles are less nucleophilic as well as less Lewis basic than isothioureas. While the kinetic and thermodynamic properties of most isothioureas investigated are comparable to those of DMAP, DABCO is a stronger nucleophile than all isothioureas investigated, while its Lewis basicity is comparable to those of the least basic isothioureas.

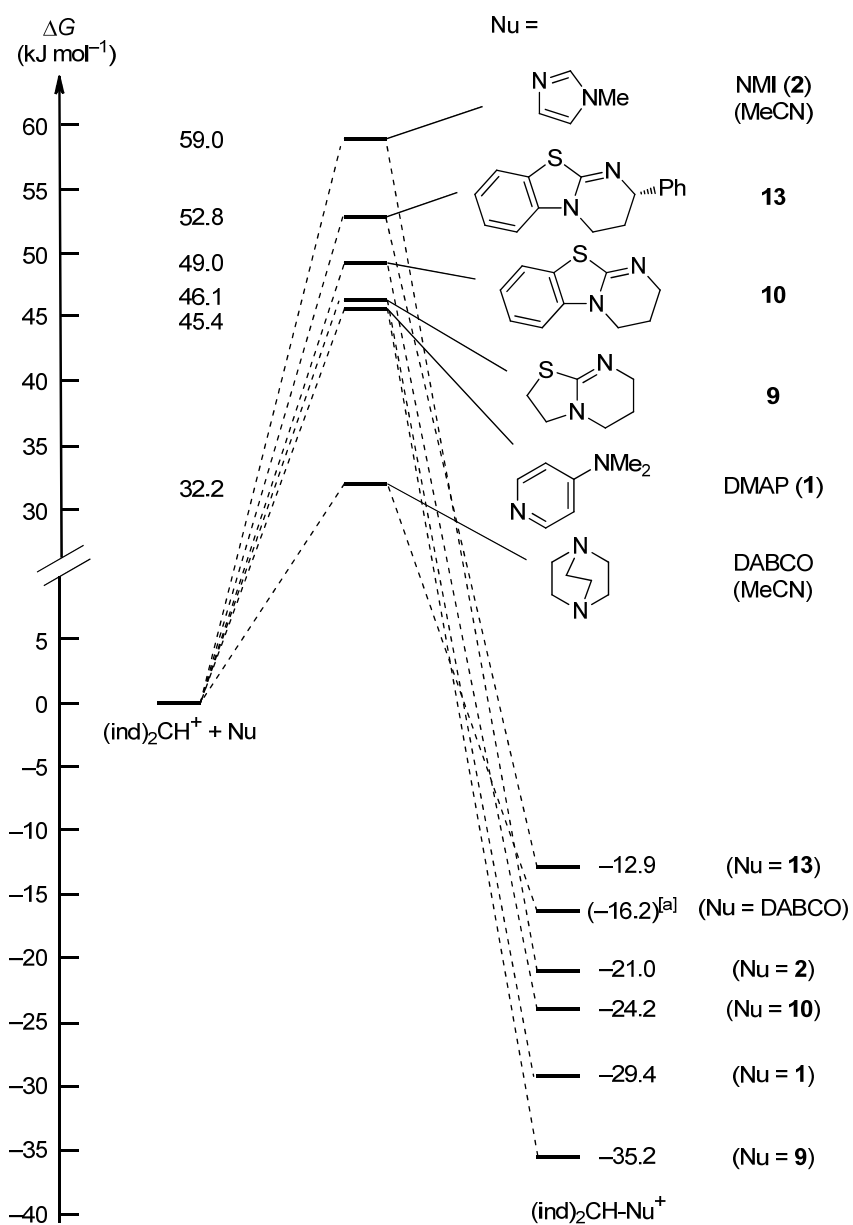


**Figure 6.** Gibbs energy profiles for the reactions of various nucleophilic organocatalysts with the benzhydrylium ion  $(\text{ind})_2\text{CH}^+$  in  $\text{CH}_2\text{Cl}_2$  at  $20^\circ\text{C}$  ( $\Delta G^\ddagger$  and  $\Delta G^0$  values from Table 3 or from ref. [20]). <sup>[a]</sup>  $\Delta G^0$  was estimated in ref. [20e].

## 4 Experimental Section

In order to identify my contributions to this multiauthor publication, only the experiments, which were performed by me, are described in chapter 4.2, 4.3, 4.4 and 4.5 of this Experimental Section.

### 4.1 General

#### *Material and Analytcs.*

CH<sub>2</sub>Cl<sub>2</sub> was freshly distilled over CaH<sub>2</sub>. Isothioureas were synthesized according to literature procedures.<sup>[7,15,18]</sup> Benzhydrylium tetrafluoroborates were prepared as described before.<sup>[19a]</sup> All other chemicals were purchased from commercial sources and (if necessary) purified by recrystallization or distillation prior to use. <sup>1</sup>H and <sup>13</sup>C NMR spectra were recorded on NMR-systems (400 MHz) in *d*<sub>6</sub>-DMSO or CD<sub>3</sub>CN and the chemical shifts in ppm refer to the solvent residual signal as internal standard ( $\delta_{\text{H}}(\text{CD}_3\text{CN}) = 1.94$ ,  $\delta_{\text{C}}(\text{CD}_3\text{CN}) = 1.4$  ppm;  $\delta_{\text{H}}(d_6\text{-DMSO}) = 2.50$ ,  $\delta_{\text{C}}(d_6\text{-DMSO}) = 39.5$  ppm).

#### *Kinetics.*

The rates of all investigated reactions were determined photometrically. The temperature of the solutions during all kinetic studies was kept constant ( $20.0 \pm 0.1$  °C) by using a circulating bath thermostat. The kinetic experiments with isothioureas were carried out with freshly prepared stock solutions of isothioureas in CH<sub>2</sub>Cl<sub>2</sub>. The nucleophiles were always employed as major component (high excess) in the reactions with the electrophiles resulting in first-order kinetics. For the evaluation of fast kinetics ( $\tau_{1/2} < 15\text{--}20$  s) stopped-flow spectrophotometer systems (Hi-Tech SF-61DX2 or Applied Photophysics SX.18MV-R) were used. The rates of slow reactions ( $\tau_{1/2} > 15\text{--}20$  s) were determined by using a J&M TIDAS diode array spectrophotometer controlled by Labcontrol Spectacle software and connected to a Hellma 661.502-QX quartz Suprasil immersion probe (5 mm light path) via fiber optic cables and standard SMA connectors. Rate constants  $k_{\text{obs}}$  (s<sup>-1</sup>) were obtained by fitting the single exponential  $A_t = A_0 \exp(-k_{\text{obs}}t) + C$  (exponential decrease) to the observed time-dependent absorbance (averaged from at least 3 kinetic runs for each nucleophile concentration in case of stopped-flow method).

### 4.2 Product Studies

**6P-BF<sub>4</sub>**: To a blue solution of (dma)<sub>2</sub>CH<sup>+</sup>BF<sub>4</sub><sup>-</sup> (21 mg, 0.062 mmol) in CH<sub>2</sub>Cl<sub>2</sub> (1 mL) was added drop by drop a solution of **6** (7.9 mg, 0.062 mmol) in dry CH<sub>2</sub>Cl<sub>2</sub> (1 mL) under

nitrogen at room temperature. After the disappearance of the blue color of the solution the solvent was evaporated and the residue was washed with *i*-hexane to afford **6P**-BF<sub>4</sub>: 27 mg (0.058 mmol, 93%, viscous liquid). **6P**-BF<sub>4</sub>: <sup>1</sup>H NMR (CD<sub>3</sub>CN, 400 MHz): δ 2.93 (s, 12 H), 3.59–3.66 (m, 4 H), 3.72–3.77 (m, 2 H), 4.03–4.08 (m, 2 H), 5.67 (s, 1 H), 6.74 (d, *J* = 8.9 Hz, 4 H), 7.11 ppm (d, *J* = 8.9 Hz). <sup>13</sup>C NMR (CD<sub>3</sub>CN, 100 MHz): δ 38.0 (t), 40.6 (q), 47.4 (t), 48.1 (t), 56.6 (t), 66.9 (d), 113.2 (d), 124.0 (s), 130.7 (d), 152.1 (s), 177.5 ppm (s). HRMS (ESI) calculated for C<sub>22</sub>H<sub>29</sub>N<sub>4</sub><sup>32</sup>S [M<sup>+</sup>] 381.2107, found 381.2112.

**7P**-BF<sub>4</sub>: Equimolar amounts of (dma)<sub>2</sub>CH<sup>+</sup>BF<sub>4</sub><sup>-</sup> (16 mg, 0.047 mmol) and **7** (8.3 mg, 0.047 mmol) were mixed in d<sub>6</sub>-DMSO (0.6 mL) in an NMR tube under nitrogen and the NMR was taken after few minutes of shaking. **7P**-BF<sub>4</sub>: <sup>1</sup>H NMR (d<sub>6</sub>-DMSO, 400 MHz): δ 2.93 (s, 12 H), 4.27–4.32 (m, 2 H), 4.53–4.58 (m, 2 H), 5.91 (s, 1 H), 6.77 (d, *J* = 8.8 Hz, 4 H), 7.25 (d, *J* = 8.8 Hz, 4 H), 7.30–7.35 (m, 1 H), 7.55 (d, *J* = 3.9 Hz, 2 H), 7.93 ppm (d, *J* = 8.1 Hz, 1 H). <sup>13</sup>C NMR (d<sub>6</sub>-DMSO, 100 MHz): δ 39.9 (q), 44.8 (t), 55.1 (t), 65.2 (d), 112.0 (d), 112.2 (d), 123.0 (s), 124.3 (d), 124.4 (d), 127.5 (s), 128.1 (d), 129.5 (d), 134.0 (s), 150.4 (s), 168.8 ppm (s).

**9P**-BF<sub>4</sub>: To a blue solution of (dma)<sub>2</sub>CH<sup>+</sup>BF<sub>4</sub><sup>-</sup> (22 mg, 0.065 mmol) in CH<sub>2</sub>Cl<sub>2</sub> (1 mL) was added drop by drop a solution of **9** (9.2 mg, 0.062 mmol) in dry CH<sub>2</sub>Cl<sub>2</sub> (1 mL) under nitrogen at room temperature. After the disappearance of the blue color of the solution the solvent was evaporated and the residue was washed with *i*-hexane to get **9P**-BF<sub>4</sub>: 27 mg (0.058 mmol, 89%, viscous liquid). **9P**-BF<sub>4</sub>: <sup>1</sup>H NMR (CD<sub>3</sub>CN, 400 MHz): δ 2.02–2.07 (m, 2 H), 2.94 (s, 12 H), 3.17–3.20 (m, 2 H), 3.41–3.47 (m, 4 H), 4.00 (t, 2 H, *J* = 7.7 Hz), 5.98 (s, 1 H), 6.75 (d, 2 H, *J* = 8.9 Hz), 7.03 ppm (d, 4 H, *J* = 8.4 Hz). <sup>13</sup>C NMR (CD<sub>3</sub>CN, 100 MHz): δ 20.2 (t), 29.2 (t), 40.6 (q), 44.5 (t), 45.6 (t), 57.0 (t), 72.9 (d), 113.3 (d), 124.3 (s), 130.4 (d), 151.8 (s), 168.3 ppm (s). HRMS (ESI) calculated for C<sub>23</sub>H<sub>31</sub>N<sub>4</sub><sup>32</sup>S [M<sup>+</sup>] 395.2264, found 395.2265.

**10P**-BF<sub>4</sub>: Equimolar amounts of (dma)<sub>2</sub>CH<sup>+</sup>BF<sub>4</sub><sup>-</sup> (13 mg, 0.038 mmol) and DHPB **10** (7.3 mg, 0.038 mmol) were mixed in d<sub>6</sub>-DMSO (0.6 mL) in an NMR tube under nitrogen and the NMR was taken after few minutes of shaking. **10P**-BF<sub>4</sub>: <sup>1</sup>H NMR (d<sub>6</sub>-DMSO, 400 MHz): δ 2.28–2.31 (m, 2 H), 2.92 (s, 12 H), 3.43–3.45 (m, 2 H), 4.23 (t, *J* = 5.9, 2 H), 6.12 (s, 1 H), 6.76 (d, *J* = 8.9 Hz, 4 H), 7.15 (d, *J* = 8.7 Hz, 4 H), 7.41–7.45 (m, 1 H), 7.59–7.63 (m, 1 H), 7.69 (d, *J* = 7.8, 1 H), 8.04 ppm (d, *J* = 8.0, 1 H). <sup>13</sup>C NMR (d<sub>6</sub>-DMSO, 100 MHz): δ 18.4 (t), 39.9 (q), 43.0 (t), 45.0 (t), 70.9 (d), 112.2 (d), 112.9 (d), 121.9 (s), 122.4 (s), 123.3 (d), 125.0 (d), 128.0 (d), 129.4 (d), 138.8 (s), 150.3 (s), 164.3 ppm (s).

4.3 Kinetics of the reactions of isothiureas with benzhydrylium ions ( $\text{Ar}_2\text{CH}^+$ )

The rates of the reactions of the isothiureas (**5–10** and **13–17**) with the colored benzhydrylium ions were measured under pseudo-first-order conditions (excess of isothiurea) at or close to the absorption maxima of  $\text{Ar}_2\text{CH}^+$  by UV-Vis spectrometry using the stopped-flow technique described previously<sup>[19a]</sup> at 20 °C in dry  $\text{CH}_2\text{Cl}_2$ . First-order rate constants  $k_{\text{obs}}$  ( $\text{s}^{-1}$ ) were obtained by least-squares fitting of the absorbances to the mono-exponential curve  $A_t = A_0 \exp(-k_{\text{obs}}t) + C$ . Because of  $k_{\text{obs}} = k[\text{Nu}]$ , second-order rate constants  $k$  ( $\text{M}^{-1} \text{s}^{-1}$ ) were derived from the slopes of the linear plots of  $k_{\text{obs}}$  ( $\text{s}^{-1}$ ) vs.  $[\text{Nu}]$ .

**Table 5.** Kinetics of the reactions of 3,5,6,7-tetrahydro-2H-imidazo[2,1-b][1,3]thiazine (**5**) with  $(\text{Ar})_2\text{CH}^+$  in  $\text{CH}_2\text{Cl}_2$  at 20 °C.

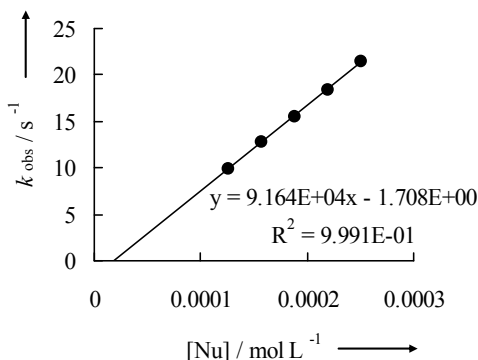
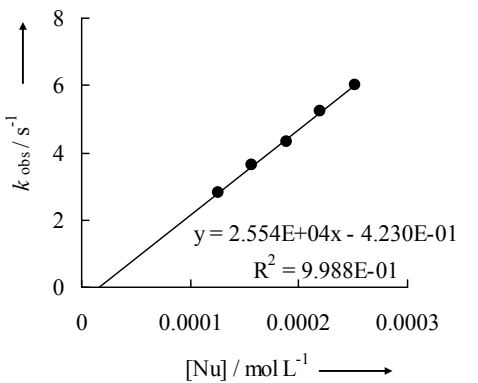
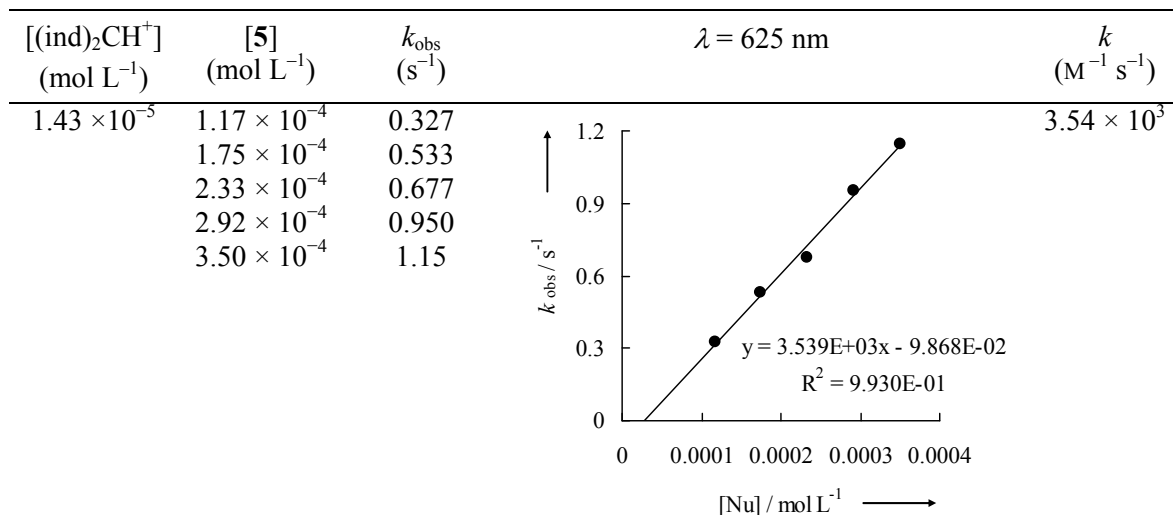
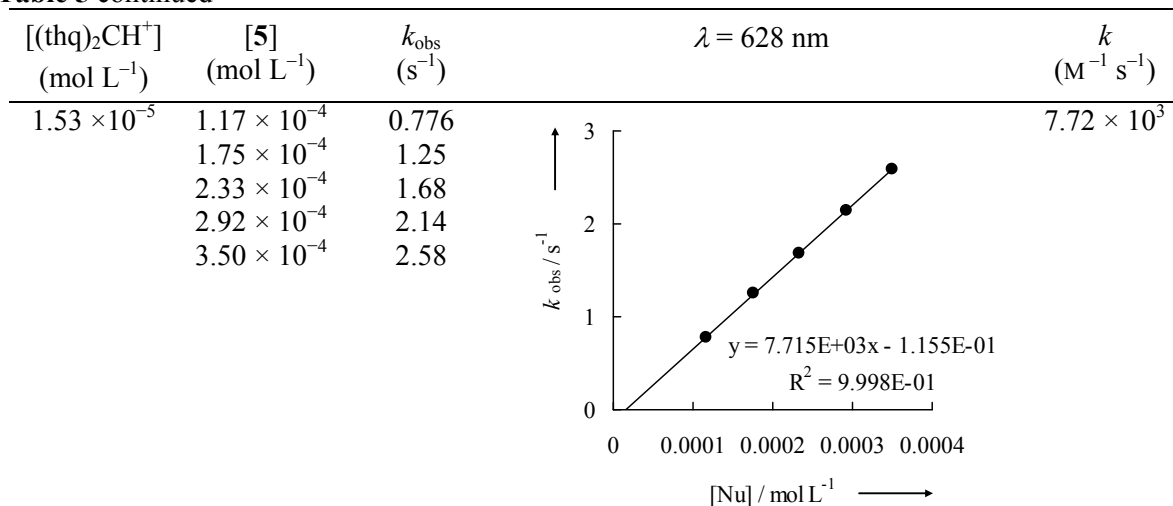
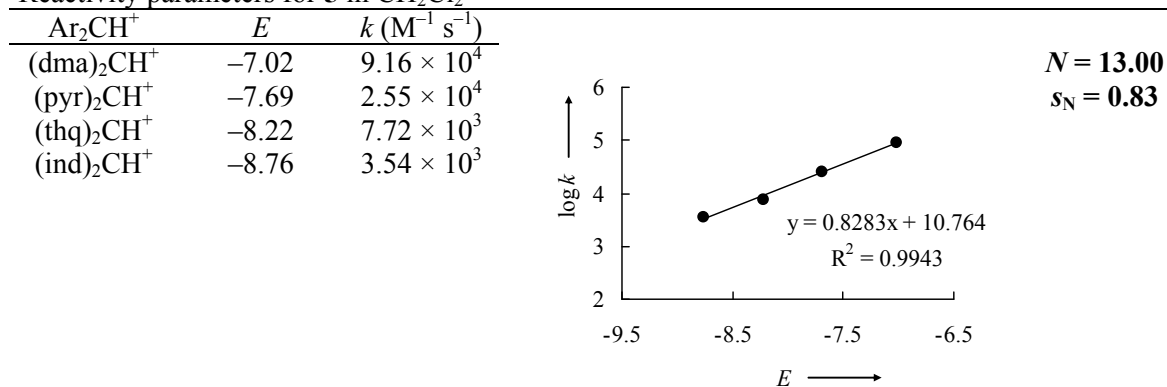
$[(\text{dma})_2\text{CH}^+]$ ( $\text{mol L}^{-1}$ )	<b>[5]</b> ( $\text{mol L}^{-1}$ )	$k_{\text{obs}}$ ( $\text{s}^{-1}$ )	$\lambda = 613 \text{ nm}$	$k$ ( $\text{M}^{-1} \text{s}^{-1}$ )
$1.41 \times 10^{-5}$	$1.26 \times 10^{-4}$	9.88		$9.16 \times 10^4$
	$1.57 \times 10^{-4}$	12.8		
	$1.89 \times 10^{-4}$	15.4		
	$2.20 \times 10^{-4}$	18.4		
	$2.52 \times 10^{-4}$	21.5		
$[(\text{pyr})_2\text{CH}^+]$ ( $\text{mol L}^{-1}$ )	<b>[5]</b> ( $\text{mol L}^{-1}$ )	$k_{\text{obs}}$ ( $\text{s}^{-1}$ )	$\lambda = 620 \text{ nm}$	$k$ ( $\text{M}^{-1} \text{s}^{-1}$ )
$1.40 \times 10^{-5}$	$1.26 \times 10^{-4}$	2.79		$2.55 \times 10^4$
	$1.57 \times 10^{-4}$	3.63		
	$1.89 \times 10^{-4}$	4.33		
	$2.20 \times 10^{-4}$	5.22		
	$2.52 \times 10^{-4}$	6.02		

Table 5 continued

Reactivity parameters for **5** in CH<sub>2</sub>Cl<sub>2</sub>

**Table 6.** Kinetics of the reactions of 2,3,5,6-tetrahydroimidazo[2,1-b]thiazole (**6**) with (Ar)<sub>2</sub>CH<sup>+</sup> in CH<sub>2</sub>Cl<sub>2</sub> at 20°C

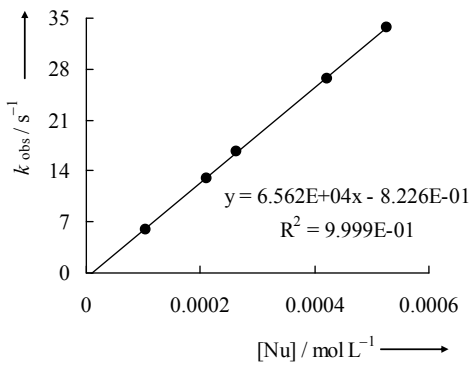
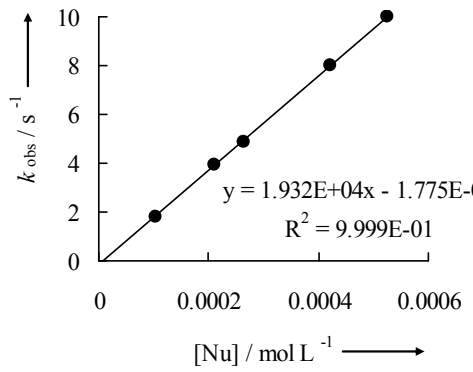
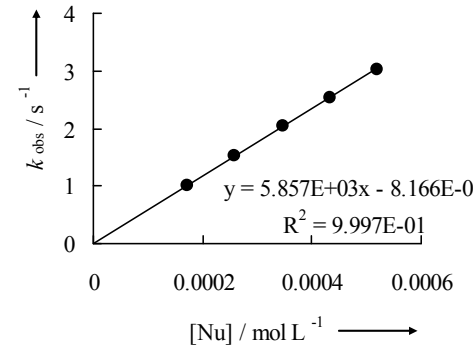
[(dma) <sub>2</sub> CH <sup>+</sup> ] (mol L <sup>-1</sup> )	[ <b>6</b> ] (mol L <sup>-1</sup> )	<i>k</i> <sub>obs</sub> (s <sup>-1</sup> )	<i>λ</i> = 613 nm	<i>k</i> (M <sup>-1</sup> s <sup>-1</sup> )
1.41 × 10 <sup>-5</sup>	1.05 × 10 <sup>-4</sup>	5.96		6.56 × 10 <sup>4</sup>
	2.11 × 10 <sup>-4</sup>	13.0		
	2.63 × 10 <sup>-4</sup>	16.7		
	4.21 × 10 <sup>-4</sup>	26.7		
	5.27 × 10 <sup>-4</sup>	33.7		
[(pyr) <sub>2</sub> CH <sup>+</sup> ] (mol L <sup>-1</sup> )	[ <b>6</b> ] (mol L <sup>-1</sup> )	<i>k</i> <sub>obs</sub> (s <sup>-1</sup> )	<i>λ</i> = 620 nm	<i>k</i> (M <sup>-1</sup> s <sup>-1</sup> )
1.47 × 10 <sup>-5</sup>	1.05 × 10 <sup>-4</sup>	1.82		1.93 × 10 <sup>4</sup>
	2.11 × 10 <sup>-4</sup>	3.94		
	2.63 × 10 <sup>-4</sup>	4.89		
	4.21 × 10 <sup>-4</sup>	8.00		
	5.27 × 10 <sup>-4</sup>	9.97		
[(thq) <sub>2</sub> CH <sup>+</sup> ] (mol L <sup>-1</sup> )	[ <b>6</b> ] (mol L <sup>-1</sup> )	<i>k</i> <sub>obs</sub> (s <sup>-1</sup> )	<i>λ</i> = 628 nm	<i>k</i> (M <sup>-1</sup> s <sup>-1</sup> )
1.34 × 10 <sup>-5</sup>	1.73 × 10 <sup>-4</sup>	0.997		5.86 × 10 <sup>3</sup>
	2.60 × 10 <sup>-4</sup>	1.51		
	3.46 × 10 <sup>-4</sup>	2.04		
	4.33 × 10 <sup>-4</sup>	2.53		
	5.19 × 10 <sup>-4</sup>	3.02		

Table 6 continued

$[(\text{ind})_2\text{CH}^+]$ (mol L <sup>-1</sup> )	<b>[6]</b> (mol L <sup>-1</sup> )	$k_{\text{obs}}$ (s <sup>-1</sup> )	$\lambda = 625 \text{ nm}$	$k$ (M <sup>-1</sup> s <sup>-1</sup> )
$1.54 \times 10^{-5}$	$1.73 \times 10^{-4}$	0.425		$2.79 \times 10^3$
	$2.60 \times 10^{-4}$	0.663		
	$3.46 \times 10^{-4}$	0.904		
	$4.33 \times 10^{-4}$	1.16		
	$5.19 \times 10^{-4}$	1.38		

Reactivity parameters for **6** in CH<sub>2</sub>Cl<sub>2</sub>

Ar <sub>2</sub> CH <sup>+</sup>	$E$	$k$ (M <sup>-1</sup> s <sup>-1</sup> )
(dma) <sub>2</sub> CH <sup>+</sup>	-7.02	$6.56 \times 10^4$
(pyr) <sub>2</sub> CH <sup>+</sup>	-7.69	$1.94 \times 10^4$
(thq) <sub>2</sub> CH <sup>+</sup>	-8.22	$5.85 \times 10^3$
(ind) <sub>2</sub> CH <sup>+</sup>	-8.76	$2.79 \times 10^3$

**Table 7.** Kinetics of the reactions of **7** with (Ar)<sub>2</sub>CH<sup>+</sup> in CH<sub>2</sub>Cl<sub>2</sub> at 20°C

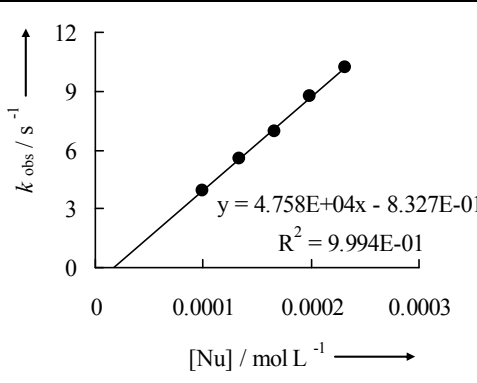
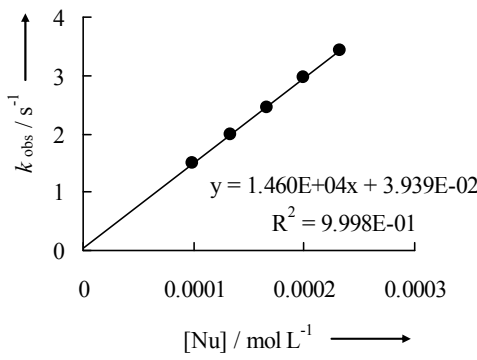
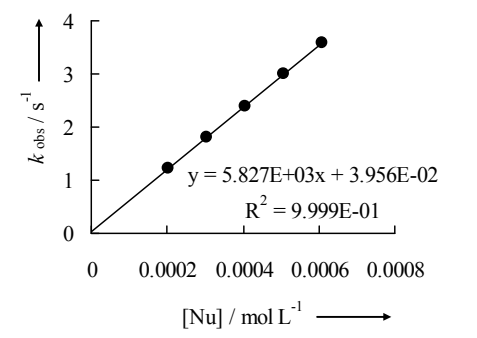
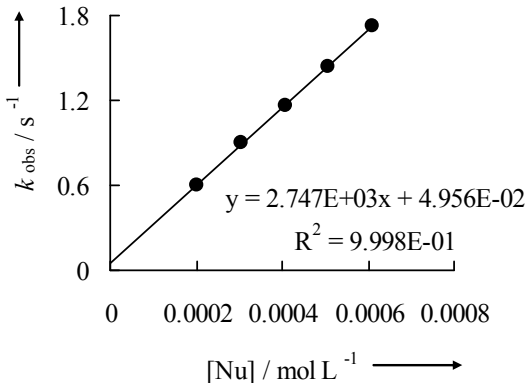
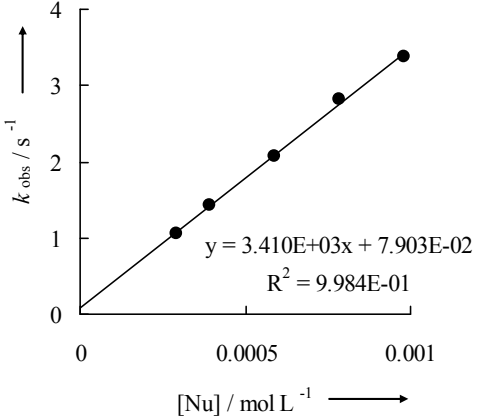
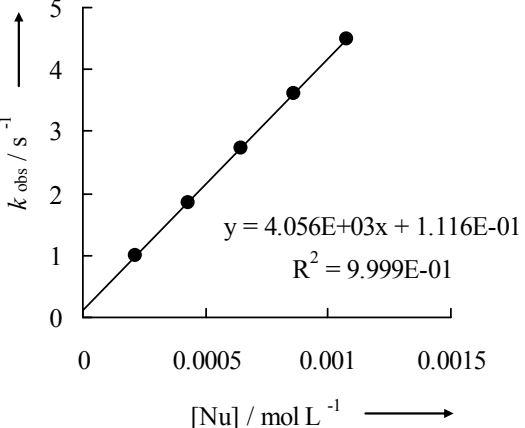
[(dma) <sub>2</sub> CH <sup>+</sup> ] (mol L <sup>-1</sup> )	[ <b>7</b> ] (mol L <sup>-1</sup> )	<i>k</i> <sub>obs</sub> (s <sup>-1</sup> )	λ = 613 nm	<i>k</i> (M <sup>-1</sup> s <sup>-1</sup> )
1.47 × 10 <sup>-5</sup>	9.96 × 10 <sup>-5</sup>	3.92		4.76 × 10 <sup>4</sup>
	1.33 × 10 <sup>-4</sup>	5.52		
	1.66 × 10 <sup>-4</sup>	6.97		
	1.99 × 10 <sup>-4</sup>	8.70		
	2.32 × 10 <sup>-4</sup>	10.2		
[(pyr) <sub>2</sub> CH <sup>+</sup> ] (mol L <sup>-1</sup> )	[ <b>7</b> ] (mol L <sup>-1</sup> )	<i>k</i> <sub>obs</sub> (s <sup>-1</sup> )	λ = 620 nm	<i>k</i> (M <sup>-1</sup> s <sup>-1</sup> )
1.68 × 10 <sup>-5</sup>	9.96 × 10 <sup>-5</sup>	1.49		1.46 × 10 <sup>4</sup>
	1.33 × 10 <sup>-4</sup>	1.99		
	1.66 × 10 <sup>-4</sup>	2.45		
	1.99 × 10 <sup>-4</sup>	2.96		
	2.32 × 10 <sup>-4</sup>	3.42		
[(thq) <sub>2</sub> CH <sup>+</sup> ] (mol L <sup>-1</sup> )	[ <b>7</b> ] (mol L <sup>-1</sup> )	<i>k</i> <sub>obs</sub> (s <sup>-1</sup> )	λ = 628 nm	<i>k</i> (M <sup>-1</sup> s <sup>-1</sup> )
1.47 × 10 <sup>-5</sup>	2.03 × 10 <sup>-4</sup>	1.23		5.83 × 10 <sup>3</sup>
	3.05 × 10 <sup>-4</sup>	1.81		
	4.06 × 10 <sup>-4</sup>	2.39		
	5.08 × 10 <sup>-4</sup>	3.01		
	6.09 × 10 <sup>-4</sup>	3.60		

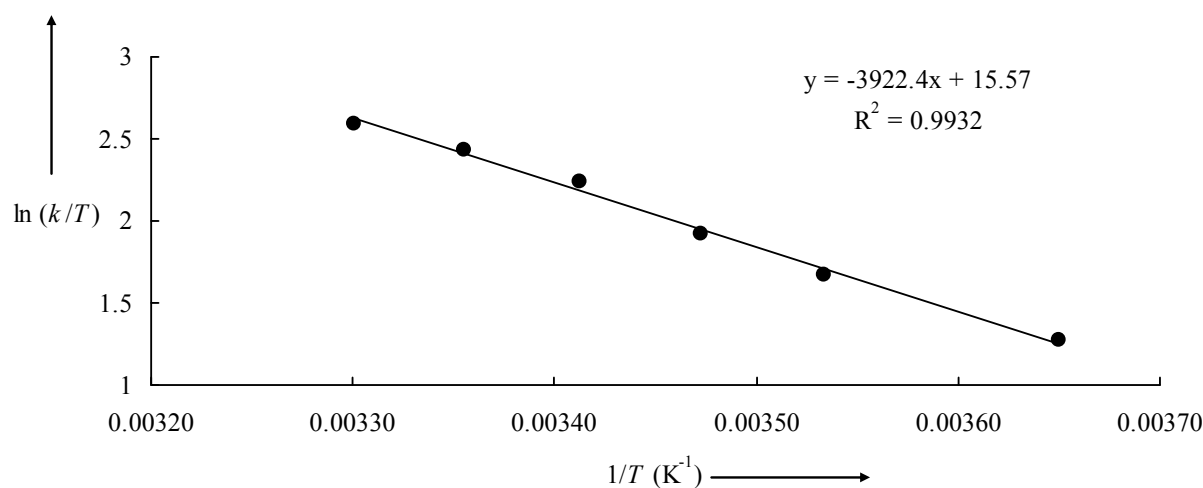
Table 7 continued

Table 7a: Kinetics of the Reactions of (7) with  $(\text{ind})_2\text{CH}^+$  in  $\text{CH}_2\text{Cl}_2$  at different temperature.

$T$ ( $^\circ\text{C}$ )	$[(\text{ind})_2\text{CH}^+]$ ( $\text{mol L}^{-1}$ )	$[\text{7}]$ ( $\text{mol L}^{-1}$ )	$k_{\text{obs}}$ ( $\text{s}^{-1}$ )	$\lambda = 625 \text{ nm}$	$k$ ( $\text{M}^{-1} \text{ s}^{-1}$ )
1.0	$1.56 \times 10^{-5}$	$2.05 \times 10^{-4}$	0.197		$9.82 \times 10^2$
		$4.11 \times 10^{-4}$	0.399		
		$6.16 \times 10^{-4}$	0.596		
		$8.22 \times 10^{-4}$	0.798		
		$1.03 \times 10^{-3}$	1.01		
10.0	$1.87 \times 10^{-5}$	$2.16 \times 10^{-4}$	0.307		$1.50 \times 10^3$
		$4.31 \times 10^{-4}$	0.647		
		$6.47 \times 10^{-4}$	0.962		
		$8.62 \times 10^{-4}$	1.28		
		$1.08 \times 10^{-3}$	1.61		
15.0	$1.56 \times 10^{-5}$	$2.94 \times 10^{-4}$	0.676		$1.96 \times 10^3$
		$3.92 \times 10^{-4}$	0.894		
		$5.87 \times 10^{-4}$	1.26		
		$7.83 \times 10^{-4}$	1.68		
		$9.79 \times 10^{-4}$	2.02		

Table 7a continued

$T$ (°C)	$[(\text{ind})_2\text{CH}^+]$ (mol L <sup>-1</sup> )	$[7]$ (mol L <sup>-1</sup> )	$k_{\text{obs}}$ (s <sup>-1</sup> )	$\lambda = 625 \text{ nm}$	$k$ (M <sup>-1</sup> s <sup>-1</sup> )
20.0	$1.47 \times 10^{-5}$	$2.03 \times 10^{-4}$	0.603		$2.75 \times 10^3$
		$3.05 \times 10^{-4}$	0.896		
		$4.06 \times 10^{-4}$	1.66		
		$5.08 \times 10^{-4}$	1.44		
		$6.09 \times 10^{-4}$	1.72		
25.0	$1.56 \times 10^{-5}$	$2.94 \times 10^{-4}$	1.07		$3.41 \times 10^3$
		$3.92 \times 10^{-4}$	1.42		
		$5.87 \times 10^{-4}$	2.06		
		$7.83 \times 10^{-4}$	2.81		
		$9.79 \times 10^{-4}$	3.38		
30.0	$1.87 \times 10^{-5}$	$2.16 \times 10^{-4}$	0.992		$4.06 \times 10^3$
		$4.31 \times 10^{-4}$	1.86		
		$6.47 \times 10^{-4}$	2.72		
		$8.62 \times 10^{-4}$	3.62		
		$1.08 \times 10^{-3}$	4.47		

Eyring Plot for the reactions of **7** with  $(\text{ind})_2\text{CH}^+\text{BF}_4^-$ 

Eyring-parameters:

$$\Delta H^\ddagger = (32.6 \pm 1.3) \text{ kJ mol}^{-1}$$

$$\Delta S^\ddagger = (-68.0 \pm 4.7) \text{ J mol}^{-1} \text{ K}^{-1}$$

Coefficient of correlation: 0.9932

Arrhenius-parameters:

$$E_A = (35.0 \pm 1.3) \text{ kJ mol}^{-1}$$

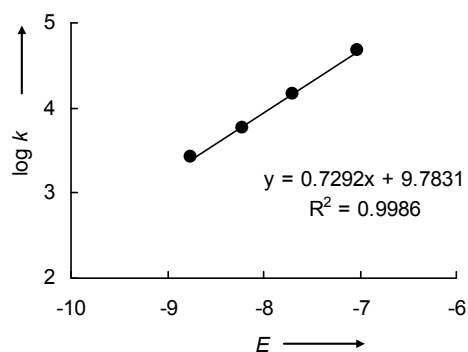
$$\ln A = 22.2 \pm 5.6$$

Coefficient of correlation: 0.9941

$$k(20^\circ\text{C}) = 2.60 \times 10^3 \text{ M}^{-1} \text{ s}^{-1}$$

Reactivity parameters for **7** in  $\text{CH}_2\text{Cl}_2$ 

$\text{Ar}_2\text{CH}^+$	$E$	$k \text{ (M}^{-1} \text{ s}^{-1}\text{)}$
$(\text{dma})_2\text{CH}^+$	-7.02	$4.76 \times 10^4$
$(\text{pyr})_2\text{CH}^+$	-7.69	$1.46 \times 10^4$
$(\text{thq})_2\text{CH}^+$	-8.22	$5.83 \times 10^3$
$(\text{ind})_2\text{CH}^+$	-8.76	$2.60 \times 10^3$

 $N = 13.42$  $s_N = 0.73$

**Table 8.** Kinetics of the Reactions of 2,3,4,6,7,8-hexahydropyrimido[2,1-b][1,3]thiazine (**8**) with  $(\text{Ar})_2\text{CH}^+$  in  $\text{CH}_2\text{Cl}_2$  at  $20^\circ\text{C}$ .

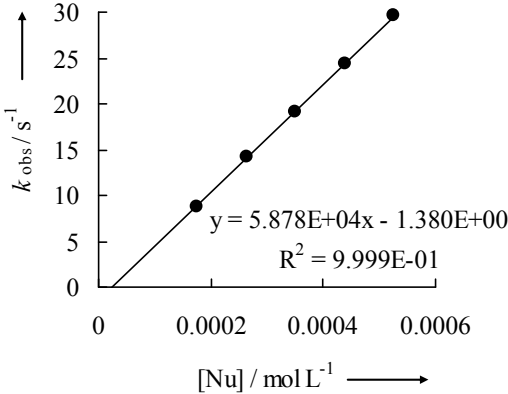
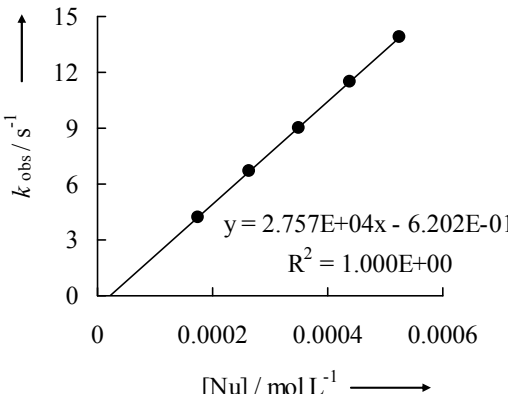
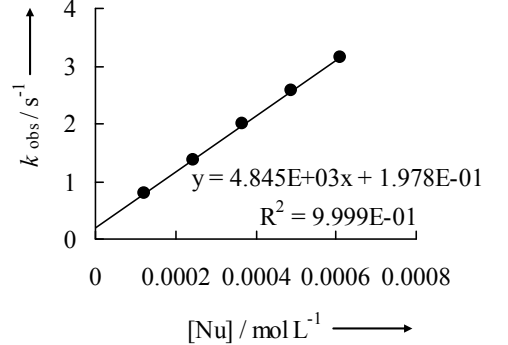
$[(\text{thq})_2\text{CH}^+]$ (mol L <sup>-1</sup> )	[ <b>8</b> ] (mol L <sup>-1</sup> )	$k_{\text{obs}}$ (s <sup>-1</sup> )	$\lambda = 628 \text{ nm}$	$k$ (M <sup>-1</sup> s <sup>-1</sup> )
$1.47 \times 10^{-5}$	$1.75 \times 10^{-4}$	8.86		$5.88 \times 10^4$
	$2.63 \times 10^{-4}$	14.2		
	$3.51 \times 10^{-4}$	19.2		
	$4.38 \times 10^{-4}$	24.3		
	$5.26 \times 10^{-4}$	29.6		
$[(\text{ind})_2\text{CH}^+]$ (mol L <sup>-1</sup> )	[ <b>8</b> ] (mol L <sup>-1</sup> )	$k_{\text{obs}}$ (s <sup>-1</sup> )	$\lambda = 625 \text{ nm}$	$k$ (M <sup>-1</sup> s <sup>-1</sup> )
$1.45 \times 10^{-5}$	$1.75 \times 10^{-4}$	4.22		$2.76 \times 10^4$
	$2.63 \times 10^{-4}$	6.65		
	$3.51 \times 10^{-4}$	9.03		
	$4.38 \times 10^{-4}$	11.5		
	$5.26 \times 10^{-4}$	13.9		
$[(\text{jul})_2\text{CH}^+]$ (mol L <sup>-1</sup> )	[ <b>8</b> ] (mol L <sup>-1</sup> )	$k_{\text{obs}}$ (s <sup>-1</sup> )	$\lambda = 642 \text{ nm}$	$k$ (M <sup>-1</sup> s <sup>-1</sup> )
$1.69 \times 10^{-5}$	$1.22 \times 10^{-4}$	0.788		$4.85 \times 10^3$
	$2.44 \times 10^{-4}$	1.37		
	$3.67 \times 10^{-4}$	1.99		
	$4.89 \times 10^{-4}$	2.57		
	$6.11 \times 10^{-4}$	3.15		

Table 8 continued

$[(\text{lil})_2\text{CH}^+]$ (mol L <sup>-1</sup> )	[8] (mol L <sup>-1</sup> )	$k_{\text{obs}}$ (s <sup>-1</sup> )	$\lambda = 639 \text{ nm}$	$k$ (M <sup>-1</sup> s <sup>-1</sup> )
$1.59 \times 10^{-5}$	$1.22 \times 10^{-4}$	0.361		$2.27 \times 10^3$
	$2.44 \times 10^{-4}$	0.620		
	$3.67 \times 10^{-4}$	0.897		
	$4.89 \times 10^{-4}$	1.18		
	$6.11 \times 10^{-4}$	1.47		

Reactivity parameters for 2,3,4,6,7,8-hexahydropyrimido[2,1-b][1,3]thiazine (8) in CH<sub>2</sub>Cl<sub>2</sub>

Ar <sub>2</sub> CH <sup>+</sup>	$E$	$k$ (M <sup>-1</sup> s <sup>-1</sup> )		
(thq) <sub>2</sub> CH <sup>+</sup>	-8.22	$5.88 \times 10^4$		$N = 14.10$ $s_N = 0.82$
(ind) <sub>2</sub> CH <sup>+</sup>	-8.76	$2.76 \times 10^4$		
(jul) <sub>2</sub> CH <sup>+</sup>	-9.45	$4.85 \times 10^3$		
(lil) <sub>2</sub> CH <sup>+</sup>	-10.04	$2.27 \times 10^3$		

Table 9. Kinetics of the reactions of THTP (9) with (Ar)<sub>2</sub>CH<sup>+</sup> in CH<sub>2</sub>Cl<sub>2</sub> at 20°C

$[(\text{thq})_2\text{CH}^+]$ (mol L <sup>-1</sup> )	[THTP] (mol L <sup>-1</sup> )	$k_{\text{obs}}$ (s <sup>-1</sup> )	$\lambda = 628 \text{ nm}$	$k$ (M <sup>-1</sup> s <sup>-1</sup> )
$7.14 \times 10^{-6}$	$4.54 \times 10^{-5}$	3.63		$7.09 \times 10^4$
	$9.07 \times 10^{-5}$	6.07		
	$1.36 \times 10^{-4}$	9.41		
	$1.81 \times 10^{-4}$	13.0		
	$2.72 \times 10^{-4}$	18.9		
	$3.63 \times 10^{-4}$	26.0		

Table 9 continued

Table 9a: Kinetics of the Reactions of THTP (9) with (ind)<sub>2</sub>CH<sup>+</sup> in CH<sub>2</sub>Cl<sub>2</sub> at different temperature.

<i>T</i> (°C)	[(ind) <sub>2</sub> CH <sup>+</sup> ] (mol L <sup>-1</sup> )	[THTP] (mol L <sup>-1</sup> )	<i>k</i> <sub>obs</sub> (s <sup>-1</sup> )	<i>k</i> (M <sup>-1</sup> s <sup>-1</sup> )
1.0	1.56 × 10 <sup>-5</sup>	1.74 × 10 <sup>-4</sup>	2.35	1.47 × 10 <sup>4</sup>
		3.47 × 10 <sup>-4</sup>	4.88	
		5.21 × 10 <sup>-4</sup>	7.36	
		6.95 × 10 <sup>-4</sup>	9.97	
		8.68 × 10 <sup>-4</sup>	12.6	
10.0	1.56 × 10 <sup>-5</sup>	1.74 × 10 <sup>-4</sup>	3.73	2.38 × 10 <sup>4</sup>
		3.47 × 10 <sup>-4</sup>	7.67	
		5.21 × 10 <sup>-4</sup>	11.7	
		6.95 × 10 <sup>-4</sup>	15.8	
		8.68 × 10 <sup>-4</sup>	20.3	
20.0	6.59 × 10 <sup>-6</sup>	4.54 × 10 <sup>-5</sup>	1.84	3.70 × 10 <sup>4</sup>
		9.07 × 10 <sup>-5</sup>	3.23	
		1.36 × 10 <sup>-4</sup>	4.97	
		1.81 × 10 <sup>-4</sup>	6.81	
		2.27 × 10 <sup>-4</sup>	8.44	

$k_{\text{obs}} / \text{s}^{-1}$

$y = 1.473\text{E}+04x - 2.431\text{E}-01$

$R^2 = 9.999\text{E}-01$

$[\text{Nu}] / \text{mol L}^{-1}$

$k_{\text{obs}} / \text{s}^{-1}$

$y = 2.376\text{E}+04x - 5.277\text{E}-01$

$R^2 = 9.995\text{E}-01$

$[\text{Nu}] / \text{mol L}^{-1}$

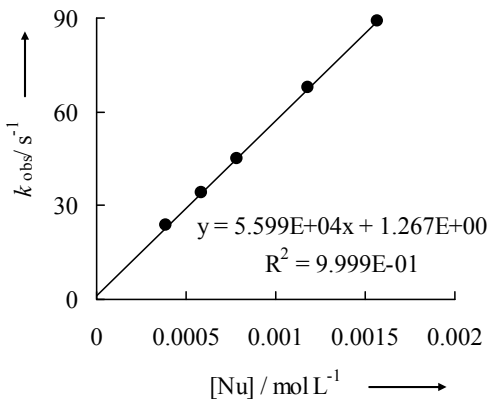
$k_{\text{obs}} / \text{s}^{-1}$

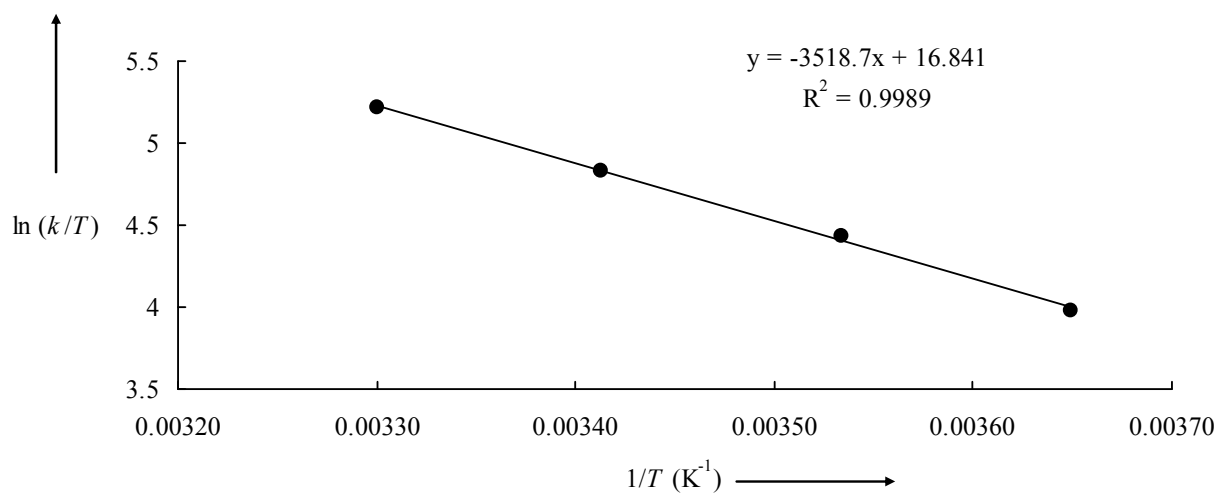
$y = 3.699\text{E}+04x + 2.559\text{E}-02$

$R^2 = 9.980\text{E}-01$

$[\text{Nu}] / \text{mol L}^{-1}$

Table 9a continued

$T$ (°C)	$[(\text{ind})_2\text{CH}^+]$ (mol L <sup>-1</sup> )	[THTP] (mol L <sup>-1</sup> )	$k_{\text{obs}}$ (s <sup>-1</sup> )	$\lambda = 625 \text{ nm}$	$k$ (M <sup>-1</sup> s <sup>-1</sup> )
30.0	$1.56 \times 10^{-5}$	$3.92 \times 10^{-4}$	23.5		$5.60 \times 10^4$
		$5.89 \times 10^{-4}$	34.0		
		$7.85 \times 10^{-4}$	44.8		
		$1.18 \times 10^{-3}$	67.7		
		$1.57 \times 10^{-3}$	89.1		

Eyring Plot for the reaction of THTP (9) with (ind)<sub>2</sub>CHBF<sub>4</sub>

Eyring-parameters:

$$\Delta H^\ddagger = (29.3 \pm 0.7) \text{ kJ mol}^{-1}$$

$$\Delta S^\ddagger = (-57.3 \pm 2.5) \text{ J mol}^{-1} \text{ K}^{-1}$$

Coefficient of correlation: 0.9988

Arrhenius-parameters:

$$E_A = (31.7 \pm 0.7) \text{ kJ mol}^{-1}$$

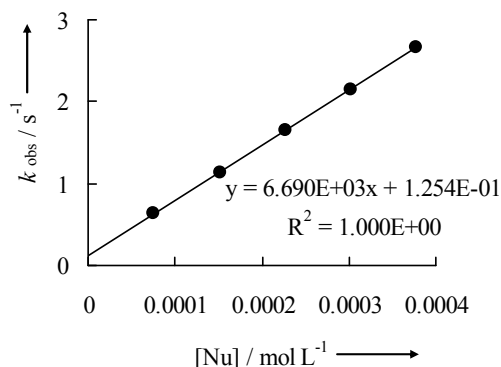
$$\ln A = 23.5 \pm 0.3$$

Coefficient of correlation: 0.9991

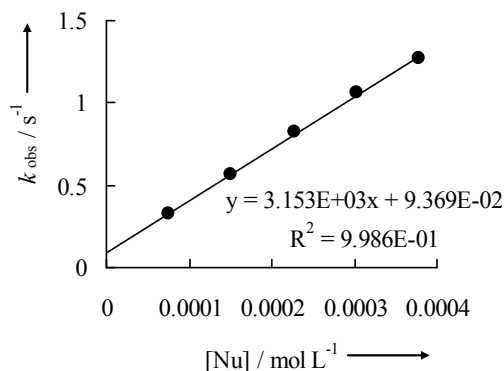
$$k(20 \text{ }^\circ\text{C}) = 3.68 \times 10^4 \text{ M}^{-1} \text{ s}^{-1}$$

Table 9 continued

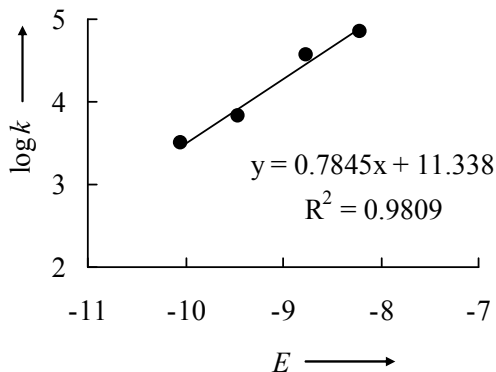
$[(\text{jul})_2\text{CH}^+]$ (mol L <sup>-1</sup> )	[THTP] (mol L <sup>-1</sup> )	$k_{\text{obs}}$ (s <sup>-1</sup> )	$\lambda = 642 \text{ nm}$	$k$ (M <sup>-1</sup> s <sup>-1</sup> )
$6.75 \times 10^{-6}$	$7.56 \times 10^{-5}$	0.633		$6.69 \times 10^3$
	$1.51 \times 10^{-4}$	1.14		
	$2.27 \times 10^{-4}$	1.64		
	$3.02 \times 10^{-4}$	2.15		
	$3.78 \times 10^{-4}$	2.66		



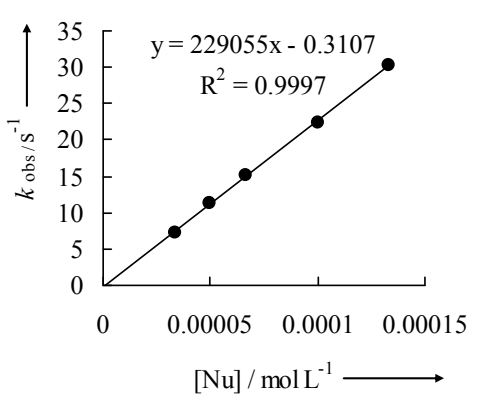
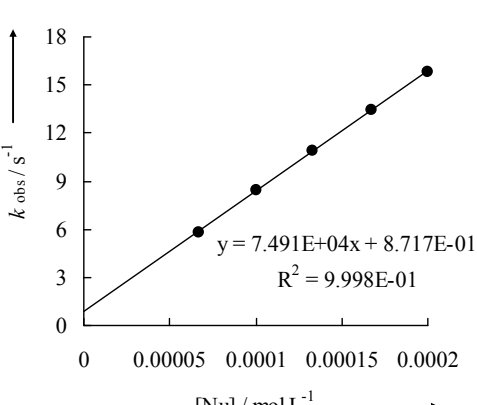
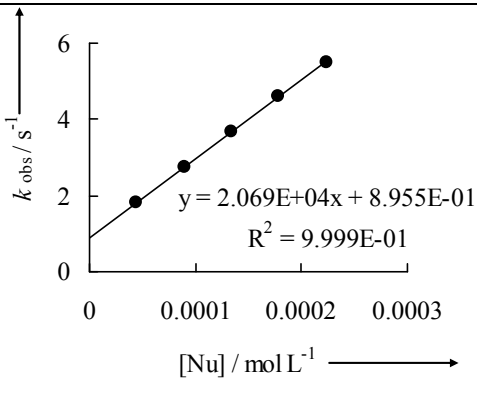
$[(\text{lil})_2\text{CH}^+]$ (mol L <sup>-1</sup> )	[THTP] (mol L <sup>-1</sup> )	$k_{\text{obs}}$ (s <sup>-1</sup> )	$\lambda = 639 \text{ nm}$	$k$ (M <sup>-1</sup> s <sup>-1</sup> )
$7.21 \times 10^{-6}$	$7.56 \times 10^{-5}$	0.324		$3.15 \times 10^3$
	$1.51 \times 10^{-4}$	0.568		
	$2.27 \times 10^{-4}$	0.821		
	$3.02 \times 10^{-4}$	1.06		
	$3.78 \times 10^{-4}$	1.27		

Reactivity parameters for THTP (9) in CH<sub>2</sub>Cl<sub>2</sub>

Ar <sub>2</sub> CH <sup>+</sup>	$E$	$k$ (M <sup>-1</sup> s <sup>-1</sup> )	$N = 14.45$ $s_N = 0.78$
(thq) <sub>2</sub> CH <sup>+</sup>	-8.22	$7.09 \times 10^4$	
(ind) <sub>2</sub> CH <sup>+</sup>	-8.76	$3.68 \times 10^4$	
(jul) <sub>2</sub> CH <sup>+</sup>	-9.45	$6.69 \times 10^3$	
(lil) <sub>2</sub> CH <sup>+</sup>	-10.04	$3.15 \times 10^3$	



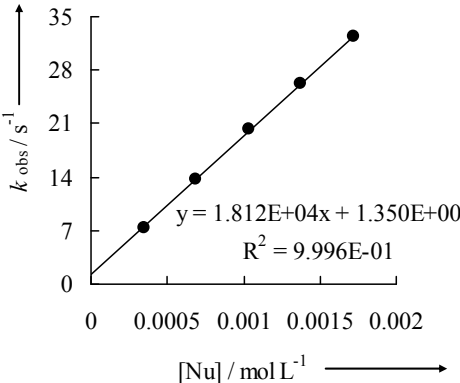
**Table 10.** Kinetics of the reactions of DHPB (**10**) with  $(\text{Ar})_2\text{CH}^+$  in  $\text{CH}_2\text{Cl}_2$  at 20 °C.

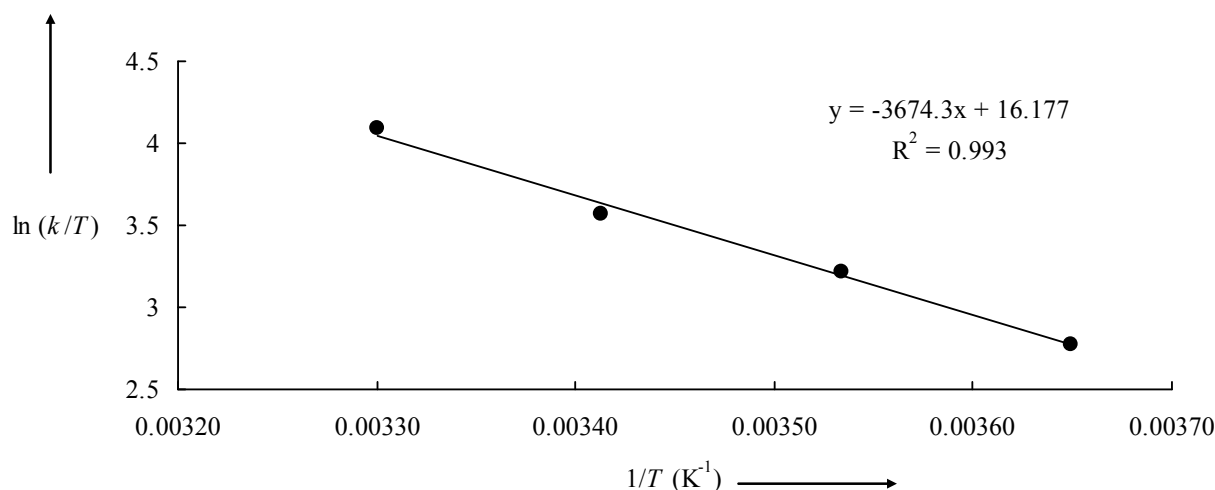
$[(\text{dma})_2\text{CH}^+]$ (mol L <sup>-1</sup> )	[DHPB] (mol L <sup>-1</sup> )	$k_{\text{obs}}$ (s <sup>-1</sup> )	$\lambda = 613 \text{ nm}$	$k$ (M <sup>-1</sup> s <sup>-1</sup> )
$7.00 \times 10^{-6}$	$3.34 \times 10^{-5}$	7.22		$2.29 \times 10^5$
	$5.01 \times 10^{-5}$	11.2		
	$6.67 \times 10^{-5}$	15.2		
	$1.00 \times 10^{-4}$	22.4		
	$1.33 \times 10^{-4}$	30.2		
$[(\text{pyr})_2\text{CH}^+]$ (mol L <sup>-1</sup> )	[DHPB] (mol L <sup>-1</sup> )	$k_{\text{obs}}$ (s <sup>-1</sup> )	$\lambda = 620 \text{ nm}$	$k$ (M <sup>-1</sup> s <sup>-1</sup> )
$7.01 \times 10^{-6}$	$6.67 \times 10^{-5}$	5.81		$7.49 \times 10^4$
	$1.00 \times 10^{-4}$	8.39		
	$1.33 \times 10^{-4}$	10.9		
	$1.67 \times 10^{-4}$	13.4		
	$2.00 \times 10^{-4}$	15.8		
$[(\text{thq})_2\text{CH}^+]$ (mol L <sup>-1</sup> )	[DHPB] (mol L <sup>-1</sup> )	$k_{\text{obs}}$ (s <sup>-1</sup> )	$\lambda = 628 \text{ nm}$	$k$ (M <sup>-1</sup> s <sup>-1</sup> )
$6.25 \times 10^{-6}$	$4.47 \times 10^{-5}$	1.83		$2.07 \times 10^4$
	$8.94 \times 10^{-5}$	2.73		
	$1.34 \times 10^{-4}$	3.66		
	$1.79 \times 10^{-4}$	4.61		
	$2.23 \times 10^{-4}$	5.51		

**Table 10a:** Kinetics of the Reactions of DHPB (**10**) with  $(\text{ind})_2\text{CH}^+$  in  $\text{CH}_2\text{Cl}_2$  at different temperature

$T$ ( $^{\circ}\text{C}$ )	$[(\text{ind})_2\text{CH}^+]$ ( $\text{mol L}^{-1}$ )	$[\text{DHPB}]$ ( $\text{mol L}^{-1}$ )	$k_{\text{obs}}$ ( $\text{s}^{-1}$ )	$\lambda = 625 \text{ nm}$	$k$ ( $\text{M}^{-1} \text{ s}^{-1}$ )
1.0	$1.56 \times 10^{-5}$	$2.55 \times 10^{-4}$	1.11		$4.40 \times 10^3$
		$3.83 \times 10^{-4}$	1.67		
		$5.11 \times 10^{-4}$	2.23		
		$6.39 \times 10^{-4}$	2.82		
		$7.66 \times 10^{-4}$	3.35		
10.0	$1.56 \times 10^{-5}$	$2.55 \times 10^{-4}$	1.87		$7.03 \times 10^3$
		$3.83 \times 10^{-4}$	2.72		
		$5.11 \times 10^{-4}$	3.61		
		$6.39 \times 10^{-4}$	4.54		
		$7.66 \times 10^{-4}$	5.45		
20.0	$6.59 \times 10^{-6}$	$4.47 \times 10^{-5}$	1.05		$1.04 \times 10^4$
		$8.94 \times 10^{-5}$	1.51		
		$1.34 \times 10^{-4}$	1.98		
		$1.79 \times 10^{-4}$	2.45		
		$2.23 \times 10^{-4}$	2.90		

Table 10a continued

$T$ (°C)	$[(\text{ind})_2\text{CH}^+]$ (mol L <sup>-1</sup> )	[DHPB] (mol L <sup>-1</sup> )	$k_{\text{obs}}$ (s <sup>-1</sup> )	$\lambda = 625 \text{ nm}$	$k$ (M <sup>-1</sup> s <sup>-1</sup> )
30.0	$1.56 \times 10^{-5}$	$3.44 \times 10^{-4}$	7.43		$1.81 \times 10^4$
		$6.87 \times 10^{-4}$	13.8		
		$1.03 \times 10^{-3}$	20.4		
		$1.37 \times 10^{-3}$	26.2		
		$1.72 \times 10^{-3}$	32.4		

Eyring Plot for the reaction of DHPB (**10**) with  $(\text{ind})_2\text{CHBF}_4$ 

Eyring-parameters:

$$\Delta H^\ddagger = (30.6 \pm 1.8) \text{ kJ mol}^{-1}$$

$$\Delta S^\ddagger = (-63.0 \pm 6.3) \text{ J mol}^{-1} \text{ K}^{-1}$$

Coefficient of correlation: 0.9930

Arrhenius-parameter:

$$E_A = (33.0 \pm 1.8) \text{ kJ mol}^{-1}$$

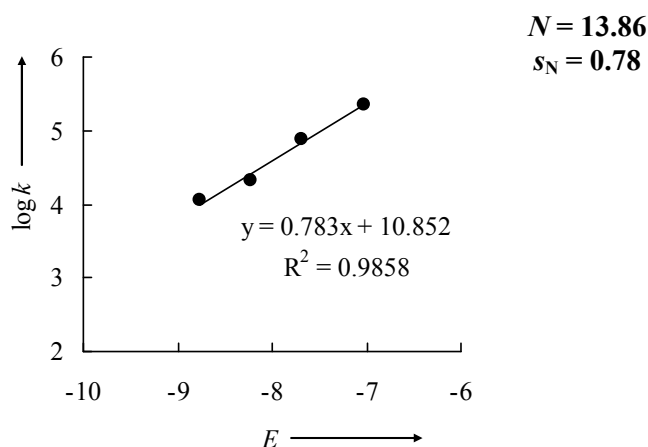
$$\ln A = 22.8 \pm 0.8$$

Coefficient of correlation: 0.9939

$$k(20 \text{ }^\circ\text{C}) = 1.11 \times 10^4 \text{ M}^{-1} \text{ s}^{-1}$$

Reactivity parameters for DHPB (**10**) in CH<sub>2</sub>Cl<sub>2</sub>

Ar <sub>2</sub> CH <sup>+</sup>	<i>E</i>	<i>k</i> (M <sup>-1</sup> s <sup>-1</sup> )
(dma) <sub>2</sub> CH <sup>+</sup>	-7.02	2.29 × 10 <sup>4</sup>
(pyr) <sub>2</sub> CH <sup>+</sup>	-7.69	7.49 × 10 <sup>4</sup>
(thq) <sub>2</sub> CH <sup>+</sup>	-8.22	2.07 × 10 <sup>4</sup>
(ind) <sub>2</sub> CH <sup>+</sup>	-8.76	1.11 × 10 <sup>4</sup>



#### 4.4 Equilibrium constants (*K*) for the reactions of benzhydrylium ions (Ar<sub>2</sub>CH<sup>+</sup>) with isothioureas in CH<sub>2</sub>Cl<sub>2</sub>.

Equilibrium constants were measured by UV-vis spectroscopy in CH<sub>2</sub>Cl<sub>2</sub> as follows: To a solution of the benzhydrylium tetrafluoroborates in dichloromethane small volumes of stock solutions of isothioureas were added and the resulting absorptions of the benzhydrylium ions were monitored. When the absorbance was constant, another portion of the stock solution was added. This procedure was repeated two to eight times for each benzhydrylium salt solution.

In some cases where initially generated adducts underwent slow subsequent reactions, the equilibrium constants were determined by UV-vis spectroscopy using a stopped-flow instrument in CH<sub>2</sub>Cl<sub>2</sub>. In these cases different concentrations of nucleophiles were mixed with solutions of the electrophiles. The end absorbances were obtained by least-squares fitting of the exponential absorbance decay to the mono-exponential function  $A_t = A_0 \exp(-k_{\text{obs}}t) + C$ , i.e.  $A = C$ .

Assuming a proportionality between the absorbances and the concentrations of the benzhydrylium ions, the equilibrium constants (*K*) can be expressed by the absorbances of the benzhydrylium ions before (*A*<sub>0</sub>) and after (*A*) the addition of isothioureas using equation (2) and (3).

The temperature of the solutions during all equilibrium studies was kept constant at (20.0 ± 0.1) °C using a circulating bath thermostat.

**Table 11.** Determination of the equilibrium constant for the reaction of  $(\text{thq})_2\text{CH}^+$  with **7**.  
 $\varepsilon[(\text{thq})_2\text{CH}^+$  at 628 nm] =  $1.78 \times 10^5 \text{ M}^{-1} \text{ cm}^{-1}$  and  $d = 0.5 \text{ cm}$ .  
 DCM at 20.0 °C.

Entry	$[\mathbf{7}]_0$ (mol L <sup>-1</sup> )	$A$	$[(\text{thq})_2\text{CH}^+]_{\text{eq}}$ (mol L <sup>-1</sup> )	$K$ (L mol <sup>-1</sup> )
0	0	0.668	$7.512 \times 10^{-6}$	
1	$3.177 \times 10^{-5}$	0.403	$4.534 \times 10^{-6}$	$2.27 \times 10^4$
2	$6.340 \times 10^{-5}$	0.281	$3.164 \times 10^{-6}$	$2.31 \times 10^4$
3	$9.488 \times 10^{-5}$	0.173	$1.946 \times 10^{-6}$	$3.17 \times 10^4$
4	$1.262 \times 10^{-4}$	0.144	$1.621 \times 10^{-6}$	$2.98 \times 10^4$
5	$1.574 \times 10^{-4}$	0.124	$1.393 \times 10^{-6}$	$2.86 \times 10^4$
0	0	0.676	$7.608 \times 10^{-6}$	
1	$3.200 \times 10^{-5}$	0.398	$4.480 \times 10^{-6}$	$2.40 \times 10^4$
2	$6.385 \times 10^{-5}$	0.277	$3.118 \times 10^{-6}$	$2.41 \times 10^4$
3	$9.555 \times 10^{-5}$	0.212	$2.381 \times 10^{-6}$	$2.40 \times 10^4$
4	$1.271 \times 10^{-4}$	0.170	$1.914 \times 10^{-6}$	$2.42 \times 10^4$
5	$1.585 \times 10^{-4}$	0.142	$1.597 \times 10^{-6}$	$2.43 \times 10^4$
6	$1.898 \times 10^{-4}$	0.122	$1.373 \times 10^{-6}$	$2.43 \times 10^4$
0	0	0.679	$7.632 \times 10^{-6}$	
1	$3.200 \times 10^{-5}$	0.394	$4.431 \times 10^{-6}$	$2.57 \times 10^4$
2	$6.385 \times 10^{-5}$	0.271	$3.052 \times 10^{-6}$	$2.56 \times 10^4$
3	$9.555 \times 10^{-5}$	0.205	$2.307 \times 10^{-6}$	$2.58 \times 10^4$
4	$1.271 \times 10^{-4}$	0.166	$1.863 \times 10^{-6}$	$2.56 \times 10^4$
5	$1.585 \times 10^{-4}$	0.140	$1.570 \times 10^{-6}$	$2.53 \times 10^4$
6	$1.898 \times 10^{-4}$	0.119	$1.337 \times 10^{-6}$	$2.56 \times 10^4$

$$K_{\text{av}}(20 \text{ °C}) = 2.56 \times 10^4 \text{ L mol}^{-1}$$

**Table 12.** Determination of the equilibrium constant for the reaction of  $(\text{ind})_2\text{CH}^+$  with **7**.  
 $\varepsilon[(\text{ind})_2\text{CH}^+$  at 628 nm] =  $1.32 \times 10^5 \text{ M}^{-1} \text{ cm}^{-1}$  and  $d = 0.5 \text{ cm}$ .  
 DCM at 1.0 °C.

Entry	$[\mathbf{7}]_0$ (mol L <sup>-1</sup> )	$A$	$[(\text{ind})_2\text{CH}^+]_{\text{eq}}$ (mol L <sup>-1</sup> )	$K$ (L mol <sup>-1</sup> )
0	0	1.098	$1.666 \times 10^{-5}$	
1	$2.627 \times 10^{-5}$	0.451	$6.835 \times 10^{-6}$	$8.71 \times 10^4$
2	$5.247 \times 10^{-5}$	0.259	$3.933 \times 10^{-6}$	$8.11 \times 10^4$
3	$7.861 \times 10^{-5}$	0.175	$2.648 \times 10^{-6}$	$8.15 \times 10^4$
4	$1.047 \times 10^{-4}$	0.131	$1.994 \times 10^{-6}$	$8.12 \times 10^4$
5	$1.307 \times 10^{-4}$	0.105	$1.587 \times 10^{-6}$	$8.15 \times 10^4$
0	0	1.187	$1.801 \times 10^{-5}$	
1	$2.627 \times 10^{-5}$	0.499	$7.574 \times 10^{-6}$	$8.67 \times 10^4$
2	$5.247 \times 10^{-5}$	0.277	$4.197 \times 10^{-6}$	$8.48 \times 10^4$
3	$7.861 \times 10^{-5}$	0.185	$2.814 \times 10^{-6}$	$8.47 \times 10^4$
4	$1.047 \times 10^{-4}$	0.140	$2.121 \times 10^{-6}$	$8.38 \times 10^4$

$$K_{\text{av}}(1 \text{ °C}) = 8.36 \times 10^4 \text{ L mol}^{-1}$$

DCM at 10.0 °C.

Entry	$[7]_0$ (mol L <sup>-1</sup> )	$A$	$[(\text{ind})_2\text{CH}^+]_{\text{eq}}$ (mol L <sup>-1</sup> )	$K$ (L mol <sup>-1</sup> )
0	0	1.911	$2.899 \times 10^{-5}$	
1	$2.624 \times 10^{-5}$	1.187	$1.801 \times 10^{-5}$	$3.97 \times 10^4$
2	$5.241 \times 10^{-5}$	0.783	$1.189 \times 10^{-5}$	$4.05 \times 10^4$
3	$7.852 \times 10^{-5}$	0.565	$8.571 \times 10^{-6}$	$4.07 \times 10^4$
4	$1.046 \times 10^{-4}$	0.435	$6.599 \times 10^{-6}$	$4.10 \times 10^4$
5	$1.306 \times 10^{-4}$	0.354	$5.367 \times 10^{-6}$	$4.08 \times 10^4$
6	$1.565 \times 10^{-4}$	0.297	$4.511 \times 10^{-6}$	$4.07 \times 10^4$
0	0	1.127	$1.710 \times 10^{-5}$	
1	$2.636 \times 10^{-5}$	0.652	$9.896 \times 10^{-6}$	$3.78 \times 10^4$
2	$5.267 \times 10^{-5}$	0.428	$6.492 \times 10^{-6}$	$3.87 \times 10^4$
3	$7.890 \times 10^{-5}$	0.311	$4.723 \times 10^{-6}$	$3.92 \times 10^4$
4	$1.051 \times 10^{-4}$	0.243	$3.686 \times 10^{-6}$	$3.94 \times 10^4$
5	$1.312 \times 10^{-4}$	0.200	$3.034 \times 10^{-6}$	$3.93 \times 10^4$
6	$1.572 \times 10^{-4}$	0.169	$2.570 \times 10^{-6}$	$3.93 \times 10^4$

$$K_{\text{av}}(10\text{ °C}) = 3.98 \times 10^4 \text{ L mol}^{-1}$$

DCM at 20.0 °C.

Entry	$[7]_0$ (mol L <sup>-1</sup> )	$A$	$[(\text{ind})_2\text{CH}^+]_{\text{eq}}$ (mol L <sup>-1</sup> )	$K$ (L mol <sup>-1</sup> )
0	0	0.925	$1.404 \times 10^{-5}$	
1	$4.915 \times 10^{-5}$	0.489	$7.414 \times 10^{-6}$	$2.08 \times 10^4$
2	$9.794 \times 10^{-5}$	0.322	$4.888 \times 10^{-6}$	$2.08 \times 10^4$
3	$1.464 \times 10^{-4}$	0.239	$3.625 \times 10^{-6}$	$2.08 \times 10^4$
4	$1.945 \times 10^{-4}$	0.189	$2.874 \times 10^{-6}$	$2.08 \times 10^4$
5	$2.423 \times 10^{-4}$	0.157	$2.376 \times 10^{-6}$	$2.08 \times 10^4$
0	0	0.917	$1.391 \times 10^{-5}$	
1	$4.950 \times 10^{-5}$	0.484	$7.346 \times 10^{-6}$	$2.06 \times 10^4$
2	$9.865 \times 10^{-5}$	0.317	$4.804 \times 10^{-6}$	$2.09 \times 10^4$
3	$1.474 \times 10^{-4}$	0.235	$3.571 \times 10^{-6}$	$2.08 \times 10^4$
4	$1.959 \times 10^{-4}$	0.187	$2.830 \times 10^{-6}$	$2.08 \times 10^4$
5	$2.440 \times 10^{-4}$	0.154	$2.344 \times 10^{-6}$	$2.08 \times 10^4$
0	0	0.888	$1.348 \times 10^{-5}$	
1	$4.794 \times 10^{-5}$	0.478	$7.259 \times 10^{-6}$	$2.03 \times 10^4$
2	$9.555 \times 10^{-5}$	0.317	$4.802 \times 10^{-6}$	$2.05 \times 10^4$
3	$1.428 \times 10^{-4}$	0.234	$3.549 \times 10^{-6}$	$2.07 \times 10^4$
4	$1.898 \times 10^{-4}$	0.194	$2.938 \times 10^{-6}$	$1.96 \times 10^4$
5	$2.364 \times 10^{-4}$	0.159	$2.409 \times 10^{-6}$	$1.99 \times 10^4$

$$K_{\text{av}}(20\text{ °C}) = 2.06 \times 10^4 \text{ L mol}^{-1}$$

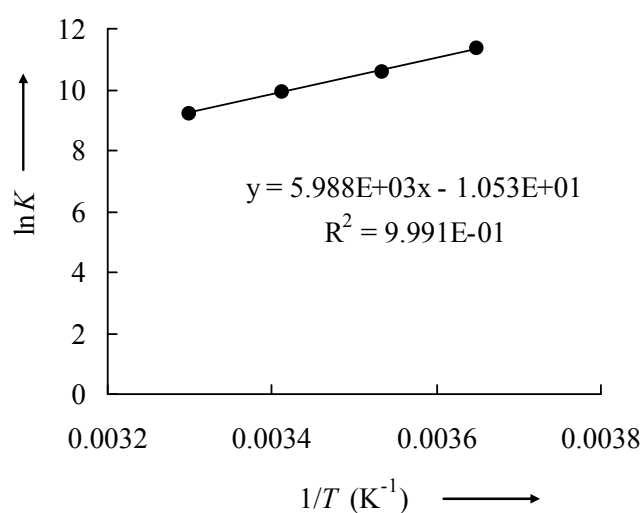
DCM at 30.0 °C.

Entry	[7] <sub>0</sub> (mol L <sup>-1</sup> )	A	[(ind) <sub>2</sub> CH <sup>+</sup> ] <sub>eq</sub> (mol L <sup>-1</sup> )	K (L mol <sup>-1</sup> )
0	0	1.047	1.588 × 10 <sup>-5</sup>	
1	2.598 × 10 <sup>-5</sup>	0.847	1.284 × 10 <sup>-5</sup>	1.02 × 10 <sup>4</sup>
2	5.190 × 10 <sup>-5</sup>	0.706	1.071 × 10 <sup>-5</sup>	1.02 × 10 <sup>4</sup>
3	7.776 × 10 <sup>-5</sup>	0.599	9.087 × 10 <sup>-6</sup>	1.04 × 10 <sup>4</sup>
4	1.036 × 10 <sup>-4</sup>	0.520	7.894 × 10 <sup>-6</sup>	1.05 × 10 <sup>4</sup>
5	1.293 × 10 <sup>-4</sup>	0.461	6.990 × 10 <sup>-6</sup>	1.04 × 10 <sup>4</sup>
6	1.550 × 10 <sup>-4</sup>	0.412	6.256 × 10 <sup>-6</sup>	1.04 × 10 <sup>4</sup>
0	0	1.040	1.578 × 10 <sup>-5</sup>	
1	5.209 × 10 <sup>-5</sup>	0.717	1.087 × 10 <sup>-5</sup>	9.49 × 10 <sup>3</sup>
2	1.039 × 10 <sup>-4</sup>	0.532	8.070 × 10 <sup>-6</sup>	9.83 × 10 <sup>3</sup>
3	1.555 × 10 <sup>-4</sup>	0.421	6.385 × 10 <sup>-6</sup>	9.94 × 10 <sup>3</sup>
4	2.069 × 10 <sup>-4</sup>	0.345	5.239 × 10 <sup>-6</sup>	1.01 × 10 <sup>4</sup>
5	2.580 × 10 <sup>-4</sup>	0.293	4.450 × 10 <sup>-6</sup>	1.01 × 10 <sup>4</sup>
6	3.088 × 10 <sup>-4</sup>	0.254	3.853 × 10 <sup>-6</sup>	1.02 × 10 <sup>4</sup>
0	0	1.055	1.600 × 10 <sup>-5</sup>	
1	5.228 × 10 <sup>-5</sup>	0.719	1.090 × 10 <sup>-5</sup>	9.48 × 10 <sup>3</sup>
2	1.043 × 10 <sup>-4</sup>	0.529	8.024 × 10 <sup>-6</sup>	9.99 × 10 <sup>3</sup>
3	1.561 × 10 <sup>-4</sup>	0.417	6.330 × 10 <sup>-6</sup>	1.01 × 10 <sup>4</sup>
4	2.076 × 10 <sup>-4</sup>	0.342	5.194 × 10 <sup>-6</sup>	1.02 × 10 <sup>4</sup>
5	2.589 × 10 <sup>-4</sup>	0.290	4.402 × 10 <sup>-6</sup>	1.03 × 10 <sup>4</sup>
6	3.100 × 10 <sup>-4</sup>	0.250	3.799 × 10 <sup>-6</sup>	1.04 × 10 <sup>4</sup>

$$K_{av}(30\text{ °C}) = 1.01 \times 10^4 \text{ L mol}^{-1}$$

**Table 13.** van't Hoff plot for the reaction of (ind)<sub>2</sub>CH<sup>+</sup> with 7 in DCM.

T (°C)	K (L mol <sup>-1</sup> )
1.0	8.36 × 10 <sup>4</sup>
10.0	3.98 × 10 <sup>4</sup>
20.0	2.06 × 10 <sup>4</sup>
30.0	1.01 × 10 <sup>4</sup>



$$\Delta H^\circ = -49.8 \text{ kJ mol}^{-1}$$

$$\Delta S^\circ = -87.7 \text{ J mol}^{-1} \text{ K}^{-1}$$

$$K(20\text{ °C}) = 2.00 \times 10^4 \text{ L mol}^{-1}$$

**Table 14.** Determination of the equilibrium constant for the reaction of  $(\text{ind})_2\text{CH}^+$  with THTP (9).

$\varepsilon[(\text{ind})_2\text{CH}^+ \text{ at } 625 \text{ nm}] = 1.318 \times 10^5 \text{ M}^{-1} \text{ cm}^{-1}$  and  $d = 0.5 \text{ cm}$   
DCM at  $10.0 \text{ }^\circ\text{C}$ .

Entry	[THTP] <sub>0</sub> (mol L <sup>-1</sup> )	A	[(ind) <sub>2</sub> CH <sup>+</sup> ] <sub>eq</sub> (mol L <sup>-1</sup> )	K (L mol <sup>-1</sup> )
0	0	1.195	$1.813 \times 10^{-5}$	
1	$1.874 \times 10^{-5}$	0.100	$1.511 \times 10^{-6}$	$5.11 \times 10^6$
0	0	1.218	$1.847 \times 10^{-5}$	
1	$2.516 \times 10^{-5}$	0.036	$5.401 \times 10^{-7}$	$4.68 \times 10^6$
0	0	1.203	$1.825 \times 10^{-5}$	
1	$2.516 \times 10^{-5}$	0.034	$5.120 \times 10^{-7}$	$4.75 \times 10^6$
0	0	1.217	$1.847 \times 10^{-5}$	
1	$2.489 \times 10^{-5}$	0.036	$5.417 \times 10^{-7}$	$4.66 \times 10^6$
0	0	1.125	$1.707 \times 10^{-5}$	
1	$1.881 \times 10^{-5}$	0.081	$1.233 \times 10^{-6}$	$4.38 \times 10^6$

$$K_{\text{av}}(10 \text{ }^\circ\text{C}) = 4.72 \times 10^6 \text{ L mol}^{-1}$$

DCM at  $20.0 \text{ }^\circ\text{C}$ .

Entry	[THTP] <sub>0</sub> (mol L <sup>-1</sup> )	A	[(ind) <sub>2</sub> CH <sup>+</sup> ] <sub>eq</sub> (mol L <sup>-1</sup> )	K (L mol <sup>-1</sup> )
0	0	1.064	$1.613 \times 10^{-5}$	
1	$1.891 \times 10^{-5}$	0.182	$2.760 \times 10^{-6}$	$8.73 \times 10^5$
2	$3.781 \times 10^{-5}$	0.030	$4.572 \times 10^{-7}$	$1.55 \times 10^6$
3	$5.669 \times 10^{-5}$	0.016	$2.466 \times 10^{-7}$	$1.58 \times 10^6$
0	0	1.060	$1.607 \times 10^{-5}$	
1	$1.891 \times 10^{-5}$	0.156	$2.360 \times 10^{-6}$	$1.12 \times 10^6$
2	$3.781 \times 10^{-5}$	0.029	$4.444 \times 10^{-7}$	$1.58 \times 10^6$
3	$5.669 \times 10^{-5}$	0.015	$2.341 \times 10^{-7}$	$1.65 \times 10^6$
0	0	1.063	$1.613 \times 10^{-5}$	
1	$1.891 \times 10^{-5}$	0.116	$1.755 \times 10^{-6}$	$1.80 \times 10^6$
2	$3.781 \times 10^{-5}$	0.021	$3.169 \times 10^{-7}$	$2.26 \times 10^6$
3	$5.669 \times 10^{-5}$	0.012	$1.748 \times 10^{-7}$	$2.23 \times 10^6$
0	0	1.061	$1.610 \times 10^{-5}$	
1	$1.891 \times 10^{-5}$	0.094	$1.431 \times 10^{-6}$	$2.43 \times 10^6$
2	$3.781 \times 10^{-5}$	0.021	$3.114 \times 10^{-7}$	$2.30 \times 10^6$
3	$5.669 \times 10^{-5}$	0.012	$1.801 \times 10^{-7}$	$2.17 \times 10^6$
0	0	1.099	$1.667 \times 10^{-5}$	
1	$1.328 \times 10^{-5}$	0.266	$4.029 \times 10^{-6}$	$2.97 \times 10^6$
2	$2.652 \times 10^{-5}$	0.041	$6.251 \times 10^{-7}$	$2.30 \times 10^6$
3	$3.973 \times 10^{-5}$	0.020	$3.080 \times 10^{-7}$	$2.17 \times 10^6$

$$K_{\text{av}}(20 \text{ }^\circ\text{C}) = 1.95 \times 10^6 \text{ L mol}^{-1}$$

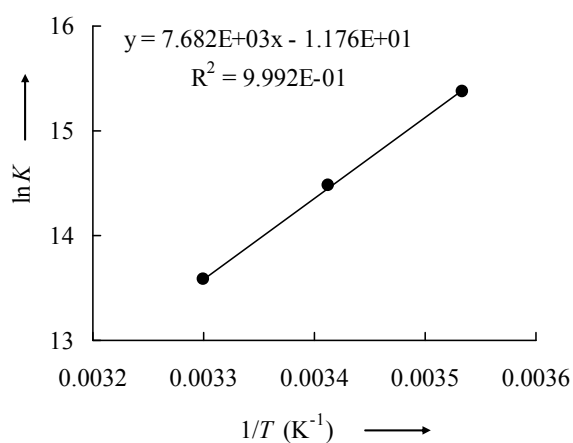
DCM at 30.0 °C.

Entry	[THTP] <sub>0</sub> (mol L <sup>-1</sup> )	A	[(ind) <sub>2</sub> CH <sup>+</sup> ] <sub>eq</sub> (mol L <sup>-1</sup> )	K (L mol <sup>-1</sup> )
0	0	1.270	1.927 × 10 <sup>-5</sup>	
1	1.874 × 10 <sup>-5</sup>	0.315	4.782 × 10 <sup>-6</sup>	7.06 × 10 <sup>5</sup>
2	3.743 × 10 <sup>-5</sup>	0.075	1.143 × 10 <sup>-6</sup>	8.16 × 10 <sup>5</sup>
3	5.607 × 10 <sup>-5</sup>	0.039	5.965 × 10 <sup>-7</sup>	8.31 × 10 <sup>5</sup>
0	0	1.290	1.958 × 10 <sup>-5</sup>	
1	2.498 × 10 <sup>-5</sup>	0.181	2.752 × 10 <sup>-6</sup>	7.45 × 10 <sup>5</sup>
2	4.986 × 10 <sup>-5</sup>	0.049	7.372 × 10 <sup>-7</sup>	8.19 × 10 <sup>5</sup>
0	0	1.261	1.913 × 10 <sup>-5</sup>	
1	2.489 × 10 <sup>-5</sup>	0.170	2.577 × 10 <sup>-6</sup>	7.56 × 10 <sup>5</sup>
2	4.968 × 10 <sup>-5</sup>	0.046	7.033 × 10 <sup>-7</sup>	8.28 × 10 <sup>5</sup>

$$K_{av}(30\text{ °C}) = 7.86 \times 10^5 \text{ L mol}^{-1}$$

**Table 15.**van't Hoff plot for the reaction of (ind)<sub>2</sub>CH<sup>+</sup> with THTP (9) in DCM.

T (°C)	K (L mol <sup>-1</sup> )
10.0	4.72 × 10 <sup>6</sup>
20.0	1.95 × 10 <sup>6</sup>
30.0	7.86 × 10 <sup>5</sup>



$$\Delta H^\circ = -63.9 \text{ kJ mol}^{-1}$$

$$\Delta S^\circ = -97.9 \text{ J mol}^{-1} \text{ K}^{-1}$$

$$K(20\text{ °C}) = 1.90 \times 10^6 \text{ L mol}^{-1}$$

**Table 16.** Determination of the equilibrium constant for the reaction of (jul)<sub>2</sub>CH<sup>+</sup> with THTP (9).

$\varepsilon[(\text{jul})_2\text{CH}^+ \text{ at } 642 \text{ nm}] = 2.24 \times 10^5 \text{ M}^{-1} \text{ cm}^{-1}$  and  $d = 0.5 \text{ cm}$   
DCM at 20.0 °C.

Entry	[THTP] <sub>0</sub> (mol L <sup>-1</sup> )	<i>A</i>	[(jul) <sub>2</sub> CH <sup>+</sup> ] <sub>eq</sub> (mol L <sup>-1</sup> )	<i>K</i> (L mol <sup>-1</sup> )
0	0	0.794	$7.095 \times 10^{-6}$	
1	$5.645 \times 10^{-5}$	0.194	$1.735 \times 10^{-6}$	$6.04 \times 10^4$
2	$1.128 \times 10^{-4}$	0.101	$9.063 \times 10^{-7}$	$6.39 \times 10^4$
3	$1.689 \times 10^{-4}$	0.071	$6.326 \times 10^{-7}$	$6.26 \times 10^4$
4	$2.250 \times 10^{-4}$	0.053	$4.746 \times 10^{-7}$	$6.35 \times 10^4$
5	$2.809 \times 10^{-4}$	0.043	$3.861 \times 10^{-7}$	$6.30 \times 10^4$
0	0	1.161	$1.037 \times 10^{-5}$	
1	$5.477 \times 10^{-5}$	0.300	$2.684 \times 10^{-6}$	$6.07 \times 10^4$
2	$1.094 \times 10^{-4}$	0.164	$1.462 \times 10^{-6}$	$6.05 \times 10^4$
3	$1.639 \times 10^{-4}$	0.112	$1.003 \times 10^{-6}$	$6.02 \times 10^4$
4	$2.183 \times 10^{-4}$	0.084	$7.517 \times 10^{-7}$	$6.10 \times 10^4$
5	$2.726 \times 10^{-4}$	0.068	$6.056 \times 10^{-7}$	$6.10 \times 10^4$
6	$3.267 \times 10^{-4}$	0.057	$5.070 \times 10^{-7}$	$6.10 \times 10^4$
0	0	1.170	$1.045 \times 10^{-5}$	
1	$5.516 \times 10^{-5}$	0.303	$2.707 \times 10^{-6}$	$6.02 \times 10^4$
2	$1.102 \times 10^{-4}$	0.160	$1.429 \times 10^{-6}$	$6.22 \times 10^4$
3	$1.651 \times 10^{-4}$	0.111	$9.887 \times 10^{-7}$	$6.12 \times 10^4$
4	$2.199 \times 10^{-4}$	0.083	$7.445 \times 10^{-7}$	$6.17 \times 10^4$
5	$2.745 \times 10^{-4}$	0.067	$5.971 \times 10^{-7}$	$6.19 \times 10^4$
6	$3.290 \times 10^{-4}$	0.056	$5.034 \times 10^{-7}$	$6.14 \times 10^4$

$$K_{\text{av}}(20 \text{ }^\circ\text{C}) = 6.16 \times 10^4 \text{ L mol}^{-1}$$

**Table 17.** Determination of the equilibrium constant for the reaction of (lil)<sub>2</sub>CH<sup>+</sup> with THTP (9).

$\varepsilon[(\text{lil})_2\text{CH}^+ \text{ at } 639 \text{ nm}] = 1.58 \times 10^5 \text{ M}^{-1} \text{ cm}^{-1}$  and  $d = 0.5 \text{ cm}$   
DCM at 20.0 °C.

Entry	[THTP] <sub>0</sub> (mol L <sup>-1</sup> )	<i>A</i>	[(lil) <sub>2</sub> CH <sup>+</sup> ] <sub>eq</sub> (mol L <sup>-1</sup> )	<i>K</i> (L mol <sup>-1</sup> )
0	0	0.517	$6.519 \times 10^{-6}$	
1	$5.758 \times 10^{-5}$	0.123	$1.550 \times 10^{-6}$	$6.08 \times 10^4$
2	$1.150 \times 10^{-4}$	0.067	$8.485 \times 10^{-7}$	$6.09 \times 10^4$
3	$1.723 \times 10^{-4}$	0.046	$5.789 \times 10^{-7}$	$6.14 \times 10^4$
4	$2.295 \times 10^{-4}$	0.035	$4.407 \times 10^{-7}$	$6.14 \times 10^4$
0	0	1.023	$1.292 \times 10^{-5}$	
1	$5.503 \times 10^{-5}$	0.263	$3.313 \times 10^{-6}$	$6.37 \times 10^4$
2	$1.099 \times 10^{-4}$	0.138	$1.746 \times 10^{-6}$	$6.46 \times 10^4$
3	$1.647 \times 10^{-4}$	0.093	$1.178 \times 10^{-6}$	$6.48 \times 10^4$
4	$2.193 \times 10^{-4}$	0.069	$8.760 \times 10^{-7}$	$6.59 \times 10^4$
5	$2.738 \times 10^{-4}$	0.055	$6.938 \times 10^{-7}$	$6.69 \times 10^4$
0	0	1.002	$1.265 \times 10^{-5}$	
1	$5.583 \times 10^{-5}$	0.268	$3.388 \times 10^{-6}$	$5.86 \times 10^4$
2	$1.115 \times 10^{-4}$	0.139	$1.753 \times 10^{-6}$	$6.15 \times 10^4$
3	$1.671 \times 10^{-4}$	0.094	$1.182 \times 10^{-6}$	$6.20 \times 10^4$
4	$2.225 \times 10^{-4}$	0.070	$8.846 \times 10^{-7}$	$6.27 \times 10^4$
5	$2.778 \times 10^{-4}$	0.056	$7.102 \times 10^{-7}$	$6.28 \times 10^4$
6	$3.330 \times 10^{-4}$	0.047	$5.912 \times 10^{-7}$	$6.30 \times 10^4$

$$K_{\text{av}}(20 \text{ }^\circ\text{C}) = 6.27 \times 10^4 \text{ L mol}^{-1}$$

**Table 18.** Determination of the equilibrium constant for the reaction of  $(\text{pyr})_2\text{CH}^+$  with DHPB (10).

$\varepsilon[(\text{pyr})_2\text{CH}^+ \text{ at } 620 \text{ nm}] = 1.74 \times 10^5 \text{ M}^{-1} \text{ cm}^{-1}$  and  $d = 0.5 \text{ cm}$   
DCM at 20.0 °C

Entry	[DHPB] <sub>0</sub> (mol L <sup>-1</sup> )	<i>A</i>	[(pyr) <sub>2</sub> CH <sup>+</sup> ] <sub>eq</sub> (mol L <sup>-1</sup> )	<i>K</i> (L mol <sup>-1</sup> )
0	0	0.664	$7.639 \times 10^{-6}$	
1	$1.265 \times 10^{-5}$	0.395	$4.548 \times 10^{-6}$	$7.08 \times 10^4$
2	$2.528 \times 10^{-5}$	0.256	$2.945 \times 10^{-6}$	$7.71 \times 10^4$
3	$3.787 \times 10^{-5}$	0.188	$2.164 \times 10^{-6}$	$7.76 \times 10^4$
4	$5.044 \times 10^{-5}$	0.148	$1.701 \times 10^{-6}$	$7.79 \times 10^4$
5	$6.297 \times 10^{-5}$	0.121	$1.391 \times 10^{-6}$	$7.85 \times 10^4$
0	0	0.674	$7.763 \times 10^{-6}$	
1	$1.545 \times 10^{-5}$	0.356	$4.098 \times 10^{-6}$	$7.56 \times 10^4$
2	$3.086 \times 10^{-5}$	0.228	$2.626 \times 10^{-6}$	$7.57 \times 10^4$
3	$4.624 \times 10^{-5}$	0.165	$1.903 \times 10^{-6}$	$7.58 \times 10^4$
4	$6.158 \times 10^{-5}$	0.130	$1.493 \times 10^{-6}$	$7.54 \times 10^4$
5	$7.688 \times 10^{-5}$	0.106	$1.225 \times 10^{-6}$	$7.53 \times 10^4$
6	$9.215 \times 10^{-5}$	0.090	$1.038 \times 10^{-6}$	$7.51 \times 10^4$
0	0	0.694	$7.991 \times 10^{-6}$	
1	$1.562 \times 10^{-5}$	0.362	$4.168 \times 10^{-6}$	$7.75 \times 10^4$
2	$3.121 \times 10^{-5}$	0.227	$2.608 \times 10^{-6}$	$7.96 \times 10^4$
3	$4.675 \times 10^{-5}$	0.163	$1.875 \times 10^{-6}$	$7.98 \times 10^4$
4	$6.226 \times 10^{-5}$	0.126	$1.445 \times 10^{-6}$	$8.08 \times 10^4$
5	$7.773 \times 10^{-5}$	0.103	$1.182 \times 10^{-6}$	$8.05 \times 10^4$
6	$9.316 \times 10^{-5}$	0.087	$9.964 \times 10^{-6}$	$8.07 \times 10^4$

$$K_{\text{av}}(20 \text{ °C}) = 7.73 \times 10^4 \text{ L mol}^{-1}$$

**Table 19.** Determination of the equilibrium constant for the reaction of  $(\text{thq})_2\text{CH}^+$  with DHPB (10).

$\varepsilon[(\text{thq})_2\text{CH}^+ \text{ at } 628 \text{ nm}] = 1.78 \times 10^5 \text{ M}^{-1} \text{ cm}^{-1}$  and  $d = 0.5 \text{ cm}$   
DCM at 20.0 °C.

Entry	[DHPB] <sub>0</sub> (mol L <sup>-1</sup> )	<i>A</i>	[(thq) <sub>2</sub> CH <sup>+</sup> ] <sub>eq</sub> (mol L <sup>-1</sup> )	<i>K</i> (L mol <sup>-1</sup> )
0	0	1.325	$1.490 \times 10^{-5}$	
1	$1.295 \times 10^{-5}$	1.063	$1.196 \times 10^{-5}$	$2.43 \times 10^4$
2	$2.586 \times 10^{-5}$	0.861	$9.678 \times 10^{-6}$	$2.59 \times 10^4$
3	$3.875 \times 10^{-5}$	0.717	$8.064 \times 10^{-6}$	$2.63 \times 10^4$
0	0	0.974	$1.095 \times 10^{-5}$	
1	$1.268 \times 10^{-5}$	0.747	$8.397 \times 10^{-6}$	$2.98 \times 10^4$
2	$2.534 \times 10^{-5}$	0.599	$6.742 \times 10^{-6}$	$2.93 \times 10^4$
3	$3.796 \times 10^{-5}$	0.498	$5.599 \times 10^{-6}$	$2.90 \times 10^4$
4	$5.056 \times 10^{-5}$	0.431	$4.844 \times 10^{-6}$	$2.81 \times 10^4$
5	$6.312 \times 10^{-5}$	0.373	$4.196 \times 10^{-6}$	$2.82 \times 10^4$
6	$8.817 \times 10^{-5}$	0.296	$3.332 \times 10^{-6}$	$2.80 \times 10^4$
0	0	0.900	$1.013 \times 10^{-5}$	
1	$1.172 \times 10^{-5}$	0.718	$8.078 \times 10^{-6}$	$2.60 \times 10^4$
2	$2.342 \times 10^{-5}$	0.579	$6.512 \times 10^{-6}$	$2.78 \times 10^4$
3	$3.509 \times 10^{-5}$	0.488	$5.484 \times 10^{-6}$	$2.76 \times 10^4$
4	$4.674 \times 10^{-5}$	0.419	$4.708 \times 10^{-6}$	$2.76 \times 10^4$
5	$5.836 \times 10^{-5}$	0.368	$4.138 \times 10^{-6}$	$2.73 \times 10^4$
6	$9.307 \times 10^{-5}$	0.267	$3.000 \times 10^{-6}$	$2.73 \times 10^4$

$$K_{\text{av}}(20 \text{ °C}) = 2.75 \times 10^4 \text{ L mol}^{-1}$$

**Table 20.** Determination of the equilibrium constant for the reaction of  $(\text{ind})_2\text{CH}^+$  with DHPB (**10**).

$\varepsilon[(\text{ind})_2\text{CH}^+ \text{ at } 625 \text{ nm}] = 1.32 \times 10^5 \text{ M}^{-1} \text{ cm}^{-1}$  and  $d = 0.5 \text{ cm}$   
DCM at  $1.0 \text{ }^\circ\text{C}$ .

Entry	[DHPB] <sub>0</sub> (mol L <sup>-1</sup> )	<i>A</i>	[(ind) <sub>2</sub> CH <sup>+</sup> ] <sub>eq</sub> (mol L <sup>-1</sup> )	<i>K</i> (L mol <sup>-1</sup> )
0	0	1.163	$1.764 \times 10^{-5}$	
1	$2.615 \times 10^{-5}$	0.484	$7.348 \times 10^{-6}$	$8.81 \times 10^4$
2	$5.223 \times 10^{-5}$	0.262	$3.978 \times 10^{-6}$	$8.87 \times 10^4$
3	$7.826 \times 10^{-5}$	0.178	$2.694 \times 10^{-6}$	$8.72 \times 10^4$
4	$1.042 \times 10^{-4}$	0.131	$1.995 \times 10^{-6}$	$8.80 \times 10^4$
5	$1.301 \times 10^{-4}$	0.103	$1.567 \times 10^{-6}$	$8.93 \times 10^4$
0	0	1.183	$1.794 \times 10^{-5}$	
1	$2.587 \times 10^{-5}$	0.504	$7.652 \times 10^{-6}$	$8.61 \times 10^4$
2	$5.167 \times 10^{-5}$	0.276	$4.190 \times 10^{-6}$	$8.62 \times 10^4$
3	$7.741 \times 10^{-5}$	0.187	$2.830 \times 10^{-6}$	$8.53 \times 10^4$
4	$1.031 \times 10^{-4}$	0.140	$2.126 \times 10^{-6}$	$8.47 \times 10^4$
5	$1.287 \times 10^{-4}$	0.112	$1.697 \times 10^{-6}$	$8.45 \times 10^4$
6	$1.543 \times 10^{-4}$	0.093	$1.416 \times 10^{-6}$	$8.40 \times 10^4$
0	0	1.162	$1.762 \times 10^{-5}$	
1	$1.536 \times 10^{-5}$	0.485	$7.355 \times 10^{-6}$	$9.47 \times 10^4$
2	$3.813 \times 10^{-5}$	0.271	$4.115 \times 10^{-6}$	$8.87 \times 10^4$
3	$6.275 \times 10^{-5}$	0.184	$2.787 \times 10^{-6}$	$8.70 \times 10^4$
4	$8.793 \times 10^{-5}$	0.137	$2.082 \times 10^{-6}$	$8.69 \times 10^4$
5	$1.133 \times 10^{-4}$	0.110	$1.665 \times 10^{-6}$	$8.64 \times 10^4$
6	$1.388 \times 10^{-4}$	0.092	$1.399 \times 10^{-6}$	$8.52 \times 10^4$

$$K_{\text{av}}(1 \text{ }^\circ\text{C}) = 8.33 \times 10^4 \text{ L mol}^{-1}$$

DCM at  $10.0 \text{ }^\circ\text{C}$ .

Entry	[DHPB] <sub>0</sub> (mol L <sup>-1</sup> )	<i>A</i>	[(ind) <sub>2</sub> CH <sup>+</sup> ] <sub>eq</sub> (mol L <sup>-1</sup> )	<i>K</i> (L mol <sup>-1</sup> )
0	0	1.183	$1.795 \times 10^{-5}$	
1	$2.596 \times 10^{-5}$	0.665	$1.009 \times 10^{-5}$	$4.29 \times 10^4$
2	$5.186 \times 10^{-5}$	0.426	$6.465 \times 10^{-6}$	$4.38 \times 10^4$
3	$7.769 \times 10^{-5}$	0.309	$4.689 \times 10^{-6}$	$4.37 \times 10^4$
4	$1.035 \times 10^{-4}$	0.242	$3.666 \times 10^{-6}$	$4.34 \times 10^4$
5	$1.292 \times 10^{-4}$	0.197	$2.985 \times 10^{-6}$	$4.36 \times 10^4$
6	$1.548 \times 10^{-4}$	0.166	$2.526 \times 10^{-6}$	$4.34 \times 10^4$
0	0	1.168	$1.772 \times 10^{-5}$	
1	$2.605 \times 10^{-5}$	0.661	$1.002 \times 10^{-5}$	$4.17 \times 10^4$
2	$5.204 \times 10^{-5}$	0.426	$6.464 \times 10^{-6}$	$4.25 \times 10^4$
3	$7.797 \times 10^{-5}$	0.309	$4.690 \times 10^{-6}$	$4.25 \times 10^4$
4	$1.038 \times 10^{-4}$	0.241	$3.658 \times 10^{-6}$	$4.25 \times 10^4$
5	$1.296 \times 10^{-4}$	0.197	$2.993 \times 10^{-6}$	$4.25 \times 10^4$
0	0	0.161	$2.450 \times 10^{-6}$	
1	$2.615 \times 10^{-5}$	0.648	$9.835 \times 10^{-6}$	$4.42 \times 10^4$
2	$5.223 \times 10^{-5}$	0.416	$6.313 \times 10^{-6}$	$4.44 \times 10^4$
3	$7.826 \times 10^{-5}$	0.305	$4.627 \times 10^{-6}$	$4.34 \times 10^4$
4	$1.042 \times 10^{-4}$	0.235	$3.565 \times 10^{-6}$	$4.40 \times 10^4$
5	$1.301 \times 10^{-4}$	0.193	$2.921 \times 10^{-6}$	$4.38 \times 10^4$

$$K_{\text{av}}(10 \text{ }^\circ\text{C}) = 4.33 \times 10^4 \text{ L mol}^{-1}$$

DCM at 20.0 °C.

Entry	[DHPB] <sub>0</sub> (mol L <sup>-1</sup> )	<i>A</i>	[(ind) <sub>2</sub> CH <sup>+</sup> ] <sub>eq</sub> (mol L <sup>-1</sup> )	<i>K</i> (L mol <sup>-1</sup> )
0	0	0.855	1.298 × 10 <sup>-5</sup>	
1	2.611 × 10 <sup>-5</sup>	0.594	9.016 × 10 <sup>-6</sup>	1.96 × 10 <sup>4</sup>
2	5.210 × 10 <sup>-5</sup>	0.448	6.801 × 10 <sup>-6</sup>	1.95 × 10 <sup>4</sup>
3	7.796 × 10 <sup>-5</sup>	0.355	5.380 × 10 <sup>-6</sup>	1.98 × 10 <sup>4</sup>
4	1.037 × 10 <sup>-4</sup>	0.293	4.446 × 10 <sup>-6</sup>	1.98 × 10 <sup>4</sup>
5	1.293 × 10 <sup>-4</sup>	0.250	3.796 × 10 <sup>-6</sup>	1.98 × 10 <sup>4</sup>
0	0	1.052	1.595 × 10 <sup>-5</sup>	
1	2.405 × 10 <sup>-5</sup>	0.759	1.152 × 10 <sup>-5</sup>	1.94 × 10 <sup>4</sup>
2	4.800 × 10 <sup>-5</sup>	0.581	8.815 × 10 <sup>-6</sup>	1.96 × 10 <sup>4</sup>
3	7.184 × 10 <sup>-5</sup>	0.468	7.094 × 10 <sup>-6</sup>	1.96 × 10 <sup>4</sup>
4	9.557 × 10 <sup>-5</sup>	0.390	5.915 × 10 <sup>-6</sup>	1.95 × 10 <sup>4</sup>
5	1.192 × 10 <sup>-4</sup>	0.340	5.156 × 10 <sup>-6</sup>	1.90 × 10 <sup>4</sup>
6	1.427 × 10 <sup>-4</sup>	0.293	4.451 × 10 <sup>-6</sup>	1.93 × 10 <sup>4</sup>
7	1.661 × 10 <sup>-4</sup>	0.260	3.946 × 10 <sup>-6</sup>	1.93 × 10 <sup>4</sup>

$$K_{av}(20\text{ °C}) = 1.95 \times 10^4 \text{ L mol}^{-1}$$

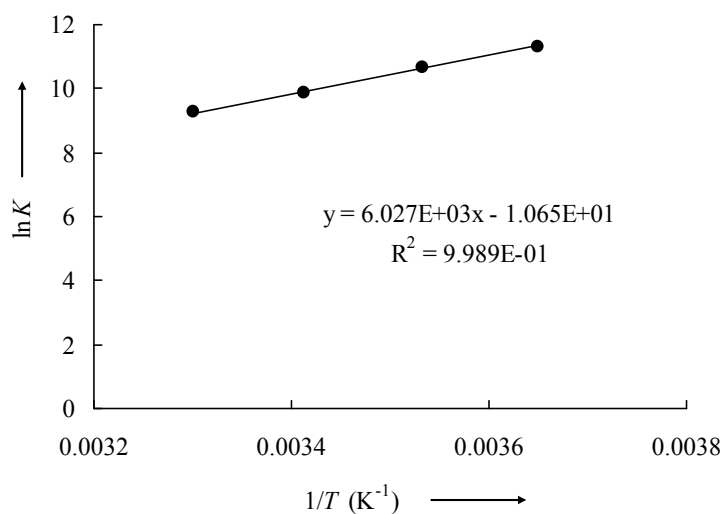
DCM at 30.0 °C.

Entry	[DHPB] <sub>0</sub> (mol L <sup>-1</sup> )	<i>A</i>	[(ind) <sub>2</sub> CH <sup>+</sup> ] <sub>eq</sub> (mol L <sup>-1</sup> )	<i>K</i> (L mol <sup>-1</sup> )
0	0	1.146	1.739 × 10 <sup>-5</sup>	
1	5.204 × 10 <sup>-5</sup>	0.771	1.170 × 10 <sup>-5</sup>	1.04 × 10 <sup>4</sup>
2	1.038 × 10 <sup>-4</sup>	0.568	8.612 × 10 <sup>-6</sup>	1.06 × 10 <sup>4</sup>
3	1.554 × 10 <sup>-4</sup>	0.448	6.803 × 10 <sup>-6</sup>	1.06 × 10 <sup>4</sup>
4	2.067 × 10 <sup>-4</sup>	0.368	5.584 × 10 <sup>-6</sup>	1.07 × 10 <sup>4</sup>
5	2.577 × 10 <sup>-4</sup>	0.315	4.779 × 10 <sup>-6</sup>	1.06 × 10 <sup>4</sup>
0	0	1.123	1.703 × 10 <sup>-5</sup>	
1	5.204 × 10 <sup>-5</sup>	0.750	1.137 × 10 <sup>-5</sup>	1.06 × 10 <sup>4</sup>
2	1.038 × 10 <sup>-4</sup>	0.555	8.420 × 10 <sup>-6</sup>	1.06 × 10 <sup>4</sup>
3	1.554 × 10 <sup>-4</sup>	0.438	6.645 × 10 <sup>-6</sup>	1.06 × 10 <sup>4</sup>
4	2.067 × 10 <sup>-4</sup>	0.361	5.480 × 10 <sup>-6</sup>	1.06 × 10 <sup>4</sup>
5	2.577 × 10 <sup>-4</sup>	0.307	4.659 × 10 <sup>-6</sup>	1.06 × 10 <sup>4</sup>
0	0	1.143	1.733 × 10 <sup>-5</sup>	
1	5.167 × 10 <sup>-5</sup>	0.769	1.167 × 10 <sup>-5</sup>	9.58 × 10 <sup>3</sup>
2	1.031 × 10 <sup>-4</sup>	0.567	8.596 × 10 <sup>-6</sup>	1.01 × 10 <sup>4</sup>
3	1.543 × 10 <sup>-4</sup>	0.448	6.791 × 10 <sup>-6</sup>	1.02 × 10 <sup>4</sup>
4	2.052 × 10 <sup>-4</sup>	0.370	5.606 × 10 <sup>-6</sup>	1.02 × 10 <sup>4</sup>
5	2.559 × 10 <sup>-4</sup>	0.314	4.769 × 10 <sup>-6</sup>	1.03 × 10 <sup>4</sup>
6	3.064 × 10 <sup>-4</sup>	0.272	4.127 × 10 <sup>-6</sup>	1.03 × 10 <sup>4</sup>
7	3.566 × 10 <sup>-4</sup>	0.240	3.646 × 10 <sup>-6</sup>	1.04 × 10 <sup>4</sup>

$$K_{av}(30\text{ °C}) = 1.04 \times 10^4 \text{ L mol}^{-1}$$

**Table 21.**van't Hoff plot for the reaction of  $(\text{ind})_2\text{CH}^+$  and DHPB (**10**) in DCM.

$T$ (°C)	$K$ (L mol <sup>-1</sup> )
1.0	$8.33 \times 10^4$
10.0	$4.33 \times 10^4$
20.0	$1.95 \times 10^4$
30.0	$1.04 \times 10^4$



$$\Delta H^\circ = -50.2 \text{ kJ mol}^{-1}$$

$$\Delta S^\circ = -88.7 \text{ J mol}^{-1} \text{ K}^{-1}$$

$$K(20 \text{ }^\circ\text{C}) = 2.02 \times 10^4 \text{ L mol}^{-1}$$

**Table 22.** Determination of the equilibrium constant for the reaction of  $(\text{ind})_2\text{CH}^+$  with **13**. $\varepsilon[(\text{ind})_2\text{CH}^+ \text{ at } 625 \text{ nm}] = 1.318 \times 10^5 \text{ M}^{-1} \text{ cm}^{-1}$  and  $d = 0.5 \text{ cm}$ .DCM at  $-10.0 \text{ }^\circ\text{C}$ .

Entry	$[\mathbf{13}]_0$ (mol L <sup>-1</sup> )	$A$	$[(\text{ind})_2\text{CH}^+]_{\text{eq}}$ (mol L <sup>-1</sup> )	$K$ (L mol <sup>-1</sup> )
0	0	0.483	$7.328 \times 10^{-6}$	
1	$5.222 \times 10^{-5}$	0.445	$6.751 \times 10^{-6}$	$1.60 \times 10^3$
2	$1.559 \times 10^{-4}$	0.379	$5.749 \times 10^{-6}$	$1.72 \times 10^3$
3	$2.586 \times 10^{-4}$	0.336	$5.096 \times 10^{-6}$	$1.64 \times 10^3$
4	$3.603 \times 10^{-4}$	0.298	$4.519 \times 10^{-6}$	$1.66 \times 10^3$
0	0	0.553	$8.392 \times 10^{-6}$	
1	$1.054 \times 10^{-4}$	0.475	$7.204 \times 10^{-6}$	$1.51 \times 10^3$
2	$2.099 \times 10^{-4}$	0.415	$6.293 \times 10^{-6}$	$1.53 \times 10^3$
3	$3.137 \times 10^{-4}$	0.368	$5.579 \times 10^{-6}$	$1.54 \times 10^3$
0	0	0.465	$7.057 \times 10^{-6}$	
1	$1.062 \times 10^{-4}$	0.389	$5.895 \times 10^{-6}$	$1.80 \times 10^3$
2	$2.116 \times 10^{-4}$	0.334	$5.066 \times 10^{-6}$	$1.79 \times 10^3$
3	$3.162 \times 10^{-4}$	0.293	$4.445 \times 10^{-6}$	$1.78 \times 10^3$
4	$4.199 \times 10^{-4}$	0.259	$3.933 \times 10^{-6}$	$1.81 \times 10^3$
5	$5.227 \times 10^{-4}$	0.234	$3.556 \times 10^{-6}$	$1.79 \times 10^3$

$$K_{\text{av}}(-10 \text{ }^\circ\text{C}) = 1.68 \times 10^3 \text{ L mol}^{-1}$$

DCM at  $-20.0\text{ }^{\circ}\text{C}$ .

Entry	$[\mathbf{13}]_0$ (mol L $^{-1}$ )	$A$	$[(\text{ind})_2\text{CH}^+]_{\text{eq}}$ (mol L $^{-1}$ )	$K$ (L mol $^{-1}$ )
0	0	0.494	$7.493 \times 10^{-6}$	
1	$1.120 \times 10^{-4}$	0.358	$5.428 \times 10^{-6}$	$3.40 \times 10^3$
2	$1.676 \times 10^{-4}$	0.313	$4.741 \times 10^{-6}$	$3.45 \times 10^3$
3	$2.229 \times 10^{-4}$	0.275	$4.166 \times 10^{-6}$	$3.56 \times 10^3$
0	0	0.542	$8.218 \times 10^{-6}$	
1	$1.034 \times 10^{-4}$	0.402	$6.105 \times 10^{-6}$	$3.35 \times 10^3$
2	$2.059 \times 10^{-4}$	0.321	$4.867 \times 10^{-6}$	$3.32 \times 10^3$
3	$3.074 \times 10^{-4}$	0.269	$4.076 \times 10^{-6}$	$3.26 \times 10^3$
0	0	0.524	$7.955 \times 10^{-6}$	
1	$1.034 \times 10^{-4}$	0.397	$6.028 \times 10^{-6}$	$3.09 \times 10^3$
2	$2.059 \times 10^{-4}$	0.317	$4.810 \times 10^{-6}$	$3.15 \times 10^3$
3	$3.074 \times 10^{-4}$	0.264	$4.002 \times 10^{-6}$	$3.16 \times 10^3$
4	$4.079 \times 10^{-4}$	0.230	$3.482 \times 10^{-6}$	$3.08 \times 10^3$
5	$5.075 \times 10^{-4}$	0.203	$3.079 \times 10^{-6}$	$3.03 \times 10^3$

$$K_{\text{av}}(-20\text{ }^{\circ}\text{C}) = 3.26 \times 10^3 \text{ L mol}^{-1}$$

DCM at  $-30.0\text{ }^{\circ}\text{C}$ .

Entry	$[\mathbf{13}]_0$ (mol L $^{-1}$ )	$A$	$[(\text{ind})_2\text{CH}^+]_{\text{eq}}$ (mol L $^{-1}$ )	$K$ (L mol $^{-1}$ )
0	0	0.523	$7.934 \times 10^{-6}$	
1	$5.715 \times 10^{-5}$	0.360	$5.468 \times 10^{-6}$	$8.18 \times 10^3$
0	0	0.489	$7.419 \times 10^{-6}$	
1	$8.439 \times 10^{-5}$	0.294	$4.462 \times 10^{-6}$	$8.06 \times 10^3$
0	0	0.507	$7.684 \times 10^{-6}$	
1	$1.132 \times 10^{-4}$	0.275	$4.178 \times 10^{-6}$	$7.57 \times 10^3$
0	0	0.510	$7.737 \times 10^{-6}$	
1	$1.623 \times 10^{-4}$	0.230	$3.489 \times 10^{-6}$	$7.41 \times 10^3$
0	0	0.498	$7.548 \times 10^{-6}$	
1	$2.168 \times 10^{-4}$	0.189	$2.866 \times 10^{-6}$	$7.42 \times 10^3$

$$K_{\text{av}}(-30\text{ }^{\circ}\text{C}) = 7.73 \times 10^3 \text{ L mol}^{-1}$$

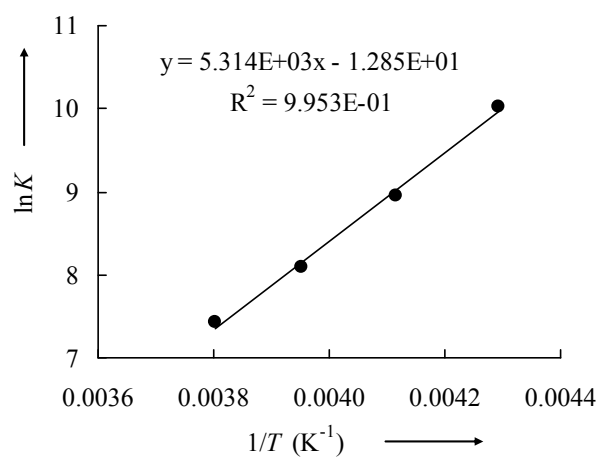
DCM at  $-40.0\text{ }^{\circ}\text{C}$ .

Entry	$[\mathbf{13}]_0$ (mol L $^{-1}$ )	$A$	$[(\text{ind})_2\text{CH}^+]_{\text{eq}}$ (mol L $^{-1}$ )	$K$ (L mol $^{-1}$ )
0	0	0.929	$1.410 \times 10^{-5}$	
1	$5.243 \times 10^{-5}$	0.446	$6.769 \times 10^{-6}$	$2.39 \times 10^4$
0	0	0.926	$1.404 \times 10^{-5}$	
1	$7.598 \times 10^{-5}$	0.371	$5.622 \times 10^{-6}$	$2.20 \times 10^4$
0	0	0.942	$1.429 \times 10^{-5}$	
1	$1.012 \times 10^{-4}$	0.315	$4.972 \times 10^{-6}$	$2.15 \times 10^4$

$$K_{\text{av}}(-40\text{ }^{\circ}\text{C}) = 2.25 \times 10^4 \text{ L mol}^{-1}$$

**Table 23.**van't Hoff plot for the reaction of  $(\text{ind})_2\text{CH}^+$  with **13** in DCM.

$T$ ( $^{\circ}\text{C}$ )	$K$ ( $\text{L mol}^{-1}$ )
-10.0	$1.68 \times 10^3$
-20.0	$3.26 \times 10^3$
-30.0	$7.73 \times 10^3$
-40.0	$2.25 \times 10^4$



$$\Delta H^{\circ} = -44.2 \text{ kJ mol}^{-1}$$
$$\Delta S^{\circ} = -106.9 \text{ J mol}^{-1} \text{ K}^{-1}$$
$$K(20 \text{ }^{\circ}\text{C}) = 1.98 \times 10^2 \text{ L mol}^{-1}$$

4.5 Nucleofugalities of isothiureas in CH<sub>2</sub>Cl<sub>2</sub> at 20 °C.Table 24. Heterolysis rate constants in CH<sub>2</sub>Cl<sub>2</sub> at 20 °C.

Nucleofuge	Electrofuge	$E_f$ [a]	$k_{\leftarrow}$ (s <sup>-1</sup> ) [b]	$N_f$ [c]	$N_f(\text{average})$
<b>7</b>	(thq) <sub>2</sub> CH <sup>+</sup>	5.22	$2.28 \times 10^{-1}$	-5.86	-5.79
	(ind) <sub>2</sub> CH <sup>+</sup>	4.83	$1.30 \times 10^{-1}$	-5.72	
<b>9 (THTP)</b>	(ind) <sub>2</sub> CH <sup>+</sup>	4.83	$1.94 \times 10^{-2}$	-6.54	-6.49
	(jul) <sub>2</sub> CH <sup>+</sup>	5.61	$1.09 \times 10^{-1}$	-6.57	
	(lil) <sub>2</sub> CH <sup>+</sup>	5.05	$5.02 \times 10^{-2}$	-6.35	
<b>10 (DHPB)</b>	(pyr) <sub>2</sub> CH <sup>+</sup>	5.35	$9.69 \times 10^{-1}$	-5.36	-5.26
	(thq) <sub>2</sub> CH <sup>+</sup>	5.22	$7.53 \times 10^{-1}$	-5.34	
	(ind) <sub>2</sub> CH <sup>+</sup>	4.83	$5.50 \times 10^{-1}$	-5.09	
<b>13</b>	(mpa) <sub>2</sub> CH <sup>+</sup>	3.46	$4.89 \times 10^{-1}$	-3.77	-3.98
	(dma) <sub>2</sub> CH <sup>+</sup>	4.84	$4.81 \times 10^0$	-4.16	
	(pyr) <sub>2</sub> CH <sup>+</sup>	5.35	$1.56 \times 10^1$	-4.16	
	(thq) <sub>2</sub> CH <sup>+</sup>	5.22	$1.39 \times 10^1$	-4.08	
	(ind) <sub>2</sub> CH <sup>+</sup>	4.83	$1.20 \times 10^1$	-3.75	
<b>14</b>	(dma) <sub>2</sub> CH <sup>+</sup>	4.84	$2.27 \times 10^0$	-4.48	-4.24
	(pyr) <sub>2</sub> CH <sup>+</sup>	5.35	$1.05 \times 10^1$	-4.33	
	(thq) <sub>2</sub> CH <sup>+</sup>	5.22	$1.05 \times 10^1$	-4.20	
	(ind) <sub>2</sub> CH <sup>+</sup>	4.83	$7.34 \times 10^0$	-3.96	
<b>15</b>	(mpa) <sub>2</sub> CH <sup>+</sup>	3.46	$2.94 \times 10^0$	-2.99	-3.15
	(dma) <sub>2</sub> CH <sup>+</sup>	4.84	$3.40 \times 10^1$	-3.31	
<b>16</b>	(mpa) <sub>2</sub> CH <sup>+</sup>	3.46	$1.04 \times 10^0$	-3.44	-3.57
	(dma) <sub>2</sub> CH <sup>+</sup>	4.84	$1.38 \times 10^1$	-3.70	
<b>17</b>	(mor) <sub>2</sub> CH <sup>+</sup>	3.03	$1.51 \times 10^0$	-2.85	-2.75
	(mpa) <sub>2</sub> CH <sup>+</sup>	3.46	$6.45 \times 10^0$	-2.65	

[a]  $E_f$  parameters from ref. 24. [b]  $k_{\leftarrow} = k/K$  see Table 3 in main text. [c] From equation  $\log k_{\leftarrow}(25 \text{ }^\circ\text{C}) = s_f(E_f + N_f)$  assuming  $s_f = 1.0$ ; temperature difference (20 and 25 °C) neglected.

## 5 References

- [1] For an excellent review, see: S. E. Denmark, G. L. Beutner, *Angew. Chem. Int. Ed.* **2008**, *47*, 1560–1638.
- [2] a) G. Höfle, W. Steglich, A. Vorbrüggen, *Angew. Chem. Int. Ed.* **1978**, *17*, 569–583; b) R. Murugan, E. F. V. Scriven, *Aldrichim. Acta* **2003**, *36*, 21–27; c) A. C. Spivey, S. Arseniyadis, *Angew. Chem. Int. Ed.* **2004**, *43*, 5436–5441; d) For mechanistic interpretations, see: S. Xu, I. Held, B. Kempf, H. Mayr, W. Steglich, H. Zipse, *Chem. Eur. J.* **2005**, *11*, 4751–4757; e) V. Lutz, J. Glatthaar, C. Würtele, M. Serafin, H. Hausmann, P. R. Schreiner, *Chem. Eur. J.* **2009**, *15*, 8548–8557.
- [3] For a select example, see: K. A. Connors, N. K. Pandit, *Anal. Chem.* **1978**, *50*, 1542–1545.
- [4] For select examples, see: a) B. G. G. Lohmeijer, R. C. Pratt, F. Leibfarth, J. W. Logan, D. A. Long, A. P. Dove, F. Nederberg, J. Choi, C. Wade, R. M. Waymouth, J. L. Hedrick, *Macromolecules* **2006**, *39*, 8574–8583; b) W-C. Shieh, S. Dell, O. Repic, *J. Org. Chem.* **2002**, *67*, 2188–2191; c) W. Zhang, M. Shi, *Org. Biomol. Chem.* **2006**, *4*, 1671–1674; d) K. E. Price, C. Larrivéé-Aboussafy, B. M. Lillie, R. W. McLaughlin, J. Mustakis, K. W. Hettenbach, J. M. Hawkins, R. Vaidyanathan, *Org. Lett.* **2009**, *11*, 2003–2006; e) C. Larrivéé-Aboussafy, B. P. Jones, K. E. Price, M. A. Hardink, R. W. McLaughlin, B. M. Lillie, J. M. Hawkins, R. Vaidyanathan, *Org. Lett.* **2010**, *12*, 324–327; f) J. E. Taylor, M. D. Jones, J. M. J. Williams, S. D. Bull, *Org. Lett.* **2010**, *12*, 5740–5743.
- [5] a) V. B. Birman, E. W. Uffman, H. Jiang, X. Li, C. J. Kilbane, *J. Am. Chem. Soc.* **2004**, *126*, 12226–12227; b) V. B. Birman, H. Jiang, *Org. Lett.* **2005**, *7*, 3445–3447; c) V. B. Birman, X. Li, H. Jiang, E. W. Uffman, *Tetrahedron* **2006**, *62*, 285–294.
- [6] M. Kobayashi, S. Okamoto, *Tetrahedron Lett.* **2006**, *47*, 4347–4350.
- [7] V. B. Birman, X. Li, Z. Han, *Org. Lett.* **2007**, *9*, 37–40.
- [8] a) C. Joannesse, C. Simal, C. Concellón, J. E. Thomson, C. D. Campbell, A. M. Z. Slawin, A. D. Smith, *Org. Biomol. Chem.* **2008**, *6*, 2900–2907; b) P. A. Woods, L. C. Morrill, T. Lebl, A. M. Z. Slawin, R. A. Bragg, A. D. Smith, *Org. Lett.* **2010**, *12*, 2660–2663.
- [9] V. B. Birman, X. Li, *Org. Lett.* **2006**, *8*, 1351–1354.
- [10] For kinetic resolutions using anhydrides as acylating agents, see: a) V. B. Birman, H. Jiang, X. Li, V. Geo, E. W. Uffman, *J. Am. Chem. Soc.* **2006**, *128*, 6536–6537; b) ref.

- [9]; c) V. B. Birman, L. Geo, *Org. Lett.* **2006**, *8*, 4859–4861. d) V. B. Birman, X. Li, *Org. Lett.* **2008**, *10*, 1115–1118; e) X. Yang, V. B. Birman, *Adv. Synth. Catal.* **2009**, *351*, 2525–2529; f) Q. Xu, H. Zhou, X. Geng, P. Chen, *Tetrahedron*, **2009**, *65*, 2232–2238; For kinetic resolutions using carboxylic acids as acylating agents utilising in-situ formation of a reactive mixed anhydride, see: g) I. Shiina, K. Nakata, *Tetrahedron. Lett.* **2007**, *48*, 8314–8317; h) I. Shiina, K. Nakata, M. Sugimoto, Y. Onda, T. Iizumi, K. Ono, *Heterocycles* **2009**, *77*, 801–810; i) X. Yang, V. B. Birman, *Adv. Synth. Catal.* **2009**, *351*, 2301–2304; j) I. Shiina, K. Nakata, *Heterocycles* **2010**, *80*, 169–175; k) I. Shiina, K. Nakata, Y. Onda, *Eur. J. Org. Chem.* **2008**, 5887–5890; l) I. Shiina, K. Nakata, K. Ono, M. Sugimoto, A. Sekiguchi, *Chem. Eur. J.* **2010**, *16*, 167–172; m) K. Nakata, Y. Onda, K. Ono, I. Shiina, *Tetrahedron. Lett.* **2010**, *51*, 5666–5669; n) I. Shiina, K. Ono, K. Nakata, *Chem. Lett.* **2011**, *40*, 147–149.
- [11] V. B. Birman, H. Jiang, X. Li, *Org. Lett.* **2007**, *9*, 3237–3240.
- [12] J. A. Kalow, A. G. Doyle, *J. Am. Chem. Soc.* **2010**, *132*, 3268–3269.
- [13] X. Yang, G. Lu, V. B. Birman, *Org. Lett.* **2010**, *12*, 892–895.
- [14] a) V. C. Purohit, A. S. Matla, D. Romo, *J. Am. Chem. Soc.* **2008**, *130*, 10478–10479; b) C. A. Leverett, V. C. Purohit, D. Romo, *Angew. Chem. Int. Ed.* **2010**, *49*, 9479–9483; c) D. Belmessieri, L. C. Morrill, C. Simal, A. M. Z. Slawin, A. D. Smith, *J. Am. Chem. Soc.* **2011**, *133*, 2714–2720; For other Lewis base mediated reactions utilising carboxylic acids as ammonium enolate precursors, see: d) G. S. Cortez, R. L. Tennyson, D. Romo, *J. Am. Chem. Soc.* **2001**, *123*, 7945–7946; e) G. S. Cortez, S. H. Oh, D. Romo, *Synthesis* **2001**, 1731–1736; f) S. H. Oh, G. S. Cortez, D. Romo, *J. Org. Chem.* **2005**, *70*, 2835–2838; g) H. Henry-Riyad, C. Lee, V. C. Purohit, D. Romo, *Org. Lett.* **2006**, *8*, 4363–4366; h) G. Ma, H. Nguyen, D. Romo, *Org. Lett.* **2007**, *9*, 2143–2146; i) H. Nguyen, G. Ma, D. Romo, *Chem. Commun.* **2010**, *46*, 4803–4805; j) K. A. Morris, K. M. Arendt, S. H. Oh, D. Romo, *Org. Lett.* **2010**, *12*, 3764–3767; k) H. Nguyen, G. Ma, T. Gladysheva, T. Fremgen, D. Romo, *J. Org. Chem.* **2011**, *76*, 2–12.
- [15] C. Joannesse, C. P. Johnston, C. Concellón, C. Simal, D. Philp, A. D. Smith, *Angew. Chem. Int. Ed.* **2009**, *48*, 8914–8918.
- [16] a) G. C. Fu, *Acc. Chem. Res.* **2000**, *33*, 412–420; b) G. C. Fu, *Acc. Chem. Res.* **2004**, *37*, 542–547; c) S. A. Shaw, P. Aleman, E. Vedejs, *J. Am. Chem. Soc.* **2003**, *125*, 13368–13369; d) S. A. Shaw, P. Aleman, J. Christy, J. W. Kampf, P. Va, E. Vedejs, *J.*

- Am. Chem. Soc.* **2006**, *128*, 925–934; e) H. V. Nguyen, D. C. D. Butler, C. J. Richards, *Org. Lett.* **2006**, *8*, 769–772.
- [17] Y. Zhanga, V. B. Birman, *Adv. Synth. Catal.* **2009**, *351*, 2525–2529.
- [18] D. Belmessieri, C. Joannesse, P. A. Woods, C. MacGregor, C. Jones, C. D. Campbell, C. P. Johnston, N. Duguet, C. Concellón, R. A. Bragg, A. D. Smith, *Org. Biomol. Chem.* **2011**, *9*, 559–570.
- [19] Reviews on nucleophilicities: a) H. Mayr, T. Bug, M. F. Gotta, N. Hering, B. Irrgang, B. Janker, B. Kempf, R. Loos, A. R. Ofial, G. Remennikov, H. Schimmel, *J. Am. Chem. Soc.* **2001**, *123*, 9500–9512; b) H. Mayr, B. Kempf, A. R. Ofial, *Acc. Chem. Res.* **2003**, *36*, 66–77; c) H. Mayr, A. R. Ofial, *J. Phys. Org. Chem.* **2008**, *21*, 584–595; d) H. Mayr, A. R. Ofial, *Pure Appl. Chem.* **2005**, *77*, 1807–1821; e) For a comprehensive listing of nucleophilicity parameters  $N$  and electrophilicity parameters  $E$ , see <http://www.cup.uni-muenchen.de/oc/mayr/DBintro.html>.
- [20] a) For pyridines, see: F. Brotzel, B. Kempf, T. Singer, H. Zipse, H. Mayr, *Chem. Eur. J.* **2007**, *13*, 336–345; b) N. De Rycke, G. Berionni, F. Couty, H. Mayr, R. Goumont, O. R. P. David, *Org. Lett.* **2011**, *13*, 530–533; c) For azoles, see: M. Baidya, F. Brotzel, H. Mayr, *Org. Biomol. Chem.* **2010**, *8*, 1929–1935; d) For  $\text{Ph}_3\text{P}$ , see: B. Kempf, H. Mayr, *Chem. Eur. J.* **2005**, *11*, 917–927; e) For DBU and DBN, see: M. Baidya, H. Mayr, *Chem. Commun.* **2008**, 1792–1794; f) For DABCO, see: M. Baidya, S. Kobayashi, F. Brotzel, U. Schmidhammer, E. Riedle, H. Mayr, *Angew. Chem. Int. Ed.* **2007**, *46*, 6176–6179.
- [21] J. Vana, M. Sedlak, J. Hanusek, *J. Org. Chem.* **2010**, *75*, 3729–3736, and cited refs.
- [22] a) R. A. Marcus, *J. Phys. Chem.* **1968**, *72*, 891–899; b) W. J. Albery, *Annu. Rev. Phys. Chem.* **1980**, *31*, 227–263.
- [23] H. F. Schaller, A. A. Tishkov, X. Feng, H. Mayr, *J. Am. Chem. Soc.* **2008**, *130*, 3012–3022.
- [24] N. Streidl, B. Denegri, O. Kronja, H. Mayr, *Acc. Chem. Res.* **2010**, *43*, 1537–1549.

## Chapter 3

**Guanidines: Highly Nucleophilic Organocatalysts**

B. Maji, D. S. Stephenson, H. Mayr, *ChemCatChem* **2012**, *4*, 993–999.

**1 Introduction**

Guanidines **1** are well known as superbases<sup>[1]</sup> and have successfully been used as Brønsted and Lewis bases catalyzing a large number of transformations.<sup>[2]</sup> Despite their similar Brønsted basicities<sup>[3]</sup> triazabicyclodecene **1g** (TBD,  $pK_{aH}$  in THF = 26) was found to be a far more efficient catalyst than triazabicyclooctene **1e** (TBO), methyltriazabicyclodecene **1h** (MTBD,  $pK_{aH}$  in THF = 25), or diazabicycloundecene (DBU,  $pK_{aH}$  in THF = 24) for the ring-opening-polymerization of cyclic esters, e.g. lactide polymerization.<sup>[4]</sup> Theoretical and kinetic studies explained the high catalytic activity of TBD by bifunctional catalysis, where TBD acts 1) as general base/H-bond donor activating the alcohol and stabilizing the tetrahedral intermediate, and 2) as a nucleophile reversibly reacting with esters to generate acyl-TBD.<sup>[4]</sup> Guanidines have also successfully been used as nucleophilic catalysts in Baylis-Hilman,<sup>[5]</sup> aldol,<sup>[6]</sup> and Strecker reactions,<sup>[7]</sup> silylations of alcohols,<sup>[8]</sup> electrophilic brominations,<sup>[9]</sup> and activation of CO<sub>2</sub>.<sup>[10]</sup> They are the source of nitrogen in the aziridination of epoxides via nucleophilic ring opening.<sup>[11]</sup>

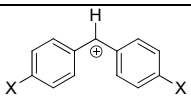
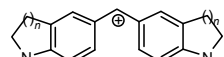
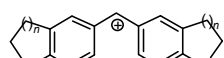
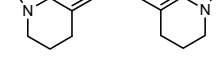
As recently stated by Fu and Tan, most synthetic applications of guanidines employ their high Brønsted basicities by the dual hydrogen bond donation of the guanidinium ions while their use as a nucleophilic catalyst has less extensively been explored.<sup>[2]</sup> In many guanidine-catalyzed reactions nucleophilic additions may compete with Brønsted base catalysis.<sup>[2]</sup> Knowledge of their nucleophilic reactivities is, therefore, crucial for understanding the catalytic activities of guanidines. Previous work of this group demonstrated that the rates of the reactions of nucleophiles with carbocations and Michael acceptors can be described by the linear-free-energy relationship (1),

$$\log k_{20^\circ\text{C}} = s_N(N + E) \quad (1)$$

where electrophiles are characterized by the electrophilicity parameter  $E$ , nucleophiles are characterized by the nucleophilicity parameters  $N$  and sensitivity parameter  $s_N$ , and  $k$  ( $\text{M}^{-1} \text{s}^{-1}$ ) is the second-order rate constant at  $20^\circ\text{C}$ . On the basis of eq. (1) it was possible to develop the most comprehensive nucleophilicity scale presently available, currently covering 40 orders of magnitude.<sup>[12]</sup>

We will now report on the determination of the nucleophilicity parameters of the guanidines **1** using the benzhydrylium methodology<sup>[12]</sup> and we will compare the nucleophilic reactivities of guanidines with those of other nucleophilic organocatalysts.<sup>[13]</sup> Finally, we will demonstrate that these parameters can be used to predict the rate constants for the additions of guanidines to various Michael acceptors with known electrophilicity parameters.<sup>[14]</sup>

**Table 1.** Abbreviations and electrophilicity parameters for the benzhydrylium ions **2** used for this work.

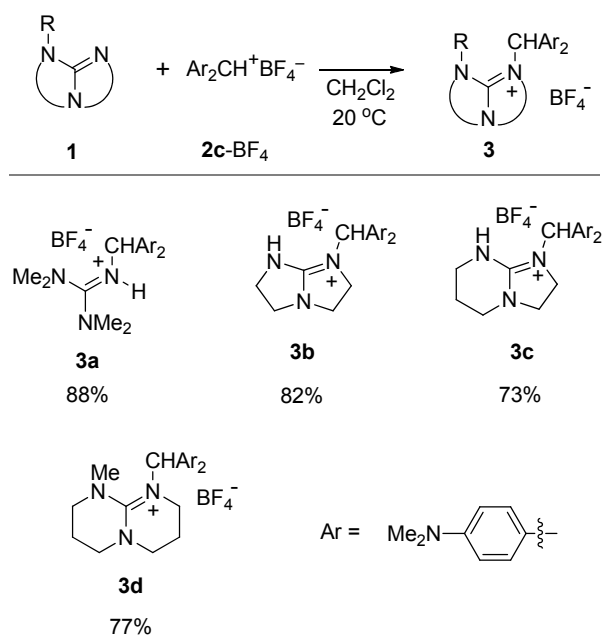
			
X		Abbreviations	$E^{[a]}$
N(CH <sub>2</sub> CH <sub>2</sub> ) <sub>2</sub> O	<b>2a</b>	(mor) <sub>2</sub> CH <sup>+</sup>	-5.53
N(Ph)CH <sub>3</sub>	<b>2b</b>	(mpa) <sub>2</sub> CH <sup>+</sup>	-5.89
N(CH <sub>3</sub> ) <sub>2</sub>	<b>2c</b>	(dma) <sub>2</sub> CH <sup>+</sup>	-7.02
N(CH <sub>2</sub> ) <sub>4</sub>	<b>2d</b>	(pyr) <sub>2</sub> CH <sup>+</sup>	-7.69
	<b>2e</b>	$n = 2$ (thq) <sub>2</sub> CH <sup>+</sup>	-8.22
	<b>2f</b>	$n = 1$ (ind) <sub>2</sub> CH <sup>+</sup>	-8.76
	<b>2g</b>	$n = 2$ (jul) <sub>2</sub> CH <sup>+</sup>	-9.45
	<b>2h</b>	$n = 1$ (lil) <sub>2</sub> CH <sup>+</sup>	-10.04

[a] Electrophilicity parameters  $E$  for benzhydrylium ions from ref. 12.

## 2 Results and Discussion

### 2.1 Product characterizations

As shown in Scheme 1, the dimethylamino-substituted benzhydrylium ion **2c** was employed to elucidate the course of these reactions. Addition of the guanidines **1** to the blue solutions of **2c**-BF<sub>4</sub> (for the structure of **2c**-BF<sub>4</sub> see Table 1) in CH<sub>2</sub>Cl<sub>2</sub> led to decolorization due to the formation of the ammonium salts **3**, which have been isolated and characterized as described in the Experimental Section. The structure of the unsymmetrical compound **3c** was assigned by 2D-NMR experiments (COSY, HSQC and HMBC).



**Scheme 1.** Products and isolated yields from the reactions of guanidines with **2c**-BF<sub>4</sub>.

### 2.2 Kinetics

The kinetics of the reactions of the guanidines **1** with the benzhydrylium ions **2** (Table 1) were studied in CH<sub>2</sub>Cl<sub>2</sub> at 20 °C. The reactions were monitored by UV-Vis spectroscopy at or close to the absorption maxima of (Ar)<sub>2</sub>CH<sup>+</sup> employing stopped-flow techniques as described previously.<sup>[12]</sup> The nucleophiles were used in excess to achieve pseudo-first-order conditions. The first-order rate constants  $k_{\text{obs}}$  (s<sup>-1</sup>) were obtained by fitting the decay of the absorbances of the benzhydrylium ions to the mono-exponential function  $A = A_0 e^{-k_{\text{obs}} t} + C$ . Plots of  $k_{\text{obs}}$  vs. the concentration of **1** gave linear correlations as required by Eq. (2) (Figure 1). The slopes of these correlation lines yielded the second-order rate constants  $k$  (M<sup>-1</sup> s<sup>-1</sup>) which are collected in Table 2.

$$-d[2]/dt = k[1][2]; \text{ for } [1] \gg [2], k_{\text{obs}} = k[1] \quad (2)$$

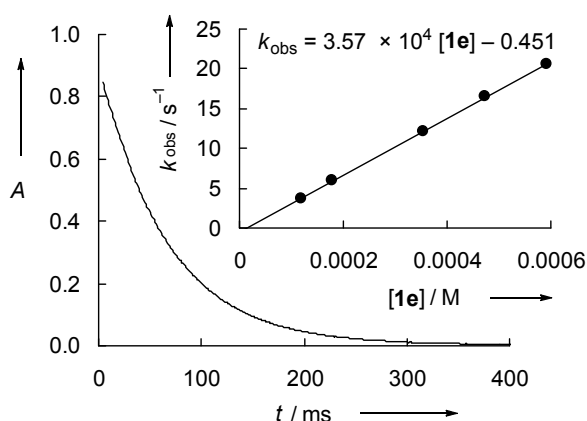


**Figure 1.** Exponential decay of the absorbance at 625 nm during the reaction of **1e** ( $3.55 \times 10^{-4}$  M) with **2f**-BF<sub>4</sub> ( $1.32 \times 10^{-5}$  M) at 20 °C in CH<sub>2</sub>Cl<sub>2</sub> ( $k_{\text{obs}} = 12.2 \text{ s}^{-1}$ ). Insert: Determination of the second-order rate constant  $k = 3.57 \times 10^4 \text{ M}^{-1} \text{ s}^{-1}$  from the dependence of  $k_{\text{obs}}$  on the concentration of **1e**.

**Table 2.** Second-order rate constants  $k$  for the reactions of the guanidines **1** and DBN with the benzhydrylium ions (Ar<sub>2</sub>CH<sup>+</sup>, Table 1) in CH<sub>2</sub>Cl<sub>2</sub> at 20 °C.

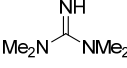
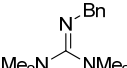
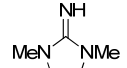
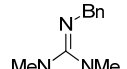
Guanidine	$N, s_N$ <sup>[a]</sup>	Ar <sub>2</sub> CH <sup>+</sup>	$k$ (M <sup>-1</sup> s <sup>-1</sup> )
 <b>1a</b> TMG	13.58, 0.77	(thq) <sub>2</sub> CH <sup>+</sup>	$1.33 \times 10^4$
		(ind) <sub>2</sub> CH <sup>+</sup>	$4.94 \times 10^3$
		(jul) <sub>2</sub> CH <sup>+</sup>	$1.44 \times 10^3$
		(lil) <sub>2</sub> CH <sup>+</sup>	$5.32 \times 10^2$
 <b>1b</b>	14.36, 0.79	(thq) <sub>2</sub> CH <sup>+</sup>	$6.73 \times 10^4$
		(ind) <sub>2</sub> CH <sup>+</sup>	$2.59 \times 10^4$
		(jul) <sub>2</sub> CH <sup>+</sup>	$7.37 \times 10^3$
		(lil) <sub>2</sub> CH <sup>+</sup>	$2.49 \times 10^3$
 <b>1c</b>	12.46, 0.87	(pyr) <sub>2</sub> CH <sup>+</sup>	$1.42 \times 10^4$
		(ind) <sub>2</sub> CH <sup>+</sup>	$1.92 \times 10^3$
		(jul) <sub>2</sub> CH <sup>+</sup>	$3.47 \times 10^2$
		(lil) <sub>2</sub> CH <sup>+</sup>	$1.42 \times 10^2$
 <b>1d</b>	14.00, 0.70	(mor) <sub>2</sub> CH <sup>+</sup>	$8.01 \times 10^5$
		(mpa) <sub>2</sub> CH <sup>+</sup>	$4.67 \times 10^5$
		(dma) <sub>2</sub> CH <sup>+</sup>	$7.83 \times 10^4$
		(pyr) <sub>2</sub> CH <sup>+</sup>	$2.46 \times 10^4$

Table 2 continued.

Guanidine	$N, s_N$ [a]	$Ar_2CH^+$	$k$ ( $M^{-1}s^{-1}$ )
 <b>1e</b> TBO	14.44, 0.79	(thq) <sub>2</sub> CH <sup>+</sup>	$7.85 \times 10^4$
		(ind) <sub>2</sub> CH <sup>+</sup>	$3.57 \times 10^4$
		(jul) <sub>2</sub> CH <sup>+</sup>	$7.72 \times 10^3$
		(lil) <sub>2</sub> CH <sup>+</sup>	$3.16 \times 10^3$
 <b>1f</b> TBN	16.15, 0.73	(thq) <sub>2</sub> CH <sup>+</sup>	$5.58 \times 10^5$
		(ind) <sub>2</sub> CH <sup>+</sup>	$2.42 \times 10^5$
		(jul) <sub>2</sub> CH <sup>+</sup>	$6.38 \times 10^4$
		(lil) <sub>2</sub> CH <sup>+</sup>	$2.86 \times 10^4$
 <b>1g</b> TBD	16.16, 0.75	(ind) <sub>2</sub> CH <sup>+</sup>	$3.84 \times 10^5$
		(jul) <sub>2</sub> CH <sup>+</sup>	$9.72 \times 10^4$
		(lil) <sub>2</sub> CH <sup>+</sup>	$4.24 \times 10^4$
 <b>1h</b> MTBD	14.43, 0.81	(thq) <sub>2</sub> CH <sup>+</sup>	$1.07 \times 10^5$
		(ind) <sub>2</sub> CH <sup>+</sup>	$4.85 \times 10^4$
		(jul) <sub>2</sub> CH <sup>+</sup>	$1.06 \times 10^4$
		(lil) <sub>2</sub> CH <sup>+</sup>	$3.85 \times 10^3$
 DBN	15.50, 0.76 [b]	(thq) <sub>2</sub> CH <sup>+</sup>	$3.20 \times 10^5$
		(ind) <sub>2</sub> CH <sup>+</sup>	$1.50 \times 10^5$
		(jul) <sub>2</sub> CH <sup>+</sup>	$3.20 \times 10^4$
		(lil) <sub>2</sub> CH <sup>+</sup>	$1.51 \times 10^4$

[a] Defined by Eq. (1). [b] For  $N, s_N$  in  $CH_3CN$  see Ref. [13e].

### 2.3 Nucleophilicity parameters

According to eq (1), linear correlations were obtained when  $\log k$  for the reactions of the guanidines **1** with the benzhydrylium ions **2** were plotted against their electrophilicity parameters  $E$ , as shown for some representative examples in Figure 2.<sup>[12]</sup> The slopes of these correlations correspond to the nucleophile-specific sensitivity parameter  $s_N$ , whereas the negative intercepts on the abscissa ( $\log k = 0$ ) yield the nucleophilicity parameters  $N$ , which are also listed in Table 2.

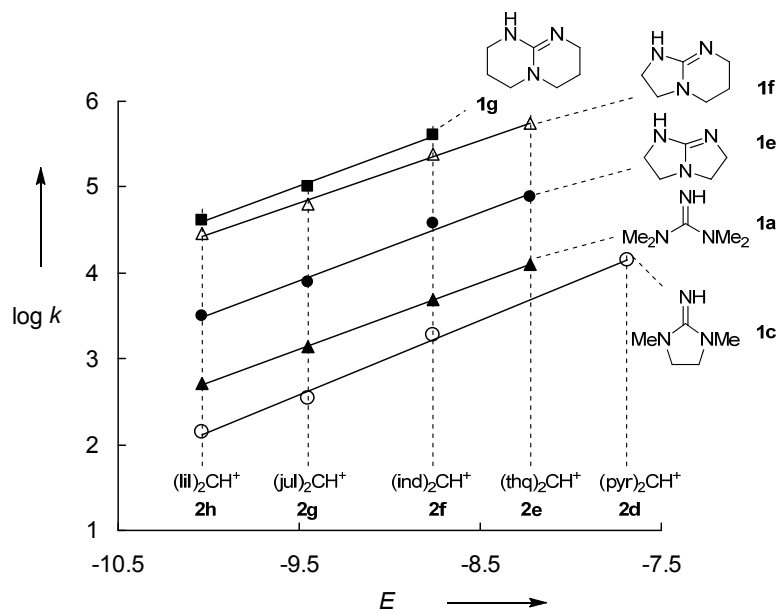
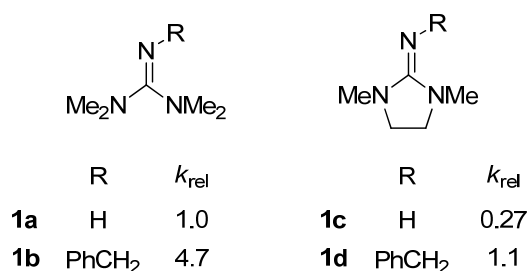


**Figure 2.** Plots of  $\log k$  for the reactions of the guanidines **1** with benzhydrylium ions versus their electrophilicity parameters  $E$  in  $\text{CH}_2\text{Cl}_2$  at  $20^\circ\text{C}$ .

## 2.4 Structure reactivity relationships

The similarity of the sensitivity parameters  $s_N$  listed in Table 2, which is reflected by the almost parallel correlation lines in Figure 2, implies that the relative reactivities of the guanidines **1a–h** depend only slightly on the nature of the electrophiles.

Scheme 2 shows that the cyclic guanidines **1c** and **1d** are almost 4 times less reactive than their acyclic analogues **1a** and **1b**, respectively, and that replacement of the NH proton by a benzyl group increases the reactivity by a factor of 4 to 5.



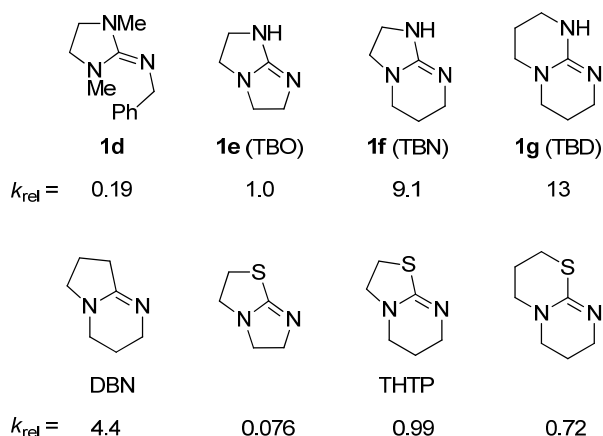
**Scheme 2.** Relative nucleophilic reactivities of the guanidines **1a–d** toward  $(\text{lil})_2\text{CH}^+$  in  $\text{CH}_2\text{Cl}_2$ .

Scheme 3 shows that the bicyclic guanidines **1e–g** are one to two orders of magnitude more reactive than the monocyclic guanidine **1d**, which can be explained by a combination of electronic and steric effects. Scheme 3, furthermore, demonstrates that the bicyclo[4.4.0]decene derivative **1g** is one order of magnitude more nucleophilic than the

bicyclo[3.3.0]octene derivative **1e**, mirroring the reactivity order for the structurally analogous isothioureas depicted below them.

The relative reactivities of the isothiourea derivatives in Scheme 3 unequivocally show that only the size of the ring comprising the nucleophilic reaction center, i.e., the imino-nitrogen, is relevant for the rate of the reaction, while the size of the annulated sulphur-containing ring has little effect. The analysis is less straightforward in the guanidine series **1e–g**. As **1f** exist as a mixture of rapidly equilibrating tautomers with similar concentrations in CD<sub>2</sub>Cl<sub>2</sub> solution (NOESY)<sup>[15]</sup> one may assume that the high reactivity of **1f** is also due to the reaction of the depicted tautomer to give an adduct with benzhydryl at the six-membered ring, which subsequently isomerizes to the NMR-spectroscopically identified adduct **3c** (Scheme 1).

Comparison of the guanidines **1e** and **1g** with the isothiourea derivatives below them, furthermore shows that replacement of the NH group by S reduces the nucleophilicity by approximately one order of magnitude. The nucleophilic reactivity of the bicyclic amidine DBN (Scheme 3, bottom left) is in between those of the guanidines **1e** and **1f,g**, indicating that structurally analogous amidines and guanidines have similar nucleophilicities.



**Scheme 3.** Effect of ring size on the relative nucleophilic reactivities of the guanidines toward (lil)<sub>2</sub>CH<sup>+</sup> (**2h**) and comparison with the amidine DBN and structurally related isothioureas<sup>[13f]</sup> (CH<sub>2</sub>Cl<sub>2</sub>, 20 °C).

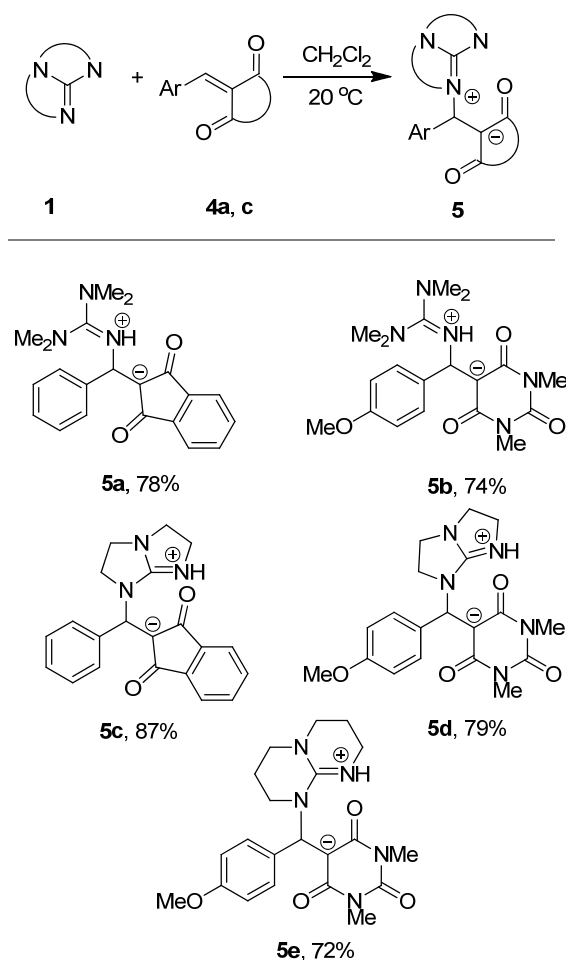
In line with the relative reactivities shown in Scheme 3, **1g** (TDB) has previously been reported to catalyze amidation of benzyl acetate significantly faster than **1e** (**1g**:  $1.9 \times 10^{-3} \text{ M}^{-1} \text{ s}^{-1}$  at 298 K; **1e**:  $2.3 \times 10^{-4} \text{ M}^{-1} \text{ s}^{-1}$  at 343 K).<sup>[4f]</sup>

The observed ring-size effects are in line with DFT calculations, which revealed a significantly higher charge (Gaussian natural bond orbital analysis) at the imine nitrogen of **1g** (−0.658) compared with **1e** (−0.591).<sup>[16]</sup> This difference was explained by the lower degree

of pyramidalization of the bridgehead nitrogen in **1g** leading to a higher degree of conjugation of the C=N group with the lone pair orbital.<sup>[2g]</sup>

## 2.5 Reactions with Michael acceptors

To examine the applicability of the  $N$  and  $s_N$  parameters of the guanidines **1** in Table 2 for reactions with other types of electrophiles we have studied their reactions with the Michael acceptors **4**, whose electrophilicity parameters have previously been reported.<sup>[14]</sup> The reactions of **4a** and **4c** with **1a**, **1e**, and **1g** proceed smoothly in  $\text{CH}_2\text{Cl}_2$  at room temperature to give the Michael addition products **5** in 74–87% yield (Scheme 4). The zwitterionic structure of **5c** was confirmed by its crystal structure (Figure 3),<sup>[17]</sup> which shows a planar quaternary carbon atom C8 (sum of the angles =  $359.9^\circ$ ) and a weak H-bonding between N2–H and one of the carbonyl oxygens (N2H $\cdots$ O1 distance = 184.3 pm). In  $\text{CD}_3\text{CN}$  solution, the rotation around C1–C8 is very fast that the two carbonyl carbons (C9 and C16), become equivalent in the  $^{13}\text{C}$  NMR spectrum.



**Scheme 4.** Products and isolated yields from the reactions of guanidines **1** with the Michael acceptors **4** in  $\text{CH}_2\text{Cl}_2$  at  $20^\circ\text{C}$ .

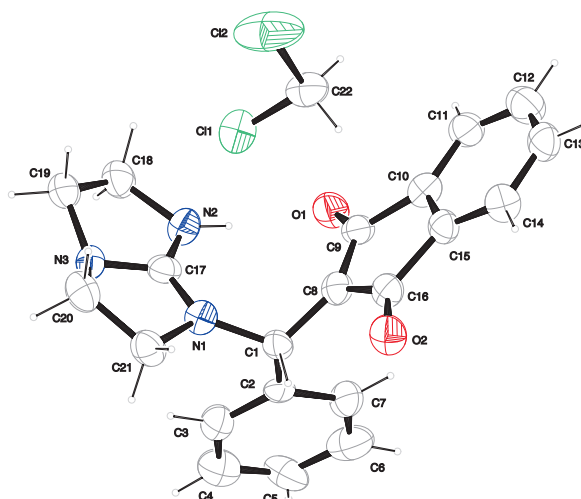
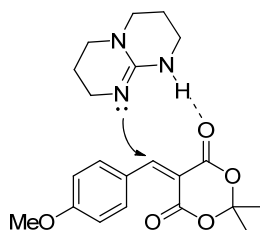


**Figure 3.** X-ray crystal structure of **5c**·CH<sub>2</sub>Cl<sub>2</sub> (50% probability ellipsoids).<sup>[17]</sup> Selected bond lengths (pm): C9-O1 = 127.1, C8-C9 = 139.8, C8-C16 = 143.1, C16-O2 = 123.9, N1-C17 = 134.3, C17-N2 = 128.9. Sum of the angle around C8 = 359.9°.

The kinetics were followed in same way as described for the reactions with benzhydrylium ions, and the second-order-rate constants are listed in Table 3. Since **1b** has been found to be a stronger nucleophile than **1a** (Table 2), its failure to react with any of **4a–d** must be due to the high reversibility of these reactions.

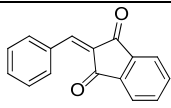
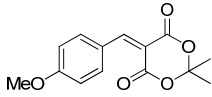
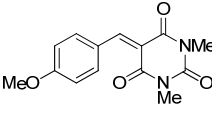
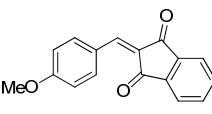
While the equilibrium constants for the reactions of **1h** with **4a** and **4d** are so small that we were unable to measure the rates of these reactions, rate and equilibrium constants could be determined for the reactions of **1h** with **4b** and **4c** (see below).

Comparison of the experimental rate constants with those calculated by eq. 1 using the  $N$  and  $s_N$  values from Table 2 and  $E$  values from ref. [14] shows agreement generally within a factor of 3. Only **1e** and **1g** react 12 to 32 times faster with **4b** and **4c** than calculated. Though we commonly refrain from interpreting deviations of less than factor  $10^2$  from the predictions of eq. (1), one might speculate that the consistently higher  $k^{\text{exp}}$  values in these four cases are indicative of a bifunctional interaction as illustrated in Scheme 5.



**Scheme 5.** Potential bifunctional interaction.

**Table 3.** Comparison of calculated and experimental second-order rate constants  $k$  for the reactions of the guanidines **1** with the Michael acceptors **4** in  $\text{CH}_2\text{Cl}_2$  at 20 °C.

Electrophile	$E$ [a]	Guanidine	$k^{\text{exp}}$	$k^{\text{calc}}$ [b]
 <b>4a</b>	-10.11	<b>1a</b>	$1.81 \times 10^2$	$4.45 \times 10^2$
		<b>1b</b>	h.r. [c]	$2.28 \times 10^3$
		<b>1e</b>	$2.61 \times 10^3$	$2.81 \times 10^3$
		<b>1g</b>	$2.95 \times 10^4$	$2.90 \times 10^4$
		<b>1h</b>	h.r. [c]	$3.16 \times 10^3$
 <b>4b</b>	-10.28	<b>1a</b>	$1.76 \times 10^3$	$3.30 \times 10^3$
		<b>1b</b>	h.r. [c]	$1.67 \times 10^3$
		<b>1e</b>	$6.57 \times 10^4$	$2.05 \times 10^3$
		<b>1g</b>	$3.67 \times 10^5$	$2.08 \times 10^4$
		<b>1h</b>	$2.19 \times 10^3$	$2.30 \times 10^3$
 <b>4c</b>	-10.37	<b>1a</b>	$8.62 \times 10^2$	$2.81 \times 10^2$
		<b>1b</b>	h.r. [c]	$1.42 \times 10^3$
		<b>1e</b>	$2.30 \times 10^4$	$1.74 \times 10^3$
		<b>1g</b>	$2.11 \times 10^5$	$1.74 \times 10^4$
		<b>1h</b>	$2.33 \times 10^3$	$1.94 \times 10^3$
 <b>4d</b>	-11.32	<b>1a</b>	h.r. [c]	$5.50 \times 10^1$
		<b>1b</b>	h.r. [c]	$2.52 \times 10^2$
		<b>1e</b>	$7.91 \times 10^2$	$3.02 \times 10^2$
		<b>1g</b>	$7.37 \times 10^3$	$2.72 \times 10^3$
		<b>1h</b>	h.r. [c]	$3.30 \times 10^2$

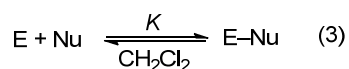
[a] Electrophilicity parameters  $E$  from ref. [14]. [b] Calculated by eq. 1 using  $N/s_N$  values from Table 2 and  $E$  values from Table 4. [c] Highly reversible.

As there is not a single case in Table 3, where  $k^{\text{exp}}$  deviates from  $k^{\text{calc}}$  by more than a factor of 32, we can conclude that the rates of the reactions of the guanidines **1** with electrophiles of known electrophilicity parameters can generally be predicted by eq. (1) using the  $N$  and  $s_N$  parameters reported in Table 2.

## 2.6 Equilibrium constants

As discussed above, some of the reactions of the guanidines **1** with the benzhydrylium tetrafluoroborates **2**- $\text{BF}_4$  and the Michael acceptors **4** proceed incompletely. Since the reactions of the colored electrophiles **2** and **4** with **1** give colorless products, the equilibrium constants (eq. 3) can be measured by UV-Vis spectroscopy. Assuming proportionality

between the absorbances of the electrophiles **2** and **4** and their concentrations (Lambert-Beer's law) the equilibrium constants  $K$  for the reactions in eq. 3 can be expressed by the absorbances of electrophiles before ( $A_0$ ) and after ( $A$ ) addition of the guanidines **1**.



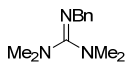
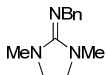
$$K = \frac{[E\text{-Nu}]}{[E][Nu]} = \frac{A_0 - A}{A[Nu]} \quad (4)$$

Where  $[Nu] = [Nu]_0 - [(A_0 - A)/\epsilon d]$

$\epsilon$  = molar absorption coefficient

$d$  = path length

**Table 4.** Equilibrium constants  $K$  for the reactions of guanidines with benzhydrylium ions ( $\text{Ar}_2\text{CH}^+$ ) in  $\text{CH}_2\text{Cl}_2$  at 20 °C.

Guanidine	$\text{Ar}_2\text{CH}^+$	$K [\text{M}^{-1}]$
	<b>1b</b> (ind) <sub>2</sub> CH <sup>+</sup>	$1.5 \times 10^6$
	(jul) <sub>2</sub> CH <sup>+</sup>	$4.39 \times 10^4$
	(lil) <sub>2</sub> CH <sup>+</sup>	$4.38 \times 10^4$
	<b>1d</b> (pyr) <sub>2</sub> CH <sup>+</sup>	$(3.9 \times 10^4)^{[a]}$
	(ind) <sub>2</sub> CH <sup>+</sup>	$(1.9 \times 10^4)^{[a]}$
	<b>1h</b> (jul) <sub>2</sub> CH <sup>+</sup>	$1.54 \times 10^5$
	(lil) <sub>2</sub> CH <sup>+</sup>	$1.73 \times 10^5$

[a] Approximate values of the equilibrium constants are given, since the final absorbance of  $\text{Ar}_2\text{CH}^+$  was not stable after its reactions with **1d**.

Table 4 shows that **1b** is an 83-times stronger Lewis base than **1d** (reference: (ind)<sub>2</sub>CH<sup>+</sup>) and a 4-times weaker Lewis base than **1h** (reference: (lil)<sub>2</sub>CH<sup>+</sup>). Comparison with Table 2 indicates that 39% of the difference in Lewis basicities of **1h** and **1b** are reflected by the relative nucleophilicities. Since the equilibrium constants for **1d** in Table 4 have a high uncertainty, an analogous comparison has not been performed for the couple **1b** vs **1d**.

**Table 5.** Comparison of the Lewis basicities of **1b** and **1h** with DBU, DBN and DMAP (For structures see Figure 4).

	<b>1b</b>	<b>1h</b>	DBU	DBN	DMAP
<b>4b</b>	$< 10^2$	$(2.9 \times 10^2)^{[a]}$	$(1-7) \times 10^4^{[b]}$	large	$1.96 \times 10^2^{[b]}$
<b>4c</b>	$< 10^2$	$(2.8 \times 10^2)^{[a]}$	$(2-8) \times 10^4^{[b]}$	large	$2.41 \times 10^2^{[b]}$

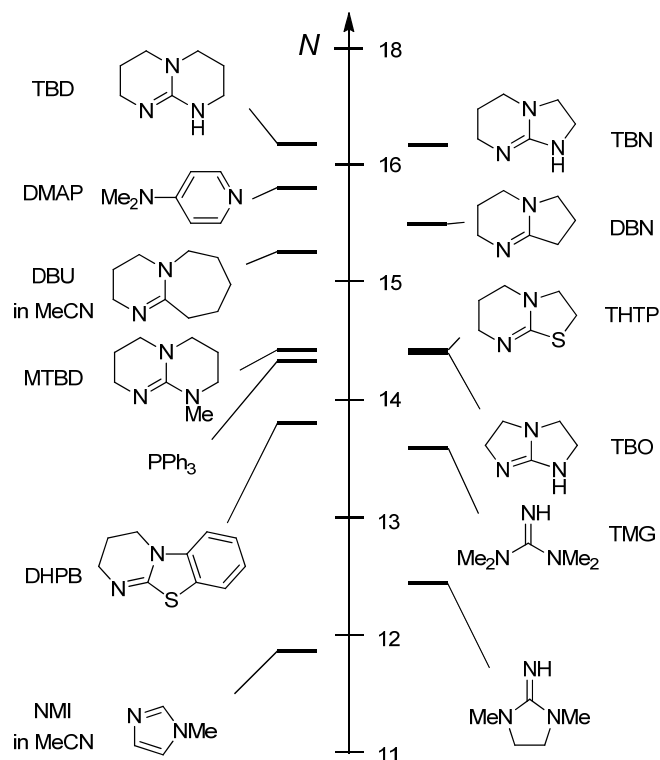
[a] Approximate value since the final absorbance of **4b** and **4c** was not stable after its reactions with **1h**. [b] From ref. [13e] in  $\text{CH}_3\text{CN}$ .

Table 5 compares the equilibrium constants for the reactions of **1b** and **1h** with the Michael acceptors **4b** and **4c** with the corresponding equilibrium constants for DBU, DBN, and DMAP. Though the equilibrium constants refer to different solvents, one can see that **1h** has a similar Lewis basicity as DMAP, while **1b** is a much weaker Lewis base.

### 3 Conclusion

The rate constants for the reactions of guanidines with benzhydrylium ions follow the linear-free energy relationship (Eq. 1), thus allowing us to include these nucleophiles into our comprehensive nucleophilicity scale and compare them with commonly used nucleophilic organocatalysts (Figure 4).<sup>[12, 13]</sup> With  $14 < N < 17$  the guanidines **1** have similar nucleophilicities as bicyclic isothiourea derivatives (subtle differences have been discussed above), DMAP, triphenylphosphane, and the bicyclic amidines DBU and DBN. While N-methyl imidazole is on the lower end of this scale, DABCO is by far the strongest nucleophile of this series despite its previously discussed low Lewis basicity.<sup>[13]</sup>

TBD (**1g**) was found to be the strongest nucleophile in the guanidine series and is approximately 1.5 orders of magnitude more nucleophilic than MTBD (**1h**) or TBO (**1e**) and 1 order of magnitude more nucleophilic than DBU, which may explain its superior catalytic efficiency in the ring-opening-polymerization of cyclic esters.<sup>[4]</sup>



**Figure 4.** Comparison of the nucleophilicities  $N$  of guanidines **1** with other nucleophilic organocatalysts (solvent is  $\text{CH}_2\text{Cl}_2$  unless otherwise stated,  $N$  from Table 2 and ref. [13]).

## 4 Experimental Section

### 4.1 General

#### Materials.

CH<sub>2</sub>Cl<sub>2</sub> was freshly distilled over CaH<sub>2</sub> prior to use. TBD (**1g**) and MTBD (**1h**) were purchased from Aldrich) and used without further purification. TMG (**1a**) was purchased from Acros Organics and distilled prior to use. **1b**,<sup>[5a]</sup> **1c**,<sup>[18]</sup> **1d**,<sup>[11a]</sup> TBO (**1e**)<sup>[15]</sup> and TBN (**1f**)<sup>[15]</sup> were synthesized according to the literature procedure. Benzhydrylium tetrafluoroborates<sup>[12b]</sup> and Michael acceptors<sup>[14]</sup> were prepared as described before.

#### Analytcs.

<sup>1</sup>H- and <sup>13</sup>C-NMR spectra were recorded on *Varian* NMR-systems (300 and 400 MHz) in *d*<sub>6</sub>-DMSO or CD<sub>3</sub>CN and the chemical shifts in ppm refer to the solvent residual signal as internal standard (in CD<sub>3</sub>CN: δ<sub>H</sub> = 1.96, δ<sub>C</sub> = 1.4 ppm; in *d*<sub>6</sub>-DMSO: δ<sub>H</sub> = 2.50, δ<sub>C</sub> = 39.5 ppm). The following abbreviations were used for chemical shift mutiplicities: brs = broad singlet, s = singlet, d = doublet, t = triplet, q = quartet, m = multiplet. For reasons of simplicity, the <sup>1</sup>H-NMR signals of AA'BB'-spin systems of *p*-disubstituted aromatic rings are treated as doublets. NMR signal assignments are based on additional 2D-NMR experiments (COSY, HSQC, and HMBC). (HR-)MS has been performed on a *Finnigan MAT 95* (EI) or a *Thermo Finnigan LTQ FT* (ESI) mass spectrometer. Melting points were determined on a Büchi B-540.

### 4.2 Reactions products

#### 4.2.1 Reactions products for the reaction of the guanidines with 2c-BF<sub>4</sub>.

**3a**: To a blue solution of **2c**-BF<sub>4</sub> (34 mg, 0.10 mmol) in dry CH<sub>2</sub>Cl<sub>2</sub> (2 mL) was added dropwise a solution of TMG (**1a**, 12.6 mg, 0.110 mmol) in CH<sub>2</sub>Cl<sub>2</sub> (2 mL). The solution was concentrated under vacuum, and the product **3a** was then precipitated by adding *n*-pentane, washed several times with *n*-pentane and dried: 40 mg (0.088 mmol, 88%). <sup>1</sup>H-NMR (CD<sub>3</sub>CN, 400 MHz): δ = 2.84 (s, 12 H, <sup>+</sup>N=C(N(CH<sub>3</sub>)<sub>2</sub>)<sub>2</sub>), 2.91 (s, 12 H, 2 × Ar-N(CH<sub>3</sub>)<sub>2</sub>), 5.50 (s, 1 H, Ar<sub>2</sub>CH), 6.33 (brs, 1 H, NH), 6.73 (d, *J* = 8.9 Hz, 4 H, Ar), 7.13 (d, *J* = 8.9 Hz, 4 H, Ar) ppm. <sup>13</sup>C-NMR (CD<sub>3</sub>CN, 100 MHz): δ = 40.5 (q, <sup>+</sup>N=C(N(CH<sub>3</sub>)<sub>2</sub>)<sub>2</sub>), 40.7 (q, Ar-N(CH<sub>3</sub>)<sub>2</sub>), 63.5 (d, Ar<sub>2</sub>CH), 113.5 (d, Ar), 128.8 (d, Ar), 129.4 (s, Ar), 151.4 (s, Ar), 161.9 (s, <sup>+</sup>N=C(N(CH<sub>3</sub>)<sub>2</sub>)<sub>2</sub>) ppm. HRMS (ESI+): Calculated for C<sub>17</sub>H<sub>21</sub>N<sub>2</sub><sup>+</sup> [M-TMG]<sup>+</sup> is 253.1699; found 253.1698.

**3b:** As described above for the formation of **3a**. **3b** was obtained from TBO (**1e**, 12.9 mg, 0.116 mmol) and **2c**-BF<sub>4</sub> (39.4 mg, 0.116 mmol): 43 mg (0.095 mmol, 82 %). <sup>1</sup>H-NMR (CD<sub>3</sub>CN, 400 MHz): δ = 2.93 (s, 12 H, 2 × Ar-N(CH<sub>3</sub>)<sub>2</sub>), 3.43-3.47 (m, 5 H), 3.81 (t, *J* = 8.0 Hz, 2 H), 3.89 (t, *J* = 8.0 Hz, 2 H), 3.97-4.01 (m, 1 H), 5.68 (s, 1 H, Ar<sub>2</sub>CH), 6.75 (d, *J* = 8.7 Hz, 4 H, Ar), 7.09 (d, *J* = 8.7 Hz, 4 H, Ar) ppm. <sup>13</sup>C-NMR (CD<sub>3</sub>CN, 100 MHz): δ = 40.7 (q, 2 × Ar-N(CH<sub>3</sub>)<sub>2</sub>), 45.6 (t, CH<sub>2</sub>), 46.6 (t, CH<sub>2</sub>), 50.4 (s), 50.6 (t, CH<sub>2</sub>), 53.9 (t, CH<sub>2</sub>), 64.2 (d, Ar<sub>2</sub>CH<sup>+</sup>), 113.4 (d, Ar), 125.3 (s, Ar), 129.9 (d, Ar), 151.8 (s, Ar), 165.7 (s, C=N<sup>+</sup>) ppm. HRMS (ESI+): Calculated for C<sub>22</sub>H<sub>30</sub>N<sub>5</sub><sup>+</sup> [M<sup>+</sup>] is 364.2496; found 364.2493.

**3c:** As described above for the formation of **3a**. **3c** was obtained from **1f** (12.5 mg, 0.100 mmol) and **2c**-BF<sub>4</sub> (34 mg, 0.10 mmol): 34 mg (0.073 mmol, 73 %). <sup>1</sup>H-NMR (CD<sub>3</sub>CN, 400 MHz): δ = 1.95-2.01 (m, 2 H, CH<sub>2</sub>), 2.93 (s, 12 H, 2 × Ar-N(CH<sub>3</sub>)<sub>2</sub>), 3.25-3.34 (m, 6 H, CH<sub>2</sub>), 3.54-3.59 (m, 2 H, CH<sub>2</sub>), 5.74 (s, 1 H, Ar<sub>2</sub>CH), 6.42 (br s, 1 H, NH), 6.74 (d, *J* = 8.7 Hz, 4 H, Ar), 7.04 (d, *J* = 8.7 Hz, 4 H, Ar) ppm. <sup>13</sup>C-NMR (CD<sub>3</sub>CN, 100 MHz): δ = 20.8 (t, CH<sub>2</sub>), 39.4 (t, CH<sub>2</sub>), 40.7 (q, 2 × Ar-N(CH<sub>3</sub>)<sub>2</sub>), 43.4 (t, CH<sub>2</sub>), 45.1 (t, CH<sub>2</sub>), 47.8 (t, CH<sub>2</sub>), 61.8 (d, Ar<sub>2</sub>CH<sup>+</sup>), 113.3 (d, Ar), 125.9 (s, Ar), 130.0 (d, Ar), 151.6 (s, Ar), 155.1 (s, C=N<sup>+</sup>) ppm. HRMS (ESI+): Calculated for C<sub>23</sub>H<sub>32</sub>N<sub>5</sub><sup>+</sup> [M<sup>+</sup>] is 378.2652; found 378.2653.

**3d:** As described above for the formation of **3a**. **3d** was obtained from MTBD (**1h**, 7.2 mg, 0.050 mmol) and **2c**-BF<sub>4</sub> (17 mg, 0.050 mmol): 19 mg (0.039 mmol, 77 %). <sup>1</sup>H-NMR (CD<sub>3</sub>CN, 400 MHz): δ = 1.08-1.14 (m, 2 H), 1.99-2.05 (m, 2 H), 2.85 (s, 3 H, NCH<sub>3</sub>), 2.93 (s, 12 H, 2 × Ar-N(CH<sub>3</sub>)<sub>2</sub>), 3.19 (t, *J* = 6.9 Hz, 2 H), 3.26-3.36 (m, 6 H), 5.98 (s, 1 H, Ar<sub>2</sub>CH), 6.74 (d, *J* = 8.9 Hz, 4 H, Ar), 7.04 (d, *J* = 9.0 Hz, 4 H, Ar) ppm. <sup>13</sup>C-NMR (CD<sub>3</sub>CN, 100 MHz): δ = 21.8 (t), 21.9 (t), 40.7 (q, 2 × Ar-N(CH<sub>3</sub>)<sub>2</sub>), 41.6 (q, NCH<sub>3</sub>), 42.5 (t), 48.9 (t), 49.1 (t), 49.5 (t), 68.3 (d, Ar<sub>2</sub>CH<sup>+</sup>), 113.2 (d, Ar), 126.3 (s, Ar), 130.4 (d, Ar), 151.5 (s, Ar), 159.3 (s, C=N<sup>+</sup>) ppm. HRMS (ESI+): Calculated for C<sub>25</sub>H<sub>36</sub>N<sub>5</sub><sup>+</sup> [M<sup>+</sup>] is 406.2965; found 406.2970.

#### 4.2.2 Product studies for the reaction of guanidines with Michael acceptors.

**5a:** To a stirred solution of TMG (**1a**, 23.5 mg, 0.204 mmol) in CH<sub>2</sub>Cl<sub>2</sub> (2 mL) under nitrogen was added a solution of 2-benzylidene-1H-indene-1,3(2H)-dione (**4a**, 45 mg, 0.19 mmol) in CH<sub>2</sub>Cl<sub>2</sub> (2 mL) and the mixture was allowed to stir for another 5 min. The reaction mixture was then concentrated under vacuum, and the product **5a** was then precipitated by adding *n*-pentane, washed several times with *n*-pentane and dried: 52 mg (0.15 mmol, 78%). <sup>1</sup>H-NMR (d<sub>6</sub>-DMSO, 400 MHz): δ = 2.70 (s, 6 H), 2.99 (s, 6 H), 5.37 (s, 1 H, ArCH<sub>2</sub><sup>+</sup>NH),

7.01-7.06 (m, 2 H, Ar), 7.18-7.20 (m, 3 H, Ar), 7.28 (dd,  $J = 7.0, 8.1$  Hz, 2 H, Ar), 7.50 (dd,  $J = 1.2, 8.3$  Hz, 2 H, Ar), 8.44 (brs, 1 H, NH) ppm.  $^{13}\text{C}$ -NMR ( $\text{d}_6$ -DMSO, 100 MHz):  $\delta = 39.2$  (q,  $\text{N}(\text{CH}_3)_2$ ), 55.5 (d,  $\text{ArCH}^+\text{NH}$ ), 103.4 (s,  $\text{C}^-$ -CO), 116.8 (d, Ar), 126.4 (d, Ar), 126.6 (d, Ar), 128.1 (d, Ar), 128.2 (d, Ar), 140.0 (s), 143.7 (s), 160.3 (s,  $\text{C}=\text{NH}^+$ ), 187.4 (s,  $\text{C}=\text{O}$ ) ppm. HRMS (ESI+): Calculated for  $\text{C}_{21}\text{H}_{24}\text{O}_2\text{N}_3^+ [\text{M}^+]$  is 350.1869; found 350.1863.

**5b:** As described above for the formation of **5a**. **5b** was obtained from TMG (**1a**, 26.0 mg, 0.226 mmol) and 5-(4-methoxybenzylidene)-1,3-dimethylpyrimidine-2,4,6(1H,3H,5H)-trione (**4c**, 56.3 mg, 0.205 mmol): 59 mg (0.15 mmol, 74%).  $^1\text{H}$ -NMR ( $\text{CD}_3\text{CN}$ , 400 MHz):  $\delta = 2.88$  (brs, 12 H,  $^+\text{N}=\text{C}(\text{N}(\text{CH}_3)_2)_2$ ), 3.12 (s, 6 H,  $2 \times \text{NCH}_3$ ), 3.74 (s, 3 H,  $\text{OCH}_3$ ), 5.70 (d,  $J = 8.4$  Hz, 1 H,  $\text{ArCH}^+\text{NH}$ ), 6.82 (d,  $J = 8.8$  Hz, 2 H, Ar), 7.41 (d,  $J = 8.9$  Hz, 2 H, Ar), 9.32 (d,  $J = 8.0$  Hz, 1 H,  $\text{ArCH}^+\text{NH}$ ) ppm.  $^{13}\text{C}$ -NMR ( $\text{CD}_3\text{CN}$ , 100 MHz):  $\delta = 27.4$  (q,  $2 \times \text{NCH}_3$ ), 40.0 (q,  $\text{C}(\text{N}(\text{CH}_3)_2)_2$ ), 40.5 (q,  $\text{C}(\text{N}(\text{CH}_3)_2)_2$ ), 55.9 (q,  $\text{OCH}_3$ ), 57.1 (d,  $\text{ArCH}^+\text{NH}$ ), 87.8 (s,  $\text{C}^-$ -CO), 114.4 (d, Ar), 128.2 (d, Ar), 137.8 (s), 154.2 (s,  $\text{C}=\text{O}$ ), 159.6 (s), 162.3 (s,  $\text{C}=\text{O}$ ), 163.5 (s,  $\text{C}=\text{NH}^+$ ) ppm. HRMS (ESI+): Calculated for  $\text{C}_{19}\text{H}_{28}\text{O}_4\text{N}_5^+ [\text{M}^+]$  is 390.2141; found 390.2133.

**5c:** As described above for the formation of **5a**. **5c** was obtained from TBO (**1e**, 21.2 mg, 0.191 mmol) and 2-benzylidene-1H-indene-1,3(2H)-dione (**4a**, 45 mg, 0.19 mmol): 57 mg (0.17 mmol, 87%). Small amount of **5c** was crystallized by vapour diffusion of *n*-pentane into its  $\text{CH}_2\text{Cl}_2$ -EtOAc (10:1) solution to give crystals suitable for single crystal X-ray structure analysis. M.p.: 127–129 °C (decomp,  $\text{CH}_2\text{Cl}_2$ -EtOAc-*n*-pentane).  $^1\text{H}$ -NMR ( $\text{CD}_3\text{CN}$ , 400 MHz):  $\delta = 3.34$ -3.52 (m, 4 H,  $2 \times \text{CH}_2$ ), 3.85-3.99 (m, 2 H,  $\text{CH}_2$ ), 4.11-4.24 (m, 2 H,  $\text{CH}_2$ ), 5.62 (s, 1 H,  $\text{ArCH}^+\text{NH}$ ), 7.20-7.25 (m, 3 H, Ar), 7.28-7.32 (m, 5 H, Ar) ppm.  $^{13}\text{C}$ -NMR ( $\text{CD}_3\text{CN}$ , 100 MHz):  $\delta = 46.4$  (t), 47.9 (t), 50.8 (t), 54.7 (d,  $\text{ArCH}^+\text{NH}$ ), 56.7 (t), 104.4 (s,  $\text{C}^-$ -CO), 118.4 (d, Ar), 127.5 (d, Ar), 127.8 (d, Ar), 129.4 (d, Ar), 131.0 (d, Ar), 140.6 (s), 140.8 (s), 166.8 (s,  $\text{C}=\text{NH}^+$ ), 191.1 (s,  $\text{C}=\text{O}$ ) ppm. HRMS (ESI+): Calculated for  $\text{C}_{21}\text{H}_{20}\text{O}_4\text{N}_5^+ [\text{M}^+]$  is 346.1556; found 346.1550.

Crystallographic data for **5c**·CH<sub>2</sub>Cl<sub>2</sub>:

net formula	C <sub>22</sub> H <sub>21</sub> Cl <sub>2</sub> N <sub>3</sub> O <sub>2</sub>
<i>M<sub>r</sub></i> /g mol <sup>-1</sup>	430.327
crystal size/mm	0.20 × 0.08 × 0.02
<i>T</i> /K	173(2)
radiation	MoKα
diffractometer	'KappaCCD'
crystal system	monoclinic
space group	<i>P</i> 2 <sub>1</sub>
<i>a</i> /Å	9.1456(13)
<i>b</i> /Å	11.5117(8)
<i>c</i> /Å	10.3089(13)
α/°	90
β/°	109.687(4)
γ/°	90
<i>V</i> /Å <sup>3</sup>	1021.9(2)
<i>Z</i>	2
calc. density/g cm <sup>-3</sup>	1.3985(3)
μ/mm <sup>-1</sup>	0.342
absorption correction	none
refls. measured	5796
<i>R</i> <sub>int</sub>	0.0890
mean σ( <i>I</i> )/ <i>I</i>	0.1047
θ range	3.54–25.43
observed refls.	2496
<i>x</i> , <i>y</i> (weighting scheme)	0.1043, 1.3622
hydrogen refinement	constr
Flack parameter	–0.03(18)
refls in refinement	3559
parameters	263
restraints	1
<i>R</i> ( <i>F</i> <sub>obs</sub> )	0.0865
<i>R</i> <sub>w</sub> ( <i>F</i> <sup>2</sup> )	0.2367
<i>S</i>	1.075
shift/error <sub>max</sub>	0.001
max electron density/e Å <sup>-3</sup>	0.498
min electron density/e Å <sup>-3</sup>	–0.358

**5d**: As described above for the formation of **5a**. **5d** was obtained from TBO (**1e**, 22.3 mg, 0.200 mmol) and 5-(4-methoxybenzylidene)-1,3-dimethylpyrimidine-2,4,6(1H,3H,5H)-trione (**4c**, 54.8 mg, 0.200 mmol): 61 mg (0.16 mmol, 79 %). <sup>1</sup>H-NMR (CD<sub>3</sub>CN, 400 MHz): δ = 3.13 (s, 6 H, 2 × NCH<sub>3</sub>), 3.38–3.49 (m, 4 H, 2 × CH<sub>2</sub>), 3.75 (s, 3 H, OCH<sub>3</sub>), 3.81–3.88 (m, 2 H, CH<sub>2</sub>), 4.15 (t, *J* = 8.0, 8.0 Hz, 2 H, CH<sub>2</sub>), 6.07 (s, 1 H, ArCH–<sup>+</sup>NH), 6.82 (d, *J* = 8.8 Hz, 2 H, Ar), 7.13 (dd, *J* = 1.0, 8.9 Hz, 2 H, Ar), 7.72 (bs s, 1 H, ArCH–<sup>+</sup>NH) ppm. <sup>13</sup>C-NMR (CD<sub>3</sub>CN, 100 MHz): δ = 27.9 (q, 2 × NCH<sub>3</sub>), 46.5 (t), 47.8 (t), 50.5 (t), 55.9 (q, OCH<sub>3</sub>), 56.5

(t), 57.4 (d, ArCH<sup>+</sup>NH), 86.7 (s, C<sup>-</sup>-CO), 114.4 (d, Ar), 128.4 (d, Ar), 132.4 (s), 154.1 (s, C=O), 159.3 (s), 165.0 (s, C=O), 167.0 (s, C=NH<sup>+</sup>) ppm. HRMS (ESI+): Calculated for C<sub>19</sub>H<sub>24</sub>O<sub>4</sub>N<sub>5</sub><sup>+</sup> [M<sup>+</sup>] is 386.1828; found 386.1822.

**5e**: As described above for the formation of **5a**. **5e** was obtained from TBD (**1g**, 34 mg, 0.24 mmol) and 5-(4-methoxybenzylidene)-1,3-dimethylpyrimidine-2,4,6(1H,3H,5H)-trione (**4c**, 66 mg, 0.24 mmol): 72 mg (0.17 mmol, 72%). <sup>1</sup>H-NMR (CD<sub>3</sub>CN, 400 MHz): δ = 1.78-1.96 (m, 4 H, 2 × CH<sub>2</sub>, overlapped with solvent residual peak), 3.13-3.16 (m, 8 H, CH<sub>2</sub> + 2 × NCH<sub>3</sub>), 3.23-3.28 (m, 4 H, CH<sub>2</sub>), 3.40-3.47 (m, 1 H, CH<sub>2</sub>), 3.53-3.58 (m, 1 H, CH<sub>2</sub>), 3.75 (s, 3 H, OCH<sub>3</sub>), 6.10 (s, 1 H, ArCH<sup>+</sup>NH), 6.83 (d, *J* = 8.8 Hz, 2 H, Ar), 7.13 (dd, *J* = 0.9, 8.9 Hz, 2 H, Ar), 9.37 (bs s, 1 H, ArCH<sup>+</sup>NH) ppm. <sup>13</sup>C-NMR (CD<sub>3</sub>CN, 100 MHz): δ = 21.7 (t), 22.5 (t), 27.9 (q, 2 × NCH<sub>3</sub>), 39.4 (t), 46.7 (t), 48.47 (t), 48.52 (t), 55.9 (q, OCH<sub>3</sub>), 60.7 (d, ArCH<sup>+</sup>NH), 85.3 (s, C<sup>-</sup>-CO), 114.3 (d, Ar), 129.5 (d, Ar), 131.3 (s), 152.4 (s, C=O), 154.2 (s, C=O), 159.3 (s) 165.2 (s, C=NH<sup>+</sup>) ppm. HRMS (ESI+): Calculated for C<sub>21</sub>H<sub>28</sub>O<sub>4</sub>N<sub>5</sub><sup>+</sup> [M<sup>+</sup>] is 414.2141; found 414.2135.

## 4.3 Kinetics

4.3.1 Determination of the rate constants for the reactions of guanidines **1** and DBN with benzhydrylium ions **2**

The rates of the reaction between the guanidines **1** and DBN with the reference electrophiles **2** were measured photometrically under pseudo-first-order condition (excess of the guanidines **1**) at or close to the absorption maximum of **2** by conventional stopped-flow technique at 20 °C in dry CH<sub>2</sub>Cl<sub>2</sub> as described previously.<sup>[S1]</sup> First-order rate constants  $k_{\text{obs}}$  (s<sup>-1</sup>) were obtained by least-squares fitting of the absorbances to the mono-exponential function  $A_t = A_0 \exp(-k_{\text{obs}}t) + C$ . Since  $k_{\text{obs}} = k[\text{Nu}]$ , the second-order rate constants  $k$  (M<sup>-1</sup> s<sup>-1</sup>) were derived from the slopes of the linear plots of  $k_{\text{obs}}$  (s<sup>-1</sup>) vs. [Nu].

**Table 6.** Kinetics of the reactions of 1,1,3,3-tetramethylguanidine (TMG, **1a**) with (Ar)<sub>2</sub>CH<sup>+</sup> in CH<sub>2</sub>Cl<sub>2</sub> at 20 °C.

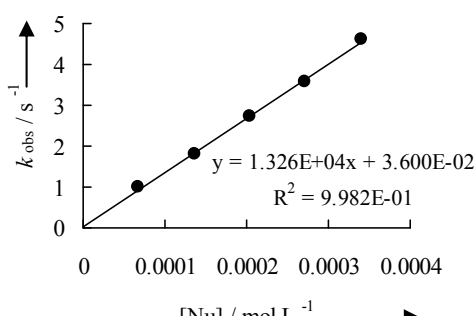
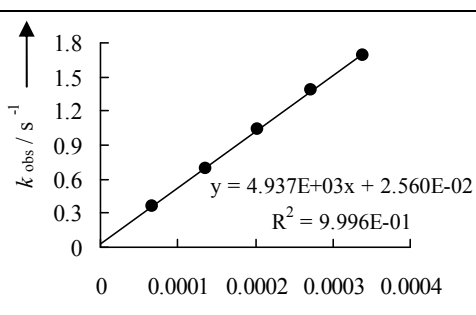
[(thq) <sub>2</sub> CH <sup>+</sup> ] (mol L <sup>-1</sup> )	[ <b>1a</b> ] (mol L <sup>-1</sup> )	$k_{\text{obs}}$ (s <sup>-1</sup> )	$\lambda = 626 \text{ nm}$	$k$ (M <sup>-1</sup> s <sup>-1</sup> )
$7.16 \times 10^{-6}$	$6.79 \times 10^{-5}$	0.985		$1.33 \times 10^4$
	$1.36 \times 10^{-4}$	1.80		
	$2.04 \times 10^{-4}$	2.74		
	$2.72 \times 10^{-4}$	3.57		
	$3.40 \times 10^{-4}$	4.61		
[(ind) <sub>2</sub> CH <sup>+</sup> ] (mol L <sup>-1</sup> )	[ <b>1a</b> ] (mol L <sup>-1</sup> )	$k_{\text{obs}}$ (s <sup>-1</sup> )	$\lambda = 626 \text{ nm}$	$k$ (M <sup>-1</sup> s <sup>-1</sup> )
$6.59 \times 10^{-6}$	$6.79 \times 10^{-5}$	0.357		$4.94 \times 10^3$
	$1.36 \times 10^{-4}$	0.692		
	$2.04 \times 10^{-4}$	1.04		
	$2.72 \times 10^{-4}$	1.38		
	$3.40 \times 10^{-4}$	1.69		

Table 6 continued

$[(\text{jul})_2\text{CH}^+]$ (mol L <sup>-1</sup> )	$[\mathbf{1a}]$ (mol L <sup>-1</sup> )	$k_{\text{obs}}$ (s <sup>-1</sup> )	$\lambda = 642 \text{ nm}$	$k$ (M <sup>-1</sup> s <sup>-1</sup> )
$7.20 \times 10^{-6}$	$8.47 \times 10^{-5}$	0.120		$1.44 \times 10^3$
	$1.69 \times 10^{-4}$	0.230		
	$2.54 \times 10^{-4}$	0.360		
	$3.39 \times 10^{-4}$	0.474		
	$4.23 \times 10^{-4}$	0.609		
$[(\text{lil})_2\text{CH}^+]$ (mol L <sup>-1</sup> )	$[\mathbf{1a}]$ (mol L <sup>-1</sup> )	$k_{\text{obs}}$ (s <sup>-1</sup> )	$\lambda = 639 \text{ nm}$	$k$ (M <sup>-1</sup> s <sup>-1</sup> )
$8.07 \times 10^{-6}$	$8.47 \times 10^{-5}$	$3.83 \times 10^{-2}$		$5.35 \times 10^2$
	$1.69 \times 10^{-4}$	$8.36 \times 10^{-2}$		
	$2.54 \times 10^{-4}$	0.125		
	$3.39 \times 10^{-4}$	0.173		
	$4.23 \times 10^{-4}$	0.220		
Reactivity parameters for 1,1,3,3-tetramethylguanidine (TMG, <b>1a</b> ) in CH <sub>2</sub> Cl <sub>2</sub>				
Ar <sub>2</sub> CH <sup>+</sup>	<i>E</i>	<i>k</i> (M <sup>-1</sup> s <sup>-1</sup> )		
(thq) <sub>2</sub> CH <sup>+</sup>	-8.22	$1.33 \times 10^4$		<i>N</i> = 13.58 <i>s<sub>N</sub></i> = 0.77
(ind) <sub>2</sub> CH <sup>+</sup>	-8.76	$4.94 \times 10^3$		
(jul) <sub>2</sub> CH <sup>+</sup>	-9.45	$1.44 \times 10^3$		
(lil) <sub>2</sub> CH <sup>+</sup>	-10.04	$5.35 \times 10^2$		

**Table 7.** Kinetics of the reactions of 2-benzyl-1,1,3,3-tetramethylguanidine (**1b**) with  $(\text{Ar})_2\text{CH}^+$  in  $\text{CH}_2\text{Cl}_2$  at 20 °C.

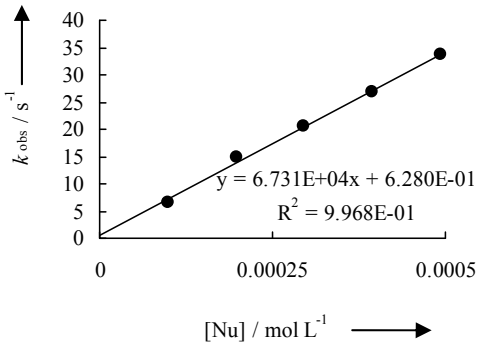
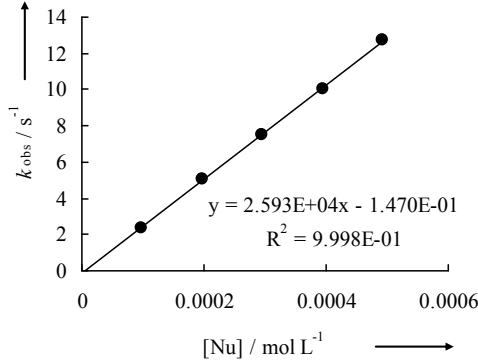
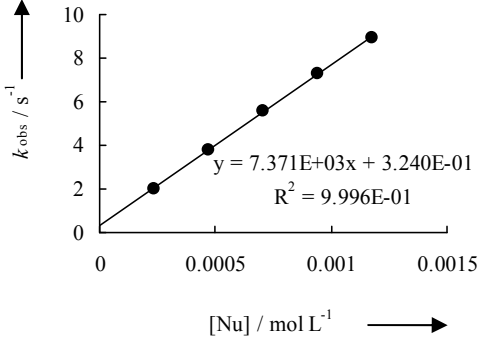
$[(\text{thq})_2\text{CH}^+]$ (mol L <sup>-1</sup> )	<b>[1b]</b> (mol L <sup>-1</sup> )	$k_{\text{obs}}$ (s <sup>-1</sup> )	$\lambda = 626 \text{ nm}$	$k$ (M <sup>-1</sup> s <sup>-1</sup> )
$1.61 \times 10^{-5}$	$9.86 \times 10^{-5}$	6.61		$6.73 \times 10^4$
	$1.97 \times 10^{-4}$	14.8		
	$2.96 \times 10^{-4}$	20.7		
	$3.95 \times 10^{-4}$	26.8		
	$4.93 \times 10^{-4}$	33.8		
$[(\text{ind})_2\text{CH}^+]$ (mol L <sup>-1</sup> )	<b>[1b]</b> (mol L <sup>-1</sup> )	$k_{\text{obs}}$ (s <sup>-1</sup> )	$\lambda = 626 \text{ nm}$	$k$ (M <sup>-1</sup> s <sup>-1</sup> )
$1.43 \times 10^{-5}$	$9.86 \times 10^{-5}$	2.40		$2.59 \times 10^4$
	$1.97 \times 10^{-4}$	5.03		
	$2.96 \times 10^{-4}$	7.49		
	$3.95 \times 10^{-4}$	10.0		
	$4.93 \times 10^{-4}$	12.7		
$[(\text{jul})_2\text{CH}^+]$ (mol L <sup>-1</sup> )	<b>[1b]</b> (mol L <sup>-1</sup> )	$k_{\text{obs}}$ (s <sup>-1</sup> )	$\lambda = 640 \text{ nm}$	$k$ (M <sup>-1</sup> s <sup>-1</sup> )
$1.35 \times 10^{-5}$	$2.35 \times 10^{-4}$	2.03		$7.37 \times 10^3$
	$4.71 \times 10^{-4}$	3.77		
	$7.06 \times 10^{-4}$	5.60		
	$9.41 \times 10^{-4}$	7.29		
	$1.18 \times 10^{-3}$	8.94		

Table 7 Continued

$[(\text{il})_2\text{CH}^+]$ (mol L <sup>-1</sup> )	<b>[1b]</b> (mol L <sup>-1</sup> )	$k_{\text{obs}}$ (s <sup>-1</sup> )	$\lambda = 640 \text{ nm}$	$k$ (M <sup>-1</sup> s <sup>-1</sup> )
$1.37 \times 10^{-5}$	$2.36 \times 10^{-4}$	0.705		$2.49 \times 10^3$
	$4.73 \times 10^{-4}$	1.27		
	$7.09 \times 10^{-4}$	1.86		
	$9.45 \times 10^{-4}$	2.44		
	$1.18 \times 10^{-3}$	3.06		

Reactivity parameters for 2-benzyl-1,1,3,3-tetramethylguanidine (**1b**) in CH<sub>2</sub>Cl<sub>2</sub>

Ar <sub>2</sub> CH <sup>+</sup>	<i>E</i>	$k$ (M <sup>-1</sup> s <sup>-1</sup> )
(thq) <sub>2</sub> CH <sup>+</sup>	-8.22	$6.73 \times 10^4$
(ind) <sub>2</sub> CH <sup>+</sup>	-8.76	$2.59 \times 10^4$
(jul) <sub>2</sub> CH <sup>+</sup>	-9.45	$7.37 \times 10^3$
(il) <sub>2</sub> CH <sup>+</sup>	-10.04	$2.49 \times 10^3$

Table 8. Kinetics of the reactions of 1,3-dimethylimidazolidin-2-imine (**1c**) with (Ar)<sub>2</sub>CH<sup>+</sup> in CH<sub>2</sub>Cl<sub>2</sub> at 20 °C.

$[(\text{pyr})_2\text{CH}^+]$ (mol L <sup>-1</sup> )	<b>[1c]</b> (mol L <sup>-1</sup> )	$k_{\text{obs}}$ (s <sup>-1</sup> )	$\lambda = 626 \text{ nm}$	$k$ (M <sup>-1</sup> s <sup>-1</sup> )
$6.12 \times 10^{-6}$	$6.83 \times 10^{-5}$	2.55		$1.42 \times 10^4$
	$1.37 \times 10^{-4}$	3.29		
	$2.05 \times 10^{-4}$	4.48		
	$2.73 \times 10^{-4}$	5.22		
	$3.41 \times 10^{-4}$	6.43		

Table 8 Continued.

$[(\text{ind})_2\text{CH}^+]$ (mol L <sup>-1</sup> )	$[\mathbf{1c}]$ (mol L <sup>-1</sup> )	$k_{\text{obs}}$ (s <sup>-1</sup> )	$\lambda = 626 \text{ nm}$	$k$ (M <sup>-1</sup> s <sup>-1</sup> )
$9.20 \times 10^{-6}$	$6.83 \times 10^{-5}$	$1.75 \times 10^{-1}$		$1.92 \times 10^3$
	$1.37 \times 10^{-4}$	$2.95 \times 10^{-1}$		
	$2.05 \times 10^{-4}$	$4.57 \times 10^{-1}$		
	$2.73 \times 10^{-4}$	$5.54 \times 10^{-1}$		
	$3.41 \times 10^{-4}$	$7.00 \times 10^{-1}$		
$[(\text{jul})_2\text{CH}^+]$ (mol L <sup>-1</sup> )	$[\mathbf{1c}]$ (mol L <sup>-1</sup> )	$k_{\text{obs}}$ (s <sup>-1</sup> )	$\lambda = 640 \text{ nm}$	$k$ (M <sup>-1</sup> s <sup>-1</sup> )
$8.10 \times 10^{-5}$	$2.94 \times 10^{-4}$	$4.04 \times 10^{-1}$		$3.47 \times 10^2$
	$5.89 \times 10^{-4}$	$5.03 \times 10^{-1}$		
	$8.83 \times 10^{-4}$	$6.09 \times 10^{-1}$		
	$1.18 \times 10^{-3}$	$7.08 \times 10^{-1}$		
	$1.47 \times 10^{-3}$	$8.12 \times 10^{-1}$		
$[(\text{liI})_2\text{CH}^+]$ (mol L <sup>-1</sup> )	$[\mathbf{1c}]$ (mol L <sup>-1</sup> )	$k_{\text{obs}}$ (s <sup>-1</sup> )	$\lambda = 640 \text{ nm}$	$k$ (M <sup>-1</sup> s <sup>-1</sup> )
$7.95 \times 10^{-6}$	$2.94 \times 10^{-4}$	$1.16 \times 10^{-1}$		$1.42 \times 10^2$
	$5.89 \times 10^{-4}$	$1.49 \times 10^{-1}$		
	$8.83 \times 10^{-4}$	$1.89 \times 10^{-1}$		
	$1.18 \times 10^{-3}$	$2.34 \times 10^{-1}$		
	$1.47 \times 10^{-3}$	$2.82 \times 10^{-1}$		

**Table 8** Continued.

Reactivity parameters for 1,3-dimethylimidazolidin-2-imine ( <b>1c</b> ) in CH <sub>2</sub> Cl <sub>2</sub>		
Ar <sub>2</sub> CH <sup>+</sup>	<i>E</i>	<i>k</i> (M <sup>-1</sup> s <sup>-1</sup> )
(pyr) <sub>2</sub> CH <sup>+</sup>	-7.69	1.42 × 10 <sup>4</sup>
(ind) <sub>2</sub> CH <sup>+</sup>	-8.76	1.92 × 10 <sup>3</sup>
(jul) <sub>2</sub> CH <sup>+</sup>	-9.45	3.47 × 10 <sup>2</sup>
(lil) <sub>2</sub> CH <sup>+</sup>	-10.04	1.42 × 10 <sup>2</sup>

  
**Table 9.** Kinetics of the reactions of N-(1,3-dimethylimidazolidin-2-ylidene)-1-phenylmethanamine (**1d**) with (Ar)<sub>2</sub>CH<sup>+</sup> in CH<sub>2</sub>Cl<sub>2</sub> at 20 °C.

[(mor) <sub>2</sub> CH <sup>+</sup> ] (mol L <sup>-1</sup> )	[ <b>1d</b> ] (mol L <sup>-1</sup> )	<i>k</i> <sub>obs</sub> (s <sup>-1</sup> )	<i>λ</i> = 620 nm	<i>k</i> (M <sup>-1</sup> s <sup>-1</sup> )
1.41 × 10 <sup>-5</sup>	7.01 × 10 <sup>-5</sup>	46.5		8.01 × 10 <sup>5</sup>
	9.35 × 10 <sup>-5</sup>	63.0		
	1.17 × 10 <sup>-4</sup>	86.1		
	1.40 × 10 <sup>-4</sup>	101		
	1.64 × 10 <sup>-4</sup>	121		

[(mpa) <sub>2</sub> CH <sup>+</sup> ] (mol L <sup>-1</sup> )	[ <b>1d</b> ] (mol L <sup>-1</sup> )	<i>k</i> <sub>obs</sub> (s <sup>-1</sup> )	<i>λ</i> = 622 nm	<i>k</i> (M <sup>-1</sup> s <sup>-1</sup> )
1.31 × 10 <sup>-5</sup>	7.01 × 10 <sup>-5</sup>	29.1		4.67 × 10 <sup>5</sup>
	9.35 × 10 <sup>-5</sup>	38.3		
	1.17 × 10 <sup>-4</sup>	50.7		
	1.40 × 10 <sup>-4</sup>	59.7		
	1.64 × 10 <sup>-4</sup>	72.9		

Table 9 Continued

$[(\text{dma})_2\text{CH}^+]$ (mol L <sup>-1</sup> )	<b>[1d]</b> (mol L <sup>-1</sup> )	$k_{\text{obs}}$ (s <sup>-1</sup> )	$\lambda = 613 \text{ nm}$	$k$ (M <sup>-1</sup> s <sup>-1</sup> )
$1.59 \times 10^{-5}$	$1.23 \times 10^{-4}$	9.72		$7.83 \times 10^4$
	$1.54 \times 10^{-4}$	11.9		
	$1.84 \times 10^{-4}$	14.5		
	$2.15 \times 10^{-4}$	16.8		
	$2.46 \times 10^{-4}$	19.3		
$[(\text{pyr})_2\text{CH}^+]$ (mol L <sup>-1</sup> )	<b>[1d]</b> (mol L <sup>-1</sup> )	$k_{\text{obs}}$ (s <sup>-1</sup> )	$\lambda = 620 \text{ nm}$	$k$ (M <sup>-1</sup> s <sup>-1</sup> )
$1.54 \times 10^{-5}$	$1.23 \times 10^{-4}$	7.31		$2.46 \times 10^4$
	$1.54 \times 10^{-4}$	7.96		
	$1.84 \times 10^{-4}$	8.89		
	$2.15 \times 10^{-4}$	9.53		
	$2.46 \times 10^{-4}$	10.3		
Reactivity parameters for N-(1,3-dimethylimidazolidin-2-ylidene)-1-phenylmethanamine ( <b>1d</b> ) in CH <sub>2</sub> Cl <sub>2</sub>				
Ar <sub>2</sub> CH <sup>+</sup>	<i>E</i>	$k$ (M <sup>-1</sup> s <sup>-1</sup> )		
(mor) <sub>2</sub> CH <sup>+</sup>	-5.53	$8.01 \times 10^5$		<b><i>N</i> = 14.00</b> <b><i>s<sub>N</sub></i> = 0.70</b>
(mpa) <sub>2</sub> CH <sup>+</sup>	-5.89	$4.67 \times 10^5$		
(dma) <sub>2</sub> CH <sup>+</sup>	-7.02	$7.83 \times 10^4$		
(pyr) <sub>2</sub> CH <sup>+</sup>	-7.69	$2.46 \times 10^4$		

**Table 10.** Kinetics of the reactions of 2,3,5,6-tetrahydro-1H-imidazo[1,2-a]imidazole (TBO, **1e**) with  $(\text{Ar})_2\text{CH}^+$  in  $\text{CH}_2\text{Cl}_2$  at 20 °C.

$[(\text{thq})_2\text{CH}^+]$ (mol L <sup>-1</sup> )	<b>[1e]</b> (mol L <sup>-1</sup> )	$k_{\text{obs}}$ (s <sup>-1</sup> )	$\lambda = 628 \text{ nm}$	$k$ (M <sup>-1</sup> s <sup>-1</sup> )
$1.58 \times 10^{-5}$	$1.18 \times 10^{-4}$	7.87		$7.85 \times 10^4$
	$1.78 \times 10^{-4}$	13.1		
	$3.55 \times 10^{-4}$	27.1		
	$4.74 \times 10^{-4}$	36.0		
	$5.92 \times 10^{-4}$	45.3		
$[(\text{ind})_2\text{CH}^+]$ (mol L <sup>-1</sup> )	<b>[1e]</b> (mol L <sup>-1</sup> )	$k_{\text{obs}}$ (s <sup>-1</sup> )	$\lambda = 625 \text{ nm}$	$k$ (M <sup>-1</sup> s <sup>-1</sup> )
$1.32 \times 10^{-5}$	$1.18 \times 10^{-4}$	3.63		$3.57 \times 10^4$
	$1.78 \times 10^{-4}$	6.03		
	$3.55 \times 10^{-4}$	12.2		
	$4.74 \times 10^{-4}$	16.6		
	$5.92 \times 10^{-4}$	20.6		
$[(\text{jul})_2\text{CH}^+]$ (mol L <sup>-1</sup> )	<b>[1e]</b> (mol L <sup>-1</sup> )	$k_{\text{obs}}$ (s <sup>-1</sup> )	$\lambda = 642 \text{ nm}$	$k$ (M <sup>-1</sup> s <sup>-1</sup> )
$1.45 \times 10^{-5}$	$1.71 \times 10^{-4}$	1.23		$7.72 \times 10^3$
	$3.43 \times 10^{-4}$	2.54		
	$5.14 \times 10^{-4}$	3.84		
	$6.86 \times 10^{-4}$	5.23		
	$8.57 \times 10^{-4}$	6.50		

Table 10 Continued.

$[(\text{il})_2\text{CH}^+]$ (mol L <sup>-1</sup> )	$[\mathbf{1e}]$ (mol L <sup>-1</sup> )	$k_{\text{obs}}$ (s <sup>-1</sup> )	$\lambda = 639 \text{ nm}$	$k$ (M <sup>-1</sup> s <sup>-1</sup> )
$1.35 \times 10^{-5}$	$1.71 \times 10^{-4}$	0.434		$3.16 \times 10^3$
	$3.43 \times 10^{-4}$	1.02		
	$5.14 \times 10^{-4}$	1.56		
	$6.86 \times 10^{-4}$	2.08		
	$8.57 \times 10^{-4}$	2.61		

Reactivity parameters for 2,3,5,6-tetrahydro-1H-imidazo[1,2-a]imidazole (TBO, <b>1e</b> ) in CH <sub>2</sub> Cl <sub>2</sub>		
Ar <sub>2</sub> CH <sup>+</sup>	$E$	$k$ (M <sup>-1</sup> s <sup>-1</sup> )
(thq) <sub>2</sub> CH <sup>+</sup>	-8.22	$7.85 \times 10^4$
(ind) <sub>2</sub> CH <sup>+</sup>	-8.76	$3.75 \times 10^4$
(jul) <sub>2</sub> CH <sup>+</sup>	-9.45	$7.72 \times 10^3$
(il) <sub>2</sub> CH <sup>+</sup>	-10.04	$3.16 \times 10^3$

		$N = 14.44$
$\log k$	$E$	$s_N = 0.79$
	-10.04	
	-9.45	
	-8.76	
	-8.22	

Table 11. Kinetics of the reactions of 1,2,3,5,6,7-hexahydroimidazo[1,2-a]pyrimidine (TBN, **1f**) with (Ar)<sub>2</sub>CH<sup>+</sup> in CH<sub>2</sub>Cl<sub>2</sub> at 20 °C.

$[(\text{thq})_2\text{CH}^+]$ (mol L <sup>-1</sup> )	$[\mathbf{1f}]$ (mol L <sup>-1</sup> )	$k_{\text{obs}}$ (s <sup>-1</sup> )	$\lambda = 626 \text{ nm}$	$k$ (M <sup>-1</sup> s <sup>-1</sup> )
$7.65 \times 10^{-6}$	$4.15 \times 10^{-5}$	22.2		$5.58 \times 10^5$
	$8.31 \times 10^{-5}$	42.0		
	$1.25 \times 10^{-4}$	67.4		
	$1.66 \times 10^{-4}$	92.0		
	$2.08 \times 10^{-4}$	113		

Table 11 Continued.

$[(\text{ind})_2\text{CH}^+]$ (mol L <sup>-1</sup> )	$[\mathbf{1f}]$ (mol L <sup>-1</sup> )	$k_{\text{obs}}$ (s <sup>-1</sup> )	$\lambda = 626 \text{ nm}$	$k$ (M <sup>-1</sup> s <sup>-1</sup> )
$7.00 \times 10^{-6}$	$4.15 \times 10^{-5}$	10.2		$2.42 \times 10^5$
	$8.31 \times 10^{-5}$	18.7		
	$1.25 \times 10^{-4}$	29.7		
	$1.66 \times 10^{-4}$	40.7		
	$2.08 \times 10^{-4}$	49.3		
$[(\text{jul})_2\text{CH}^+]$ (mol L <sup>-1</sup> )	$[\mathbf{1f}]$ (mol L <sup>-1</sup> )	$k_{\text{obs}}$ (s <sup>-1</sup> )	$\lambda = 640 \text{ nm}$	$k$ (M <sup>-1</sup> s <sup>-1</sup> )
$7.20 \times 10^{-6}$	$9.15 \times 10^{-5}$	4.91		$6.38 \times 10^4$
	$1.83 \times 10^{-4}$	10.8		
	$2.74 \times 10^{-4}$	16.6		
	$3.66 \times 10^{-4}$	22.8		
	$4.57 \times 10^{-4}$	28.1		
$[(\text{lil})_2\text{CH}^+]$ (mol L <sup>-1</sup> )	$[\mathbf{1f}]$ (mol L <sup>-1</sup> )	$k_{\text{obs}}$ (s <sup>-1</sup> )	$\lambda = 640 \text{ nm}$	$k$ (M <sup>-1</sup> s <sup>-1</sup> )
$7.93 \times 10^{-6}$	$9.15 \times 10^{-5}$	1.94		$2.86 \times 10^4$
	$1.83 \times 10^{-4}$	4.29		
	$2.74 \times 10^{-4}$	7.00		
	$3.66 \times 10^{-4}$	9.73		
	$4.57 \times 10^{-4}$	12.3		

**Table 11** Continued.Reactivity parameters for 1,2,3,5,6,7-hexahydroimidazo[1,2-a]pyrimidine (TBN, **1f**) in CH<sub>2</sub>Cl<sub>2</sub>

Ar <sub>2</sub> CH <sup>+</sup>	<i>E</i>	<i>k</i> (M <sup>-1</sup> s <sup>-1</sup> )
(thq) <sub>2</sub> CH <sup>+</sup>	-8.22	5.58 × 10 <sup>5</sup>
(ind) <sub>2</sub> CH <sup>+</sup>	-8.76	2.42 × 10 <sup>5</sup>
(jul) <sub>2</sub> CH <sup>+</sup>	-9.45	6.38 × 10 <sup>4</sup>
(lil) <sub>2</sub> CH <sup>+</sup>	-10.04	2.86 × 10 <sup>4</sup>

  
**Table 12.** Kinetics of the reactions of 2,3,4,6,7,8-hexahydro-1H-pyrimido[1,2-a]pyrimidine (TBD, **1g**) with (Ar)<sub>2</sub>CH<sup>+</sup> in CH<sub>2</sub>Cl<sub>2</sub> at 20 °C.

[(ind) <sub>2</sub> CH <sup>+</sup> ] (mol L <sup>-1</sup> )	[ <b>1g</b> ] (mol L <sup>-1</sup> )	<i>k</i> <sub>obs</sub> (s <sup>-1</sup> )	λ = 625 nm	<i>k</i> (M <sup>-1</sup> s <sup>-1</sup> )
1.60 × 10 <sup>-5</sup>	1.72 × 10 <sup>-4</sup>	59.1		3.84 × 10 <sup>5</sup>
	2.16 × 10 <sup>-4</sup>	77.3		
	3.02 × 10 <sup>-4</sup>	113		
	3.45 × 10 <sup>-4</sup>	124		

[(jul) <sub>2</sub> CH <sup>+</sup> ] (mol L <sup>-1</sup> )	[ <b>1g</b> ] (mol L <sup>-1</sup> )	<i>k</i> <sub>obs</sub> (s <sup>-1</sup> )	λ = 642 nm	<i>k</i> (M <sup>-1</sup> s <sup>-1</sup> )
1.50 × 10 <sup>-5</sup>	1.72 × 10 <sup>-4</sup>	14.1		9.72 × 10 <sup>4</sup>
	2.16 × 10 <sup>-4</sup>	18.6		
	3.02 × 10 <sup>-4</sup>	27.3		
	3.45 × 10 <sup>-4</sup>	31.1		
	3.88 × 10 <sup>-4</sup>	35.0		

Table 12 Continued.

$[(\text{lil})_2\text{CH}^+]$ (mol L <sup>-1</sup> )	$[\mathbf{1g}]$ (mol L <sup>-1</sup> )	$k_{\text{obs}}$ (s <sup>-1</sup> )	$\lambda = 639 \text{ nm}$	$k$ (M <sup>-1</sup> s <sup>-1</sup> )
$1.50 \times 10^{-6}$	$2.08 \times 10^{-4}$	6.69		$4.24 \times 10^4$
	$2.60 \times 10^{-4}$	8.74		
	$3.13 \times 10^{-4}$	10.9		
	$3.65 \times 10^{-4}$	13.1		
	$4.17 \times 10^{-4}$	15.6		

$\text{Ar}_2\text{CH}^+$	$E$	$k$ (M <sup>-1</sup> s <sup>-1</sup> )	$N = 16.16$ $s_N = 0.75$
$(\text{ind})_2\text{CH}^+$	-8.76	$3.84 \times 10^5$	
$(\text{jul})_2\text{CH}^+$	-9.45	$9.72 \times 10^4$	
$(\text{lil})_2\text{CH}^+$	-10.04	$4.24 \times 10^4$	

Table 13. Kinetics of the reactions of 1-methyl-2,3,4,6,7,8-hexahydro-1H-pyrimido[1,2-a]pyrimidine (MTBD, **1h**) with  $(\text{Ar})_2\text{CH}^+$  in  $\text{CH}_2\text{Cl}_2$  at 20 °C.

$[(\text{thq})_2\text{CH}^+]$ (mol L <sup>-1</sup> )	$[\mathbf{1h}]$ (mol L <sup>-1</sup> )	$k_{\text{obs}}$ (s <sup>-1</sup> )	$\lambda = 625 \text{ nm}$	$k$ (M <sup>-1</sup> s <sup>-1</sup> )
$1.38 \times 10^{-5}$	$1.20 \times 10^{-4}$	12.7		$1.07 \times 10^5$
	$2.40 \times 10^{-4}$	26.7		
	$3.60 \times 10^{-4}$	40.1		
	$4.80 \times 10^{-4}$	52.0		
	$6.00 \times 10^{-4}$	64.5		

Table 13 Continued

$[(\text{ind})_2\text{CH}^+]$ (mol L <sup>-1</sup> )	$[\mathbf{1h}]$ (mol L <sup>-1</sup> )	$k_{\text{obs}}$ (s <sup>-1</sup> )	$\lambda = 625 \text{ nm}$	$k$ (M <sup>-1</sup> s <sup>-1</sup> )
$1.44 \times 10^{-5}$	$1.20 \times 10^{-4}$	5.11		$4.85 \times 10^4$
	$2.40 \times 10^{-4}$	11.1		
	$3.60 \times 10^{-4}$	17.3		
	$4.80 \times 10^{-4}$	22.8		
	$6.00 \times 10^{-4}$	28.4		
$[(\text{jul})_2\text{CH}^+]$ (mol L <sup>-1</sup> )	$[\mathbf{1h}]$ (mol L <sup>-1</sup> )	$k_{\text{obs}}$ (s <sup>-1</sup> )	$\lambda = 641 \text{ nm}$	$k$ (M <sup>-1</sup> s <sup>-1</sup> )
$1.42 \times 10^{-5}$	$2.15 \times 10^{-4}$	1.96		$1.06 \times 10^4$
	$3.23 \times 10^{-4}$	3.14		
	$4.31 \times 10^{-4}$	4.15		
	$5.38 \times 10^{-4}$	5.41		
$[(\text{lil})_2\text{CH}^+]$ (mol L <sup>-1</sup> )	$[\mathbf{1h}]$ (mol L <sup>-1</sup> )	$k_{\text{obs}}$ (s <sup>-1</sup> )	$\lambda = 639 \text{ nm}$	$k$ (M <sup>-1</sup> s <sup>-1</sup> )
$1.58 \times 10^{-5}$	$2.36 \times 10^{-4}$	0.841		$3.84 \times 10^3$
	$4.71 \times 10^{-4}$	1.75		
	$7.07 \times 10^{-4}$	2.61		
	$9.42 \times 10^{-4}$	3.55		
	$1.18 \times 10^{-3}$	4.46		

**Table 13** ContinuedReactivity parameters for 1-methyl-2,3,4,6,7,8-hexahydro-1H-pyrimido[1,2-a]pyrimidine (MTBD, **1h**) in CH<sub>2</sub>Cl<sub>2</sub>

Ar <sub>2</sub> CH <sup>+</sup>	<i>E</i>	<i>k</i> (M <sup>-1</sup> s <sup>-1</sup> )
(thq) <sub>2</sub> CH <sup>+</sup>	-8.22	1.07 × 10 <sup>5</sup>
(ind) <sub>2</sub> CH <sup>+</sup>	-8.76	4.85 × 10 <sup>4</sup>
(jul) <sub>2</sub> CH <sup>+</sup>	-9.45	1.06 × 10 <sup>4</sup>
(lil) <sub>2</sub> CH <sup>+</sup>	-10.04	3.84 × 10 <sup>3</sup>

  
**Table 14.** Kinetics of the reactions of 1,5-diazabicyclo(4.3.0)non-5-ene (DBN) with (Ar)<sub>2</sub>CH<sup>+</sup> in CH<sub>2</sub>Cl<sub>2</sub> at 20 °C.

[(thq) <sub>2</sub> CH <sup>+</sup> ] (mol L <sup>-1</sup> )	[DBN] (mol L <sup>-1</sup> )	<i>k</i> <sub>obs</sub> (s <sup>-1</sup> )	<i>λ</i> = 626 nm	<i>k</i> (M <sup>-1</sup> s <sup>-1</sup> )
1.61 × 10 <sup>-5</sup>	1.23 × 10 <sup>-4</sup>	33.6		3.20 × 10 <sup>5</sup>
	1.85 × 10 <sup>-4</sup>	53.0		
	2.46 × 10 <sup>-4</sup>	69.0		
	3.70 × 10 <sup>-4</sup>	112		
	4.93 × 10 <sup>-4</sup>	151		
[(ind) <sub>2</sub> CH <sup>+</sup> ] (mol L <sup>-1</sup> )	[DBN] (mol L <sup>-1</sup> )	<i>k</i> <sub>obs</sub> (s <sup>-1</sup> )	<i>λ</i> = 626 nm	<i>k</i> (M <sup>-1</sup> s <sup>-1</sup> )
1.43 × 10 <sup>-5</sup>	1.23 × 10 <sup>-4</sup>	17.8		1.50 × 10 <sup>5</sup>
	1.85 × 10 <sup>-4</sup>	28.3		
	2.46 × 10 <sup>-4</sup>	34.7		
	3.70 × 10 <sup>-4</sup>	54.4		
	4.93 × 10 <sup>-4</sup>	73.7		

Table 14 Continued

$[(\text{jul})_2\text{CH}^+]$ (mol L <sup>-1</sup> )	[DBN] (mol L <sup>-1</sup> )	$k_{\text{obs}}$ (s <sup>-1</sup> )	$\lambda = 640 \text{ nm}$	$k$ (M <sup>-1</sup> s <sup>-1</sup> )
$1.35 \times 10^{-5}$	$1.25 \times 10^{-4}$	3.16		$3.20 \times 10^4$
	$2.50 \times 10^{-4}$	6.70		
	$5.00 \times 10^{-4}$	14.5		
	$7.50 \times 10^{-4}$	23.1		
$[(\text{lil})_2\text{CH}^+]$ (mol L <sup>-1</sup> )	[DBN] (mol L <sup>-1</sup> )	$k_{\text{obs}}$ (s <sup>-1</sup> )	$\lambda = 640 \text{ nm}$	$k$ (M <sup>-1</sup> s <sup>-1</sup> )
$1.37 \times 10^{-5}$	$1.25 \times 10^{-4}$	1.47		$1.51 \times 10^4$
	$2.50 \times 10^{-4}$	3.34		
	$5.00 \times 10^{-4}$	6.94		
	$7.50 \times 10^{-4}$	11.0		
	$1.00 \times 10^{-3}$	14.6		
Reactivity parameters for 1,5-Diazabicyclo(4.3.0)non-5-ene (DBN) in CH <sub>2</sub> Cl <sub>2</sub>				
Ar <sub>2</sub> CH <sup>+</sup>	<i>E</i>	$k$ (M <sup>-1</sup> s <sup>-1</sup> )		
(thq) <sub>2</sub> CH <sup>+</sup>	-8.22	$3.20 \times 10^5$	$N = 15.50$	
(ind) <sub>2</sub> CH <sup>+</sup>	-8.76	$1.50 \times 10^5$	$s_N = 0.76$	
(jul) <sub>2</sub> CH <sup>+</sup>	-9.45	$3.20 \times 10^4$		
(lil) <sub>2</sub> CH <sup>+</sup>	-10.04	$1.51 \times 10^4$		

### 4.3.2 Determination of the Rate Constants for the Reactions of Guanidines (1) with Michael Acceptors (4).

The rates of the reaction between the guanidines **1** with the Michael acceptors (**4**) were measured photometrically, under pseudo-first-order conditions (excess of guanidine) at or close to the absorption maximum of **4** by conventional stopped flow technique at 20 °C in dry CH<sub>2</sub>Cl<sub>2</sub> as described previously.<sup>[12b]</sup> First-order rate constants  $k_{\text{obs}}$  were obtained by least-squares fitting of the absorbances to the mono-exponential  $A_t = A_0 \exp(-k_{\text{obs}}t) + C$ . Since  $k_{\text{obs}} = k[\text{Nu}]$ , the second-order rate constants  $k$  (M<sup>-1</sup> s<sup>-1</sup>) were derived from the slopes of the linear plots of  $k_{\text{obs}}$  (s<sup>-1</sup>) vs. [Nu].

**Table 15.** Kinetics of the reactions of 2-benzylidene-1H-indene-1,3(2H)-dione (**4a**) with the guanidines **1** in CH<sub>2</sub>Cl<sub>2</sub> at 20 °C.

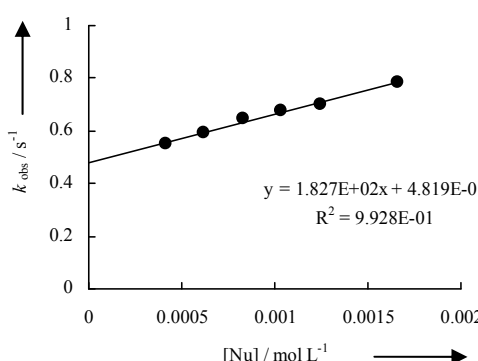
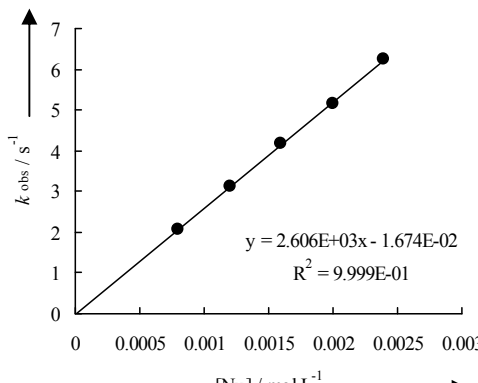
[ <b>4a</b> ] (mol L <sup>-1</sup> )	[ <b>1a</b> ] (mol L <sup>-1</sup> )	$k_{\text{obs}}$ (s <sup>-1</sup> )	$\lambda = 340 \text{ nm}$	$k$ (M <sup>-1</sup> s <sup>-1</sup> )
$5.12 \times 10^{-5}$	$4.15 \times 10^{-4}$	0.553		$1.81 \times 10^2$
	$6.23 \times 10^{-4}$	0.592		
	$8.30 \times 10^{-4}$	0.644		
	$1.04 \times 10^{-3}$	0.678		
	$1.25 \times 10^{-3}$	0.702		
	$1.66 \times 10^{-3}$	0.782		
[ <b>4a</b> ] (mol L <sup>-1</sup> )	[ <b>1e</b> ] (mol L <sup>-1</sup> )	$k_{\text{obs}}$ (s <sup>-1</sup> )	$\lambda = 340 \text{ nm}$	$k$ (M <sup>-1</sup> s <sup>-1</sup> )
$6.00 \times 10^{-5}$	$7.99 \times 10^{-4}$	2.06		$2.61 \times 10^3$
	$1.20 \times 10^{-3}$	3.11		
	$1.60 \times 10^{-3}$	4.16		
	$2.00 \times 10^{-3}$	5.15		
	$2.40 \times 10^{-3}$	6.24		

Table 15 continued.

[4a] (mol L <sup>-1</sup> )	[1g] (mol L <sup>-1</sup> )	<i>k</i> <sub>obs</sub> (s <sup>-1</sup> )	λ = 340 nm	<i>k</i> (M <sup>-1</sup> s <sup>-1</sup> )
3.00 × 10 <sup>-5</sup>	2.03 × 10 <sup>-4</sup>	4.56		2.95 × 10 <sup>4</sup>
	2.70 × 10 <sup>-4</sup>	6.63		
	3.38 × 10 <sup>-4</sup>	9.03		
	4.05 × 10 <sup>-4</sup>	10.8		
	5.40 × 10 <sup>-4</sup>	14.6		
	6.08 × 10 <sup>-4</sup>	16.9		
	6.75 × 10 <sup>-4</sup>	18.5		

Table 16. Kinetics of the reactions of 5-(4-methoxybenzylidene)-2,2-dimethyl-1,3-dioxane-4,6-dione (**4b**) with the guanidines **1** in CH<sub>2</sub>Cl<sub>2</sub> at 20 °C.

[4b] (mol L <sup>-1</sup> )	[1a] (mol L <sup>-1</sup> )	<i>k</i> <sub>obs</sub> (s <sup>-1</sup> )	λ = 366 nm	<i>k</i> (M <sup>-1</sup> s <sup>-1</sup> )
4.64 × 10 <sup>-5</sup>	4.15 × 10 <sup>-4</sup>	0.770		1.76 × 10 <sup>3</sup>
	6.23 × 10 <sup>-4</sup>	1.13		
	8.30 × 10 <sup>-4</sup>	1.50		
	1.04 × 10 <sup>-3</sup>	1.84		
	1.25 × 10 <sup>-3</sup>	2.24		
[4b] (mol L <sup>-1</sup> )	[1e] (mol L <sup>-1</sup> )	<i>k</i> <sub>obs</sub> (s <sup>-1</sup> )	λ = 366 nm	<i>k</i> (M <sup>-1</sup> s <sup>-1</sup> )
5.87 × 10 <sup>-5</sup>	7.99 × 10 <sup>-4</sup>	50.2		6.57 × 10 <sup>4</sup>
	1.20 × 10 <sup>-3</sup>	76.2		
	1.60 × 10 <sup>-3</sup>	103		
	2.00 × 10 <sup>-3</sup>	129		
	2.40 × 10 <sup>-3</sup>	155		

Table 16 continued

[4b] (mol L <sup>-1</sup> )	[1g] (mol L <sup>-1</sup> )	<i>k</i> <sub>obs</sub> (s <sup>-1</sup> )	λ = 366 nm	<i>k</i> (M <sup>-1</sup> s <sup>-1</sup> )
8.42 × 10 <sup>-5</sup>	3.06 × 10 <sup>-4</sup>	111		3.67 × 10 <sup>5</sup>
	3.57 × 10 <sup>-4</sup>	131		
	4.08 × 10 <sup>-4</sup>	152		
	4.59 × 10 <sup>-4</sup>	176		
	5.10 × 10 <sup>-4</sup>	182		
[4b] (mol L <sup>-1</sup> )	[1h] (mol L <sup>-1</sup> )	<i>k</i> <sub>obs</sub> (s <sup>-1</sup> )	λ = 380 nm	<i>k</i> (M <sup>-1</sup> s <sup>-1</sup> )
6.41 × 10 <sup>-5</sup>	1.45 × 10 <sup>-3</sup>	12.1		2.19 × 10 <sup>3</sup>
	2.17 × 10 <sup>-3</sup>	13.3		
	2.89 × 10 <sup>-3</sup>	15.3		
	4.34 × 10 <sup>-3</sup>	18.5		
	5.78 × 10 <sup>-3</sup>	21.4		

Table 17. Kinetics of the reactions of 5-(4-methoxybenzylidene)-1,3-dimethylpyrimidine-2,4,6(1H,3H,5H)-trione (4c) with the guanidines 1 in CH<sub>2</sub>Cl<sub>2</sub> at 20 °C.

[4c] (mol L <sup>-1</sup> )	[1a] (mol L <sup>-1</sup> )	<i>k</i> <sub>obs</sub> (s <sup>-1</sup> )	λ = 378 nm	<i>k</i> (M <sup>-1</sup> s <sup>-1</sup> )
3.78 × 10 <sup>-5</sup>	4.15 × 10 <sup>-4</sup>	0.353		8.62 × 10 <sup>2</sup>
	6.23 × 10 <sup>-4</sup>	0.533		
	8.30 × 10 <sup>-4</sup>	0.720		
	1.04 × 10 <sup>-3</sup>	0.888		
	1.25 × 10 <sup>-3</sup>	1.07		

Table 17 continued.

[4c] (mol L <sup>-1</sup> )	[1e] (mol L <sup>-1</sup> )	<i>k</i> <sub>obs</sub> (s <sup>-1</sup> )	λ = 378 nm	<i>k</i> (M <sup>-1</sup> s <sup>-1</sup> )
5.10 × 10 <sup>-5</sup>	4.34 × 10 <sup>-4</sup>	10.2		2.30 × 10 <sup>4</sup>
	8.69 × 10 <sup>-4</sup>	20.7		
	1.30 × 10 <sup>-3</sup>	31.3		
	1.74 × 10 <sup>-3</sup>	41.1		
	2.17 × 10 <sup>-3</sup>	50.0		
[4c] (mol L <sup>-1</sup> )	[1g] (mol L <sup>-1</sup> )	<i>k</i> <sub>obs</sub> (s <sup>-1</sup> )	λ = 380 nm	<i>k</i> (M <sup>-1</sup> s <sup>-1</sup> )
6.45 × 10 <sup>-5</sup>	5.09 × 10 <sup>-4</sup>	92.7		2.11 × 10 <sup>5</sup>
	5.82 × 10 <sup>-4</sup>	104		
	6.55 × 10 <sup>-4</sup>	125		
	7.27 × 10 <sup>-4</sup>	139		
	8.00 × 10 <sup>-4</sup>	152		
[4c] (mol L <sup>-1</sup> )	[1h] (mol L <sup>-1</sup> )	<i>k</i> <sub>obs</sub> (s <sup>-1</sup> )	λ = 380 nm	<i>k</i> (M <sup>-1</sup> s <sup>-1</sup> )
5.83 × 10 <sup>-5</sup>	1.45 × 10 <sup>-3</sup>	13.5		2.33 × 10 <sup>3</sup>
	2.17 × 10 <sup>-3</sup>	15.4		
	2.89 × 10 <sup>-3</sup>	17.1		
	4.34 × 10 <sup>-3</sup>	20.3		
	5.78 × 10 <sup>-3</sup>	23.7		

**Table 18.** Kinetics of the reactions of 2-(4-methoxybenzylidene)-1H-indene-1,3(2H)-dione (**4d**) with the guanidines **1** in CH<sub>2</sub>Cl<sub>2</sub> at 20 °C.

[ <b>4d</b> ] (mol L <sup>-1</sup> )	[ <b>1e</b> ] (mol L <sup>-1</sup> )	<i>k</i> <sub>obs</sub> (s <sup>-1</sup> )	λ = 384 nm	<i>k</i> (M <sup>-1</sup> s <sup>-1</sup> )
6.32 × 10 <sup>-5</sup>	4.34 × 10 <sup>-4</sup>	0.562		7.91 × 10 <sup>2</sup>
	8.69 × 10 <sup>-4</sup>	0.908		
	1.30 × 10 <sup>-3</sup>	1.26		
	1.74 × 10 <sup>-3</sup>	1.61		
	2.17 × 10 <sup>-3</sup>	1.93		
[ <b>4d</b> ] (mol L <sup>-1</sup> )	[ <b>1g</b> ] (mol L <sup>-1</sup> )	<i>k</i> <sub>obs</sub> (s <sup>-1</sup> )	λ = 384 nm	<i>k</i> (M <sup>-1</sup> s <sup>-1</sup> )
3.75 × 10 <sup>-5</sup>	2.03 × 10 <sup>-4</sup>	1.47		7.37 × 10 <sup>3</sup>
	2.70 × 10 <sup>-4</sup>	1.86		
	3.38 × 10 <sup>-4</sup>	2.58		
	5.40 × 10 <sup>-4</sup>	4.02		
	6.75 × 10 <sup>-4</sup>	4.90		

#### 4.4 Equilibrium constants ( $K$ ) for the reactions of the electrophiles **2** and **4** with guanidines (**1**) in $\text{CH}_2\text{Cl}_2$ .

Equilibrium constants were measured by UV-vis spectroscopy in  $\text{CH}_2\text{Cl}_2$  as follows: To a solution of the electrophiles **2** and **4** in dichloromethane small volumes of stock solutions of guanidines (**1**) were added and the resulting absorptions of the electrophiles **2** and **4** were monitored. When the absorbance was constant, another portion of the stock solution was added. This procedure was repeated two to four times for each electrophile solution.

Assuming a proportionality between the absorbances and the concentrations of electrophiles, the equilibrium constants ( $K$ ) can be expressed by the absorbances of **2** and **4** before ( $A_0$ ) and after ( $A$ ) the addition of guanidines using equation (3) and (4).

The temperature of the solutions during all equilibrium studies was kept constant at  $(20.0 \pm 0.1)^\circ\text{C}$  using a circulating bath thermostat.

**Table 19.** Determination of the equilibrium constant for the reaction of  $(\text{ind})_2\text{CH}^+$  with 2-benzyl-1,1,3,3-tetramethylguanidine (**1b**).

$\varepsilon[(\text{ind})_2\text{CH}^+ \text{ at } 625 \text{ nm}] = 1.32 \times 10^5 \text{ M}^{-1} \text{ cm}^{-1}$  and  $d = 0.5 \text{ cm}$ ,  $\text{CH}_2\text{Cl}_2$  at  $20.0^\circ\text{C}$ .

Entry	$[\mathbf{1b}]_0$ (mol L <sup>-1</sup> )	$A$	$[(\text{ind})_2\text{CH}^+]_{\text{eq}}$ (mol L <sup>-1</sup> )	$K$ (L mol <sup>-1</sup> )
0	0	0.899	$1.364 \times 10^{-5}$	
1	$2.693 \times 10^{-5}$	0.039	$5.9 \times 10^{-7}$	$1.6 \times 10^6$
0	0	0.868	$1.316 \times 10^{-5}$	
1	$5.406 \times 10^{-5}$	0.014	$2.1 \times 10^{-7}$	$1.5 \times 10^6$
0	0	0.844	$1.280 \times 10^{-5}$	
1	$2.664 \times 10^{-5}$	0.036	$5.5 \times 10^{-7}$	$1.5 \times 10^6$
2	$5.316 \times 10^{-5}$	0.014	$2.1 \times 10^{-7}$	$1.5 \times 10^6$
0	0	0.851	$1.290 \times 10^{-5}$	
1	$2.693 \times 10^{-5}$	0.039	$5.9 \times 10^{-7}$	$1.4 \times 10^6$
2	$5.373 \times 10^{-5}$	0.014	$2.2 \times 10^{-7}$	$1.4 \times 10^6$

$$K_{\text{av}}(20^\circ\text{C}) = 1.5 \times 10^6 \text{ L mol}^{-1}$$

**Table 20.** Determination of the equilibrium constant for the reaction of (jul)<sub>2</sub>CH<sup>+</sup> with 2-benzyl-1,1,3,3-tetramethylguanidine (**1b**). $\varepsilon[(\text{jul})_2\text{CH}^+ \text{ at } 642 \text{ nm}] = 2.24 \times 10^5 \text{ M}^{-1} \text{ cm}^{-1}$  and  $d = 0.5 \text{ cm}$ , CH<sub>2</sub>Cl<sub>2</sub> at 20.0 °C.

Entry	[ <b>1b</b> ] <sub>0</sub> (mol L <sup>-1</sup> )	<i>A</i>	[(jul) <sub>2</sub> CH <sup>+</sup> ] <sub>eq</sub> (mol L <sup>-1</sup> )	<i>K</i> (L mol <sup>-1</sup> )
0	0	0.814	$7.271 \times 10^{-6}$	
1	$2.655 \times 10^{-5}$	0.408	$3.645 \times 10^{-6}$	$4.33 \times 10^4$
0	0	0.782	$6.988 \times 10^{-6}$	
1	$5.285 \times 10^{-5}$	0.249	$2.228 \times 10^{-6}$	$4.40 \times 10^4$
0	0	0.794	$7.089 \times 10^{-6}$	
1	$8.060 \times 10^{-5}$	0.185	$1.655 \times 10^{-6}$	$4.44 \times 10^4$
0	0	0.792	$7.078 \times 10^{-6}$	
1	$1.073 \times 10^{-4}$	0.145	$1.294 \times 10^{-6}$	$4.46 \times 10^4$
0	0	0.798	$7.132 \times 10^{-6}$	
1	$1.340 \times 10^{-4}$	0.124	$1.107 \times 10^{-6}$	$4.30 \times 10^4$

$$K_{\text{av}}(20 \text{ }^\circ\text{C}) = 4.39 \times 10^4 \text{ L mol}^{-1}$$

**Table 21.** Determination of the equilibrium constant for the reaction of (lil)<sub>2</sub>CH<sup>+</sup> with 2-benzyl-1,1,3,3-tetramethylguanidine (**1b**). $\varepsilon[(\text{lil})_2\text{CH}^+ \text{ at } 639 \text{ nm}] = 1.59 \times 10^5 \text{ M}^{-1} \text{ cm}^{-1}$  and  $d = 0.5 \text{ cm}$ , CH<sub>2</sub>Cl<sub>2</sub> at 20.0 °C.

Entry	[ <b>1b</b> ] <sub>0</sub> (mol L <sup>-1</sup> )	<i>A</i>	[(lil) <sub>2</sub> CH <sup>+</sup> ] <sub>eq</sub> (mol L <sup>-1</sup> )	<i>K</i> (L mol <sup>-1</sup> )
0	0	0.785	$9.908 \times 10^{-6}$	
1	$2.658 \times 10^{-5}$	0.406	$5.127 \times 10^{-6}$	$4.26 \times 10^4$
0	0	0.781	$9.850 \times 10^{-6}$	
1	$5.367 \times 10^{-5}$	0.257	$3.248 \times 10^{-6}$	$4.38 \times 10^4$
0	0	0.780	$9.842 \times 10^{-6}$	
1	$8.012 \times 10^{-5}$	0.190	$2.399 \times 10^{-6}$	$4.29 \times 10^4$
0	0	0.759	$9.575 \times 10^{-6}$	
1	$1.063 \times 10^{-4}$	0.143	$1.800 \times 10^{-6}$	$4.38 \times 10^4$
0	0	0.795	$1.003 \times 10^{-5}$	
1	$1.356 \times 10^{-4}$	0.118	$1.494 \times 10^{-6}$	$4.61 \times 10^4$

$$K_{\text{av}}(20 \text{ }^\circ\text{C}) = 4.38 \times 10^4 \text{ L mol}^{-1}$$

**Table 22.** Determination of the equilibrium constant for the reaction of (pyr)<sub>2</sub>CH<sup>+</sup> with N-(1,3-dimethylimidazolidin-2-ylidene)-1-phenylmethanamine (**1d**). $\varepsilon$  [(pyr)<sub>2</sub>CH<sup>+</sup> at 639 nm] =  $1.74 \times 10^5 \text{ M}^{-1} \text{ cm}^{-1}$  and  $d = 0.5 \text{ cm}$ , CH<sub>2</sub>Cl<sub>2</sub> at 20.0 °C.Since the final absorbance of (pyr)<sub>2</sub>CH<sup>+</sup> was not stable after its reactions with **1d** the equilibrium constant mentioned in this table is approximate.

Entry	[ <b>1d</b> ] <sub>0</sub> (mol L <sup>-1</sup> )	<i>A</i>	[(pyr) <sub>2</sub> CH <sup>+</sup> ] <sub>eq</sub> (mol L <sup>-1</sup> )	<i>K</i> (L mol <sup>-1</sup> )
0	0	0.580	$6.675 \times 10^{-6}$	
1	$1.435 \times 10^{-5}$	0.423	$4.871 \times 10^{-6}$	$2.94 \times 10^4$
0	0	0.589	$6.780 \times 10^{-6}$	
1	$2.808 \times 10^{-5}$	0.308	$3.548 \times 10^{-6}$	$3.47 \times 10^4$
0	0	0.574	$6.601 \times 10^{-6}$	
1	$4.222 \times 10^{-5}$	0.281	$3.234 \times 10^{-6}$	$2.56 \times 10^4$
0	0	0.578	$6.651 \times 10^{-6}$	
1	$5.6222 \times 10^{-5}$	0.170	$1.961 \times 10^{-6}$	$4.49 \times 10^4$
0	0	0.577	$6.642 \times 10^{-6}$	
1	$6.479 \times 10^{-5}$	0.114	$1.311 \times 10^{-6}$	$6.07 \times 10^4$

$$K_{\text{av}}(20 \text{ }^\circ\text{C}) = 3.9 \times 10^4 \text{ L mol}^{-1}$$

**Table 23.** Determination of the equilibrium constant for the reaction of (ind)<sub>2</sub>CH<sup>+</sup> with N-(1,3-dimethylimidazolidin-2-ylidene)-1-phenylmethanamine (**1d**). $\varepsilon$  [(ind)<sub>2</sub>CH<sup>+</sup> at 625 nm] =  $1.32 \times 10^5 \text{ M}^{-1} \text{ cm}^{-1}$  and  $d = 0.5 \text{ cm}$ , CH<sub>2</sub>Cl<sub>2</sub> at 20.0 °C.Since the final absorbance of (ind)<sub>2</sub>CH<sup>+</sup> was not stable after its reactions with **1d** equilibrium constant mentioned in this table is approximate.

Entry	[ <b>1d</b> ] <sub>0</sub> (mol L <sup>-1</sup> )	<i>A</i>	[(ind) <sub>2</sub> CH <sup>+</sup> ] <sub>eq</sub> (mol L <sup>-1</sup> )	<i>K</i> (L mol <sup>-1</sup> )
0	0	0.594	$9.009 \times 10^{-6}$	
1	$5.663 \times 10^{-5}$	0.306	$4.642 \times 10^{-6}$	$1.78 \times 10^4$
0	0	0.615	$9.324 \times 10^{-6}$	
1	$8.354 \times 10^{-5}$	0.216	$3.269 \times 10^{-6}$	$2.31 \times 10^4$
0	0	0.618	$9.376 \times 10^{-6}$	
1	$2.818 \times 10^{-5}$	0.445	$6.747 \times 10^{-6}$	$1.47 \times 10^4$

$$K_{\text{av}}(20 \text{ }^\circ\text{C}) = 1.9 \times 10^4 \text{ L mol}^{-1}$$

**Table 24.** Determination of the equilibrium constant for the reaction of (jul)<sub>2</sub>CH<sup>+</sup> with 1-methyl-2,3,4,6,7,8-hexahydro-1H-pyrimido[1,2-a]pyrimidine (**1h**). $\varepsilon$  [(jul)<sub>2</sub>CH<sup>+</sup> at 642 nm] =  $2.24 \times 10^5 \text{ M}^{-1} \text{ cm}^{-1}$  and  $d = 0.5 \text{ cm}$ , CH<sub>2</sub>Cl<sub>2</sub> at 20.0 °C.

Entry	[ <b>1h</b> ] <sub>0</sub> (mol L <sup>-1</sup> )	<i>A</i>	[(jul) <sub>2</sub> CH <sup>+</sup> ] <sub>eq</sub> (mol L <sup>-1</sup> )	<i>K</i> (L mol <sup>-1</sup> )
0	0	0.822	$7.346 \times 10^{-6}$	
1	$2.398 \times 10^{-5}$	0.215	$1.920 \times 10^{-6}$	$1.52 \times 10^5$
2	$4.773 \times 10^{-5}$	0.111	$9.916 \times 10^{-7}$	$1.53 \times 10^5$
0	0	0.823	$7.355 \times 10^{-6}$	
1	$2.406 \times 10^{-5}$	0.216	$1.928 \times 10^{-6}$	$1.51 \times 10^5$
2	$4.789 \times 10^{-5}$	0.109	$9.702 \times 10^{-7}$	$1.58 \times 10^5$
0	0	0.822	$7.347 \times 10^{-6}$	
1	$2.441 \times 10^{-5}$	0.213	$1.902 \times 10^{-6}$	$1.55 \times 10^5$
2	$4.858 \times 10^{-5}$	0.110	$9.791 \times 10^{-7}$	$1.56 \times 10^5$

$$K_{\text{av}}(20 \text{ }^\circ\text{C}) = 1.54 \times 10^5 \text{ L mol}^{-1}$$

**Table 25.** Determination of the equilibrium constant for the reaction of  $(\text{lil})_2\text{CH}^+$  with 1-methyl-2,3,4,6,7,8-hexahydro-1H-pyrimido[1,2-a]pyrimidine (**1h**). $\varepsilon[(\text{lil})_2\text{CH}^+ \text{ at } 639 \text{ nm}] = 1.59 \times 10^5 \text{ M}^{-1} \text{ cm}^{-1}$  and  $d = 0.5 \text{ cm}$ ,  $\text{CH}_2\text{Cl}_2$  at  $20.0 \text{ }^\circ\text{C}$ .

Entry	[ <b>1h</b> ] <sub>0</sub> (mol L <sup>-1</sup> )	<i>A</i>	[(lil) <sub>2</sub> CH <sup>+</sup> ] <sub>eq</sub> (mol L <sup>-1</sup> )	<i>K</i> (L mol <sup>-1</sup> )
0	0	0.816	$7.292 \times 10^{-6}$	
1	$2.426 \times 10^{-5}$	0.201	$1.795 \times 10^{-6}$	$1.63 \times 10^5$
2	$4.829 \times 10^{-5}$	0.0983	$8.778 \times 10^{-7}$	$1.73 \times 10^5$
0	0	0.817	$7.299 \times 10^{-6}$	
1	$2.480 \times 10^{-5}$	0.194	$1.732 \times 10^{-6}$	$1.73 \times 10^5$
2	$4.935 \times 10^{-5}$	0.0956	$8.536 \times 10^{-7}$	$1.79 \times 10^5$
0	0	0.778	$6.949 \times 10^{-6}$	
1	$2.444 \times 10^{-5}$	0.182	$1.627 \times 10^{-6}$	$1.73 \times 10^5$
2	$4.864 \times 10^{-5}$	0.0903	$8.066 \times 10^{-7}$	$1.79 \times 10^5$

$$K_{\text{av}}(20 \text{ }^\circ\text{C}) = 1.73 \times 10^5 \text{ L mol}^{-1}$$

**Table 26.** Determination of the equilibrium constant for the reaction of **4b** with 1-methyl-2,3,4,6,7,8-hexahydro-1H-pyrimido[1,2-a]pyrimidine (**1h**). $\varepsilon[\mathbf{4b} \text{ at } 366 \text{ nm}] = 2.61 \times 10^4 \text{ M}^{-1} \text{ cm}^{-1}$  and  $d = 0.5 \text{ cm}$ ,  $\text{CH}_2\text{Cl}_2$  at  $20.0 \text{ }^\circ\text{C}$ .Since the final absorbance of **4b** was not stable after its reactions with **1h** equilibrium constant mentioned in this table is approximate.

Entry	[ <b>1h</b> ] <sub>0</sub> (mol L <sup>-1</sup> )	<i>A</i>	[ <b>4b</b> ] <sub>eq</sub> (mol L <sup>-1</sup> )	<i>K</i> (L mol <sup>-1</sup> )
0	0	0.387	$2.963 \times 10^{-5}$	
1	$1.647 \times 10^{-4}$	0.367	$2.809 \times 10^{-5}$	$3.21 \times 10^2$
2	$3.257 \times 10^{-4}$	0.348	$2.663 \times 10^{-5}$	$3.30 \times 10^2$
3	$4.917 \times 10^{-5}$	0.331	$2.535 \times 10^{-5}$	$3.30 \times 10^2$
0	0	0.380	$2.914 \times 10^{-5}$	
1	$3.309 \times 10^{-4}$	0.345	$2.646 \times 10^{-5}$	$3.17 \times 10^2$
2	$6.587 \times 10^{-4}$	0.314	$2.405 \times 10^{-5}$	$3.20 \times 10^2$
3	$9.834 \times 10^{-4}$	0.286	$2.192 \times 10^{-5}$	$3.28 \times 10^2$
0	0	0.388	$2.969 \times 10^{-5}$	
1	$3.274 \times 10^{-4}$	0.352	$2.695 \times 10^{-5}$	$2.22 \times 10^2$
2	$6.517 \times 10^{-4}$	0.320	$2.455 \times 10^{-5}$	$2.65 \times 10^2$
3	$9.730 \times 10^{-4}$	0.293	$2.246 \times 10^{-5}$	$2.84 \times 10^2$
4	$1.291 \times 10^{-3}$	0.270	$2.072 \times 10^{-5}$	$2.92 \times 10^2$
0	0	0.387	$2.969 \times 10^{-5}$	
1	$3.286 \times 10^{-4}$	0.352	$2.697 \times 10^{-5}$	$2.31 \times 10^2$
2	$6.540 \times 10^{-4}$	0.321	$2.460 \times 10^{-5}$	$2.67 \times 10^2$
3	$9.764 \times 10^{-4}$	0.294	$2.251 \times 10^{-5}$	$2.85 \times 10^2$

$$K_{\text{av}}(20 \text{ }^\circ\text{C}) = 2.92 \times 10^2 \text{ L mol}^{-1}$$

**Table 27.** Determination of the equilibrium constant for the reaction of **4c** with 1-methyl-2,3,4,6,7,8-hexahydro-1H-pyrimido[1,2-a]pyrimidine (**1h**). $\varepsilon[\mathbf{4c}] \text{ at } 378 \text{ nm} = 2.94 \times 10^4 \text{ M}^{-1} \text{ cm}^{-1}$  and  $d = 0.5 \text{ cm}$ ,  $\text{CH}_2\text{Cl}_2$  at  $20.0 \text{ }^\circ\text{C}$ .Since the final absorbance of **4c** was not stable after its reactions with **1h** equilibrium constant mentioned in this table is approximate.

Entry	[ <b>1h</b> ] <sub>0</sub> (mol L <sup>-1</sup> )	<i>A</i>	[ <b>4b</b> ] <sub>eq</sub> (mol L <sup>-1</sup> )	<i>K</i> (L mol <sup>-1</sup> )
0	0	0.537	$3.656 \times 10^{-5}$	
1	$3.341 \times 10^{-4}$	0.493	$3.352 \times 10^{-5}$	$2.58 \times 10^2$
0	0	0.316	$2.149 \times 10^{-5}$	
1	$6.918 \times 10^{-4}$	0.266	$1.812 \times 10^{-5}$	$3.23 \times 10^2$
0	0	0.315	$2.141 \times 10^{-5}$	
1	$1.021 \times 10^{-3}$	0.246	$1.674 \times 10^{-5}$	$2.92 \times 10^2$
0	0	0.320	$2.176 \times 10^{-5}$	
1	$1.355 \times 10^{-3}$	0.235	$1.600 \times 10^{-5}$	$2.75 \times 10^2$
0	0	0.301	$2.049 \times 10^{-5}$	
1	$1.614 \times 10^{-3}$	0.211	$1.433 \times 10^{-5}$	$2.33 \times 10^2$

$$K_{\text{av}}(20 \text{ }^\circ\text{C}) = 2.76 \times 10^2 \text{ L mol}^{-1}$$

## 5 References

- [1] *Superbases for Organic Synthesis* (T. Ishikawa, ed.), Wiley, Chichester, **2009**.
- [2] a) S. E. Denmark, G. L. Beutner, *Angew. Chem. Int. Ed.* **2008**, *47*, 1560–1638; b) N. De Rycke, F. Couty, O. R. P. David, *Chem. Eur. J.* **2011**, *17*, 12852–12871; c) J. E. Taylor, S. D. Bull, J. M. J. Williams, *Chem. Soc. Rev.* **2012**, *41*, 2109–2121; d) T. Ishikawa, T. Isobe, *Chem. Eur. J.* **2002**, *8*, 552–557; e) K. Nagasawa, Y. Hashimoto, *Chem. Rec.* **2003**, *3*, 201–211; f) T. Ishikawa, T. Kumamoto, *Synthesis* **2006**, 737–752; g) M. P. Coles, *Chem. Commun.* **2009**, 3659–3676; h) D. Leow, C.-H. Tan, *Chem. Asian J.* **2009**, *4*, 488–507; i) D. Leow, C.-H. Tan, *Synlett* **2010**, 1589–1605; j) X. Fu, C.-H. Tan, *Chem. Commun.* **2011**, *47*, 8210–8222.
- [3] I. Kaljurand, A. Kütt, L. Sooväli, T. Rodima, V. Mäemets, I. Leito, I. A. Koppel, *J. Org. Chem.* **2005**, *70*, 1019–1028.
- [4] a) B. G. G. Lohmeijer, R. C. Pratt, F. Leibfarth, J. W. Logan, D. A. Long, A. P. Dove, F. Nederberg, J. Choi, C. Wade, R. M. Waymouth, J. L. Hedrick, *Macromolecules* **2006**, *39*, 8574–8583; b) R. C. Pratt, B. G. G. Lohmeijer, D. A. Long, R. M. Waymouth, J. L. Hedrick, *J. Am. Chem. Soc.* **2006**, *128*, 4556–4557; c) N. E. Kamber, W. Jeong, R. M. Waymouth, R. C. Pratt, B. G. G. Lohmeijer, J. L. Hedrick, *Chem. Rev.* **2007**, *107*, 5813–5840; d) A. Chuma, H. W. Horn, W. C. Swope, R. C. Pratt, L. Zhang, B. G. G. Lohmeijer, C. G. Wade, R. M. Waymouth, J. L. Hedrick, J. E. Rice, *J. Am. Chem. Soc.* **2008**, *130*, 6749–6754; e) X. Sun, J. P. Gao, Z. Y. Wang, *J. Am.*

- Chem. Soc.* **2008**, *130*, 8130–8131; f) M. K. Kiesewetter, M. D. Scholten, N. Kirn, R. L. Weber, J. L. Hedrick, R. M. Waymouth, *J. Org. Chem.* **2009**, *74*, 9490–9496; g) L. Zhang, R. C. Pratt, F. Nederberg, H. W. Horn, J. E. Rice, R. M. Waymouth, C. G. Wade, J. L. Hedrick, *Macromolecules* **2010**, *43*, 1660–1664.
- [5] a) N. E. Leadbeater, C. van der Pol, *J. Chem. Soc., Perkin Trans. 1* **2001**, 2831–2835; b) R. S. Grainger, N. E. Leadbeater, A. Masdéu Pàmies, *Catal. Commun.* **2002**, *3*, 449–452; c) V. K. Aggarwal, A. Mereu, *Chem. Commun.* **1999**, 2311–2312.
- [6] a) C. Ghobril, C. Sabot, C. Mioskowski, R. Baati, *Eur. J. Org. Chem.* **2008**, 4104–4108; b) P. Hammar, C. Ghobril, C. Antheaume, A. Wagner, R. Baati, F. Himo, *J. Org. Chem.* **2010**, *75*, 4728–4736; c) C. Ghobril, P. Hammar, S. Kodepelly, B. Spiess, A. Wagner, F. Himo, R. Baati, *ChemCatChem* **2010**, *2*, 1573–1581.
- [7] a) E. J. Corey, M. J. Grogan, *Org. Lett.* **1999**, *1*, 157–160; b) L. Wang, X. Huang, J. Jiang, X. Liu, X. Feng, *Tetrahedron Lett.* **2006**, *47*, 1581–1584.
- [8] a) S. Kim, H. Chang, *Synth. Commun.* **1984**, *14*, 899–904; b) T. Isobe, K. Fukuda, Y. Araki, T. Ishikawa, *Chem. Commun.* **2001**, 243–244.
- [9] S. M. Ahmad, D. C. Braddock, G. Cansell, S. A. Hermitage, *Tetrahedron Lett.* **2007**, *48*, 915–918.
- [10] a) S. Huang, J. Ma, J. Li, N. Zhao, W. Wei, Y. Sun, *Catal. Commun.* **2008**, *9*, 276–280; b) M. Costa, G. P. Chiusoli, M. Rizzardi, *Chem. Commun.* **1996**, 1699–1700; c) A. Barbarini, R. Maggi, A. Mazzacani, G. Mori, G. Sartori, R. Sartorio, *Tetrahedron Lett.* **2003**, *44*, 2931–2934.
- [11] a) Y. Tsuchiya, T. Kumamoto, T. Ishikawa, *J. Org. Chem.* **2004**, *69*, 8504–8505; b) W. Disadee, T. Ishikawa, M. Kawahata, K. Yamaguchi, *J. Org. Chem.* **2006**, *71*, 6600–6603.
- [12] a) H. Mayr, M. Patz, *Angew. Chem. Int. Ed. Engl.* **1994**, *33*, 938–957; b) H. Mayr, T. Bug, M. F. Gotta, N. Hering, B. Irrgang, B. Janker, B. Kempf, R. Loos, A. R. Ofial, G. Remennikov, H. Schimmel, *J. Am. Chem. Soc.* **2001**, *123*, 9500–9512; c) R. Lucius, R. Loos, H. Mayr, *Angew. Chem. Int. Ed.* **2002**, *41*, 91–95; d) H. Mayr, B. Kempf, A. R. Ofial, *Acc. Chem. Res.* **2003**, *36*, 66–77; e) H. Mayr, A. R. Ofial, *Pure Appl. Chem.* **2005**, *77*, 1807–1821; f) H. Mayr, *Angew. Chem. Int. Ed.* **2011**, *50*, 3612–3618; g) For a comprehensive listing of nucleophilicity parameters  $N$  and electrophilicity parameters  $E$ , see <http://www.cup.uni-muenchen.de/oc/mayr/DBintro.html>.

- [13] For pyridines see: a) F. Brotzel, B. Kempf, T. Singer, H. Zipse, H. Mayr, *Chem. Eur. J.* **2007**, *13*, 336–345; b) N. De Rycke, G. Berionni, F. Couty, H. Mayr, R. Goumont, O. R. P. David, *Org. Lett.* **2011**, *13*, 530–533; For azoles see: c) M. Baidya, F. Brotzel, H. Mayr, *Org. Biomol. Chem.* **2010**, *8*, 1929–1935; For phosphanes see: d) B. Kempf, H. Mayr, *Chem. Eur. J.* **2005**, *11*, 917–927; For DBU and DBN see: e) M. Baidya, H. Mayr, *Chem. Commun.* **2008**, 1792–1794; For isothioureas see: f) B. Maji, C. Joannesse, T. A. Nigst, A. D. Smith, H. Mayr, *J. Org. Chem.* **2011**, *76*, 5104–5112.
- [14] a) O. Kaumanns, H. Mayr, *J. Org. Chem.* **2008**, *73*, 2738–2745; b) F. Seeliger, S. T. A. Berger, G. Y. Remennikov, K. Polborn, H. Mayr, *J. Org. Chem.* **2007**, *72*, 9170–9180; c) S. T. A. Berger, F. H. Seeliger, F. Hofbauer, H. Mayr, *Org. Biomol. Chem.* **2007**, *5*, 3020–3026.
- [15] A crystal structure analysis revealed the constitution with NH group in the six-membered ring: F. A. Cotton, C. A. Murillo, X. Wang, C. C. Wilkinson, *Inorg. Chem.* **2006**, *45*, 5493–5500.
- [16] M. S. Khalaf, M. P. Coles, P. B. Hitchcock, *Dalton Trans.* **2008**, 4288 – 4295.
- [17] CCDC-873492 contains the supplementary crystallographic data for **5c**·CH<sub>2</sub>Cl<sub>2</sub> reported in this paper. These data can be obtained free of charge from The Cambridge Crystallographic Data Centre via [www.ccdc.cam.ac.uk/data\\_request/cif](http://www.ccdc.cam.ac.uk/data_request/cif).
- [18] J. V. Greenhill, M. J. Ismail, P. N. Edwards, P. J. Taylor, *J. Chem. Soc. Perkin Trans. 2* **1985**, 1255–1264.

## Chapter 4

# Nucleophilic Reactivities of 2-Imidazoline, Thiazoline, and Oxazoline

B. Maji, M. Baidya, S. Kobayashi, J. Ammer, P. Mayer, A. R. Ofial, H. Mayr, *Eur. J. Org. Chem.* **2012**, in preparation

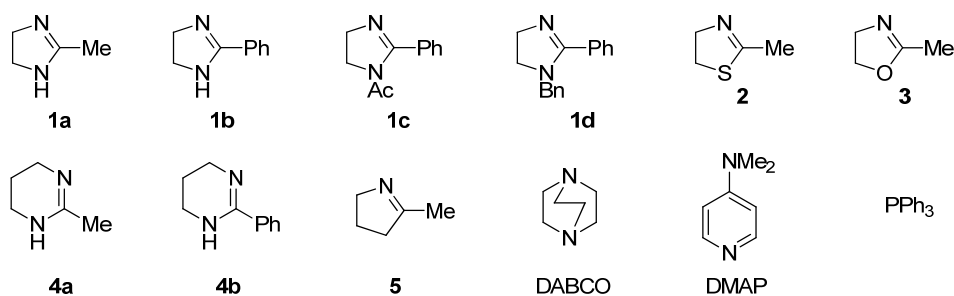
### 1 Introduction

Imidazolines (**1**), oxazolines (**2**) and thiazolines (**3**) are important building blocks in natural products and pharmaceutical chemistry.<sup>[1,2]</sup> They are often used as chiral auxiliaries and ligands in coordination chemistry and homogeneous catalysis.<sup>[3]</sup> Protonated chiral imidazolines have been employed as Brønsted acidic organocatalysts<sup>[4]</sup> in asymmetric Diels-Alder, Friedel-Crafts, and Michael reactions.<sup>[5]</sup> Recently, Lectka et al. reported anionic sulfonated analogues of 4,5-dihydro-1H-imidazole to be efficient nucleophilic catalysts in diastereoselective Staudinger  $\beta$ -lactam synthesis by activating the *in situ* generated ketenes.<sup>[6]</sup> In 2006, Tan and coworkers successfully used chiral imidazoline catalysts in asymmetric Morita-Baylis-Hilman reaction.<sup>[7,8]</sup>

In numerous publications it was shown that the rate constants ( $\log k$ ) for the reactions of nucleophiles with carbocations and Michael acceptors can be described by the linear-free-energy relationship (1),<sup>[9]</sup> where electrophiles are characterized by the solvent-independent electrophilicity parameters  $E$ , and the nucleophiles are characterized by two solvent-dependent parameters, nucleophilicity parameter  $N$  and the sensitivity parameter  $s_N$ .

$$\log k (20\text{ }^\circ\text{C}) = s_N(N + E) \quad (1)$$

In this work we have used the benzhydrylium methodology to characterize the nucleophilicity parameters for the 2-imidazolines **1a-d**, 2-methylthiazoline **2**, and 2-methyloxazoline **3** and to compare their reactivities with those of the tetrahydropyrimidines **4a,b**, dihydropyrrole **5**, and previously characterized nucleophilic organocatalysts (Scheme 1).<sup>[10]</sup>

**Scheme 1.** Selected nitrogen-containing heterocycles.**Table 1.** Abbreviations and the electrophilicity parameters for the benzhydrylium ions used for this work.

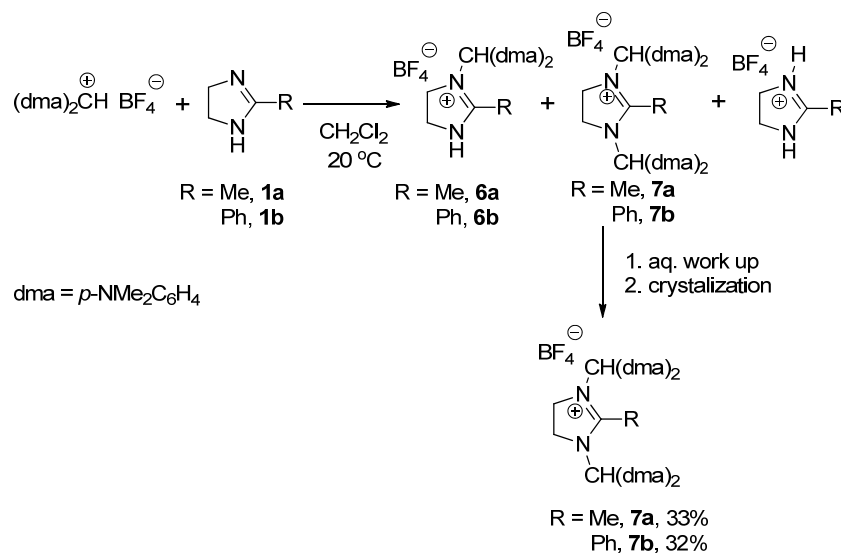
		Abbreviations	$E^{[a]}$
OMe	Me	(ani)(tol)CH <sup>+</sup>	1.48
OMe	OPh	(ani)(POP)CH <sup>+</sup>	0.61
OMe	OMe	(ani) <sub>2</sub> CH <sup>+</sup>	0
		(ani)(fur)CH <sup>+</sup>	-0.56
		(fur) <sub>2</sub> CH <sup>+</sup>	-1.36
N(Ph)CH <sub>2</sub> CF <sub>3</sub>	N(Ph)CH <sub>2</sub> CF <sub>3</sub>	(pfa) <sub>2</sub> CH <sup>+</sup>	-3.14
N(CH <sub>3</sub> )CH <sub>2</sub> CF <sub>3</sub>	N(CH <sub>3</sub> )CH <sub>2</sub> CF <sub>3</sub>	(mfa) <sub>2</sub> CH <sup>+</sup>	-3.85
N(CH <sub>2</sub> CH <sub>2</sub> ) <sub>2</sub> O	N(CH <sub>2</sub> CH <sub>2</sub> ) <sub>2</sub> O	(mor) <sub>2</sub> CH <sup>+</sup>	-5.53
N(Ph)CH <sub>3</sub>	N(Ph)CH <sub>3</sub>	(mpa) <sub>2</sub> CH <sup>+</sup>	-5.89
N(CH <sub>3</sub> ) <sub>2</sub>	N(CH <sub>3</sub> ) <sub>2</sub>	(dma) <sub>2</sub> CH <sup>+</sup>	-7.02
N(CH <sub>2</sub> ) <sub>4</sub>	N(CH <sub>2</sub> ) <sub>4</sub>	(pyr) <sub>2</sub> CH <sup>+</sup>	-7.69
		n = 2 (thq) <sub>2</sub> CH <sup>+</sup>	-8.22
		n = 1 (ind) <sub>2</sub> CH <sup>+</sup>	-8.76
		n = 2 (jul) <sub>2</sub> CH <sup>+</sup>	-9.45
		n = 1 (lil) <sub>2</sub> CH <sup>+</sup>	-10.04

<sup>[a]</sup> Electrophilicity parameters  $E$  for benzhydrylium ions from ref. [9b].

## 2 Results and Discussion

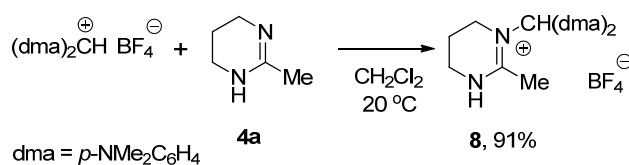
### 2.1 Reaction products

Addition of a dichloromethane solution of **1a** or **1b** to an equimolar amount of  $(\text{dma})_2\text{CH}^+\text{BF}_4^-$  in dichloromethane gave a mixture of mono-substituted **6a,b** and bis-substituted products **7a,b** in ~1 : 3 ratio (Scheme 2). The formation of the bis-substituted products **7a,b** can be explained by subsequent reaction of the deprotonated (by a second molecule of **1a** or **1b**) monosubstituted products **6a,b** with  $(\text{dma})_2\text{CH}^+\text{BF}_4^-$ . While we were unable to isolate the mono substituted products, the bis-substituted products **7a,b** can be isolated by subsequent aqueous workup and crystallization. Crystals suitable for single crystal X-ray structure analysis of **7b** (Figure 1) have been grown by diffusion of *n*-pentane vapour into a dichloromethane-ethyl acetate solution (10 : 1) of **7b**.<sup>[11]</sup>



**Scheme 2.** Reaction products for the reaction of **1a,b** with the  $(\text{dma})_2\text{CH}^+\text{BF}_4^-$  in  $\text{CH}_2\text{Cl}_2$  at  $20^\circ\text{C}$ .

The higher homologue of **1a**, 2-methyl-1,4,5,6-tetrahydropyrimidine **4a**, however, reacts smoothly with  $(\text{dma})_2\text{CH}^+\text{BF}_4^-$  to give only the mono-substituted product **8** in 91% yield (Scheme 3).



**Scheme 3.** Reaction products for the reaction of **4a** with the  $(\text{dma})_2\text{CH}^+\text{BF}_4^-$  in  $\text{CH}_2\text{Cl}_2$  at  $20^\circ\text{C}$ .

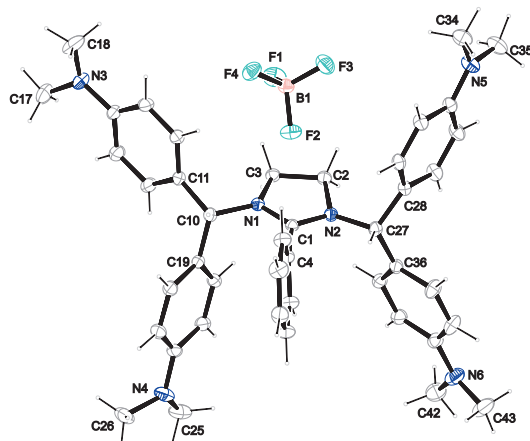
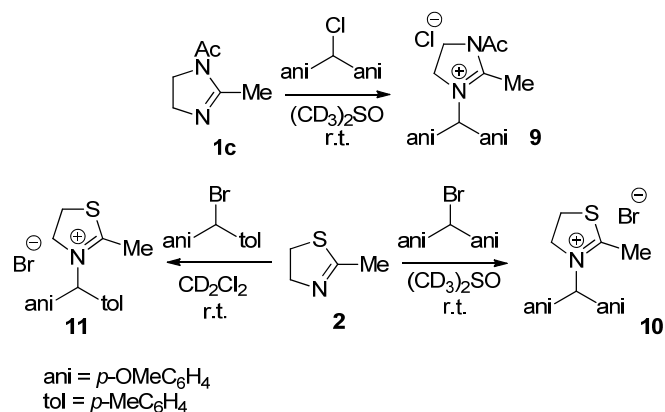


**Figure 1.** Crystal structure of **7b** (50% probability ellipsoids).<sup>[11]</sup>

Compounds **1c**, **2**, and **3** do not react with  $(\text{dma})_2\text{CH}^+\text{BF}_4^-$  indicating that they are weaker nucleophile and/or Lewis base than compounds **1** and **4**. Mixing of **1c** and **2** with an equimolar amount of benzhydryl chloride or bromide gave the addition products **9–11** in greater than 90% yields which were characterized by NMR spectroscopy (Scheme 4).



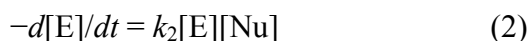
**Scheme 4.** Reaction products for the reaction of **1c** and **2** with with the benzhydryl chloride or bromide.

## 2.2 Kinetics

Most reactions of the nucleophiles **1–5** with benzhydrylium ions (Table 1) were investigated photometrically in  $\text{CH}_2\text{Cl}_2$  at 20 °C by using stopped-flow techniques as described previously.<sup>[9]</sup> Kinetics of the reactions of **4a** with benzhydrylium ions were also studied in  $\text{CH}_3\text{CN}$  and DMSO.

For the fast reactions ( $k > 10^6 \text{ M}^{-1} \text{ s}^{-1}$ ), benzhydrylium ions were generated by laser-flash photolysis (7-ns pulse, 266 nm) of substituted benzhydryl phosphonium tetrafluoroborates in the presence of **2** and **3** as described in ref. [12]. In all cases an excess of the nucleophiles (more than 10 equivalents) over electrophiles were used to achieve pseudo-first-order

conditions. The pseudo-first order rate constants  $k_{\text{obs}}$  ( $\text{s}^{-1}$ ) were obtained by a least squares fit of the exponential decays of the absorbances of  $\text{Ar}_2\text{CH}^+$  to the function  $A = A_0e^{-k_{\text{obs}}t} + C$ . The plots of  $k_{\text{obs}}$  against the concentrations of nucleophiles were linear with negligible intercepts as shown in the insert of Figure 2, indicating a second-order rate law [Eq. (2)].



The slopes of these correlation lines yielded the second-order rate constants  $k$  ( $\text{M}^{-1} \text{s}^{-1}$ ) which are collected in Table 2.

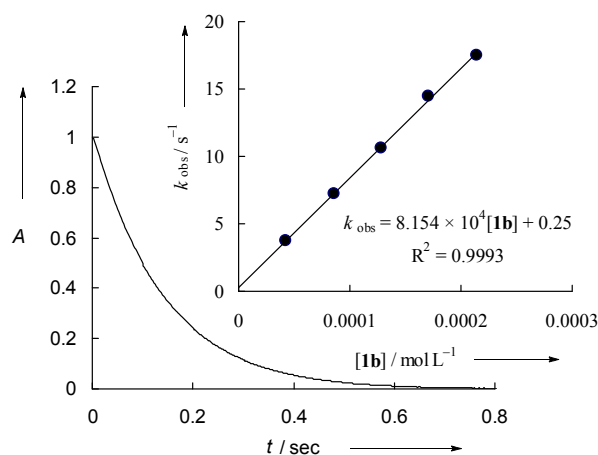


**Figure 2.** Exponential decay of the absorbance  $A$  at 622 nm during the reaction of **1b** ( $1.28 \times 10^{-4}$  M) with  $(\text{mpa})_2\text{CH}^+$  ( $1.00 \times 10^{-5}$  M) in  $\text{CH}_2\text{Cl}_2$  at 20 °C ( $k_{\text{obs}} = 10.7 \text{ s}^{-1}$ ). Insert: Determination of the second-order rate constant  $k = 8.15 \times 10^4 \text{ M}^{-1}\text{s}^{-1}$  from the dependence of  $k_{\text{obs}}$  on the concentration of **1b**.

### 2.3 Nucleophilicity parameters

When the logarithms of the second-order-rate constants (Table 2) for the reactions of the nucleophiles **1–5** with the reference electrophiles  $\text{Ar}_2\text{CH}^+$  were plotted against the empirical electrophilicity parameters  $E$  of  $\text{Ar}_2\text{CH}^+$  (Table 1), linear correlations were obtained as shown for some of the representative examples in Figure 3. As described above, kinetics of the reactions of the nucleophiles **2** and **3** with benzhydrylium ions were measured by two different methods, stopped-flow and Laser-flash photolysis. Linear correlations (as shown for **2** in Figure 4) between the logarithms of the rate constants  $k$  measured by the two methods with the electrophilicity parameters  $E$  reflect the consistency of our measurements.

**Table 2:** Second-order rate constants ( $k$ ) for the reactions of benzhydrylium ion with the nucleophiles **1–5** in dichloromethane at 20 °C.

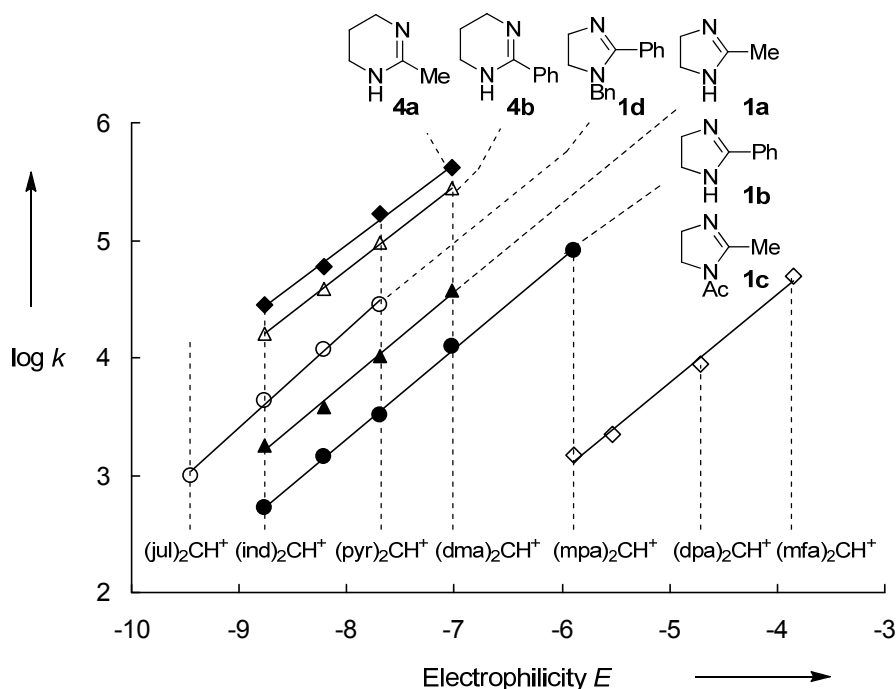
Nucleophile	Solvent	$N, s_N^{[a]}$	(Ar) <sub>2</sub> CH <sup>+</sup>	$k / \text{M}^{-1}\text{s}^{-1}$
 <b>1a</b>	CH <sub>2</sub> Cl <sub>2</sub>	12.92, 0.77	(dma) <sub>2</sub> CH <sup>+</sup>	$3.73 \times 10^4$
			(pyr) <sub>2</sub> CH <sup>+</sup>	$1.04 \times 10^4$
			(thq) <sub>2</sub> CH <sup>+</sup>	$3.75 \times 10^3$
			(ind) <sub>2</sub> CH <sup>+</sup>	$1.76 \times 10^3$
 <b>1b</b>	CH <sub>2</sub> Cl <sub>2</sub>	12.31, 0.77	(mpa) <sub>2</sub> CH <sup>+</sup>	$8.15 \times 10^4$
			(dma) <sub>2</sub> CH <sup>+</sup>	$1.26 \times 10^4$
			(pyr) <sub>2</sub> CH <sup>+</sup>	$3.25 \times 10^3$
			(thq) <sub>2</sub> CH <sup>+</sup>	$1.24 \times 10^3$
 <b>1c</b>	CH <sub>2</sub> Cl <sub>2</sub>	10.03, 0.75	(mfa) <sub>2</sub> CH <sup>+</sup>	$4.91 \times 10^4$
			(dpa) <sub>2</sub> CH <sup>+</sup>	$8.81 \times 10^3$
			(mor) <sub>2</sub> CH <sup>+</sup>	$2.25 \times 10^3$
			(mpa) <sub>2</sub> CH <sup>+</sup>	$1.48 \times 10^3$
 <b>1d</b>	CH <sub>2</sub> Cl <sub>2</sub>	13.11, 0.83	(pyr) <sub>2</sub> CH <sup>+</sup>	$2.82 \times 10^4$
			(thq) <sub>2</sub> CH <sup>+</sup>	$1.18 \times 10^4$
			(ind) <sub>2</sub> CH <sup>+</sup>	$4.31 \times 10^3$
			(jul) <sub>2</sub> CH <sup>+</sup>	$9.97 \times 10^2$
 <b>2</b>	CH <sub>2</sub> Cl <sub>2</sub>	10.22, 0.71	(ani)(tol)CH <sup>+</sup>	$1.35 \times 10^8$
			(ani)(POP)CH <sup>+</sup>	$3.91 \times 10^7$
			(ani) <sub>2</sub> CH <sup>+</sup>	$2.05 \times 10^7$
			(ani)(fur)CH <sup>+</sup>	$7.47 \times 10^6$
			(fur) <sub>2</sub> CH <sup>+</sup>	$2.41 \times 10^6$
			(pfa) <sub>2</sub> CH <sup>+</sup>	$1.09 \times 10^5$
			(mfa) <sub>2</sub> CH <sup>+</sup>	$3.65 \times 10^4$
			(dpa) <sub>2</sub> CH <sup>+</sup>	$5.99 \times 10^3$
			(mor) <sub>2</sub> CH <sup>+</sup>	$1.86 \times 10^3$

Table 2 continued

Nucleophile	Solvent	$N, s_N^{[a]}$	$(Ar)_2CH^+$	$k / M^{-1}s^{-1}$
 <b>3</b>	CH <sub>2</sub> Cl <sub>2</sub>	9.83, 0.76	(ani)(POP)CH <sup>+</sup>	$6.16 \times 10^7$
			(ani) <sub>2</sub> CH <sup>+</sup>	$3.09 \times 10^7$
			(ani)(fur)CH <sup>+</sup>	$1.55 \times 10^7$
			(fur) <sub>2</sub> CH <sup>+</sup>	$5.35 \times 10^6$
			(mfa) <sub>2</sub> CH <sup>+</sup>	$3.86 \times 10^4$
			(dpa) <sub>2</sub> CH <sup>+</sup>	$7.02 \times 10^3$
			(mor) <sub>2</sub> CH <sup>+</sup>	$1.70 \times 10^3$
 <b>4a</b>	CH <sub>2</sub> Cl <sub>2</sub>	15.21, 0.69	(dma) <sub>2</sub> CH <sup>+</sup>	$4.19 \times 10^5$
			(pyr) <sub>2</sub> CH <sup>+</sup>	$1.68 \times 10^5$
			(thq) <sub>2</sub> CH <sup>+</sup>	$5.90 \times 10^4$
			(ind) <sub>2</sub> CH <sup>+</sup>	$2.82 \times 10^4$
	CH <sub>3</sub> CN	14.43, 0.79	(pyr) <sub>2</sub> CH <sup>+</sup>	$2.30 \times 10^5$
			(thq) <sub>2</sub> CH <sup>+</sup>	$7.29 \times 10^4$
			(ind) <sub>2</sub> CH <sup>+</sup>	$2.89 \times 10^4$
	DMSO	14.48, 0.79	(pyr) <sub>2</sub> CH <sup>+</sup>	$3.24 \times 10^5$
			(thq) <sub>2</sub> CH <sup>+</sup>	$9.34 \times 10^4$
			(ind) <sub>2</sub> CH <sup>+</sup>	$3.29 \times 10^4$
 <b>4b</b>	CH <sub>2</sub> Cl <sub>2</sub>	14.62, 0.72	(dma) <sub>2</sub> CH <sup>+</sup>	$2.75 \times 10^5$
			(pyr) <sub>2</sub> CH <sup>+</sup>	$9.61 \times 10^4$
			(thq) <sub>2</sub> CH <sup>+</sup>	$3.79 \times 10^4$
			(ind) <sub>2</sub> CH <sup>+</sup>	$1.58 \times 10^4$
 <b>5</b>	CH <sub>2</sub> Cl <sub>2</sub>	13.12, 0.69	(mpa) <sub>2</sub> CH <sup>+</sup>	$9.53 \times 10^4$
			(dma) <sub>2</sub> CH <sup>+</sup>	$2.02 \times 10^4$
			(pyr) <sub>2</sub> CH <sup>+</sup>	$5.57 \times 10^3$
			(thq) <sub>2</sub> CH <sup>+</sup>	$2.37 \times 10^3$

[a] Nucleophilicity parameters  $N$  and  $s_N$  derived by using Eq. 1.

According to equation (1), the slopes of these correlation lines give the nucleophile-specific sensitivity parameters  $s_N$  and the intercepts on the abscissa give the nucleophilicity parameters  $N$  of **1–5**, which are listed in Table 2.<sup>[9]</sup>



**Figure 3.** Plots of  $\log k$  for the reactions of the N-heterocyclic compounds **1** and **4** with benzhydrylium ions versus their electrophilicity parameters  $E$  in  $\text{CH}_2\text{Cl}_2$  at  $20^\circ\text{C}$ .

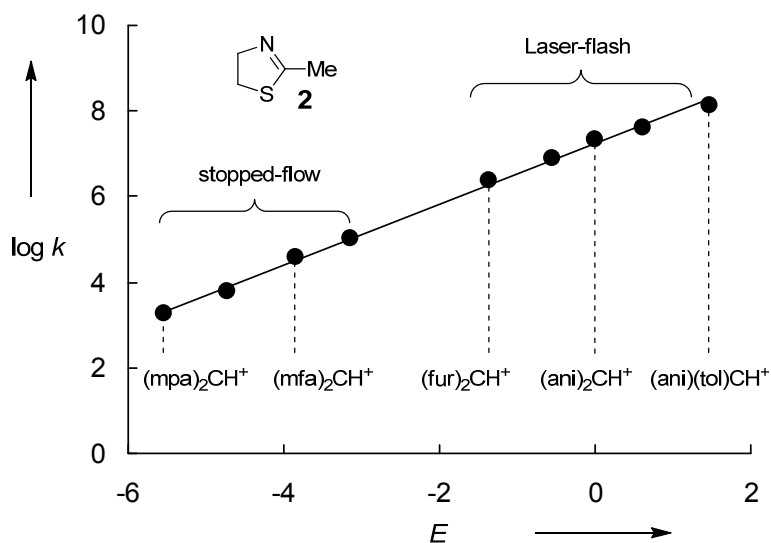
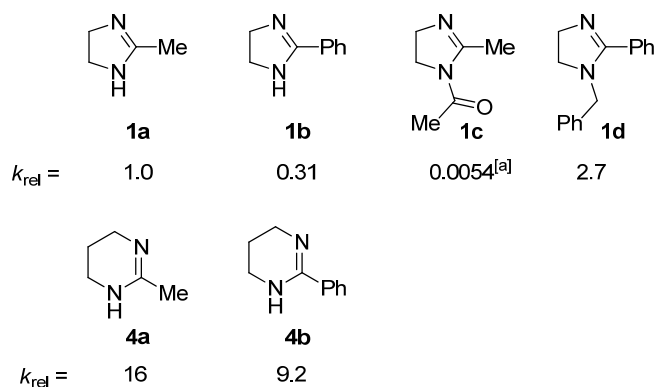


**Figure 4.** Plots of  $\log k$  for the reactions of the nucleophiles **2** with benzhydrylium ions versus their electrophilicity parameters  $E$  in  $\text{CH}_2\text{Cl}_2$  at  $20^\circ\text{C}$ .

#### 2.4 Relationship between structures and nucleophilicities

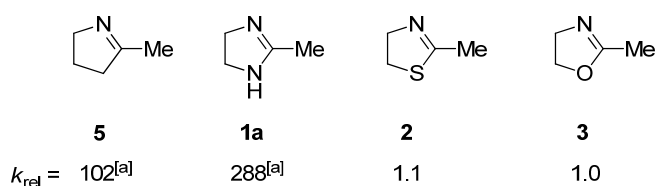
The similarities of the slopes of the correlation lines in Figure 3, which are numerically expressed by sensitivity parameters  $s_N$  in Table 2 indicate that the relative nucleophilicities of the N-heterocycles **1–5**, depend only slightly on the nature of the electrophiles.

Scheme 5 shows that the tetrahydropyrimidine derivatives **4a** and **4b** are 16 and 30 times more nucleophilic than the imidazolines **1a** and **1b**. This ring size effect goes in parallel to the previously observed reactivities for cyclic guanidines<sup>[10g]</sup> and isothiouras,<sup>[10f]</sup> i.e. six-membered amidine rings are generally one order of magnitude more nucleophilic than the corresponding five-membered amidine rings.<sup>[10e-g]</sup>



**Scheme 5.** Relative nucleophilic reactivities of the nucleophiles **1a–d**, and **4a,b** toward  $(\text{pyr})_2\text{CH}^+$  in  $\text{CH}_2\text{Cl}_2$ . [a]  $k [(\text{pyr})_2\text{CH}^+]$  was calculated using  $N$  and  $s_N$  value from Table 2.

Scheme 5, furthermore, shows that replacement of the 2-methyl group by a phenyl group (**1a/1b** and **4a/4b**) reduces the reactivity by a factor of 3 and 1.6. Whereas replacement of the NH proton of **1a** by the electron withdrawing acetyl group (**1a** → **1c**) decreases the reactivity by a factor of 183 and replacement of the NH proton of **1b** by the electron donating benzyl group (**1b** → **1d**) increases the reactivity by a factor of 8.7.



**Scheme 6.** Relative nucleophilic reactivities of the nucleophiles **1a**, **2**, **3**, and **5** toward  $(\text{mor})_2\text{CH}^+$  in  $\text{CH}_2\text{Cl}_2$ . [a]  $k [(\text{mor})_2\text{CH}^+]$  was calculated using  $N$  and  $s_N$  value from Table 2.

Scheme 6 shows the effect of heteroatoms in 3-position 2-methyl pyrroline **5**. Replacement of ‘CH<sub>2</sub>’ by ‘O’ (**5** → **3**) reduces the reactivity by a factor of 10<sup>2</sup>. Since the electrophilic attack takes place at the sp<sup>2</sup> lone pair of nitrogen which resides in the plane of the ring, the reduction of nucleophilicity can be explained by the inductive effect of ‘O’ which overcompensates the mesomeric effect. Replacement of ‘O’ by ‘S’ (**3** → **2**) does not have any influence on the nucleophilic reactivities of the N-heterocycles. Obviously, the lower electronegativity and weaker +M-effect of ‘S’ compared to ‘O’ are compensating each other. Compensation of two

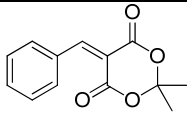
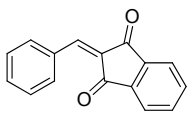
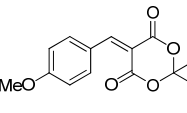
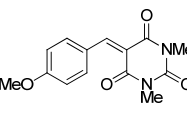
opposing, inductive and resonance, effects also explains that introduction of the ‘NH’ group in place of ‘CH<sub>2</sub>’ (**5** → **1a**) has only a marginal effect on nucleophilicity.

### 2.5 Reaction with Michael acceptors

To examine the applicability of the nucleophilicity parameters ( $N$  and  $s_N$ ) in Table 2 for the reactions with other types of nucleophiles we have studied the rates of the reactions of the N-heterocyclic compounds **1** and **4** with ordinary Michael acceptors **7** whose electrophilicity parameters have previously been determined.<sup>[13]</sup>

The rates of the reactions of **1** and **4** with **7a-d** were measured by the same photometric method as described above for their reactions with benzhydrylium ions, i.e., by following the decay of the absorbances of **7a-d** at or close to their absorption maxima at 20 °C in CH<sub>2</sub>Cl<sub>2</sub>. The resulting second-order-rate constants are listed in Table 3. Although **1d** is 2.7 times more nucleophilic than **1a**, it does not react with any one of the Michael acceptors studied because of the high reversibility of these reactions.

**Table 3.** Comparison of Calculated and Experimental Second-Order Rate Constants  $k$  (in M<sup>-1</sup> s<sup>-1</sup>) for the Reactions of the Nucleophiles **1** and **4** with the Michael Acceptors **7a-d** in CH<sub>2</sub>Cl<sub>2</sub> at 20 °C.

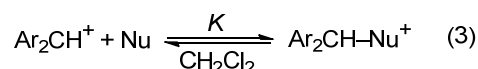
Electrophile	$E$ <sup>[a]</sup>	Nucleophile	$k^{\text{exp}}$	$k^{\text{calc}}$ <sup>[b]</sup>
 <b>7a</b>	-9.15	<b>1a</b>	$7.37 \times 10^3$	$8.00 \times 10^2$
		<b>1d</b>	h.r. <sup>[c]</sup>	$1.94 \times 10^3$
		<b>4a</b>	$7.38 \times 10^4$	$1.52 \times 10^4$
 <b>7b</b>	-10.11	<b>1a</b>	h.r. <sup>[c]</sup>	$1.46 \times 10^2$
		<b>1d</b>	h.r. <sup>[c]</sup>	$3.09 \times 10^2$
		<b>4a</b>	$2.91 \times 10^2$	$3.30 \times 10^3$
 <b>7c</b>	-10.28	<b>1a</b>	$7.88 \times 10^2$	$1.08 \times 10^2$
		<b>1d</b>	h.r. <sup>[c]</sup>	$2.23 \times 10^2$
		<b>4a</b>	$1.00 \times 10^4$	$2.52 \times 10^3$
 <b>7d</b>	-10.37	<b>1a</b>	$4.76 \times 10^2$	$9.19 \times 10^1$
		<b>1d</b>	h.r. <sup>[c]</sup>	$1.88 \times 10^2$
		<b>4a</b>	$6.15 \times 10^3$	$2.19 \times 10^3$

<sup>[a]</sup> Electrophilicity parameters  $E$  from ref. [13]. <sup>[b]</sup> Calculated by eq. 1 using  $N/s_N$  values from Table 2 and  $E$  values from Table 3. <sup>[c]</sup> Highly reversible.

Comparison of the experimental rate constants  $k_{\text{exp}}$  with the rate constants calculated  $k^{\text{calc}}$  by eq (1) from the  $N$  and  $s_N$  parameters in Table 2 and the  $E$  values from ref. [13], shows agreement within factors of 3 to 11. In view of the simplicity of the three parameter equation (1) we consider these deviations acceptable, since the electrophilicities of the Michael acceptors **7** were determined from their reactions with carbanions in DMSO, and the nucleophilicity parameters of **1** and **4** are derived from their reactions with benzhydrylium ions in  $\text{CH}_2\text{Cl}_2$  (Table 2). We, therefore, conclude that rates of reactions of the nucleophiles **1** and **4** with electrophiles of known electrophilicity parameters can be predicted by equation (1) using  $N$  and  $s_N$  parameter reported in Table 2.

## 2.6 Equilibrium constants and intrinsic barriers

As the reactions of the nucleophiles **1–5** with the colored benzhydrylium ions give colorless products, equilibrium constants for these reactions were also measured photometrically. Because of the proportionality between the concentrations and absorbances of the blue benzhydrylium ions, the equilibrium constants  $K$  for the reactions in equation (3), which are listed in Table 4 were calculated by equation (4), where  $A_0$  and  $A$  are the absorbances of  $\text{Ar}_2\text{CH}^+$  before and after addition of the nucleophiles, respectively.



$$K = \frac{[\text{Ar}_2\text{CH}-\text{Nu}^+]}{[\text{Ar}_2\text{CH}^+][\text{Nu}]} = \frac{A_0 - A}{A [\text{Nu}]} \quad (4)$$

Where  $[\text{Nu}] = [\text{Nu}]_0 - [(A_0 - A)/\epsilon d]$

$\epsilon$  = molar absorption coefficient

$d$  = path length

Table 4 shows that the 2-methylimidazoline derivative **1c** is a 50 times stronger Lewis base than 2-methylthiazoline (**2**, reference  $(\text{mor})_2\text{CH}^+$ ) and a 8 times stronger Lewis base than 2-methyloxazoline (**3**, reference  $(\text{mor})_2\text{CH}^+$ ). Although a direct comparison of the equilibrium constants is not possible, Table 4 shows that N-benzylated 2-methylimidazoline (**1d**) is a far stronger Lewis base than **1c**, **2**, and **3**, because it gives adducts even with the weakly Lewis-acidic benzhydrylium ions  $(\text{lil})_2\text{CH}^+$ ,  $(\text{jul})_2\text{CH}^+$ , and  $(\text{ind})_2\text{CH}^+$ .

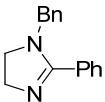
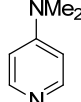
Comparison of the rate and equilibrium constants for the reactions of benzhydrylium ions with the imidazoline derivative **1d** and other commonly used nucleophilic organocatalysts (Scheme 7) shows that **1d** reacts with electrophiles similarly fast as  $\text{PPh}_3$ , and 10 and  $10^4$  times more slowly than DMAP and DABCO, respectively. However, **1d** is a 200 to 300 times stronger Lewis base than  $\text{PPh}_3$  and DABCO, comparable to that of DMAP.<sup>[10]</sup> This break-

down of the rate-equilibrium-relationship indicates that these reactions proceed via different Marcus intrinsic barriers  $\Delta G_0^\ddagger$ , the barriers of the corresponding reactions without any thermodynamic driving force ( $\Delta G^0 = 0$ ).<sup>[14]</sup>

**Table 4:** Equilibrium Constants  $K$  ( $M^{-1}$ ), Activation Free Energies  $\Delta G^\ddagger$  ( $\text{kJ mol}^{-1}$ ), Reaction Free Energies  $\Delta G^0$  ( $\text{kJ mol}^{-1}$ ), and Intrinsic Barriers  $\Delta G_0^\ddagger$  ( $\text{kJ mol}^{-1}$ ) for the Reactions of Nucleophiles **1**, **2**, and **3** with Benzhydrylium Ions ( $\text{Ar}_2\text{CH}^+$ ) in  $\text{CH}_2\text{Cl}_2$  at 20 °C.

Nucleophile	$\text{Ar}_2\text{CH}^+$	$K$	$\Delta G^\ddagger$ <sup>[a]</sup>	$\Delta G^0$ <sup>[b]</sup>	$\Delta G_0^\ddagger$ <sup>[c]</sup>
 <b>1c</b>	(mor) <sub>2</sub> CH <sup>+</sup>	$3.10 \times 10^4$	52.9	-25.2	64.9
	(mpa) <sub>2</sub> CH <sup>+</sup>	$3.51 \times 10^3$	53.9	-19.9	63.5
 <b>1d</b>	(ind) <sub>2</sub> CH <sup>+</sup>	$2.67 \times 10^5$	51.3	-30.4	65.7
	(jul) <sub>2</sub> CH <sup>+</sup>	$7.00 \times 10^3$	54.9	-21.6	65.2
	(lil) <sub>2</sub> CH <sup>+</sup>	$8.10 \times 10^3$	57.4	-21.9	67.9
 <b>2</b>	(mfa) <sub>2</sub> CH <sup>+</sup>	$2.27 \times 10^4$	41.6	-24.4	57.7
	(dpa) <sub>2</sub> CH <sup>+</sup>	$7.20 \times 10^3$	50.5	-21.6	60.9
	(mor) <sub>2</sub> CH <sup>+</sup>	$6.38 \times 10^2$	53.4	-15.7	61.0
 <b>3</b>	(mor) <sub>2</sub> CH <sup>+</sup>	$4.07 \times 10^3$	53.6	-20.2	63.3
	(mpa) <sub>2</sub> CH <sup>+</sup>	$6.57 \times 10^2$	54.7	-15.8	62.4

<sup>[a]</sup> From rate constants in Table 2 using the Eyring equation. <sup>[b]</sup> From equilibrium constants  $K$  in this table ( $-RT \ln K$ ). <sup>[c]</sup> From equation (5)

	 <b>1d</b>	 DABCO	 DMAP	 Ph <sub>3</sub> P
$k / M^{-1}s^{-1}$	$4.31 \times 10^3$	$1.10 \times 10^7$ <sup>[a]</sup>	$4.96 \times 10^4$ <sup>[b]</sup>	$4.17 \times 10^3$ <sup>[b]</sup>
$K / M^{-1}$	$2.67 \times 10^5$	$(8.7 \times 10^2)$ <sup>[a]</sup>	$1.71 \times 10^5$ <sup>[b]</sup>	$1.21 \times 10^3$ <sup>[b]</sup>
$\Delta G_0^\ddagger / \text{kJ mol}^{-1}$	65.7	(40.3) <sup>[a]</sup>	59.2 <sup>[b]</sup>	59.7 <sup>[b]</sup>

**Scheme 7:** Comparison of the rate and equilibrium constants for the reactions of (ind)<sub>2</sub>CH<sup>+</sup> with **1d**, DABCO, DMAP, and PPh<sub>3</sub>. Solvent:  $\text{CH}_2\text{Cl}_2$ . [a] In  $\text{CH}_3\text{CN}$  from ref. [10h]. [b] From ref. [10a,d]

Substitution of the activation free energies  $\Delta G^\ddagger$  (derived from the rate constants in Table 2 by the Eyring equation) and Gibbs free energies  $\Delta G^0$  ( $= -RT \ln K$ ) into the Marcus equation (5) yields the intrinsic barriers  $\Delta G_0^\ddagger$  for these reactions which are listed in Table 4.

$$\Delta G^\ddagger = \Delta G_0^\ddagger + 0.5 \Delta G^0 + ((\Delta G^0)^2 / 16 \Delta G_0^\ddagger) \quad (5)$$

Table 5 shows that the intrinsic barrier  $\Delta G_0^\ddagger$  for the reactions benzhydrylium ion  $(\text{mor})_2\text{CH}^+$  with **2** is  $2 \text{ kJ mol}^{-1}$  smaller than that for the reaction with **3** and  $4 \text{ kJ mol}^{-1}$  smaller than that for the reactions with **1c**. Obviously, the product stabilizing mesomeric effect  $\text{S} < \text{O} < \text{N} < \text{Ac}$  is only partially developed at the transition state.

Scheme 7 shows that the reaction of  $(\text{ind})_2\text{CH}^+$  with the imidazoline derivative **1d** has a much higher intrinsic barrier ( $\Delta\Delta G_0^\ddagger = 6 \text{ kJ mol}^{-1}$ ) than the corresponding reactions with DMAP and  $\text{PPh}_3$ . Although **1d** is a  $10^2$  times stronger Lewis base than  $\text{PPh}_3$ , **1d** and  $\text{PPh}_3$  attack electrophiles with similar rates. On the other hand, despite similar Lewis basicities of **1d** and DMAP, the imidazole **1d** reacts 10-times more slowly than DMAP because of the higher reorganization energy needed for the formation of resonance stabilized amidinium ion from **1d**. The higher nucleophilicity ( $>10^3$  times) of the weakly Lewis basic ( $>10^2$  times) DABCO can analogously be explained by lower intrinsic barriers ( $\Delta\Delta G_0^\ddagger = 20 \text{ kJ mol}^{-1}$ ) of its reactions with electrophiles.

## 2.7 Nucleofugalities

Equation (6), which is formally analogous to equation (1), has recently been suggested as a basis for a nucleofugality scale, which allows to calculate the rate of heterolytic cleavage  $k_{\leftarrow}$   $\text{s}^{-1}$  at  $25 \text{ }^\circ\text{C}$  from the electrofugality parameters  $E_f$  of the electrofuges, and nucleofugality ( $N_f$ ), and nucleofuge-specific sensitivity parameters  $s_f$ .<sup>[15]</sup>

$$\log k_{\leftarrow} (25 \text{ }^\circ\text{C}) = s_f(E_f + N_f) \quad (6)$$

**Table 5:** Reverse Rate Constants ( $k_{\leftarrow}$ ) for the Reactions of Nucleophiles **1**, **2** and **3** with Benzhydrylium Ions ( $\text{Ar}_2\text{CH}^+$ ) in  $\text{CH}_2\text{Cl}_2$  at  $20 \text{ }^\circ\text{C}$ .

Nucleophile	$\text{Ar}_2\text{CH}^+$	$k_{\leftarrow}^{[a]} / [\text{s}^{-1}]$	$N_f^{[b]}$
 <b>1c</b>	$(\text{mor})_2\text{CH}^+$	$7.26 \times 10^{-2}$	-4.0
	$(\text{mpa})_2\text{CH}^+$	$4.22 \times 10^{-2}$	
 <b>1d</b>	$(\text{ind})_2\text{CH}^+$	$1.61 \times 10^{-2}$	-6.5
	$(\text{jul})_2\text{CH}^+$	$1.42 \times 10^{-1}$	
	$(\text{lil})_2\text{CH}^+$	$4.36 \times 10^{-2}$	
 <b>2</b>	$(\text{mfa})_2\text{CH}^+$	1.61	-2.5
	$(\text{dpa})_2\text{CH}^+$	$8.32 \times 10^{-1}$	
	$(\text{mor})_2\text{CH}^+$	2.96	
 <b>3</b>	$(\text{mor})_2\text{CH}^+$	$4.18 \times 10^{-1}$	-3.3
	$(\text{mpa})_2\text{CH}^+$	1.63	

<sup>[a]</sup>  $k_{\leftarrow} = k/K$ . <sup>[b]</sup> From equation (6).

In analogy to the  $N$  and  $s_N$  parameters, the  $N_f$  and  $s_f$  parameters are obtained from linear plots of  $\log k_{\leftarrow}$  (25 °C) vs the electrofugality parameters ( $E_f$ ) of the benzhydrylium ions reported in ref [15]. However, as the number of  $k_{\leftarrow}$  values in Table 5 available for each of the nucleofuges is not sufficient to derive a reliable values for  $s_f$ , we followed previously recommended procedure<sup>[15]</sup> and assumed  $s_f = 1.0$  to calculate the nucleofugality parameters of the N-heterocycles in Table 5 and they are compared with previously published nucleofuges in Figure 5.

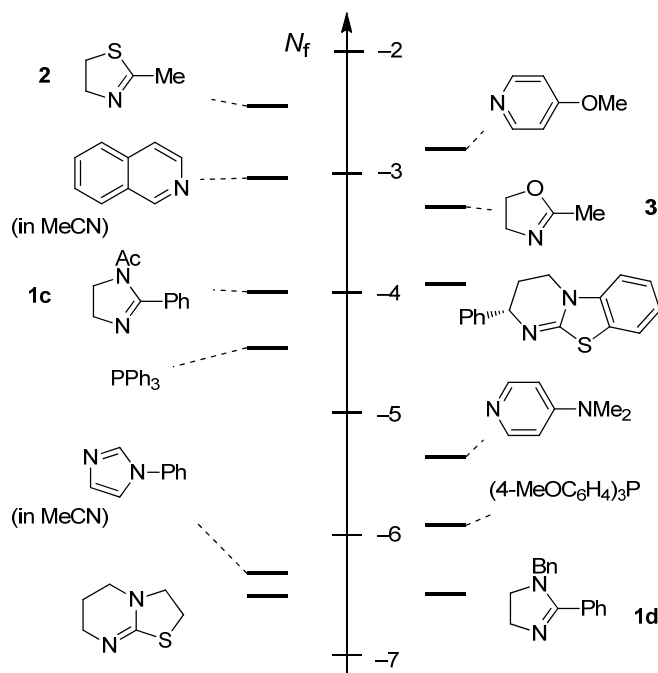


**Figure 5.** Comparison of the nucleofugalities  $N_f$  of the nucleophiles **1–3** with other nucleophilic organocatalysts (solvent is  $\text{CH}_2\text{Cl}_2$  unless otherwise stated,  $N_f$  from Table 5 and ref. [10f and 15]).

### 3 Conclusion

In conclusion we have found that rate constants of reactions of the N-heterocyclic compounds **1–5** with benzhydrylium ions follow the linear-free-energy equation (2), which allowed us to determine nucleophilicity parameters ( $N$  and  $s_N$ ) of **1–5** and to compare them with those of commonly used nucleophilic organocatalysts (Figure 6). The  $N$  values in Figure 6 show that the imidazoline derivatives **1** are among the moderately reactive  $N$ -nucleophiles. While they are 10 to  $10^3$  times less nucleophilic than DHPB,  $\text{PPh}_3$ , DBU, DBN, or DMAP the imidazolines **1** are 10 to  $10^2$  times more nucleophilic than imidazoles and benzimidazoles. On the other hand, the tetrahydropyrimidine derivatives **4** have similar nucleophilicities as THTP, DBU, and DBN.

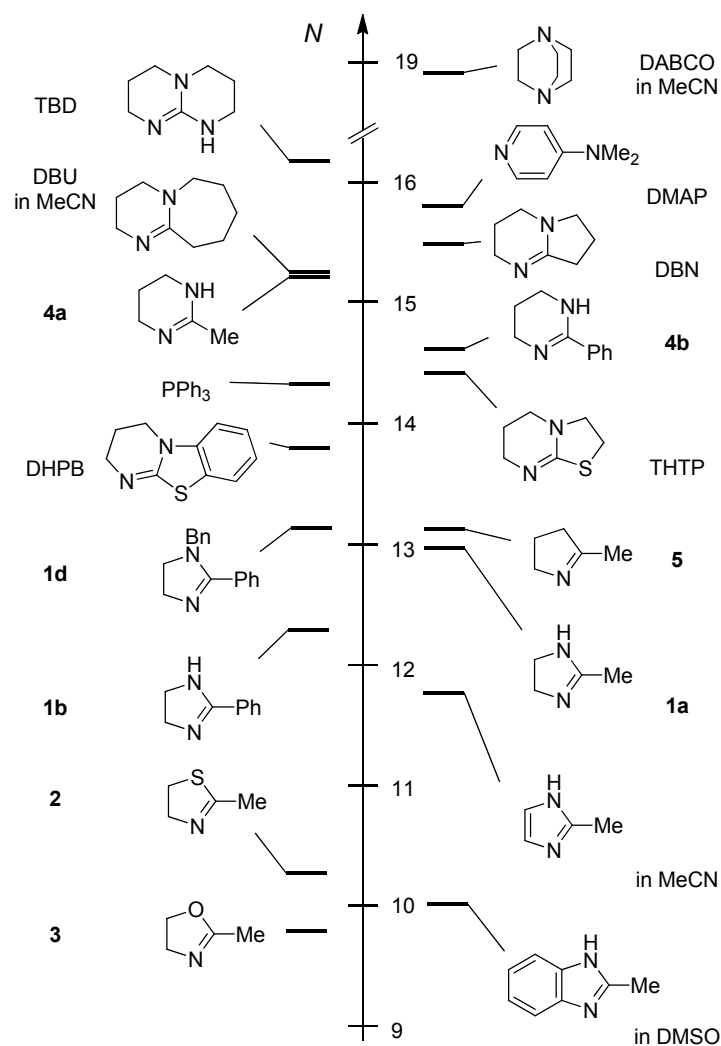


**Figure 6.** Comparison of the nucleophilicities  $N$  of the nucleophiles **1–5** with other nucleophilic organocatalysts (solvent is  $\text{CH}_2\text{Cl}_2$  unless otherwise stated,  $N$  from Table 2 and ref. [9g]).

Since the electrophiles attack at the lone pair in the plane of the N-heterocycles, the nucleophilic reactivity order  $3 \approx 2 \ll 5 \approx 1\mathbf{a}$  can be analyzed by the inductive effects of the hetero atoms in 3-position of the ring.

Substitution of the rate and equilibrium constants into Marcus equation derived that the reactions of the benzhydrylium ions with imidazoline derivatives requires higher intrinsic barriers than those with  $\text{PPh}_3$ , DMAP, or DABCO. As a result **1d** is a weaker nucleophile than comparable Lewis basic DMAP and a stronger Lewis base than comparable nucleophilic  $\text{PPh}_3$ .

## 4 Experimental Section

### 4.1 General

#### *Materials*

CH<sub>2</sub>Cl<sub>2</sub> was freshly distilled over CaH<sub>2</sub> prior to use. Commercially available acetonitrile (VWR, Prolabo, HPLC-gradient grade) and DMSO (Acros, 99.9%, Extra Dry, AcroSeal) was used as received. Compounds **1a** (ABCR), **1b** (Aldrich), **2** (Aldrich), and **3** (ABCR) were purchased and used without further purification. **5** was purchased from Aldrich and distilled prior to use. **1c**,<sup>[16a]</sup> **1d**,<sup>[16b]</sup> **4a**,<sup>[16c]</sup> and **4b**<sup>[16c]</sup> were synthesized according to the literature procedure. Benzhydrylium tetrafluoroborates<sup>[9b]</sup> and Michael acceptors<sup>[13]</sup> were prepared as described before.

#### *Analytcs*

<sup>1</sup>H- and <sup>13</sup>C-NMR spectra were recorded on *Varian* NMR-systems (300 and 400 MHz) in CDCl<sub>3</sub>, *d*<sub>6</sub>-DMSO or CD<sub>2</sub>Cl<sub>2</sub> and the chemical shifts in ppm refer to the solvent residual signal as internal standard (in CDCl<sub>3</sub>: δ<sub>H</sub> = 7.26, δ<sub>C</sub> = 77.2; in *d*<sub>6</sub>-DMSO: δ<sub>H</sub> = 2.50, δ<sub>C</sub> = 39.5 ppm; in CD<sub>2</sub>Cl<sub>2</sub>: δ<sub>H</sub> = 5.32, δ<sub>C</sub> = 53.8). The following abbreviations were used for chemical shift mutiplicities: brs = broad singlet, s = singlet, d = doublet, t = triplet, q = quartet, m = multiplet. For reasons of simplicity, the <sup>1</sup>H-NMR signals of AA'BB'-spin systems of *p*-disubstituted aromatic rings are treated as doublets. NMR signal assignments are based on additional 2D-NMR experiments (COSY, HSQC, and HMBC). (HR-)MS has been performed on a *Finnigan MAT 95* (EI) or a *Thermo Finnigan LTQ FT* (ESI) mass spectrometer. Melting points were determined on a Büchi B-540.

#### *Kinetics*

As described previously, the reactions of the nucleophiles **1–5** with the benzhydrylium ions and Michael acceptors **7** were followed photometrically at or close to the absorption maxima of Ar<sub>2</sub>CH<sup>+</sup> and **7**. A circulating bath thermostat was used to keep the temperature of the solutions constant at 20.0 ± 0.1 °C during all kinetic experiments.

For the evaluation of kinetics with τ<sub>1/2</sub> < 15–20 s the spectrophotometer system Applied Photophysics SX.18MV-R or Hi-Tech SF-61DX stopped-flow reaction analyser was used.

Reactions with τ<sub>1/2</sub> < 10 ms were analyzed by laser flash photolytic generation of benzhydrylium ions (Ar<sub>2</sub>CH<sup>+</sup>) from phosphonium ion precursor salts (P-salt) in presence of excess **2** and **3**. A solution of known concentration of P-salt in CH<sub>3</sub>CN (≈ 10<sup>-5</sup> mol L<sup>-1</sup>) was mixed with a solution of known concentration of **2** and **3** (≈ 10<sup>-4</sup> to 10<sup>-3</sup> mol L<sup>-1</sup>) in CH<sub>2</sub>Cl<sub>2</sub>. The resulting colorless solution was then irradiated with 6.5-ns laser pulses (266 nm) from a

quadrupled Nd:YAG laser (266 nm, 40-60 mJ/pulse) to generate the benzhydrylium ions  $\text{Ar}_2\text{CH}^+$ .

The decay of the absorbance of  $\text{Ar}_2\text{CH}^+$  was monitored by UV/Vis spectroscopy at the corresponding absorption maxima. The pseudo-first-order rate constants  $k_{\text{obs}}$  ( $\text{s}^{-1}$ ) were obtained by least-squares fitting of the absorbances to the monoexponential function  $A_t = A_0 \exp(-k_{\text{obs}}t) + C$ . The second-order rate constants  $k$  ( $\text{M}^{-1} \text{s}^{-1}$ ) were obtained from the slopes of the linear plots of  $k_{\text{obs}}$  against the nucleophile concentrations.

#### 4.2 Reaction products

**7a:** To a solution of  $(\text{dma})_2\text{CH}^+\text{BF}_4^-$  (68 mg, 0.20 mmol) in  $\text{CH}_2\text{Cl}_2$  (3 mL) a solution of **1a** (17 mg, 0.20 mmol) in  $\text{CH}_2\text{Cl}_2$  (2 mL) was added drop wise under nitrogen atmosphere and then the mixture was allowed to stir for another 2–3 minutes. Then the solution was evaporated and  $^1\text{H}$  NMR of the crude product showed a mixture of mono- and bis-substituted product in  $\sim 1 : 3$ . The crude mixture was then dissolved in  $\text{CH}_2\text{Cl}_2$  (15 mL) and washed several time (5-6 times) with water, dried over  $\text{Na}_2\text{SO}_4$ , concentrated ( $\sim 2$  ml) and then crystallized by slow diffusion of *n*-pentane into it to give 45 mg (67  $\mu\text{mol}$ , 33%) of **7a** as blue powder. M.p. ( $\text{CH}_2\text{Cl}_2$ -*n*-pentane): 134–136 °C.  $^1\text{H}$ -NMR ( $\text{CD}_2\text{Cl}_2$ , 400 MHz):  $\delta = 2.24$  (s, 3 H,  $\text{CH}_3$ ), 2.96 (s, 24 H,  $\text{N}(\text{CH}_3)_2$ ), 3.55 (s, 4 H,  $\text{CH}_2$ ), 6.08 (s, 2 H,  $\text{Ar}_2\text{CH}-\text{N}^+$ ), 6.72 (d,  $J = 8.8$  Hz, 8 H, Ar), 7.05 (d,  $J = 8.8$  Hz, 8 H, Ar) ppm.  $^{13}\text{C}$ -NMR ( $\text{CD}_2\text{Cl}_2$ , 100 MHz):  $\delta = 12.9$  (q,  $\text{CH}_3$ ), 40.7 (q,  $\text{N}(\text{CH}_3)_2$ ), 46.8 (t,  $\text{CH}_2$ ), 64.4 (d,  $\text{Ar}_2\text{CH}-\text{N}$ ), 112.9 (d, Ar), 124.2 (s, Ar), 129.4 (d, Ar), 151.2 (s, Ar), 166.8 (s,  $\text{C}=\text{N}^+$ ) ppm. HRMS (ESI $^+$ ): calculated for  $\text{C}_{38}\text{H}_{49}\text{N}_6^+$  ( $\text{M}^+$ ) is 589.4013; found 589.4012.

**7b:** To a solution of  $(\text{dma})_2\text{CH}^+\text{BF}_4^-$  (34 mg, 0.10 mmol) in  $\text{CH}_2\text{Cl}_2$  (3 mL) a solution of **1b** (15 mg, 0.10 mmol) in  $\text{CH}_2\text{Cl}_2$  (2 mL) was added drop wise under nitrogen atmosphere and then the mixture was allowed to stir for another 2–3 minutes. Then the solution was evaporated and  $^1\text{H}$  NMR of the crude product showed a mixture of mono- and bis-substituted product in  $\sim 1 : 3$ . The crude mixture was then dissolved in  $\text{CH}_2\text{Cl}_2$  (15 mL) and washed several time (5-6 times) with water, dried over  $\text{Na}_2\text{SO}_4$ , concentrated ( $\sim 2$  ml), added few drops of ethylacetate and then crystallized by slow diffusion of *n*-pentane into it to give 24 mg (32  $\mu\text{mol}$ , 32%) of **7b** as blue shiny crystals. M.p. ( $\text{CH}_2\text{Cl}_2$ -EtOAc-*n*-pentane): 168–170 °C.  $^1\text{H}$ -NMR ( $\text{CDCl}_3$ , 300 MHz):  $\delta = 2.94$  (s, 24 H,  $\text{N}(\text{CH}_3)_2$ ), 3.94 (s, 4 H,  $\text{CH}_2$ ), 5.66 (s, 2 H,  $\text{Ar}_2\text{CH}-\text{N}^+$ ), 6.68 (d,  $J = 8.7$  Hz, 8 H, Ar), 6.94 (d,  $J = 8.7$  Hz, 8 H, Ar), 7.33-7.36 (m, 2 H, Ar), 7.49-7.54 (m, 2 H, Ar), 7.58-7.67 (m, 1 H, Ar) ppm.  $^{13}\text{C}$ -NMR ( $\text{CDCl}_3$ , 75 MHz):  $\delta =$

40.6 (q, N(CH<sub>3</sub>)<sub>2</sub>), 45.7 (t, CH<sub>2</sub>), 64.7 (d, Ar<sub>2</sub>CH-N), 112.7 (d, Ar), 123.1 (d, Ar), 123.4 (s, Ar), 127.9 (d, Ar), 129.2 (d, Ar), 130.1 (d, Ar), 133.0 (s, Ar), 150.1 (s, Ar), 166.3 (s, C=N<sup>+</sup>) ppm. HRMS (ESI<sup>+</sup>): calculated for C<sub>43</sub>H<sub>51</sub>N<sub>6</sub><sup>+</sup> (M<sup>+</sup>) is 651.4170; found 651.4172.

**Crystallographic data for 7b:**

net formula	C <sub>43</sub> H <sub>51</sub> BF <sub>4</sub> N <sub>6</sub>
<i>M<sub>r</sub></i> /g mol <sup>-1</sup>	738.710
crystal size/mm	0.252 × 0.183 × 0.113
<i>T</i> /K	200(2)
radiation	MoKα
diffractometer	'KappaCCD'
crystal system	monoclinic
space group	<i>P</i> 2 <sub>1</sub> / <i>c</i>
<i>a</i> /Å	12.9344(2)
<i>b</i> /Å	24.2468(5)
<i>c</i> /Å	12.7879(2)
α/°	90
β/°	97.1823(10)
γ/°	90
<i>V</i> /Å <sup>3</sup>	3979.04(12)
<i>Z</i>	4
calc. density/g cm <sup>-3</sup>	1.2331(6)
μ/mm <sup>-1</sup>	0.086
absorption correction	none
refls. measured	26794
<i>R</i> <sub>int</sub>	0.0317
mean σ( <i>I</i> )/ <i>I</i>	0.0284
θ range	3.17–25.34
observed refls.	5577
<i>x</i> , <i>y</i> (weighting scheme)	0.0575, 1.0544
hydrogen refinement	constr
refls in refinement	7255
parameters	495
restraints	0
<i>R</i> ( <i>F</i> <sub>obs</sub> )	0.0440
<i>R</i> <sub>w</sub> ( <i>F</i> <sup>2</sup> )	0.1198
<i>S</i>	1.034
shift/error <sub>max</sub>	0.001
max electron density/e Å <sup>-3</sup>	0.173
min electron density/e Å <sup>-3</sup>	-0.193

**8:** To a solution of (dma)<sub>2</sub>CH<sup>+</sup>BF<sub>4</sub><sup>-</sup> (52.3 mg, 0.154 mmol) in CH<sub>2</sub>Cl<sub>2</sub> (2 mL) a solution of **4a** (15.1 mg, 0.154 mmol) in CH<sub>2</sub>Cl<sub>2</sub> (1 mL) was added drop wise under nitrogen atmosphere and then the mixture was allowed to stir for another 2–3 minutes. Then the solution was evaporated and the resulting residue was washed with dry *i*-hexane to get a greenish powder (62 mg, 0.14 mmol, 91%). M.p. (CH<sub>2</sub>Cl<sub>2</sub>-*i*-hexane): 102–105 °C (decomp.). <sup>1</sup>H-NMR

(DMSO- $d_6$ , 400 MHz):  $\delta$  = 1.89-1.91 (m, 2 H,  $N^+CH_2CH_2CH_2N$ ), 2.34 (s, 3 H,  $CH_3$ ), 2.91 (s, 12 H,  $N(CH_3)_2$ ), 3.06 (t,  $J$  = 5.4, Hz, 2 H,  $N^+CH_2CH_2CH_2N$ ), 3.29 (t,  $J$  = 5.7, 2 H,  $N^+CH_2CH_2CH_2N$ ), 6.28 (s, 1 H,  $Ar_2CH-N^+$ ), 6.74 (d,  $J$  = 8.8 Hz, 4 H, Ar), 7.02 (d,  $J$  = 8.8 Hz, 4 H, Ar), 9.59 (bs, 1 H,  $N^+-H$ ) ppm.  $^{13}C$ -NMR (DMSO- $d_6$ , 100 MHz):  $\delta$  = 18.5 (t,  $N^+CH_2CH_2CH_2N$ ), 18.7 (q,  $CH_3$ ), 38.4 (t,  $N^+CH_2CH_2CH_2N$ ), 39.9 (q,  $N(CH_3)_2$ ), 42.8 (t,  $N^+CH_2CH_2CH_2N$ ), 65.3 (d,  $Ar_2CH-N$ ), 112.2 (d, Ar), 124.4 (s, Ar), 129.0 (d, Ar), 149.9 (s, Ar), 160.9 (s,  $C=N^+$ ) ppm. HRMS (ESI $^+$ ): calculated for  $C_{17}H_{21}N_2^+$  ( $M-4a^+$ ) is 253.1699; found 253.1698.

**9:** Equimolar solution of (ani) $_2$ CHCl (26.3 mg, 0.100 mmol) and **1c** (12.6 mg, 0.100 mmol) were mixed in  $d_6$ -DMSO (0.8 mL) in an NMR tube under argon and after few minutes of shaking the NMR was recorded.  $^1H$ -NMR ( $d_6$ -DMSO, 400 MHz):  $\delta$  = 2.33 (s, 3 H,  $CH_3$ ), 2.72 (s, 3 H,  $CH_3$ ), 3.65-3.70 (m, 2 H,  $CH_2$ ), 2.78 (s, 6 H,  $OCH_3$ ), 4.25-4.30 (m, 2 H,  $CH_2$ ), 6.81 (s, 1 H,  $Ar_2CH-N^+$ ), 7.00 (d,  $J$  = 8.8 Hz, 4 H, Ar), 7.28 (d,  $J$  = 8.8 Hz, 4 H, Ar) ppm.  $^{13}C$ -NMR (DMSO- $d_6$ , 100 MHz):  $\delta$  = 15.3 (q,  $CH_3$ ), 24.6 (q,  $CH_3$ ), 45.8 (t,  $CH_2$ ), 47.9 (t,  $CH_2$ ), 55.2 (q,  $OCH_3$ ), 62.5 (d,  $Ar_2CH-N$ ), 114.2 (d, Ar), 127.7 (s, Ar), 129.9 (d, Ar), 159.3 (s, Ar), 168.5 (s,  $C=N^+$ ), 170.5 (s,  $C=O$ ) ppm.

**10:** Equimolar solution of (ani) $_2$ CHBr (30.7 mg, 0.100 mmol) and **2** (10.1 mg, 0.100 mmol) were mixed in  $d_6$ -DMSO (0.8 mL) in an NMR tube under argon and after few minutes of shaking the NMR was recorded.  $^1H$ -NMR ( $d_6$ -DMSO, 400 MHz):  $\delta$  = 2.67 (s, 3 H,  $CH_3$ ), 3.67-3.72 (m, 2 H,  $CH_2$ ), 2.78 (s, 6 H,  $OCH_3$ ), 4.14 (t,  $J$  = 9.2, Hz, 2 H,  $CH_2$ ), 6.87 (s, 1 H,  $Ar_2CH-N^+$ ), 7.02 (d,  $J$  = 8.8 Hz, 4 H, Ar), 7.30 (d,  $J$  = 8.8 Hz, 4 H, Ar) ppm.  $^{13}C$ -NMR (DMSO- $d_6$ , 100 MHz):  $\delta$  = 18.2 (q,  $CH_3$ ), 29.0 (t,  $CH_2$ ), 55.3 (q,  $OCH_3$ ), 58.3 (t,  $CH_2$ ), 66.4 (d,  $Ar_2CH-N$ ), 114.4 (d, Ar), 127.5 (s, Ar), 129.9 (d, Ar), 159.4 (s, Ar), 191.9 (s,  $C=N^+$ ) ppm.

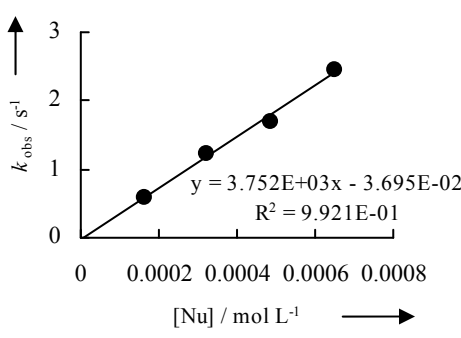
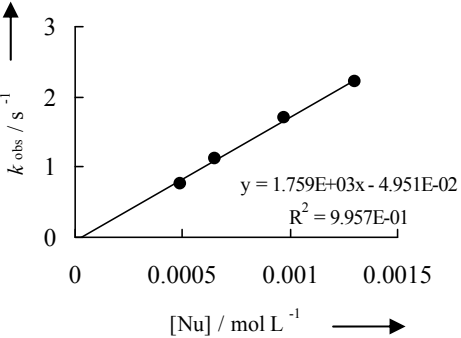
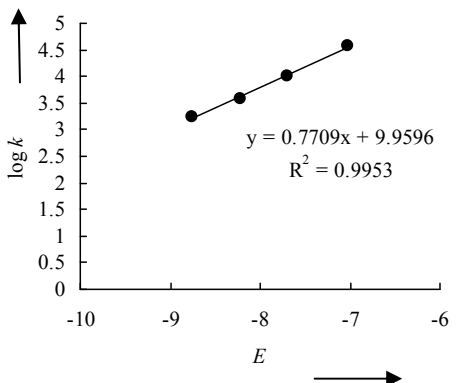
**11:** Equimolar solution of (ani)(tol)CHBr (29.1 mg, 0.100 mmol) and **2** (10.1 mg, 0.100 mmol) were mixed in  $CD_2Cl_2$  (0.8 mL) in an NMR tube under argon and after few minutes of shaking the NMR was recorded.  $^1H$ -NMR ( $CD_2Cl_2$ , 400 MHz):  $\delta$  = 2.36 (s, 3 H,  $CH_3$ ), 2.74 (s, 3 H,  $CH_3$ ), 3.75-3.81 (m, 2 H + 3 H,  $CH_2$  +  $OCH_3$ ), 4.17-4.30 (m, 2 H,  $CH_2$ ), 6.94 (d,  $J$  = 8.7 Hz, 2 H, Ar), 6.98 (s, 1 H,  $Ar_2CH-N^+$ ), 7.24-7.26 (m, 2 H + 2 H, Ar), 7.40 (d,  $J$  = 8.7 Hz, 2 H, Ar) ppm.  $^{13}C$ -NMR ( $CD_2Cl_2$ , 100 MHz):  $\delta$  = 20.6 (q,  $CH_3$ ), 21.4 (q,  $CH_3$ ), 30.3 (t,  $CH_2$ ), 55.9 (q,  $OCH_3$ ), 60.2 (t,  $CH_2$ ), 69.1 (d,  $Ar_2CH-N$ ), 115.1 (d, Ar), 127.6 (s, Ar), 128.5 (d, Ar), 130.6 (d, Ar), 131.0 (d, Ar), 132.9 (s, Ar), 140.0 (s, Ar), 160.9 (s, Ar), 192.7 (s,  $C=N^+$ ) ppm.

## 4.3 Kinetics

4.3.1 Kinetics of the reactions of 1–5 with benzhydrylium ions ( $\text{Ar}_2\text{CH}^+$ )**Table 6.** Kinetics of the reactions of 2-methyl-4,5-dihydro-1H-imidazole (**1a**) with  $(\text{Ar})_2\text{CH}^+$  in  $\text{CH}_2\text{Cl}_2$  at 20 °C.

$[(\text{dma})_2\text{CH}^+]$ (mol L <sup>-1</sup> )	[ <b>1a</b> ] (mol L <sup>-1</sup> )	$k_{\text{obs}}$ (s <sup>-1</sup> )	$\lambda = 613$ nm (Stopped-flow)	$k$ (M <sup>-1</sup> s <sup>-1</sup> )
$1.50 \times 10^{-5}$	$6.50 \times 10^{-5}$	2.00		$3.73 \times 10^4$
	$1.30 \times 10^{-4}$	4.37		
	$1.63 \times 10^{-4}$	5.64		
	$2.28 \times 10^{-4}$	8.05		
$[(\text{pyr})_2\text{CH}^+]$ (mol L <sup>-1</sup> )	[ <b>1a</b> ] (mol L <sup>-1</sup> )	$k_{\text{obs}}$ (s <sup>-1</sup> )	$\lambda = 620$ nm (Stopped-flow)	$k$ (M <sup>-1</sup> s <sup>-1</sup> )
$1.60 \times 10^{-5}$	$3.23 \times 10^{-4}$	4.28		$1.04 \times 10^4$
	$4.85 \times 10^{-4}$	5.42		
	$6.47 \times 10^{-4}$	7.38		
	$8.08 \times 10^{-4}$	9.21		

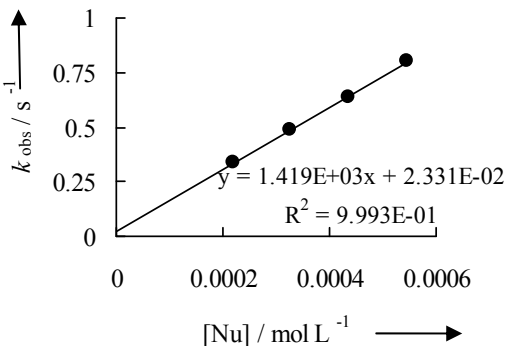
Table 6 continued

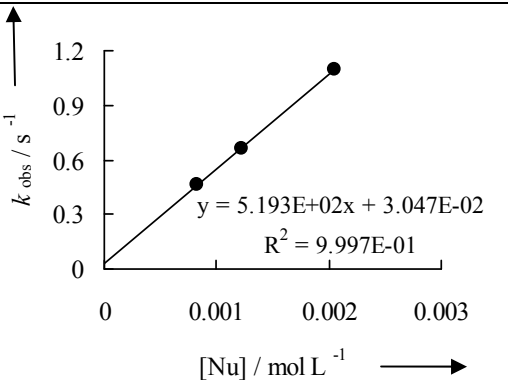
$[(\text{thq})_2\text{CH}^+]$ (mol L <sup>-1</sup> )	[ <b>1a</b> ] (mol L <sup>-1</sup> )	$k_{\text{obs}}$ (s <sup>-1</sup> )	$\lambda = 628$ nm (Stopped-flow)	$k$ (M <sup>-1</sup> s <sup>-1</sup> )
$2.00 \times 10^{-5}$	$1.63 \times 10^{-4}$	0.587		$3.75 \times 10^3$
	$3.25 \times 10^{-4}$	1.21		
	$4.88 \times 10^{-4}$	1.69		
	$6.50 \times 10^{-4}$	2.46		
$[(\text{ind})_2\text{CH}^+]$ (mol L <sup>-1</sup> )	[ <b>1a</b> ] (mol L <sup>-1</sup> )	$k_{\text{obs}}$ (s <sup>-1</sup> )	$\lambda = 625$ nm (Stopped-flow)	$k$ (M <sup>-1</sup> s <sup>-1</sup> )
$1.43 \times 10^{-5}$	$4.88 \times 10^{-4}$	0.766		$1.76 \times 10^3$
	$6.50 \times 10^{-4}$	1.13		
	$9.75 \times 10^{-4}$	1.70		
	$1.30 \times 10^{-4}$	2.21		
Reactivity parameters for <b>1a</b> in CH <sub>2</sub> Cl <sub>2</sub>				
Ar <sub>2</sub> CH <sup>+</sup>	<i>E</i>	$k$ (M <sup>-1</sup> s <sup>-1</sup> )		<i>N</i> = 12.92 <i>s<sub>N</sub></i> = 0.77
(dma) <sub>2</sub> CH <sup>+</sup>	-7.02	$3.73 \times 10^4$		
(pyr) <sub>2</sub> CH <sup>+</sup>	-7.69	$1.04 \times 10^4$		
(thq) <sub>2</sub> CH <sup>+</sup>	-8.22	$3.75 \times 10^4$		
(ind) <sub>2</sub> CH <sup>+</sup>	-8.76	$1.76 \times 10^4$		

**Table 7.** Kinetics of the reactions of 2-phenyl-4,5-dihydro-1H-imidazole (**1b**) with (Ar)<sub>2</sub>CH<sup>+</sup> in CH<sub>2</sub>Cl<sub>2</sub> at 20°C

[(mpa) <sub>2</sub> CH <sup>+</sup> ] (mol L <sup>-1</sup> )	[ <b>1b</b> ] (mol L <sup>-1</sup> )	<i>k</i> <sub>obs</sub> (s <sup>-1</sup> )	λ = 622 nm (Stopped-flow)	<i>k</i> (M <sup>-1</sup> s <sup>-1</sup> )
1.00 × 10 <sup>-5</sup>	4.28 × 10 <sup>-5</sup>	3.71		8.15 × 10 <sup>4</sup>
	8.55 × 10 <sup>-4</sup>	7.22		
	1.28 × 10 <sup>-4</sup>	10.7		
	1.71 × 10 <sup>-4</sup>	14.4		
	2.14 × 10 <sup>-4</sup>	17.5		
[(dma) <sub>2</sub> CH <sup>+</sup> ] (mol L <sup>-1</sup> )	[ <b>1b</b> ] (mol L <sup>-1</sup> )	<i>k</i> <sub>obs</sub> (s <sup>-1</sup> )	λ = 613 nm (Stopped-flow)	<i>k</i> (M <sup>-1</sup> s <sup>-1</sup> )
1.50 × 10 <sup>-5</sup>	1.09 × 10 <sup>-4</sup>	1.26		1.26 × 10 <sup>4</sup>
	2.18 × 10 <sup>-4</sup>	2.69		
	3.27 × 10 <sup>-4</sup>	4.03		
	4.36 × 10 <sup>-4</sup>	5.40		
[(pyr) <sub>2</sub> CH <sup>+</sup> ] (mol L <sup>-1</sup> )	[ <b>1b</b> ] (mol L <sup>-1</sup> )	<i>k</i> <sub>obs</sub> (s <sup>-1</sup> )	λ = 620 nm (Stopped-flow)	<i>k</i> (M <sup>-1</sup> s <sup>-1</sup> )
2.00 × 10 <sup>-5</sup>	2.18 × 10 <sup>-4</sup>	0.760		3.25 × 10 <sup>3</sup>
	3.27 × 10 <sup>-4</sup>	1.10		
	4.36 × 10 <sup>-4</sup>	1.46		
	5.46 × 10 <sup>-4</sup>	1.82		

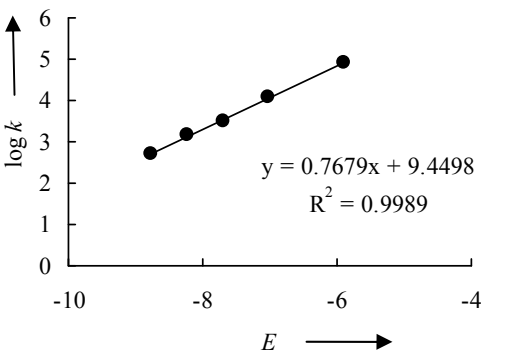
Table 7 continued

$[(\text{thq})_2\text{CH}^+]$ (mol L <sup>-1</sup> )	[1b] (mol L <sup>-1</sup> )	$k_{\text{obs}}$ (s <sup>-1</sup> )	$\lambda = 628$ nm (Stopped-flow)	$k$ (M <sup>-1</sup> s <sup>-1</sup> )
$2.00 \times 10^{-5}$	$2.18 \times 10^{-4}$	0.336		$1.42 \times 10^3$
	$3.27 \times 10^{-4}$	0.487		
	$4.36 \times 10^{-4}$	0.635		
	$5.46 \times 10^{-4}$	0.803		

$[(\text{ind})_2\text{CH}^+]$ (mol L <sup>-1</sup> )	[1b] (mol L <sup>-1</sup> )	$k_{\text{obs}}$ (s <sup>-1</sup> )	$\lambda = 625$ nm (Stopped-flow)	$k$ (M <sup>-1</sup> s <sup>-1</sup> )
$2.00 \times 10^{-5}$	$8.20 \times 10^{-4}$	0.460		$5.19 \times 10^2$
	$1.23 \times 10^{-3}$	0.663		
	$2.05 \times 10^{-3}$	1.10		

Reactivity parameters for 1b in CH<sub>2</sub>Cl<sub>2</sub>

Ar <sub>2</sub> CH <sup>+</sup>	$E$	$k$ (M <sup>-1</sup> s <sup>-1</sup> )
(mpa) <sub>2</sub> CH <sup>+</sup>	-5.89	$8.15 \times 10^4$
(dma) <sub>2</sub> CH <sup>+</sup>	-7.02	$1.26 \times 10^4$
(pyr) <sub>2</sub> CH <sup>+</sup>	-7.69	$3.25 \times 10^4$
(thq) <sub>2</sub> CH <sup>+</sup>	-8.22	$1.42 \times 10^3$
(ind) <sub>2</sub> CH <sup>+</sup>	-8.76	$5.19 \times 10^2$

$N = 12.31$   
 $s_N = 0.77$

**Table 8.** Kinetics of the reactions of 1-(2-methyl-4,5-dihydro-1H-imidazol-1-yl)ethanone **1c** with  $(\text{Ar})_2\text{CH}^+$  in  $\text{CH}_2\text{Cl}_2$  at  $20^\circ\text{C}$ 

$[(\text{mfa})_2\text{CH}^+]$ (mol L <sup>-1</sup> )	<b>[1c]</b> (mol L <sup>-1</sup> )	$k_{\text{obs}}$ (s <sup>-1</sup> )	$\lambda = 593 \text{ nm}$ (Stopped-flow)	$k$ (M <sup>-1</sup> s <sup>-1</sup> )
$5.54 \times 10^{-6}$	$8.05 \times 10^{-5}$	3.80		$4.91 \times 10^4$
	$1.61 \times 10^{-4}$	8.23		
	$2.41 \times 10^{-4}$	12.0		
	$3.22 \times 10^{-4}$	16.3		
	$4.02 \times 10^{-4}$	19.5		
$[(\text{dpa})_2\text{CH}^+]$ (mol L <sup>-1</sup> )	<b>[1c]</b> (mol L <sup>-1</sup> )	$k_{\text{obs}}$ (s <sup>-1</sup> )	$\lambda = 672 \text{ nm}$ (Stopped-flow)	$k$ (M <sup>-1</sup> s <sup>-1</sup> )
$8.92 \times 10^{-6}$	$8.05 \times 10^{-5}$	0.640		$8.81 \times 10^3$
	$1.61 \times 10^{-4}$	1.40		
	$2.41 \times 10^{-4}$	2.05		
	$3.22 \times 10^{-4}$	2.78		
	$4.02 \times 10^{-4}$	3.49		
$[(\text{mor})_2\text{CH}^+]$ (mol L <sup>-1</sup> )	<b>[1c]</b> (mol L <sup>-1</sup> )	$k_{\text{obs}}$ (s <sup>-1</sup> )	$\lambda = 620 \text{ nm}$ (Stopped-flow)	$k$ (M <sup>-1</sup> s <sup>-1</sup> )
$6.13 \times 10^{-6}$	$2.30 \times 10^{-4}$	0.610		$2.25 \times 10^3$
	$4.61 \times 10^{-4}$	1.30		
	$5.76 \times 10^{-4}$	1.39		
	$9.21 \times 10^{-4}$	2.15		
	$1.15 \times 10^{-3}$	2.67		

Table 8 continued

$[(\text{thq})_2\text{CH}^+]$ (mol L <sup>-1</sup> )	$[\mathbf{1c}]$ (mol L <sup>-1</sup> )	$k_{\text{obs}}$ (s <sup>-1</sup> )	$\lambda = 622 \text{ nm}$ (Stopped-flow)	$k$ (M <sup>-1</sup> s <sup>-1</sup> )
$6.46 \times 10^{-6}$	$2.30 \times 10^{-4}$	0.997		$1.48 \times 10^3$
	$4.61 \times 10^{-4}$	1.35		
	$5.76 \times 10^{-4}$	1.53		
	$9.21 \times 10^{-4}$	2.05		
	$1.15 \times 10^{-3}$	2.34		

Reactivity parameters for **1c** in CH<sub>2</sub>Cl<sub>2</sub>

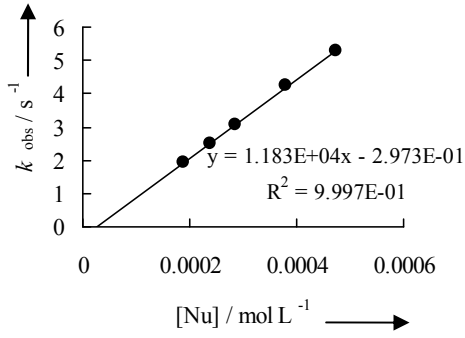
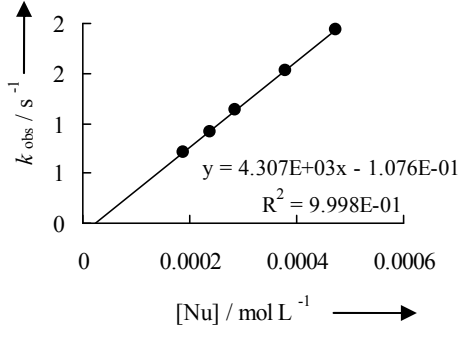
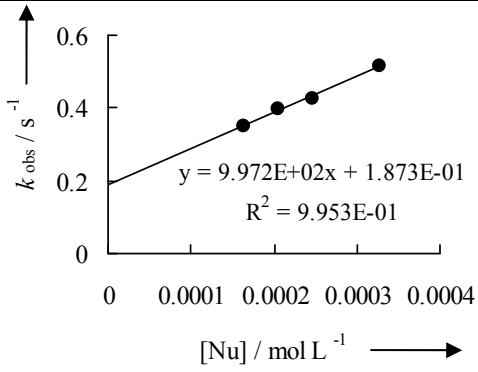
Ar <sub>2</sub> CH <sup>+</sup>	<i>E</i>	$k$ (M <sup>-1</sup> s <sup>-1</sup> )
(mfa) <sub>2</sub> CH <sup>+</sup>	-3.85	$4.91 \times 10^4$
(dpa) <sub>2</sub> CH <sup>+</sup>	-4.72	$8.81 \times 10^3$
(mor) <sub>2</sub> CH <sup>+</sup>	-5.53	$2.25 \times 10^3$
(mpa) <sub>2</sub> CH <sup>+</sup>	-5.89	$1.48 \times 10^3$

Table 9. Kinetics of the reactions of 1-benzyl-2-phenyl-4,5-dihydro-1H-imidazole **1d** with (Ar)<sub>2</sub>CH<sup>+</sup> in CH<sub>2</sub>Cl<sub>2</sub> at 20°C

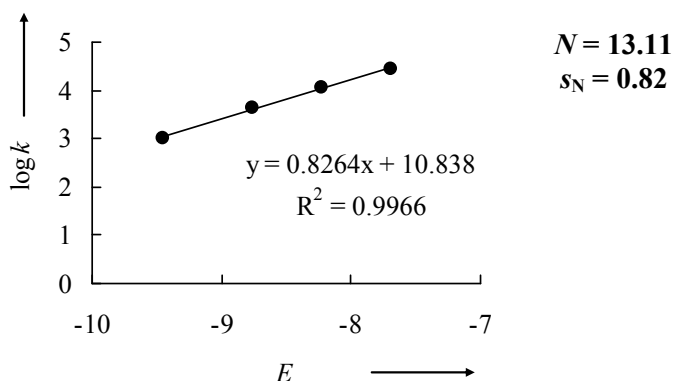
$[(\text{pyr})_2\text{CH}^+]$ (mol L <sup>-1</sup> )	$[\mathbf{1d}]$ (mol L <sup>-1</sup> )	$k_{\text{obs}}$ (s <sup>-1</sup> )	$\lambda = 620 \text{ nm}$ (Stopped-flow)	$k$ (M <sup>-1</sup> s <sup>-1</sup> )
$1.34 \times 10^{-5}$	$1.64 \times 10^{-4}$	3.86		$2.82 \times 10^4$
	$2.05 \times 10^{-4}$	4.87		
	$2.46 \times 10^{-4}$	5.96		
	$3.28 \times 10^{-4}$	7.99		
	$4.10 \times 10^{-4}$	10.9		

Table 9 continued

$[(\text{thq})_2\text{CH}^+]$ (mol L <sup>-1</sup> )	<b>[1d]</b> (mol L <sup>-1</sup> )	$k_{\text{obs}}$ (s <sup>-1</sup> )	$\lambda = 622 \text{ nm}$ (Stopped-flow)	$k$ (M <sup>-1</sup> s <sup>-1</sup> )
$1.50 \times 10^{-5}$	$1.90 \times 10^{-4}$	1.94		$1.18 \times 10^4$
	$2.37 \times 10^{-4}$	2.50		
	$2.84 \times 10^{-4}$	3.06		
	$3.79 \times 10^{-4}$	4.23		
	$4.74 \times 10^{-4}$	5.28		
$[(\text{ind})_2\text{CH}^+]$ (mol L <sup>-1</sup> )	<b>[1d]</b> (mol L <sup>-1</sup> )	$k_{\text{obs}}$ (s <sup>-1</sup> )	$\lambda = 626 \text{ nm}$ (Stopped-flow)	$k$ (M <sup>-1</sup> s <sup>-1</sup> )
$1.54 \times 10^{-5}$	$1.90 \times 10^{-4}$	0.702		$4.31 \times 10^3$
	$2.37 \times 10^{-4}$	0.913		
	$2.84 \times 10^{-4}$	1.13		
	$3.79 \times 10^{-4}$	1.52		
	$4.74 \times 10^{-4}$	1.93		
$[(\text{jul})_2\text{CH}^+]$ (mol L <sup>-1</sup> )	<b>[1d]</b> (mol L <sup>-1</sup> )	$k_{\text{obs}}$ (s <sup>-1</sup> )	$\lambda = 642 \text{ nm}$ (Stopped-flow)	$k$ (M <sup>-1</sup> s <sup>-1</sup> )
$1.55 \times 10^{-5}$	$1.64 \times 10^{-4}$	0.350		$9.97 \times 10^2$
	$2.05 \times 10^{-4}$	0.398		
	$2.46 \times 10^{-4}$	0.427		
	$3.28 \times 10^{-4}$	0.516		

**Table 9** continuedReactivity parameters for **1d** in CH<sub>2</sub>Cl<sub>2</sub>

Ar <sub>2</sub> CH <sup>+</sup>	<i>E</i>	<i>k</i> (M <sup>-1</sup> s <sup>-1</sup> )
(pyr) <sub>2</sub> CH <sup>+</sup>	-7.69	2.82 × 10 <sup>4</sup>
(thq) <sub>2</sub> CH <sup>+</sup>	-8.22	1.18 × 10 <sup>4</sup>
(ind) <sub>2</sub> CH <sup>+</sup>	-8.76	4.31 × 10 <sup>3</sup>
(jul) <sub>2</sub> CH <sup>+</sup>	-9.45	9.97 × 10 <sup>2</sup>

**Table 10.** Kinetics of the reactions of 2-methyl-1,4,5,6-tetrahydropyrimidine **2a** with (Ar)<sub>2</sub>CH<sup>+</sup> in CH<sub>2</sub>Cl<sub>2</sub> at 20°C

[(dma) <sub>2</sub> CH <sup>+</sup> ] (mol L <sup>-1</sup> )	[ <b>2a</b> ] (mol L <sup>-1</sup> )	<i>k</i> <sub>obs</sub> (s <sup>-1</sup> )	$\lambda = 613$ nm (Stopped-flow)	<i>k</i> (M <sup>-1</sup> s <sup>-1</sup> )
7.63 × 10 <sup>-6</sup>	5.04 × 10 <sup>-5</sup>	24.7	<p><math>y = 4.193E+05x + 3.847E+00</math> <math>R^2 = 9.924E-01</math></p>	4.19 × 10 <sup>5</sup>
	1.01 × 10 <sup>-4</sup>	43.3		
	1.51 × 10 <sup>-4</sup>	71.7		
	2.52 × 10 <sup>-4</sup>	108		
[(pyr) <sub>2</sub> CH <sup>+</sup> ] (mol L <sup>-1</sup> )	[ <b>2a</b> ] (mol L <sup>-1</sup> )	<i>k</i> <sub>obs</sub> (s <sup>-1</sup> )	$\lambda = 620$ nm (Stopped-flow)	<i>k</i> (M <sup>-1</sup> s <sup>-1</sup> )
5.61 × 10 <sup>-6</sup>	5.04 × 10 <sup>-5</sup>	8.42	<p><math>y = 1.682E+05x + 8.032E-02</math> <math>R^2 = 9.999E-01</math></p>	1.68 × 10 <sup>5</sup>
	1.01 × 10 <sup>-4</sup>	17.3		
	1.51 × 10 <sup>-4</sup>	33.9		
	2.52 × 10 <sup>-4</sup>	42.5		

Table 10 continued

$[(\text{thq})_2\text{CH}^+]$ (mol L <sup>-1</sup> )	<b>[2a]</b> (mol L <sup>-1</sup> )	$k_{\text{obs}}$ (s <sup>-1</sup> )	$\lambda = 628 \text{ nm}$ (Stopped-flow)	$k$ (M <sup>-1</sup> s <sup>-1</sup> )
$7.01 \times 10^{-6}$	$1.23 \times 10^{-4}$	6.61		$5.90 \times 10^4$
	$2.47 \times 10^{-4}$	14.7		
	$3.70 \times 10^{-4}$	20.9		
	$4.93 \times 10^{-4}$	28.8		
$[(\text{jul})_2\text{CH}^+]$ (mol L <sup>-1</sup> )	<b>[2a]</b> (mol L <sup>-1</sup> )	$k_{\text{obs}}$ (s <sup>-1</sup> )	$\lambda = 625 \text{ nm}$ (Stopped-flow)	$k$ (M <sup>-1</sup> s <sup>-1</sup> )
$7.69 \times 10^{-6}$	$1.23 \times 10^{-4}$	3.32		$2.82 \times 10^4$
	$2.47 \times 10^{-4}$	6.84		
	$3.70 \times 10^{-4}$	9.97		
	$4.93 \times 10^{-4}$	13.9		
Reactivity parameters for <b>2a</b> in CH <sub>2</sub> Cl <sub>2</sub>				
Ar <sub>2</sub> CH <sup>+</sup>	$E$	$k$ (M <sup>-1</sup> s <sup>-1</sup> )		
(dma) <sub>2</sub> CH <sup>+</sup>	-7.02	$4.19 \times 10^5$		
(pyr) <sub>2</sub> CH <sup>+</sup>	-7.69	$1.68 \times 10^5$		
(thq) <sub>2</sub> CH <sup>+</sup>	-8.22	$5.90 \times 10^4$		
(ind) <sub>2</sub> CH <sup>+</sup>	-8.76	$2.82 \times 10^4$		
			$N = 15.21$	
			$s_N = 0.69$	

**Table 11.** Kinetics of the reactions of 2-methyl-1,4,5,6-tetrahydropyrimidine **2a** with  $(\text{Ar})_2\text{CH}^+$  in  $\text{CH}_3\text{CN}$  at  $20^\circ\text{C}$ 

$[(\text{pyr})_2\text{CH}^+]$ (mol L <sup>-1</sup> )	<b>[2a]</b> (mol L <sup>-1</sup> )	$k_{\text{obs}}$ (s <sup>-1</sup> )	$\lambda = 620 \text{ nm}$ (Stopped-flow)	$k$ (M <sup>-1</sup> s <sup>-1</sup> )
$1.53 \times 10^{-5}$	$1.09 \times 10^{-4}$	24.5		$2.30 \times 10^5$
	$1.64 \times 10^{-4}$	36.7		
	$2.18 \times 10^{-4}$	47.2		
	$2.73 \times 10^{-4}$	63.7		
	$3.27 \times 10^{-4}$	73.6		
$[(\text{thq})_2\text{CH}^+]$ (mol L <sup>-1</sup> )	<b>[2a]</b> (mol L <sup>-1</sup> )	$k_{\text{obs}}$ (s <sup>-1</sup> )	$\lambda = 628 \text{ nm}$ (Stopped-flow)	$k$ (M <sup>-1</sup> s <sup>-1</sup> )
$1.52 \times 10^{-5}$	$1.09 \times 10^{-4}$	7.97		$7.29 \times 10^4$
	$1.64 \times 10^{-4}$	12.0		
	$2.18 \times 10^{-4}$	15.9		
	$3.27 \times 10^{-4}$	23.9		
$[(\text{ind})_2\text{CH}^+]$ (mol L <sup>-1</sup> )	<b>[2a]</b> (mol L <sup>-1</sup> )	$k_{\text{obs}}$ (s <sup>-1</sup> )	$\lambda = 625 \text{ nm}$ (Stopped-flow)	$k$ (M <sup>-1</sup> s <sup>-1</sup> )
$1.45 \times 10^{-5}$	$9.98 \times 10^{-5}$	3.02		$2.89 \times 10^4$
	$2.00 \times 10^{-4}$	5.97		
	$3.00 \times 10^{-4}$	8.97		
	$3.99 \times 10^{-4}$	11.7		
	$4.99 \times 10^{-4}$	14.6		

**Table 11** continued

$[(\text{jul})_2\text{CH}^+]$ (mol L <sup>-1</sup> )	<b>[2a]</b> (mol L <sup>-1</sup> )	$k_{\text{obs}}$ (s <sup>-1</sup> )	$\lambda = 642 \text{ nm}$ (Stopped-flow)	$k$ (M <sup>-1</sup> s <sup>-1</sup> )
$1.84 \times 10^{-5}$	$9.98 \times 10^{-5}$	0.996		$9.09 \times 10^3$
	$2.00 \times 10^{-4}$	1.98		
	$3.00 \times 10^{-4}$	2.91		
	$3.99 \times 10^{-4}$	3.77		
	$4.99 \times 10^{-4}$	4.64		

Reactivity parameters for **2a** in CH<sub>3</sub>CN

Ar <sub>2</sub> CH <sup>+</sup>	$E$	$k$ (M <sup>-1</sup> s <sup>-1</sup> )
(pyr) <sub>2</sub> CH <sup>+</sup>	-7.69	$2.30 \times 10^5$
(thq) <sub>2</sub> CH <sup>+</sup>	-8.22	$7.29 \times 10^4$
(ind) <sub>2</sub> CH <sup>+</sup>	-8.76	$2.89 \times 10^4$
(jul) <sub>2</sub> CH <sup>+</sup>	-9.45	$9.09 \times 10^3$

  
**Table 12.** Kinetics of the reactions of 2-methyl-1,4,5,6-tetrahydropyrimidine **2a** with (Ar)<sub>2</sub>CH<sup>+</sup> in DMSO at 20°C

$[(\text{pyr})_2\text{CH}^+]$ (mol L <sup>-1</sup> )	<b>[2a]</b> (mol L <sup>-1</sup> )	$k_{\text{obs}}$ (s <sup>-1</sup> )	$\lambda = 620 \text{ nm}$ (Stopped-flow)	$k$ (M <sup>-1</sup> s <sup>-1</sup> )
$9.18 \times 10^{-6}$	$7.74 \times 10^{-5}$	25.5		$3.24 \times 10^5$
	$1.16 \times 10^{-4}$	38.5		
	$1.55 \times 10^{-4}$	51.0		
	$1.94 \times 10^{-4}$	63.7		
	$2.32 \times 10^{-4}$	75.6		

Table 12 continued

$[(\text{thq})_2\text{CH}^+]$ (mol L <sup>-1</sup> )	<b>[2a]</b> (mol L <sup>-1</sup> )	$k_{\text{obs}}$ (s <sup>-1</sup> )	$\lambda = 628 \text{ nm}$ (Stopped-flow)	$k$ (M <sup>-1</sup> s <sup>-1</sup> )
$8.92 \times 10^{-6}$	$6.16 \times 10^{-5}$	5.12		$9.34 \times 10^4$
	$1.23 \times 10^{-4}$	10.8		
	$1.85 \times 10^{-4}$	16.7		
	$2.47 \times 10^{-4}$	22.3		
	$3.08 \times 10^{-4}$	28.2		
$[(\text{ind})_2\text{CH}^+]$ (mol L <sup>-1</sup> )	<b>[2a]</b> (mol L <sup>-1</sup> )	$k_{\text{obs}}$ (s <sup>-1</sup> )	$\lambda = 625 \text{ nm}$ (Stopped-flow)	$k$ (M <sup>-1</sup> s <sup>-1</sup> )
$8.24 \times 10^{-6}$	$7.74 \times 10^{-5}$	2.16		$3.29 \times 10^4$
	$1.16 \times 10^{-4}$	3.32		
	$1.55 \times 10^{-4}$	4.75		
	$1.94 \times 10^{-4}$	5.99		
	$2.32 \times 10^{-4}$	7.19		
$[(\text{jul})_2\text{CH}^+]$ (mol L <sup>-1</sup> )	<b>[2a]</b> (mol L <sup>-1</sup> )	$k_{\text{obs}}$ (s <sup>-1</sup> )	$\lambda = 642 \text{ nm}$ (Stopped-flow)	$k$ (M <sup>-1</sup> s <sup>-1</sup> )
$1.84 \times 10^{-5}$	$6.16 \times 10^{-5}$	0.734		$1.31 \times 10^4$
	$1.23 \times 10^{-4}$	1.53		
	$1.85 \times 10^{-4}$	2.38		
	$2.47 \times 10^{-4}$	3.19		
	$3.08 \times 10^{-4}$	3.94		

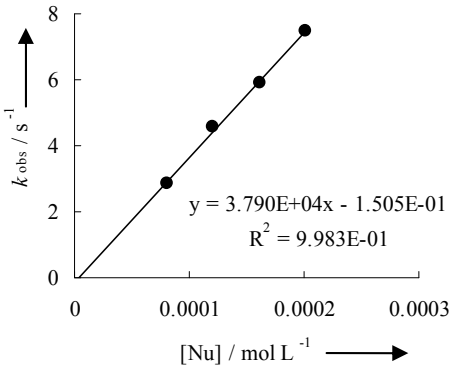
**Table 12** continued

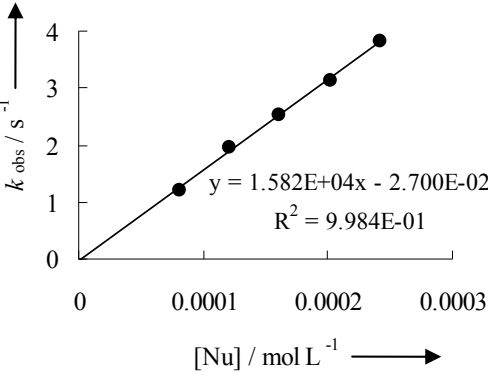
Reactivity parameters for <b>2a</b> in DMSO		
$\text{Ar}_2\text{CH}^+$	$E$	$k$ ( $\text{M}^{-1} \text{s}^{-1}$ )
(pyr) <sub>2</sub> CH <sup>+</sup>	-7.69	$3.24 \times 10^5$
(thq) <sub>2</sub> CH <sup>+</sup>	-8.22	$9.34 \times 10^4$
(ind) <sub>2</sub> CH <sup>+</sup>	-8.76	$3.29 \times 10^4$
(jul) <sub>2</sub> CH <sup>+</sup>	-9.45	$1.31 \times 10^4$

  
**Table 13.** Kinetics of the reactions of 2-phenyl-1,4,5,6-tetrahydropyrimidine **2b** with  $(\text{Ar})_2\text{CH}^+$  in  $\text{CH}_2\text{Cl}_2$  at 20°C

$[(\text{dma})_2\text{CH}^+]$ ( $\text{mol L}^{-1}$ )	<b>[2b]</b> ( $\text{mol L}^{-1}$ )	$k_{\text{obs}}$ ( $\text{s}^{-1}$ )	$\lambda = 613 \text{ nm}$ (Stopped-flow)	$k$ ( $\text{M}^{-1} \text{s}^{-1}$ )
$7.06 \times 10^{-6}$	$4.65 \times 10^{-5}$	16.1		$2.75 \times 10^5$
	$9.30 \times 10^{-5}$	32.6		
	$1.40 \times 10^{-4}$	44.1		
	$1.86 \times 10^{-4}$	54.9		
$[(\text{pyr})_2\text{CH}^+]$ ( $\text{mol L}^{-1}$ )	<b>[2b]</b> ( $\text{mol L}^{-1}$ )	$k_{\text{obs}}$ ( $\text{s}^{-1}$ )	$\lambda = 622 \text{ nm}$ (Stopped-flow)	$k$ ( $\text{M}^{-1} \text{s}^{-1}$ )
$8.29 \times 10^{-6}$	$4.65 \times 10^{-5}$	4.37		$9.61 \times 10^4$
	$9.30 \times 10^{-5}$	9.30		
	$1.40 \times 10^{-4}$	13.4		
	$1.86 \times 10^{-4}$	17.9		
	$2.33 \times 10^{-4}$	22.4		

Table 13 continued

$[(\text{thq})_2\text{CH}^+]$ (mol L <sup>-1</sup> )	<b>[2b]</b> (mol L <sup>-1</sup> )	$k_{\text{obs}}$ (s <sup>-1</sup> )	$\lambda = 628 \text{ nm}$ (Stopped-flow)	$k$ (M <sup>-1</sup> s <sup>-1</sup> )
$6.50 \times 10^{-6}$	$8.07 \times 10^{-5}$	2.85		$3.79 \times 10^4$
	$1.21 \times 10^{-4}$	4.56		
	$1.61 \times 10^{-4}$	5.92		
	$2.02 \times 10^{-4}$	7.49		

$[(\text{ind})_2\text{CH}^+]$ (mol L <sup>-1</sup> )	<b>[2b]</b> (mol L <sup>-1</sup> )	$k_{\text{obs}}$ (s <sup>-1</sup> )	$\lambda = 625 \text{ nm}$ (Stopped-flow)	$k$ (M <sup>-1</sup> s <sup>-1</sup> )
$7.55 \times 10^{-6}$	$8.07 \times 10^{-5}$	1.21		$1.58 \times 10^4$
	$1.21 \times 10^{-4}$	1.95		
	$1.61 \times 10^{-4}$	2.53		
	$2.02 \times 10^{-4}$	3.14		
	$2.42 \times 10^{-4}$	3.81		

Reactivity parameters for **2b** in CH<sub>2</sub>Cl<sub>2</sub>

Ar <sub>2</sub> CH <sup>+</sup>	$E$	$k$ (M <sup>-1</sup> s <sup>-1</sup> )
(dma) <sub>2</sub> CH <sup>+</sup>	-7.02	$2.75 \times 10^5$
(pyr) <sub>2</sub> CH <sup>+</sup>	-7.69	$9.61 \times 10^4$
(thq) <sub>2</sub> CH <sup>+</sup>	-8.22	$3.79 \times 10^4$
(ind) <sub>2</sub> CH <sup>+</sup>	-8.76	$1.58 \times 10^4$

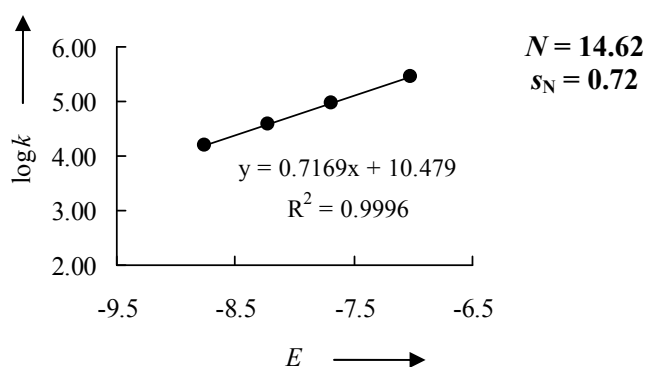


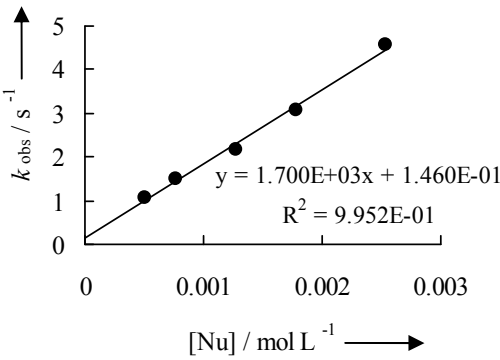
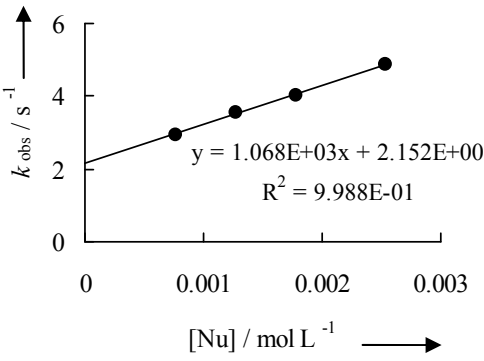
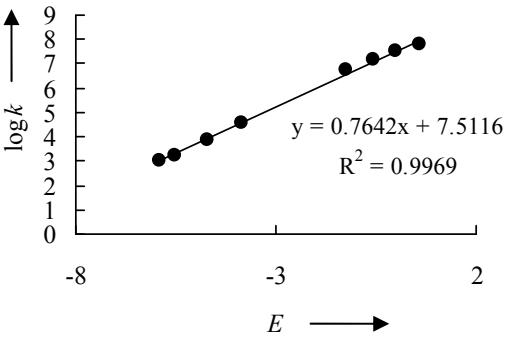
**Table 14.** Kinetics of the reactions of 2-methyl-4,5-dihydrooxazole **3** with (Ar)<sub>2</sub>CH<sup>+</sup> in CH<sub>2</sub>Cl<sub>2</sub> at 20°C

[(ani)(POP)CH- PPh <sub>3</sub> <sup>+</sup> BF <sub>4</sub> <sup>-</sup> ] (mol L <sup>-1</sup> )	[ <b>3</b> ] (mol L <sup>-1</sup> )	<i>k</i> <sub>obs</sub> (s <sup>-1</sup> )	λ = 516 nm (laser-flash photolysis)	<i>k</i> (M <sup>-1</sup> s <sup>-1</sup> )
6.60 × 10 <sup>-5</sup>	7.78 × 10 <sup>-4</sup>	5.97 × 10 <sup>4</sup>		6.16 × 10 <sup>7</sup>
	1.56 × 10 <sup>-3</sup>	1.10 × 10 <sup>5</sup>		
	2.33 × 10 <sup>-3</sup>	1.59 × 10 <sup>5</sup>		
	3.11 × 10 <sup>-3</sup>	2.06 × 10 <sup>5</sup>		
	3.89 × 10 <sup>-3</sup>	2.51 × 10 <sup>5</sup>		
[(ani) <sub>2</sub> CH- PPh <sub>3</sub> <sup>+</sup> BF <sub>4</sub> <sup>-</sup> ] (mol L <sup>-1</sup> )	[ <b>3</b> ] (mol L <sup>-1</sup> )	<i>k</i> <sub>obs</sub> (s <sup>-1</sup> )	λ = 515 nm (laser-flash photolysis)	<i>k</i> (M <sup>-1</sup> s <sup>-1</sup> )
5.20 × 10 <sup>-5</sup>	8.65 × 10 <sup>-4</sup>	3.50 × 10 <sup>4</sup>		3.09 × 10 <sup>7</sup>
	1.73 × 10 <sup>-3</sup>	6.15 × 10 <sup>4</sup>		
	2.60 × 10 <sup>-3</sup>	8.78 × 10 <sup>4</sup>		
	3.46 × 10 <sup>-3</sup>	1.17 × 10 <sup>5</sup>		
	4.33 × 10 <sup>-3</sup>	1.41 × 10 <sup>5</sup>		
[(ani)(fur)CH- PPh <sub>3</sub> <sup>+</sup> BF <sub>4</sub> <sup>-</sup> ] (mol L <sup>-1</sup> )	[ <b>3</b> ] (mol L <sup>-1</sup> )	<i>k</i> <sub>obs</sub> (s <sup>-1</sup> )	λ = 528 nm (laser-flash photolysis)	<i>k</i> (M <sup>-1</sup> s <sup>-1</sup> )
4.76 × 10 <sup>-5</sup>	7.78 × 10 <sup>-4</sup>	1.44 × 10 <sup>4</sup>		1.55 × 10 <sup>7</sup>
	1.56 × 10 <sup>-3</sup>	2.61 × 10 <sup>4</sup>		
	2.33 × 10 <sup>-3</sup>	3.83 × 10 <sup>4</sup>		
	3.11 × 10 <sup>-3</sup>	5.04 × 10 <sup>4</sup>		
	3.89 × 10 <sup>-3</sup>	6.25 × 10 <sup>4</sup>		

Table 14 continued

$[(\text{fur})_2\text{CH}-\text{PPh}_3^+\text{BF}_4^-]$ (mol L <sup>-1</sup> )	[3] (mol L <sup>-1</sup> )	$k_{\text{obs}}$ (s <sup>-1</sup> )	$\lambda = 530 \text{ nm}$ (laser-flash photolysis)	$k$ (M <sup>-1</sup> s <sup>-1</sup> )
$7.44 \times 10^{-5}$	$8.65 \times 10^{-4}$	$8.27 \times 10^3$		$5.35 \times 10^6$
	$1.73 \times 10^{-3}$	$1.26 \times 10^4$		
	$2.60 \times 10^{-3}$	$1.75 \times 10^4$		
	$3.46 \times 10^{-3}$	$2.25 \times 10^4$		
	$4.33 \times 10^{-3}$	$2.65 \times 10^4$		
$[(\text{mfa})_2\text{CH}^+]$ (mol L <sup>-1</sup> )	[3] (mol L <sup>-1</sup> )	$k_{\text{obs}}$ (s <sup>-1</sup> )	$\lambda = 593 \text{ nm}$ (stopped flow)	$k$ (M <sup>-1</sup> s <sup>-1</sup> )
$2.00 \times 10^{-5}$	$2.21 \times 10^{-4}$	8.01		$3.86 \times 10^4$
	$3.68 \times 10^{-4}$	13.8		
	$7.37 \times 10^{-4}$	29.3		
	$1.47 \times 10^{-3}$	56.3		
$[(\text{dpa})_2\text{CH}^+]$ (mol L <sup>-1</sup> )	[3] (mol L <sup>-1</sup> )	$k_{\text{obs}}$ (s <sup>-1</sup> )	$\lambda = 672 \text{ nm}$ (stopped flow)	$k$ (M <sup>-1</sup> s <sup>-1</sup> )
$2.00 \times 10^{-5}$	$3.68 \times 10^{-4}$	2.59		$7.02 \times 10^3$
	$7.37 \times 10^{-4}$	5.10		
	$1.11 \times 10^{-3}$	8.00		
	$1.47 \times 10^{-3}$	9.92		
	$1.84 \times 10^{-3}$	13.1		

Table 14 continued

$[(\text{mor})_2\text{CH}^+]$ (mol L <sup>-1</sup> )	[ <b>3</b> ] (mol L <sup>-1</sup> )	$k_{\text{obs}}$ (s <sup>-1</sup> )	$\lambda = 620 \text{ nm}$ (Stopped-flow)	$k$ (M <sup>-1</sup> s <sup>-1</sup> )
$2.00 \times 10^{-5}$	$5.03 \times 10^{-4}$	1.08		$1.70 \times 10^3$
	$7.61 \times 10^{-4}$	1.48		
	$1.27 \times 10^{-3}$	2.18		
	$1.78 \times 10^{-3}$	3.09		
	$2.54 \times 10^{-3}$	4.55		
$[(\text{mpa})_2\text{CH}^+]$ (mol L <sup>-1</sup> )	[ <b>3</b> ] (mol L <sup>-1</sup> )	$k_{\text{obs}}$ (s <sup>-1</sup> )	$\lambda = 622 \text{ nm}$ (Stopped-flow)	$k$ (M <sup>-1</sup> s <sup>-1</sup> )
$2.00 \times 10^{-5}$	$7.61 \times 10^{-4}$	2.95		$1.07 \times 10^3$
	$1.27 \times 10^{-3}$	3.54		
	$1.78 \times 10^{-3}$	4.02		
	$2.54 \times 10^{-3}$	4.87		
Reactivity parameters for <b>3</b> in CH <sub>2</sub> Cl <sub>2</sub>				
Ar <sub>2</sub> CH <sup>+</sup>	<i>E</i>	$k$ (M <sup>-1</sup> s <sup>-1</sup> )		
(dma)(pop)CH <sup>+</sup>	0.61	$6.16 \times 10^7$		<i>N</i> = 9.83 <i>s<sub>N</sub></i> = 0.76
(ani) <sub>2</sub> CH <sup>+</sup>	0	$3.09 \times 10^7$		
(ani)(fur)CH <sup>+</sup>	-0.56	$1.55 \times 10^7$		
(fur) <sub>2</sub> CH <sup>+</sup>	-1.26	$5.35 \times 10^6$		
(mfa) <sub>2</sub> CH <sup>+</sup>	-3.85	$3.86 \times 10^4$		
(dpa) <sub>2</sub> CH <sup>+</sup>	-4.72	$7.02 \times 10^3$		
(mor) <sub>2</sub> CH <sup>+</sup>	-5.53	$1.70 \times 10^3$		
(mpa) <sub>2</sub> CH <sup>+</sup>	-5.89	$1.07 \times 10^3$		

**Table 15.** Kinetics of the reactions of 2-methyl-4,5-dihydrothiazole **4** with (Ar)<sub>2</sub>CH<sup>+</sup> in CH<sub>2</sub>Cl<sub>2</sub> at 20°C

[(ani)(tol)CH- PPh <sub>3</sub> <sup>+</sup> BF <sub>4</sub> <sup>-</sup> ] (mol L <sup>-1</sup> )	[ <b>4</b> ] (mol L <sup>-1</sup> )	<i>k</i> <sub>obs</sub> (s <sup>-1</sup> )	λ = 516 nm (laser-flash photolysis)	<i>k</i> (M <sup>-1</sup> s <sup>-1</sup> )
5.00 × 10 <sup>-5</sup>	8.15 × 10 <sup>-4</sup>	1.25 × 10 <sup>5</sup>		1.35 × 10 <sup>8</sup>
	1.63 × 10 <sup>-3</sup>	2.38 × 10 <sup>5</sup>		
	2.44 × 10 <sup>-3</sup>	3.57 × 10 <sup>5</sup>		
	3.26 × 10 <sup>-3</sup>	4.58 × 10 <sup>5</sup>		
	4.07 × 10 <sup>-3</sup>	5.65 × 10 <sup>5</sup>		
[(ani)(pop)CH- PPh <sub>3</sub> <sup>+</sup> BF <sub>4</sub> <sup>-</sup> ] (mol L <sup>-1</sup> )	[ <b>4</b> ] (mol L <sup>-1</sup> )	<i>k</i> <sub>obs</sub> (s <sup>-1</sup> )	λ = 516 nm (laser-flash photolysis)	<i>k</i> (M <sup>-1</sup> s <sup>-1</sup> )
4.40 × 10 <sup>-5</sup>	8.15 × 10 <sup>-4</sup>	4.03 × 10 <sup>4</sup>		3.91 × 10 <sup>7</sup>
	1.63 × 10 <sup>-3</sup>	7.21 × 10 <sup>4</sup>		
	2.44 × 10 <sup>-3</sup>	1.02 × 10 <sup>5</sup>		
	3.26 × 10 <sup>-3</sup>	1.37 × 10 <sup>5</sup>		
	4.07 × 10 <sup>-3</sup>	1.67 × 10 <sup>5</sup>		
[(ani) <sub>2</sub> CH- PPh <sub>3</sub> <sup>+</sup> BF <sub>4</sub> <sup>-</sup> ] (mol L <sup>-1</sup> )	[ <b>4</b> ] (mol L <sup>-1</sup> )	<i>k</i> <sub>obs</sub> (s <sup>-1</sup> )	λ = 515 nm (laser-flash photolysis)	<i>k</i> (M <sup>-1</sup> s <sup>-1</sup> )
5.20 × 10 <sup>-5</sup>	8.15 × 10 <sup>-4</sup>	2.41 × 10 <sup>4</sup>		2.05 × 10 <sup>7</sup>
	1.63 × 10 <sup>-3</sup>	4.08 × 10 <sup>4</sup>		
	2.44 × 10 <sup>-3</sup>	5.73 × 10 <sup>4</sup>		
	3.26 × 10 <sup>-3</sup>	7.41 × 10 <sup>4</sup>		
	4.07 × 10 <sup>-3</sup>	9.08 × 10 <sup>4</sup>		

Table 15 continued

$[(\text{ani})(\text{fur})\text{CH}-\text{PPh}_3^+\text{BF}_4^-]$ (mol L <sup>-1</sup> )	[4] (mol L <sup>-1</sup> )	$k_{\text{obs}}$ (s <sup>-1</sup> )	$\lambda = 528 \text{ nm}$ (laser-flash photolysis)	$k$ (M <sup>-1</sup> s <sup>-1</sup> )
$5.78 \times 10^{-5}$	$7.63 \times 10^{-4}$	$1.04 \times 10^4$		$7.47 \times 10^6$
	$1.53 \times 10^{-3}$	$1.63 \times 10^4$		
	$2.29 \times 10^{-3}$	$2.24 \times 10^4$		
	$3.05 \times 10^{-3}$	$2.79 \times 10^4$		
	$3.82 \times 10^{-3}$	$3.31 \times 10^4$		
$[(\text{fur})_2\text{CH}-\text{PPh}_3^+\text{BF}_4^-]$ (mol L <sup>-1</sup> )	[4] (mol L <sup>-1</sup> )	$k_{\text{obs}}$ (s <sup>-1</sup> )	$\lambda = 530 \text{ nm}$ (laser-flash photolysis)	$k$ (M <sup>-1</sup> s <sup>-1</sup> )
$4.33 \times 10^{-5}$	$1.53 \times 10^{-3}$	$6.02 \times 10^3$		$2.41 \times 10^6$
	$1.91 \times 10^{-3}$	$6.87 \times 10^3$		
	$2.29 \times 10^{-3}$	$7.89 \times 10^3$		
$[(\text{pfa})_2\text{CH}^+]$ (mol L <sup>-1</sup> )	[4] (mol L <sup>-1</sup> )	$k_{\text{obs}}$ (s <sup>-1</sup> )	$\lambda = 601 \text{ nm}$ (stopped flow)	$k$ (M <sup>-1</sup> s <sup>-1</sup> )
$2.00 \times 10^{-5}$	$9.16 \times 10^{-5}$	9.61		$1.09 \times 10^5$
	$2.29 \times 10^{-4}$	24.0		
	$3.21 \times 10^{-4}$	33.5		
	$4.58 \times 10^{-4}$	48.8		
	$6.87 \times 10^{-4}$	74.1		

Table 15 continued

$[(\text{mfa})_2\text{CH}^+]$ (mol L <sup>-1</sup> )	[4] (mol L <sup>-1</sup> )	$k_{\text{obs}}$ (s <sup>-1</sup> )	$\lambda = 593$ nm (Stopped-flow)	$k$ (M <sup>-1</sup> s <sup>-1</sup> )
$2.00 \times 10^{-5}$	$1.30 \times 10^{-4}$	6.96		$3.65 \times 10^4$
	$2.61 \times 10^{-4}$	11.3		
	$3.91 \times 10^{-4}$	16.0		
	$5.22 \times 10^{-4}$	20.7		
	$6.52 \times 10^{-4}$	26.1		
$[(\text{dpa})_2\text{CH}^+]$ (mol L <sup>-1</sup> )	[4] (mol L <sup>-1</sup> )	$k_{\text{obs}}$ (s <sup>-1</sup> )	$\lambda = 672$ nm (Stopped-flow)	$k$ (M <sup>-1</sup> s <sup>-1</sup> )
$2.00 \times 10^{-5}$	$2.29 \times 10^{-4}$	2.07		$5.99 \times 10^3$
	$4.58 \times 10^{-4}$	3.33		
	$6.87 \times 10^{-4}$	4.78		
	$9.16 \times 10^{-4}$	5.99		
	$1.15 \times 10^{-3}$	7.60		
$[(\text{mor})_2\text{CH}^+]$ (mol L <sup>-1</sup> )	[4] (mol L <sup>-1</sup> )	$k_{\text{obs}}$ (s <sup>-1</sup> )	$\lambda = 620$ nm (Stopped-flow)	$k$ (M <sup>-1</sup> s <sup>-1</sup> )
$2.61 \times 10^{-5}$	$5.22 \times 10^{-4}$	4.18		$1.86 \times 10^3$
	$7.83 \times 10^{-4}$	4.56		
	$1.30 \times 10^{-3}$	5.50		
	$1.83 \times 10^{-3}$	6.51		
	$2.61 \times 10^{-3}$	8.02		

**Table 15** continued

Reactivity parameters for <b>4</b> in CH <sub>2</sub> Cl <sub>2</sub>		
Ar <sub>2</sub> CH <sup>+</sup>	<i>E</i>	<i>k</i> (M <sup>-1</sup> s <sup>-1</sup> )
(ani)(pop)CH <sup>+</sup>	1.48	1.35 × 10 <sup>8</sup>
(ani)(pop)CH <sup>+</sup>	0.61	3.91 × 10 <sup>7</sup>
(ani) <sub>2</sub> CH <sup>+</sup>	0	2.05 × 10 <sup>7</sup>
(ani)(fur)CH <sup>+</sup>	-0.56	7.47 × 10 <sup>6</sup>
(fur) <sub>2</sub> CH <sup>+</sup>	-1.26	2.41 × 10 <sup>6</sup>
(pfa) <sub>2</sub> CH <sup>+</sup>	-3.14	1.09 × 10 <sup>5</sup>
(mfa) <sub>2</sub> CH <sup>+</sup>	-3.85	3.65 × 10 <sup>4</sup>
(dpa) <sub>2</sub> CH <sup>+</sup>	-4.72	5.99 × 10 <sup>3</sup>
(mor) <sub>2</sub> CH <sup>+</sup>	-5.53	1.86 × 10 <sup>3</sup>

  
**Table 16.** Kinetics of the reactions of 5-methyl-3,4-dihydro-2H-pyrrole **5** with (Ar)<sub>2</sub>CH<sup>+</sup> in CH<sub>2</sub>Cl<sub>2</sub> at 20°C

[(mpa) <sub>2</sub> CH <sup>+</sup> ] (mol L <sup>-1</sup> )	[ <b>5</b> ] (mol L <sup>-1</sup> )	<i>k</i> <sub>obs</sub> (s <sup>-1</sup> )	λ = 622 nm (Stopped-flow)	<i>k</i> (M <sup>-1</sup> s <sup>-1</sup> )
6.46 × 10 <sup>-6</sup>	1.77 × 10 <sup>-4</sup>	14.1		9.53 × 10 <sup>4</sup>
	2.65 × 10 <sup>-4</sup>	21.7		
	3.54 × 10 <sup>-4</sup>	30.5		
	4.42 × 10 <sup>-4</sup>	39.1		
	5.30 × 10 <sup>-4</sup>	47.5		
[(dma) <sub>2</sub> CH <sup>+</sup> ] (mol L <sup>-1</sup> )	[ <b>5</b> ] (mol L <sup>-1</sup> )	<i>k</i> <sub>obs</sub> (s <sup>-1</sup> )	λ = 613 nm (Stopped-flow)	<i>k</i> (M <sup>-1</sup> s <sup>-1</sup> )
7.50 × 10 <sup>-6</sup>	8.84 × 10 <sup>-5</sup>	2.34		2.02 × 10 <sup>4</sup>
	1.77 × 10 <sup>-4</sup>	3.93		
	2.65 × 10 <sup>-4</sup>	5.36		
	3.54 × 10 <sup>-4</sup>	7.57		
	4.42 × 10 <sup>-4</sup>	9.44		

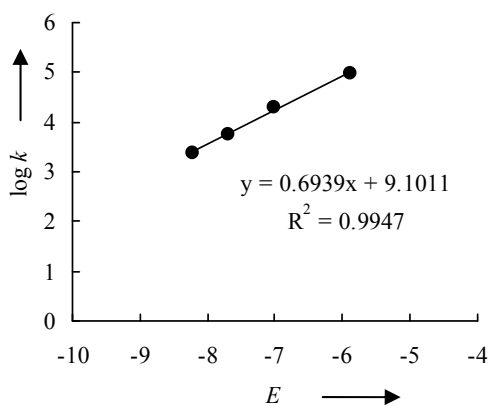
Table 16 continued

$[(\text{pyr})_2\text{CH}^+]$ (mol L <sup>-1</sup> )	[ <b>5</b> ] (mol L <sup>-1</sup> )	$k_{\text{obs}}$ (s <sup>-1</sup> )	$\lambda = 620 \text{ nm}$ (Stopped-flow)	$k$ (M <sup>-1</sup> s <sup>-1</sup> )
$7.01 \times 10^{-6}$	$1.67 \times 10^{-4}$	4.18		$5.57 \times 10^3$
	$2.78 \times 10^{-4}$	4.71		
	$3.89 \times 10^{-4}$	5.36		
	$5.01 \times 10^{-4}$	5.91		
	$6.68 \times 10^{-4}$	6.97		

$[(\text{thq})_2\text{CH}^+]$ (mol L <sup>-1</sup> )	[ <b>5</b> ] (mol L <sup>-1</sup> )	$k_{\text{obs}}$ (s <sup>-1</sup> )	$\lambda = 628 \text{ nm}$ (Stopped-flow)	$k$ (M <sup>-1</sup> s <sup>-1</sup> )
$6.11 \times 10^{-6}$	$2.78 \times 10^{-4}$	2.94		$2.37 \times 10^3$
	$3.89 \times 10^{-4}$	3.18		
	$5.01 \times 10^{-4}$	3.47		
	$6.68 \times 10^{-4}$	3.82		
	$8.90 \times 10^{-4}$	4.39		

Reactivity parameters for **5** in CH<sub>2</sub>Cl<sub>2</sub>

Ar <sub>2</sub> CH <sup>+</sup>	$E$	$k$ (M <sup>-1</sup> s <sup>-1</sup> )
(mpa) <sub>2</sub> CH <sup>+</sup>	-5.89	$9.53 \times 10^4$
(dma) <sub>2</sub> CH <sup>+</sup>	-7.02	$2.02 \times 10^4$
(pyr) <sub>2</sub> CH <sup>+</sup>	-7.69	$5.57 \times 10^3$
(thq) <sub>2</sub> CH <sup>+</sup>	-8.22	$2.37 \times 10^3$



### 4.3.2 Determination of the Rate Constants for the Reactions of 1a and 2a with Michael acceptors.

**Table 17.** Kinetics of the reactions of 2-methyl-4,5-dihydro-1H-imidazole (**1a**) with the Michael acceptors in CH<sub>2</sub>Cl<sub>2</sub> at 20 °C.

[7a] (mol L <sup>-1</sup> )	[1a] (mol L <sup>-1</sup> )	<i>k</i> <sub>obs</sub> (s <sup>-1</sup> )	λ = 320 nm	<i>k</i> (M <sup>-1</sup> s <sup>-1</sup> )
4.96 × 10 <sup>-5</sup>	4.49 × 10 <sup>-4</sup>	3.71		7.37 × 10 <sup>3</sup>
	5.62 × 10 <sup>-4</sup>	4.71		
	6.74 × 10 <sup>-4</sup>	5.39		
	7.86 × 10 <sup>-4</sup>	6.29		
	8.99 × 10 <sup>-4</sup>	7.05		
[7c] (mol L <sup>-1</sup> )	[1a] (mol L <sup>-1</sup> )	<i>k</i> <sub>obs</sub> (s <sup>-1</sup> )	λ = 392 nm	<i>k</i> (M <sup>-1</sup> s <sup>-1</sup> )
4.81 × 10 <sup>-5</sup>	6.74 × 10 <sup>-4</sup>	4.21		7.88 × 10 <sup>2</sup>
	8.99 × 10 <sup>-4</sup>	4.35		
	1.12 × 10 <sup>-3</sup>	4.48		
	1.35 × 10 <sup>-3</sup>	4.59		
	2.02 × 10 <sup>-3</sup>	5.27		
[7d] (mol L <sup>-1</sup> )	[1a] (mol L <sup>-1</sup> )	<i>k</i> <sub>obs</sub> (s <sup>-1</sup> )	λ = 380 nm	<i>k</i> (M <sup>-1</sup> s <sup>-1</sup> )
6.45 × 10 <sup>-5</sup>	6.54 × 10 <sup>-4</sup>	0.863		4.76 × 10 <sup>2</sup>
	9.81 × 10 <sup>-4</sup>	1.01		
	1.31 × 10 <sup>-3</sup>	1.14		
	1.63 × 10 <sup>-3</sup>	1.32		
	1.96 × 10 <sup>-3</sup>	1.49		

**Table 18.** Kinetics of the reactions of 2-methyl-1,4,5,6-tetrahydropyrimidine (**2a**) with the Michael acceptors in CH<sub>2</sub>Cl<sub>2</sub> at 20 °C.

[ <b>7a</b> ] (mol L <sup>-1</sup> )	[ <b>2a</b> ] (mol L <sup>-1</sup> )	<i>k</i> <sub>obs</sub> (s <sup>-1</sup> )	$\lambda = 320 \text{ nm}$	<i>k</i> (M <sup>-1</sup> s <sup>-1</sup> )
4.00 × 10 <sup>-5</sup>	1.88 × 10 <sup>-4</sup>	13.3		7.38 × 10 <sup>4</sup>
	2.82 × 10 <sup>-4</sup>	20.4		
	3.76 × 10 <sup>-4</sup>	28.1		
	4.70 × 10 <sup>-4</sup>	34.7		
	5.64 × 10 <sup>-4</sup>	40.8		
[ <b>7b</b> ] (mol L <sup>-1</sup> )	[ <b>2a</b> ] (mol L <sup>-1</sup> )	<i>k</i> <sub>obs</sub> (s <sup>-1</sup> )	$\lambda = 340 \text{ nm}$	<i>k</i> (M <sup>-1</sup> s <sup>-1</sup> )
4.00 × 10 <sup>-5</sup>	2.63 × 10 <sup>-3</sup>	9.98		2.91 × 10 <sup>2</sup>
	3.76 × 10 <sup>-3</sup>	10.3		
	5.26 × 10 <sup>-3</sup>	10.7		
[ <b>7c</b> ] (mol L <sup>-1</sup> )	[ <b>2a</b> ] (mol L <sup>-1</sup> )	<i>k</i> <sub>obs</sub> (s <sup>-1</sup> )	$\lambda = 392 \text{ nm}$	<i>k</i> (M <sup>-1</sup> s <sup>-1</sup> )
4.88 × 10 <sup>-5</sup>	2.82 × 10 <sup>-4</sup>	7.38		1.00 × 10 <sup>4</sup>
	3.76 × 10 <sup>-4</sup>	8.42		
	4.70 × 10 <sup>-4</sup>	9.40		
	5.64 × 10 <sup>-4</sup>	10.3		
	7.52 × 10 <sup>-4</sup>	12.6		
	9.40 × 10 <sup>-4</sup>	13.8		

Table 18 continued.

[7d] (mol L <sup>-1</sup> )	[2a] (mol L <sup>-1</sup> )	<i>k</i> <sub>obs</sub> (s <sup>-1</sup> )	$\lambda = 380 \text{ nm}$	<i>k</i> (M <sup>-1</sup> s <sup>-1</sup> )
$6.45 \times 10^{-5}$	$6.46 \times 10^{-4}$	5.36		$6.15 \times 10^3$
	$8.07 \times 10^{-4}$	6.43		
	$9.69 \times 10^{-4}$	7.30		
	$1.13 \times 10^{-3}$	8.32		
	$1.29 \times 10^{-3}$	9.38		

Table 19. Kinetics of the reactions of 2-methyl-1,4,5,6-tetrahydropyrimidine (2a) with the Michael acceptors in CH<sub>3</sub>CN at 20 °C.

[7a] (mol L <sup>-1</sup> )	[2a] (mol L <sup>-1</sup> )	<i>k</i> <sub>obs</sub> (s <sup>-1</sup> )	$\lambda = 322 \text{ nm}$	<i>k</i> (M <sup>-1</sup> s <sup>-1</sup> )
$8.52 \times 10^{-5}$	$3.27 \times 10^{-4}$	52.7		$1.92 \times 10^5$
	$3.82 \times 10^{-4}$	64.9		
	$4.36 \times 10^{-4}$	73.7		
	$4.91 \times 10^{-4}$	83.8		
	$5.45 \times 10^{-4}$	95.6		

[7b] (mol L <sup>-1</sup> )	[2a] (mol L <sup>-1</sup> )	<i>k</i> <sub>obs</sub> (s <sup>-1</sup> )	$\lambda = 340 \text{ nm}$	<i>k</i> (M <sup>-1</sup> s <sup>-1</sup> )
$3.82 \times 10^{-5}$	$5.99 \times 10^{-4}$	4.59		$6.58 \times 10^3$
	$6.99 \times 10^{-4}$	5.30		
	$7.99 \times 10^{-4}$	5.94		
	$9.98 \times 10^{-4}$	7.20		
	$1.20 \times 10^{-3}$	8.57		

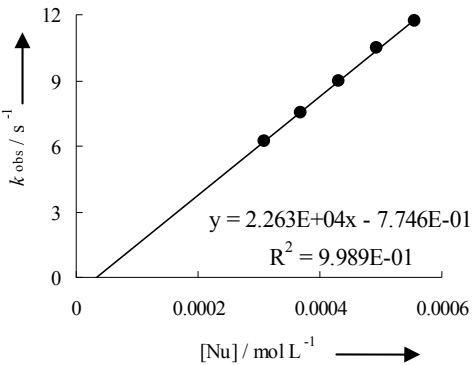
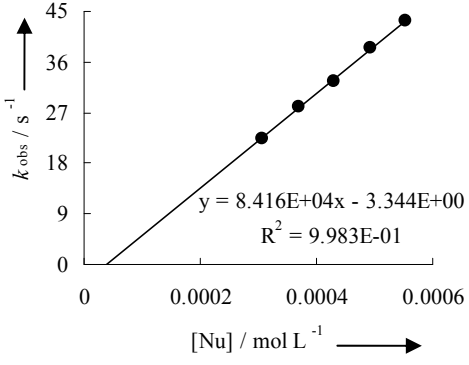
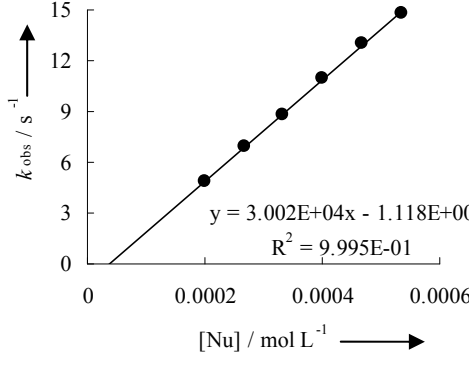
Table 19 continued.

[7c] (mol L <sup>-1</sup> )	[2a] (mol L <sup>-1</sup> )	<i>k</i> <sub>obs</sub> (s <sup>-1</sup> )	λ = 392 nm	<i>k</i> (M <sup>-1</sup> s <sup>-1</sup> )
5.34 × 10 <sup>-5</sup>	3.82 × 10 <sup>-4</sup>	12.4		3.44 × 10 <sup>4</sup>
	4.36 × 10 <sup>-4</sup>	14.2		
	4.91 × 10 <sup>-4</sup>	16.0		
	5.45 × 10 <sup>-4</sup>	17.9		
	6.54 × 10 <sup>-4</sup>	21.7		
[7d] (mol L <sup>-1</sup> )	[2a] (mol L <sup>-1</sup> )	<i>k</i> <sub>obs</sub> (s <sup>-1</sup> )	λ = 370 nm	<i>k</i> (M <sup>-1</sup> s <sup>-1</sup> )
5.24 × 10 <sup>-5</sup>	3.00 × 10 <sup>-4</sup>	4.46		1.70 × 10 <sup>4</sup>
	3.99 × 10 <sup>-4</sup>	6.02		
	4.99 × 10 <sup>-4</sup>	7.66		
	5.99 × 10 <sup>-4</sup>	9.54		
	6.99 × 10 <sup>-4</sup>	11.2		

Table 20. Kinetics of the reactions of 2-methyl-1,4,5,6-tetrahydropyrimidine (2a) with the Michael acceptors in DMSO at 20 °C.

[7a] (mol L <sup>-1</sup> )	[2a] (mol L <sup>-1</sup> )	<i>k</i> <sub>obs</sub> (s <sup>-1</sup> )	λ = 322 nm	<i>k</i> (M <sup>-1</sup> s <sup>-1</sup> )
7.40 × 10 <sup>-5</sup>	2.00 × 10 <sup>-4</sup>	65.8		4.33 × 10 <sup>5</sup>
	2.67 × 10 <sup>-4</sup>	92.6		
	3.34 × 10 <sup>-4</sup>	118		
	4.00 × 10 <sup>-4</sup>	153		
	4.67 × 10 <sup>-4</sup>	180		

Table 20 continued

[7b] (mol L <sup>-1</sup> )	[2a] (mol L <sup>-1</sup> )	<i>k</i> <sub>obs</sub> (s <sup>-1</sup> )	λ = 340 nm	<i>k</i> (M <sup>-1</sup> s <sup>-1</sup> )
4.61 × 10 <sup>-5</sup>	3.08 × 10 <sup>-4</sup>	6.21		2.26 × 10 <sup>4</sup>
	3.70 × 10 <sup>-4</sup>	7.55		
	4.31 × 10 <sup>-4</sup>	8.99		
	4.93 × 10 <sup>-4</sup>	10.5		
	5.55 × 10 <sup>-4</sup>	11.7		
[7c] (mol L <sup>-1</sup> )	[2a] (mol L <sup>-1</sup> )	<i>k</i> <sub>obs</sub> (s <sup>-1</sup> )	λ = 392 nm	<i>k</i> (M <sup>-1</sup> s <sup>-1</sup> )
5.55 × 10 <sup>-5</sup>	3.08 × 10 <sup>-4</sup>	22.5		8.42 × 10 <sup>4</sup>
	3.70 × 10 <sup>-4</sup>	28.1		
	4.31 × 10 <sup>-4</sup>	32.5		
	4.93 × 10 <sup>-4</sup>	38.5		
	5.55 × 10 <sup>-4</sup>	43.3		
[7d] (mol L <sup>-1</sup> )	[2a] (mol L <sup>-1</sup> )	<i>k</i> <sub>obs</sub> (s <sup>-1</sup> )	λ = 364 nm	<i>k</i> (M <sup>-1</sup> s <sup>-1</sup> )
5.10 × 10 <sup>-5</sup>	2.00 × 10 <sup>-4</sup>	4.87		3.00 × 10 <sup>4</sup>
	2.67 × 10 <sup>-4</sup>	6.94		
	3.34 × 10 <sup>-4</sup>	8.80		
	4.00 × 10 <sup>-4</sup>	10.9		
	4.67 × 10 <sup>-4</sup>	13.0		
	5.34 × 10 <sup>-4</sup>	14.8		

#### 4.4 Equilibrium constants ( $K$ ) for the reactions of benzhydrylium ions ( $\text{Ar}_2\text{CH}^+$ ) with the nucleophiles **1**, **3** and **4** in $\text{CH}_2\text{Cl}_2$ .

Equilibrium constants were measured by UV-vis spectroscopy in  $\text{CH}_2\text{Cl}_2$  as follows: To a solution of the benzhydrylium tetrafluoroborates in dichloromethane small volumes of stock solutions of the nucleophiles **1**, **3** and **4** were added and the resulting absorptions of the benzhydrylium ions were monitored. When the absorbance was constant, another portion of the stock solution was added. This procedure was repeated two to eight times for each benzhydrylium salt solution.

Assuming a proportionality between the absorbances and the concentrations of the benzhydrylium ions, the equilibrium constants ( $K$ ) can be expressed by the absorbances of the benzhydrylium ions before ( $A_0$ ) and after ( $A$ ) the addition of nucleophiles using equation (3) and (4).

The temperature of the solutions during all equilibrium studies was kept constant at  $(20.0 \pm 0.1)$  °C using a circulating bath thermostat.

**Table 21.** Determination of the equilibrium constant for the reaction of  $(\text{mor})_2\text{CH}^+$  with 1-(2-methyl-4,5-dihydro-1H-imidazol-1-yl)ethanone (**1c**).

$\varepsilon[(\text{mor})_2\text{CH}^+ \text{ at } 620 \text{ nm}] = 1.45 \times 10^5 \text{ M}^{-1} \text{ cm}^{-1}$  and  $d = 0.5 \text{ cm}$  DCM at 20.0 °C.

Entry	$[\mathbf{1c}]_0$ (mol L <sup>-1</sup> )	$A$	$[(\text{mor})_2\text{CH}^+]_{\text{eq}}$ (mol L <sup>-1</sup> )	$K$ (L mol <sup>-1</sup> )
0	0	1.165	$1.612 \times 10^{-5}$	
1	$1.640 \times 10^{-4}$	0.205	$2.841 \times 10^{-6}$	$3.09 \times 10^4$
2	$3.272 \times 10^{-4}$	0.110	$1.528 \times 10^{-6}$	$3.04 \times 10^4$
3	$4.897 \times 10^{-4}$	0.076	$1.055 \times 10^{-6}$	$2.99 \times 10^4$
4	$6.514 \times 10^{-4}$	0.058	$8.019 \times 10^{-7}$	$2.97 \times 10^4$
0	0	1.190	$1.647 \times 10^{-5}$	
1	$8.354 \times 10^{-5}$	0.354	$4.900 \times 10^{-6}$	$3.27 \times 10^4$
2	$1.669 \times 10^{-4}$	0.198	$2.742 \times 10^{-6}$	$3.26 \times 10^4$
3	$2.500 \times 10^{-4}$	0.141	$1.948 \times 10^{-6}$	$3.15 \times 10^4$
4	$3.330 \times 10^{-4}$	0.110	$1.521 \times 10^{-6}$	$3.07 \times 10^4$
5	$4.157 \times 10^{-4}$	0.091	$1.266 \times 10^{-6}$	$2.98 \times 10^4$
6	$4.983 \times 10^{-4}$	0.079	$1.086 \times 10^{-6}$	$2.91 \times 10^4$
0	0	1.208	$1.672 \times 10^{-5}$	
1	$8.237 \times 10^{-5}$	0.341	$4.713 \times 10^{-6}$	$3.61 \times 10^4$
2	$1.645 \times 10^{-4}$	0.206	$2.849 \times 10^{-6}$	$3.22 \times 10^4$
3	$2.465 \times 10^{-4}$	0.146	$2.017 \times 10^{-6}$	$3.13 \times 10^4$
4	$3.283 \times 10^{-4}$	0.114	$1.584 \times 10^{-6}$	$3.04 \times 10^4$
5	$4.099 \times 10^{-4}$	0.094	$1.307 \times 10^{-6}$	$2.97 \times 10^4$
6	$4.914 \times 10^{-4}$	0.081	$1.122 \times 10^{-6}$	$2.90 \times 10^4$

$$K_{\text{av}}(20 \text{ °C}) = 3.10 \times 10^4 \text{ L mol}^{-1}$$

**Table 22.** Determination of the equilibrium constant for the reaction of  $(\text{mpa})_2\text{CH}^+$  with 1-(2-methyl-4,5-dihydro-1H-imidazol-1-yl)ethanone (**1c**). $\varepsilon[(\text{mpa})_2\text{CH}^+ \text{ at } 622 \text{ nm}] = 1.41 \times 10^5 \text{ M}^{-1} \text{ cm}^{-1}$  and  $d = 0.5 \text{ cm}$  DCM at 20.0 °C.

Entry	[ <b>1c</b> ] <sub>0</sub> (mol L <sup>-1</sup> )	<i>A</i>	$[(\text{mpa})_2\text{CH}^+]_{\text{eq}}$ (mol L <sup>-1</sup> )	<i>K</i> (L mol <sup>-1</sup> )
0	0	1.208	$1.710 \times 10^{-5}$	
1	$1.687 \times 10^{-4}$	0.753	$1.066 \times 10^{-5}$	$3.70 \times 10^3$
2	$3.365 \times 10^{-4}$	0.564	$7.979 \times 10^{-6}$	$3.46 \times 10^3$
3	$5.036 \times 10^{-4}$	0.453	$6.410 \times 10^{-6}$	$3.35 \times 10^3$
4	$6.699 \times 10^{-4}$	0.377	$5.338 \times 10^{-6}$	$3.30 \times 10^3$
5	$8.354 \times 10^{-4}$	0.324	$4.587 \times 10^{-6}$	$3.26 \times 10^3$
6	$1.000 \times 10^{-3}$	0.285	$4.028 \times 10^{-6}$	$3.23 \times 10^3$
7	$1.164 \times 10^{-3}$	0.252	$3.563 \times 10^{-6}$	$3.23 \times 10^3$
0	0	1.289	$1.825 \times 10^{-5}$	
1	$8.923 \times 10^{-5}$	0.957	$1.355 \times 10^{-5}$	$4.08 \times 10^3$
2	$1.782 \times 10^{-4}$	0.775	$1.098 \times 10^{-5}$	$3.85 \times 10^3$
3	$2.670 \times 10^{-4}$	0.655	$9.280 \times 10^{-6}$	$3.72 \times 10^3$
4	$3.556 \times 10^{-4}$	0.573	$8.114 \times 10^{-6}$	$3.58 \times 10^3$
5	$4.439 \times 10^{-4}$	0.507	$7.175 \times 10^{-6}$	$3.53 \times 10^3$
6	$5.321 \times 10^{-4}$	0.449	$6.358 \times 10^{-6}$	$3.55 \times 10^3$
0	0	1.251	$1.771 \times 10^{-5}$	
1	$1.717 \times 10^{-4}$	0.768	$1.088 \times 10^{-5}$	$3.79 \times 10^3$
2	$3.427 \times 10^{-4}$	0.570	$8.072 \times 10^{-6}$	$3.55 \times 10^3$
3	$5.127 \times 10^{-4}$	0.455	$6.443 \times 10^{-6}$	$3.45 \times 10^3$
4	$6.820 \times 10^{-4}$	0.379	$5.362 \times 10^{-6}$	$3.39 \times 10^3$
5	$8.505 \times 10^{-4}$	0.324	$4.588 \times 10^{-6}$	$3.36 \times 10^3$
6	$1.018 \times 10^{-3}$	0.283	$4.006 \times 10^{-6}$	$3.34 \times 10^3$

$$K_{\text{av}}(20 \text{ °C}) = 3.51 \times 10^3 \text{ L mol}^{-1}$$

**Table 23.** Determination of the equilibrium constant for the reaction of  $(\text{mpa})_2\text{CH}^+$  with 1-benzyl-2-phenyl-4,5-dihydro-1H-imidazole (**1d**). $\varepsilon[(\text{ind})_2\text{CH}^+ \text{ at } 622 \text{ nm}] = 1.41 \times 10^5 \text{ M}^{-1} \text{ cm}^{-1}$  and  $d = 0.5 \text{ cm}$  DCM at 20.0 °C.

Entry	[ <b>1d</b> ] <sub>0</sub> (mol L <sup>-1</sup> )	<i>A</i>	$[(\text{ind})_2\text{CH}^+]_{\text{eq}}$ (mol L <sup>-1</sup> )	<i>K</i> (L mol <sup>-1</sup> )
0	0	0.943	$1.431 \times 10^{-5}$	
1	$1.953 \times 10^{-5}$	0.274	$4.151 \times 10^{-6}$	$2.60 \times 10^5$
2	$3.901 \times 10^{-5}$	0.117	$1.774 \times 10^{-6}$	$2.66 \times 10^5$
3	$5.844 \times 10^{-5}$	0.073	$1.108 \times 10^{-6}$	$2.62 \times 10^5$
4	$7.783 \times 10^{-5}$	0.053	$8.022 \times 10^{-7}$	$2.60 \times 10^5$
0	0	0.917	$1.391 \times 10^{-5}$	
1	$1.918 \times 10^{-5}$	0.268	$4.067 \times 10^{-6}$	$2.66 \times 10^5$
2	$3.831 \times 10^{-5}$	0.114	$1.732 \times 10^{-6}$	$2.72 \times 10^5$
3	$5.739 \times 10^{-5}$	0.070	$1.068 \times 10^{-6}$	$2.72 \times 10^5$
4	$7.643 \times 10^{-5}$	0.050	$7.646 \times 10^{-7}$	$2.73 \times 10^5$
0	0	0.932	$1.414 \times 10^{-5}$	
1	$1.911 \times 10^{-5}$	0.269	$4.080 \times 10^{-6}$	$2.64 \times 10^5$
2	$3.817 \times 10^{-5}$	0.116	$1.763 \times 10^{-6}$	$2.66 \times 10^5$
3	$5.718 \times 10^{-5}$	0.071	$1.071 \times 10^{-6}$	$2.71 \times 10^5$
4	$7.616 \times 10^{-5}$	0.052	$7.822 \times 10^{-7}$	$2.67 \times 10^5$

$$K_{\text{av}}(20 \text{ °C}) = 2.67 \times 10^5 \text{ L mol}^{-1}$$

**Table 24.** Determination of the equilibrium constant for the reaction of  $(\text{mpa})_2\text{CH}^+$  with 1-benzyl-2-phenyl-4,5-dihydro-1H-imidazole (**1d**). $\varepsilon[(\text{jul})_2\text{CH}^+ \text{ at } 642 \text{ nm}] = 2.24 \times 10^5 \text{ M}^{-1} \text{ cm}^{-1}$  and  $d = 0.5 \text{ cm}$  DCM at 20.0 °C.

Entry	[ <b>1d</b> ] <sub>0</sub> (mol L <sup>-1</sup> )	<i>A</i>	[(jul) <sub>2</sub> CH <sup>+</sup> ] <sub>eq</sub> (mol L <sup>-1</sup> )	<i>K</i> (L mol <sup>-1</sup> )
0	0	0.858	$7.661 \times 10^{-6}$	
1	$3.882 \times 10^{-5}$	0.680	$6.078 \times 10^{-6}$	$6.91 \times 10^3$
2	$7.745 \times 10^{-5}$	0.566	$5.055 \times 10^{-6}$	$6.79 \times 10^3$
3	$1.159 \times 10^{-4}$	0.481	$4.296 \times 10^{-6}$	$6.84 \times 10^3$
4	$1.542 \times 10^{-4}$	0.418	$3.732 \times 10^{-6}$	$6.87 \times 10^3$
5	$1.922 \times 10^{-4}$	0.368	$3.288 \times 10^{-6}$	$6.93 \times 10^3$
6	$2.301 \times 10^{-4}$	0.329	$2.936 \times 10^{-6}$	$6.97 \times 10^3$
7	$2.678 \times 10^{-4}$	0.297	$2.650 \times 10^{-6}$	$7.01 \times 10^3$
0	0	0.839	$7.496 \times 10^{-6}$	
1	$3.840 \times 10^{-5}$	0.663	$5.924 \times 10^{-6}$	$7.12 \times 10^3$
2	$7.661 \times 10^{-5}$	0.548	$4.894 \times 10^{-6}$	$7.08 \times 10^3$
3	$1.146 \times 10^{-4}$	0.466	$4.167 \times 10^{-6}$	$7.06 \times 10^3$
4	$1.525 \times 10^{-4}$	0.405	$3.621 \times 10^{-6}$	$7.06 \times 10^3$
5	$1.902 \times 10^{-4}$	0.358	$3.195 \times 10^{-6}$	$7.09 \times 10^3$
6	$2.277 \times 10^{-4}$	0.320	$2.862 \times 10^{-6}$	$7.09 \times 10^3$
7	$2.650 \times 10^{-4}$	0.290	$2.591 \times 10^{-6}$	$7.09 \times 10^3$
8	$3.021 \times 10^{-4}$	0.264	$2.357 \times 10^{-6}$	$7.14 \times 10^3$

$$K_{\text{av}}(20 \text{ °C}) = 7.00 \times 10^3 \text{ L mol}^{-1}$$

**Table 25.** Determination of the equilibrium constant for the reaction of  $(\text{mpa})_2\text{CH}^+$  with 1-benzyl-2-phenyl-4,5-dihydro-1H-imidazole (**1d**). $\varepsilon[(\text{lil})_2\text{CH}^+ \text{ at } 642 \text{ nm}] = 1.59 \times 10^5 \text{ M}^{-1} \text{ cm}^{-1}$  and  $d = 0.5 \text{ cm}$  DCM at 20.0 °C.

Entry	[ <b>1d</b> ] <sub>0</sub> (mol L <sup>-1</sup> )	<i>A</i>	[(lil) <sub>2</sub> CH <sup>+</sup> ] <sub>eq</sub> (mol L <sup>-1</sup> )	<i>K</i> (L mol <sup>-1</sup> )
0	0	0.728	9.182E-06	
1	$6.052 \times 10^{-5}$	0.493	6.222E-06	$8.16 \times 10^3$
2	$1.206 \times 10^{-4}$	0.375	4.733E-06	$7.96 \times 10^3$
3	$1.802 \times 10^{-4}$	0.300	3.787E-06	$7.99 \times 10^3$
4	$2.394 \times 10^{-4}$	0.248	3.136E-06	$8.07 \times 10^3$
5	$2.981 \times 10^{-4}$	0.211	2.666E-06	$8.16 \times 10^3$
6	$3.564 \times 10^{-4}$	0.183	2.311E-06	$8.25 \times 10^3$
0	0	0.707	8.926E-06	
1	$5.712 \times 10^{-4}$	0.486	6.127E-06	$8.31 \times 10^3$
2	$1.138 \times 10^{-4}$	0.372	4.698E-06	$8.08 \times 10^3$
3	$1.701 \times 10^{-4}$	0.300	3.782E-06	$8.09 \times 10^3$
4	$2.260 \times 10^{-4}$	0.251	3.173E-06	$8.04 \times 10^3$
5	$2.816 \times 10^{-4}$	0.217	2.733E-06	$8.02 \times 10^3$
6	$3.367 \times 10^{-4}$	0.189	2.391E-06	$8.04 \times 10^3$

$$K_{\text{av}}(20 \text{ °C}) = 8.10 \times 10^3 \text{ L mol}^{-1}$$

**Table 26.** Determination of the equilibrium constant for the reaction of  $(\text{mor})_2\text{CH}^+$  with 2-methyl-4,5-dihydrooxazole (**3**). $\varepsilon[(\text{mor})_2\text{CH}^+ \text{ at } 620 \text{ nm}] = 1.45 \times 10^5 \text{ M}^{-1} \text{ cm}^{-1}$  and  $d = 0.5 \text{ cm}$ 

DCM at 20.0 °C.

Entry	$[\mathbf{3}]_0$ (mol L <sup>-1</sup> )	$A$	$[(\text{mor})_2\text{CH}^+]_{\text{eq}}$ (mol L <sup>-1</sup> )	$K$ (L mol <sup>-1</sup> )
0	0	0.497	$6.878 \times 10^{-6}$	
1	$4.239 \times 10^{-4}$	0.188	$2.601 \times 10^{-6}$	$3.89 \times 10^3$
2	$8.444 \times 10^{-4}$	0.117	$1.615 \times 10^{-6}$	$3.84 \times 10^3$
3	$1.261 \times 10^{-3}$	0.084	$1.158 \times 10^{-6}$	$3.88 \times 10^3$
4	$1.675 \times 10^{-3}$	0.064	$8.844 \times 10^{-7}$	$3.98 \times 10^3$
0	0	0.639	$8.838 \times 10^{-6}$	
1	$2.064 \times 10^{-4}$	0.341	$4.718 \times 10^{-6}$	$4.30 \times 10^3$
2	$4.121 \times 10^{-4}$	0.236	$3.263 \times 10^{-6}$	$4.18 \times 10^3$
3	$6.169 \times 10^{-4}$	0.181	$2.505 \times 10^{-6}$	$4.11 \times 10^3$
4	$8.208 \times 10^{-4}$	0.148	$2.049 \times 10^{-6}$	$4.03 \times 10^3$
5	$1.024 \times 10^{-3}$	0.124	$1.719 \times 10^{-6}$	$4.02 \times 10^3$
0	0	0.653	$9.029 \times 10^{-6}$	
1	$3.150 \times 10^{-4}$	0.281	$3.886 \times 10^{-6}$	$4.25 \times 10^3$
2	$6.281 \times 10^{-4}$	0.181	$2.501 \times 10^{-6}$	$4.16 \times 10^3$
3	$9.394 \times 10^{-4}$	0.133	$1.842 \times 10^{-6}$	$4.14 \times 10^3$
4	$1.249 \times 10^{-3}$	0.105	$1.456 \times 10^{-6}$	$4.13 \times 10^3$
5	$1.556 \times 10^{-3}$	0.088	$1.219 \times 10^{-6}$	$4.07 \times 10^3$

$$K_{\text{av}}(20 \text{ }^\circ\text{C}) = 4.07 \times 10^3 \text{ L mol}^{-1}$$

**Table 27.** Determination of the equilibrium constant for the reaction of  $(\text{mpa})_2\text{CH}^+$  with 2-methyl-4,5-dihydrooxazole (**3**). $\varepsilon[(\text{mpa})_2\text{CH}^+ \text{ at } 622 \text{ nm}] = 1.41 \times 10^5 \text{ M}^{-1} \text{ cm}^{-1}$  and  $d = 0.5 \text{ cm}$ 

DCM at 20.0 °C.

Entry	$[\mathbf{3}]_0$ (mol L <sup>-1</sup> )	$A$	$[(\text{mpa})_2\text{CH}^+]_{\text{eq}}$ (mol L <sup>-1</sup> )	$K$ (L mol <sup>-1</sup> )
0	0	0.811	$1.149 \times 10^{-5}$	
1	$2.968 \times 10^{-4}$	0.684	$9.685 \times 10^{-6}$	$6.15 \times 10^2$
2	$5.912 \times 10^{-4}$	0.590	$8.351 \times 10^{-6}$	$6.20 \times 10^2$
3	$8.833 \times 10^{-4}$	0.516	$7.301 \times 10^{-6}$	$6.31 \times 10^2$
4	$1.173 \times 10^{-3}$	0.456	$6.460 \times 10^{-6}$	$6.42 \times 10^2$
0	0	0.864	$1.223 \times 10^{-5}$	
1	$4.726 \times 10^{-4}$	0.664	$9.408 \times 10^{-6}$	$6.21 \times 10^2$
2	$9.393 \times 10^{-4}$	0.537	$7.599 \times 10^{-6}$	$6.30 \times 10^2$
3	$1.400 \times 10^{-3}$	0.445	$6.301 \times 10^{-6}$	$6.49 \times 10^2$
4	$1.855 \times 10^{-3}$	0.374	$5.292 \times 10^{-6}$	$6.78 \times 10^2$
5	$2.305 \times 10^{-3}$	0.318	$4.504 \times 10^{-6}$	$7.10 \times 10^2$
0	0	0.860	$1.218 \times 10^{-5}$	
1	$6.309 \times 10^{-4}$	0.621	$8.794 \times 10^{-6}$	$5.95 \times 10^2$
2	$1.251 \times 10^{-3}$	0.475	$6.724 \times 10^{-6}$	$6.27 \times 10^2$
3	$1.861 \times 10^{-3}$	0.374	$5.299 \times 10^{-6}$	$6.69 \times 10^2$
4	$2.461 \times 10^{-3}$	0.300	$4.243 \times 10^{-6}$	$7.24 \times 10^2$
5	$3.051 \times 10^{-3}$	0.242	$3.430 \times 10^{-6}$	$7.91 \times 10^2$

$$K_{\text{av}}(20 \text{ }^\circ\text{C}) = 6.57 \times 10^2 \text{ L mol}^{-1}$$

**Table 28.** Determination of the equilibrium constant for the reaction of  $(\text{mfa})_2\text{CH}^+$  with 2-methyl-4,5-dihydrothiazole (**4**). $\varepsilon[(\text{mfa})_2\text{CH}^+ \text{ at } 593 \text{ nm}] = 1.38 \times 10^5 \text{ M}^{-1} \text{ cm}^{-1}$  and  $d = 0.5 \text{ cm}$  DCM at 20.0 °C.

Entry	$[\mathbf{4}]_0$ (mol L <sup>-1</sup> )	$A$	$[(\text{mfa})_2\text{CH}^+]_{\text{eq}}$ (mol L <sup>-1</sup> )	$K$ (L mol <sup>-1</sup> )
0	0	1.184	$1.715 \times 10^{-5}$	
1	$1.363 \times 10^{-4}$	0.319	$4.620 \times 10^{-6}$	$2.18 \times 10^4$
2	$2.720 \times 10^{-4}$	0.177	$2.563 \times 10^{-6}$	$2.20 \times 10^4$
3	$4.071 \times 10^{-4}$	0.119	$1.729 \times 10^{-6}$	$2.26 \times 10^4$
4	$5.416 \times 10^{-4}$	0.090	$1.298 \times 10^{-6}$	$2.30 \times 10^4$
5	$6.754 \times 10^{-4}$	0.072	$1.047 \times 10^{-6}$	$2.30 \times 10^4$
0	0	1.120	$1.623 \times 10^{-5}$	
1	$6.357 \times 10^{-5}$	0.514	$7.453 \times 10^{-6}$	$2.14 \times 10^4$
2	$1.270 \times 10^{-4}$	0.326	$4.730 \times 10^{-6}$	$2.10 \times 10^4$
3	$1.903 \times 10^{-4}$	0.237	$3.439 \times 10^{-6}$	$2.09 \times 10^4$
4	$2.535 \times 10^{-4}$	0.183	$2.649 \times 10^{-6}$	$2.13 \times 10^4$
5	$3.165 \times 10^{-4}$	0.148	$2.142 \times 10^{-6}$	$2.16 \times 10^4$
6	$3.794 \times 10^{-4}$	0.125	$1.812 \times 10^{-6}$	$2.16 \times 10^4$
0	0	1.206	$1.748 \times 10^{-5}$	
1	$1.987 \times 10^{-4}$	0.220	$3.188 \times 10^{-6}$	$2.42 \times 10^4$
2	$3.961 \times 10^{-4}$	0.117	$1.699 \times 10^{-6}$	$2.42 \times 10^4$
3	$5.921 \times 10^{-4}$	0.079	$1.144 \times 10^{-6}$	$2.45 \times 10^4$
4	$7.869 \times 10^{-4}$	0.059	$8.574 \times 10^{-7}$	$2.48 \times 10^4$
5	$9.803 \times 10^{-4}$	0.047	$6.763 \times 10^{-7}$	$2.53 \times 10^4$

$$K_{\text{av}}(20 \text{ }^\circ\text{C}) = 2.27 \times 10^4 \text{ L mol}^{-1}$$

**Table 29.** Determination of the equilibrium constant for the reaction of  $(\text{dpa})_2\text{CH}^+$  with 2-methyl-4,5-dihydrothiazole (**4**). $\varepsilon[(\text{dpa})_2\text{CH}^+ \text{ at } 672 \text{ nm}] = 9.55 \times 10^4 \text{ M}^{-1} \text{ cm}^{-1}$  and  $d = 0.5 \text{ cm}$  DCM at 20.0 °C.

Entry	$[\mathbf{4}]_0$ (mol L <sup>-1</sup> )	$A$	$[(\text{dpa})_2\text{CH}^+]_{\text{eq}}$ (mol L <sup>-1</sup> )	$K$ (L mol <sup>-1</sup> )
0	0	0.578	$1.210 \times 10^{-5}$	
1	$1.737 \times 10^{-4}$	0.254	$5.328 \times 10^{-6}$	$7.58 \times 10^2$
0	0	0.571	$1.196 \times 10^{-5}$	
1	$3.327 \times 10^{-4}$	0.170	$3.562 \times 10^{-6}$	$7.23 \times 10^2$
0	0	0.566	$1.185 \times 10^{-5}$	
1	$4.963 \times 10^{-4}$	0.125	$2.624 \times 10^{-6}$	$7.15 \times 10^2$
0	0	0.525	$1.099 \times 10^{-5}$	
1	$6.095 \times 10^{-4}$	0.101	$2.107 \times 10^{-6}$	$6.95 \times 10^2$
0	0	0.559	$1.170 \times 10^{-5}$	
1	$8.154 \times 10^{-4}$	0.082	$1.726 \times 10^{-6}$	$7.09 \times 10^2$

$$K_{\text{av}}(20 \text{ }^\circ\text{C}) = 7.20 \times 10^3 \text{ L mol}^{-1}$$

**Table 30.** Determination of the equilibrium constant for the reaction of  $(\text{mor})_2\text{CH}^+$  with 2-methyl-4,5-dihydrothiazole (**4**). $\varepsilon[(\text{mor})_2\text{CH}^+ \text{ at } 620 \text{ nm}] = 1.45 \times 10^5 \text{ M}^{-1} \text{ cm}^{-1}$  and  $d = 0.5 \text{ cm}$  DCM at 20.0 °C.

Entry	[ <b>4</b> ] <sub>0</sub> (mol L <sup>-1</sup> )	<i>A</i>	$[(\text{mor})_2\text{CH}^+]_{\text{eq}}$ (mol L <sup>-1</sup> )	<i>K</i> (L mol <sup>-1</sup> )
0	0	0.649	$8.984 \times 10^{-6}$	
1	$3.026 \times 10^{-4}$	0.548	$7.581 \times 10^{-6}$	$5.99 \times 10^2$
0	0	0.655	$9.071 \times 10^{-6}$	
1	$4.502 \times 10^{-4}$	0.509	$7.042 \times 10^{-6}$	$6.25 \times 10^2$
0	0	0.649	$8.977 \times 10^{-6}$	
1	$5.955 \times 10^{-4}$	0.463	$6.408 \times 10^{-6}$	$6.57 \times 10^2$
0	0	0.697	$9.642 \times 10^{-6}$	
1	$7.953 \times 10^{-4}$	0.456	$6.310 \times 10^{-6}$	$6.46 \times 10^2$
0	0	0.531	$7.345 \times 10^{-6}$	
1	$8.039 \times 10^{-4}$	0.345	$4.776 \times 10^{-6}$	$6.50 \times 10^2$
0	0	0.380	$5.255 \times 10^{-6}$	
1	$8.402 \times 10^{-4}$	0.240	$3.318 \times 10^{-6}$	$6.52 \times 10^2$

$$K_{\text{av}}(20 \text{ }^\circ\text{C}) = 6.38 \times 10^2 \text{ L mol}^{-1}$$

#### 4.5 Nucleofugalities of N-heterocycles in CH<sub>2</sub>Cl<sub>2</sub> at 20 °C.

**Table 31.** Heterolysis rate constants in CH<sub>2</sub>Cl<sub>2</sub> at 20 °C.

Nucleofuge	Electrofuge	$E_f$ <sup>[a]</sup>	$k_{\leftarrow}$ (s <sup>-1</sup> ) <sup>[b]</sup>	$N_f$ <sup>[b]</sup>	$N_f$ (average)
<b>1c</b>	$(\text{mor})_2\text{CH}^+$	3.03	$7.26 \times 10^{-2}$	-4.17	-4.00
	$(\text{mpa})_2\text{CH}^+$	3.46	$4.22 \times 10^{-2}$	-3.84	
<b>1d</b>	$(\text{ind})_2\text{CH}^+$	4.83	$1.61 \times 10^{-2}$	-6.62	-6.50
	$(\text{jul})_2\text{CH}^+$	5.61	$1.42 \times 10^{-1}$	-6.64	
	$(\text{lil})_2\text{CH}^+$	5.05	$4.36 \times 10^{-2}$	-6.41	
<b>2</b>	$(\text{mfa})_2\text{CH}^+$	3.13	1.61	-2.92	-2.45
	$(\text{dpa})_2\text{CH}^+$	1.78	$8.32 \times 10^{-1}$	-1.86	
	$(\text{mor})_2\text{CH}^+$	3.03	2.96	-2.56	
<b>3</b>	$(\text{mor})_2\text{CH}^+$	3.03	$4.18 \times 10^{-1}$	-3.41	-3.33
	$(\text{mpa})_2\text{CH}^+$	3.46	1.63	-3.25	

<sup>[a]</sup>  $E_f$  parameters from ref. [15]. <sup>[b]</sup>  $k_{\leftarrow} = k/K$  see Table 5. <sup>[c]</sup> From equation  $\log k_{\leftarrow}(25 \text{ }^\circ\text{C}) = s_f(E_f + N_f)$  assuming  $s_f = 1.0$ ; temperature difference (20 and 25 °C) neglected.

## 5 References

- [1] M. R. Grimmett, in: *Comprehensive Heterocyclic Chemistry*, (Eds.: A. R. Katritzky, C. W. Rees, E. F. V. Scriven), Pergamon, Oxford, **1996**, Vol. 3, pp 77–120.
- [2] a) S. Tsujii, K. L. Rinehart, Y. Kashman, S. S. Cross, M. S. Lui, S. A. Pomponi, M. C. Diaz, *J. Org. Chem.* **1988**, *53*, 5446–5453; b) P. Bousquet, J. Feldman, J. Schwartz, J.

- Pharmacol. Exp. Ther.* **1984**, *230*, 232–236; c) C. Dardonville, I. Rozas, *Med. Res. Rev.* **2004**, *24*, 639–661.
- [3] a) A. K. Ghosh, P. Mathivanan, J. Cappiello, *Tetrahedron: Asymmetry* **1998**, *9*, 1–45; b) M. Gomez, G. Muller, M. Rocamora, *Coord. Chem. Rev.* **1999**, *193–195*, 769–835; c) H. A. McManus, P. J. Guiry, *Chem. Rev.* **2004**, *104*, 4151–4202; d) J. Zhou, Y. Tang, *Chem. Soc. Rev.* **2005**, *34*, 664–676. e) G. Desimoni, G. Faita, K. A. Jorgensen, *Chem. Rev.* **2006**, *106*, 3561–3651; f) H. Liua, D.-M. Du, *Adv. Synth. Catal.* **2009**, *351*, 489–519; g) H. A. McManus, P. J. Guiry, *Chem. Rev.* **2004**, *104*, 4151–4202; h) C. E. Anderson, L. E. Overman, *J. Am. Chem. Soc.* **2003**, *125*, 12412–12413; i) T. Arai, T. Mizukami, N. Yokoyama, D. Nakazato, A. Yanagisawa, *Synlett* **2005**, 2670–2672; j) S. Bhor, G. Anilkumar, M. K. Tse, M. Klawonn, C. Döbler, B. Bitterlich, A. Grotevendt, M. Beller, *Org. Lett.* **2005**, *7*, 3393–3396; k) C. A. Busacca, J. C. Lorenz, N. Grinberg, N. Haddad, H. Lee, Z. Li, M. Liang, D. Reeves, A. Saha, R. Varsolona, C. H. Senanayake, *Org. Lett.* **2007**, *10*, 341–344.
- [4] For reviews in Brønsted acid organocatalysts see: a) A. G. Doyle, E. N. Jacobsen, *Chem. Rev.* **2007**, *107*, 5713–5743; b) P. M. Pihko, *Angew. Chem. Int. Ed.* **2004**, *43*, 2062–2064; c) P. R. Schreiner, *Chem. Soc. Rev.* **2003**, *32*, 289–296. d) T. Akiyama, *Chem. Rev.* **2007**, *107*, 5744–5758; e) D. Uraguchi, M. Terada, *J. Am. Chem. Soc.* **2004**, *126*, 5356–5357; f) D. Nakashima, H. Yamamoto, *J. Am. Chem. Soc.* **2006**, *128*, 9626–9627; g) C. H. Cheon, H. Yamamoto, *J. Am. Chem. Soc.* **2008**, *130*, 9246–9247; h) Y. Huang, A. K. Unni, A. N. Thadani, V. H. Rawal, *Nature* **2003**, *424*, 146–146.
- [5] a) S. B. Tsogoeva, G. Dürner, M. Bolte, M.W. Gcbel, *Eur. J. Org. Chem.* **2003**, 1661–1664; b) D. Akalay, G. Drner, J. W. Bats, M. Bolte, M.W. Gcbel, *J. Org. Chem.* **2007**, *72*, 5618–5624; c) K. Murai, S. Fukushima, S. Hayashi, Y. Takahara, H. Fujioka, *Org. Lett.* **2010**, *12*, 964–966.
- [6] A. Weatherwax, C. J. Abraham, T. Lectka, *Org. Lett.* **2005**, *7*, 3461–3464.
- [7] J. Xu, Y. Guan, S. Yang, Y. Ng, G. Peh, C.-H. Tan, *Chem. Asian J.* **2006**, *1*, 724–729.
- [8] For selected reviews on Baylis-Hilman reactions, see: a) D. Basavaiah, A. J. Rao, T. Satyanarayana, *Chem. Rev.* **2003**, *103*, 811–891; b) G. Masson, C. Housseman, J. Zhu, *Angew. Chem. Int. Ed.* **2007**, *46*, 4614–4628.
- [9] a) H. Mayr, M. Patz, *Angew. Chem. Int. Ed. Engl.* **1994**, *33*, 938–957; b) H. Mayr, T. Bug, M. F. Gotta, N. Hering, B. Irrgang, B. Janker, B. Kempf, R. Loos, A. R. Ofial, G. Remennikov, H. Schimmel, *J. Am. Chem. Soc.* **2001**, *123*, 9500–9512; c) R. Lucius, R. Loos, H. Mayr, *Angew. Chem. Int. Ed.* **2002**, *41*, 91–95; d) H. Mayr, B.

- Kempf, A. R. Ofial, *Acc. Chem. Res.* **2003**, *36*, 66–77; e) H. Mayr, A. R. Ofial, *Pure Appl. Chem.* **2005**, *77*, 1807–1821; f) H. Mayr, *Angew. Chem. Int. Ed.* **2011**, *50*, 3612–3618; g) For a comprehensive listing of nucleophilicity parameters  $N$  and electrophilicity parameters  $E$ , see <http://www.cup.uni-muenchen.de/oc/mayr/DBintro.html>.
- [10] For pyridines see: a) F. Brotzel, B. Kempf, T. Singer, H. Zipse, H. Mayr, *Chem. Eur. J.* **2007**, *13*, 336–345; b) N. De Rycke, G. Berionni, F. Couty, H. Mayr, R. Goumont, O. R. P. David, *Org. Lett.* **2011**, *13*, 530–533; For azoles see: c) M. Baidya, F. Brotzel, H. Mayr, *Org. Biomol. Chem.* **2010**, *8*, 1929–1935; For phosphanes see: d) B. Kempf, H. Mayr, *Chem. Eur. J.* **2005**, *11*, 917–927; For DBU and DBN see: e) M. Baidya, H. Mayr, *Chem. Commun.* **2008**, 1792–1794; For isothioureas see: f) B. Maji, C. Joannesse, T. A. Nigst, A. D. Smith, H. Mayr, *J. Org. Chem.* **2011**, *76*, 5104–5112; For guanidines see: g) B. Maji, D. A. Stephenson, H. Mayr, *ChemCatChem* **2012**, DOI: 10.1002/cctc.201200143; For DABCO and DMAP see: h) M. Baidya, S. Kobayashi, F. Brotzel, U. Schmidhammer, E. Riedle, H. Mayr, *Angew. Chem. Int. Ed.* **2007**, *46*, 6176–6179.
- [11] CCDC 891470 (**7b**) contains the supplementary crystallographic data for this paper. These data can be obtained free of charge from The Cambridge Crystallographic Data Centre via [www.ccdc.cam.ac.uk/data\\_request/cif](http://www.ccdc.cam.ac.uk/data_request/cif).
- [12] a) J. Ammer, M. Baidya, S. Kobayashi, H. Mayr, *J. Phys. Org. Chem.* **2010**, *23*, 1029–1035; b) X.-H. Duan, B. Maji, H. Mayr, *Org. Biomol. Chem.* **2011**, *9*, 8046–8050.
- [13] a) O. Kaumanns, H. Mayr, *J. Org. Chem.* **2008**, *73*, 2738–2745; b) F. Seeliger, S. T. A. Berger, G. Y. Remennikov, K. Polborn, H. Mayr, *J. Org. Chem.* **2007**, *72*, 9170–9180; c) S. T. A. Berger, F. H. Seeliger, F. Hofbauer, H. Mayr, *Org. Biomol. Chem.* **2007**, *5*, 3020–3026.
- [14] a) R. A. Marcus, *J. Phys. Chem.* **1968**, *72*, 891–899; b) W. J. Albery, *Annu. Rev. Phys. Chem.* **1980**, *31*, 227–263.
- [15] N. Streidl, B. Denegri, O. Kronja, H. Mayr, *Acc. Chem. Res.* **2010**, *43*, 1537–1549.
- [16] a) D. Li, Y. Zhang, G. Zhou, W. Guo, *Synlett.* **2008**, 225–228; b) J.-F. Gong, X.-H. Fan, C. Xu, J.-L. Li, Y.-J. Wu, M.-P. Song, *J. Orgmet. Chem.* **2007**, *692*, 2006–2013; c) R. N. Butler, K. J. Fitzgerald, *J. Chem. Soc. Perkin Trans. 1*, **1989**, 155–157.

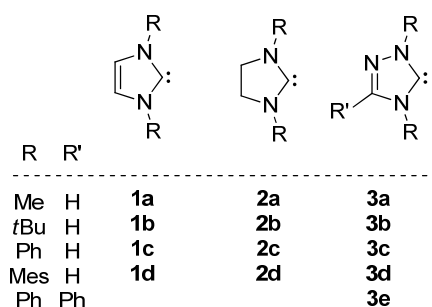
## Chapter 5

# What Makes N-Heterocyclic Carbenes Special in Organocatalysis?

B. Maji, M. Breugst, H. Mayr, *Angew. Chem. Int. Ed.* **2011**, *50*, 6915–6919.

## 1 Introduction

Since the first isolation and characterization of stable N-heterocyclic carbenes (NHCs) by Arduengo and coworkers in 1991,<sup>[1]</sup> these compounds have attracted great interest in various fields of chemistry. As molecules with divalent carbon atoms, NHCs (e.g., **1–3**, Scheme 1) are not only of theoretical interest<sup>[2]</sup> but also of practical relevance as ligands in metal complexes<sup>[3]</sup> and as nucleophilic organocatalysts.<sup>[4]</sup>



**Scheme 1.** Important N-heterocyclic carbenes.

Despite the extensive use of NHCs as organocatalysts, quantitative investigations of their catalytic activities are rare.<sup>[5]</sup> Since the relative reactivities of different nucleophiles towards electrophiles correlate only poorly<sup>[6]</sup> with the corresponding Brønsted basicities ( $pK_{aH}$ ),<sup>[7]</sup> we have recently employed benzhydrylium ions and structurally related quinone methides **4** (Table 1) with widely varying reactivities as reference compounds<sup>[8]</sup> to compare the nucleophilicities and Lewis basicities of various organocatalysts.<sup>[9]</sup>

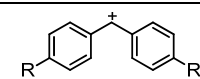
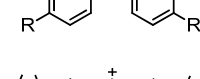
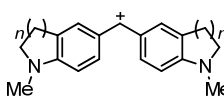
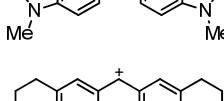
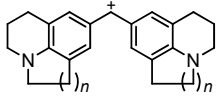
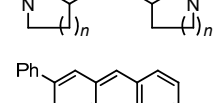
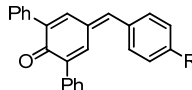
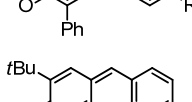
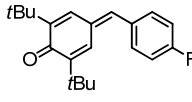
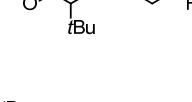
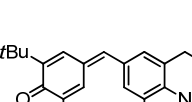
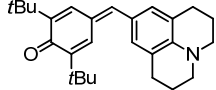
It was demonstrated that the rates of the reactions of carbocations and Michael acceptors with *n*-,  $\pi$ -, and  $\sigma$ -nucleophiles can be described by the linear free-energy relationship in Equation (1), where electrophiles are characterized by one solvent-independent electrophilicity

parameter  $E$ , and nucleophiles are characterized by two solvent-dependent parameters, the nucleophilicity parameter  $N$ , and a nucleophile-specific sensitivity parameter  $s_N$ .<sup>[8]</sup>

$$\lg k_2 = s_N(N + E) \quad (1)$$

We now report on the use of the benzhydrylium methodology for characterizing the nucleophilicities of three representative NHCs **1d**, **2d**, and **3e** and for comparing them with other nucleophilic organocatalysts.

**Table 1.** Benzhydrylium Ions **4a–f**  $\text{BF}_4^-$  and Quinone Methides **4g–l** Employed as Reference Electrophiles in this Work.

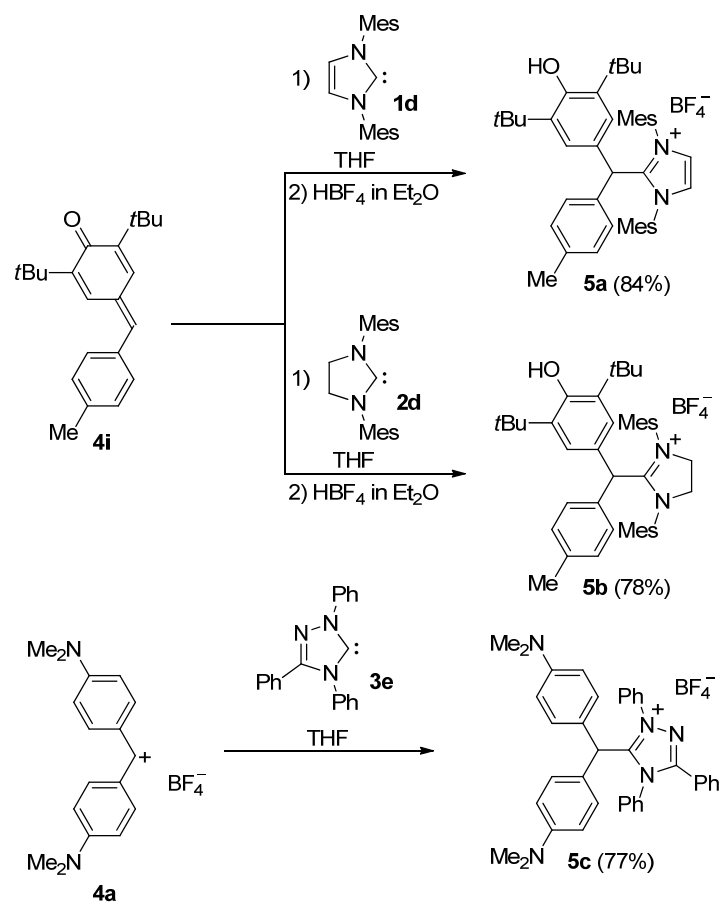
Electrophile		$E^{[a]}$	$\lambda_{\text{max}}^{[b]}$ [nm]
	R = NMe <sub>2</sub>	<b>4a</b> -7.02	611
	R = N(CH <sub>2</sub> ) <sub>4</sub>	<b>4b</b> -7.69	618
	$n = 2$	<b>4c</b> -8.22	626
	$n = 1$	<b>4d</b> -8.76	622
	$n = 2$	<b>4e</b> -9.45	637
	$n = 1$	<b>4f</b> -10.04	635
	R = OMe	<b>4g</b> -12.18	411
	R = NMe <sub>2</sub>	<b>4h</b> -13.39	499
	R = Me	<b>4i</b> -15.83	362
	R = OMe	<b>4j</b> -16.11	384
	R = NMe <sub>2</sub>	<b>4k</b> -17.29	460
		<b>4l</b> -17.90	492

[a] Electrophilicity parameters  $E$  for **4a–f** from ref. [8c], for **4g–l** from ref. [8d] [b] in THF.

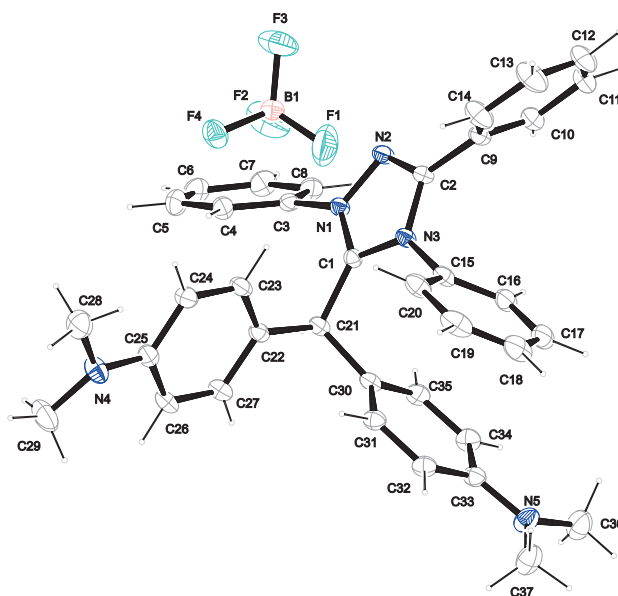
## 2 Results and discussions

Representative combinations of the carbenes **1d**, **2d**, and **3e** with the reference electrophiles **4a** or **4i** showed the course of the reactions (Scheme 2). The products formed from **1d** and **2d** and the quinone methide **4i** in THF were subsequently treated with one equivalent of  $\text{HBF}_4$  to generate the salts **5a,b** which were isolated and characterized as described in the Experimental Section 4.2.1 and 4.2.2. Addition of Enders' carbene **3e** to the blue solution of the benzhydrylium tetrafluoroborate **4a-BF<sub>4</sub>** in THF at ambient temperature led to

decolorization and formation of the adduct **5c** which has been isolated and characterized by X-ray crystallography (Figure 1).<sup>[10]</sup>

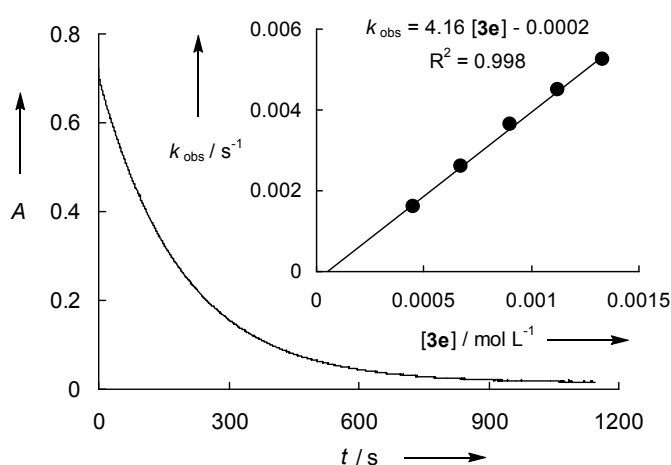
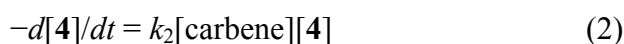


**Scheme 2.** Products of the reactions of the N-heterocyclic carbenes **1d**, **2d**, and **3e** with reference electrophiles in THF.



**Figure 1.** Crystal structure of **5c** (50 % probability ellipsoids).

The kinetic investigations were performed in THF at 20 °C by photometrically following the disappearance of the colored electrophiles **4** (Table 1, Figure 2).<sup>[11]</sup> The NHCs were used in high excess to achieve pseudo-first-order conditions. Because of the strong overlap of the UV-bands of **4i** with those of its adducts with **1d**, **2d**, and **3e**, we were unable to determine the kinetics of these reactions. The first-order rate constants  $k_{\text{obs}}$  ( $\text{s}^{-1}$ ) were obtained by fitting the experimentally observed decay of the absorbances to the mono-exponential function  $A = A_0 e^{-k_{\text{obs}} t} + C$ . The plots of  $k_{\text{obs}}$  against the concentrations of **1–3** were linear with negligible intercepts (Figure 2) indicating a second-order rate law [Eq. (2)].

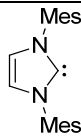
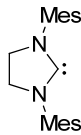
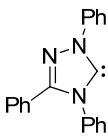
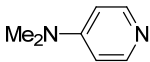
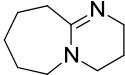


**Figure 2.** Exponential decay of the absorbance at 499 nm during the reaction of **3e** ( $1.33 \times 10^{-3} \text{ mol L}^{-1}$ ) with **4h** ( $3.98 \times 10^{-5} \text{ mol L}^{-1}$ ) at 20 °C in THF ( $k_{\text{obs}} = 5.26 \times 10^{-3} \text{ s}^{-1}$ ). Insert: Determination of second-order rate constant  $k_2 = 4.16 \text{ L mol}^{-1} \text{ s}^{-1}$  from the dependence of  $k_{\text{obs}}$  on the concentration of **3e**.

The slopes of these linear plots give the second-order rate constants  $k_2$  ( $\text{L mol}^{-1} \text{ s}^{-1}$ ) which are listed in Table 2. As the nucleophilicities of triphenylphosphane (**6**), DMAP (**7**), and DBU (**8**) have previously only been determined in other solvents,<sup>[9]</sup> their reactivities towards the reference electrophiles **4** have now also been measured in THF solution (Table 2) in order to allow a comparison of the corresponding rate constants under the same conditions.<sup>[11]</sup>

Figure 3 shows linear plots of  $\lg k_2$  for the reactions of the N-heterocyclic carbenes **1d**, **2d**, and **3e** with the reference electrophiles **4** versus the previously published electrophilicity parameters  $E$  of **4a–I** (Table 1), from which the nucleophile-specific parameters  $N$  and  $s_N$  [Eq. (1)], listed in Table 2, have been derived. Small, but systematic deviations of the reactivities of **3e** from these correlations are noticed and are commented on Experimental Section 4.3.4.

**Table 2.** Second-Order Rate Constants for the Reactions of the NHCs **1d**, **2d**, **3e**, PPh<sub>3</sub> (**6**), DMAP (**7**), and DBU (**8**) with the Reference Electrophiles **4** in THF at 20 °C.

Nucleophile	<i>N</i> , <i>s<sub>N</sub></i>	Electrophile	<i>k</i> <sub>2</sub> / L mol <sup>-1</sup> s <sup>-1</sup>
 <b>1d</b>	21.72, 0.45	<b>4g</b>	2.27 × 10 <sup>4</sup>
		<b>4h</b>	4.64 × 10 <sup>3</sup>
		<b>4j</b>	3.45 × 10 <sup>2</sup>
		<b>4k</b>	7.03 × 10 <sup>1</sup>
		<b>4l</b>	7.03 × 10 <sup>1</sup>
 <b>2d</b>	23.35, 0.40	<b>4h</b>	1.04 × 10 <sup>4</sup>
		<b>4k</b>	2.53 × 10 <sup>2</sup>
		<b>4l</b>	1.69 × 10 <sup>2</sup>
 <b>3e</b>	14.07, 0.84	<b>4c</b>	4.96 × 10 <sup>4</sup>
		<b>4d</b>	2.08 × 10 <sup>4</sup>
		<b>4e</b>	1.28 × 10 <sup>4</sup>
		<b>4f</b>	4.91 × 10 <sup>3</sup>
		<b>4g</b>	2.11 × 10 <sup>1</sup>
		<b>4h</b>	4.16
		<b>4i</b>	4.16
 <b>6</b>	13.59, 0.66 <sup>[a]</sup>	<b>4a</b>	1.93 × 10 <sup>4</sup>
		<b>4b</b>	7.80 × 10 <sup>3</sup>
		<b>4d</b>	1.42 × 10 <sup>3</sup>
		<b>4e</b>	1.42 × 10 <sup>3</sup>
 <b>7</b>	15.90, 0.66 <sup>[a]</sup>	<b>4a</b>	7.14 × 10 <sup>5</sup>
		<b>4b</b>	3.63 × 10 <sup>5</sup>
		<b>4c</b>	1.18 × 10 <sup>5</sup>
		<b>4d</b>	4.32 × 10 <sup>4</sup>
		<b>4e</b>	2.21 × 10 <sup>4</sup>
		<b>4f</b>	7.62 × 10 <sup>3</sup>
		<b>4g</b>	7.62 × 10 <sup>3</sup>
 <b>8</b>	16.12, 0.67 <sup>[a]</sup>	<b>4c</b>	2.13 × 10 <sup>5</sup>
		<b>4d</b>	8.12 × 10 <sup>4</sup>
		<b>4e</b>	3.01 × 10 <sup>4</sup>
		<b>4f</b>	3.01 × 10 <sup>4</sup>
		<b>4g</b>	1.24 × 10 <sup>4</sup>

[a] For *N* and *s<sub>N</sub>* of these nucleophiles in CH<sub>2</sub>Cl<sub>2</sub> and CH<sub>3</sub>CN, see ref.<sup>[12]</sup>.

Though the relative reactivities of carbenes depend slightly on the nature of the reference electrophile, one can see in Figure 3 that the carbenes derived from imidazolium (**1d**) and imidazolium (**2d**) salts are roughly 10<sup>3</sup> times more nucleophilic than Enders' carbene **3e**.

On the other hand, the triazole-5-ylidene **3e** has a similar nucleophilicity as DMAP (**7**) and DBU (**8**).

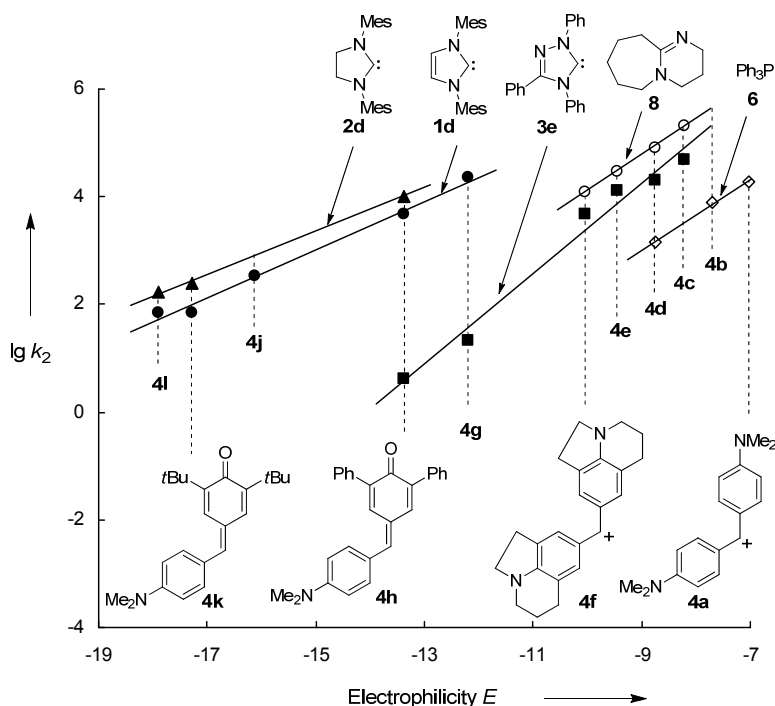
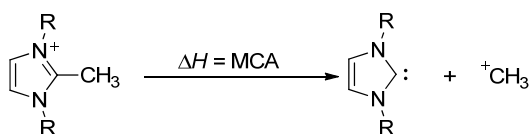


**Figure 3.** Plot of  $\lg k_2$  for the reaction of NHCs **1d**, **2d**, and **3e**,  $\text{PPh}_3$  (**6**), and DBU (**8**) with the reference electrophiles **4** in THF at 20 °C versus their electrophilicity parameters.

This gradation of the rate constants differs significantly from that of the Lewis basicities of these compounds. While **3e** combines quantitatively with **4g** and **4h**,  $\text{PPh}_3$  (**6**) and DMAP (**7**) do not react at all with these two quinone methides though Eq. (1) predicts relatively high rate constants for these reactions. The corresponding reactions of DBU (**8**) with **4g** and **4h** proceed incompletely. The Arduengo carbenes **1d** and **2d** are so strong Lewis bases that they react quantitatively even with **4k** and **4l**, the weakest electrophiles of this series.

As all attempts to measure the equilibrium constants for the reactions of these N-heterocyclic carbenes with **4** were unsuccessful, we have investigated the methyl cation affinities (Scheme 3) of differently substituted carbenes on the MP2/6-31+G(2d,p)//B98/6-31G(d) level of theory using Gaussian 09.<sup>[13]</sup> This method has previously been shown to offer a practicable and reliable approach to methyl cation affinities for various organic bases.<sup>[14]</sup>

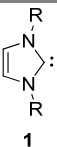
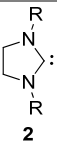
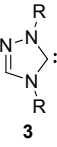
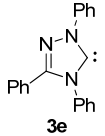


**Scheme 3.** Methyl cation affinities (MCA) of N-heterocyclic carbenes.

The two nonbonding electrons of carbenes can either reside in the same orbital with anti-parallel spins (singlet) or in two different orbitals with parallel spins (triplets).<sup>[2h,15]</sup> In line with previous investigations<sup>[2h,16]</sup> the singlet structures of the NHCs **1–3** were found to be much more stable than the corresponding triplets (290–360 kJ mol<sup>-1</sup>).

The calculated bond lengths and angles (Table 3) of the cyclic framework deviate by less than 0.04 Å or 0.7° from the experimental values obtained by X-ray crystallography.<sup>[16,17]</sup> The five-membered ring is planar for most carbenes, and only the carbene derived from di-*tert*-butyl imidazoline (**2b**) adopts a twist conformation with an N-C-C-N-dihedral angle of 18°. While the phenyl groups in (**1–3**)**c** are coplanar with the five-membered ring or only slightly distorted out of plane (interplanar angle 25° for **1c** and 27° for **3c**), the mesityl substituents are almost perpendicular to the plane of the heterocyclic ring (interplanar angle 77–78° in **1d**, **2d**, and **3d**). In contrast, all phenyl and mesityl groups are almost perpendicular to the heterocyclic ring in the azolium ions obtained by methylation of the carbenes (**1–3**)**c** and (**1–3**)**d**, which can be explained by the steric interaction of the aryl groups with the methyl group at the former carbene center.

**Table 3.** Methyl Cation Affinities (MCA, in kJ mol<sup>-1</sup>) [MP2/6-31+G(2d,p)//B98/6-31G(d)] and NCN Angles of the Carbenes **1–3**.

 <b>1</b>		<b>1a</b>	<b>1b</b>	<b>1c</b>	<b>1d</b>
		R = CH <sub>3</sub>	R = <i>t</i> Bu	R = Ph	R = Mes
	MCA	718.0	714.3	742.4	767.2
	ΔNCN	101.4°	102.6°	101.8°	101.3°
 <b>2</b>		<b>2a</b>	<b>2b</b>	<b>2c</b>	<b>2d</b>
		R = CH <sub>3</sub>	R = <i>t</i> Bu	R = Ph	R = Mes
	MCA	719.3	699.4	722.9	768.9
	ΔNCN	105.1°	106.6°	105.7°	105.4°
 <b>3</b>		<b>3a</b>	<b>3b</b>	<b>3c</b>	<b>3d</b>
		R = CH <sub>3</sub>	R = <i>t</i> Bu	R = Ph	R = Mes
	MCA	674.4	676.8	694.4	728.4
	ΔNCN	99.8°	100.7°	100.3°	100.0°
 <b>3e</b>		<b>3e</b>			
	MCA	712.2			
	ΔNCN	103.7°			

The calculated  $H_{298}$  values for the carbenes **1–3** and the corresponding  $H_{298}$  values for the methylated azolium ions have been combined with  $H_{298}$  of the methyl cation to give the methyl cation affinities (MCA) as defined in Scheme 3 (Table 3).

Table 3 shows that the methyl substituted imidazole- and imidazoline-derived carbenes **1a** and **2a** have the same methyl cation affinities indicating that the extra double bond in **1a** does not affect its Lewis basicity. Analogously, the mesityl substituted carbenes **1d** and **2d** have approximately the same methyl cation affinities. The 50 kJ mol<sup>-1</sup> higher MCA of **1d** and **2d** relative to **1a** and **2a** can be attributed to the inductive electron-withdrawing effect of the mesityl groups which are almost perpendicular to the heterocyclic rings in the carbenes **1d** and **2d** as well as in the corresponding azolium ions and, therefore, cannot operate through mesomeric electron donation.

Both phenyl-substituted carbenes **1c** and **2c** are weaker Lewis bases than their mesityl analogues **1d** and **2d** because the phenyl groups can mesomerically interact with the empty *p*-orbital at C-2 of the heterocyclic ring in the carbenes **1c** and **2c** but not in the resulting amidinium ions, where the phenyl group is distorted out of the plane by the methyl group. As the mesomeric stabilization of the ground state is more efficient in **2c** (interplanar angle 0°; phenyl staggered with the CH<sub>2</sub> group) than in **1c** (interplanar angle 25°; interaction between phenyl and the vinylic CH), **2c** is a weaker Lewis base than **1c**.

While **1a**, **1b**, and **2a** have similar methyl cation affinities, the MCA of the *tert*-butyl substituted carbene **2b** is smaller by 15 to 20 kJ mol<sup>-1</sup> because methylation of **2b** forces the twist conformation of the CH<sub>2</sub>-CH<sub>2</sub>-bridge in **2b** into a strained planar ring conformation.

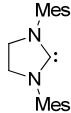
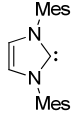
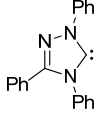
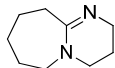
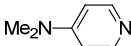
The substituent effects on the triazole-derived carbenes **3a–d** are similar as in the isoelectronic series **1a–d**. The electron-withdrawing effect of the additional nitrogen in **3a–d** accounts for the fact that their methyl cation affinities are 38 to 48 kJ mol<sup>-1</sup> smaller than those of the analogously substituted carbenes **1a–d**. The 18 kJ mol<sup>-1</sup> increase of the methyl cation affinity from **3c** to **3e** can, finally, be assigned to the mesomeric effect of the additional phenyl group.

Table 4 shows that the MCAs of the NHCs **2d**, **1d**, and **3e** are more than 100 kJ mol<sup>-1</sup> greater than those of PPh<sub>3</sub> (**6**) and of the N-nucleophiles **7–9**, in accord with our observation that the weakly Lewis acidic quinone methides **4g,h** react quantitatively with these three NHCs but not with PPh<sub>3</sub> (**6**), DMAP (**7**), and DABCO (**9**).

The similar methyl cation affinities of **2d** and **1d** are reflected by their similar nucleophilicities, expressed by the relative reactivities of these two carbenes towards **4h**

(Table 4). The extra nitrogen in **3e** reduces the methyl cation affinity by 55 kJ mol<sup>-1</sup> and the nucleophilicity by a factor of 10<sup>3</sup> [ $k_{\text{rel}}(\mathbf{4h})$ ].

**Table 4.** Methyl Cation Affinities [MCA, MP2/6-31+G(2d,p)//B98/6-31G(d), in kJ mol<sup>-1</sup>] and Relative Rate Constants towards **4h** and **4d** for Different Organocatalysts.

Substrate	MCA	$k_{\text{rel}}(\mathbf{4h})$	$k_{\text{rel}}(\mathbf{4d})$
 <b>2d</b>	768.9	$2.5 \times 10^3$	
 <b>1d</b>	767.2	$1.1 \times 10^3$	
 <b>3e</b>	712.2	1.0	1.0
 <b>6</b>	618.4 <sup>[a]</sup>		$6.8 \times 10^{-2}$
 <b>8</b>	609.6 <sup>[b]</sup>		3.9
 <b>7</b>	581.2 <sup>[b]</sup>		2.1
 <b>9</b>	562.2 <sup>[c]</sup>		$5.3 \times 10^{2[d]}$

[a] From ref. [14c]. [b] from ref. [14a]. [c] from ref. [14b]. [d] in MeCN at 20 °C:  $k_2 = 1.10 \times 10^7$  L mol<sup>-1</sup> s<sup>-1</sup>, from ref. [6d].

The lower part of Table 4 shows that the MCAs of **3e** and **6–9** do not correlate with the corresponding nucleophilicities. DABCO (**9**), the compound with the lowest MCA, has by far the highest nucleophilicity. Enders' carbene **3e** is a slightly weaker nucleophile than DBU (**8**) and DMAP (**7**) [ $k_{\text{rel}}(\mathbf{4d})$ ] despite its much higher methyl cation affinity.

In previous work we have derived relative Lewis basicities of **7–9** from equilibrium constants of their reactions with benzhydrylium ions and structurally related Michael acceptors. The ordering **8** > **7** > **9** was the same as for the methyl cation affinities in Table 4.<sup>[6d,9d]</sup> The fact that DABCO (**9**) is a much stronger nucleophile and at the same time a much weaker Lewis base than DMAP (**7**), as well as the observation that DBU (**8**) has a similar nucleophilicity as DMAP (**7**) yet a much higher Lewis basicity was explained by widely differing Marcus intrinsic barriers in the order **8** > **7** > **9**.<sup>[6d,9d]</sup>

As compounds **7** and **8** have similar nucleophilic reactivities as Enders' carbene **3e** while their methyl cation affinities are more than 100 kJ mol<sup>-1</sup> lower, one has to conclude that NHCs must react via much higher intrinsic barriers than compounds **6–9**.<sup>[18]</sup>

### 3 Conclusion

The ability of NHCs to act as umpolung reagents<sup>[19]</sup> has been explained by the high acidity of the former aldehyde proton in the initially formed adduct which gives rise to the formation of the Breslow intermediate.<sup>[20]</sup> A further specialty is their extraordinarily high Lewis basicity quantified in this work, which explains that they do not catalyze Baylis-Hillman reactions of  $\alpha,\beta$ -unsaturated aldehydes but instead induce their homoenolate chemistry through umpolung.<sup>[4d,21]</sup> As discussed elsewhere,<sup>[18]</sup> nucleophiles generally attack at the carbonyl group of  $\alpha,\beta$ -unsaturated aldehydes under conditions of kinetic control. With tertiary amines and phosphanes, this attack is reversible, and the subsequent conjugate addition gives rise to the Baylis-Hillman reactions. Because of the high Lewis basicity of N-heterocyclic carbenes, the kinetically preferred attack at the carbonyl group has a lower degree of reversibility and therefore, enables their use as umpolung reagents also of  $\alpha,\beta$ -unsaturated aldehydes.

### 4 Experimental Sections

#### 4.1 General

##### *Chemicals.*

**1d** was synthesised according to the literature procedure.<sup>[22]</sup> **2d** and **3e** were purchased from commercial sources and used without further purification. Benzhydrylium tetrafluoroborates **4a-f**<sup>[8b]</sup> and quinone methides **4g-l**<sup>[8c]</sup> were prepared as described before.

Commercially available THF (Sigma-Aldrich, purisis, p.a.) and *i*-hexane were distilled over sodium prior to use. DMSO was purchased from Acros organics (99.7 %, Extra dry, Aero seal) and used without further purification.

##### *Analytics.*

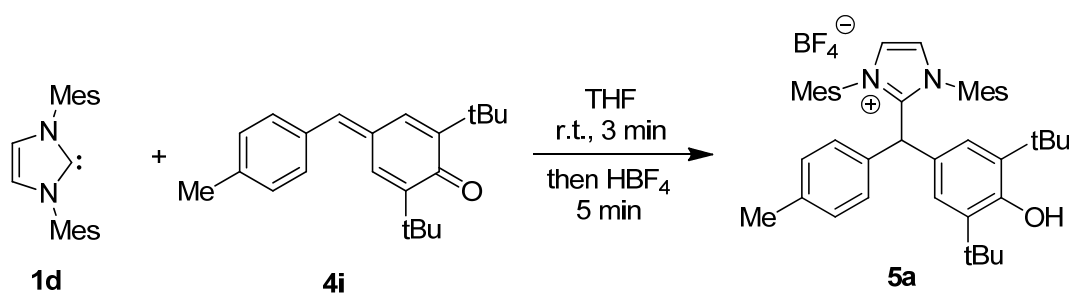
<sup>1</sup>H- and <sup>13</sup>C-NMR spectra were recorded on *Varian* NMR-systems (400) in CD<sub>3</sub>CN and the chemical shifts in ppm refer to the solvent residual signal as internal standard ( $\delta_{\text{H}}$  (CD<sub>3</sub>CN) = 1.94,  $\delta_{\text{C}}$  (CD<sub>3</sub>CN) = 1.4). The following abbreviations were used for chemical shift mutiplicities: brs = broad singlet, s = singlet, d = doublet, t = triplet, q = quartet, m = multiplet. For reasons of simplicity, the <sup>1</sup>H-NMR signals of AA'BB'-spin systems of *p*-disubstituted aromatic rings are treated as doublets. NMR signal assignments are based on additional 2D-NMR experiments (COSY, HSQC, and HMBC). (HR-MS) has been performed on a *Finnigan MAT 95* (EI) or a *Thermo Finnigan LTQ FT* (ESI) mass spectrometer. Melting points were determined on a *Büchi B-540* device and are not corrected.

*Kinetics.*

The rates of all investigated reactions were determined photometrically. The temperature of the solutions during all kinetic studies was kept constant ( $20.0 \pm 0.1^\circ\text{C}$ ) by using a circulating bath thermostat. The kinetic experiments were carried out with freshly prepared stock solutions of NHCs **1–3**, DMAP, DBU, and  $\text{PPh}_3$  in dry THF. Due to lower solubility of the benzhydrylium tetrafluoroborates (**4a–f**)- $\text{BF}_4$  in THF, these stock solutions are prepared in dry THF containing  $\sim 1\text{--}5\%$  of DMSO as cosolvent. First-order kinetics were achieved by employing more than 6 equiv. of the nucleophiles. For the evaluation of fast kinetics ( $\tau_{1/2} < 15\text{--}20$  s) the spectrophotometer system Applied Photophysics SX.18MV-R stopped-flow reaction analyser was used.

The rates of slow reactions ( $\tau_{1/2} > 15\text{--}20$  s) were determined by using a J&M TIDAS diode array spectrophotometer controlled by Labcontrol Spectacle software and connected to a Hellma 661.502-QX quartz Suprasil immersion probe (5 mm light path) via fiber optic cables and standard SMA connectors.

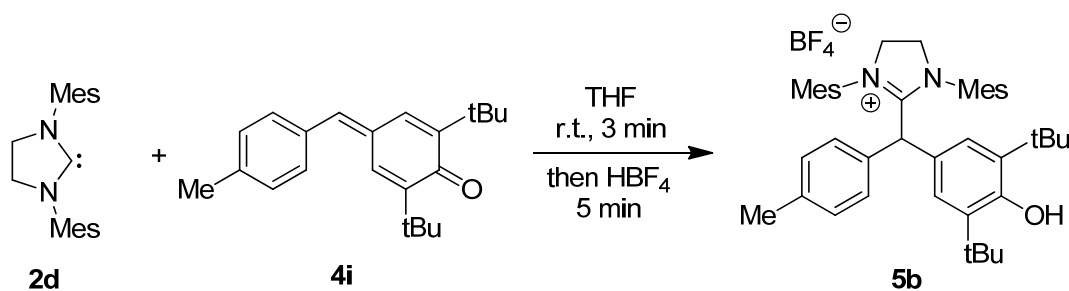
Rate constants  $k_{\text{obs}}$  ( $\text{s}^{-1}$ ) were obtained by fitting the single exponential  $A_t = A_0 \exp(-k_{\text{obs}}t) + C$  (exponential decrease) to the observed time-dependent absorbance (averaged from at least 5 kinetic runs for each nucleophile concentration in case of stopped-flow methodology).

**4.2 Product Studies****4.2.1 Product studies for the reaction of 1d with 4i.**

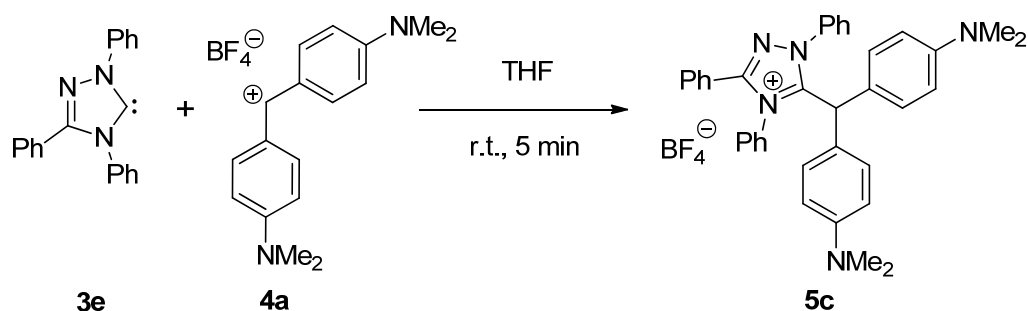
To an oven dried flask charged with a mixture of **4i** (33.0 mg, 0.107 mmol) and **1d** (30.4 mg, 0.100 mmol) was added dry THF (5 mL) and the mixture was then stirred for 2–3 min at room temperature. The reaction was then quenched with 20  $\mu\text{L}$  of 50–55% ethereal  $\text{HBF}_4$  (8.8 mg, 0.100 mmol). The solvent was then evaporated and the crude material was dissolved in minimum volume of toluene-dichloromethane ( $\sim 1:4$ ). The product **5a** was then precipitated by adding *n*-pentane and washed several times with *n*-pentane. Yellowish powder, 59 mg, 84  $\mu\text{mol}$ , 84%.  $^1\text{H-NMR}$  ( $\text{CD}_3\text{CN}$ , 400 MHz):  $\delta = 1.26$  (s, 18 H), 1.87 (s, 6 H), 2.06 (s, 6 H),

2.19 (s, 3 H), 2.28 (s, 6 H), 5.32 (s, 1 H), 5.48 (s, 1 H), 6.72 (s, 2 H), 6.82-6.85 (m, 4 H), 6.88-6.99 (m, 2 H), 6.97-6.98 (m, 2 H), 7.53 (s, 2 H) ppm.  $^{13}\text{C}$ -NMR ( $\text{CD}_3\text{CN}$ , 100 MHz):  $\delta$  = 18.5 (q,  $\text{CH}_3$ ), 18.6 (q,  $\text{CH}_3$ ), 21.1 (q,  $\text{CH}_3$ ), 21.2 (q,  $\text{CH}_3$ ), 30.2 (q,  $\text{CH}_3$ ), 35.2 (q,  $\text{CH}_3$ ), 51.6 (d,  $\text{Ar}_2\text{CH}$ ), 126.1 (d, Ar), 126.9 (d, Ar), 128.1 (s, Ar), 129.8 (d, Ar), 129.9 (d, Ar), 130.7 (d, Ar), 130.8 (d, Ar), 132.0 (s, Ar), 132.4 (s, Ar), 135.2 (s, Ar), 135.4 (s, Ar), 138.3 (s, Ar), 139.3 (s, Ar), 142.1 (s, Ar), 148.5 (s,  $\text{C}=\text{N}^+$ ), 154.7 (s, Ar) ppm. HR-MS (ESI) [ $\text{M}^+$ ]: calculated for  $[\text{C}_{43}\text{H}_{53}\text{N}_2\text{O}]^+$  is 613.4152; found 613.4158.

#### 4.2.2 Product studies for the reaction of **2d** with **4i**.



To an oven dried flask charged with a mixture of **4i** (33.9 mg, 0.110 mmol) and **2d** (30.6 mg, 0.100 mmol) was added dry THF (5 mL) and the mixture was then stirred for 2–3 min at room temperature. The reaction was then quenched with 20  $\mu\text{L}$  of 50-55% ethereal  $\text{HBF}_4$  (8.8 mg, 0.100 mmol). The solvent was then evaporated and the crude material was dissolved in minimum volume of toluene-dichloromethane (~1:4). The product **5b** was then precipitated by adding *n*-pentane and washed several times with *n*-pentane. Off white powder 55 mg, 78  $\mu\text{mol}$ , 78%.  $^1\text{H}$ -NMR ( $\text{CD}_3\text{CN}$ , 400 MHz):  $\delta$  = 1.28 (s, 18 H), 2.06 (s, 6 H), 2.16 (s, 3 H), 2.22 (s, 6 H), 2.34 (s, 6 H), 4.24 (s, 4 H), 4.87 (s, 1 H), 5.48 (s, 1 H), 6.71 (s, 4 H), 6.79 (d,  $J$  = 8.3 Hz, 2 H), 6.87-6.90 (m, 4 H) ppm.  $^{13}\text{C}$ -NMR ( $\text{CD}_3\text{CN}$ , 100 MHz):  $\delta$  = 18.8 (q,  $\text{CH}_3$ ), 18.9 (q,  $\text{CH}_3$ ), 21.06 (q,  $\text{CH}_3$ ), 21.11 (q,  $\text{CH}_3$ ), 30.2 (q,  $\text{CH}_3$ ), 35.2 (q,  $\text{CH}_3$ ), 52.2 (t,  $\text{CH}_2$ ), 52.6 (d,  $\text{Ar}_2\text{CH}$ ), 127.1 (d, Ar), 127.3 (s, Ar), 129.6 (d, Ar), 130.0 (d, Ar), 131.0 (d, Ar), 131.1 (d, Ar), 131.6 (s, Ar), 132.3 (s, Ar), 135.8 (s, Ar), 136.2 (s, Ar), 138.2 (s, Ar), 139.3 (s, Ar), 141.2 (s, Ar), 154.8 (s, Ar), 170.0 (s,  $\text{C}=\text{N}^+$ ) ppm. HR-MS (ESI) [ $\text{M}^+$ ]: calculated for  $[\text{C}_{43}\text{H}_{55}\text{N}_2\text{O}]^+$  is 615.4309; found 615.4306.

4.2.3 Product studies for the reaction of **4** with **4a**.

To a oven dried flask charged with a mixture of **4a** (34.0 mg, 0.100 mmol) and **3e** (31.2 mg, 0.105 mmol) was added dry THF (10 mL) and the mixture was then stirred for 5 min at room temperature. Then, the solvent was evaporated and the residue was washed with dry *i*-hexane. The crude product was dissolved in dichloromethane-ethyl acetate mixture (~9:1) and crystallized by vapour diffusion of *n*-pentane into the above solvent mixture at room temperature to get bluish shiny crystals of **5c** (49 mg, 77  $\mu\text{mol}$ , 77%). *m.p.* (dichloromethane, ethyl acetate, *n*-pentane) >209 °C (decomposition).  $^1\text{H-NMR}$  ( $\text{CD}_3\text{CN}$ , 400 MHz):  $\delta$  = 2.88 (s, 12 H,  $\text{N}(\text{CH}_3)_2$ ), 5.82 (s, 1 H,  $\text{Ar}_2\text{CH}$ ), 6.49 (d,  $J$  = 8.9 Hz, 4 H, Ar), 6.73 (d,  $J$  = 8.7 Hz, 4 H, Ar), 7.26-7.29 (m, 2 H, Ar), 7.33-7.43 (m, 8 H, Ar), 7.48-7.56 (m, 5 H, Ar) ppm.  $^{13}\text{C-NMR}$  ( $\text{CD}_3\text{CN}$ , 101 MHz):  $\delta$  = 40.7 (q,  $\text{N}(\text{CH}_3)_2$ ), 47.9 (d,  $\text{Ar}_2\text{CH}$ ), 113.3 (d, Ar), 123.0 (s), 124.0 (s), 127.5 (d, Ar), 128.9 (d, Ar), 130.0 (d, Ar), 130.6 (d, Ar), 130.7 (d, Ar), 131.1 (d, Ar), 132.3 (d, Ar), 132.56 (s), 132.59 (d, Ar), 133.2 (d, Ar), 136.6 (s), 151.5 (s), 155.0 (s), 157.0 (s) ppm. HR-MS (ESI) [ $\text{M}^+$ ]: calculated for  $[\text{C}_{37}\text{H}_{36}\text{N}_5]^+$  is 550.2965; found 550.2967.

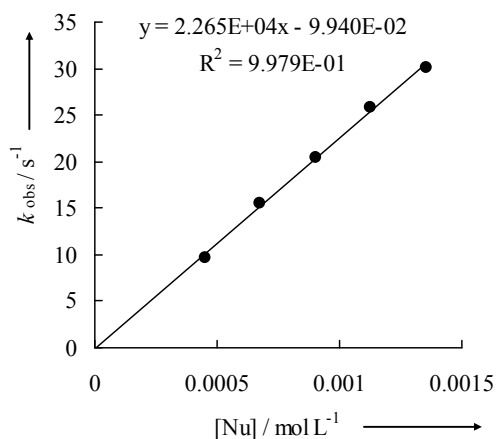
**Crystallographic data for 5c:**

net formula	C <sub>37</sub> H <sub>36</sub> BF <sub>4</sub> N <sub>5</sub>
<i>M<sub>r</sub></i> /g mol <sup>-1</sup>	637.520
crystal size/mm	0.31 × 0.22 × 0.10
<i>T</i> /K	173(2)
radiation	MoKα
diffractometer	'Oxford XCalibur'
crystal system	monoclinic
space group	<i>P</i> 2 <sub>1</sub> / <i>c</i>
<i>a</i> /Å	10.6683(3)
<i>b</i> /Å	13.8062(4)
<i>c</i> /Å	22.7356(7)
α/°	90
β/°	100.361(3)
γ/°	90
<i>V</i> /Å <sup>3</sup>	3294.09(17)
<i>Z</i>	4
calc. density/g cm <sup>-3</sup>	1.28550(7)
μ/mm <sup>-1</sup>	0.092
absorption correction	'multi-scan'
transmission factor range	0.98039–1.00000
refls. measured	23689
<i>R</i> <sub>int</sub>	0.0353
mean σ( <i>I</i> )/ <i>I</i>	0.0580
θ range	4.25–25.25
observed refls.	3466
<i>x</i> , <i>y</i> (weighting scheme)	0.1046, 0
hydrogen refinement	constr
refls in refinement	5927
parameters	428
restraints	0
<i>R</i> ( <i>F</i> <sub>obs</sub> )	0.0588
<i>R</i> <sub>w</sub> ( <i>F</i> <sup>2</sup> )	0.1743
<i>S</i>	0.975
shift/error <sub>max</sub>	0.001
max electron density/e Å <sup>-3</sup>	0.877
min electron density/e Å <sup>-3</sup>	-0.379

## 4.3 Kinetics

4.3.1 Kinetics of the Reactions of the Carbene **1d** with the Reference Electrophiles **4**.**Table 5:** Kinetics of the reaction of **1d** with **4g** at 20 °C in THF (stopped-flow,  $\lambda = 418$  nm).

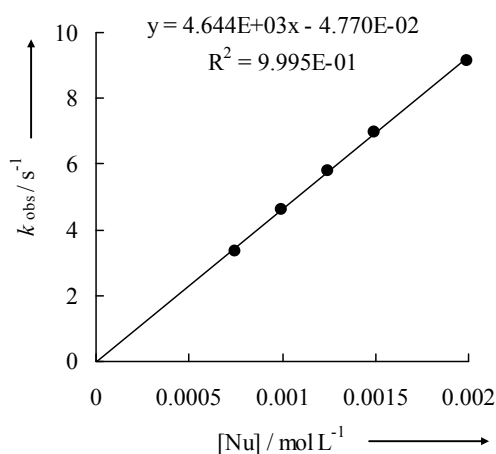
[ <b>4g</b> ] / mol L <sup>-1</sup>	[ <b>1d</b> ] / mol L <sup>-1</sup>	$k_{\text{obs}}$ / s <sup>-1</sup>
$8.78 \times 10^{-5}$	$4.51 \times 10^{-4}$	9.72
$8.78 \times 10^{-5}$	$6.77 \times 10^{-4}$	$1.56 \times 10^1$
$8.78 \times 10^{-5}$	$9.02 \times 10^{-4}$	$2.04 \times 10^1$
$8.78 \times 10^{-5}$	$1.13 \times 10^{-3}$	$2.58 \times 10^1$
$8.78 \times 10^{-5}$	$1.35 \times 10^{-3}$	$3.02 \times 10^1$



$$k_2 = 2.27 \times 10^4 \text{ L mol}^{-1} \text{ s}^{-1}$$

**Table 6:** Kinetics of the reaction of **1d** with **4h** at 20 °C in THF (stopped-flow,  $\lambda = 530$  nm).

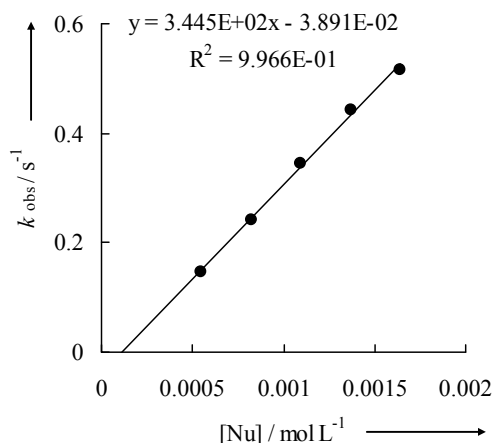
[ <b>4h</b> ] / mol L <sup>-1</sup>	[ <b>1d</b> ] / mol L <sup>-1</sup>	$k_{\text{obs}}$ / s <sup>-1</sup>
$5.30 \times 10^{-5}$	$7.48 \times 10^{-4}$	3.37
$5.30 \times 10^{-5}$	$9.97 \times 10^{-4}$	4.60
$5.30 \times 10^{-5}$	$1.25 \times 10^{-3}$	5.78
$5.30 \times 10^{-5}$	$1.50 \times 10^{-3}$	6.95
$5.30 \times 10^{-5}$	$1.99 \times 10^{-3}$	9.16



$$k_2 = 4.64 \times 10^3 \text{ L mol}^{-1} \text{ s}^{-1}$$

**Table 7:** Kinetics of the reaction of **1d** with **4j** at 20 °C in THF (stopped-flow,  $\lambda = 383$  nm).

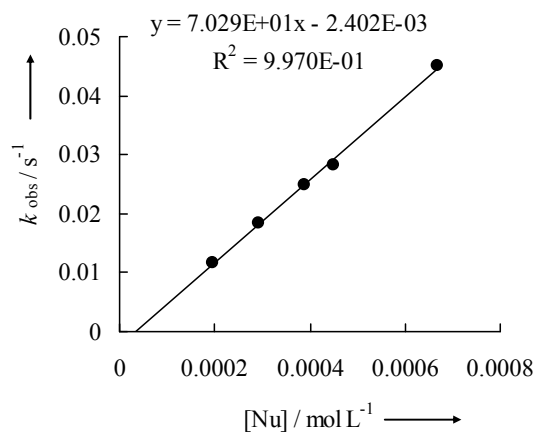
[ <b>4j</b> ] / mol L <sup>-1</sup>	[ <b>1d</b> ] / mol L <sup>-1</sup>	$k_{\text{obs}} / \text{s}^{-1}$
$7.02 \times 10^{-5}$	$5.47 \times 10^{-4}$	$1.46 \times 10^{-1}$
$7.02 \times 10^{-5}$	$8.21 \times 10^{-4}$	$2.40 \times 10^{-1}$
$7.02 \times 10^{-5}$	$1.09 \times 10^{-3}$	$3.44 \times 10^{-1}$
$7.02 \times 10^{-5}$	$1.37 \times 10^{-3}$	$4.44 \times 10^{-1}$
$7.02 \times 10^{-5}$	$1.64 \times 10^{-3}$	$5.16 \times 10^{-1}$



$$k_2 = 3.45 \times 10^2 \text{ L mol}^{-1} \text{ s}^{-1}$$

**Table 8:** Kinetics of the reaction of **1d** with **4k** at 20 °C in THF (diode array,  $\lambda = 460$  nm).

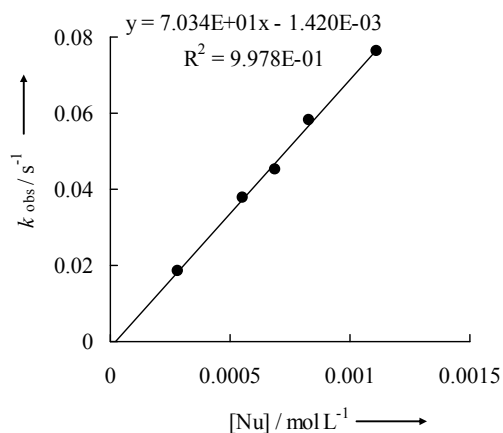
[ <b>4k</b> ] / mol L <sup>-1</sup>	[ <b>1d</b> ] / mol L <sup>-1</sup>	$k_{\text{obs}} / \text{s}^{-1}$
$4.30 \times 10^{-5}$	$1.95 \times 10^{-4}$	$1.18 \times 10^{-2}$
$4.30 \times 10^{-5}$	$2.93 \times 10^{-4}$	$1.84 \times 10^{-2}$
$4.28 \times 10^{-5}$	$3.89 \times 10^{-4}$	$2.49 \times 10^{-2}$
$3.97 \times 10^{-5}$	$4.51 \times 10^{-4}$	$2.82 \times 10^{-2}$
$4.20 \times 10^{-5}$	$6.68 \times 10^{-4}$	$4.52 \times 10^{-2}$



$$k_2 = 7.03 \times 10^1 \text{ L mol}^{-1} \text{ s}^{-1}$$

**Table 9:** Kinetics of the reaction of the ImMes **1d** with **4l** at 20 °C in THF (diode array  $\lambda = 493$  nm).

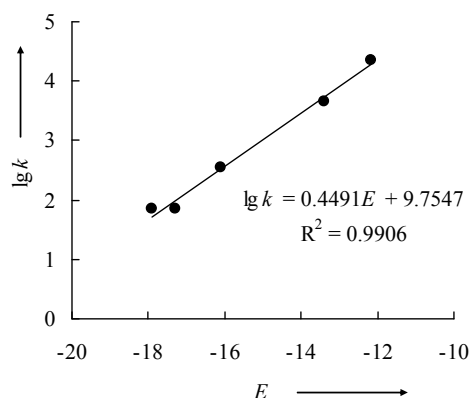
[ <b>4l</b> ] / mol L <sup>-1</sup>	[ <b>1d</b> ] / mol L <sup>-1</sup>	$k_{\text{obs}} / \text{s}^{-1}$
$3.88 \times 10^{-5}$	$2.80 \times 10^{-4}$	$1.84 \times 10^{-2}$
$3.82 \times 10^{-5}$	$5.51 \times 10^{-4}$	$3.77 \times 10^{-2}$
$3.81 \times 10^{-5}$	$6.88 \times 10^{-4}$	$4.54 \times 10^{-2}$
$3.82 \times 10^{-5}$	$8.27 \times 10^{-4}$	$5.80 \times 10^{-2}$
$3.84 \times 10^{-5}$	$1.11 \times 10^{-3}$	$7.65 \times 10^{-2}$



$$k_2 = 7.03 \times 10^1 \text{ L mol}^{-1} \text{ s}^{-1}$$

**Table 10:** Determination of the parameters  $N$  and  $s_N$  for **1d** in THF.

Electrophiles	$E$	$k_2$ ( $\text{M}^{-1} \text{s}^{-1}$ )
<b>4g</b>	-12.18	$2.27 \times 10^4$
<b>4h</b>	-13.39	$4.64 \times 10^3$
<b>4j</b>	-16.11	$3.45 \times 10^2$
<b>4k</b>	-17.29	$7.03 \times 10^1$
<b>4l</b>	-17.90	$7.03 \times 10^1$



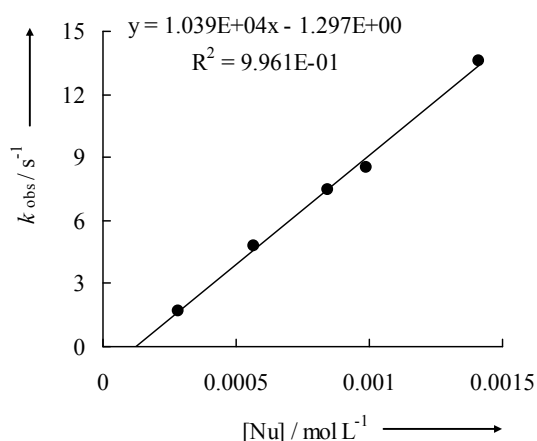
$$N = 21.72$$

$$s_N = 0.45$$

### 4.3.2 Kinetics of the Reactions of the Carbene **2d** with the Reference Electrophiles **4**.

**Table 11:** Kinetics of the reaction of **2d** with **4h** at 20 °C in THF (stopped-flow,  $\lambda = 530$  nm).

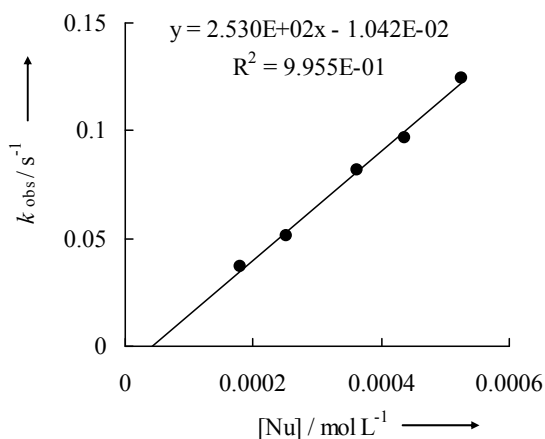
[ <b>4h</b> ] / $\text{mol L}^{-1}$	[ <b>2d</b> ] / $\text{mol L}^{-1}$	$k_{\text{obs}}$ / $\text{s}^{-1}$
$7.28 \times 10^{-5}$	$2.82 \times 10^{-4}$	1.67
$7.28 \times 10^{-5}$	$5.65 \times 10^{-4}$	4.77
$7.28 \times 10^{-5}$	$8.47 \times 10^{-4}$	7.47
$7.28 \times 10^{-5}$	$9.88 \times 10^{-4}$	8.51
$7.28 \times 10^{-5}$	$1.41 \times 10^{-3}$	$1.36 \times 10^1$



$$k_2 = 1.04 \times 10^4 \text{ L mol}^{-1} \text{ s}^{-1}$$

**Table 12:** Kinetics of the reaction of **2d** with **4k** at 20 °C in THF (diode array,  $\lambda = 463$  nm).

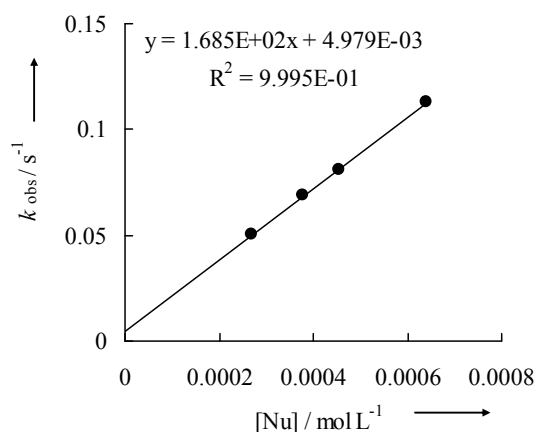
[ <b>4k</b> ] / $\text{mol L}^{-1}$	[ <b>2d</b> ] / $\text{mol L}^{-1}$	$k_{\text{obs}}$ / $\text{s}^{-1}$
$3.96 \times 10^{-5}$	$1.81 \times 10^{-4}$	$3.70 \times 10^{-2}$
$3.68 \times 10^{-5}$	$2.51 \times 10^{-4}$	$5.14 \times 10^{-2}$
$3.96 \times 10^{-5}$	$3.61 \times 10^{-4}$	$8.21 \times 10^{-2}$
$3.83 \times 10^{-5}$	$4.37 \times 10^{-4}$	$9.69 \times 10^{-2}$
$3.84 \times 10^{-5}$	$5.26 \times 10^{-4}$	$1.25 \times 10^{-1}$



$$k_2 = 2.53 \times 10^2 \text{ L mol}^{-1} \text{ s}^{-1}$$

**Table 13:** Kinetics of the reaction of **2d** with **4l** at 20 °C in THF (diode array,  $\lambda = 493$  nm).

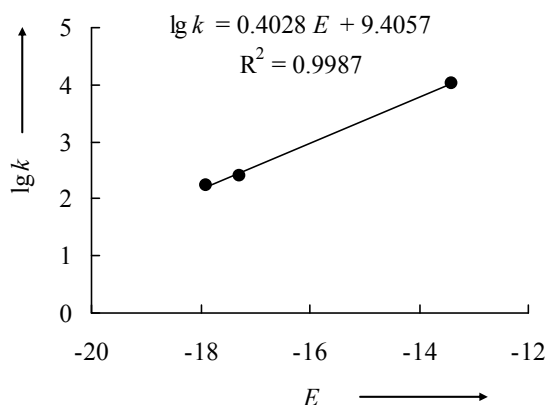
[ <b>4l</b> ] / mol L <sup>-1</sup>	[ <b>2d</b> ] / mol L <sup>-1</sup>	$k_{\text{obs}} / \text{s}^{-1}$
$3.63 \times 10^{-5}$	$2.69 \times 10^{-4}$	$5.04 \times 10^{-2}$
$3.82 \times 10^{-5}$	$3.77 \times 10^{-4}$	$6.91 \times 10^{-2}$
$3.69 \times 10^{-5}$	$4.56 \times 10^{-4}$	$8.10 \times 10^{-2}$
$3.69 \times 10^{-5}$	$6.39 \times 10^{-4}$	$1.13 \times 10^{-1}$



$$k_2 = 1.69 \times 10^2 \text{ L mol}^{-1} \text{ s}^{-1}$$

**Table 14:** Determination of the parameters  $N$  and  $s_N$  **2d** in THF.

Electrophiles	$E$	$k_2 (\text{M}^{-1} \text{s}^{-1})$
<b>4h</b>	-13.39	$1.04 \times 10^4$
<b>4k</b>	-17.29	$2.53 \times 10^2$
<b>4l</b>	-17.90	$1.69 \times 10^2$



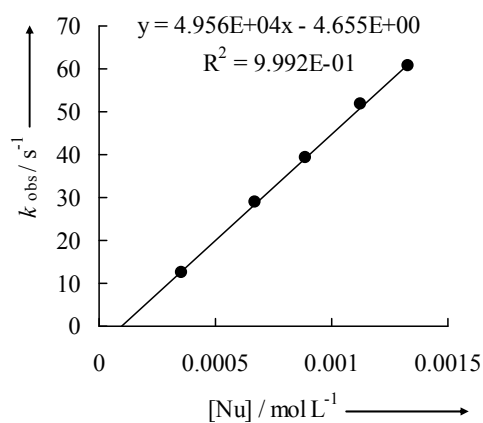
$$N = 23.35$$

$$s = 0.40$$

#### 4.3.3 Kinetics of the Reactions of the Carbene **3e** with the Reference Electrophiles **4**.

**Table 15:** Kinetics of the reaction of the 1,3,4-triphenyl triazol-5-ylidenes **3e** with **4c** at 20 °C in THF (stopped-flow,  $\lambda = 612$  nm).

[ <b>4c</b> ] / mol L <sup>-1</sup>	[ <b>3e</b> ] / mol L <sup>-1</sup>	$k_{\text{obs}} / \text{s}^{-1}$
$3.10 \times 10^{-5}$	$3.53 \times 10^{-4}$	$1.25 \times 10^1$
$3.10 \times 10^{-5}$	$6.73 \times 10^{-4}$	$2.91 \times 10^1$
$3.10 \times 10^{-5}$	$8.91 \times 10^{-4}$	$3.93 \times 10^1$
$3.10 \times 10^{-5}$	$1.13 \times 10^{-3}$	$5.19 \times 10^1$
$3.10 \times 10^{-5}$	$1.33 \times 10^{-3}$	$6.06 \times 10^1$

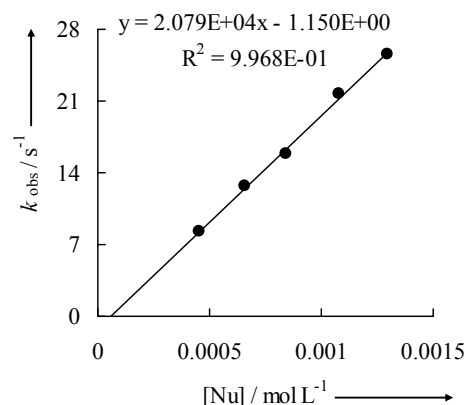


$$k_2 = 4.96 \times 10^4 \text{ L mol}^{-1} \text{ s}^{-1}$$

**Table 16:** Kinetics of the reaction of the 1,3,4-triphenyl triazol-5-ylidenes **3e** with **4d** at 20 °C in THF (stopped-flow,  $\lambda = 616$  nm).

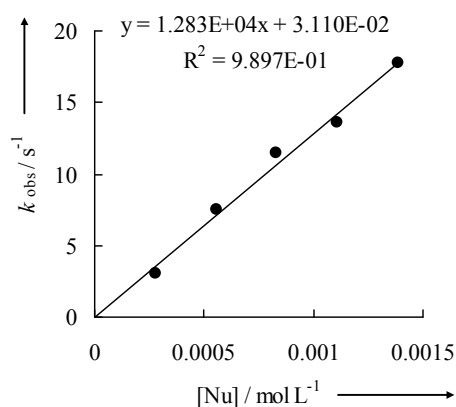
[ <b>4d</b> ] / mol L <sup>-1</sup>	[ <b>3e</b> ] / mol L <sup>-1</sup>	$k_{\text{obs}} / \text{s}^{-1}$
$1.60 \times 10^{-5}$	$4.54 \times 10^{-4}$	8.26
$1.60 \times 10^{-5}$	$6.56 \times 10^{-4}$	$1.27 \times 10^1$
$1.60 \times 10^{-5}$	$8.41 \times 10^{-4}$	$1.58 \times 10^1$
$1.60 \times 10^{-5}$	$1.08 \times 10^{-3}$	$2.18 \times 10^1$
$1.60 \times 10^{-5}$	$1.29 \times 10^{-3}$	$2.55 \times 10^1$

$$k_2 = 2.08 \times 10^4 \text{ L mol}^{-1} \text{ s}^{-1}$$

**Table 17:** Kinetics of the reaction of the 1,3,4-triphenyl triazol-5-ylidenes **3e** with **4e** at 20 °C in THF (stopped-flow,  $\lambda = 630$  nm).

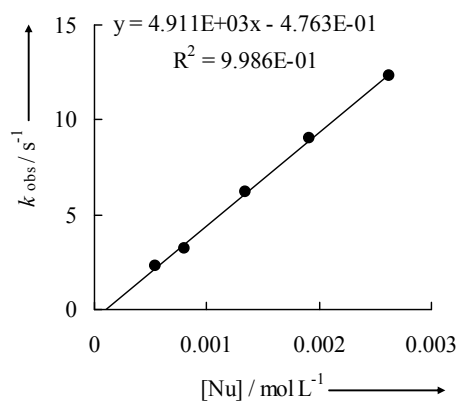
[ <b>4e</b> ] / mol L <sup>-1</sup>	[ <b>3e</b> ] / mol L <sup>-1</sup>	$k_{\text{obs}} / \text{s}^{-1}$
$2.81 \times 10^{-5}$	$2.77 \times 10^{-4}$	3.09
$2.81 \times 10^{-5}$	$5.54 \times 10^{-4}$	7.51
$2.81 \times 10^{-5}$	$8.31 \times 10^{-4}$	$1.15 \times 10^1$
$2.81 \times 10^{-5}$	$1.11 \times 10^{-3}$	$1.37 \times 10^1$
$2.81 \times 10^{-5}$	$1.39 \times 10^{-3}$	$1.78 \times 10^1$

$$k_2 = 1.28 \times 10^4 \text{ L mol}^{-1} \text{ s}^{-1}$$

**Table 18:** Kinetics of the reaction of the 1,3,4-triphenyl triazol-5-ylidenes **3e** with **4f** at 20 °C in THF (stopped-flow,  $\lambda = 631$  nm).

[ <b>4f</b> ] / mol L <sup>-1</sup>	[ <b>3e</b> ] / mol L <sup>-1</sup>	$k_{\text{obs}} / \text{s}^{-1}$
$2.40 \times 10^{-5}$	$5.38 \times 10^{-4}$	2.31
$2.40 \times 10^{-5}$	$8.07 \times 10^{-4}$	3.24
$2.40 \times 10^{-5}$	$1.35 \times 10^{-3}$	6.21
$2.40 \times 10^{-5}$	$1.92 \times 10^{-3}$	9.01
$2.40 \times 10^{-5}$	$2.62 \times 10^{-3}$	$1.24 \times 10^1$

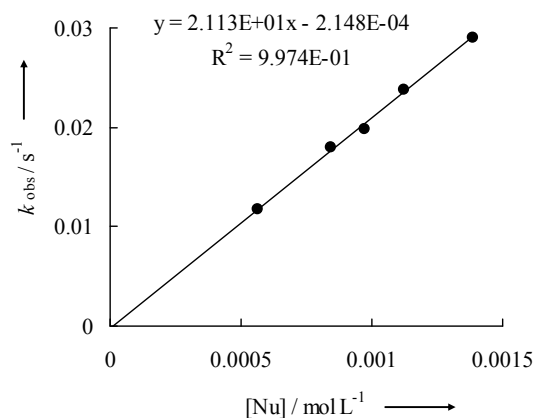
$$k_2 = 4.91 \times 10^3 \text{ L mol}^{-1} \text{ s}^{-1}$$



**Table 19:** Kinetics of the reaction of the 1,3,4-triphenyl triazol-5-ylidenes **3e** with **4g** at 20 °C in THF (diode array,  $\lambda = 430$  nm).

[ <b>4g</b> ] / mol L <sup>-1</sup>	[ <b>3e</b> ] / mol L <sup>-1</sup>	$k_{\text{obs}}$ / s <sup>-1</sup>
$9.08 \times 10^{-5}$	$5.66 \times 10^{-4}$	$1.17 \times 10^{-2}$
$9.04 \times 10^{-5}$	$8.46 \times 10^{-4}$	$1.79 \times 10^{-2}$
$8.93 \times 10^{-5}$	$9.74 \times 10^{-4}$	$1.99 \times 10^{-2}$
$9.00 \times 10^{-5}$	$1.12 \times 10^{-3}$	$2.38 \times 10^{-2}$
$8.91 \times 10^{-5}$	$1.39 \times 10^{-3}$	$2.91 \times 10^{-2}$

$$k_2 = 2.11 \times 10^1 \text{ L mol}^{-1} \text{ s}^{-1}$$

**Table 20:** Kinetics of the reaction of the 1,3,4-triphenyl triazol-5-ylidenes **3e** with **4h** at 20 °C in THF (diode array,  $\lambda = 499$  nm).

[ <b>4h</b> ] / mol L <sup>-1</sup>	[ <b>3e</b> ] / mol L <sup>-1</sup>	$k_{\text{obs}}$ / s <sup>-1</sup>
$3.98 \times 10^{-5}$	$4.50 \times 10^{-4}$	$1.61 \times 10^{-3}$
$3.98 \times 10^{-5}$	$6.76 \times 10^{-4}$	$2.61 \times 10^{-3}$
$3.98 \times 10^{-5}$	$9.02 \times 10^{-4}$	$3.63 \times 10^{-3}$
$3.97 \times 10^{-5}$	$1.12 \times 10^{-3}$	$4.50 \times 10^{-3}$
$3.93 \times 10^{-5}$	$1.33 \times 10^{-3}$	$5.26 \times 10^{-3}$

$$k_2 = 4.16 \text{ L mol}^{-1} \text{ s}^{-1}$$

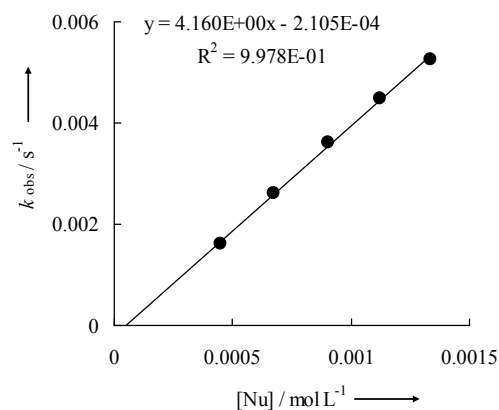
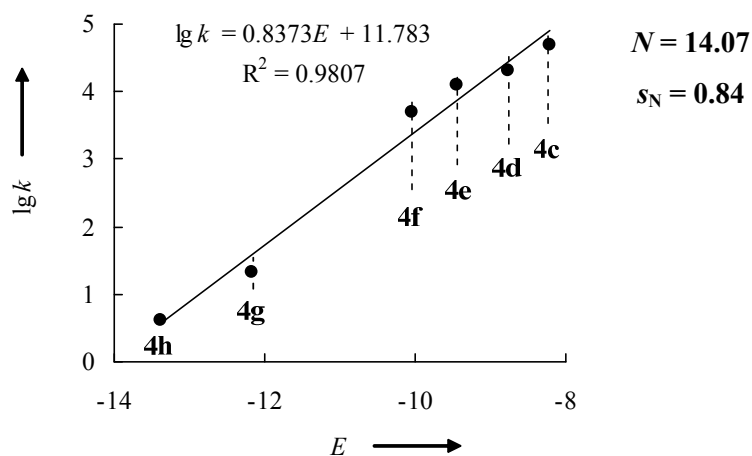


**Table 21:** Determination of the parameters  $N$  and  $s_N$  for 1,3,4-triphenyl triazol-5-ylidenes **3e** in THF.

Electrophiles	$E$	$k_2$ ( $M^{-1} s^{-1}$ )
<b>4c</b>	-8.22	$4.96 \times 10^4$
<b>4d</b>	-8.76	$2.08 \times 10^4$
<b>4e</b>	-9.45	$1.28 \times 10^4$
<b>4f</b>	-10.04	$4.91 \times 10^3$
<b>4g</b>	-12.18	$2.11 \times 10^1$
<b>4h</b>	-13.39	4.16

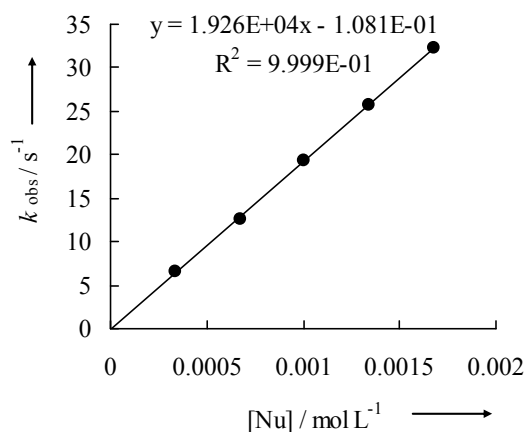


It appears as if the reactions of **3e** with the benzhydrylium ions **4b-f** on one side and the quinone methides **4g,h** on the other followed separate correlations. This separation may be due to the fact that the relative electrophilicities of benzhydrylium ions and quinone methides were derived from reactions carbanions with the two classes of electrophiles in DMSO. Whereas the good fit of data within the two groups of electrophiles shows that the electrophilicity parameters within the two groups of electrophiles can again be treated as solvent independent, the relative electrophilicities of the charged electrophiles on the right and the neutral electrophiles on the left may differ more in THF than in DMSO and acetonitrile. Kinetic studies of other nucleophiles in THF are needed to examine this hypothesis.

#### 4.3.4 Kinetics of the Reactions of $PPh_3$ (**6**) with the Reference Electrophiles **4**.

**Table 22:** Kinetics of the reaction of **6** with **4a** at 20 °C in THF (stopped-flow,  $\lambda = 605$  nm).

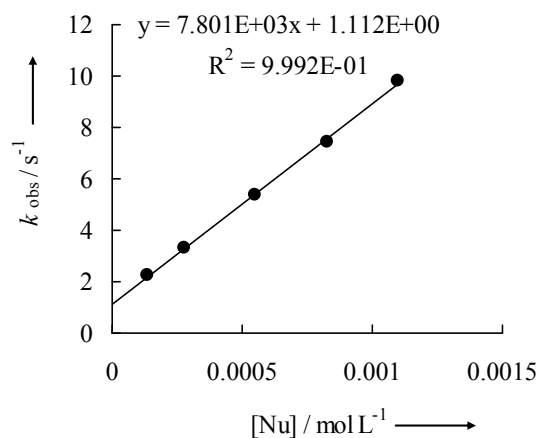
[ <b>4a</b> ] / mol L <sup>-1</sup>	[ $PPh_3$ ] / mol L <sup>-1</sup>	$k_{obs}$ / s <sup>-1</sup>
$2.00 \times 10^{-5}$	$3.36 \times 10^{-4}$	6.49
$2.00 \times 10^{-5}$	$6.71 \times 10^{-4}$	$1.26 \times 10^1$
$2.00 \times 10^{-5}$	$1.01 \times 10^{-3}$	$1.93 \times 10^1$
$2.00 \times 10^{-5}$	$1.34 \times 10^{-3}$	$2.57 \times 10^1$
$2.00 \times 10^{-5}$	$1.68 \times 10^{-3}$	$3.22 \times 10^1$



$$k_2 = 1.93 \times 10^4 \text{ L mol}^{-1} \text{ s}^{-1}$$

**Table 23:** Kinetics of the reaction of PPh<sub>3</sub> **6** with **4b** at 20 °C in THF (stopped-flow,  $\lambda = 615$  nm).

[ <b>4b</b> ] / mol L <sup>-1</sup>	[PPh <sub>3</sub> ] / mol L <sup>-1</sup>	$k_{\text{obs}} / \text{s}^{-1}$
$2.29 \times 10^{-5}$	$1.38 \times 10^{-4}$	2.22
$2.29 \times 10^{-5}$	$2.75 \times 10^{-4}$	3.30
$2.29 \times 10^{-5}$	$5.51 \times 10^{-4}$	5.35
$2.29 \times 10^{-5}$	$8.26 \times 10^{-4}$	7.44
$2.29 \times 10^{-5}$	$1.10 \times 10^{-3}$	9.81

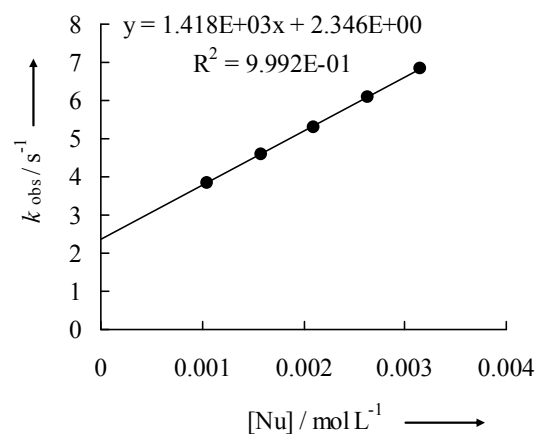


$$k_2 = 7.80 \times 10^3 \text{ L mol}^{-1} \text{ s}^{-1}$$

Reaction does not proceed quantitatively.

**Table 24:** Kinetics of the reaction of **6** with **4d** at 20 °C in THF (detected at  $\lambda = 615$  nm).

[ <b>4d</b> ] / mol L <sup>-1</sup>	[PPh <sub>3</sub> ] / mol L <sup>-1</sup>	$k_{\text{obs}} / \text{s}^{-1}$
$2.20 \times 10^{-5}$	$1.05 \times 10^{-3}$	3.85
$2.20 \times 10^{-5}$	$1.58 \times 10^{-3}$	4.60
$2.20 \times 10^{-5}$	$2.10 \times 10^{-3}$	5.28
$2.20 \times 10^{-5}$	$2.63 \times 10^{-3}$	6.06
$2.20 \times 10^{-5}$	$3.16 \times 10^{-3}$	6.85

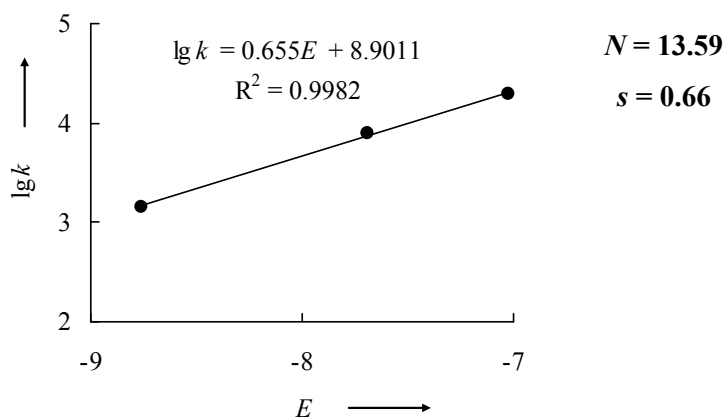


$$k_2 = 1.42 \times 10^3 \text{ L mol}^{-1} \text{ s}^{-1}$$

Reaction does not proceed quantitatively.

**Table 25:** Determination of the parameters  $N$  and  $s_N$  for PPh<sub>3</sub> (**6**) in THF.

Electrophiles	$E$	$k_2 (\text{M}^{-1} \text{ s}^{-1})$
<b>4a</b>	-7.02	$1.93 \times 10^4$
<b>4b</b>	-7.69	$7.80 \times 10^3$
<b>4d</b>	-8.76	$1.42 \times 10^3$

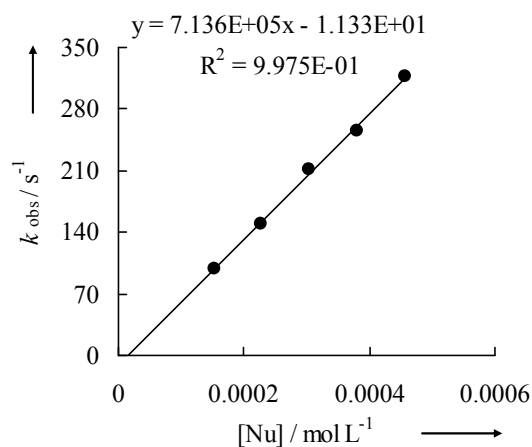


## 4.3.5 Kinetics of the Reactions of the DMAP (7) with the Reference Electrophiles 4.

**Table 26:** Kinetics of the reaction of 7 with 4a at 20 °C in THF (stopped-flow,  $\lambda = 606$  nm).

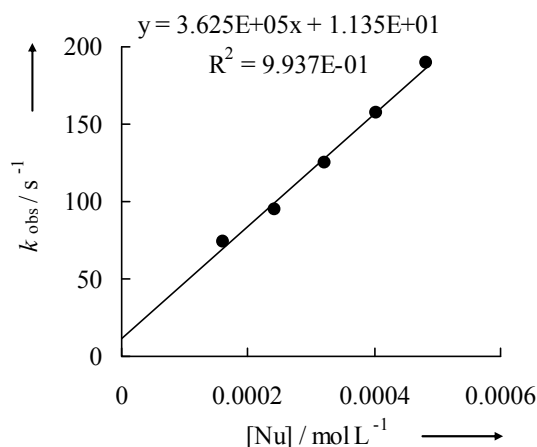
[4a] / mol L <sup>-1</sup>	[DMAP] / mol L <sup>-1</sup>	$k_{\text{obs}} / \text{s}^{-1}$
$2.00 \times 10^{-5}$	$1.52 \times 10^{-4}$	$9.86 \times 10^1$
$2.00 \times 10^{-5}$	$2.28 \times 10^{-4}$	$1.49 \times 10^2$
$2.00 \times 10^{-5}$	$3.04 \times 10^{-4}$	$2.11 \times 10^2$
$2.00 \times 10^{-5}$	$3.81 \times 10^{-4}$	$2.55 \times 10^2$
$2.00 \times 10^{-5}$	$4.57 \times 10^{-4}$	$3.17 \times 10^2$

$$k_2 = 7.14 \times 10^5 \text{ L mol}^{-1} \text{ s}^{-1}$$

**Table 27:** Kinetics of the reaction of 7 with 4b at 20 °C in THF (stopped-flow,  $\lambda = 615$  nm).

[4b] / mol L <sup>-1</sup>	[DMAP] / mol L <sup>-1</sup>	$k_{\text{obs}} / \text{s}^{-1}$
$2.29 \times 10^{-5}$	$1.61 \times 10^{-4}$	$7.44 \times 10^1$
$2.29 \times 10^{-5}$	$2.42 \times 10^{-4}$	$9.68 \times 10^1$
$2.29 \times 10^{-5}$	$3.23 \times 10^{-4}$	$1.28 \times 10^2$
$2.29 \times 10^{-5}$	$4.03 \times 10^{-4}$	$1.59 \times 10^2$
$2.29 \times 10^{-5}$	$4.84 \times 10^{-4}$	$1.89 \times 10^2$

$$k_2 = 3.63 \times 10^5 \text{ L mol}^{-1} \text{ s}^{-1}$$

**Table 28:** Kinetics of the reaction of 7 with 4c at 20 °C in THF (stopped-flow,  $\lambda = 615$  nm).

[4c] / mol L <sup>-1</sup>	[DMAP] / mol L <sup>-1</sup>	$k_{\text{obs}} / \text{s}^{-1}$
$2.17 \times 10^{-5}$	$1.61 \times 10^{-4}$	$2.59 \times 10^1$
$2.17 \times 10^{-5}$	$2.42 \times 10^{-4}$	$3.30 \times 10^1$
$2.17 \times 10^{-5}$	$3.23 \times 10^{-4}$	$4.29 \times 10^1$
$2.17 \times 10^{-5}$	$4.03 \times 10^{-4}$	$5.29 \times 10^1$
$2.17 \times 10^{-5}$	$4.84 \times 10^{-4}$	$6.36 \times 10^1$

$$k_2 = 1.18 \times 10^5 \text{ L mol}^{-1} \text{ s}^{-1}$$

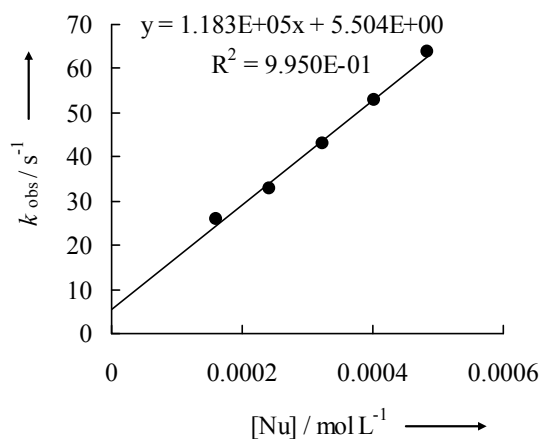
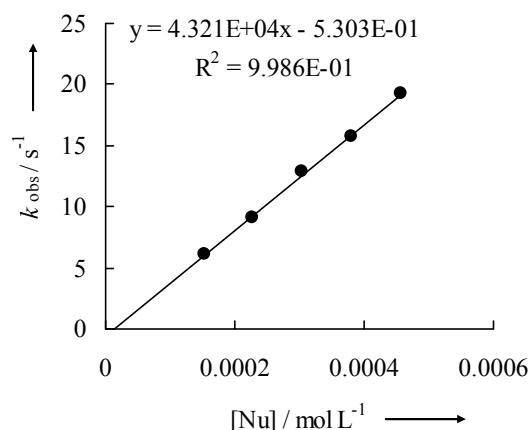


**Table 29:** Kinetics of the reaction of **7** with **4d** at 20 °C in THF (stopped-flow,  $\lambda = 616$  nm).

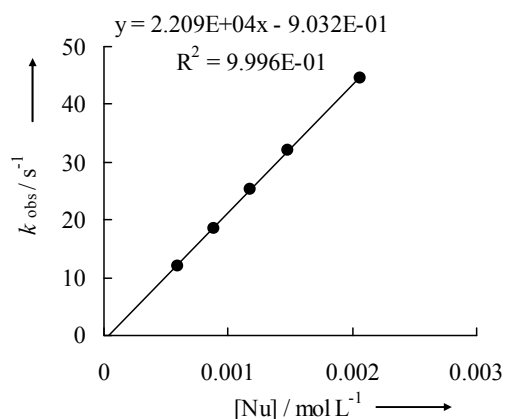
[ <b>4d</b> ] / mol L <sup>-1</sup>	[DMAP] / mol L <sup>-1</sup>	$k_{\text{obs}} / \text{s}^{-1}$
$2.20 \times 10^{-5}$	$1.52 \times 10^{-4}$	6.11
$2.20 \times 10^{-5}$	$2.28 \times 10^{-4}$	9.12
$2.20 \times 10^{-5}$	$3.04 \times 10^{-4}$	$1.29 \times 10^1$
$2.20 \times 10^{-5}$	$3.81 \times 10^{-4}$	$1.58 \times 10^1$
$2.20 \times 10^{-5}$	$4.57 \times 10^{-4}$	$1.92 \times 10^1$



$$k_2 = 4.32 \times 10^4 \text{ L mol}^{-1} \text{ s}^{-1}$$

**Table 30:** Kinetics of the reaction of **7** with **4e** at 20 °C in THF (stopped-flow,  $\lambda = 630$  nm).

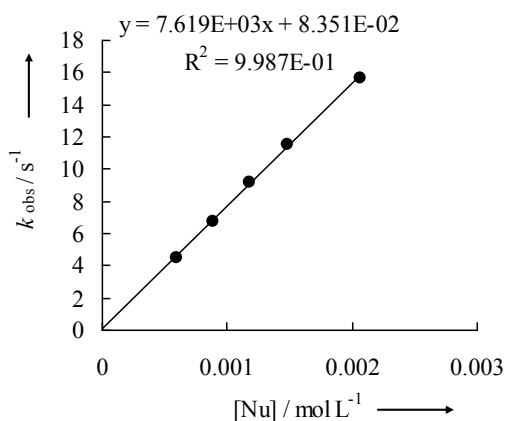
[ <b>4e</b> ] / mol L <sup>-1</sup>	[DMAP] / mol L <sup>-1</sup>	$k_{\text{obs}} / \text{s}^{-1}$
$2.16 \times 10^{-5}$	$5.91 \times 10^{-4}$	$1.20 \times 10^1$
$2.16 \times 10^{-5}$	$8.86 \times 10^{-4}$	$1.85 \times 10^1$
$2.16 \times 10^{-5}$	$1.18 \times 10^{-3}$	$2.54 \times 10^1$
$2.16 \times 10^{-5}$	$1.48 \times 10^{-3}$	$3.21 \times 10^1$
$2.16 \times 10^{-5}$	$2.07 \times 10^{-3}$	$4.45 \times 10^1$



$$k_2 = 2.21 \times 10^4 \text{ L mol}^{-1} \text{ s}^{-1}$$

**Table 31:** Kinetics of the reaction of **7** with **4f** at 20 °C in THF (stopped-flow,  $\lambda = 636$  nm).

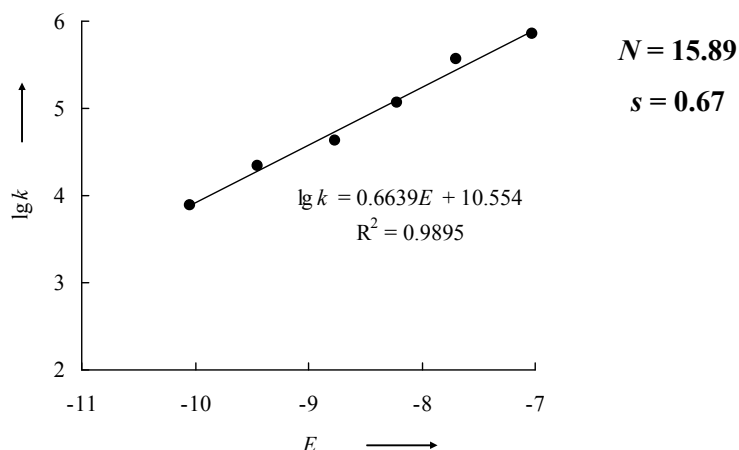
[ <b>4f</b> ] / mol L <sup>-1</sup>	[DMAP] / mol L <sup>-1</sup>	$k_{\text{obs}} / \text{s}^{-1}$
$1.82 \times 10^{-5}$	$5.91 \times 10^{-4}$	4.47
$1.82 \times 10^{-5}$	$8.86 \times 10^{-4}$	6.78
$1.82 \times 10^{-5}$	$1.18 \times 10^{-3}$	9.20
$1.82 \times 10^{-5}$	$1.48 \times 10^{-3}$	$1.15 \times 10^1$
$1.82 \times 10^{-5}$	$2.07 \times 10^{-3}$	$1.57 \times 10^1$



$$k_2 = 7.62 \times 10^3 \text{ L mol}^{-1} \text{ s}^{-1}$$

**Table 32:** Determination of the parameters  $N$  and  $s_N$  for DMAP (**7**) in THF.

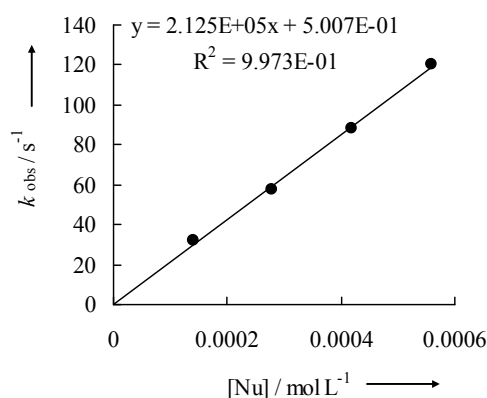
Electrophiles	$E$	$k_2$ ( $\text{M}^{-1} \text{s}^{-1}$ )
<b>4a</b>	-7.02	$7.14 \times 10^5$
<b>4b</b>	-7.69	$3.63 \times 10^5$
<b>4c</b>	-8.22	$1.18 \times 10^5$
<b>4d</b>	-8.76	$4.32 \times 10^4$
<b>4e</b>	-9.45	$2.21 \times 10^4$
<b>4f</b>	-10.04	$7.62 \times 10^3$



#### 4.3.6 Kinetics of the Reactions of the DBU (**8**) with the Reference Electrophiles **4**.

**Table 33:** Kinetics of the reaction of **8** with **4c** at 20 °C in THF (stopped-flow,  $\lambda = 616$  nm).

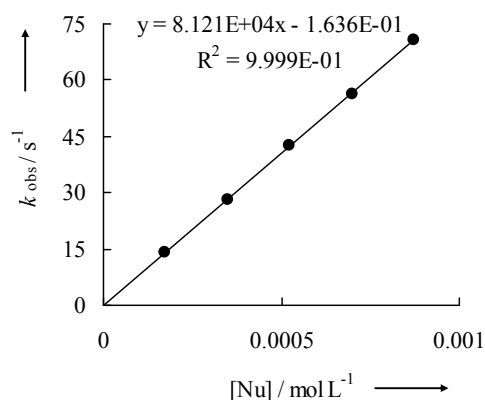
$[\mathbf{4c}] / \text{mol L}^{-1}$	$[\text{DBU}] / \text{mol L}^{-1}$	$k_{\text{obs}} / \text{s}^{-1}$
$1.91 \times 10^{-5}$	$1.40 \times 10^{-4}$	$3.20 \times 10^1$
$1.91 \times 10^{-5}$	$2.79 \times 10^{-4}$	$5.76 \times 10^1$
$1.91 \times 10^{-5}$	$4.19 \times 10^{-4}$	$8.83 \times 10^1$
$1.91 \times 10^{-5}$	$5.58 \times 10^{-4}$	$1.21 \times 10^2$



$$k_2 = 2.13 \times 10^5 \text{ L mol}^{-1} \text{ s}^{-1}$$

**Table 34:** Kinetics of the reaction of **8** with **4d** at 20 °C in THF (stopped-flow,  $\lambda = 616$  nm).

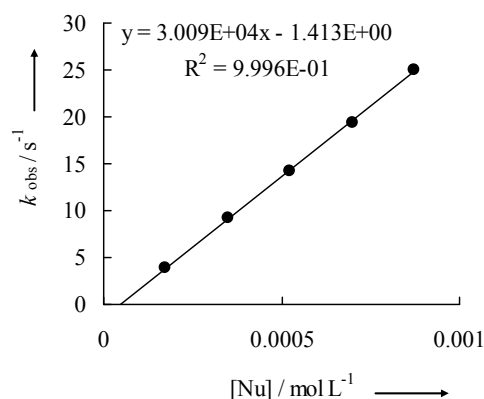
$[\mathbf{4d}] / \text{mol L}^{-1}$	$[\text{DBU}] / \text{mol L}^{-1}$	$k_{\text{obs}} / \text{s}^{-1}$
$2.00 \times 10^{-5}$	$1.74 \times 10^{-4}$	$1.40 \times 10^1$
$2.00 \times 10^{-5}$	$3.49 \times 10^{-4}$	$2.81 \times 10^1$
$2.00 \times 10^{-5}$	$5.23 \times 10^{-4}$	$4.25 \times 10^1$
$2.00 \times 10^{-5}$	$6.98 \times 10^{-4}$	$5.62 \times 10^1$
$2.00 \times 10^{-5}$	$8.72 \times 10^{-4}$	$7.08 \times 10^1$



$$k_2 = 8.12 \times 10^4 \text{ L mol}^{-1} \text{ s}^{-1}$$

**Table 35:** Kinetics of the reaction of **8** with **4e** at 20 °C in THF (stopped-flow,  $\lambda = 630$  nm).

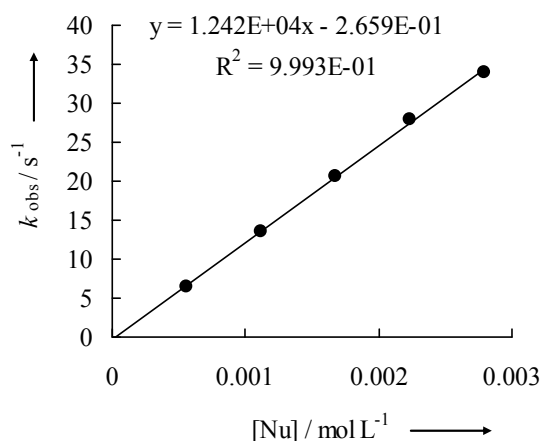
[ <b>4e</b> ] / mol L <sup>-1</sup>	[DBU] / mol L <sup>-1</sup>	$k_{\text{obs}} / \text{s}^{-1}$
$2.16 \times 10^{-5}$	$1.74 \times 10^{-4}$	3.86
$2.16 \times 10^{-5}$	$3.49 \times 10^{-4}$	9.22
$2.16 \times 10^{-5}$	$5.23 \times 10^{-4}$	$1.42 \times 10^1$
$2.16 \times 10^{-5}$	$6.98 \times 10^{-4}$	$1.94 \times 10^1$
$2.16 \times 10^{-5}$	$8.72 \times 10^{-4}$	$2.50 \times 10^1$



$$k_2 = 3.01 \times 10^4 \text{ L mol}^{-1} \text{ s}^{-1}$$

**Table 36:** Kinetics of the reaction of **8** with **4f** at 20 °C in THF (stopped-flow,  $\lambda = 630$  nm).

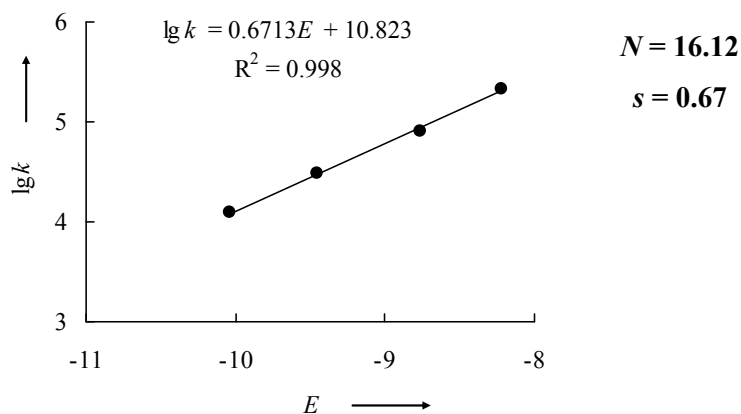
[ <b>4f</b> ] / mol L <sup>-1</sup>	[DBU] / mol L <sup>-1</sup>	$k_{\text{obs}} / \text{s}^{-1}$
$2.05 \times 10^{-5}$	$5.58 \times 10^{-4}$	6.54
$2.05 \times 10^{-5}$	$1.12 \times 10^{-3}$	$1.36 \times 10^1$
$2.05 \times 10^{-5}$	$1.67 \times 10^{-3}$	$2.06 \times 10^1$
$2.05 \times 10^{-5}$	$2.23 \times 10^{-3}$	$2.79 \times 10^1$
$2.05 \times 10^{-5}$	$2.79 \times 10^{-3}$	$3.41 \times 10^1$

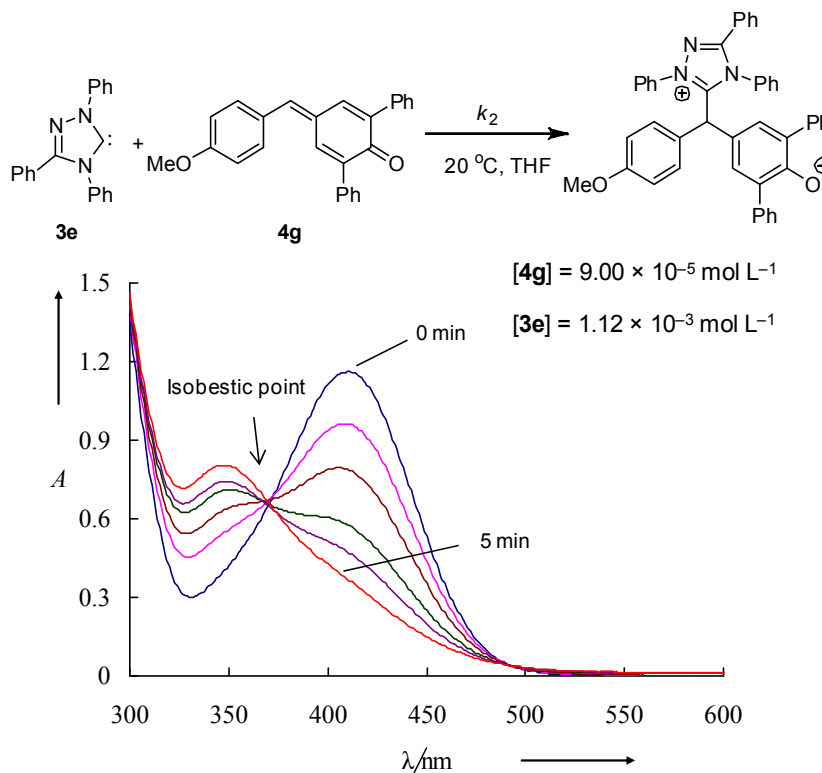
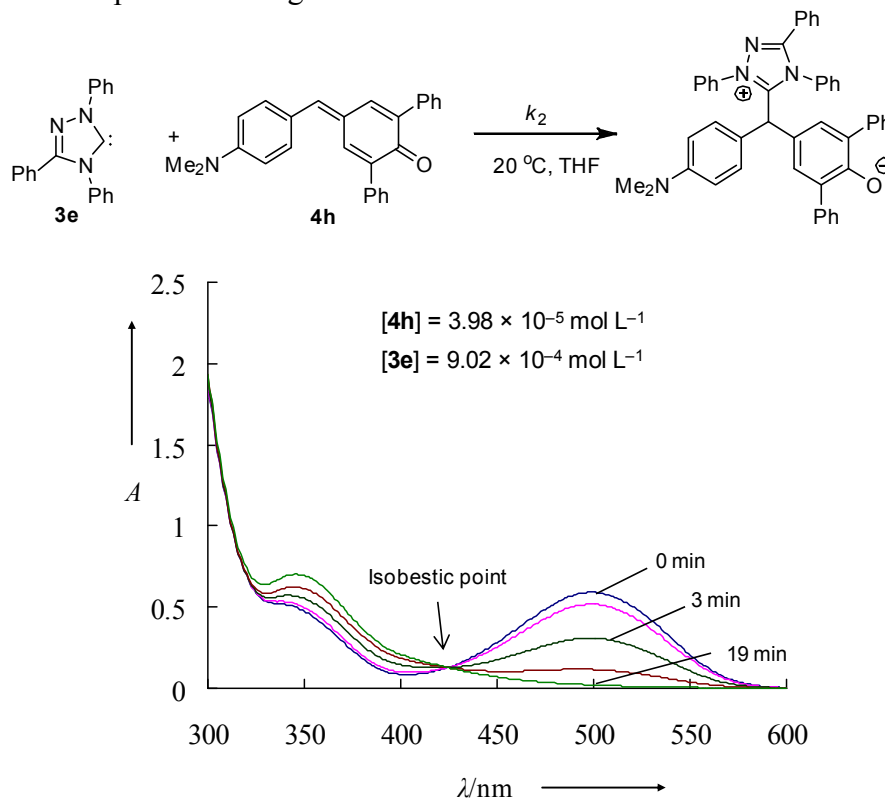


$$k_2 = 1.24 \times 10^4 \text{ L mol}^{-1} \text{ s}^{-1}$$

**Table 37:** Determination of the parameters  $N$  and  $s_N$  for DBU (**8**) in THF.

Electrophiles	$E$	$k_2 (\text{M}^{-1} \text{ s}^{-1})$
<b>4c</b>	-8.22	$2.13 \times 10^5$
<b>4d</b>	-8.76	$8.12 \times 10^4$
<b>4e</b>	-9.45	$3.01 \times 10^4$
<b>4f</b>	-10.04	$1.24 \times 10^4$



4.4 Tracing the reactions of **3e** with **4g** and **4h** by UV-Vis spectroscopy.4.4.1 UV-spectroscopic monitoring of the reaction of **3e** with **4g**.4.4.2 UV-spectroscopic monitoring of the reaction of **3e** with **4h**.

## 5 References

- [1] A. J. Arduengo III, R. L. Harlow, M. Kline, *J. Am. Chem. Soc.* **1991**, *113*, 361–363.
- [2] a) C. Heinemann, T. Müller, Y. Apeloig, H. Schwarz, *J. Am. Chem. Soc.* **1996**, *118*, 2023–2038; b) C. Boehme, G. Frenking, *J. Am. Chem. Soc.* **1996**, *118*, 2039–2046; c) W. A. Herrmann, C. Köcher, *Angew. Chem. Int. Ed. Engl.* **1997**, *36*, 2162–2187; d) D. Bourissou, O. Guerret, F. P. Gabbaï, G. Bertrand, *Chem. Rev.* **2000**, *100*, 39–91; e) R. Tonner, G. Frenking, *Chem. Eur. J.* **2008**, *14*, 3260–3272; f) R. Tonner, G. Frenking, *Chem. Eur. J.* **2008**, *14*, 3273–3289; g) A. K. Guha, S. Sarmah, A. K. Phukan, *Dalton Trans.* **2010**, *39*, 7374–7383; h) S. Gronert, J. R. Keeffe, R. A. More O’Ferrall, *J. Am. Chem. Soc.* **2011**, *133*, 3381–3389.
- [3] a) *N-Heterocyclic Carbenes in Synthesis* (Ed. S. P. Nolan), Wiley-VCH, Weinheim, **2006**; b) W. A. Herrmann, *Angew. Chem. Int. Ed.* **2002**, *41*, 1290–1309; c) V. César, S. Bellemin-Laponnaz, L. H. Gade, *Chem. Soc. Rev.* **2004**, *33*, 619–636; d) F. Kauer Zinn, M. S. Viciu, S. P. Nolan, *Annu. Rep. Prog. Chem., Sect. B: Org. Chem.* **2004**, *100*, 231–249; e) V. Nair, S. Bindu, V. Sreekumar, *Angew. Chem. Int. Ed.* **2004**, *43*, 5130–5135; f) S. Díez-González, S. P. Nolan, *Annu. Rep. Prog. Chem., Sect. B: Org. Chem.* **2005**, *101*, 171–191; g) F. Glorius (Ed.), *Top. Heterocycl. Chem.* **2007**, *21*, 1–231; h) S. Würtz, F. Glorius, *Acc. Chem. Res.* **2008**, *41*, 1523–1533; i) F. E. Hahn, M. C. Jahnke, *Angew. Chem. Int. Ed.* **2008**, *47*, 3122–3172; j) S. Díez-González, N. Marion, S. P. Nolan, *Chem. Rev.* **2009**, *109*, 3612–3676.
- [4] a) D. Enders, T. Balensiefer, *Acc. Chem. Res.* **2004**, *37*, 534–541; b) D. Enders, O. Niemeier, A. Henseler, *Chem. Rev.* **2007**, *107*, 5606–5655; c) N. Marion, S. Díez-González, S. P. Nolan, *Angew. Chem. Int. Ed.* **2007**, *46*, 2988–3000; d) V. Nair, S. Vellalath, B. P. Babu, *Chem. Soc. Rev.* **2008**, *37*, 2691–2698; e) J. L. Moore, T. Rovis in *Top. Curr. Chem.* **2009**, *291* (Ed.: B. List), Springer, Berlin, 77–144; f) P.-C. Chiang, J. W. Bode in *N-Heterocyclic Carbenes: From Laboratory Curiosities to Efficient Synthetic Tools* (Ed.: S. S. Díez-González), Royal Society of Chemistry: Cambridge, **2010**, pp. 399–435; g) K. Zeitler, *Angew. Chem. Int. Ed.* **2005**, *44*, 7506–7510; h) M. Padmanaban, A. T. Biju, F. Glorius, *Org. Lett.* **2011**, *13*, 98–101.
- [5] For physicochemical data of NHCs see: a) T. Dröge, F. Glorius, *Angew. Chem. Int. Ed.* **2010**, *49*, 6940–6952; For kinetic data on carbenes see: b) J. H. Teles, J.-P. Melder, K. Ebel, R. Schneider, E. Gehrler, W. Harder, S. Bode, D. Enders, K. Breuer, G. Raabe, *Helv. Chim. Acta.* **1996**, *79*, 61–83; c) M. J. White, F. J. Leeper, *J. Org.*

- Chem.* **2001**, *66*, 5124–5131. For NMR characterizations of intermediates in NHC catalyzed reactions see: d) A. Berkessel, S. Elfert, K. Etzenbach-Effers, J. H. Teles, *Angew. Chem. Int. Ed.* **2010**, *49*, 7120–7124; e) J. Mahatthananchai, P. Zheng, J. W. Bode, *Angew. Chem. Int. Ed.* **2011**, *50*, 1673–1677.
- [6] a) J. E. Leffler, E. Grunwald, *Rates and Equilibria of Organic Reactions*, John Wiley and Sons, New York, **1963**; b) A. Williams, *Free Energy Relationships in Organic and Bio-Organic Chemistry*, The Royal Society of Chemistry, Cambridge, **2003**; c) F. G. Bordwell, T. A. Cripe, D. L. Hughes, in *Nucleophilicity* (Eds.: J. M. Harris, S. P. McManus), American Chemical Society, Chicago, **1987**, pp. 137–153; d) M. Baidya, S. Kobayashi, F. Brotzel, U. Schmidhammer, E. Riedle, H. Mayr, *Angew. Chem. Int. Ed.* **2007**, *46*, 6176–6179.
- [7] For  $pK_{\text{aH}}$  values of several carbenes see: a) R. W. Alder, P. R. Allen, S. J. Williams, *J. Chem. Soc., Chem. Commun.* **1995**, 1267–1268; b) T. L. Amyes, S. T. Diver, J. P. Richard, F. M. Rivas, K. Toth, *J. Am. Chem. Soc.* **2004**, *126*, 4366–4374; c) Y. Chu, H. Deng, J.-P. Cheng, *J. Org. Chem.* **2007**, *72*, 7790–7793; d) E. M. Higgins, J. A. Sherwood, A. G. Lindsay, J. Armstrong, R. S. Massey, R. W. Alder, A. C. O'Donoghue, *Chem. Commun.* **2011**, *47*, 1559–1561.
- [8] a) H. Mayr, M. Patz, *Angew. Chem. Int. Ed. Engl.* **1994**, *33*, 938–957; b) H. Mayr, T. Bug, M. F. Gotta, N. Hering, B. Irrgang, B. Janker, B. Kempf, R. Loos, A. R. Ofial, G. Remennikov, H. Schimmel, *J. Am. Chem. Soc.* **2001**, *123*, 9500–9512; c) R. Lucius, R. Loos, H. Mayr, *Angew. Chem. Int. Ed.* **2002**, *41*, 91–95; d) H. Mayr, B. Kempf, A. R. Ofial, *Acc. Chem. Res.* **2003**, *36*, 66–77; e) H. Mayr, A. R. Ofial, *Pure Appl. Chem.* **2005**, *77*, 1807–1821; f) H. Mayr, *Angew. Chem. Int. Ed.* **2011**, *50*, 3612–3618.
- [9] For pyridines see: a) F. Brotzel, B. Kempf, T. Singer, H. Zipse, H. Mayr, *Chem. Eur. J.* **2007**, *13*, 336–345; For azoles see: b) M. Baidya, F. Brotzel, H. Mayr, *Org. Biomol. Chem.* **2010**, *8*, 1929–1935; For phosphanes see: c) B. Kempf, H. Mayr, *Chem. Eur. J.* **2005**, *11*, 917–927; For DBU and DBN see: d) M. Baidya, H. Mayr, *Chem. Commun.* **2008**, 1792–1794; For isothioureas see: e) B. Maji, C. Joannesse, T. A. Nigst, A. D. Smith, H. Mayr, *J. Org. Chem.* **2011**, *76*, 5104–5112.
- [10] CCDC 826211 (**5c**) contains the supplementary crystallographic data for this paper. These data can be obtained free of charge from The Cambridge Crystallographic Data Centre via [www.ccdc.cam.ac.uk/data\\_request/cif](http://www.ccdc.cam.ac.uk/data_request/cif).

- [11] Since NHCs are known to react with CH<sub>2</sub>Cl<sub>2</sub>, CH<sub>3</sub>CN, or DMSO, the organic solvents commonly used for our kinetic measurements, we have performed the kinetic studies of carbenes in THF solution: A. J. Arduengo III, J. C. Calabrese, F. Davidson, H. V. R. Dias, J. R. Goerlich, R. Krafczyk, W. J. Marshall, M. Tamm, R. Schmutzler, *Helv. Chim. Acta* **1999**, *82*, 2348–2364.
- [12] For a comprehensive listing of nucleophilicity parameters *N* and electrophilicity parameters *E*, see <http://www.cup.uni-muenchen.de/oc/mayr/DBintro.html>.
- [13] Gaussian09, Revision A.02, M. J. Frisch et al., Gaussian, Inc., Wallingford CT, **2009**.
- [14] a) Y. Wei, G. N. Sastry, H. Zipse, *J. Am. Chem. Soc.* **2008**, *130*, 3473–3477; b) Y. Wei, T. Singer, H. Mayr, G. N. Sastry, H. Zipse, *J. Comput. Chem.* **2008**, *29*, 291–297; c) C. Lindner, B. Maryasin, F. Richter, H. Zipse, *J. Phys. Org. Chem.* **2010**, *23*, 1036–1042.
- [15] a) P. H. Mueller, N. G. Rondan, K. N. Houk, J. F. Harrison, D. Hooper, B. H. Willen, J. F. Liebman, *J. Am. Chem. Soc.* **1981**, *103*, 5049–5052; b) H. F. Schaefer III, *Science* **1986**, *231*, 1100–1107; c) A. Nemirowski, P. R. Schreiner, *J. Org. Chem.* **2007**, *72*, 9533–9540; d) K. Hirai, T. Itoh, H. Tomioka, *Chem. Rev.* **2009**, *109*, 3275–3332; e) J. Vignolle, X. Cattoën, D. Bourissou, *Chem. Rev.* **2009**, *109*, 3333–3384.
- [16] A. A. Tukov, A. T. Normand, M. S. Nechaev, *Dalton Trans.* **2009**, 7015–7028.
- [17] For crystal structures of several carbenes see: a) A. J. Arduengo III, H. V. R. Dias, R. L. Harlow, M. Kline, *J. Am. Chem. Soc.* **1992**, *114*, 5530–5534; b) A. J. Arduengo III, H. Bock, H. Chen, M. Denk, D. A. Dixon, J. C. Green, W. A. Herrmann, N. L. Jones, M. Wagner, R. West, *J. Am. Chem. Soc.* **1994**, *116*, 6641–6649; c) A. J. Arduengo III, J. R. Goerlich, W. J. Marshall, *J. Am. Chem. Soc.* **1995**, *117*, 11027–11028; d) M. K. Denk, J. M. Rodezno, S. Gupta, A. J. Lough, *J. Organomet. Chem.* **2001**, *617–618*, 242–253.
- [18] For further consequences of different intrinsic barriers, see: H. Mayr, M. Breugst, A. R. Ofial, *Angew. Chem. Int. Ed.* **2011**, *50*, 6470–6505.
- [19] D. Seebach, *Angew. Chem. Int. Ed. Engl.* **1979**, *18*, 239–258.
- [20] R. Breslow, *J. Am. Chem. Soc.* **1958**, *80*, 3719–3726.
- [21] a) S. S. Sohn, E. L. Rosen, J. W. Bode, *J. Am. Chem. Soc.* **2004**, *126*, 14370–14371; b) C. Burstein, F. Glorius, *Angew. Chem. Int. Ed.* **2004**, *43*, 6205–6208.
- [22] a) L. Hintermann, *Beilstein Journal of Organic Chemistry* **2007**, *3*, No. 22. doi:10.1186/1860-5397-3-22; b) L. Jafarpour, E. D. Stevens, S. P. Nolan, *J. Organomet. Chem.* **2000**, *606*, 49–54.

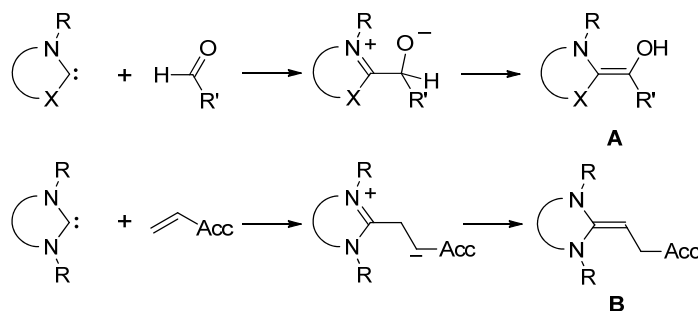
## Chapter 6

# Nucleophilic Reactivity of Deoxy-Breslow-Intermediates: How Does Aromaticity Affect the Catalytic Activity of N-Heterocyclic Carbenes?

B. Maji, M. Horn, H. Mayr, *Angew. Chem. Int. Ed.* **2012**, *51*, 6231–6235.

## 1 Introduction

N-Heterocyclic carbenes<sup>[1]</sup> (NHCs, **1**) are widely used as umpolung reagents<sup>[2]</sup> in organocatalysis.<sup>[3]</sup> In benzoin condensations<sup>[4]</sup> and Stetter reactions<sup>[5]</sup> the initially formed Breslow intermediate **A**,<sup>[6]</sup> a nucleophilic acyl anion equivalent, reacts with an aldehyde or Michael acceptor to give 1,2- or 1,4-functionalized products. Recently, Fu, Matsuoka, and Glorius independently reported the umpolung of the  $\beta$ -position of Michael acceptors, where 1,1-diaminoalkenes **B** act as key intermediates.<sup>[7]</sup> Since the structure of **B** is closely related to **A**, it has been named “deoxy-Breslow intermediate” (Scheme 1).<sup>[7c,8]</sup>



**Scheme 1.** Reactions of NHCs with aldehydes and Michael acceptors to give intermediates **A** and **B**, respectively.

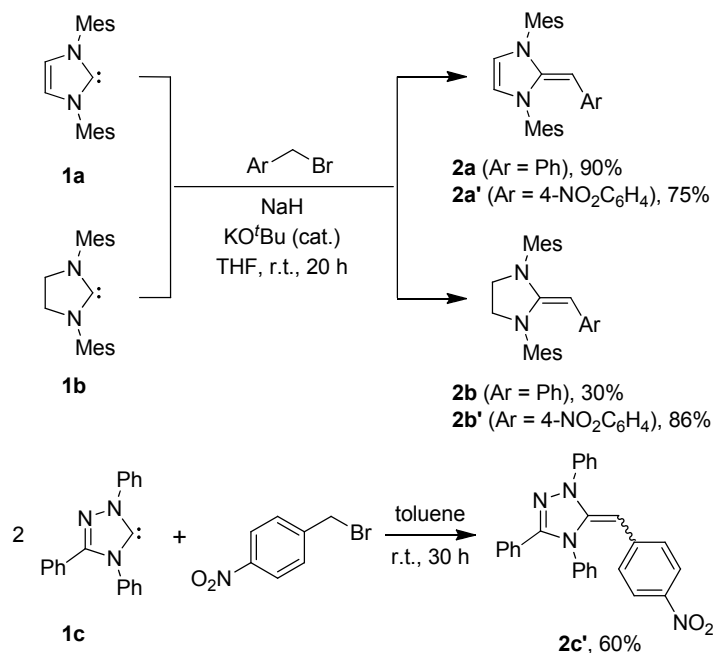
Most suitable for these reactions were 1,2,4-triazol-5-ylidines, 1,3-thiazol-2-ylidines, or imidazol-2-ylidines, while imidazolidine-2-ylidines are not effective as umpolung reagents.<sup>[3,8]</sup> This observation is surprising, because in recent work we have shown that the

imidazol-2-ylidene **1a** and imidazolidine-2-ylidene **1b** have almost the same nucleophilicities and Lewis basicities, while Ender's carbene **1c** reacted  $10^3$  times more slowly and  $55 \text{ kJ mol}^{-1}$  less exothermic with C-electrophiles.<sup>[9]</sup>

As the different catalytic activities of unsaturated and saturated carbenes thus cannot be assigned to the different properties of the carbenes themselves, the question arose whether it is due to the different reactivities of the corresponding Breslow intermediates. While characterizations of Breslow intermediates by spectroscopic and theoretical methods have been reported,<sup>[10]</sup> we are not aware of any kinetic investigations comparing the reactivities of 1,1-diaminoethenes, derived from different classes of NHCs. Therefore, we have now synthesized compounds **2**<sup>[11]</sup> and determined the kinetics of their reactions with electrophiles.

## 2 Results and discussions

The reactions of **1a** and **1b** with benzyl or 4-nitrobenzyl bromide, and subsequent deprotonation of the resulting amidinium ions with NaH in the presence of a catalytic amount of KO<sup>t</sup>Bu in THF yielded 30–90% of **2a–2b'** (Scheme 2). While **2a,a'** could also be generated with stoichiometric amounts of KO<sup>t</sup>Bu in the absence of NaH,<sup>[8]</sup> this procedure did not allow the synthesis of **2b,b'**. Attempts to synthesize **2c'** analogously, resulted in complex reaction mixtures. However, **2c'** was synthesized in 60% yield from 4-nitrobenzyl bromide and 2 equivalents of **1c** in toluene, the second molecule of **1c** acting as the base.



**Scheme 2.** Synthesis of deoxy-Breslow intermediates **2**.

In order to quantify the nucleophilic reactivities of **2** we have studied the kinetics of their reactions with the benzhydrylium ions **3a–f** and the quinone methides **3g,h** (Table 1) which have been used as reference electrophiles for characterizing the reactivities of a manifold of structurally variable nucleophiles.<sup>[12]</sup>

$$\log k = s_N(N + E) \quad (1)$$

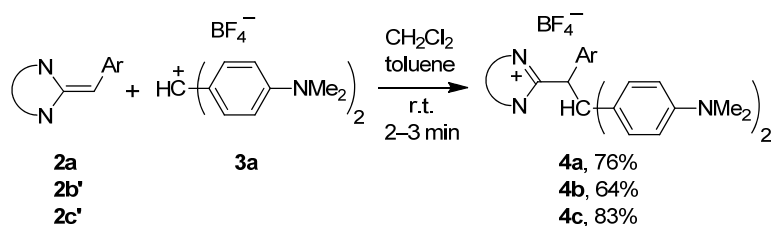
Equation (1) has been demonstrated to reliably predict second-order rate constants  $k$  for a wide range of electrophile-nucleophile combinations. In this approach, electrophiles are assigned a solvent-independent electrophilicity parameter  $E$ , whereas nucleophiles are characterized by a pair of solvent-dependent parameters ( $N$ ,  $s_N$ ).<sup>[13]</sup>

**Table 1.** Benzhydrylium Ions **3a–f** and Quinone Methides **3g,h** Employed as Reference Electrophiles in this Work.

Electrophile		$E^{[a]}$
	R = NMe <sub>2</sub>	<b>3a</b> -7.02
	R = N(CH <sub>2</sub> ) <sub>4</sub>	<b>3b</b> -7.69
	n = 2	<b>3c</b> -8.22
	n = 1	<b>3d</b> -8.76
	n = 2	<b>3e</b> -9.45
	n = 1	<b>3f</b> -10.04
	R = OMe	<b>3g</b> -12.18
	R = NMe <sub>2</sub>	<b>3h</b> -13.39

[a] Electrophilicity parameters  $E$  for **3a–f** from ref. [12a], for **3g–h** from ref [12b].

Representative product studies (Scheme 3) revealed that the benzhydrylium ion **3a** attacks the exocyclic olefinic carbon atoms of the deoxy-Breslow-intermediates **2** to give the azolium salts **4a–c** which were isolated and fully characterized (**4c** by X-ray crystallography, Figure 1).<sup>[14]</sup>



**Scheme 3.** Reactions of **2a**, **2b'**, and **2c'** with the reference electrophile **3a**.

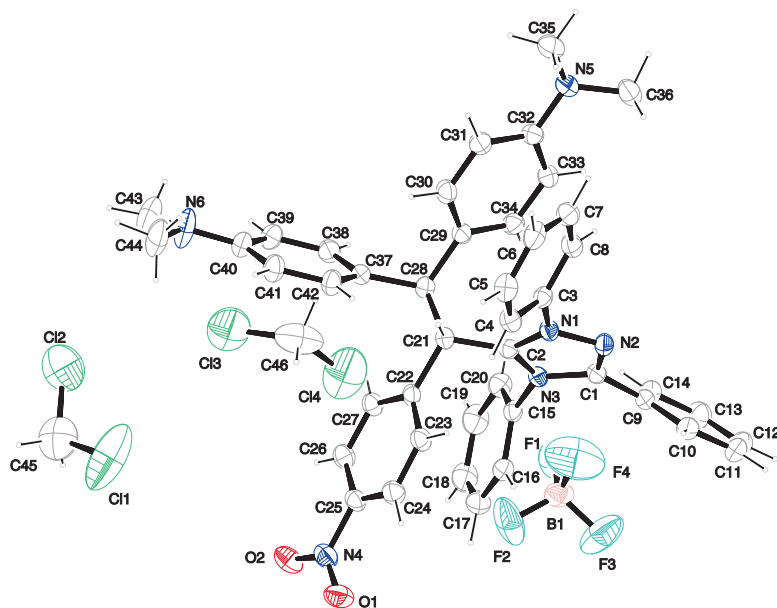


**Figure 1:** Crystal structure of **4c**.2CH<sub>2</sub>Cl<sub>2</sub> (50 % probability ellipsoids).

The kinetics of the reactions of **2** with **3** were followed photometrically in THF or DMSO at 20 °C by monitoring the disappearance of the absorbances of **3** using conventional or stopped-flow spectrophotometers. Pseudo-first-order conditions were established by using a high excess of **2**. The first-order rate constants  $k_{\text{obs}}$  (s<sup>-1</sup>) were obtained by least-squares fitting of the decay of the absorbances of **3** to the functions  $A_t = A_0 e^{-k_{\text{obs}} t} + C$ . The slopes of the linear plots of  $k_{\text{obs}}$  against the concentrations of **2** (Figure 2) gave the second-order rate constants  $k$  listed in Table 2.

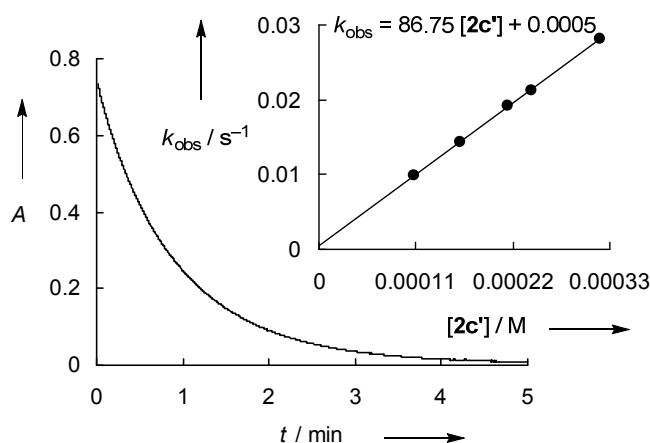


**Figure 2.** Exponential decay of the absorbance at 636 nm during the reaction of **3f**-BF<sub>4</sub><sup>-</sup> (1.41 × 10<sup>-5</sup> M) with **2c'** (2.14 × 10<sup>-4</sup> M) in THF at 20 °C ( $k_{\text{obs}} = 1.92 \times 10^{-2}$  s<sup>-1</sup>). Inset: Determination of the second-order rate constant  $k = 86.8 \text{ M}^{-1} \text{ s}^{-1}$  from the dependence of  $k_{\text{obs}}$  on the concentration of **2c'**.

**Table 2.** Second-Order Rate Constants  $k$  ( $\text{M}^{-1} \text{s}^{-1}$ ) for the Reactions of the Deoxy-Breslow Intermediates **2** with the Reference Electrophiles **3** at 20 °C.

Nucleophile	Solvent	$N, s_N$ <sup>[a]</sup>	Electrophile	$k / \text{M}^{-1} \text{s}^{-1}$
<b>2a</b>	THF	17.12, 0.80	<b>3e</b>	$1.33 \times 10^6$
			<b>3f</b>	$4.50 \times 10^5$
			<b>3g</b>	$6.10 \times 10^3$
	DMSO	17.41, 0.74	<b>3e</b>	$8.80 \times 10^5$
			<b>3f</b>	$2.30 \times 10^5$
			<b>3h</b>	$1.05 \times 10^3$
<b>2a'</b>	THF	14.45, 0.71	<b>3c</b>	$2.96 \times 10^4$
			<b>3d</b>	$7.89 \times 10^3$
			<b>3e</b>	$5.16 \times 10^3$
			<b>3f</b>	$1.16 \times 10^3$
			<b>3g</b>	$6.10 \times 10^3$
<b>2b</b>	THF	13.91, 0.64	<b>3b</b>	$9.60 \times 10^3$
			<b>3c</b>	$5.95 \times 10^3$
			<b>3d</b>	$1.53 \times 10^3$
			<b>3e</b>	$8.88 \times 10^2$
			<b>3f</b>	$3.01 \times 10^2$
			<b>3g</b>	$6.10 \times 10^3$
<b>2b'</b>	THF	11.42, 0.70	<b>3a</b>	$1.10 \times 10^3$
			<b>3b</b>	$4.35 \times 10^2$
			<b>3c</b>	$1.74 \times 10^2$
			<b>3d</b>	$6.83 \times 10^1$
			<b>3e</b>	$8.88 \times 10^2$
<b>2c'</b>	THF	12.75, 0.71	<b>3b</b>	$4.00 \times 10^3$
			<b>3d</b>	$5.91 \times 10^2$
			<b>3f</b>	$8.68 \times 10^1$

[a]  $N, s_N$  as defined by Equation (1).

When  $\log k$  were plotted against the corresponding electrophilicity parameters  $E$  of **3**, linear correlations were obtained (Figure 3). Eq. (1) can therefore, be used to evaluate the  $N$  and  $s_N$  parameters of the deoxy Breslow intermediates **2** (third column of Table 2).<sup>[12]</sup> Table 2 and Figure 3 show that the reactions are only slightly slower in DMSO than in THF (factor 1.6). The order of the nucleophilic reactivities of compounds **2** differs dramatically from the reactivity order of the corresponding precursor carbenes **1** (Scheme 4): While the carbene **1a** was found to be 2.5 times less reactive than **1b**,<sup>[9]</sup> the benzylidenimidazole **2a** reacts  $10^3$  times faster than its saturated analogue **2b**. The attenuating effect of the nitro group reduces

the reactivity ratio  $k_{2a}/k_{2b}$  to  $10^2$ , and even the triazole-derived olefin **2c'** is one order of magnitude more reactive than the imidazolidine derivative **2b'**.

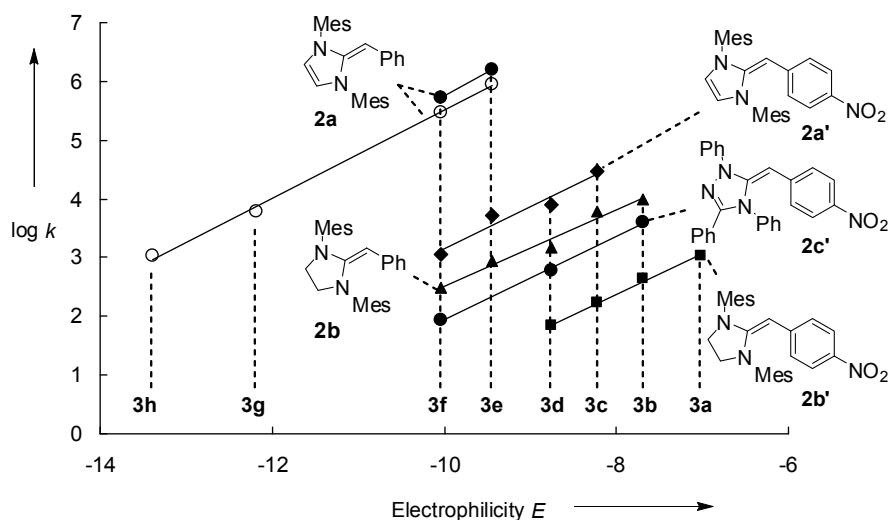
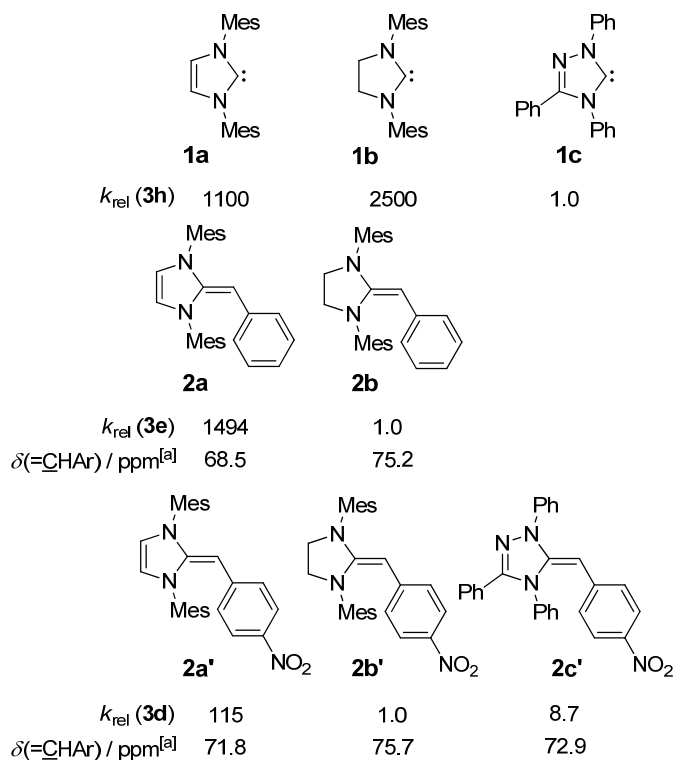


**Figure 3.** Plot of  $\log k$  for the reactions of **2** with the electrophiles **3** (THF, 20 °C) versus the corresponding electrophilicity parameters  $E$ . Open circles: Solvent is DMSO.



**Scheme 4.** Relative reactivities of the NHCs **1** towards benzhydrylium ions (ref. [9]) and comparison with the corresponding reactivities of deoxy-Breslow-intermediates **2** (THF, 20 °C). <sup>[a]</sup> In  $C_6D_6$ .

The reactivity orders  $2\mathbf{a} \gg 2\mathbf{b}$  and  $2\mathbf{a}' > 2\mathbf{c}' > 2\mathbf{b}'$  are in line with the relative charge densities at the nucleophilic carbon atoms which can be derived from the corresponding  $^{13}\text{C}$  NMR chemical shifts (Scheme 4) as well as from quantum chemical calculations (Scheme 7 in the Experimental Section).

How can one explain the high reactivity ratio  $k_{2\mathbf{a}}/k_{2\mathbf{b}} = 1494$  which contrasts the relative nucleophilicities of the precursor carbenes  $k_{1\mathbf{a}}/k_{1\mathbf{b}} = 0.44$ ? From the X-ray structures of  $2\mathbf{a}$  and  $2\mathbf{b}$  (Figure 4)<sup>[14]</sup> one can derive that the exocyclic double bond in  $2\mathbf{a}$  is only slightly elongated compared to  $2\mathbf{b}$  ( $\Delta = 0.7$  pm) indicating that the resonance structures with aromatic rings have only little significance for the ground state of  $2\mathbf{a}$  (Scheme 5).

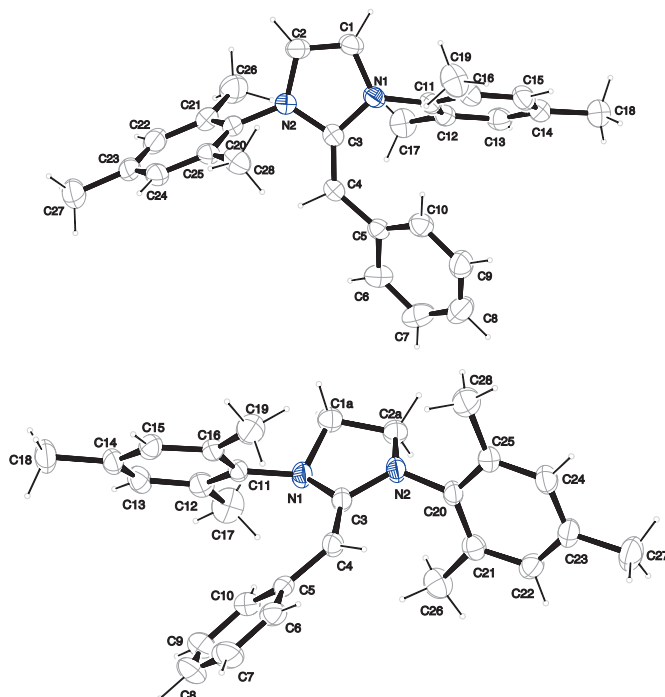
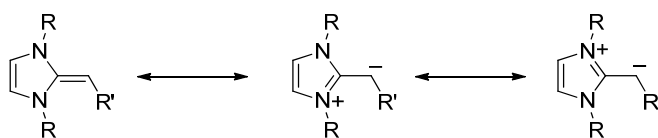


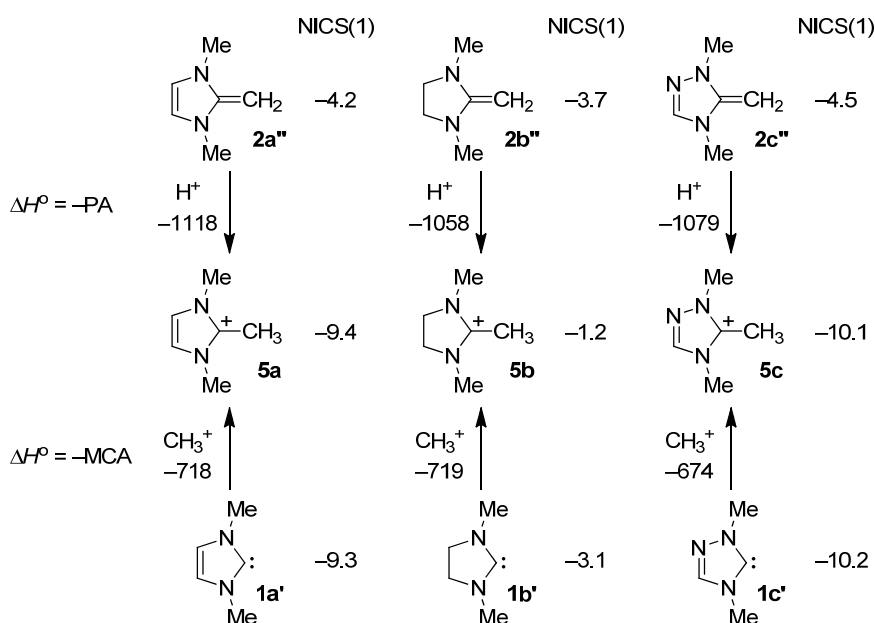
**Figure 4.** Crystal structures of  $2\mathbf{a}$  (top) and  $2\mathbf{b}$  (bottom). Only one position of the disordered C1 and C2 is shown for  $2\mathbf{b}$ . Selected bond lengths (pm) and angles ( $^\circ$ ):  $2\mathbf{a}$ : C3–C4 = 136.1, N1–C3–C4–C5 = 9.9, C3–C4–C5–C10 = 32.1;  $2\mathbf{b}$ : C3–C4 = 135.4, N1–C3–C4–C5 = 11.6, C3–C4–C5–C10 = 26.7.



**Scheme 5.** Resonance structures for 2-alkylidene imidazoles.

In order to compare the thermodynamics of these reactions, gas phase proton affinities of the 1,1-diaminoethylenes  $2\mathbf{a}''$ ,  $2\mathbf{b}''$ , and  $2\mathbf{c}''$  were calculated on the MP2/6-31+G(2d,p)//B98/6-31G(d) level of theory using the Gaussian 09 program package.<sup>[15]</sup>

Scheme 6 shows that the proton affinity of **2b''**, derived from the saturated Arduengo carbene **1b'** is 60 kJ mol<sup>-1</sup> lower than that of **2a''**. Compound **2b''** is even a weaker Brønsted base than the triazole-derived olefin **2c''** which includes an electronegative nitrogen atom ( $\Delta\text{PA} = 21 \text{ kJ mol}^{-1}$ ). The nucleophilicity order **2a'** > **2c'** > **2b'** (Scheme 4, bottom line) thus mirrors the proton affinity order **2a''** > **2c''** > **2b''** (Scheme 6, top). Analogously, the completely different nucleophilicity order of the NHCs **1a**  $\approx$  **1b**  $\gg$  **1c** (Scheme 4, first line) is also reflected by the order of methyl cation affinities **1a'**  $\approx$  **1b'**  $\gg$  **1c'** (Scheme 6, bottom).<sup>[9]</sup>



**Scheme 6.** Comparison of the proton affinities (PA) of the diaminoethylenes **2** with the methyl cation affinities (MCA, from ref. [9]) of the corresponding carbenes **1** (in kJ mol<sup>-1</sup>, MP2/6-31+G(2d,p)//B98/6-31G(d)), and the NICS(1) values of **1**, **2**, and **5** (B3LYP/6-311+G(d)).

As the carbenes **1** are attacked by electrophiles at the nonbonding lone pair in the plane of the heterocyclic ring, the  $\pi$ -system is not affected and the different reactivities of the NHCs **1** can be explained by inductive effects.<sup>[9]</sup> In contrast, electrophilic additions to **2** occur at the conjugated  $\pi$ -system, and resonance effects become important.

From the comparable NICS(1)<sup>[16]</sup> values of **2a''**, **2b''** and **2c''** one can derive that aromaticity is not important for the ground states of these compounds, as derived above from the X-ray structures of **2a** and **2b** (Figure 4, Scheme 5). Electrophilic additions to the nonaromatic **2a''** and **2c''** give rise to the formation of the aromatic azolium ions **5a** and **5c** (large NICS(1) values, Scheme 6) and thus account for the high proton affinities of **2a''** and **2c''**, respectively.<sup>[17]</sup>

In contrast, the NICS(1) values in Scheme 6 show that the aromatic character will not be changed when **5a** and **5c** are formed through methyl cation addition to the precursor carbenes **1a'** and **1c'**. For that reason the unsaturated carbenes **1a'** and **1c'** neither have greater Lewis basicity than the saturated carbene **1b'** (Scheme 6) nor do **1a** and **1c** have greater nucleophilicity than **1b** (Scheme 4). Calculations of NICS(0)<sub>πzz</sub> values<sup>[18a]</sup> led to similar conclusions.<sup>[18b]</sup>

### 3 Conclusion

We thus conclude that the different catalytic activities of saturated (e.g. **1b**) and unsaturated NHCs (e.g. **1a,c**) cannot be explained by the intrinsic properties of the carbenes, but that one of the subsequent steps must account for this difference. In this work we have shown that Breslow intermediates derived from unsaturated NHCs (e.g. **2a**) are significantly more nucleophilic than those derived from saturated NHCs (e.g. **2b**). The development of aromaticity by electrophilic attack at Breslow intermediates derived from unsaturated NHCs is, therefore, considered to be an important reason for the preferred use of such carbenes as umpolung catalysts. In coordination and transition metal chemistry, on the other hand, where the  $\sigma$ -donor ability of the carbenes plays the dominant role, saturated as well as unsaturated NHCs have been reported to be suitable ligands.<sup>[19]</sup>

## 4 Experimental Section

### 4.1 General

#### *Chemicals.*

1,3-Dimesitylimidazolium chloride **1a.HCl**,<sup>[20a]</sup> 1,3-dimesitylimidazolidium chloride **1b.HCl**,<sup>[20b]</sup> and **1c**<sup>[20c]</sup> were synthesized according to the literature procedures. Benzhydrylium tetrafluoroborates **3a-f**<sup>[12a]</sup> and quinone methides **3g,h**<sup>[12b]</sup> were prepared as described before.

For synthetic studies: Commercially available THF (Sigma-Aldrich, p.a.) and *n*-pentane were distilled over sodium prior to use. Toluene was freshly distilled over CaH<sub>2</sub>.

For kinetic studies: DMSO (Acros organics, 99.7%, Extra dry, Aero seal) and THF (Acros organics, 99.5%, Extra dry, Over Molecular Sieve, Stabilized, Aero seal) were purchased and used without further purification.

*Analytics.*

<sup>1</sup>H- and <sup>13</sup>C-NMR spectra were recorded on *Varian* NMR-systems (300, 400, and 600 MHz) in C<sub>6</sub>D<sub>6</sub>, CD<sub>3</sub>CN and CDCl<sub>3</sub>, and the chemical shifts in ppm refer to the solvent residual signal as internal standard ( $\delta_{\text{H}}$  (C<sub>6</sub>D<sub>6</sub>) = 7.16,  $\delta_{\text{C}}$  (C<sub>6</sub>D<sub>6</sub>) = 128.4;  $\delta_{\text{H}}$  (CD<sub>3</sub>CN) = 1.94,  $\delta_{\text{C}}$  (CD<sub>3</sub>CN) = 1.4;  $\delta_{\text{H}}$  (CDCl<sub>3</sub>) = 7.24,  $\delta_{\text{C}}$  (CDCl<sub>3</sub>) = 77.2). The following abbreviations were used for chemical shift multiplicities: brs = broad singlet, s = singlet, d = doublet, t = triplet, q = quartet, m = multiplet. The <sup>1</sup>H-NMR signals of AA'BB'-spin systems of *p*-disubstituted benzene rings are treated as doublets. NMR signal assignments are based on additional 2D-NMR experiments (COSY, HSQC, and HMBC). HR-MS has been performed on a *Finnigan MAT 95* (EI) or a *Thermo Finnigan LTQ FT* (ESI) mass spectrometer. Melting points were determined on a *Büchi B-540* device and are not corrected.

*Kinetics.*

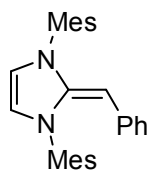
The rates of all investigated reactions were determined photometrically using dry glass apparatus under nitrogen atmosphere. The temperature of the solutions during all kinetic studies was kept constant (20.0 ± 0.1°C) by using a circulating bath thermostat. The kinetic experiments were carried out with freshly prepared stock solutions of the deoxy-Breslow-intermediates **2** dry THF. Due to lower solubility of the benzhydrylium tetrafluoroborates (**3a-f**)-BF<sub>4</sub> in THF, these stock solutions are prepared in dry THF containing ~1–5% of DMSO as cosolvent. For kinetic investigations in DMSO, stock solutions of **2a** were prepared in dry toluene and appropriately diluted with DMSO just before the kinetic runs (~1–2.5% of toluene as cosolvent). First-order kinetics were achieved by employing more than 6 equiv. of the nucleophiles **2**. For the evaluation of fast kinetics ( $\tau_{1/2} < 15\text{--}20$  s) the spectrophotometer system Applied Photophysics SX.18MV-R stopped-flow reaction analyser was used.

The rates of slow reactions ( $\tau_{1/2} > 15\text{--}20$  s) were determined by using a J&M TIDAS diode array spectrophotometer controlled by Labcontrol Spectacle software and connected to a Hellma 661.502-QX quartz Suprasil immersion probe (5 mm light path) via fiber optic cables and standard SMA connectors.

Rate constants  $k_{\text{obs}}$  (s<sup>-1</sup>) were obtained by fitting the single exponential  $A_t = A_0 \exp(-k_{\text{obs}}t) + C$  (exponential decrease) to the observed time-dependent absorbance (averaged from at least 5 kinetic runs for each nucleophile concentration in case of the stopped-flow method).

## 4.2 Synthesis of the Deoxy-Breslow Intermediates (2)

### 2-Benzylidene-1,3-dimesityl-2,3-dihydro-1*H*-imidazole (**2a**)

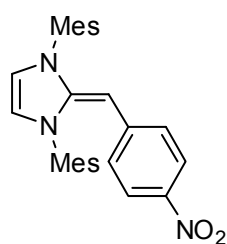


To an oven dried Schlenk-flask charged with a mixture of 1,3-dimesitylimidazolium chloride (682 mg, 2.00 mmol), *t*BuOK (11 mg, 98  $\mu$ mol), and NaH (120 mg, 5.00 mmol) was added dry THF (25 mL) and the mixture was then stirred for 15 min at room temperature under nitrogen. Then a THF solution (10 mL) of benzyl bromide (342 mg, 2.00 mmol) was slowly added. The mixture was allowed to stir for 20 h before the solvent was evaporated. The crude product mixture was then dispersed in dry toluene (30 mL) and filtered through a celite pad under nitrogen. After removing the solvent, the yellow solid was crystallized from *n*-pentane by slow evaporation to get 710 mg (1.79 mmol, 90%) of **2a**. M.P. = 137–138 °C (*n*-pentane). UV/Vis (THF):  $\lambda_{\text{max}}$  = 362 nm. IR (ATR)  $\tilde{\nu}$  ( $\text{cm}^{-1}$ ): 3020, 2954, 2916, 2852, 1620, 1581, 1561, 1484, 1431, 1414, 1373, 1339, 1290, 1236, 1194, 1175, 1029, 984, 914, 847, 745, 694.  $^1\text{H-NMR}$  ( $\text{d}_6$ -benzene, 400 MHz):  $\delta$  = 2.04 (s, 3 H,  $\text{CH}_3$ ), 2.13 (s, 3 H,  $\text{CH}_3$ ), 2.25, 2.26 (2 s, 12 H,  $\text{CH}_3$ ), 4.36 (s, 1 H,  $=\text{CHPh}$ ), 5.70 (d,  $J$  = 2.5 Hz, 1 H,  $\text{NCH}=\text{CHN}$ ), 5.72 (dd,  $J$  = 0.7, 2.5 Hz, 1 H,  $\text{NCH}=\text{CHN}$ ), 6.60-6.66 (m, 5 H, Ar), 6.79-6.83 (m, 4 H, Ar) ppm.  $^{13}\text{C-NMR}$  ( $\text{d}_6$ -benzene, 100 MHz):  $\delta$  = 18.5 (q,  $\text{CH}_3$ ), 19.1 (q,  $\text{CH}_3$ ), 21.2 (q,  $\text{CH}_3$ ), 21.4 (q,  $\text{CH}_3$ ), 68.5 (d,  $=\text{CHPh}$ ), 114.7 (d,  $\text{NCH}=\text{CHN}$ ), 116.0 (d,  $\text{NCH}=\text{CHN}$ ), 120.3 (d, Ar), 126.8 (d, Ar), 127.3 (d, Ar), 129.7 (d, Ar), 130.2 (d, Ar), 134.8 (s, Ar), 135.8 (s, Ar), 136.2 (s, Ar), 137.5 (s, Ar), 138.1 (s, Ar), 138.5 (s, Ar), 139.6 (s, Ar), 143.4 (s,  $\text{NC}=\text{CHPh}$ ) ppm. HR-MS (EI, positive)  $[\text{M}]$ : calculated for  $[\text{C}_{28}\text{H}_{30}\text{N}_2]^+$  is 394.2404; found 394.2400.

Crystallographic data for **2a**:

net formula	C <sub>28</sub> H <sub>30</sub> N <sub>2</sub>
<i>M<sub>r</sub></i> /g mol <sup>-1</sup>	394.551
crystal size/mm	0.47 × 0.32 × 0.08
/K	173(2)
radiation	MoKα
diffractometer	'Oxford XCalibur'
crystal system	monoclinic
space group	<i>P</i> 2 <sub>1</sub> / <i>c</i>
<i>a</i> /Å	11.8478(13)
<i>b</i> /Å	14.8944(18)
<i>c</i> /Å	12.8035(14)
α/°	90
β/°	96.896(10)
γ/°	90
<i>V</i> /Å <sup>3</sup>	2243.0(4)
<i>Z</i>	4
calc. density/g cm <sup>-3</sup>	1.1684(2)
μ/mm <sup>-1</sup>	0.068
absorption correction	'multi-scan'
transmission factor range	0.66624–1.00000
refls. measured	7897
<i>R</i> <sub>int</sub>	0.0344
mean σ( <i>I</i> )/ <i>I</i>	0.0576
θ range	4.22–26.37
observed refls.	3091
<i>x</i> , <i>y</i> (weighting scheme)	0.0601, 0.2327
hydrogen refinement	constr
refls in refinement	4529
parameters	277
restraints	0
<i>R</i> ( <i>F</i> <sub>obs</sub> )	0.0504
<i>R</i> <sub>w</sub> ( <i>F</i> <sup>2</sup> )	0.1415
<i>S</i>	1.034
shift/error <sub>max</sub>	0.001
max electron density/e Å <sup>-3</sup>	0.219
min electron density/e Å <sup>-3</sup>	-0.228

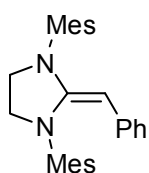
1,3-Dimesityl-2-(4-nitrobenzylidene)-2,3-dihydro-1H-imidazole (**2a'**)



To an oven dried Schlenk-flask charged with a mixture of 1,3-dimesitylimidazolium chloride (341 mg, 1.00 mmol), *t*BuOK (11 mg, 98 μmol), and NaH (60 mg, 2.5 mmol) was added dry THF (20 mL) and the mixture was stirred for 15 min at room temperature under nitrogen. Then a THF solution (10 mL) of 4-nitrobenzyl bromide (216 mg, 1.00 mmol) was slowly added. The mixture was allowed to stir for 20 h before the solvent was

evaporated. The crude product mixture was then dispersed in dry toluene (30 mL) and filtered through a celite pad under nitrogen. On concentrating the filtrate 330 mg (0.751 mmol, 75%) of **2a'** crystallized. M.P. = 151–153 °C (toluene). UV/Vis (THF):  $\lambda_{\text{max}} = 562$  nm. IR (ATR)  $\tilde{\nu}$  (cm<sup>-1</sup>): 2952, 2921, 2852, 1531, 1478, 1449, 1339, 1232, 1212, 1163, 1104, 1086, 850, 828, 691, 635. <sup>1</sup>H-NMR (d<sub>6</sub>-benzene, 300 MHz):  $\delta = 2.02$  (s, 12 H, CH<sub>3</sub>), 2.04 (s, 6 H, CH<sub>3</sub>), 4.29 (s, 1 H, =CH-4-NO<sub>2</sub>C<sub>6</sub>H<sub>4</sub>), 5.66 (s, 2 H, NCH=CHN), 6.02 (d,  $J = 9.2$  Hz, 2 H, Ar), 6.64, 6.65 (2s, 4 H, Ar), 7.73 (d,  $J = 9.2$  Hz, 2 H, Ar) ppm. <sup>13</sup>C-NMR (d<sub>6</sub>-benzene, 75 MHz):  $\delta = 18.4$  (q, CH<sub>3</sub>), 21.2 (q, CH<sub>3</sub>), 71.8 (d, =CH-4-NO<sub>2</sub>C<sub>6</sub>H<sub>4</sub>), 120.3 (d, NCH=CHN), 126.8 (d, Ar), 127.3 (d, Ar), 117.0 (d, Ar), 122.1 (d, Ar), 124.1 (d, Ar), 130.2 (d, Ar), 134.3 (s, Ar), 136.2 (s, Ar), 139.1 (s, Ar), 139.5 (s, Ar), 145.9 (s, Ar), 146.6 (s, NC=CH-4-NO<sub>2</sub>C<sub>6</sub>H<sub>4</sub>) ppm. HR-MS (EI, positive) [M + H<sup>+</sup>]: calculated for [C<sub>28</sub>H<sub>30</sub>N<sub>3</sub>O<sub>2</sub>]<sup>+</sup> 440.2333; found 440.2329.

## 2-Benzylidene-1,3-dimesitylimidazolidine (**2b**)

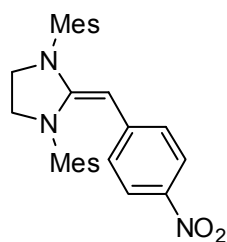


To an oven dried Schlenk-flask charged with a mixture of 1,3-dimesityl-4,5-dihydro-1H-imidazol-3-ium chloride (686 mg, 2.01 mmol), *t*BuOK (11 mg, 98  $\mu$ mol), and NaH (120 mg, 5.00 mmol) was added dry THF (25 mL) and the mixture was heated to 60 °C for 3 h under nitrogen. After cooling to room temperature, a THF solution (10 mL) of benzyl bromide (342 mg, 2.00 mmol) was slowly added. The mixture was stirred for 20 h before the solvent was evaporated. The crude product mixture was then dispersed in dry toluene (30 mL) and filtered through a celite pad under nitrogen. On concentrating, the 238 mg (0.600 mmol, 30%) of **2b** crystallized. M.P. = 148–151 °C (decomp., toluene). UV/Vis (THF):  $\lambda_{\text{max}} = 320$  nm. IR (ATR)  $\tilde{\nu}$  (cm<sup>-1</sup>): 2919, 2851, 1666, 1621, 1587, 1481, 1444, 1355, 1274, 1197, 1111, 1027, 849, 815, 753. <sup>1</sup>H-NMR (d<sub>6</sub>-benzene, 400 MHz):  $\delta = 2.00$  (s, 3 H, CH<sub>3</sub>), 2.16 (s, 3 H, CH<sub>3</sub>), 2.33 (s, 12 H, CH<sub>3</sub>), 3.21-3.32 (m, 4 H, 2  $\times$  CH<sub>2</sub>), 4.37 (s, 1 H, =CHPh), 6.59 (s, 2 H, Ar), 6.63-6.68 (m, 1 H, Ar), 6.74-6.77 (m, 2 H, Ar), 6.81-6.86 (m, 4 H, Ar) ppm. <sup>13</sup>C-NMR (d<sub>6</sub>-benzene, 75 MHz):  $\delta = 18.6$  (q, CH<sub>3</sub>), 19.2 (q, CH<sub>3</sub>), 21.1 (q, CH<sub>3</sub>), 21.4 (q, CH<sub>3</sub>), 47.8 (t, CH<sub>2</sub>), 51.2 (t, CH<sub>2</sub>), 75.2 (d, =CHPh), 121.8 (d, Ar), 127.2 (d, Ar), 127.5 (d, Ar), 130.1 (d, Ar), 130.4 (d, Ar), 135.6 (s, Ar), 136.0 (s, Ar), 137.2 (s, Ar), 137.6 (s, Ar), 138.4 (s, Ar), 139.15 (s, Ar), 139.18 (s, Ar), 147.9 (s, NC=CHPh) ppm. HR-MS (EI, positive) [M]: calculated for [C<sub>28</sub>H<sub>32</sub>N<sub>2</sub>]<sup>+</sup> 396.2560; found 396.2535; [M - H]<sup>+</sup>: calculated for [C<sub>28</sub>H<sub>31</sub>N<sub>2</sub>]<sup>+</sup> is 395.2482; found 395.2482.

**Crystallographic data for 2b:**

net formula	C <sub>28</sub> H <sub>32</sub> N <sub>2</sub>
<i>M<sub>r</sub></i> /g mol <sup>-1</sup>	396.567
crystal size/mm	0.43 × 0.33 × 0.25
<i>T</i> /K	173(2)
radiation	MoKα
diffractometer	'Oxford XCalibur'
crystal system	monoclinic
space group	<i>P</i> 2 <sub>1</sub> / <i>n</i>
<i>a</i> /Å	11.7727(10)
<i>b</i> /Å	13.5106(8)
<i>c</i> /Å	15.4610(14)
α/°	90
β/°	111.723(10)
γ/°	90
<i>V</i> /Å <sup>3</sup>	2284.5(3)
<i>Z</i>	4
calc. density/g cm <sup>-3</sup>	1.15303(15)
μ/mm <sup>-1</sup>	0.067
absorption correction	'multi-scan'
transmission factor range	0.87096–1.00000
refls. measured	13690
<i>R</i> <sub>int</sub>	0.0297
mean σ( <i>I</i> )/ <i>I</i>	0.0353
θ range	4.24–26.37
observed refls.	3434
<i>x</i> , <i>y</i> (weighting scheme)	0.0620, 0.9402
hydrogen refinement	constr
refls in refinement	4647
parameters	276
restraints	0
<i>R</i> ( <i>F</i> <sub>obs</sub> )	0.0517
<i>R</i> <sub>w</sub> ( <i>F</i> <sup>2</sup> )	0.1444
<i>S</i>	1.039
shift/error <sub>max</sub>	0.001
max electron density/e Å <sup>-3</sup>	0.251
min electron density/e Å <sup>-3</sup>	-0.267

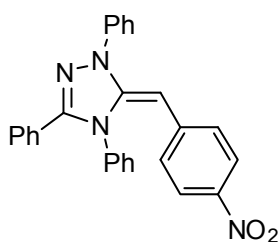
1,3-Dimesityl-2-(4-nitrobenzylidene)imidazolidine (**2b'**)



To an oven dried Schlenk-flask charged with a mixture of 1,3-dimesityl-4,5-dihydro-1H-imidazol-3-ium chloride (1.03 g, 3.00 mmol), *t*BuOK (11 mg, 98 μmol), and NaH (180 mg, 7.50 mmol) was added dry THF (25 mL) and the mixture was heated to 60 °C for 3 h under nitrogen. After cooling to room temperature, a THF solution (10 mL) of 4-nitrobenzyl bromide (648 mg, 3.00 mmol) was slowly added. The mixture was allowed to stir for 20 h

before the solvent was evaporated under vacuum. The crude product mixture was dispersed in dry toluene (30 mL) and filtered through a celite pad under nitrogen. On concentrating the filtrate, 1.14 g (2.58 mmol, 86%) of **2b'** crystallized. M.P. = 156–158 °C (decomp., toluene). UV/Vis (THF):  $\lambda_{\text{max}} = 493$  nm. IR (ATR)  $\tilde{\nu}$  (cm<sup>-1</sup>): 2951, 2913, 2858, 1538, 1468, 1441, 1262, 1234, 1177, 1108, 1085, 1000, 840, 720, 693, 659. <sup>1</sup>H-NMR (d<sub>6</sub>-benzene, 400 MHz):  $\delta = 1.91$  (s, 3 H, CH<sub>3</sub>), 2.14 (s, 9 H, CH<sub>3</sub>), 2.18 (s, 6 H, CH<sub>3</sub>), 3.09-3.13 (m, 2 H, CH<sub>2</sub>), 3.18-3.22 (m, 2 H, CH<sub>2</sub>), 4.21 (s, 1 H, =CH-4-NO<sub>2</sub>C<sub>6</sub>H<sub>4</sub>), 6.27 (d,  $J = 9.0$  Hz, 2 H, Ar), 6.51 (s, 2 H, Ar), 6.81 (s, 2 H, Ar), 7.68 (d,  $J = 9.0$  Hz, 2 H, Ar) ppm. <sup>13</sup>C-NMR (d<sub>6</sub>-benzene, 100 MHz):  $\delta = 18.3$  (q, CH<sub>3</sub>), 19.0 (q, CH<sub>3</sub>), 20.9 (q, CH<sub>3</sub>), 21.4 (q, CH<sub>3</sub>), 47.7 (t, CH<sub>2</sub>), 51.3 (t, CH<sub>2</sub>), 75.7 (d, =CH-4-NO<sub>2</sub>C<sub>6</sub>H<sub>4</sub>), 123.1 (d, Ar), 125.0 (d, Ar), 130.44 (d, Ar), 130.46 (d, Ar), 134.9 (s, Ar), 136.3 (s, Ar), 137.4 (s, Ar), 137.8 (s, Ar), 138.1 (s, Ar), 138.2 (s, Ar), 141.5 (s, Ar), 146.8 (s, Ar), 152.3 (s, NC=CH-4-NO<sub>2</sub>C<sub>6</sub>H<sub>4</sub>) ppm. HR-MS (EI, positive) [M]: calculated for [C<sub>28</sub>H<sub>31</sub>N<sub>3</sub>O<sub>2</sub>]<sup>+</sup> 441.2416; found 441.2502.

#### 5-(4-Nitrobenzylidene)-1,3,4-triphenyl-4,5-dihydro-1H-1,2,4-triazole (**2c'**)



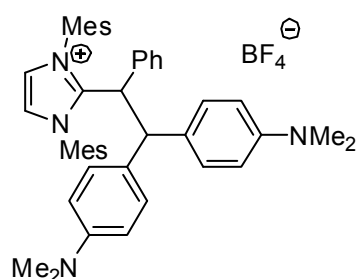
To a toluene solution (15 mL) of Enders' carbene (**1c**, 595 mg, 2.00 mmol) in an oven-dried Schlenk-flask was slowly added a toluene solution (10 mL) of 4-nitrobenzyl bromide (216 mg, 1.00 mmol) and the mixture was allowed to stir at room temperature. After complete consumption of 4-nitrobenzylbromide (indicated by <sup>1</sup>H NMR) it was filtered through a celite pad under nitrogen. On concentrating the filtrate, 259 mg (0.599 mmol, 60%) of **2c'** precipitated. M.P. 185–187 °C (decomp., toluene). UV/Vis (THF):  $\lambda_{\text{max}} = 512$  nm. IR (ATR)  $\tilde{\nu}$  (cm<sup>-1</sup>): 3064, 2923, 2853, 1608, 1564, 1543, 1492, 1476, 1304, 1278, 1236, 1156, 1104, 844, 765, 751, 689, 626. <sup>1</sup>H-NMR (d<sub>6</sub>-benzene, 400 MHz):  $\delta = 4.74$  (s, 1 H, =CH-4-NO<sub>2</sub>C<sub>6</sub>H<sub>4</sub>), 6.38 (d,  $J = 8.5$  Hz, 2 H, Ar), 6.77-6.93 (m, 9 H, Ar), 6.99 (t,  $J = 7.9$  Hz, 2 H, Ar), 7.32 (d,  $J = 7.3$  Hz, 2 H, Ar), 7.52 (d,  $J = 7.4$  Hz, 2 H, Ar), 7.81 (d,  $J = 8.8$  Hz, 2 H, Ar) ppm. <sup>13</sup>C-NMR (d<sub>6</sub>-benzene, 100 MHz):  $\delta = 72.9$  (d, =CH-4-NO<sub>2</sub>C<sub>6</sub>H<sub>4</sub>), 122.1 (d, Ar), 123.8 (d, Ar), 124.8 (d, Ar), 126.6 (d, Ar), 128.8 (d, Ar), 128.9 (d, Ar), 129.38 (d, Ar), 129.43 (d, Ar), 129.9 (d, Ar), 130.6 (d, Ar), 130.8 (d, Ar), 135.9 (s), 139.9 (s, Ar), 141.7 (s, Ar), 144.9 (s, Ar), 147.6 (s), 149.9 (s, Ar) ppm. HR-MS (EI, positive) [M]: calculated for [C<sub>27</sub>H<sub>20</sub>N<sub>4</sub>O<sub>2</sub>]<sup>+</sup> is 432.1581; found 432.1585.

### 4.3 Reactions of the deoxy-Breslow intermediates with $\text{Ar}_2\text{CH}^+$

*General Procedure (GP):*

**3a** (34 mg, 0.10 mmol) was dissolved in 2 mL of dry  $\text{CH}_2\text{Cl}_2$  in an oven-dried Schlenk-flask under nitrogen. Then a toluene solution (2 mL) of the nucleophile (**2**, 0.10 mmol) was added, and the mixture was stirred for 2-3 min. The solvent was removed under reduced pressure and the residue was purified by crystallization by vapour diffusion of n-pentane into a  $\text{CH}_2\text{Cl}_2$ -EtOAc (~10 : 1) solution of the crude mixture.

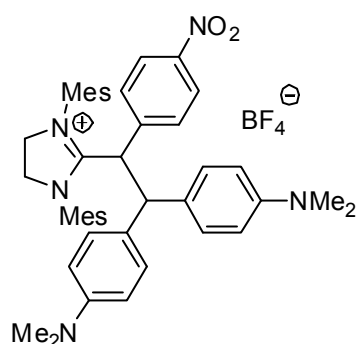
**4a**: Prepared from **3a** and **2a** according to GP. Light blue solid, 56 mg (76  $\mu\text{mol}$ , 76%).



$^1\text{H-NMR}$  ( $\text{CD}_3\text{CN}$ , 400 MHz):  $\delta$  = 1.38 (s, 6 H,  $\text{CH}_3$ ), 2.07 (s, 6 H,  $\text{CH}_3$ ), 2.47 (s, 6 H,  $\text{CH}_3$ ), 2.62 (s, 6 H,  $\text{N}(\text{CH}_3)_2$ ), 2.89 (s, 6 H,  $\text{N}(\text{CH}_3)_2$ ), 4.42 (d,  $J$  = 11.8 Hz, 1 H,  $\text{PhCHCH}(\text{dma})_2$ ), 5.16 (d,  $J$  = 11.8 Hz, 1 H,  $\text{PhCHCH}(\text{dma})_2$ ), 6.17 (d,  $J$  = 8.9 Hz, 2 H, Ar), 6.51-6.56 (m, 6 H, Ar), 6.86-6.90 (m, 4 H, Ar), 7.02-7.04 (m, 3 H, Ar), 7.27 (s, 2 H, Ar), 7.45 (s, 2 H,  $\text{NCH}=\text{CHN}$ ) ppm.

$^{13}\text{C-NMR}$  ( $\text{CD}_3\text{CN}$ , 100 MHz):  $\delta$  = 17.7 (q,  $\text{CH}_3$ ), 18.9 (q,  $\text{CH}_3$ ), 21.4 (q,  $\text{CH}_3$ ), 40.5 (q,  $\text{N}(\text{CH}_3)_2$ ), 40.9 (q,  $\text{N}(\text{CH}_3)_2$ ), 48.2 (d,  $\text{PhCHCH}(\text{dma})_2$ ), 53.0 (d,  $\text{PhCHCH}(\text{dma})_2$ ), 112.9 (d, Ar), 114.2 (d, Ar), 126.7 (d,  $\text{NCH}=\text{CHN}$ ), 128.5 (d, Ar), 128.8 (d, Ar), 129.1 (d, Ar), 129.3 (d, Ar), 130.6 (s, Ar), 131.0 (d, Ar), 131.3 (d, Ar), 132.0 (s, Ar), 132.7 (s, Ar), 132.9 (d, Ar), 135.0 (s, Ar), 136.2 (s, Ar), 137.7 (s, Ar), 142.9 (s, Ar), 148.5 (s,  $\text{N}^+=\text{C}-\text{N}$ ), 149.5 (s, Ar), 151.4 (s, Ar) ppm. HR-MS (ESI) [ $\text{M}^+$ ]: calculated for  $[\text{C}_{45}\text{H}_{51}\text{N}_4]^+$  647.4108; found 647.4112.

**4b**: Prepared from **3a** and **2b'** according to GP. Yellowish-green solid, 50 mg (64  $\mu\text{mol}$ ,



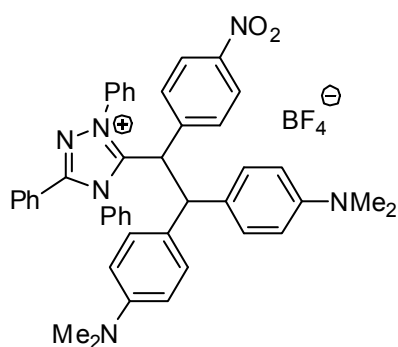
64%).

Mp. = 127-129  $^\circ\text{C}$  (decomp.,  $\text{CH}_2\text{Cl}_2$ -EtOAc-*n*-pentane).  $^1\text{H-NMR}$  ( $\text{CDCl}_3$ , 600 MHz):  $\delta$  = 1.90 (s, 6 H,  $\text{CH}_3$ ), 2.15 (s, 6 H,  $\text{CH}_3$ ), 2.38 (s, 6 H,  $\text{CH}_3$ ), 2.63 (s, 6 H,  $\text{N}(\text{CH}_3)_2$ ), 2.91 (s, 6 H,  $\text{N}(\text{CH}_3)_2$ ), 4.31-4.34 (m, 1 + 4 H,  $\text{CH}(\text{dma})_2$ ,  $\text{NCH}_2\text{CH}_2\text{N}$ ), 4.75 (d,  $J$  = 10.3 Hz, 1 H,  $4\text{-NO}_2\text{C}_6\text{H}_4\text{CH}$ ), 6.08 (d,  $J$  = 8.9 Hz, 2 H, Ar), 6.21 (d,  $J$  = 8.9 Hz, 2 H, Ar), 6.50 (d,  $J$  = 8.8 Hz, 2

H, Ar), 6.54 (d,  $J$  = 8.7 Hz, 2 H, Ar), 6.76 (d,  $J$  = 8.8 Hz, 2 H, Ar), 6.93 (s, 2 H, Ar), 7.02 (s, 2 H, Ar), 7.69 (d,  $J$  = 8.8 Hz, 2 H, Ar) ppm.  $^{13}\text{C-NMR}$  ( $\text{CDCl}_3$ , 150 MHz):  $\delta$  = 18.2 (q,  $\text{CH}_3$ ), 18.8 (q,  $\text{CH}_3$ ), 21.4, (q,  $\text{CH}_3$ ), 40.3 (q,  $\text{N}(\text{CH}_3)_2$ ), 40.7 (q,  $\text{N}(\text{CH}_3)_2$ ), 49.4 (d,  $4\text{-NO}_2\text{C}_6\text{H}_4\text{CH}$ ), 50.6 (d,  $\text{CH}(\text{dma})_2$ ), 52.0 (t,  $\text{NCH}_2\text{CH}_2\text{N}$ ), 112.2 (d, Ar), 113.1 (d, Ar), 122.4 (d, Ar), 128.0

(d, Ar), 128.7 (d, Ar), 129.1 (s, Ar), 130.7 (d, Ar), 130.8 (d, Ar), 131.1 (s, Ar), 133.0 (d, Ar), 136.0 (s, Ar), 136.8 (s, Ar), 140.2 (s, Ar), 141.5 (s, Ar), 147.1 (s, Ar), 148.7 (s, Ar), 150.3 (s, Ar), 168.0 (s, N<sup>+</sup>=C-N) ppm. HR-MS (ESI, positive): calculated for [C<sub>45</sub>H<sub>52</sub>O<sub>2</sub>N<sub>5</sub>]<sup>+</sup> 694.4116; found 694.4114.

**4c**: Prepared from **3a** and **2c'** according to GP. Light blue solid, 64 mg (83 μmol, 83%).



Mp. = 162-164 °C (decomp., CH<sub>2</sub>Cl<sub>2</sub>-EtOAc-*n*-pentane).

<sup>1</sup>H-NMR (CDCl<sub>3</sub>, 600 MHz): δ = 2.77 (s, 6 H, N(CH<sub>3</sub>)<sub>2</sub>), 2.93 (s, 6 H, N(CH<sub>3</sub>)<sub>2</sub>), 4.80 (d, *J* = 12.3 Hz, 1 H, CH(dma)<sub>2</sub>), 5.36 (d, *J* = 12.3 Hz, 1 H, 4-NO<sub>2</sub>C<sub>6</sub>H<sub>4</sub>CH), 6.39 (d, *J* = 8.9 Hz, 2 H, Ar), 6.51 (d, *J* = 8.9 Hz, 2 H, Ar), 6.63-6.65 (m, 2 + 2 H, Ar), 7.00-7.04 (m, 2 H, Ar), 7.24-7.26 (m, 3 H, Ar, overlapped with CDCl<sub>3</sub>), 7.35-7.38 (m, 3

H, Ar), 7.41-7.45 (m, 4 H, Ar), 7.48 (t, *J* = 7.6 Hz, 1 H, Ar), 7.56 (t, *J* = 7.5 Hz, 1 H, Ar), 7.65 (t, *J* = 7.4 Hz, 1 H, Ar), 7.79 (d, *J* = 8.9 Hz, 2 H, Ar), 8.07 (d, *J* = 8.9 Hz, 2 H, Ar) ppm.

<sup>13</sup>C-NMR (CDCl<sub>3</sub>, 150 MHz): δ = 40.4 (q, N(CH<sub>3</sub>)<sub>2</sub>), 40.7 (q, N(CH<sub>3</sub>)<sub>2</sub>), 46.1 (d, 4-NO<sub>2</sub>C<sub>6</sub>H<sub>4</sub>CH), 51.0 (d, CH(dma)<sub>2</sub>), 52.0 (t, NCH<sub>2</sub>CH<sub>2</sub>N), 112.7 (d, Ar), 113.1 (d, Ar), 122.6 (s, Ar), 123.5 (d, Ar), 125.8 (s, Ar), 127.4 (d, Ar), 127.6 (s, Ar), 128.1 (d, Ar), 128.6 (d, Ar), 129.0 (d, Ar), 129.1 (d, Ar), 130.0 (d, Ar), 130.1 (d, Ar), 130.4 (d, Ar), 130.5 (d, Ar), 131.3 (d, Ar), 131.4 (s, Ar), 131.95 (d, Ar), 131.99 (d, Ar), 132.1 (d, Ar), 135.2 (s, Ar), 138.9 (s, Ar), 147.2 (s, Ar), 149.4 (s, Ar), 150.3 (s, Ar), 154.3 (s, N<sup>+</sup>=C-N), 155.1 (s, Ar) ppm. HR-MS (ESI, positive): calculated for [C<sub>44</sub>H<sub>41</sub>O<sub>2</sub>N<sub>6</sub>]<sup>+</sup> 685.3286; found 685.3293.

**Crystallographic data for 4c.2CH<sub>2</sub>Cl<sub>2</sub>:**

net formula	C <sub>46</sub> H <sub>45</sub> BCl <sub>4</sub> F <sub>4</sub> N <sub>6</sub> O <sub>2</sub>
<i>M<sub>r</sub></i> /g mol <sup>-1</sup>	942.504
crystal size/mm	0.35 × 0.29 × 0.26
<i>T</i> /K	173(2)
radiation	MoKα
diffractometer	'KappaCCD'
crystal system	triclinic
space group	<i>P</i> 1bar
<i>a</i> /Å	9.3936(2)
<i>b</i> /Å	15.1675(3)
<i>c</i> /Å	16.8338(4)
α/°	103.6616(13)
β/°	90.3338(15)
γ/°	102.6776(12)
<i>V</i> /Å <sup>3</sup>	2269.55(8)
<i>Z</i>	2
calc. density/g cm <sup>-3</sup>	1.37920(5)
μ/mm <sup>-1</sup>	0.323
absorption correction	none
refls. measured	15376
<i>R</i> <sub>int</sub>	0.0218
mean σ( <i>I</i> )/ <i>I</i>	0.0356
θ range	3.16–25.33
observed refls.	6240
<i>x</i> , <i>y</i> (weighting scheme)	0.0799, 3.0183
hydrogen refinement	constr
refls in refinement	8271
parameters	600
restraints	0
<i>R</i> ( <i>F</i> <sub>obs</sub> )	0.0652
<i>R</i> <sub>w</sub> ( <i>F</i> <sup>2</sup> )	0.1828
<i>S</i>	1.052
shift/error <sub>max</sub>	0.001
max electron density/e Å <sup>-3</sup>	0.923
min electron density/e Å <sup>-3</sup>	-1.087

Three of four F atoms are disordered, split model applied, sof ratio 0.56/0.44.

## 4.4 Kinetics

### 4.4.1 Kinetics of the reactions of the 2a with the reference electrophiles 3 in DMSO.

**Table 3:** Kinetics of the reaction of 2a with 3e at 20 °C in DMSO (stopped-flow,  $\lambda = 641$  nm).

[3e] / mol L <sup>-1</sup>	[2a] / mol L <sup>-1</sup>	$k_{\text{obs}} / \text{s}^{-1}$
$1.15 \times 10^{-5}$	$9.94 \times 10^{-5}$	69.0
	$1.49 \times 10^{-4}$	105
	$1.99 \times 10^{-4}$	141
	$2.98 \times 10^{-4}$	236
	$3.97 \times 10^{-4}$	328

$$k = 8.80 \times 10^5 \text{ L mol}^{-1} \text{ s}^{-1}$$

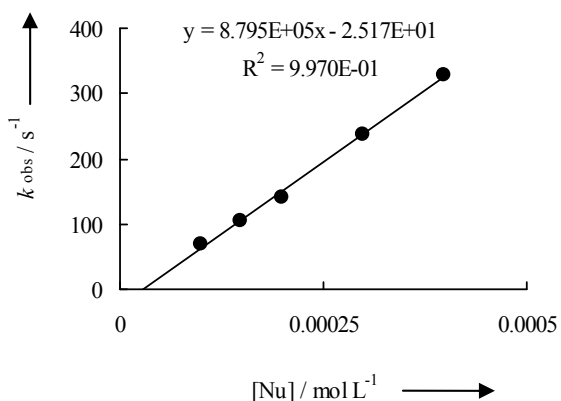


**Table 4:** Kinetics of the reaction of 2a with 3f at 20 °C in DMSO (stopped-flow,  $\lambda = 641$  nm).

[3f] / mol L <sup>-1</sup>	[2a] / mol L <sup>-1</sup>	$k_{\text{obs}} / \text{s}^{-1}$
$1.25 \times 10^{-5}$	$9.94 \times 10^{-5}$	24.0
	$1.49 \times 10^{-4}$	37.3
	$1.99 \times 10^{-4}$	48.7
	$2.98 \times 10^{-4}$	71.7
	$3.97 \times 10^{-4}$	92.9

$$k = 2.30 \times 10^5 \text{ L mol}^{-1} \text{ s}^{-1}$$

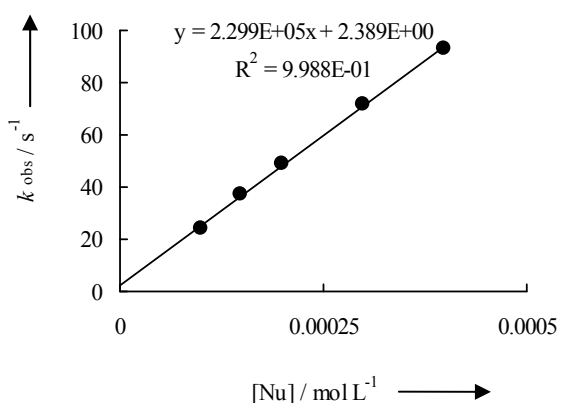


**Table 5:** Kinetics of the reaction of 2a with 3g at 20 °C in DMSO (stopped-flow,  $\lambda = 424$  nm).

[3g] / mol L <sup>-1</sup>	[2a] / mol L <sup>-1</sup>	$k_{\text{obs}} / \text{s}^{-1}$
$3.29 \times 10^{-5}$	$2.15 \times 10^{-4}$	1.39
	$4.31 \times 10^{-4}$	2.65
	$6.46 \times 10^{-4}$	3.83
	$8.62 \times 10^{-4}$	5.21
	$9.69 \times 10^{-4}$	6.05

$$k = 6.10 \times 10^3 \text{ L mol}^{-1} \text{ s}^{-1}$$

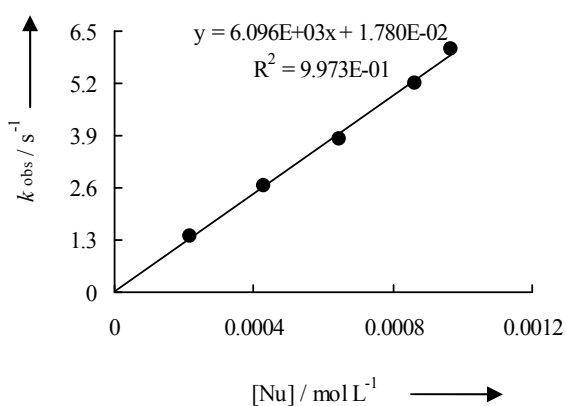
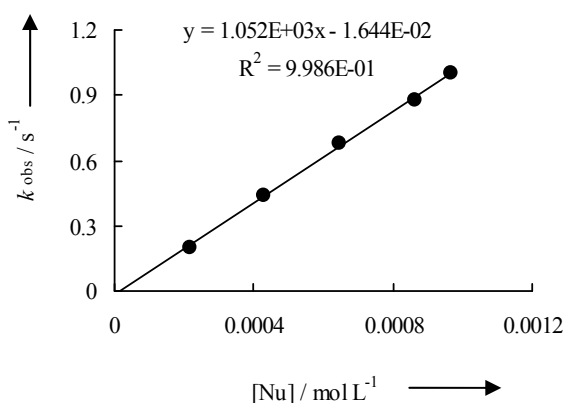


**Table 6:** Kinetics of the reaction of **2a** with **3h** at 20 °C in DMSO (stopped-flow,  $\lambda = 533$  nm).

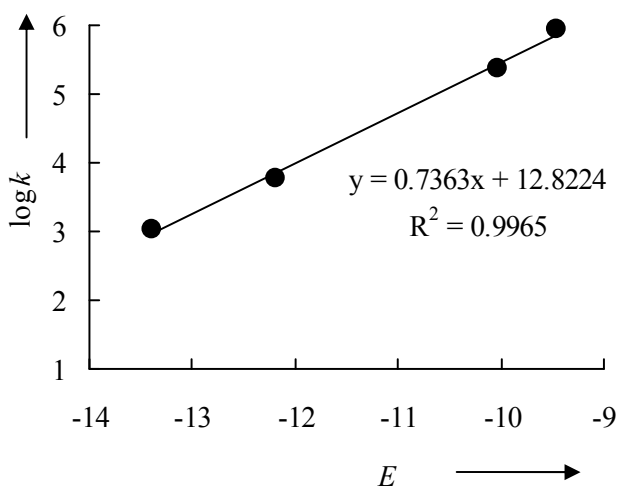
[ <b>3h</b> ] / mol L <sup>-1</sup>	[ <b>2a</b> ] / mol L <sup>-1</sup>	$k_{\text{obs}} / \text{s}^{-1}$
$1.79 \times 10^{-5}$	$2.15 \times 10^{-4}$	0.200
	$4.31 \times 10^{-4}$	0.442
	$6.46 \times 10^{-4}$	0.682
	$8.62 \times 10^{-4}$	0.880
	$9.69 \times 10^{-4}$	0.999



$$k = 1.05 \times 10^3 \text{ L mol}^{-1} \text{ s}^{-1}$$

**Table 7:** Determination of the parameters  $N$  and  $s_N$  for **2a** in DMSO.

Electrophiles	$E$	$k (\text{M}^{-1} \text{s}^{-1})$
<b>3e</b>	-9.45	$8.80 \times 10^5$
<b>3f</b>	-10.04	$2.30 \times 10^5$
<b>3g</b>	-12.18	$6.10 \times 10^3$
<b>3h</b>	-13.39	$1.05 \times 10^3$



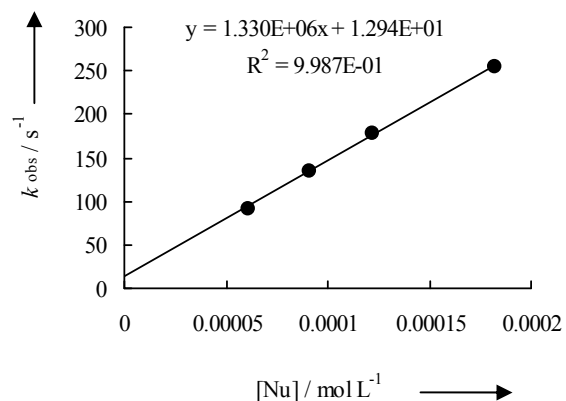
$$N = 17.41$$

$$s_N = 0.74$$

#### 4.4.2 Kinetics of the Reactions of the **2a** with the Reference Electrophiles **3** in THF.

**Table 8:** Kinetics of the reaction of **2a** with **3e** at 20 °C in THF (stopped-flow,  $\lambda = 640$  nm).

[ <b>3e</b> ] / mol L <sup>-1</sup>	[ <b>2a</b> ] / mol L <sup>-1</sup>	$k_{\text{obs}} / \text{s}^{-1}$
$1.05 \times 10^{-5}$	$6.09 \times 10^{-5}$	91.8
	$9.13 \times 10^{-5}$	135
	$1.22 \times 10^{-4}$	178
	$1.83 \times 10^{-4}$	254



$$k = 1.33 \times 10^6 \text{ L mol}^{-1} \text{ s}^{-1}$$

**Table 9:** Kinetics of the reaction of **2a** with **3f** at 20 °C in THF (stopped-flow,  $\lambda = 640$  nm).

[ <b>3f</b> ] / mol L <sup>-1</sup>	[ <b>2a</b> ] / mol L <sup>-1</sup>	$k_{\text{obs}} / \text{s}^{-1}$
$1.15 \times 10^{-5}$	$7.65 \times 10^{-5}$	30.7
	$1.02 \times 10^{-4}$	41.8
	$1.53 \times 10^{-4}$	63.6
	$2.04 \times 10^{-4}$	88.3

$$k = 4.50 \times 10^5 \text{ L mol}^{-1} \text{ s}^{-1}$$

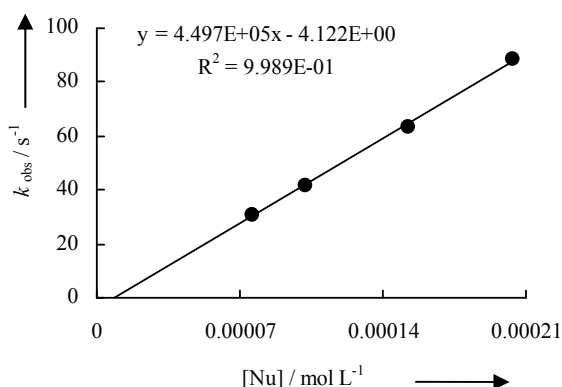
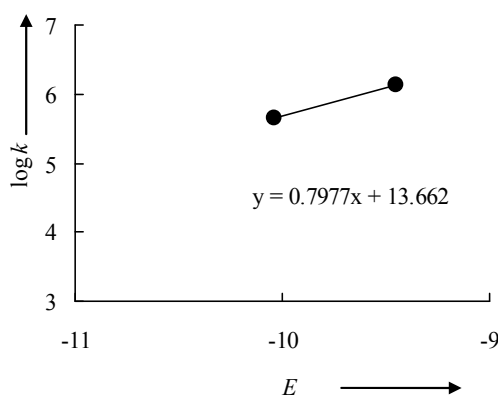


**Table 10:** Determination of the parameters  $N$  and  $s_N$  for **2a** in THF.

Electrophiles	$E$	$k (\text{M}^{-1} \text{s}^{-1})$
<b>3e</b>	-9.45	$1.33 \times 10^6$
<b>3f</b>	-10.04	$4.50 \times 10^5$



$$N = 17.12$$

$$s_N = 0.80$$

#### 4.4.3 Kinetics of the Reactions of the **2a'** with the Reference Electrophiles **3** in THF.

**Table 11:** Kinetics of the reaction of **2a'** with **3c** at 20 °C in THF (stopped-flow,  $\lambda = 626$  nm).

[ <b>3c</b> ] / mol L <sup>-1</sup>	[ <b>2a'</b> ] / mol L <sup>-1</sup>	$k_{\text{obs}} / \text{s}^{-1}$
$1.52 \times 10^{-5}$	$1.11 \times 10^{-4}$	2.98
	$1.71 \times 10^{-4}$	4.76
	$2.28 \times 10^{-4}$	6.39
	$2.84 \times 10^{-4}$	8.02
	$3.41 \times 10^{-4}$	9.84

$$k = 2.96 \times 10^4 \text{ L mol}^{-1} \text{ s}^{-1}$$

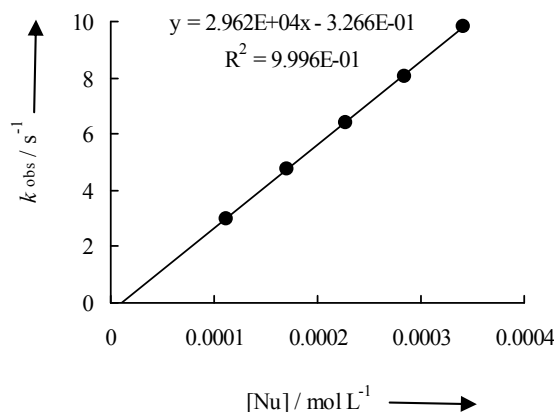
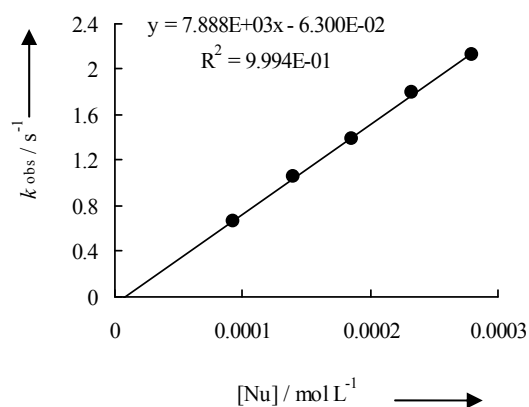


**Table 12:** Kinetics of the reaction of **2a'** with **3d** at 20 °C in THF (stopped-flow,  $\lambda = 640$  nm).

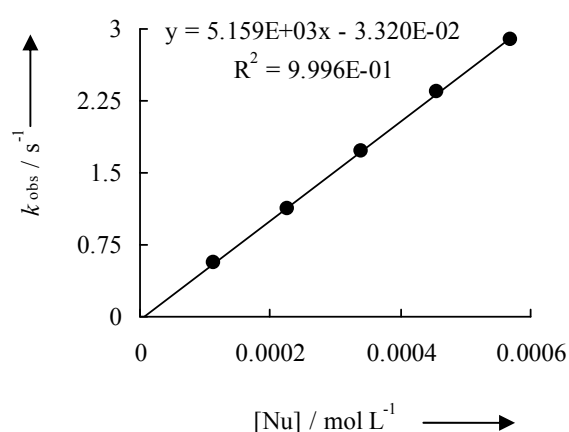
$[3d] / \text{mol L}^{-1}$	$[2a'] / \text{mol L}^{-1}$	$k_{\text{obs}} / \text{s}^{-1}$
$1.72 \times 10^{-5}$	$9.31 \times 10^{-5}$	0.665
	$1.40 \times 10^{-4}$	1.05
	$1.86 \times 10^{-4}$	1.39
	$2.33 \times 10^{-4}$	1.79
	$2.79 \times 10^{-4}$	2.13



$$k = 7.89 \times 10^3 \text{ L mol}^{-1} \text{ s}^{-1}$$

**Table 13:** Kinetics of the reaction of **2a'** with **3e** at 20 °C in THF (stopped-flow,  $\lambda = 640$  nm).

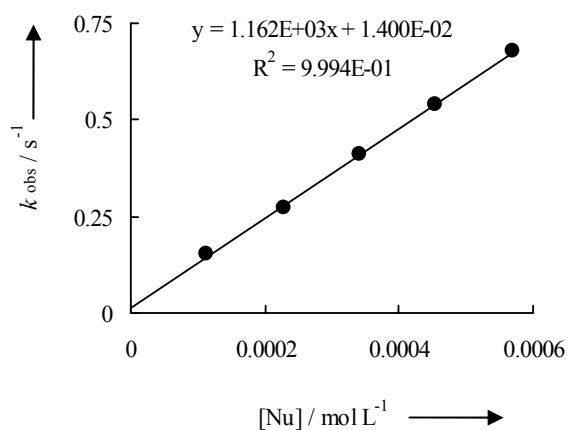
$[3e] / \text{mol L}^{-1}$	$[2a'] / \text{mol L}^{-1}$	$k_{\text{obs}} / \text{s}^{-1}$
$1.80 \times 10^{-5}$	$1.14 \times 10^{-4}$	0.566
	$2.28 \times 10^{-4}$	1.12
	$3.41 \times 10^{-4}$	1.72
	$4.55 \times 10^{-4}$	2.34
	$5.69 \times 10^{-4}$	2.89



$$k = 5.16 \times 10^3 \text{ L mol}^{-1} \text{ s}^{-1}$$

**Table 14:** Kinetics of the reaction of **2a'** with **3f** at 20 °C in THF (stopped-flow,  $\lambda = 640$  nm).

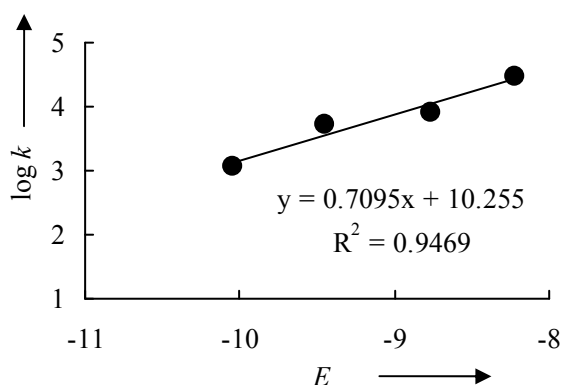
$[3f] / \text{mol L}^{-1}$	$[4b] / \text{mol L}^{-1}$	$k_{\text{obs}} / \text{s}^{-1}$
$1.79 \times 10^{-5}$	$1.14 \times 10^{-4}$	0.152
	$2.28 \times 10^{-4}$	0.270
	$3.41 \times 10^{-4}$	0.412
	$4.55 \times 10^{-4}$	0.542
	$5.69 \times 10^{-4}$	0.677



$$k = 1.16 \times 10^3 \text{ L mol}^{-1} \text{ s}^{-1}$$

**Table 15:** Determination of the parameters  $N$  and  $s_N$  for **2a'** in THF.

Electrophiles	$E$	$k$ ( $M^{-1} s^{-1}$ )
<b>3c</b>	-8.22	$2.96 \times 10^4$
<b>3d</b>	-8.76	$7.89 \times 10^3$
<b>3e</b>	-9.45	$5.16 \times 10^3$
<b>3f</b>	-10.04	$1.16 \times 10^3$



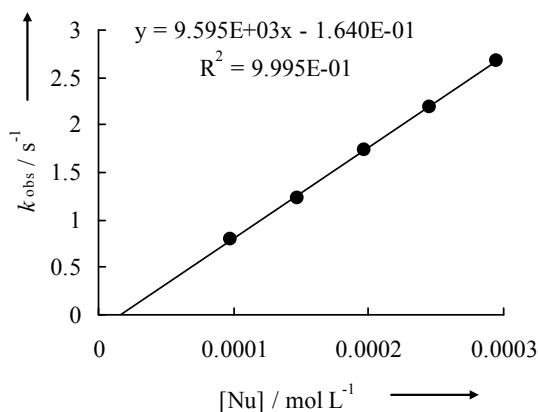
$$N = 14.45$$

$$s_N = 0.71$$

#### 4.4.4 Kinetics of the Reactions of the **2b** with the Reference Electrophiles **3** in THF.

**Table 16:** Kinetics of the reaction of **2b** with **3b** at 20 °C in THF (stopped-flow,  $\lambda = 620$  nm).

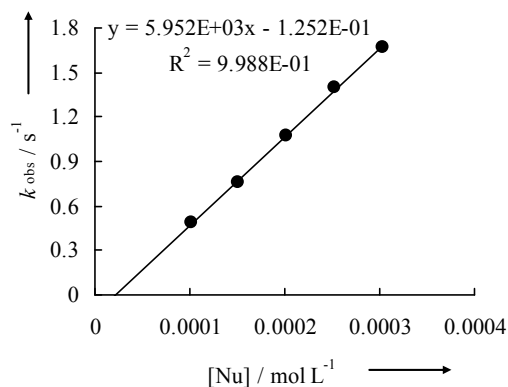
[ <b>3b</b> ] / mol L <sup>-1</sup>	[ <b>2b</b> ] / mol L <sup>-1</sup>	$k_{\text{obs}}$ / s <sup>-1</sup>
$1.34 \times 10^{-5}$	$9.83 \times 10^{-5}$	0.796
	$1.48 \times 10^{-4}$	1.23
	$1.97 \times 10^{-4}$	1.73
	$2.46 \times 10^{-4}$	2.18
	$2.95 \times 10^{-4}$	2.68



$$k = 9.60 \times 10^3 \text{ L mol}^{-1} \text{ s}^{-1}$$

**Table 17:** Kinetics of the reaction of **2b** with **3c** at 20 °C in THF (stopped-flow,  $\lambda = 622$  nm).

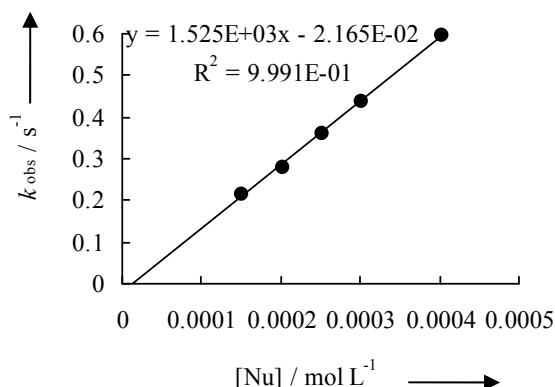
[ <b>3c</b> ] / mol L <sup>-1</sup>	[ <b>2b</b> ] / mol L <sup>-1</sup>	$k_{\text{obs}}$ / s <sup>-1</sup>
$1.66 \times 10^{-5}$	$1.01 \times 10^{-4}$	0.488
	$1.51 \times 10^{-4}$	0.758
	$2.02 \times 10^{-4}$	1.07
	$2.52 \times 10^{-4}$	1.40
	$3.03 \times 10^{-4}$	1.67



$$k = 5.95 \times 10^3 \text{ L mol}^{-1} \text{ s}^{-1}$$

**Table 18:** Kinetics of the reaction of **2b** with **3d** at 20 °C in THF (stopped-flow,  $\lambda = 625$  nm).

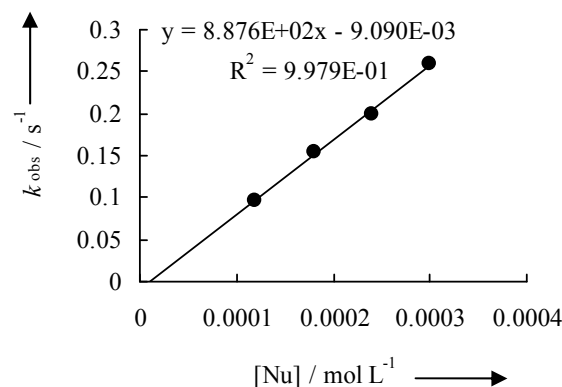
[ <b>3d</b> ] / mol L <sup>-1</sup>	[ <b>2b</b> ] / mol L <sup>-1</sup>	$k_{\text{obs}}$ / s <sup>-1</sup>
$1.65 \times 10^{-5}$	$1.51 \times 10^{-4}$	0.215
	$2.02 \times 10^{-4}$	0.280
	$2.52 \times 10^{-4}$	0.362
	$3.03 \times 10^{-4}$	0.439
	$4.03 \times 10^{-4}$	0.596



$$k = 1.53 \times 10^3 \text{ L mol}^{-1} \text{ s}^{-1}$$

**Table 19:** Kinetics of the reaction of **2b** with **3e** at 20 °C in THF (stopped-flow,  $\lambda = 638$  nm).

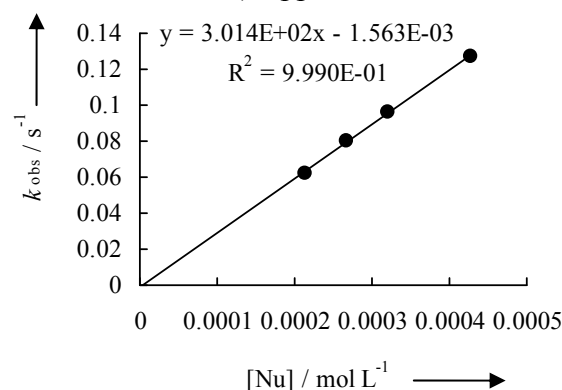
[ <b>3e</b> ] / mol L <sup>-1</sup>	[ <b>2b</b> ] / mol L <sup>-1</sup>	$k_{\text{obs}}$ / s <sup>-1</sup>
$1.61 \times 10^{-5}$	$1.20 \times 10^{-4}$	$9.67 \times 10^{-2}$
	$1.80 \times 10^{-4}$	$1.54 \times 10^{-1}$
	$2.40 \times 10^{-4}$	$2.00 \times 10^{-1}$
	$3.00 \times 10^{-4}$	$2.59 \times 10^{-1}$



$$k = 8.88 \times 10^2 \text{ L mol}^{-1} \text{ s}^{-1}$$

**Table 20:** Kinetics of the reaction of **2b** with **3f** at 20 °C in THF (stopped-flow,  $\lambda = 638$  nm).

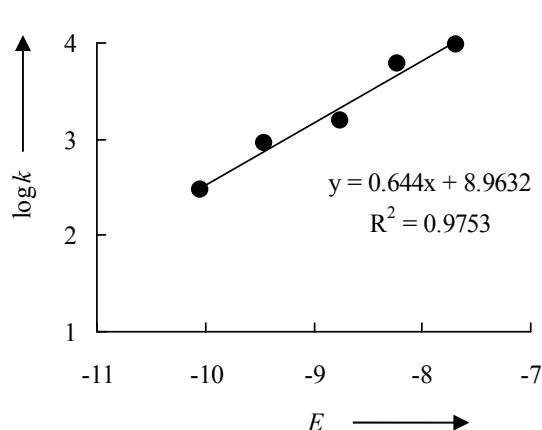
[ <b>3f</b> ] / mol L <sup>-1</sup>	[ <b>2b</b> ] / mol L <sup>-1</sup>	$k_{\text{obs}}$ / s <sup>-1</sup>
$1.67 \times 10^{-5}$	$2.14 \times 10^{-4}$	$6.22 \times 10^{-2}$
	$2.68 \times 10^{-4}$	$7.96 \times 10^{-2}$
	$3.21 \times 10^{-4}$	$9.63 \times 10^{-2}$
	$4.29 \times 10^{-4}$	$1.27 \times 10^{-1}$



$$k = 3.01 \times 10^2 \text{ L mol}^{-1} \text{ s}^{-1}$$

**Table 21:** Determination of the parameters  $N$  and  $s_N$  for **2b** in THF.

Electrophiles	$E$	$k$ ( $M^{-1} s^{-1}$ )
<b>3b</b>	-7.69	$9.60 \times 10^3$
<b>3c</b>	-8.22	$5.95 \times 10^3$
<b>3d</b>	-8.76	$1.53 \times 10^3$
<b>3e</b>	-9.45	$8.88 \times 10^2$
<b>3f</b>	-10.04	$3.01 \times 10^2$



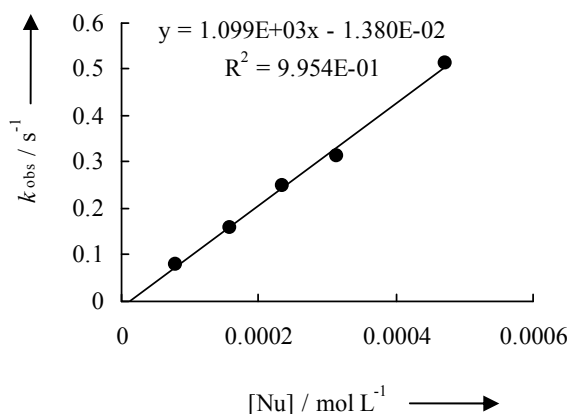
$$N = 13.91$$

$$s_N = 0.64$$

#### 4.4.5 Kinetics of the Reactions of the **2b'** with the Reference Electrophiles **3** in THF.

**Table 22:** Kinetics of the reaction of **2b'** with **3a** at 20 °C in THF (stopped-flow,  $\lambda = 610$  nm).

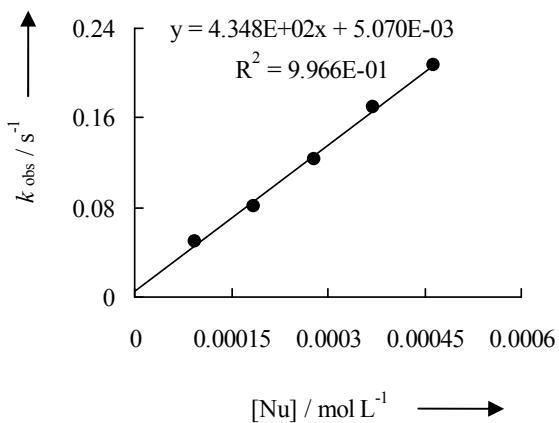
$[3a] / \text{mol L}^{-1}$	$[2b'] / \text{mol L}^{-1}$	$k_{\text{obs}} / \text{s}^{-1}$
$1.34 \times 10^{-5}$	$7.87 \times 10^{-5}$	$7.84 \times 10^{-2}$
	$1.57 \times 10^{-4}$	$1.59 \times 10^{-1}$
	$2.36 \times 10^{-4}$	$2.51 \times 10^{-1}$
	$3.15 \times 10^{-4}$	$3.13 \times 10^{-1}$
	$4.72 \times 10^{-4}$	$5.15 \times 10^{-1}$



$$k = 1.10 \times 10^3 \text{ L mol}^{-1} \text{ s}^{-1}$$

**Table 23:** Kinetics of the reaction of **2b'** with **3b** at 20 °C in THF (stopped-flow,  $\lambda = 620$  nm).

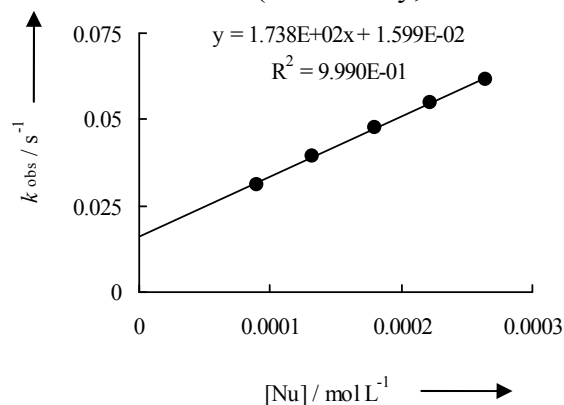
$[3b] / \text{mol L}^{-1}$	$[2b'] / \text{mol L}^{-1}$	$k_{\text{obs}} / \text{s}^{-1}$
$1.27 \times 10^{-5}$	$9.29 \times 10^{-5}$	$4.95 \times 10^{-2}$
	$1.86 \times 10^{-4}$	$8.15 \times 10^{-2}$
	$2.79 \times 10^{-4}$	$1.23 \times 10^{-1}$
	$3.71 \times 10^{-4}$	$1.70 \times 10^{-1}$
	$4.64 \times 10^{-4}$	$2.07 \times 10^{-1}$



$$k = 4.35 \times 10^2 \text{ L mol}^{-1} \text{ s}^{-1}$$

**Table 24:** Kinetics of the reaction of **2b'** with **3c** at 20 °C in THF (diode-array,  $\lambda = 626$  nm).

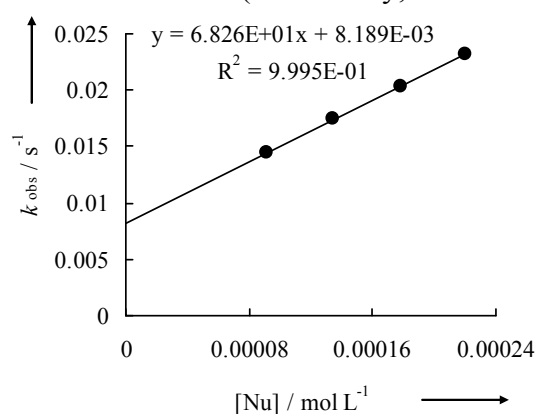
[ <b>3c</b> ] / mol L <sup>-1</sup>	[ <b>5b</b> ] / mol L <sup>-1</sup>	$k_{\text{obs}}$ / s <sup>-1</sup>
$1.93 \times 10^{-5}$	$8.94 \times 10^{-5}$	$3.11 \times 10^{-2}$
$1.39 \times 10^{-5}$	$1.32 \times 10^{-4}$	$3.92 \times 10^{-2}$
$1.43 \times 10^{-5}$	$1.80 \times 10^{-4}$	$4.78 \times 10^{-2}$
$1.41 \times 10^{-5}$	$2.22 \times 10^{-4}$	$5.47 \times 10^{-2}$
$1.40 \times 10^{-5}$	$2.65 \times 10^{-4}$	$6.17 \times 10^{-2}$



$$k = 1.74 \times 10^2 \text{ L mol}^{-1} \text{ s}^{-1}$$

**Table 25:** Kinetics of the reaction of **2b'** with **3d** at 20 °C in THF (diode-array,  $\lambda = 621$  nm).

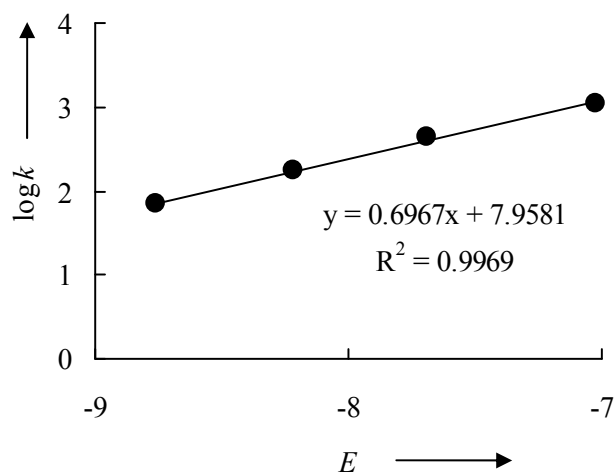
[ <b>3d</b> ] / mol L <sup>-1</sup>	[ <b>2b'</b> ] / mol L <sup>-1</sup>	$k_{\text{obs}}$ / s <sup>-1</sup>
$1.49 \times 10^{-5}$	$9.19 \times 10^{-5}$	$1.44 \times 10^{-2}$
$1.46 \times 10^{-5}$	$1.35 \times 10^{-4}$	$1.75 \times 10^{-2}$
$1.45 \times 10^{-5}$	$1.78 \times 10^{-4}$	$2.03 \times 10^{-2}$
$1.43 \times 10^{-5}$	$2.20 \times 10^{-4}$	$2.32 \times 10^{-2}$



$$k = 6.83 \times 10^1 \text{ L mol}^{-1} \text{ s}^{-1}$$

**Table 26:** Determination of the parameters  $N$  and  $s_N$  for **2b'** in THF.

Electrophiles	$E$	$k$ (M <sup>-1</sup> s <sup>-1</sup> )
<b>3a</b>	-7.02	$1.10 \times 10^3$
<b>3b</b>	-7.69	$4.35 \times 10^2$
<b>3c</b>	-8.22	$1.74 \times 10^2$
<b>3d</b>	-8.76	$6.83 \times 10^1$



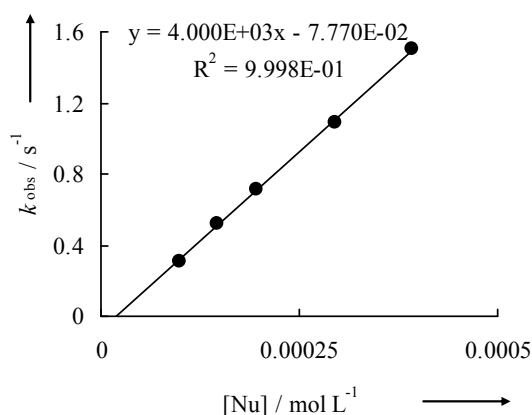
$$N = 11.42$$

$$s_N = 0.70$$

#### 4.4.6 Kinetics of the Reactions of the 2c' with the Reference Electrophiles 3 in THF.

**Table 27:** Kinetics of the reaction of 2c' with 3b at 20 °C in THF (stopped-flow,  $\lambda = 622$  nm).

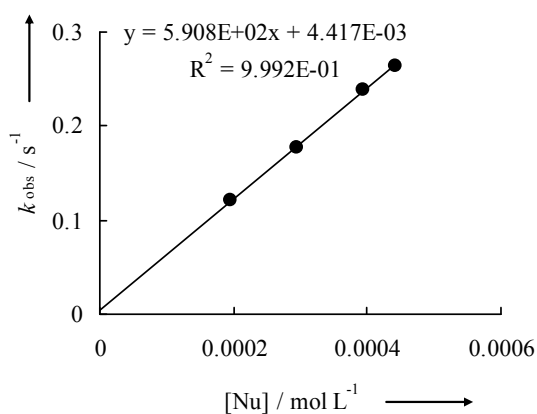
[3b] / mol L <sup>-1</sup>	[2c'] / mol L <sup>-1</sup>	$k_{\text{obs}} / \text{s}^{-1}$
$1.75 \times 10^{-5}$	$9.83 \times 10^{-5}$	$3.12 \times 10^{-1}$
	$1.47 \times 10^{-4}$	$5.17 \times 10^{-1}$
	$1.97 \times 10^{-4}$	$7.13 \times 10^{-1}$
	$2.95 \times 10^{-4}$	1.09
	$3.93 \times 10^{-4}$	1.50



$$k = 4.00 \times 10^3 \text{ L mol}^{-1} \text{ s}^{-1}$$

**Table 28:** Kinetics of the reaction of 2c' with 3d at 20 °C in THF (stopped-flow,  $\lambda = 628$  nm).

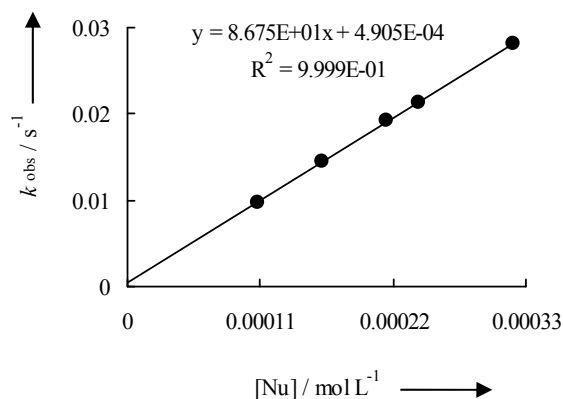
[3d] / mol L <sup>-1</sup>	[2c'] / mol L <sup>-1</sup>	$k_{\text{obs}} / \text{s}^{-1}$
$1.29 \times 10^{-5}$	$1.97 \times 10^{-4}$	$1.21 \times 10^{-1}$
	$2.95 \times 10^{-4}$	$1.77 \times 10^{-1}$
	$3.93 \times 10^{-4}$	$2.39 \times 10^{-1}$
	$4.42 \times 10^{-4}$	$2.64 \times 10^{-1}$



$$k = 5.91 \times 10^2 \text{ L mol}^{-1} \text{ s}^{-1}$$

**Table 29:** Kinetics of the reaction of 2c' with 3f at 20 °C in THF (diode-array,  $\lambda = 636$  nm).

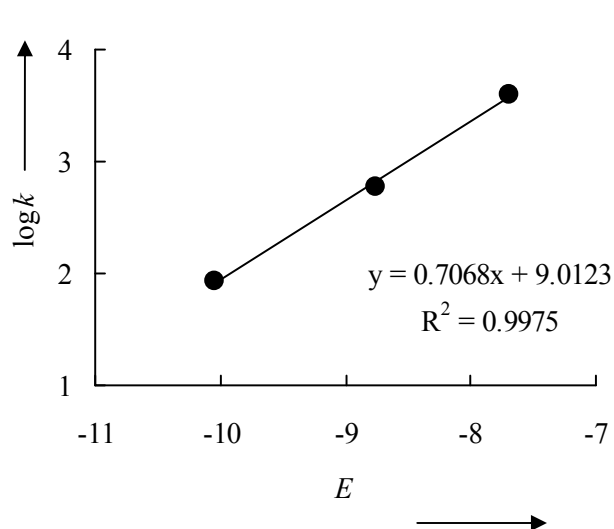
[3f] / mol L <sup>-1</sup>	[2c'] / mol L <sup>-1</sup>	$k_{\text{obs}} / \text{s}^{-1}$
$1.42 \times 10^{-5}$	$1.08 \times 10^{-4}$	$9.82 \times 10^{-3}$
$1.42 \times 10^{-5}$	$1.61 \times 10^{-4}$	$1.44 \times 10^{-2}$
$1.41 \times 10^{-5}$	$2.14 \times 10^{-4}$	$1.92 \times 10^{-2}$
$1.41 \times 10^{-5}$	$2.41 \times 10^{-4}$	$2.13 \times 10^{-2}$
$1.41 \times 10^{-5}$	$3.20 \times 10^{-4}$	$2.82 \times 10^{-2}$



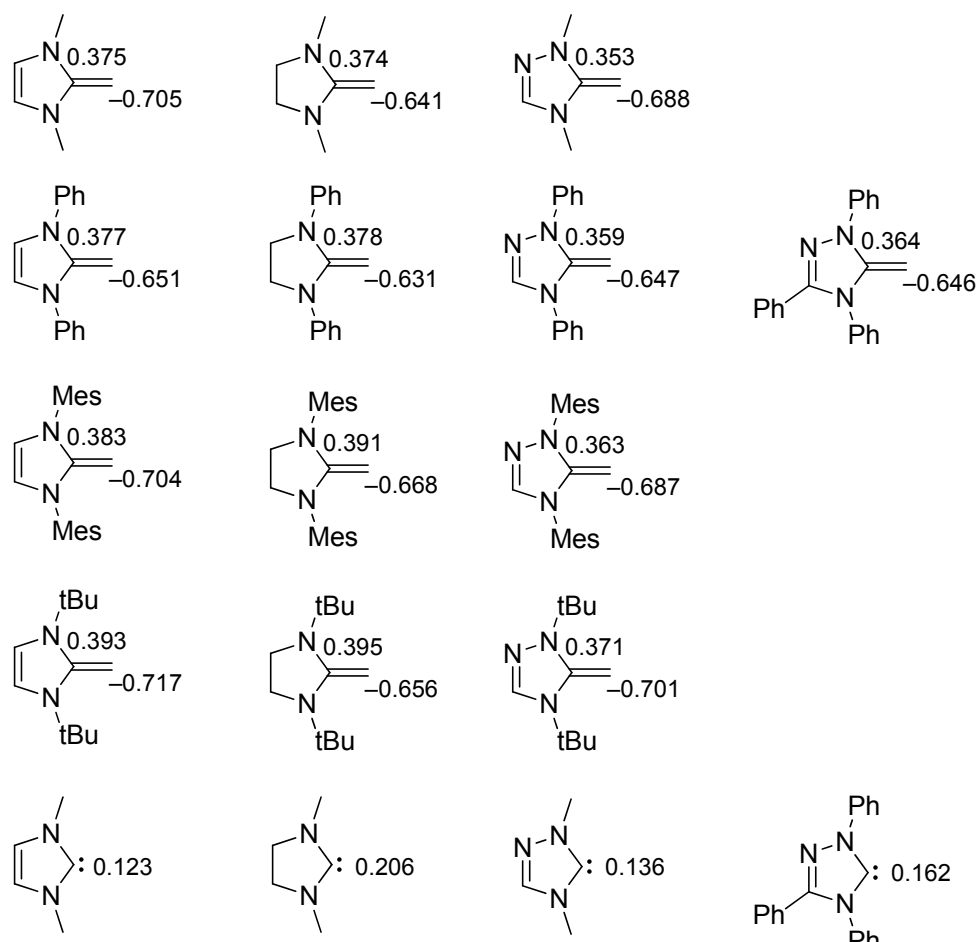
$$k = 8.68 \times 10^1 \text{ L mol}^{-1} \text{ s}^{-1}$$

**Table 30:** Determination of the parameters  $N$  and  $s_N$  for **2c'** in THF.

Electrophiles	$E$	$k$ ( $M^{-1} s^{-1}$ )
<b>3b</b>	-7.69	$4.00 \times 10^3$
<b>3d</b>	-8.76	$5.91 \times 10^2$
<b>3f</b>	-10.04	$8.68 \times 10^1$



**Scheme 7.** Selected NBO-charges of ene-1,1-diamines, carbenes, and carbene-methyl cation-adducts [B98/6-31G(d)].<sup>[a]</sup>



<sup>[a]</sup> Calculations were performed by Dr. M. Horn at Ludwig-Maximilians-Universität München.

## 5 References

- [1] a) First isolation: A. J. Arduengo III, R. L. Harlow, M. Kline, *J. Am. Chem. Soc.* **1991**, *113*, 361–363; b) For physicochemical data of NHCs see: T. Dröge, F. Glorius, *Angew. Chem. Int. Ed.* **2010**, *49*, 6940–6952.
- [2] Umpolung: a) D. Seebach, *Angew. Chem. Int. Ed. Engl.* **1979**, *18*, 239–258; b) X. Bugaut, F. Glorius, *Chem. Soc. Rev.* **2012**, *41*, 3511–3522.
- [3] For reviews of NHC catalyzed reactions see: a) D. Enders, O. Niemeier, A. Henseler, *Chem. Rev.* **2007**, *107*, 5606–5655; b) N. Marion, S. Díez-González, S. P. Nolan, *Angew. Chem. Int. Ed.* **2007**, *46*, 2988–3000; c) V. Nair, S. Vellalath, B. P. Babu, *Chem. Soc. Rev.* **2008**, *37*, 2691–2698; d) P.-C. Chiang, J. W. Bode in *N-Heterocyclic Carbenes: From Laboratory Curiosities to Efficient Synthetic Tools* (Ed.: S. S. Díez-González), Royal Society of Chemistry: Cambridge, **2010**, pp. 399–435; e) K. Zeitler, *Angew. Chem. Int. Ed.* **2005**, *44*, 7506–7510; f) J. L. Moore, T. Rovis, *Top. Curr. Chem.* **2010**, *291*, 77; g) V. Nair, R. S. Menon, A. T. Biju, C. R. Sinu, R. R. Paul, A. Jose, V. Sreekumar, *Chem. Soc. Rev.* **2011**, *40*, 5336–5346; h) A. T. Biju, N. Kuhl, F. Glorius, *Acc. Chem. Res.* **2011**, *44*, 1182–1195.
- [4] a) T. Ukai, R. Tanaka, T. Dokawa, *J. Pharm. Soc. Jpn.* **1943**, *63*, 296–300; b) For an excellent review of asymmetric benzoin condensations (from 1966 to 2003) see: D. Enders, T. Balensiefer, *Acc. Chem. Res.* **2004**, *37*, 534–541.
- [5] H. Stetter, *Angew. Chem. Int. Ed. Engl.* **1976**, *15*, 639–647.
- [6] R. Breslow, *J. Am. Chem. Soc.* **1958**, *80*, 3719–3726.
- [7] a) C. Fischer, S. W. Smith, D. A. Powell, G. C. Fu, *J. Am. Chem. Soc.* **2006**, *128*, 1472–1473; b) S. Matsuoka, Y. Ota, A. Washio, A. Katada, K. Ichioka, K. Takagi, M. Suzuki, *Org. Lett.* **2011**, *13*, 3722–3725; c) A. T. Biju, M. Padmanaban, N. E. Wurcz, F. Glorius, *Angew. Chem. Int. Ed.* **2011**, *50*, 8412–8415; d) R. L. Atienza, H. S. Roth, K. A. Scheidt, *Chem. Sci.* **2011**, *2*, 1772–1776; e) Y. Zhang, E. Y. X. Chen, *Angew. Chem. Int. Ed.* **2012**, *51*, 2465–2469.
- [8] C. E. I. Knappke, A. J. Arduengo, III, H. Jiao, J.-M. Neudörfl, A. J. von Wangelin, *Synthesis* **2011**, 3784–3795.
- [9] B. Maji, M. Breugst, H. Mayr, *Angew. Chem. Int. Ed.* **2011**, *50*, 6915–6919.
- [10] a) A. Berkessel, S. Elfert, K. Etzenbach-Effers, J. H. Teles, *Angew. Chem. Int. Ed.* **2010**, *49*, 7120–7124; b) R. Breslow, R. Kim, *Tetrahedron Lett.* **1994**, *35*, 699–702; c) Y.-T. Chen, G. L. Barletta, K. Haghjoo, J. T. Cheng, F. Jordan, *J. Org. Chem.*

- 1994, 59, 7714–7722; d) M. J. White, F. J. Leeper, *J. Org. Chem.* **2001**, 66, 5124–5131; e) W. Schrader, P. P. Handayani, C. Burstein, F. Glorius, *Chem. Commun.* **2007**, 716–718; f) J. H. Teles, J.-P. Melder, K. Ebel, R. Schneider, E. Gehrler, W. Harder, S. Bode, D. Enders, K. Breuer, G. Raabe, *Helv. Chim. Acta* **1996**, 79, 61–83; g) F. Jordan, Z. H. Kudzin, C. B. Rios, *J. Am. Chem. Soc.* **1987**, 109, 4415–4416; h) L. Pignataro, T. Papalia, A. M. Z. Slawin, S. M. Goldup, *Org. Lett.* **2009**, 11, 1643–1646; i) D. A. DiRocco, K. M. Oberg, T. Rovis, *J. Am. Chem. Soc.* **2012**, 134, 6143–6145.
- [11] For syntheses of 1,1-diaminoalkenes see: a) N. Kuhn, H. Bohnen, J. Kreutzberg, D. Bläser, R. Boese, *J. Chem. Soc., Chem. Commun.* **1993**, 1136–1137; b) A. J. Arduengo III, F. Davidson, H. V. R. Dias, J. R. Goerlich, D. Khasnis, W. J. Marshall, T. K. Prakasha, *J. Am. Chem. Soc.* **1997**, 119, 12742–12749; c) O. Kaufhold, F. E. Hahn, *Angew. Chem. Int. Ed.* **2008**, 47, 4057–4060; d) A. Fürstner, M. Alcarazo, R. Goddard, C. W. Lehmann, *Angew. Chem. Int. Ed.* **2008**, 47, 3210–3214; e) K.-P. Hartmann, M. Heuschmann, *Angew. Chem. Int. Ed. Engl.* **1989**, 28, 1267–1269; f) M. Ernd, M. Heuschmann, H. Zipse, *Helv. Chim. Acta* **2005**, 88, 1491–1518; g) H. Quast, M. Ach, M. K. Kindermann, P. Rademacher, M. Schindler, *Chem. Ber.* **1993**, 126, 503–516; h) H. Quast, M. Ach, J. Balthasar, T. Hergenröther, D. Regnat, J. Lehmann, K. Banert, *Helv. Chim. Acta* **2005**, 88, 1589–1609; i) C. E. I. Knappke, J.-M. Neudörfl, A. J. von Wangelin, *Org. Biomol. Chem.* **2010**, 8, 1695–1705; j) D. Enders, K. Breuer, J. Runsink, J. H. Teles, *Liebigs Ann.* **1996**, 2019–2028.
- [12] a) H. Mayr, T. Bug, M. F. Gotta, N. Hering, B. Irrgang, B. Janker, B. Kempf, R. Loos, A. R. Ofial, G. Remennikov, H. Schimmel, *J. Am. Chem. Soc.* **2001**, 123, 9500–9512; b) R. Lucius, R. Loos, H. Mayr, *Angew. Chem. Int. Ed.* **2002**, 41, 91–95; c) H. Mayr, B. Kempf, A. R. Ofial, *Acc. Chem. Res.* **2003**, 36, 66–77; d) H. Mayr, A. R. Ofial, *Pure Appl. Chem.* **2005**, 77, 1807–1821; e) H. Mayr, *Angew. Chem. Int. Ed.* **2011**, 50, 3612–3618.
- [13] For a comprehensive listing of nucleophilicity parameters  $N$  and electrophilicity parameters  $E$ , see <http://www.cup.lmu.de/oc/mayr/DBintro.html>.
- [14] CCDC 879115 (**2a**), 879114 (**2b**), and 879116 (**4c**) contain the supplementary crystallographic data for this paper. These data can be obtained free of charge from The Cambridge Crystallographic Data Centre via [www.ccdc.cam.ac.uk/data\\_request/cif](http://www.ccdc.cam.ac.uk/data_request/cif).
- [15] Gaussian 09, Revision A.02, M. J. Frisch et al., Gaussian, Inc., Wallingford CT, **2009**.

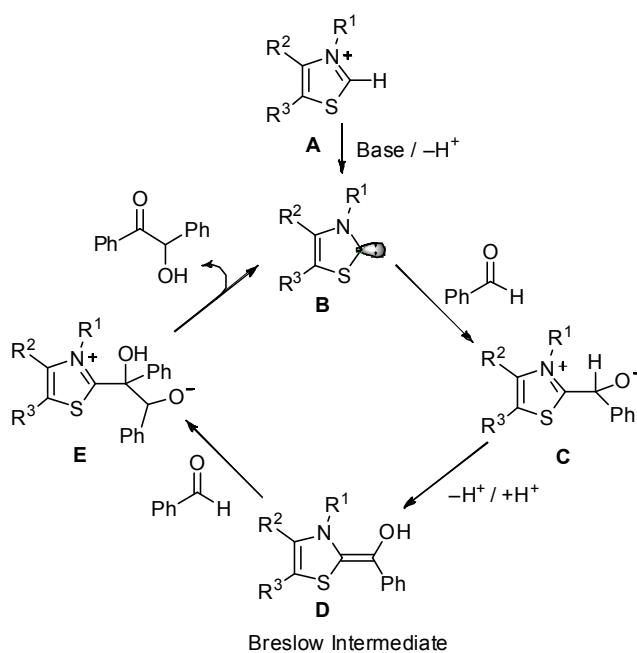
- [16] NICS(1) values (nucleus-independent chemical shift, 1 Å above the ring center) were calculated on the B3LYP/6-311+G(d) level of theory using the Gaussian 09 program package. For selected accounts on aromaticities see: a) P. von R. Schleyer, C. Maerker, A. Dransfeld, H. Jiao, N. J. R. van E. Hommes, *J. Am. Chem. Soc.* **1996**, *118*, 6317–6318; b) P. von R. Schleyer, M. Manoharan, Z. -X. Wang, B. Kiran, H. Jiao, R. Puchta, N. J. R. van E. Hommes, *Org. Lett.* **2001**, *3*, 2465–2468; c) Z. Chen, C. S. Wannere, C. Corminboeuf, R. Puchta, P. von R. Schleyer, *Chem. Rev.* **2005**, *105*, 3842–3888; d) P. von R. Schleyer in *Chemical Reactivity Theory* (Ed.: P. K. Chattaraj), Taylor & Francis/CRC Press, Boca Raton, **2009**, pp. 419–438; e) J. A. N. F. Gomes, R. B. Mallion, *Chem. Rev.* **2001**, *101*, 1349–1383; f) G. Merino, T. Heine, G. Seifert, *Chem. Eur. J.* **2004**, *10*, 4367–4371.
- [17] R. A. Kunetskiy, S. M. Polyakova, J. Vavřík, I. Císařová, J. Saame, E. R. Nerut, I. Koppel, I. A. Koppel, A. Kütt, I. Leito, I. M. Lyapkalo, *Chem. Eur. J.* **2012**, *18*, 3621–3630.
- [18] a) H. Fallah-Bagher-Shaidaei, C. S. Wannere, C. Corminboeuf, R. Puchta, P. v. R. Schleyer, *Org. Lett.* **2006**, *8*, 863–866; b) J. Wu, P. v. R. Schleyer, personal communication.
- [19] a) S. Díez-González, N. Marion, S. P. Nolan, *Chem. Rev.* **2009**, *109*, 3612–3676; b) *N-Heterocyclic Carbenes in Synthesis* (Ed. S. P. Nolan), Wiley-VCH, Weinheim, **2006**; c) V. César, S. Bellemin-Laponnaz, L. H. Gade, *Chem. Soc. Rev.* **2004**, *33*, 619–636; d) S. Würtz, F. Glorius, *Acc. Chem. Res.* **2008**, *41*, 1523–1533; e) F. E. Hahn, M. C. Jahnke, *Angew. Chem. Int. Ed.* **2008**, *47*, 3122–3172; f) G. C. Vougioukalakis, R. H. Grubbs, *Chem. Rev.* **2010**, *110*, 1746–1787; g) M. J. Fuchter, *Chem. Eur. J.* **2010**, *16*, 12286–12294; h) K. Lee, A. R. Zhugralin, A. H. Hoveyda, *J. Am. Chem. Soc.* **2009**, *131*, 7253–7255; i) J. M. O'Brien, A. H. Hoveyda, *J. Am. Chem. Soc.* **2011**, *133*, 7712–7715.
- [20] a) L. Hintermann, *Beilstein Journal of Organic Chemistry* **2007**, *3*, No. 22. doi:10.1186/1860-5397-3-22; b) K. M. Kuhn, R. H. Grubbs, *Org. Lett.* **2008**, *10*, 2075–2077; c) D. Enders, K. Breuer, U. Kallfass, T. Balensiefer, *Synthesis*, **2003**, 1292–1295.

## Chapter 7

Structures and Reactivities of O-Methylated  
Breslow IntermediatesB. Maji, H. Mayr, *Angew. Chem. Int. Ed.* **2012**, DOI: 10.1002/anie.201204524.

## 1 Introduction

Since the first report by Ukai in 1943,<sup>[1]</sup> thiamine and related thiazolium ions **A** have been known to catalyze umpolung (reversal of polarity)<sup>[2]</sup> reactions of aldehydes. The mechanism generally accepted for these reactions was proposed by Breslow in 1958,<sup>[3]</sup> when he described that the thiazolium ring first undergoes deprotonation at the most acidic position to give an ylide or carbene **B**. The subsequent nucleophilic addition of **B** to an aldehyde generates the zwitterion **C** which undergoes a proton shift to give the Breslow intermediate **D**, a nucleophilic acyl anion equivalent. Its reaction with a second molecule of aldehyde followed by a proton shift and release of **B** generates the benzoin.<sup>[3]</sup>

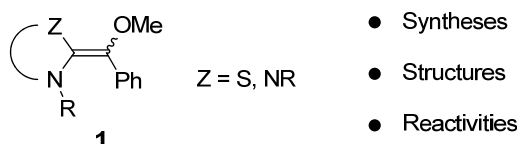


**Scheme 1.** Breslow's mechanistic proposal for thiazole-ylidene catalyzed benzoin condensation reaction.

The first isolation and characterization of stable N-heterocyclic carbenes by Arduengo in 1991<sup>[4]</sup> has triggered extensive investigations on the use of these species for umpolung reactions of aldehydes and also for the umpolung of  $\alpha,\beta$ -unsaturated aldehydes and related compounds.<sup>[5,6]</sup> However, our knowledge of structure and reactivity of Breslow intermediates has so far predominantly been based on theoretical investigations<sup>[7]</sup> since attempts to isolate Breslow intermediates or their O-protected derivatives have been unsuccessful.<sup>[7c,8]</sup>

In 1987, O-protected Breslow intermediates derived from thiazoles were generated by Jordan et al. in *d*<sub>5</sub>-pyridine solution and characterized by <sup>1</sup>H NMR spectroscopy.<sup>[9a]</sup> Three years later, Bordwell, Jordan, and coworkers determined the pK<sub>aH+</sub> values of the conjugate acids.<sup>[9b]</sup> Recently, Berkessel et al. characterized the keto form of the Breslow intermediate derived from 1,2,4-triphenyltriazol-5-ylidene.<sup>[7c]</sup> While the authors succeeded to identify a spiro-dioxolane as the resting state of the catalytic system, the enol form of the Breslow intermediate could neither be identified nor trapped.<sup>[7c]</sup>

Since the presence of the enol group makes the intermediates (**D**) inherently unstable and difficult to isolate or characterize, Rovis et al. recently replaced the enol moiety by a methylphenylamino group which allowed them to isolate and characterize aza-analogues of the Breslow intermediates derived from chiral triazole carbenes.<sup>[10]</sup> We now report on the synthesis of O-methylated Breslow intermediates **1** derived from thiazole, imidazole, and triazole carbene families and benzaldehyde, which can be considered to be the closest relatives of Breslow intermediates that can be handled as stable entities (Scheme 2).

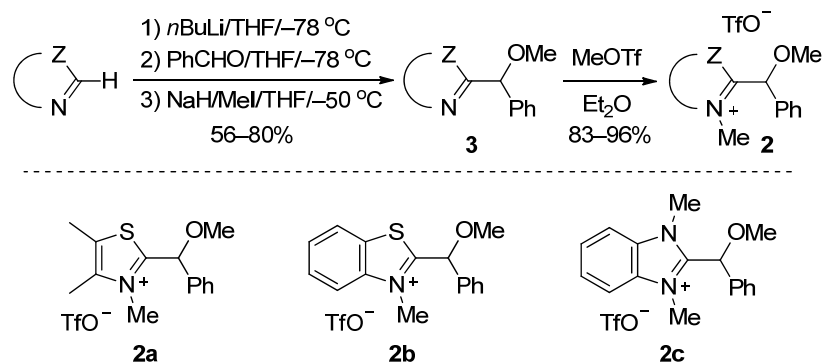


**Scheme 2.** O-methylated Breslow intermediates **1**.

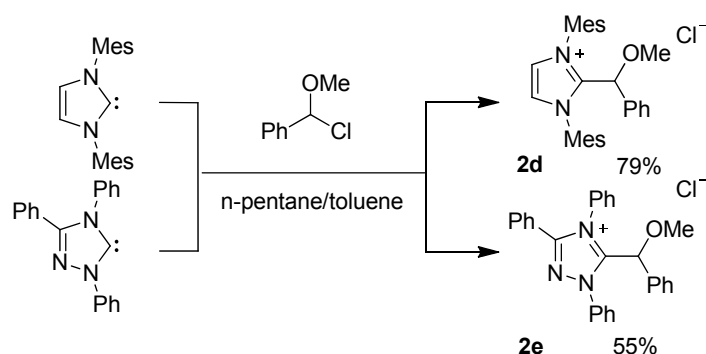
## 2 Results and Discussion

The N-alkyl substituted azolium triflates **2a-c**, precursors of **1a-c**, were readily accessible by quaternization of the nitrogen atom of **3** with MeOTf in Et<sub>2</sub>O (Scheme 3).<sup>[11]</sup>

The N-aryl substituted azolium chlorides **2d,e** were synthesized by slow addition of diluted *n*-pentane/toluene solutions of the corresponding carbenes into *n*-pentane/toluene solutions of (chloro(methoxy)methyl)benzene which was generated from benzaldehyde dimethyl acetal and acetyl chloride in toluene (Scheme 4).

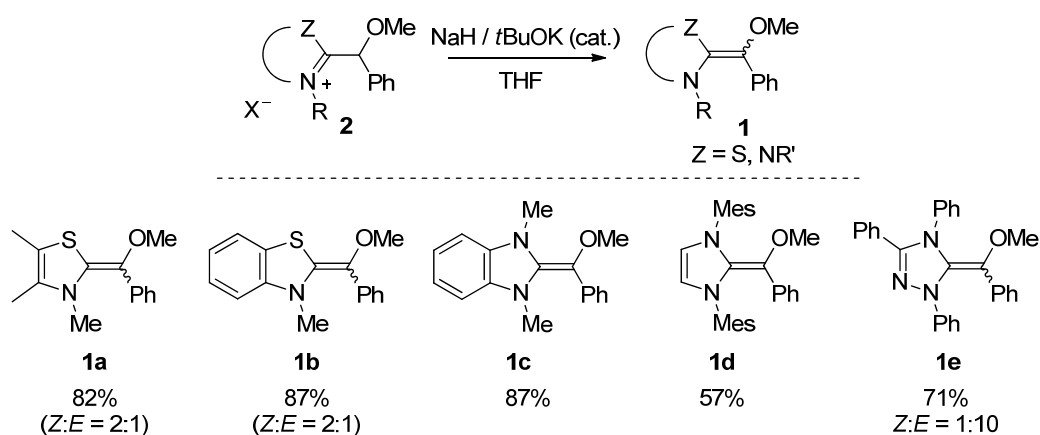


**Scheme 3.** Synthesis of the N-alkyl substituted azolium triflates **2a-c**.



**Scheme 4.** Synthesis of the N-aryl substituted azolium chlorides **2d,e**.

Treatment of the azolium salts **2** with NaH in the presence of catalytic amounts of *t*BuOK in dry THF followed by evaporation of THF and extraction of the organic materials with dry toluene yielded the O-methylated Breslow intermediates **1a-e** which can be stored in an argon-filled glove box at  $-30\text{ }^\circ\text{C}$  for several weeks without significant decomposition.



**Scheme 5.** Synthesis of the O-protected Breslow intermediates **1a-e**.

The thiazole derivatives **1a,b** are formed as mixtures of *Z* and *E* isomers (ratio *Z* : *E* = 2 : 1 in  $\text{C}_6\text{D}_6$  solution, NOESY)<sup>[9a]</sup> and the triazole derivative **1e** is formed as *Z* : *E* = 1 : 10 mixture.

The olefinic character of these species is revealed by  $^{13}\text{C}$  NMR resonances at  $\delta = 135\text{--}145$  ppm for NCZ and at  $\delta = 114\text{--}128$  ppm for  $\text{C}\text{--}\text{OMe}$ . X-ray crystallographic analyses of *Z*-**1a** and *E*-**1e**<sup>[12]</sup> show that the exocyclic double bond adopts a planar geometry with bond lengths (**1a** = 134.9 pm and **1e** = 135.8 pm) as in the corresponding deoxy-Breslow intermediates ( $\approx 136$  pm)<sup>[13]</sup> and their aza-analogues (136 pm).<sup>[10]</sup> The  $\text{S}\cdots\text{O}$  distance in **1a** (285.0 pm) is shorter than the sum of their van der Waals radii (332 pm) suggesting an intramolecular non-bonded 1,4-S $\cdots$ O interaction which might be responsible for the preferred configuration (*Z*-isomer) in the solid state.<sup>[14]</sup> In both compounds, the phenyl ring is slightly twisted ( $28^\circ$  in **1a** and  $37^\circ$  in **1e**), and the O-methyl group is almost perpendicularly oriented to the exocyclic double bond, as it is seen for the OH-group in the quantum chemically calculated structures of their non-protected analogues.<sup>[15]</sup>

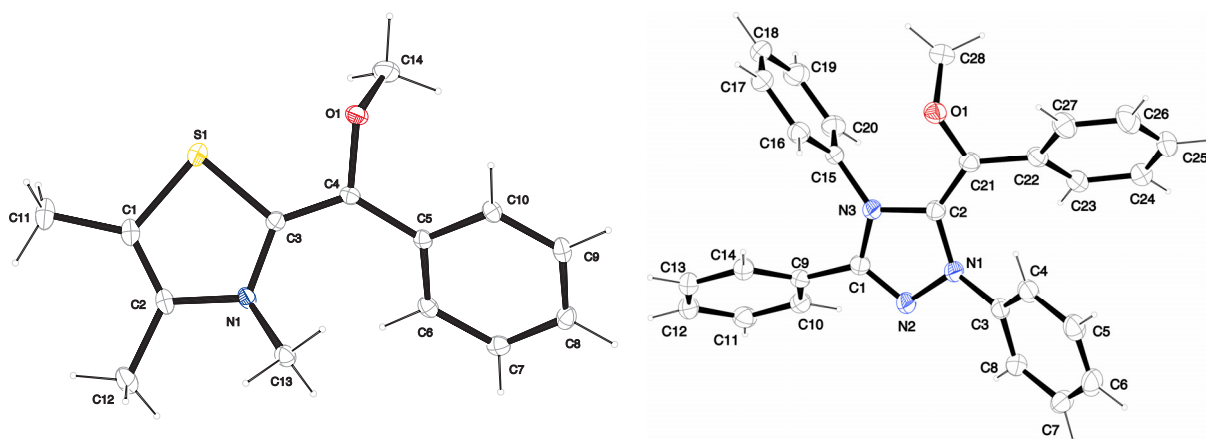


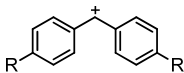
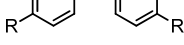
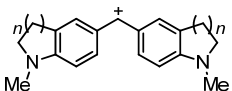
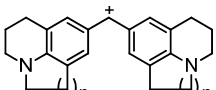
**Figure 1.** Crystal structures of *Z*-**1a** (left) and *E*-**1e** (right). Ellipsoids are shown at the 50% probability level. Selected bond lengths (pm) and angles ( $^\circ$ ): **1a**: C3-C4 = 134.9, S1-O1 = 285.0, C3-C4-O1 = 114.1, S1-C3-C4 = 120.6, S1-C3-C4-O1 = 13.4, N1-C3-C4-C5 = 14.8, C3-C4-O1-C14 =  $-110.2$ , C3-C4-C5-C6 = 28.4. **1e**: C2-C21 = 135.8, N2-N1-C3 = 116.3, C2-N1-C3 = 129.1, N3-C2-C21-O1 = 18.7, N1-C2-C21-C22 = 11.7, C2-C21-O1-C28 =  $-116.4$ , C2-C21-C22-C23 = 37.1.

In order to elucidate the relationship between structure and reactivity we have studied the kinetics of the reactions of the O-methylated Breslow intermediates **1** with the stabilized benzhydrylium ions **4a-g** (Table 1) which have previously been used to develop the most comprehensive nucleophilicity scale presently available on the basis of equation (1).<sup>[16]</sup> Herein, nucleophiles are characterized by two solvent dependent parameters (nucleophilicity parameter  $N$  and sensitivity parameter  $s_N$ ), electrophiles are characterized by one solvent

independent parameter (electrophilicity  $E$ ), and  $k$  is the second-order rate constant at 20 °C.<sup>[16]</sup>

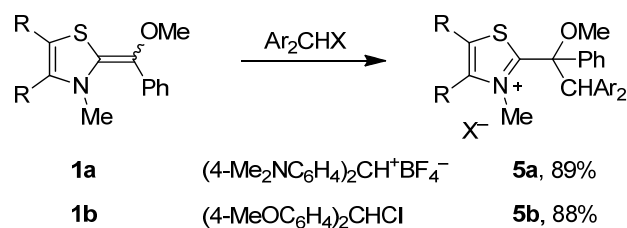
$$\log k = s_N(N + E) \quad (1)$$

**Table 1.** Benzhydrylium Ions **4a–g** Employed as Reference Electrophiles in this Work.

Electrophile	$E^{[a]}$
	R = N(CH <sub>2</sub> CH <sub>2</sub> ) <sub>2</sub> O <b>4a</b> -5.53
	R = NMe <sub>2</sub> <b>4b</b> -7.02
	R = N(CH <sub>2</sub> ) <sub>4</sub> <b>4c</b> -7.69
	$n = 2$ <b>4d</b> -8.22
	$n = 1$ <b>4e</b> -8.76
	$n = 2$ <b>4f</b> -9.45
	$n = 1$ <b>4g</b> -10.04

[a] Electrophilicity parameters  $E$  for **4a–g** from ref. [16a].

Representative combinations of the O-methylated Breslow intermediates **1a,b** with diarylcarbenium tetrafluoroborates or chlorides **4**<sup>[17]</sup> showed that the electrophiles attack at the exocyclic double bond to give the azolium salts **5a,b** which were isolated and characterized.



**Scheme 6.** Reactions of **1a,b** with diarylcarbenium ions.

The rates of the reactions of **1** with the electrophiles **4** were measured photometrically by following the decay of the absorbances of **4** in dry THF at 20 °C using a stopped-flow instrument as described previously.<sup>[16]</sup> A large excess of **1** was used in order to achieve pseudo-first-order conditions. Except for the reaction of **1b** with **4b** and **4c**, the benzhydrylium ions **4** were consumed completely in all reaction investigated. The end absorbances of **4b** and **4c** observed with variable concentrations of **1c** were used to calculate the equilibrium constants given in footnotes [b] and [c] of Table 2. The first-order rate

constants ( $k_{\text{obs}}$  in  $\text{s}^{-1}$ ) were obtained by least-squares fitting of the function  $A = A_0 e^{-k_{\text{obs}}t} + C$  to the decays of the absorbances. As shown in the insert of Figure 2, plots of  $k_{\text{obs}}$  against the concentrations of **1** were linear with slopes corresponding to the second-order rate constants  $k$  ( $\text{M}^{-1} \text{s}^{-1}$ ), which are listed in Table 2.

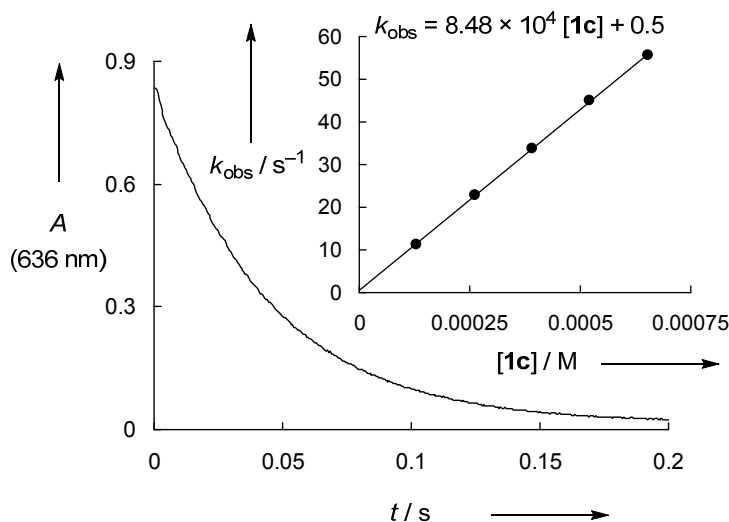


**Figure 2.** Exponential decay of the absorbance at 636 nm during the reaction of **4f** ( $1.46 \times 10^{-5} \text{ M}$ ) with **1c** ( $2.61 \times 10^{-4} \text{ M}$ ) at  $20^\circ \text{C}$  in THF ( $k_{\text{obs}} = 22.8 \text{ s}^{-1}$ ). Insert: Determination of the second-order rate constant  $k = 8.48 \times 10^4 \text{ M}^{-1} \text{ s}^{-1}$  from the dependence of  $k_{\text{obs}}$  on the concentration of **1c**.

The plots of  $\log k$  against the empirical electrophilicity parameters  $E$  of the diarylcarbenium ions **4** are linear (Figure 3), indicating that equation (1) can be used to derive the  $N$  and  $s_N$  parameters of the O-methylated Breslow intermediates **1** (Table 2).

The different slopes of the correlation lines in Figure 3 imply that the relative reactivities of the electron-rich  $\pi$ -systems **1** depend slightly on the electrophilicity of the reaction partners. As none of the reference electrophiles **4a-g** has been investigated with respect to all nucleophiles listed in Table 2, the correlations for **1a** and **1c** have been extrapolated to obtain rate constants for their reactions with **4c**, which are compared with directly measured rate constants in Scheme 7.

**Table 2.** Second-Order Rate Constants  $k$  ( $\text{M}^{-1} \text{s}^{-1}$ ) for the Reactions of the O-Methylated-Breslow-Intermediates **1** and the Deoxy-Breslow intermediate **6** with the Reference Electrophiles **4** in THF at 20 °C.

Nucleophile	$N, s_N$ <sup>[a]</sup>	Electrophile	$k / \text{M}^{-1} \text{s}^{-1}$
<b>1a</b>	14.77, 0.80	<b>4d</b>	$1.93 \times 10^5$
		<b>4e</b>	$5.22 \times 10^4$
		<b>4f</b>	$2.28 \times 10^4$
		<b>4g</b>	$5.67 \times 10^3$
<b>1b</b>	10.45, 0.81	<b>4a</b>	$9.26 \times 10^3$
		<b>4b</b>	$5.63 \times 10^2$ <sup>[b]</sup>
		<b>4c</b>	$1.71 \times 10^2$ <sup>[c]</sup>
<b>1c</b>	16.61, 0.68	<b>4d</b>	$5.88 \times 10^5$
		<b>4e</b>	$1.64 \times 10^5$
		<b>4f</b>	$8.48 \times 10^4$
		<b>4g</b>	$2.89 \times 10^4$
<b>1e</b>	15.65, 0.52	<b>4c</b>	$1.16 \times 10^4$
		<b>4d</b>	$9.85 \times 10^3$
		<b>4e</b>	$2.67 \times 10^3$
		<b>4f</b>	$1.52 \times 10^3$
		<b>4g</b>	$8.61 \times 10^2$
<b>6</b>	15.58, 0.57	<b>4c</b>	$2.79 \times 10^4$
		<b>4d</b>	$2.20 \times 10^4$
		<b>4e</b>	$6.09 \times 10^3$
		<b>4f</b>	$3.31 \times 10^3$

[a]  $N$  and  $s_N$  as defined by Equation (1). [b] Estimated equilibrium constant  $(3-5) \times 10^3 \text{M}^{-1}$ . [c] Estimated equilibrium constant  $(1-5) \times 10^2 \text{M}^{-1}$ .

Scheme 7 shows that the methyl-protected Breslow intermediate **1b** is 163 times less reactive than its deoxy analogue **6**<sup>[18]</sup> due to the inductive electron withdrawing effect of the methoxy group, which destabilizes the positively charged thiazolium ion formed by electrophilic attack. Thus, the mesomeric electron donating effect of the methoxy group, which raises the HOMO of **1b** relative to **6**, does not lead to an increase of  $k_{\text{rel}}$  (and of  $N$ ) but to an increase of the sensitivity  $s_N$ , which implies that the reactivity ratio **6/1b** decreases with increasing electrophilicity of the reaction partner. Analogous effects have previously been observed for ordinary alkenes<sup>[16c,19]</sup> and enol ethers.<sup>[16f]</sup>

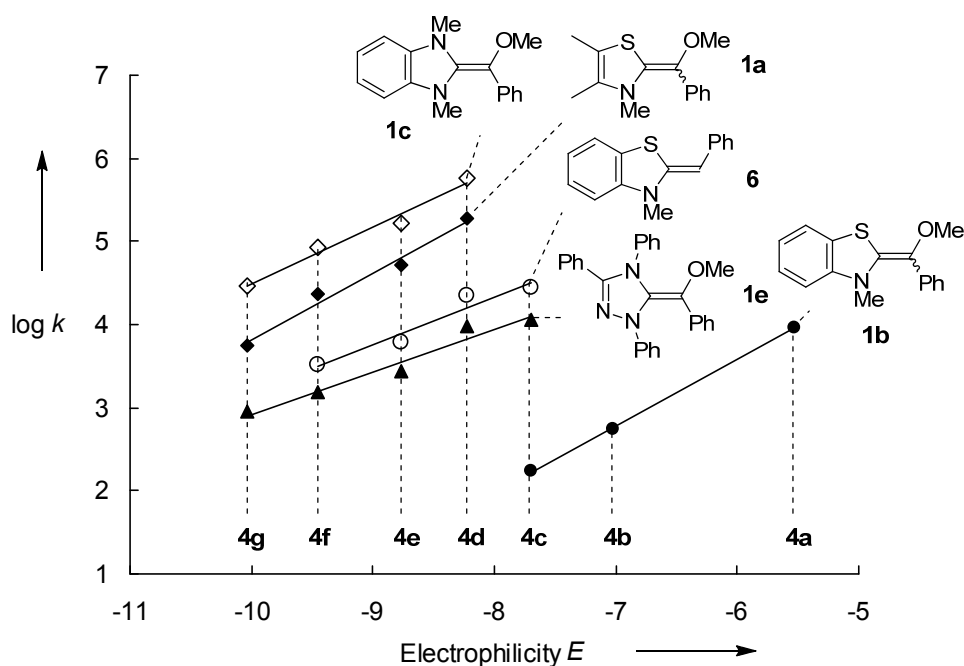
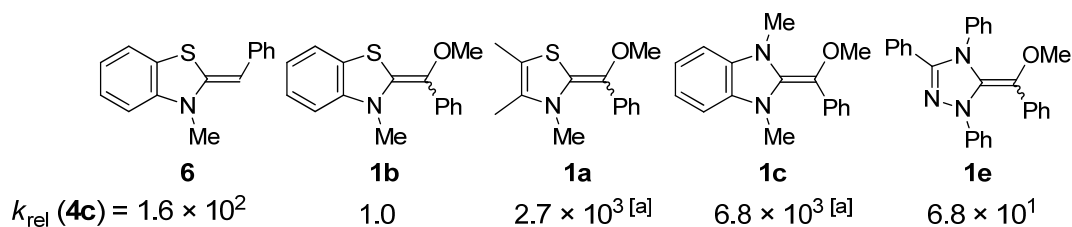


**Figure 3.** Plot of  $\log k$  (Table 2) for the reactions of **1** with the electrophiles **4** in THF at 20 °C versus the corresponding electrophilicity parameters  $E$  (Table 1).



**Scheme 7.** Relative reactivities of the O-methylated Breslow intermediates **1** and comparison with **6** (towards **4c**, THF, 20 °C). [a] From rate constant calculated by using equation (1),  $N$  and  $s_N$  from Table 2, and  $E(\mathbf{4c})$  from Table 1.

Scheme 7 also shows that replacement of the benzoannulated ring by two methyl groups (**1b**  $\rightarrow$  **1a**) increases the nucleophilic reactivity by a factor of 2700. An even higher activation (factor 6800) is observed when the sulphur atom in **1b** is replaced by the better mesomeric electron donor NMe (**1b**  $\rightarrow$  **1c**). The 100-fold lower reactivity of the triazole carbene-derived Breslow-intermediate (**1c**  $\rightarrow$  **1e**) can be explained by the electron withdrawing effect of the extra nitrogen as well as by the phenyl rings.

### 3 Conclusion

In conclusion, we have developed a method to synthesize and isolate stable O-methylated Breslow intermediates **1**, derived from the thiazole, imidazole and triazole carbene families and benzaldehyde, by deprotonation of the corresponding azolium salts **2**. This allowed us to perform structural analyses of these model systems in the solid state and to derive their nucleophilic reactivities from the kinetics of their reactions with stabilized benzhydrylium ions **3**. If the ratios **1b/6** and **1c/1b** are considered to be representative, one can conclude that O-methylated Breslow intermediates are  $10^2$  times less nucleophilic than the corresponding deoxy-Breslow intermediates and that Breslow intermediates derived from thiazoles are  $10^3$ - $10^4$  times less reactive than those derived from structurally analogous imidazoles.

## 4 Experimental Section

### 4.1 General

#### *Chemicals.*

1,3-Dimesitylimidazolium-2-ylidene,<sup>[20a,b]</sup> and 1,2,4-triphenyltriazol-5-ylidene<sup>[20c]</sup> were synthesized according to literature procedures. Benzhydrylium tetrafluoroborates **4a-g** and 4,4'-(chloromethylene)bis(methoxybenzene) were prepared as described before.<sup>[16a]</sup>

For synthetic studies: Commercially available THF (Sigma-Aldrich, p.a.) was distilled over sodium prior to use. Toluene and *n*-pentane were distilled over sodium and stored over molecular sieve (3 Å). Commercially available CH<sub>3</sub>CN (Sigma-Aldrich, puriss) was distilled over CaH<sub>2</sub> and stored over molecular sieve (3 Å). CH<sub>2</sub>Cl<sub>2</sub> was distilled over CaH<sub>2</sub> prior to use.

For kinetic studies: THF (Acros organics, 99.5%, Extra dry, Over Molecular Sieve, Stabilized, Aero seal) was purchased and used without further purification.

#### *Analytics.*

<sup>1</sup>H- and <sup>13</sup>C-NMR spectra were recorded on Varian NMR-systems (300, 400, and 600 MHz) in C<sub>6</sub>D<sub>6</sub>, *d*<sub>8</sub>-THF, CD<sub>3</sub>CN, *d*<sub>6</sub>-DMSO and CDCl<sub>3</sub>, and the chemical shifts in ppm refer to the solvent residual signal as internal standard ( $\delta_{\text{H}}(\text{C}_6\text{D}_6) = 7.16$ ,  $\delta_{\text{C}}(\text{C}_6\text{D}_6) = 128.4$ ; ( $\delta_{\text{H}}(\textit{d}_8\text{-THF}) = 1.73$ ,  $\delta_{\text{C}}(\textit{d}_8\text{-THF}) = 25.4$ ;  $\delta_{\text{H}}(\text{CD}_3\text{CN}) = 1.94$ ,  $\delta_{\text{C}}(\text{CD}_3\text{CN}) = 1.4$ ;  $\delta_{\text{H}}(\textit{d}_6\text{-DMSO}) = 2.50$ ,  $\delta_{\text{C}}(\textit{d}_6\text{-DMSO}) = 39.5$ ;  $\delta_{\text{H}}(\text{CDCl}_3) = 7.24$ ,  $\delta_{\text{C}}(\text{CDCl}_3) = 77.2$ ). The following abbreviations were used for chemical shift multiplicities: brs = broad singlet, s = singlet, d = doublet, t = triplet, q = quartet, m = multiplet. The <sup>1</sup>H-NMR signals of AA'BB'-spin systems of *p*-disubstituted

benzene rings are treated as doublets. NMR signal assignments are based on additional 2D-NMR experiments (COSY, HSQC, HMBC, and NOESY). HR-MS has been performed on a *Finnigan MAT 95* (EI) or a *Thermo Finnigan LTQ FT* (ESI) mass spectrometer. Melting points were determined on a *Büchi B-540* device and are not corrected. An IR spectrometer (*Spectrum BX* from *Perkin Elmer*) with an ATR unit (attenuated total reflection; Dura Sampler Diamond ATR from Smiths Detection) was used to record the IR spectra of neat compounds. UV-vis spectra in THF were recorded with J&M TIDAS diode array spectrophotometer (resolution: 0.8 nm) that was connected to a Hellma 661.502-QX quartz Suprasil immersion probe (5 mm light path) via fiber optic cables and standard SMA connectors.

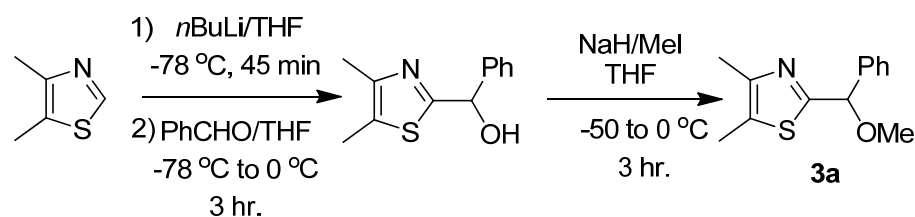
### *Kinetics.*

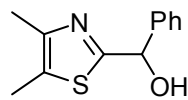
The rates of all investigated reactions were determined photometrically using oven dry glass apparatus under nitrogen atmosphere. The temperature of the solutions during all kinetic studies was kept constant ( $20.0 \pm 0.1^\circ\text{C}$ ) by using a circulating bath thermostat. The kinetic experiments were carried out with freshly prepared stock solutions of the O-methylated-Breslow-intermediates **1** or deoxy-Breslow intermediate **6** in dry THF. Due to low solubility of the benzhydrylium tetrafluoroborates (**4a-g**)- $\text{BF}_4$  in THF, these stock solutions were prepared in dry THF containing ~1–5% of DMSO as cosolvent. First-order kinetics were achieved by employing more than 6 equiv. of the nucleophiles **1**. Fast kinetics ( $\tau_{1/2} < 25\text{-}30$  s) were evaluated on the spectrophotometer system Applied Photophysics SX.18MV-R stopped-flow reaction analyser.

Rate constants  $k_{\text{obs}}$  ( $\text{s}^{-1}$ ) were obtained by fitting the single exponential  $A_t = A_0 \exp(-k_{\text{obs}}t) + C$  (exponential decrease) to the observed time-dependent absorbance (averaged from at least 5 kinetic runs for each nucleophile concentration).

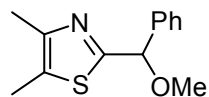
## 4.2 Synthesis of 2-(methoxy(phenyl)methyl)-azoles (**3a-c**)

### 4.2.1 Synthesis of 2-(methoxy(phenyl)methyl)-4,5-dimethylthiazole (**3a**)

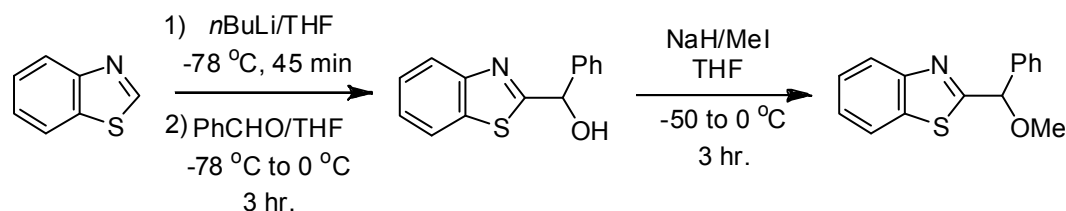


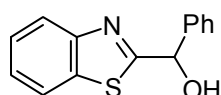
**(4,5-Dimethylthiazol-2-yl)(phenyl)methanol**

To a stirred solution of 4,5-dimethylthiazole (2.14 g, 18.9 mmol) in dry THF (10 mL) at  $-78\text{ }^{\circ}\text{C}$  was dropwise added 9.0 mL of *n*BuLi (2.5 M in THF, 23 mmol) under nitrogen. The reaction mixture was allowed to stir for 45 min before a solution of benzaldehyde (5.86 g, 55.2 mmol) in THF (7 mL) was added dropwise. The mixture was stirred at  $-78\text{ }^{\circ}\text{C}$  for 2 h and then allowed to warm to  $0\text{ }^{\circ}\text{C}$  over 1 h before it was quenched with 20 mL of water. The organic phase was separated and the aqueous phase was extracted with ethyl acetate ( $3 \times 20\text{ mL}$ ). The combined organic phases were dried with anhydrous  $\text{Na}_2\text{SO}_4$ , and concentrated in vacuum. The crude product was purified by crystallization from EtOAc-*n*-pentane mixture to give 3.55 g (16.2 mmol, 86%) of the title compound. Spectroscopic data are in accordance with the literature [8a].

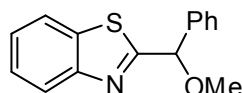
**2-(Methoxy(phenyl)methyl)-4,5-dimethylthiazole (3a)**

To a stirred suspension of NaH (0.24 g, 10 mmol) in dry THF (7 mL) at  $-50\text{ }^{\circ}\text{C}$  was added a solution of 4,5-dimethylthiazol-2-yl)(phenyl)methanol (1.10 g, 5.02 mmol) in THF (6 mL) under nitrogen. The reaction mixture was allowed to stir for 30 min, before MeI (0.375 mL, 851 mg, 6.00 mmol) was added. The mixture was then allowed to warm to room temperature over 2.5 h and quenched with 10 mL of water. The organic phase was separated and the aqueous phase was extracted with ethyl acetate ( $4 \times 10\text{ mL}$ ). The combined organic phases were dried with anhydrous  $\text{Na}_2\text{SO}_4$ , and concentrated in vacuum. The crude product was purified by column chromatography on silica gel using EtOAc-*n*-pentane as eluent to give 1.09 g (4.67 mmol, 93%) of the title compound. Mp:  $59\text{--}60\text{ }^{\circ}\text{C}$  (EtOAc-*n*-pentane).  $^1\text{H-NMR}$  ( $\text{CDCl}_3$ , 400 MHz):  $\delta = 2.27, 2.27$  (2 s, 6 H,  $\text{CH}_3$ ), 3.43 (s, 3 H,  $\text{OCH}_3$ ), 5.44 (s, 1 H,  $\text{CHPh}$ ), 7.26-7.29 (m, 1 H, Ar), 7.31-7.35 (m, 2 H, Ar), 7.42-7.45 (m, 2 H, Ar) ppm.  $^{13}\text{C-NMR}$  ( $\text{CDCl}_3$ , 100 MHz):  $\delta = 11.5$  (q,  $\text{CH}_3$ ), 14.9 (q,  $\text{CH}_3$ ), 57.7 (q,  $\text{OCH}_3$ ), 83.3 (d,  $\text{CHPh}$ ), 127.0 (d, Ar), 127.3 (s), 128.4 (d, Ar), 128.8 (d, Ar), 140.1 (s, Ar), 147.9 (s), 167.6 (s, NCS) ppm. HRMS (ESI positive):  $m/z$  calculated for  $[\text{C}_{13}\text{H}_{16}\text{NOS}]^+$  is 234.0947; found 234.0948.

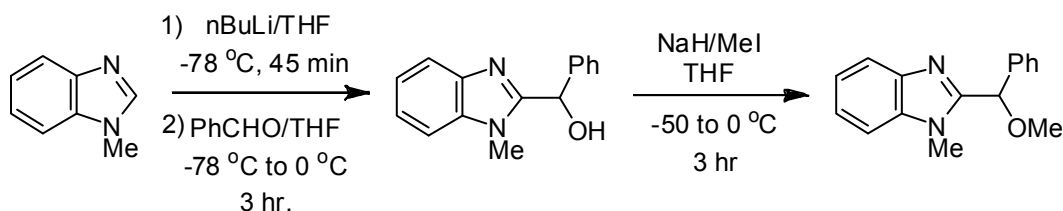
**2.2 Synthesis of 2-(methoxy(phenyl)methyl)benzo[d]thiazole (3b)**

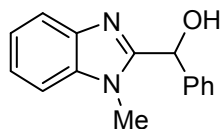
**Benzo[d]thiazol-2-yl(phenyl)methanol**

To a stirred solution of benzothiazole (2.7 g, 20 mmol) in dry THF (10 mL) at  $-78^{\circ}\text{C}$  was dropwise added 11.5 mL of *n*BuLi (2.1 M in hexane, 24 mmol) under nitrogen. The reaction mixture was allowed to stir for 45 min before a solution of benzaldehyde (2.65 g, 25.0 mmol) in THF (10 mL) was added dropwise. The mixture was stirred at  $-78^{\circ}\text{C}$  for 2 h and then allowed to warm to  $0^{\circ}\text{C}$  over 1 h before it was quenched with 20 mL of water. The organic phase was separated and the aqueous phase was extracted with ethyl acetate ( $3 \times 20$  mL). The combined organic phases were dried with anhydrous  $\text{Na}_2\text{SO}_4$ , and concentrated in vacuum. The crude product was purified by crystallization from EtOAc-*n*-pentane mixture to give 3.47 g (14.3 mmol, 72%) of the title compound. Spectroscopic data are in accordance with the literature [21a].

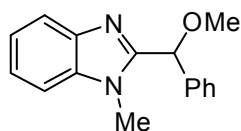
**2-(Methoxy(phenyl)methyl)benzo[d]thiazole (3b)**

To a stirred suspension of NaH (0.22 g, 9.2 mmol) in dry THF (7 mL) at  $-50^{\circ}\text{C}$  was added a solution of benzo[d]thiazol-2-yl(phenyl)methanol (1.5 g, 6.2 mmol) in THF (6 mL) under nitrogen. The reaction mixture was allowed to stir for 30 min before MeI (1.0 mL, 2.3 g, 16 mmol) was added. The mixture was then allowed to warm to room temperature over 2.5 h and the quenched with 10 mL of water. The organic phase was separated and the aqueous phase was extracted with ethyl acetate ( $4 \times 10$  mL). The combined organic phases were dried with anhydrous  $\text{Na}_2\text{SO}_4$ , and concentrated in vacuum. The crude product was purified by column chromatography on silica gel using EtOAc-*n*-pentane as eluent to give 1.24 g (4.86 mmol, 78%) of the title compound. Mp:  $63\text{--}65^{\circ}\text{C}$  (EtOAc-*n*-pentane).  $^1\text{H-NMR}$  ( $\text{CDCl}_3$ , 600 MHz):  $\delta = 3.52$  (s, 3 H,  $\text{OCH}_3$ ), 5.66 (s, 1 H,  $\text{CHPh}$ ), 7.28-7.37 (m, 4 H, Ar), 7.41-7.44 (m, 1 H, Ar), 7.51-7.52 (m, 2 H, Ar), 7.84-7.85 (m, 1 H, Ar), 7.97-7.99 (m, 1 H, Ar) ppm.  $^{13}\text{C-NMR}$  ( $\text{CDCl}_3$ , 150 MHz):  $\delta = 57.9$  (q,  $\text{OCH}_3$ ), 83.8 (d,  $\text{CHPh}$ ), 122.0 (d, Ar), 123.4 (d, Ar), 125.3 (d, Ar), 126.1 (d, Ar), 127.2 (d, Ar), 128.7 (d, Ar), 128.9 (d, Ar), 135.3 (s, Ar), 139.2 (s, Ar), 153.2 (s, Ar), 173.8 (s, NCS) ppm. HRMS (ESI positive):  $m/z$  calculated for  $[\text{C}_{15}\text{H}_{14}\text{NOS}]^+$  is 256.0791; found 256.0792.

**2.3 Synthesis of 2-(methoxy(phenyl)methyl)-1-methyl-1H-benzo[d]imidazole (3c)**

**(1-Methyl-1H-benzo[d]imidazol-2-yl)(phenyl)methanol**

To a stirred solution of N-methyl benzimidazole (1.29 g, 9.75 mmol) in dry THF (10 mL) at  $-78\text{ }^{\circ}\text{C}$  was dropwise added 5.7 mL of *n*BuLi (2.1 M in hexane, 12 mmol) under nitrogen. The reaction mixture was allowed to stir for 45 min before a solution of benzaldehyde (1.24 g, 11.7 mmol) in THF (10 mL) was added dropwise. The mixture was stirred at  $-78\text{ }^{\circ}\text{C}$  for 2 h and then allowed to warm to  $0\text{ }^{\circ}\text{C}$  over 1 h before it was quenched with 20 mL of water. The organic phase was separated and the aqueous phase was extracted with ethyl acetate ( $3 \times 30\text{ mL}$ ). The combined organic phases were dried with anhydrous  $\text{Na}_2\text{SO}_4$ , and concentrated in vacuum. The crude product was purified by column chromatography on silica gel using EtOAc-*n*-pentane as eluent 1.39 g (5.83 mmol, 60%) of the title compound. Mp:  $145\text{-}147\text{ }^{\circ}\text{C}$  (EtOAc-*n*-pentane).  $^1\text{H-NMR}$  ( $\text{CDCl}_3$ , 600 MHz):  $\delta = 3.43$  (s, 3 H,  $\text{NCH}_3$ ), 6.14 (s,  $\text{CHPh}$ ), 6.59 (brs, 1 H, OH), 7.10-7.11 (m, 1 H, Ar), 7.17-7.21 (m, 2 H, Ar), 7.24 (t,  $J = 7.2\text{ Hz}$ , 1 H, Ar), 7.28 (t,  $J = 7.3\text{ Hz}$ , 2 H, Ar), 7.36 (d,  $J = 7.6\text{ Hz}$ , 2 H, Ar), 7.65-7.66 (m, 1 H, Ar) ppm.  $^{13}\text{C-NMR}$  ( $\text{CDCl}_3$ , 150 MHz):  $\delta = 30.4$  (q,  $\text{NCH}_3$ ), 70.0 (d,  $\text{CHPh}$ ), 109.4 (d, Ar), 119.4 (d, Ar), 122.3 (d, Ar), 123.0 (d, Ar), 126.5 (d, Ar), 128.0 (d, Ar), 128.7 (d, Ar), 136.5 (s, Ar), 140.1 (s, Ar), 141.3 (s, Ar), 155.6 (s, NCN) ppm. HRMS (ESI positive):  $m/z$  calculated for  $[\text{C}_{15}\text{H}_{15}\text{N}_2\text{O}]^+$  is 239.1179; found 239.1178.

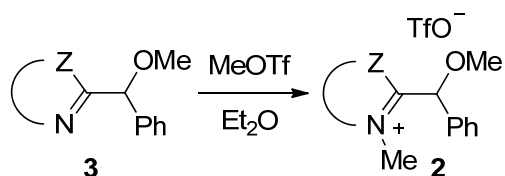
**2-(Methoxy(phenyl)methyl)-1-methyl-1H-benzo[d]imidazole (3c)**

To a stirred suspension of NaH (77 mg, 3.2 mmol) in dry THF (8 mL) at  $-50\text{ }^{\circ}\text{C}$  was dropwise added a solution of (1-methyl-1H-benzo[d]imidazol-2-yl)(phenyl)methanol (510 mg, 2.14 mmol) in THF (5 mL) under nitrogen. The reaction mixture was allowed to stir for 30 min before MeI (0.20 mL, 0.46 g, 3.2 mmol) was added. The mixture was then allowed to warm to room temperature over 2.5 h and the quenched with 20 mL of water. The organic phase was separated and the aqueous phase was extracted with ethyl acetate ( $4 \times 10\text{ mL}$ ). The combined organic phases were dried with anhydrous  $\text{Na}_2\text{SO}_4$ , and concentrated in vacuum. The crude product was purified by filtration through a short plug of silica gel to give 530 mg (2.10 mmol, 98%) of the title compound as light yellow oil.  $^1\text{H-NMR}$  ( $\text{CDCl}_3$ , 600 MHz):  $\delta = 3.51$  (s, 3 H,  $\text{OCH}_3$ ), 3.58 (s, 3 H,  $\text{NCH}_3$ ), 5.83 (s, 1 H,  $\text{CHPh}$ ), 7.26-7.29 (m, 4 H, Ar), 7.33 (t,  $J = 7.6\text{ Hz}$ , 2 H, Ar), 7.41 (d,  $J = 8.1\text{ Hz}$ , 2 H, Ar), 7.81-7.83 (m, 1 H, Ar) ppm.  $^{13}\text{C-NMR}$  ( $\text{CDCl}_3$ , 150 MHz):  $\delta = 30.4$  (q,  $\text{NCH}_3$ ), 57.8 (q,  $\text{OCH}_3$ ), 80.2 (d,  $\text{CHPh}$ ), 109.3 (d, Ar), 120.1 (d, Ar), 122.2 (d, Ar), 123.0 (d, Ar), 126.1 (d, Ar), 128.0 (d, Ar), 128.6 (d, Ar), 136.9 (s, Ar),

138.2 (s, Ar), 142.3 (s, Ar), 152.7 (s, NCN) ppm. HRMS (ESI positive):  $m/z$  calculated for  $[C_{16}H_{16}N_2ONa]^+$  is 275.1155; found 275.1155.

### 43. Synthesis of the N-alkyl azolium triflates (2a-c)

General procedure 1 (GP 1):



To a solution of 2-(methoxy(phenyl)methyl)-azole (1 eq.) in dry  $Et_2O$  (8 mL) was added MeOTf (1.5 eq.) via syringe and the reaction mixture was allowed to stir for 15h at room temperature under nitrogen. The solvent was then decanted or filtered and the residue was washed with  $Et_2O$  and then with *n*-pentane and dried under vacuum.

**2-(Methoxy(phenyl)methyl)-3,4,5-trimethylthiazol-3-ium triflate (2a)** was obtained

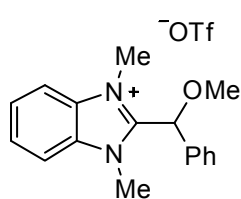
according to GP 1 from 2-(methoxy(phenyl)methyl)-4,5-dimethylthiazole (233 mg, 1.00 mmol) and MeOTf (250 mg, 1.52 mmol). Colorless sticky oil, 377 mg (0.950 mmol, 95%).  $^1H$ -NMR ( $CDCl_3$ , 600 MHz):  $\delta$  = 2.40 (s, 3 H,  $CH_3$ ), 2.44 (s, 3 H,  $CH_3$ ), 3.48 (s, 3 H,  $NCH_3$ ), 3.87 (s, 3 H,  $OCH_3$ ), 6.01 (s, 1 H,  $CHPh$ ), 7.45 (s, 5 H, Ph) ppm.  $^{13}C$ -NMR ( $CDCl_3$ , 75 MHz):  $\delta$  = 12.47 (q,  $CH_3$ ), 12.53 (q,  $CH_3$ ), 38.9 (q,  $OCH_3$ ), 58.0 (q,  $NCH_3$ ), 79.1 (d,  $CHPh$ ), 120.8 (q,  $J_{C-F}$  = 320.7 Hz,  $CF_3SO_3^-$ ), 128.6 (d, Ar), 129.8 (d, Ar), 130.7 (d, Ar), 130.8 (s), 134.3 (s, Ar), 144.0 (s), 173.0 (s,  $NCS$ ) ppm. HRMS (ESI positive):  $m/z$  calculated for  $[C_{14}H_{18}NOS]^+$  is 248.1104; found 248.1103.

**2-(Methoxy(phenyl)methyl)-3-methylbenzo[d]thiazol-3-ium triflate (2b)** was obtained

according to GP 1 from 2-(methoxy(phenyl)methyl)benzo[d]thiazole (1.10 g, 4.30 mmol) and MeOTf (1.06 g, 6.45 mmol). White powder, 1.73 g (4.12 mmol, 96%). Mp: 114-116 °C ( $Et_2O$ ). IR (ATR)  $\tilde{\nu}$  ( $cm^{-1}$ ): 1587, 1531, 1493, 1457, 1272, 1251, 1224, 1164, 1144, 1100, 1029, 966, 753, 696.  $^1H$ -NMR ( $CDCl_3$ , 600 MHz):  $\delta$  = 3.53 (s, 3 H,  $OCH_3$ ), 4.15 (s, 3 H,  $NCH_3$ ), 6.43 (s, 1 H,  $CHPh$ ), 7.44-7.45 (m, 3 H, Ar), 7.50-7.52 (m, 2 H, Ar), 7.71 (t,  $J$  = 7.5 Hz, 1 H, Ar), 7.79 (t,  $J$  = 7.5 Hz, 1 H, Ar), 8.01 (d,  $J$  = 8.6 Hz, 1 H, Ar), 8.10 (d,  $J$  = 8.2 Hz, 1 H, Ar) ppm.  $^{13}C$ -NMR ( $CDCl_3$ , 150 MHz):  $\delta$  = 38.0 (q,  $NCH_3$ ), 58.0 (q,  $OCH_3$ ), 79.7 (d,  $CHPh$ ), 116.8 (d, Ar), 120.8 (q,  $J_{C-F}$  = 320 Hz,  $CF_3SO_3^-$ ), 124.0 (d, Ar), 128.9 (d, Ar), 129.2 (d, Ar), 129.5 (s, Ar), 130.0 (d, Ar), 130.5 (d, Ar), 130.9 (d, Ar), 133.8 (s, Ar), 143.0 (s, Ar), 181.9 (s,

NCS) ppm. HRMS (ESI positive):  $m/z$  calculated for  $[C_{16}H_{16}NOS]^+$  is 270.0947; found 270.0946.

**2-(Methoxy(phenyl)methyl)-1,3-dimethyl-1H-benzo[d]imidazol-3-ium triflate (2c)** was

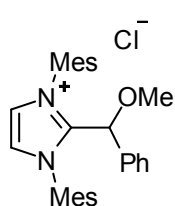


obtained according to GP 1 from 2-(methoxy(phenyl)methyl)-1-methyl-1H-benzo[d]imidazole (504 mg, 2.00 mmol) and MeOTf (410 mg, 2.50 mmol). White powder, 698 mg (1.68 mmol, 84%). Mp: 98-99 °C (Et<sub>2</sub>O).

IR (ATR)  $\tilde{\nu}$  (cm<sup>-1</sup>): 1534, 1475, 1351, 1263, 1222, 1168, 1142, 1094, 1028, 975, 930, 906, 780, 749, 702. <sup>1</sup>H-NMR (CDCl<sub>3</sub>, 300 MHz):  $\delta$  = 3.60 (s, 3 H, OCH<sub>3</sub>), 4.14 (s, 6 H, NCH<sub>3</sub>), 6.39 (s, 1 H, CHPh), 7.34-7.39 (m, 5 H, Ar), 7.58-7.64 (m, 2 H, Ar), 7.71-7.76 (m, 2 H, Ar) ppm. <sup>13</sup>C-NMR (CDCl<sub>3</sub>, 75 MHz):  $\delta$  = 33.4 (q, NCH<sub>3</sub>), 58.8 (q, OCH<sub>3</sub>), 76.8 (d, CHPh), 113.0 (d, Ar), 120.9 (q,  $J_{C-F}$  = 321 Hz, CF<sub>3</sub>SO<sub>2</sub><sup>-</sup>), 127.1 (d, Ar), 127.8 (d, Ar), 129.9 (d, Ar), 130.2 (d, Ar), 132.1 (s, Ar), 134.0 (s, Ar) 150.2 (s, NCN) ppm. HRMS (ESI positive):  $m/z$  calculated for  $[C_{17}H_{19}N_2O]^+$  is 267.1492; found 267.1490.

#### 4.4 Synthesis of the N-aryl azolium chlorides (2d,e)

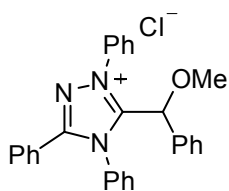
##### 1,3-Dimesityl-2-(methoxy(phenyl)methyl)-1H-imidazol-3-ium chloride (2d)



To an oven dried Schlenk-flask charged with ZnBr<sub>2</sub> (2 mg) was added toluene (5 mL) and (dimethoxymethyl)benzene (304 mg, 2.00 mmol) and the mixture was cooled to 0 °C on an ice bath. AcCl (165 mg, 2.01 mmol) was added into the above solution and stirred for 30 min at room temperature. The reaction mixture was then diluted with dry *n*-pentane (20 mL) and cooled to 0 °C. Then a 1: 2 toluene/*n*-pentane solution (20 mL) of 1,3-dimesitylimidazolium-2-ylidene (609 mg, 2.00 mmol) was slowly added and stirred for 10 min. The white precipitate was then filtered, washed with *n*-pentane and dried to give 729 mg (1.58 mmol, 79%) of the title compound as off white powder. Mp: 134-137 °C (EtOAc-*n*-pentane). IR (ATR)  $\tilde{\nu}$  (cm<sup>-1</sup>): 2921, 1606, 1561, 1503, 1452, 1383, 1234, 1205, 1179, 1164, 1091, 1072, 1037, 964, 852, 748, 734, 723. <sup>1</sup>H-NMR (CDCl<sub>3</sub>, 400 MHz):  $\delta$  = 1.64 (s, 6 H, CH<sub>3</sub>), 2.13 (s, 6 H, CH<sub>3</sub>), 2.33 (s, 6 H, CH<sub>3</sub>), 3.06 (s, 3 H, OCH<sub>3</sub>), 5.00 (s, 1 H, CHPh), 6.51 (d,  $J$  = 7.5 Hz, 2 H, Ar), 6.83 (s, 2 H, Ar), 7.01-7.06 (m, 4 H, Ar), 7.19 (t,  $J$  = 7.4 Hz, 1 H, Ar), 8.18 (s, 2 H, NCH=CHN) ppm. <sup>13</sup>C-NMR (CDCl<sub>3</sub>, 100 MHz):  $\delta$  = 17.0 (q, CH<sub>3</sub>), 17.9 (q, CH<sub>3</sub>), 21.3 (q, CH<sub>3</sub>), 58.5 (q, OCH<sub>3</sub>), 74.9 (s, CHPh), 126.6 (d, Ar), 127.0 (d, NCH=CHN), 128.8 (d, Ar), 129.75 (d, Ar), 129.82 (d, Ar), 130.12 (d, Ar), 130.16 (s, Ar), 130.9 (s, Ar), 135.1 (s, Ar), 135.2 (s, Ar), 142.0 (s, Ar), 142.8

(s, NCN) ppm. HRMS (ESI positive):  $m/z$  calculated for  $[C_{29}H_{33}N_2O]^+$  is 425.2587; found 425.2586.

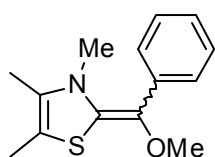
### 5-(Methoxy(phenyl)methyl)-1,3,4-triphenyl-4H-1,2,4-triazol-1-ium chloride (**2e**)



To an oven dried Schlenk-flask charged with  $ZnBr_2$  (2 mg) was added toluene (5 mL) and (dimethoxymethyl)benzene (304 mg, 2.00 mmol) and the mixture was cooled to 0 °C on an ice bath.  $AcCl$  (165 mg, 2.01 mmol) was added into the above solution and stirred for 30 min at room temperature. The reaction mixture was then diluted with dry *n*-pentane (20 mL) and cooled to 0 °C. Then a 1: 1 toluene/*n*-pentane solution (25 mL) of Enders carbene (595 mg, 2.00 mmol) was slowly added and stirred for 20 min. The white precipitate from was filtered, washed with *n*-pentane and dried to give 500 mg (1.10 mmol, 55%) of the title compound as off white powder.  $^1H$ -NMR ( $CDCl_3$ , 300 MHz):  $\delta$  = 3.24 (s, 3 H,  $OCH_3$ ), 6.01 (s, 1 H,  $CHPh$ ), 7.10-7.16 (m, 4 H, Ar), 7.24-7.29 (m, 2 H, overlapped with  $CHCl_3$ , Ar), 7.36-7.56 (m, 10 H, Ar), 7.86-8.01 (m, 4 H, Ar) ppm.  $^{13}C$ -NMR ( $CDCl_3$ , 75 MHz):  $\delta$  = 58.7 (q,  $OCH_3$ ), 76.9 (d,  $CHPh$ ), 122.6 (d, Ar), 127.1 (d, Ar), 127.7 (d, Ar), 128.3 (d, Ar), 128.62 (d, Ar), 128.64 (d, Ar), 129.0 (d, Ar), 129.2 (d, Ar), 129.8 (d, Ar), 131.0 (d, Ar), 131.3 (s, Ar), 131.7 (s, Ar), 131.9 (d, Ar), 132.5 (s, Ar), 136.0 (s, Ar), 153.2 (s, NCN), 154.0 (s,  $PhC(N)=N$ ) ppm. HRMS (ESI positive):  $m/z$  calculated for  $[C_{28}H_{24}N_3O]^+$  is 418.1914; found 418.1912.

## 4.5. Synthesis of the O-methylated Breslow intermediates (**1a-e**)

### (E)- and (Z)-2-(Methoxy(phenyl)methylene)-3,4,5-trimethyl-2,3-dihydrothiazole (**1a**)

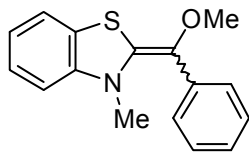


To a stirred suspension of  $NaH$  (36 mg, 1.5 mmol) in dry THF (5 mL) at – 20 °C was dropwise added a solution of 2-(methoxy(phenyl)methyl)-3,4,5-trimethylthiazol-3-ium triflate (**2a**, 397 mg, 1.00 mmol) in THF (6 mL) under nitrogen and the reaction mixture was allowed to stir for 36 h in absence of light. After warming to room temperature the solvent was removed under vacuum and the residue was suspended in dry toluene (20 mL) and filtered through a celite pad under nitrogen. Then the solvent was evaporated to give 205 mg (0.829 mmol, 83%) of the title compound as 2:1 mixture of *Z*:*E* isomers. Crystal suitable for X-ray crystallography was grown by slow evaporation of the *n*-pentane solution under nitrogen. Mp: 73–75 °C (*n*-pentane). UV/Vis (THF):  $\lambda_{max}$  = 382 nm. IR (ATR)  $\tilde{\nu}$  ( $cm^{-1}$ ): 2919, 2859, 2820, 1659, 1600, 1577, 1560, 1485, 1440, 1418, 1390, 1378, 1281, 1236, 1201, 1170, 1090, 1070, 1018, 981, 942, 871, 759, 706, 688.  $^1H$ -NMR ( $C_6D_6$ , 400 MHz):  $\delta$  = 1.32 (s, 3 H + 3 H\*,  $CH_3$ ), 1.58 (s, 3 H,  $CH_3$ ), 1.67\* (s, 3 H,  $CH_3$ ), 2.43\* (s, 3 H,  $CH_3$ ), 3.00 (s, 3 H,  $CH_3$ ), 3.35 (s, 3 H,  $CH_3$ ), 3.50\* (s, 3 H,

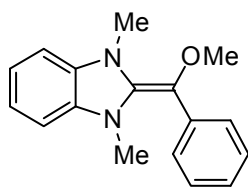
CH<sub>3</sub>), 6.96-7.02 (m, 1 H + 1 H\*, Ar), 7.18-7.23\* (m, 2 H, Ar), 7.28-7.32 (m, 2 H, Ar), 7.41-7.44\* (m, 2 H, Ar), 7.79-7.81 (m, 2 H, Ar) ppm. <sup>13</sup>C-NMR (C<sub>6</sub>D<sub>6</sub>, 100 MHz): δ = 11.7 (q, CH<sub>3</sub>), 11.8\* (q, CH<sub>3</sub>), 12.1 (q, CH<sub>3</sub>), 12.2\* (q, CH<sub>3</sub>), 35.8 (q, CH<sub>3</sub>), 38.3\* (q, CH<sub>3</sub>), 56.9\* (q, CH<sub>3</sub>), 58.8 (q, CH<sub>3</sub>), 101.4 (s, CH<sub>3</sub>CS), 106.3\* (s, CH<sub>3</sub>CS), 125.1 (d, Ar), 125.3\* (d, Ar), 125.8 (d, Ar), 126.9\* (d, Ar), 126.9 (s, =C(Ph)OCH<sub>3</sub>, overlapped), 127.9\* (s, =C(Ph)OCH<sub>3</sub>), 128.7\* (d, Ar), 129.0 (d, Ar), 131.6 (s, CH<sub>3</sub>CN), 132.6\* (s, CH<sub>3</sub>CN), 136.0\* (s, Ar), 137.4 (s, NCS), 138.6 (s, Ar), 141.6\* (s, NCS) ppm. HRMS (EI positive): m/z calculated for [C<sub>14</sub>H<sub>17</sub>NO<sup>32</sup>S]<sup>+</sup> is 247.1031; found 247.1030. \* assigned for the major stereoisomer.

### Crystallographic data for **Z-1a**:

net formula	C <sub>14</sub> H <sub>17</sub> NOS
<i>M<sub>r</sub></i> /g mol <sup>-1</sup>	247.357
crystal size/mm	0.35 × 0.25 × 0.17
<i>T</i> /K	173(2)
radiation	MoKα
diffractometer	'Oxford XCalibur'
crystal system	monoclinic
space group	<i>P</i> 2 <sub>1</sub> / <i>c</i>
<i>a</i> /Å	15.9660(7)
<i>b</i> /Å	6.8902(3)
<i>c</i> /Å	12.1520(6)
α/°	90
β/°	103.381(5)
γ/°	90
<i>V</i> /Å <sup>3</sup>	1300.54(10)
<i>Z</i>	4
calc. density/g cm <sup>-3</sup>	1.26333(10)
μ/mm <sup>-1</sup>	0.232
absorption correction	'multi-scan'
transmission factor range	0.95300–1.00000
refls. measured	9041
<i>R</i> <sub>int</sub>	0.0285
mean σ( <i>I</i> )/ <i>I</i>	0.0333
θ range	4.50–26.32
observed refls.	2023
<i>x</i> , <i>y</i> (weighting scheme)	0.0601, 0
hydrogen refinement	constr
refls in refinement	2637
parameters	158
restraints	0
<i>R</i> ( <i>F</i> <sub>obs</sub> )	0.0362
<i>R</i> <sub>w</sub> ( <i>F</i> <sup>2</sup> )	0.1043
<i>S</i>	1.079
shift/error <sub>max</sub>	0.001
max electron density/e Å <sup>-3</sup>	0.291
min electron density/e Å <sup>-3</sup>	-0.188

**(E)- and (Z)-2-(Methoxy(phenyl)methylene)-3-methyl-2,3-dihydrobenzo[d]thiazole (1b)**

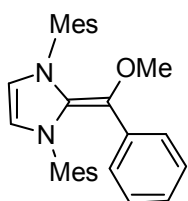
To a stirred suspension of NaH (72 mg, 3.0 mmol) and *t*BuOK (11 mg, 98  $\mu$ mol) in dry THF (5 mL) at  $-20$  °C was dropwise added a solution of 2-(methoxy(phenyl)methyl)-3-methylbenzo[d]thiazol-3-ium triflate (**2b**, 839 mg, 2.00 mmol) in THF (12 mL) under nitrogen and the reaction mixture was allowed to stir for 16 h in absence of light. After warming to room temperature the solvent was removed under vacuum and the residue was suspended in dry toluene (25 mL) and filtered through a celite pad under nitrogen. Then the solvent was evaporated to give 469 mg (1.74 mmol, 87%) of the title compound as yellow oil as 2:1 mixture of *Z*:*E* isomers. UV/Vis (THF):  $\lambda_{\text{max}} = 362$  nm. IR (ATR)  $\tilde{\nu}$  ( $\text{cm}^{-1}$ ): 3056, 2927, 2823, 1623, 1579, 1474, 1452, 1442, 1341, 1300, 1284, 1224, 1158, 1129, 1093, 1072, 1027, 971, 956, 913, 903, 866, 788, 762, 738, 700, 673.  $^1\text{H-NMR}$  ( $\text{C}_6\text{D}_6$ , 400 MHz):  $\delta = 2.40$  (s, 3 H,  $\text{NCH}_3$ )\*, 3.09 (s, 3 H,  $\text{NCH}_3$ ), 3.21 (s, 3 H,  $\text{OCH}_3$ ), 3.39 (s, 3 H,  $\text{OCH}_3$ )\*, 6.19-6.22 (m, 1 H + 1 H,  $\text{Ar}^* + \text{Ar}$ ), 6.61 (td,  $J = 1.1, 7.5$  Hz, 1 H,  $\text{Ar}$ ), 6.66 (td,  $J = 1.1, 7.5$  Hz, 1 H,  $\text{Ar}^*$ )\*, 6.77-6.80 (m, 1 H,  $\text{Ar}$ ), 6.85-6.90 (m, 1 H + 1 H,  $\text{Ar}^* + \text{Ar}$ ), 6.94-6.96 (m, 1 H,  $\text{Ar}^*$ )\*, 6.98-7.06 (m, 1 H + 1 H,  $\text{Ar}^* + \text{Ar}$ ), 7.12-7.16 (m, 2 H,  $\text{Ar}^*$ , overlapped with  $\text{C}_6\text{H}_6$ ), 7.22-7.27 (m, 2 H + 2 H,  $\text{Ar}^* + \text{Ar}$ ), 7.67-7.70 (m, 2 H,  $\text{Ar}$ ) ppm.  $^{13}\text{C-NMR}$  ( $\text{C}_6\text{D}_6$ , 100 MHz):  $\delta = 35.5$  (q,  $\text{NCH}_3$ ), 35.8 (q,  $\text{NCH}_3$ )\*, 57.0 (q,  $\text{OCH}_3$ )\*, 59.1 (q,  $\text{OCH}_3$ ), 107.9 (d,  $\text{Ar}$ ), 109.7 (d,  $\text{Ar}^*$ )\*, 120.8 (d,  $\text{Ar}$ ), 121.05 (d,  $\text{Ar}$ ), 121.05 (d,  $\text{Ar}^*$ )\*, 121.5 (d,  $\text{Ar}^*$ )\*, 124.8 (s,  $\text{NC}=\underline{\text{C}}\text{S}$ ), 126.0 (d,  $\text{Ar}^*$ )\*, 126.1 (d,  $\text{Ar}$ ), 126.7 (d,  $\text{Ar}^*$ )\*, 126.9 (d,  $\text{Ar}$ ), 127.3 (s,  $\text{NC}=\underline{\text{C}}\text{S}$ )\*, 127.4 (d,  $\text{Ar}^*$ )\*, 127.8 (s,  $=\underline{\text{C}}(\text{Ph})\text{OCH}_3$ ), 128.3 (s,  $=\underline{\text{C}}(\text{Ph})\text{OCH}_3$ )\*, 128.5 (d,  $\text{Ar}$ ), 128.7 (d,  $\text{Ar}^*$ )\*, 129.2 (d,  $\text{Ar}$ ), 133.6 (s,  $\text{NCS}$ ), 135.2 (s,  $\text{Ar}^*$ )\*, 137.1 (s,  $\text{NCS}$ )\*, 137.8 (s,  $\text{Ar}$ ), 146.1 (s,  $\text{NC}=\underline{\text{C}}\text{S}$ ), 147.7 (s,  $\text{NC}=\underline{\text{C}}\text{S}$ ) ppm. HRMS (ESI positive):  $m/z$  calculated for  $[\text{C}_{16}\text{H}_{16}\text{NO}^{32}\text{S}]^+$  is 270.0947; found 270.0946. \* assigned for the major stereoisomer.

**2-(Methoxy(phenyl)methylene)-1,3-dimethyl-2,3-dihydro-1H-benzo[d]imidazole (1c)**

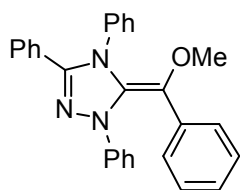
To a stirred suspension of NaH (18 mg, 0.75 mmol) *t*BuOK (2.0 mg, 18  $\mu$ mol) in dry THF (2 mL) at room temperature was dropwise added a solution of 2-(methoxy(phenyl)methyl)-1,3-dimethyl-1H-benzo[d]imidazol-3-ium triflate (**2c**, 208 mg, 0.500 mmol) in THF (5 mL) under nitrogen and the reaction mixture was allowed to stir for 15 h in absence of light. The solvent was then removed under vacuum and the residue was suspended in dry toluene (25 mL) and filtered through a celite pad under nitrogen. Then the solvent was evaporated to give 130 mg (0.488 mmol, 98%) of the title compound. Mp: 97-98 °C (toluene). UV/Vis

(THF):  $\lambda_{\text{max}} = 398$  nm. IR (ATR)  $\tilde{\nu}$  ( $\text{cm}^{-1}$ ): 2933, 1621, 1606, 1575, 1495, 14845, 1442, 1422, 1365, 1306, 1292, 1280, 1219, 1169, 1151, 1090, 1069, 1020, 966, 947, 897, 785, 754, 744, 734, 702, 678.  $^1\text{H-NMR}$  ( $\text{C}_6\text{D}_6$ , 400 MHz):  $\delta = 2.51$  (s, 3 H,  $\text{NCH}_3$ ), 3.08 (s, 3 H,  $\text{NCH}_3$ ), 3.40 (s, 3 H,  $\text{OCH}_3$ ), 6.36 (dd,  $J = 1.2, 7.4$  Hz, 1 H, Ar), 6.41 (dd,  $J = 1.2, 7.4$  Hz, 1 H, Ar), 6.80-6.88 (m, 2 H, Ar), 6.95-6.99 (m, 1 H, Ar), 7.22-7.26 (m, 2 H, Ar), 7.31-7.35 (m, 2 H, Ar) ppm.  $^{13}\text{C-NMR}$  ( $\text{C}_6\text{D}_6$ , 100 MHz):  $\delta = 32.7$  (q,  $\text{NCH}_3$ ), 37.3 (q,  $\text{NCH}_3$ ), 60.1 (q,  $\text{OCH}_3$ ), 105.7 (d, Ar), 107.3 (d, Ar), 115.7 (s,  $=\underline{\text{C}}(\text{Ph})\text{OCH}_3$ ), 120.6 (d, Ar), 121.0 (d, Ar), 123.7 (d, Ar), 125.9 (d, Ar), 128.7 (d, Ar), 138.54 (s, Ar), 138.58 (s, Ar), 139.0 (s, Ar), 144.4 (s,  $\text{NCN}$ ) ppm. HRMS (ESI positive):  $m/z$  calculated for  $[\text{C}_{17}\text{H}_{19}\text{N}_2\text{O}]^+$  is 267.1492; found 267.1492.

### 1,3-Dimesityl-2-(methoxy(phenyl)methylene)-2,3-dihydro-1H-imidazole (1d)



To an oven dried Schlenk-flask charged with 1,3-dimesityl-2-(methoxy(phenyl)methyl)-1H-imidazol-3-ium chloride (**2d**, 461 mg, 1.00 mmol), NaH (48 mg, 2.0 mmol), and *t*BuOK (11 mg, 98  $\mu\text{mol}$ ) was added dry THF (15 mL) under nitrogen and the reaction mixture was allowed to stir for 6 h in absence of light. The solvent was then removed under vacuum and the residue was suspended in dry toluene (20 mL) and filtered through a celite pad under nitrogen. Then the solvent was evaporated and the yellow residue was taken into dry *n*-pentane (30 mL) and filtered again through a celite pad under nitrogen. Evaporation of *n*-pentane gave yellow oil which solidified on standing at  $-30$   $^\circ\text{C}$  for over night to give 242 mg (0.570 mmol, 57%) of the title compound. Mp: 68-71  $^\circ\text{C}$  (decomposition, *n*-pentane). UV/Vis (THF):  $\lambda_{\text{max}} = 399$  nm. IR (ATR)  $\tilde{\nu}$  ( $\text{cm}^{-1}$ ): 2922, 2854, 1625, 1583, 1569, 1485, 1439, 1395, 1374, 1281, 1271, 1217, 1198, 1160, 1085, 1069, 970, 913, 850, 756, 749, 683, 669.  $^1\text{H-NMR}$  ( $\text{C}_6\text{D}_6$ , 400 MHz):  $\delta = 1.96$  (s, 3 H,  $\text{CH}_3$ ), 2.14 (s, 3 H,  $\text{CH}_3$ ), 2.22 (s, 6 H,  $\text{CH}_3$ ), 2.44 (s, 6 H,  $\text{CH}_3$ ), 2.67 (s, 3 H,  $\text{OCH}_3$ ), 5.69 (d,  $J = 2.5$  Hz, 1 H,  $\text{NCH}=\text{CHN}$ ), 5.71 (d,  $J = 2.5$  Hz, 1 H,  $\text{NCH}=\text{CHN}$ ), 6.52 (s, 2 H, Ar), 6.61-6.65 (m, 1 H, Ar), 6.82 (s, 2 H, Ar), 6.84-6.88 (m, 2 H, Ar), 6.96-6.99 (m, 2 H, Ar) ppm.  $^{13}\text{C-NMR}$  ( $\text{C}_6\text{D}_6$ , 100 MHz):  $\delta = 18.89$  (q,  $\text{CH}_3$ ), 18.92 (q,  $\text{CH}_3$ ), 21.1 (q,  $\text{CH}_3$ ), 21.4 (q,  $\text{CH}_3$ ), 58.0 (q,  $\text{OCH}_3$ ), 114.9 (s,  $=\underline{\text{C}}(\text{Ph})\text{OCH}_3$ ), 116.9 (d,  $\text{NCH}=\text{CHN}$ ), 117.1 (d,  $\text{NCH}=\text{CHN}$ ), 121.87 (d, Ar), 124.8 (d, Ar), 127.3 (d, Ar), 129.4 (d, Ar), 130.0 (d, Ar), 135.0 (s, Ar), 136.0 (s, Ar), 136.6 (s, Ar), 137.2 (s, Ar), 137.9 (s, Ar), 138.4 (s, Ar), 140.9 (s,  $\text{NCN}$ ) ppm. HRMS (EI positive):  $m/z$  calculated for  $[\text{C}_{29}\text{H}_{33}\text{N}_2\text{O}]^+$  is 425.2587; found 425.2603.

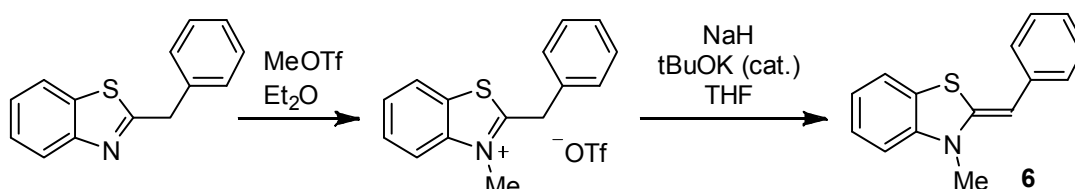
**(E)-5-(Methoxy(phenyl)methylene)-1,3,4-triphenyl-4,5-dihydro-1H-1,2,4-triazole (1e)**

To an oven dried Schlenk-flask charged with NaH (48 mg, 2.0 mmol), *t*BuOK (11 mg, 98  $\mu$ mol), and 5-(methoxy(phenyl)methyl)-1,3,4-triphenyl-4H-1,2,4-triazol-1-ium chloride (**2e**, 454 mg, 1.00 mmol) was added dry THF (15 mL) under nitrogen and the reaction mixture was allowed to stir for 4 h in absence of light. The solvent was then removed under vacuum and the residue was suspended in dry toluene (20 mL) and filtered through a celite pad under nitrogen. Then the solvent was evaporated to give 296 mg (0.709 mmol, 71%) of the title compound as 10 : 1 mixture of *E* : *Z* isomer. Crystal suitable for X-ray crystallography was grown by cooling down a saturated acetonitrile solution at  $-30$  °C under argon. Mp:  $<170$  °C (decomposition, toluene). UV/Vis (THF):  $\lambda_{\text{max}} = 368$  nm. IR (ATR)  $\tilde{\nu}$  ( $\text{cm}^{-1}$ ): 1667, 1628, 1587, 1558, 1532, 1492, 1445, 1397, 1373, 1309, 1274, 1156, 1086, 1054, 1026, 974, 965, 747, 692, 657.  $^1\text{H-NMR}$  ( $\text{C}_6\text{D}_6$ , 400 MHz):  $\delta = 2.64$  (s, 3 H,  $\text{OCH}_3$ ), 6.72-6.78 (m, 2 H, Ar), 6.86-7.00 (m, 12 H, Ar), 7.23-7.25 (m, 2 H, Ar), 7.30-7.33 (m, 2 H, Ar), 7.47-7.49 (m, 2 H, Ar), 7.53-7.56 (m, 2 H, Ar) ppm.  $^{13}\text{C-NMR}$  ( $\text{C}_6\text{D}_6$ , 100 MHz):  $\delta = 58.7$  (q,  $\text{OCH}_3$ ), 117.3 (s,  $=\text{C}(\text{Ph})\text{OCH}_3$ ), 120.9 (d, Ar), 124.1 (d, Ar), 124.6 (d, Ar), 125.6 (d, Ar), 128.2 (d, Ar, overlapped with solvent residual peak), 128.4 (d, Ar, overlapped with solvent residual peak), 128.5 (d, Ar, overlapped with solvent residual peak), 128.6 (d, Ar, overlapped with solvent residual peak), 128.7 (d, Ar), 129.1 (d, Ar), 129.9 (d, Ar), 130.6 (d, Ar), 136.7 (s, Ar), 139.7 (s, Ar), 140.3 (s, Ar), 141.4 (s, Ar), 152.2 (s, NCN) ppm. HRMS (EI positive):  $m/z$  calculated for  $[\text{C}_{28}\text{H}_{23}\text{N}_3\text{O}]^+$  is 417.1836; found 417.1839.

Crystallographic data for *E*-1e:

net formula	C <sub>28</sub> H <sub>23</sub> N <sub>3</sub> O
<i>M<sub>r</sub></i> /g mol <sup>-1</sup>	417.502
crystal size/mm	0.35 × 0.09 × 0.04
<i>T</i> /K	200(2)
radiation	MoKα
diffractometer	'KappaCCD'
crystal system	monoclinic
space group	<i>P</i> 2 <sub>1</sub> / <i>c</i>
<i>a</i> /Å	5.8831(2)
<i>b</i> /Å	10.5560(2)
<i>c</i> /Å	35.0548(8)
α/°	90
β/°	93.7490(10)
γ/°	90
<i>V</i> /Å <sup>3</sup>	2172.31(10)
<i>Z</i>	4
calc. density/g cm <sup>-3</sup>	1.27659(6)
μ/mm <sup>-1</sup>	0.079
absorption correction	none
refls. measured	12648
<i>R</i> <sub>int</sub>	0.0602
mean σ( <i>I</i> )/ <i>I</i>	0.0548
θ range	3.47–25.41
observed refls.	2649
<i>x</i> , <i>y</i> (weighting scheme)	0.0498, 0.5183
hydrogen refinement	constr
refls in refinement	3975
parameters	290
restraints	0
<i>R</i> ( <i>F</i> <sub>obs</sub> )	0.0461
<i>R</i> <sub>w</sub> ( <i>F</i> <sup>2</sup> )	0.1197
<i>S</i>	1.031
shift/error <sub>max</sub>	0.001
max electron density/e Å <sup>-3</sup>	0.136
min electron density/e Å <sup>-3</sup>	-0.168

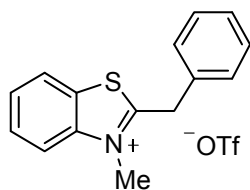
## 4.6 Synthesis of the deoxy-Breslow intermediate (6)



## 2-Benzyl-3-methylbenzo[d]thiazol-3-ium triflate

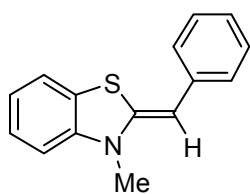
To a stirred solution of 2-benzylbenzo[d]thiazole<sup>[21b]</sup> (225 mg, 1.00 mmol) in dry Et<sub>2</sub>O (5 mL) was added MeOTf (205 mg, 1.25 mmol) via syringe and the reaction mixture was

allowed to stir for 12 h at room temperature under nitrogen. The white precipitate was then filtered and was washed with Et<sub>2</sub>O and then with *n*-pentane and dried

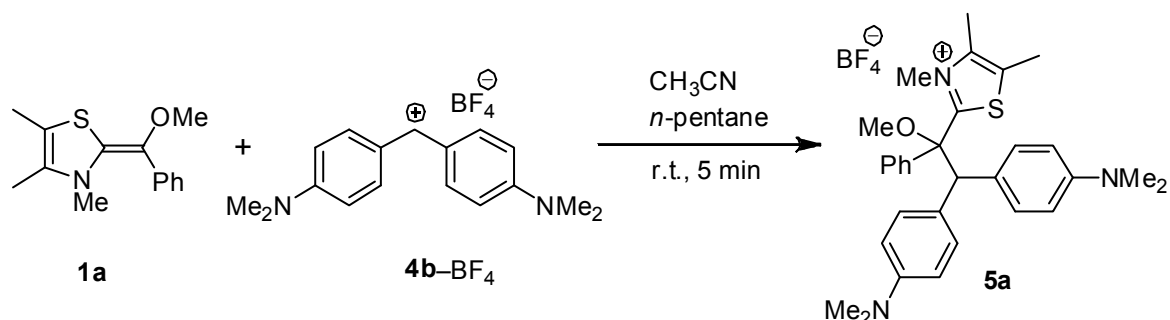


under vacuum to give 347 mg (0.892 mmol, 89%) of the title compound as white powder. Mp: 167-168 °C (Et<sub>2</sub>O). IR (ATR)  $\tilde{\nu}$  (cm<sup>-1</sup>): 3079, 1513, 1498, 1459, 1251, 1224, 1206, 1165, 1157, 1026, 772, 763, 698. <sup>1</sup>H-NMR (DMSO-d<sub>6</sub>, 400 MHz):  $\delta$  = 4.31 (s, 3 H, NCH<sub>3</sub>), 4.87 (s, 2 H, PhCH<sub>2</sub>), 7.45-7.52 (m, 5 H, Ar), 7.77-7.81 (m, 1 H, Ar), 7.89-7.94 (m, 1 H, Ar), 8.32-8.35 (m, 2 H, Ar) ppm. <sup>13</sup>C-NMR (DMSO-d<sub>6</sub>, 100 MHz):  $\delta$  = 36.38 (t, PhCH<sub>2</sub>), 36.43 (q, NCH<sub>3</sub>), 116.7 (d, Ar), 120.6 (q, *J*<sub>C-F</sub> = 322.5 Hz, CF<sub>3</sub>SO<sub>3</sub><sup>-</sup>), 124.5 (d, Ar), 128.0 (d, Ar), 128.67 (d, Ar), 128.72 (s, Ar), 129.35 (d, Ar), 129.43 (d, Ar), 130.0 (d, Ar), 133.5 (s, Ar), 142.1 (s, Ar), 182.5 (s, NCS) ppm. HRMS (ESI positive): *m/z* calculated for [C<sub>15</sub>H<sub>14</sub>NS]<sup>+</sup> is 240.0841; found 240.0840.

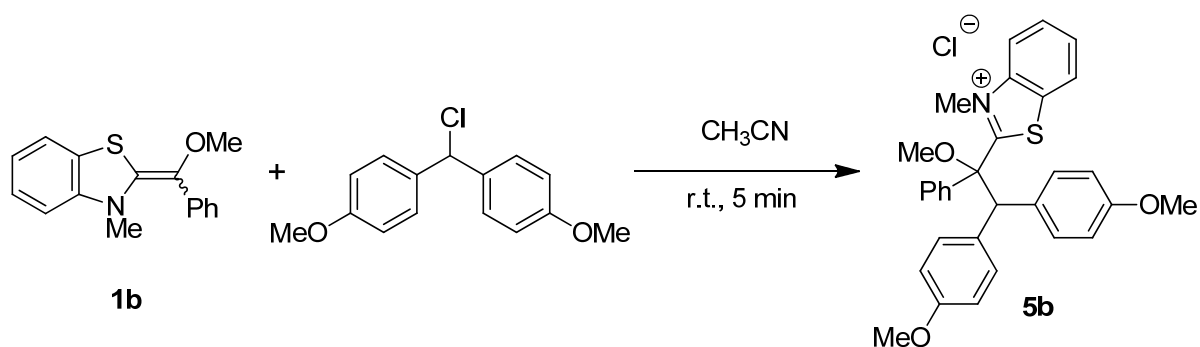
#### (Z)-2-Benzylidene-3-methyl-2,3-dihydrobenzo[d]thiazole (6)



To an oven dried Schlenk-flask charged with 2-benzyl-3-methylbenzo[d]thiazol-3-ium triflate (389 mg, 1.00 mmol), NaH (36 mg, 1.5 mmol), and *t*BuOK (11 mg, 98 μmol) was added dry and cold (0-5 °C) THF (15 mL) under nitrogen and the reaction mixture was allowed to stir for 5 h in absence of light. After warming to room temperature the solvent was removed under vacuum and the residue was suspended in dry toluene (20 mL) and filtered through a celite pad under nitrogen. Then the solvent was evaporated to give 221 mg (0.924 mmol, 92%) of the title compound as pale yellow palate. Mp: 80-82 °C (toluene). UV/Vis (THF):  $\lambda_{\text{max}}$  = 351 nm. IR (ATR)  $\tilde{\nu}$  (cm<sup>-1</sup>): 2930, 1603, 1591, 1583, 1575, 1561, 1477, 1455, 1444, 1374, 1306, 1261, 1192, 1126, 1022, 888, 831, 777, 741, 687. <sup>1</sup>H-NMR (C<sub>6</sub>D<sub>6</sub>, 300 MHz):  $\delta$  = 2.43 (s, 3 H, NCH<sub>3</sub>), 5.46 (s, 1 H, CHPh), 6.15 (d, *J* = 7.9 Hz, 1 H, Ar), 6.64 (td, *J* = 1.1, 7.5 Hz, 1 H, Ar), 6.87-6.93 (m, 2 H, Ar), 7.00-7.06 (m, 1 H, Ar), 7.30-7.36 (m, 2 H, Ar), 7.50-7.54 (m, 2 H, Ar) ppm. <sup>13</sup>C-NMR (C<sub>6</sub>D<sub>6</sub>, 75 MHz):  $\delta$  = 30.9 (q, NCH<sub>3</sub>), 92.9 (d, CHPh), 107.8 (d, Ar), 120.5 (d, Ar), 121.8 (d, Ar), 124.3 (d, Ar), 124.5 (s, NC=CS), 126.4 (d, Ar), 126.7 (d, Ar), 129.3 (d, Ar), 139.0 (s, Ar), 143.1 (s, NC=CS), 143.8 (s, NCS) ppm. HRMS (EI positive): *m/z* calculated for [C<sub>15</sub>H<sub>13</sub>N<sup>32</sup>S]<sup>+</sup> is 239.0763; found 239.0762.

4.7 Reactions of **1a,b** and **6** with diarylcarbenium ionsReaction of **1a** with  $(4\text{-Me}_2\text{NC}_6\text{H}_4)_2\text{CH}^+\text{BF}_4^-$ 

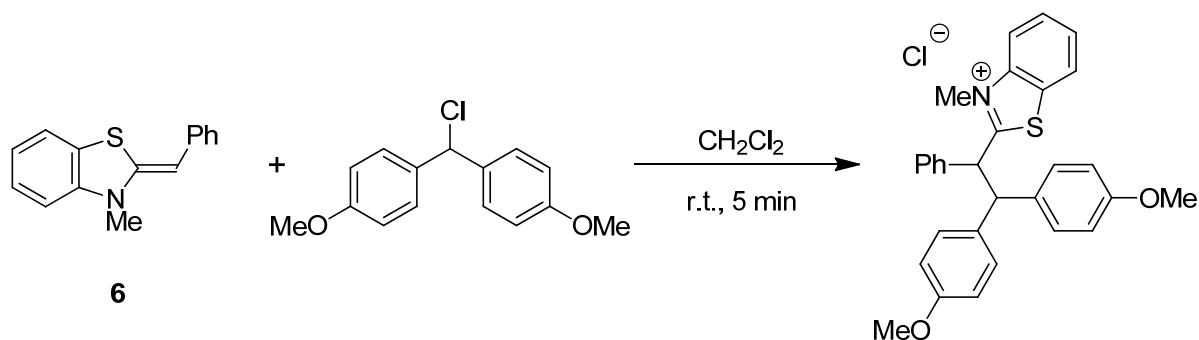
To blue solution of  $(4\text{-Me}_2\text{NC}_6\text{H}_4)_2\text{CH}^+\text{BF}_4^-$  **4b-BF<sub>4</sub><sup>-</sup>** (34 mg, 0.10 mmol) in CH<sub>3</sub>CN (2 mL) was added a yellow solution of **1a** (24.8 mg, 0.100 mmol) in *n*-pentane (2 mL) and the solution was stirred for 5 min at room temperature before the solvent was evaporated under reduced pressure and the pale blue residue was then washed with *n*-pentane and dried to give the thiazolium salt **5a** as blue solid, 52 mg, 0.089 mmol, 89%. Mp: = 102-107 °C (decomposition, CH<sub>3</sub>CN). <sup>1</sup>H-NMR (CD<sub>6</sub>CN, 400 MHz):  $\delta$  = 2.24 (s, 3 H, CH<sub>3</sub>), 2.32 (s, 3 H, CH<sub>3</sub>), 2.81 (s, 3 H, Ar-NCH<sub>3</sub>), 2.90 (s, 3 H, Ar-NCH<sub>3</sub>), 3.20 (s, 3 H, OCH<sub>3</sub>), 3.47 (s, 3 H, NCH<sub>3</sub>), 4.92 (s, Ar<sub>2</sub>CH), 6.52 (d,  $J$  = 9.0 Hz, 2 H, Ar), 6.70 (d,  $J$  = 9.0 Hz, 2 H, Ar), 7.11 (d,  $J$  = 9.0 Hz, 2 H, Ar), 7.24 (d,  $J$  = 7.7 Hz, 2 H, Ar), 7.37-7.47 (m, 5 H, Ar) ppm. <sup>13</sup>C-NMR (CD<sub>6</sub>CN, 100 MHz):  $\delta$  = 12.3 (q, CH<sub>3</sub>), 12.7 (q, CH<sub>3</sub>), 40.5 (q, NCH<sub>3</sub>), 40.7 (q, Ar-NCH<sub>3</sub>), 40.8 (q, Ar-NCH<sub>3</sub>), 55.2 (q, OCH<sub>3</sub>), 57.2 (Ar<sub>2</sub>CH), 89.3 (s, C(Ph)OCH<sub>3</sub>), 113.2 (d, Ar), 113.6 (d, Ar), 129.2 (s, Ar), 129.3 (s, Ar), 129.7 (d, Ar), 130.7 (d, Ar), 130.8 (d, Ar), 131.0 (d, Ar), 132.0 (d, Ar), 132.6 (s, Ar), 136.2 (s, Ar), 145.5 (s, Ar), 150.89 (s, Ar), 150.94 (s, Ar), 177.6 (s, NCS) ppm. HRMS (ESI positive):  $m/z$  calculated for [C<sub>31</sub>H<sub>38</sub>N<sub>3</sub>OS]<sup>+</sup> is 500.2730; found 500.2731.

Reaction of **1b** with  $(4\text{-MeOC}_6\text{H}_4)_2\text{CHCl}$ 

To solution of  $(4\text{-MeOC}_6\text{H}_4)_2\text{CHCl}$  (26.3 mg, 0.100 mmol) in CH<sub>3</sub>CN (1 mL) was added a yellow solution of **1b** (26.9 mg, 0.100 mmol) in CH<sub>3</sub>CN (1 mL) and stirred for 5 min. The

solvent was then evaporated to give 47 mg (0.088 mmol, 88%) of the thiazolium salt as off-white powder. Mp: = 142-143 °C (CH<sub>3</sub>CN). <sup>1</sup>H-NMR (CD<sub>3</sub>CN + ε CDCl<sub>3</sub>, 400 MHz): δ = 3.28 (s, 3 H, OCH<sub>3</sub>), 3.55 (s, 3 H, Ar-OCH<sub>3</sub>), 3.78 (s, 3 H, Ar-OCH<sub>3</sub>), 3.96 (s, 3 H, NCH<sub>3</sub>), 5.29 (s, 1 H, Ar<sub>2</sub>CH), 6.56 (d, *J* = 9.0 Hz, 2 H, Ar), 6.94 (d, *J* = 9.0 Hz, 2 H, Ar), 7.34-7.37 (m, 6 H, Ar), 7.47-7.51 (m, 1 H, Ar), 7.73-7.81 (m, 4 H, Ar), 8.03 (d, *J* = 8.6, 1H, Ar), 8.24 (d, *J* = 8.6 Hz, 1 H, Ar) ppm. <sup>13</sup>C-NMR (CD<sub>3</sub>CN + ε CDCl<sub>3</sub>, 100 MHz): δ = 40.0 (q, NCH<sub>3</sub>), 55.7 (q, OCH<sub>3</sub>), 55.9 (q, Ar-OCH<sub>3</sub>), 56.3 (q, Ar-OCH<sub>3</sub>), 57.0 (d, Ar<sub>2</sub>CH), 90.1 (s, C(Ph)OCH<sub>3</sub>), 114.7 (d, Ar), 115.2 (d, Ar), 117.9 (d, Ar), 124.8 (d, Ar), 129.7 (s, Ar), 129.8 (d, Ar), 130.1 (d, Ar), 130.4 (d, Ar), 130.84 (d, Ar), 130.87 (d, Ar), 131.5 (d, Ar), 132.2 (d, Ar), 133.2 (s, Ar), 133.8 (s, Ar), 134.3 (s, Ar), 144.4 (s, Ar), 159.6 (s, Ar), 159.8 (s, Ar), 188.0 (s, NCS) ppm. HRMS (ESI positive): *m/z* calculated for [C<sub>31</sub>H<sub>30</sub>NO<sub>3</sub>S]<sup>+</sup> is 496.1941; found 496.1938.

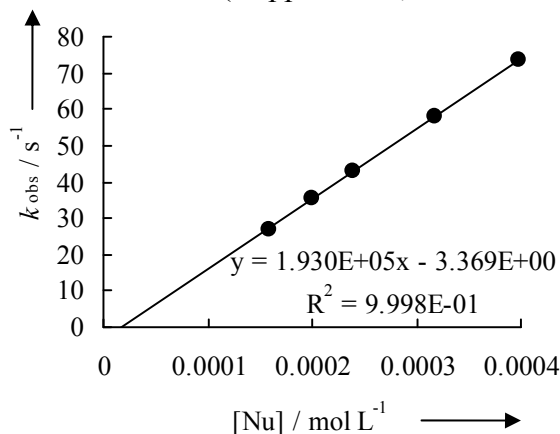
#### Reaction of **6** with (4-MeOC<sub>6</sub>H<sub>4</sub>)<sub>2</sub>CHCl



To solution of (4-MeOC<sub>6</sub>H<sub>4</sub>)<sub>2</sub>CHCl (26.3 mg, 0.10 mmol) in CH<sub>2</sub>Cl<sub>2</sub> (1 mL) was added a yellow solution of **6** (23.9 mg, 0.100 mmol) in CH<sub>2</sub>Cl<sub>2</sub> (1 mL) and stirred for 5 min. The solvent was then evaporated, washed with *n*-pentane, and dried to give 47 mg (0.094 mmol, 94%) of the thiazolium salt at white powder. Mp: = 135-137 °C (decomp., CHCl<sub>3</sub>-*n*-pentane). <sup>1</sup>H-NMR (CDCl<sub>3</sub>, 600 MHz): δ = 3.50 (s, 3 H, OCH<sub>3</sub>), 3.56 (s, 3 H, OCH<sub>3</sub>), 4.55 (s, 3 H, NCH<sub>3</sub>), 4.75 (d, *J* = 11.8 Hz, 1 H, Ar<sub>2</sub>CH), 6.55 (d, *J* = 8.7 Hz, 2 H, Ar), 6.73 (d, *J* = 8.7 Hz, 2 H, Ar), 7.06 (t, *J* = 7.33 Hz, 1 H, Ar), 7.10-7.15 (m, 3 H, CHPh + Ar), 7.45 (d, *J* = 8.7 Hz, 2 H, Ar), 7.56-7.59 (m, 3 H, Ar), 7.67 (t, *J* = 7.7 Hz, 1 H, Ar), 7.76 (d, *J* = 8.6 Hz, 2 H, Ar), 7.91 (d, *J* = 8.6 Hz, 1 H, Ar), 8.09 (d, *J* = 8.2 Hz, 1 H, Ar) ppm. <sup>13</sup>C-NMR (CDCl<sub>3</sub>, 150 MHz): δ = 39.1 (q, NCH<sub>3</sub>), 51.4 (d, CHPh), 55.1 (q, OCH<sub>3</sub>), 55.3 (q, OCH<sub>3</sub>), 57.4 (Ar<sub>2</sub>CH), 114.1 (d, Ar), 115.0 (d, Ar), 116.9 (d, Ar), 124.1 (d, Ar), 128.4 (d, Ar), 129.0 (s, Ar), 129.1 (d, Ar), 129.4 (d, Ar), 129.5 (d, Ar), 129.84 (d, Ar), 129.88 (d, Ar), 130.3 (d, Ar), 132.9 (s, Ar), 133.7 (s, Ar), 136.3 (s, Ar), 141.3 (s, Ar), 158.2 (s, Ar), 158.8 (s, Ar), 182.9 (s, NCS) ppm. HRMS (ESI positive): *m/z* calculated for [C<sub>30</sub>H<sub>28</sub>NO<sub>2</sub>S]<sup>+</sup> is 466.1835; found 466.1833.

4.8 Kinetics of the reactions of nucleophiles **1** or **6** and the diarylcarbenium ions **4**4.8.1 Kinetics of the reactions of the **1a** with the reference electrophiles **4**.**Table 3:** Kinetics of the reaction of **1a** with **4d** at 20 °C in THF (stopped-flow,  $\lambda = 625$  nm).

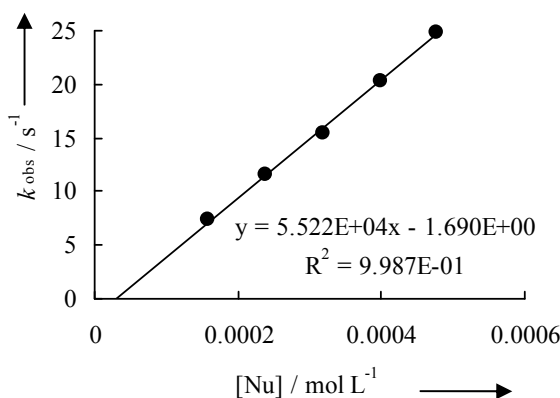
[ <b>4d</b> ] / mol L <sup>-1</sup>	[ <b>1a</b> ] / mol L <sup>-1</sup>	$k_{\text{obs}}$ / s <sup>-1</sup>
$1.53 \times 10^{-5}$	$1.59 \times 10^{-4}$	27.1
	$1.99 \times 10^{-4}$	35.4
	$2.39 \times 10^{-4}$	42.9
	$3.19 \times 10^{-4}$	57.8
	$3.98 \times 10^{-4}$	73.6



$$k = 1.93 \times 10^5 \text{ L mol}^{-1} \text{ s}^{-1}$$

**Table 4:** Kinetics of the reaction of **1a** with **4e** at 20 °C in THF (stopped-flow,  $\lambda = 625$  nm).

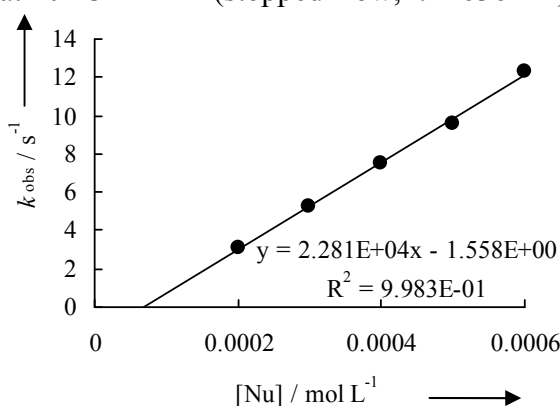
[ <b>4e</b> ] / mol L <sup>-1</sup>	[ <b>1a</b> ] / mol L <sup>-1</sup>	$k_{\text{obs}}$ / s <sup>-1</sup>
$1.37 \times 10^{-5}$	$1.59 \times 10^{-4}$	7.31
	$2.39 \times 10^{-4}$	11.5
	$3.19 \times 10^{-4}$	15.5
	$3.98 \times 10^{-4}$	20.3
	$4.78 \times 10^{-4}$	24.9



$$k = 5.22 \times 10^4 \text{ L mol}^{-1} \text{ s}^{-1}$$

**Table 5:** Kinetics of the reaction of **1a** with **4f** at 20 °C in THF (stopped-flow,  $\lambda = 636$  nm).

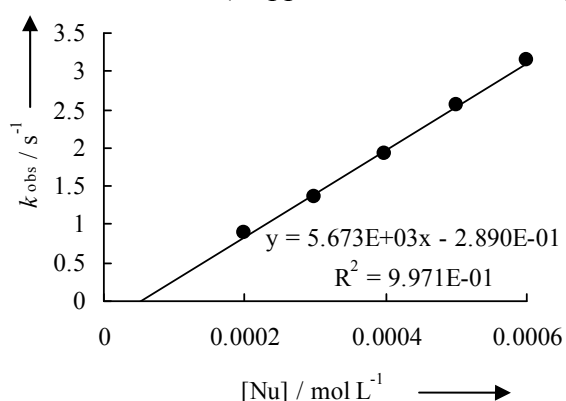
[ <b>4f</b> ] / mol L <sup>-1</sup>	[ <b>1a</b> ] / mol L <sup>-1</sup>	$k_{\text{obs}}$ / s <sup>-1</sup>
$1.86 \times 10^{-5}$	$2.00 \times 10^{-4}$	3.09
	$3.00 \times 10^{-4}$	5.27
	$3.99 \times 10^{-4}$	7.48
	$4.99 \times 10^{-4}$	9.63
	$5.99 \times 10^{-4}$	12.3



$$k = 2.28 \times 10^4 \text{ L mol}^{-1} \text{ s}^{-1}$$

**Table 6:** Kinetics of the reaction of **1a** with **4g** at 20 °C in THF (stopped-flow,  $\lambda = 636$  nm).

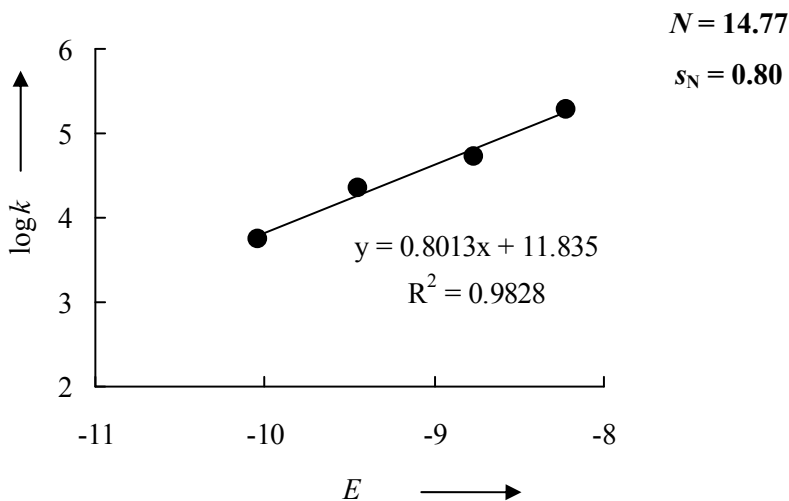
[ <b>4g</b> ] / mol L <sup>-1</sup>	[ <b>1a</b> ] / mol L <sup>-1</sup>	$k_{\text{obs}}$ / s <sup>-1</sup>
$1.54 \times 10^{-5}$	$2.00 \times 10^{-4}$	0.903
	$3.00 \times 10^{-4}$	1.36
	$3.99 \times 10^{-4}$	1.93
	$4.99 \times 10^{-4}$	2.55
	$5.99 \times 10^{-4}$	3.14



$$k = 5.67 \times 10^3 \text{ L mol}^{-1} \text{ s}^{-1}$$

**Table 7:** Determination of the parameters  $N$  and  $s_N$  for **1a** in THF.

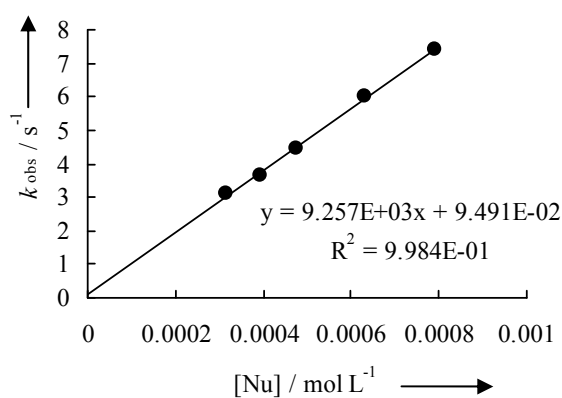
Electrophiles	$E$	$k$ (M <sup>-1</sup> s <sup>-1</sup> )
<b>4d</b>	-8.22	$1.93 \times 10^5$
<b>4e</b>	-8.76	$5.22 \times 10^4$
<b>4f</b>	-9.45	$2.28 \times 10^4$
<b>4g</b>	-10.04	$5.67 \times 10^3$



#### 4.8.2 Kinetics of the reactions of the **1b** with the reference electrophiles **4**.

**Table 8:** Kinetics of the reaction of **1b** with **4a** at 20 °C in THF (stopped-flow,  $\lambda = 618$  nm).

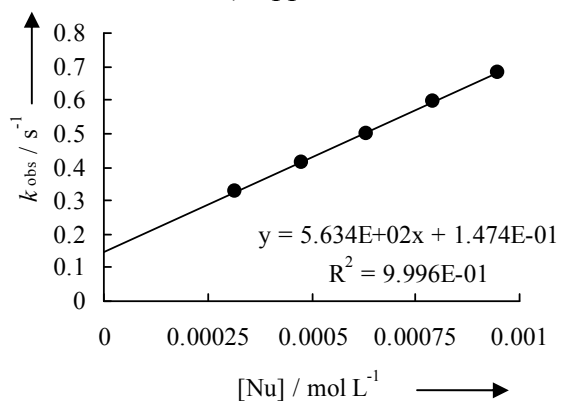
[ <b>4a</b> ] / mol L <sup>-1</sup>	[ <b>1b</b> ] / mol L <sup>-1</sup>	$k_{\text{obs}}$ / s <sup>-1</sup>
$1.70 \times 10^{-5}$	$3.16 \times 10^{-4}$	3.10
	$3.95 \times 10^{-4}$	3.66
	$4.74 \times 10^{-4}$	4.46
	$6.33 \times 10^{-4}$	6.01
	$7.91 \times 10^{-4}$	7.40



$$k = 9.26 \times 10^3 \text{ L mol}^{-1} \text{ s}^{-1}$$

**Table 9:** Kinetics of the reaction of **1b** with **4b** at 20 °C in THF (stopped-flow,  $\lambda = 611$  nm).

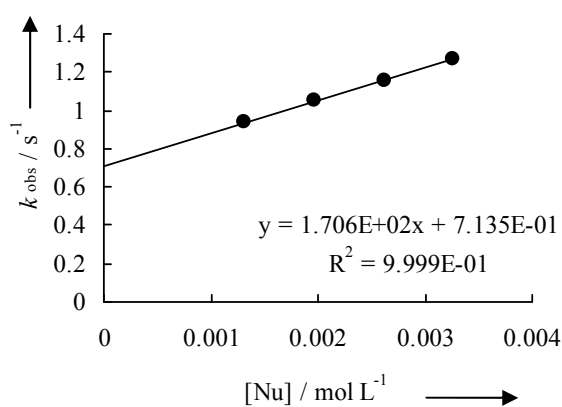
[ <b>4b</b> ] / mol L <sup>-1</sup>	[ <b>1b</b> ] / mol L <sup>-1</sup>	$k_{\text{obs}} / \text{s}^{-1}$
$1.54 \times 10^{-5}$	$3.16 \times 10^{-4}$	0.329
	$4.74 \times 10^{-4}$	0.411
	$6.33 \times 10^{-4}$	0.502
	$7.91 \times 10^{-4}$	0.594
	$9.49 \times 10^{-4}$	0.683



$$k = 5.63 \times 10^2 \text{ L mol}^{-1} \text{ s}^{-1}$$

**Table 10:** Kinetics of the reaction of **1b** with **4c** at 20 °C in THF (stopped-flow,  $\lambda = 618$  nm).

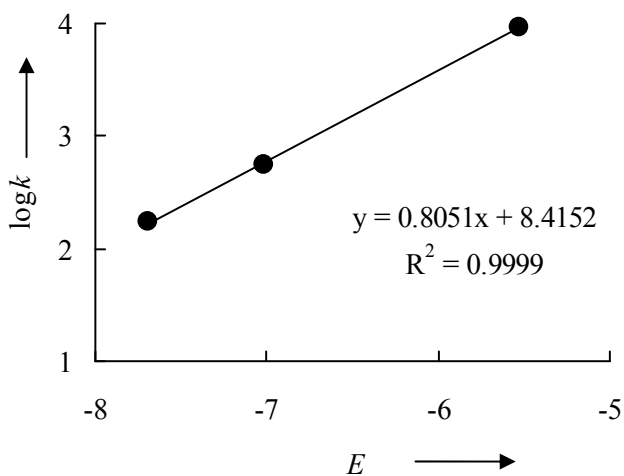
[ <b>4c</b> ] / mol L <sup>-1</sup>	[ <b>1b</b> ] / mol L <sup>-1</sup>	$k_{\text{obs}} / \text{s}^{-1}$
$1.90 \times 10^{-5}$	$1.31 \times 10^{-3}$	0.935
	$1.96 \times 10^{-3}$	1.05
	$2.61 \times 10^{-3}$	1.16
	$3.27 \times 10^{-3}$	1.27



$$k = 1.71 \times 10^2 \text{ L mol}^{-1} \text{ s}^{-1}$$

**Table 11:** Determination of the parameters  $N$  and  $s_N$  for **1b** in THF.

Electrophiles	$E$	$k$ (M <sup>-1</sup> s <sup>-1</sup> )
<b>4a</b>	-5.53	$9.26 \times 10^3$
<b>4b</b>	-7.02	$5.63 \times 10^2$
<b>4c</b>	-7.69	$1.71 \times 10^2$

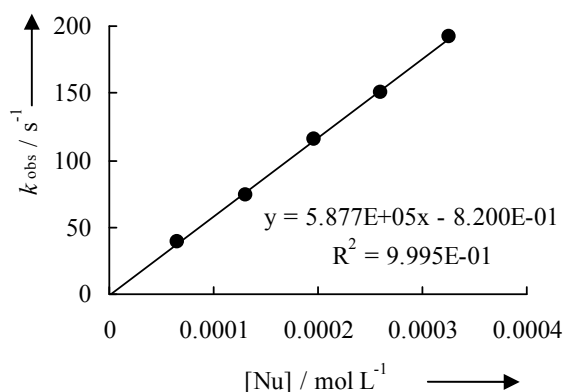


$$N = 10.45$$

$$s_N = 0.81$$

4.8.3 Kinetics of the reactions of the **1c** with the reference electrophiles **4**.**Table 12:** Kinetics of the reaction of **1c** with **4d** at 20 °C in THF (stopped-flow,  $\lambda = 625$  nm).

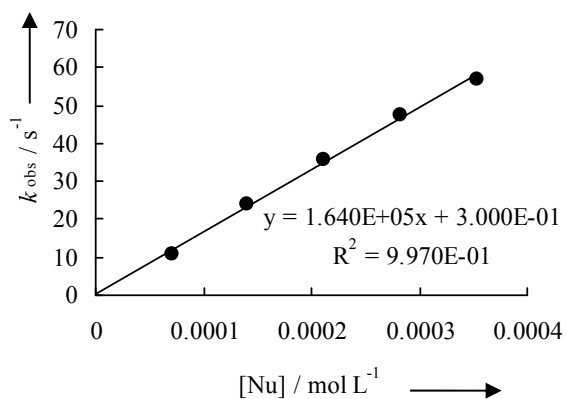
[ <b>4d</b> ] / mol L <sup>-1</sup>	[ <b>1c</b> ] / mol L <sup>-1</sup>	$k_{\text{obs}}$ / s <sup>-1</sup>
$1.07 \times 10^{-5}$	$6.52 \times 10^{-5}$	38.6
	$1.30 \times 10^{-4}$	74.4
	$1.96 \times 10^{-4}$	115
	$2.61 \times 10^{-4}$	151
	$3.26 \times 10^{-4}$	192



$$k = 5.88 \times 10^5 \text{ L mol}^{-1} \text{ s}^{-1}$$

**Table 13:** Kinetics of the reaction of **1c** with **4e** at 20 °C in THF (stopped-flow,  $\lambda = 625$  nm).

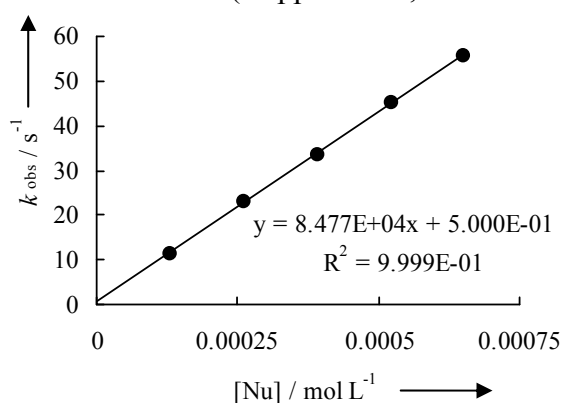
[ <b>4e</b> ] / mol L <sup>-1</sup>	[ <b>1c</b> ] / mol L <sup>-1</sup>	$k_{\text{obs}}$ / s <sup>-1</sup>
$1.17 \times 10^{-5}$	$7.06 \times 10^{-5}$	10.9
	$1.41 \times 10^{-4}$	24.0
	$2.12 \times 10^{-4}$	35.7
	$2.82 \times 10^{-4}$	47.6
	$3.53 \times 10^{-4}$	57.0



$$k = 1.64 \times 10^5 \text{ L mol}^{-1} \text{ s}^{-1}$$

**Table 14:** Kinetics of the reaction of **1c** with **4f** at 20 °C in THF (stopped-flow,  $\lambda = 636$  nm).

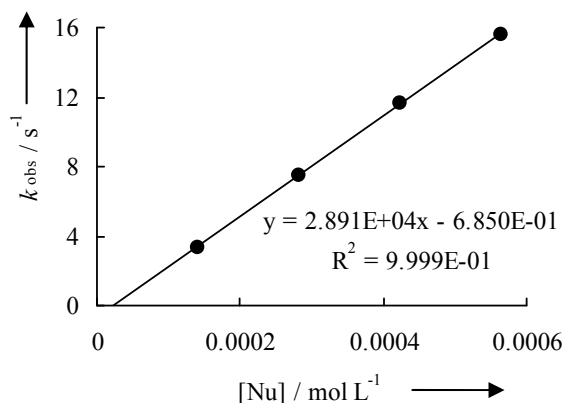
[ <b>4f</b> ] / mol L <sup>-1</sup>	[ <b>1c</b> ] / mol L <sup>-1</sup>	$k_{\text{obs}}$ / s <sup>-1</sup>
$1.46 \times 10^{-5}$	$1.30 \times 10^{-4}$	11.4
	$2.61 \times 10^{-4}$	22.8
	$3.91 \times 10^{-4}$	33.6
	$5.22 \times 10^{-4}$	45.0
	$6.52 \times 10^{-4}$	55.6



$$k = 8.48 \times 10^4 \text{ L mol}^{-1} \text{ s}^{-1}$$

**Table 15:** Kinetics of the reaction of **1c** with **4g** at 20 °C in THF (stopped-flow,  $\lambda = 636$  nm).

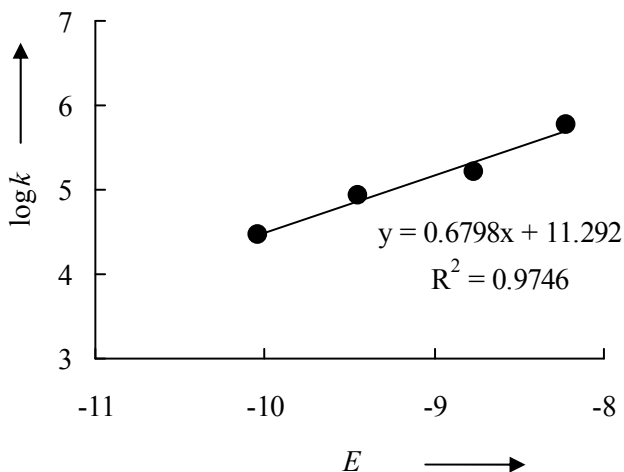
[ <b>4g</b> ] / mol L <sup>-1</sup>	[ <b>1c</b> ] / mol L <sup>-1</sup>	$k_{\text{obs}} / \text{s}^{-1}$
$1.50 \times 10^{-5}$	$1.41 \times 10^{-4}$	3.35
	$2.82 \times 10^{-4}$	7.53
	$4.24 \times 10^{-4}$	11.6
	$5.65 \times 10^{-4}$	15.6



$$k = 2.89 \times 10^4 \text{ L mol}^{-1} \text{ s}^{-1}$$

**Table 16:** Determination of the parameters  $N$  and  $s_N$  for **1c** in THF.

Electrophiles	$E$	$k$ (M <sup>-1</sup> s <sup>-1</sup> )
<b>4d</b>	-8.22	$5.88 \times 10^5$
<b>4e</b>	-8.76	$1.64 \times 10^5$
<b>4f</b>	-9.45	$8.48 \times 10^4$
<b>4g</b>	-10.04	$2.89 \times 10^4$



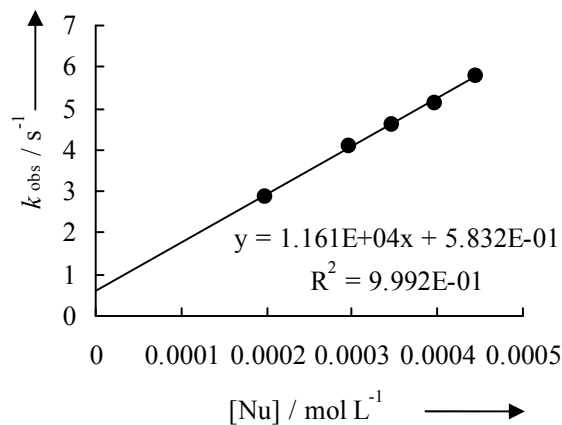
$$N = 16.61$$

$$s_N = 0.68$$

#### 4.8.4 Kinetics of the reactions of the **1e** with the reference electrophiles **4**.

**Table 17:** Kinetics of the reaction of **1e** with **4c** at 20 °C in THF (stopped-flow,  $\lambda = 625$  nm).

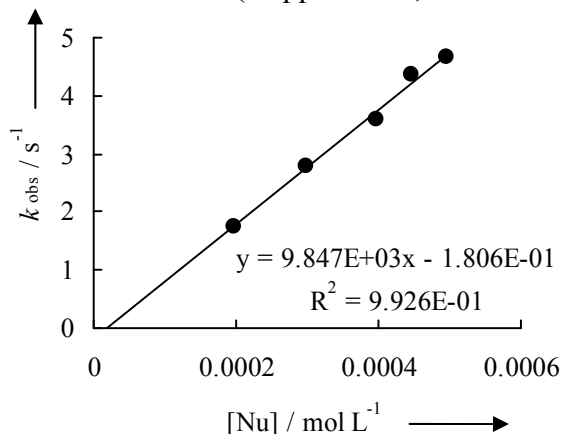
[ <b>4c</b> ] / mol L <sup>-1</sup>	[ <b>1e</b> ] / mol L <sup>-1</sup>	$k_{\text{obs}} / \text{s}^{-1}$
$1.47 \times 10^{-5}$	$1.98 \times 10^{-4}$	2.87
	$2.97 \times 10^{-4}$	4.07
	$3.47 \times 10^{-4}$	4.62
	$3.97 \times 10^{-4}$	5.15
	$4.46 \times 10^{-4}$	5.78



$$k = 1.16 \times 10^4 \text{ L mol}^{-1} \text{ s}^{-1}$$

**Table 18:** Kinetics of the reaction of **1e** with **4d** at 20 °C in THF (stopped-flow,  $\lambda = 625$  nm).

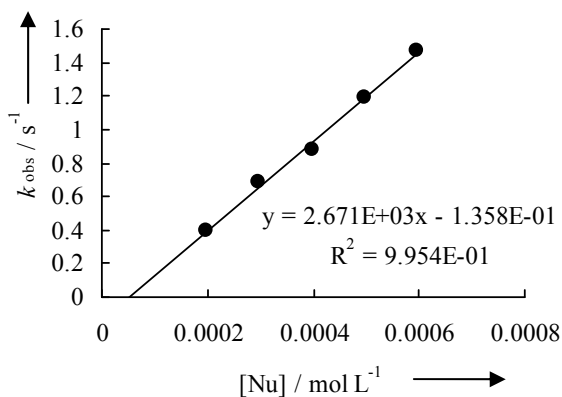
[ <b>4d</b> ] / mol L <sup>-1</sup>	[ <b>1e</b> ] / mol L <sup>-1</sup>	$k_{\text{obs}}$ / s <sup>-1</sup>
$1.71 \times 10^{-5}$	$1.98 \times 10^{-4}$	1.76
	$2.97 \times 10^{-4}$	2.80
	$3.97 \times 10^{-4}$	3.59
	$4.46 \times 10^{-4}$	4.36
	$4.96 \times 10^{-4}$	4.66



$$k = 9.85 \times 10^3 \text{ L mol}^{-1} \text{ s}^{-1}$$

**Table 19:** Kinetics of the reaction of **1e** with **4e** at 20 °C in THF (stopped-flow,  $\lambda = 625$  nm).

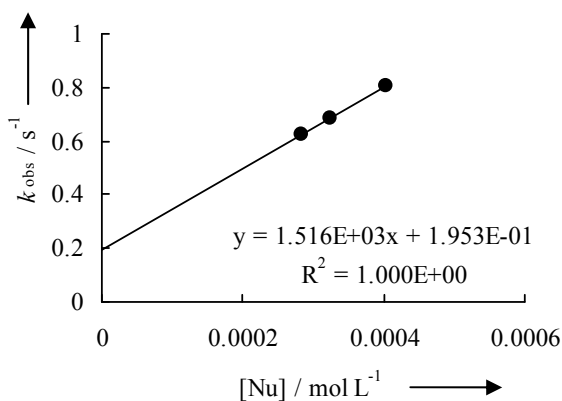
[ <b>4e</b> ] / mol L <sup>-1</sup>	[ <b>1e</b> ] / mol L <sup>-1</sup>	$k_{\text{obs}}$ / s <sup>-1</sup>
$1.36 \times 10^{-5}$	$1.98 \times 10^{-4}$	0.398
	$2.97 \times 10^{-4}$	0.685
	$3.97 \times 10^{-4}$	0.876
	$4.96 \times 10^{-4}$	1.19
	$5.95 \times 10^{-4}$	1.47



$$k = 2.67 \times 10^3 \text{ L mol}^{-1} \text{ s}^{-1}$$

**Table 20:** Kinetics of the reaction of **1e** with **4f** at 20 °C in THF (stopped-flow,  $\lambda = 636$  nm).

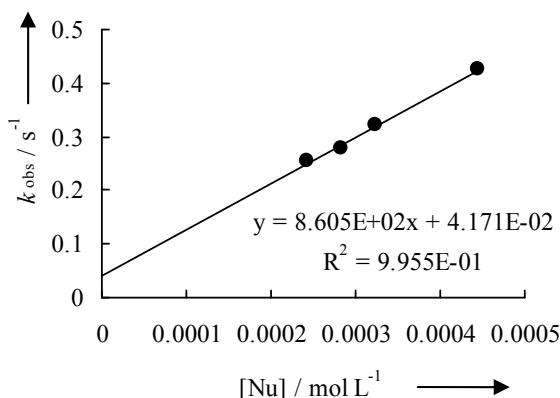
[ <b>4f</b> ] / mol L <sup>-1</sup>	[ <b>1e</b> ] / mol L <sup>-1</sup>	$k_{\text{obs}}$ / s <sup>-1</sup>
$1.62 \times 10^{-5}$	$2.83 \times 10^{-4}$	0.624
	$3.23 \times 10^{-4}$	0.686
	$4.04 \times 10^{-4}$	0.808



$$k = 1.52 \times 10^3 \text{ L mol}^{-1} \text{ s}^{-1}$$

**Table 21:** Kinetics of the reaction of **1e** with **4g** at 20 °C in THF (stopped-flow,  $\lambda = 636$  nm).

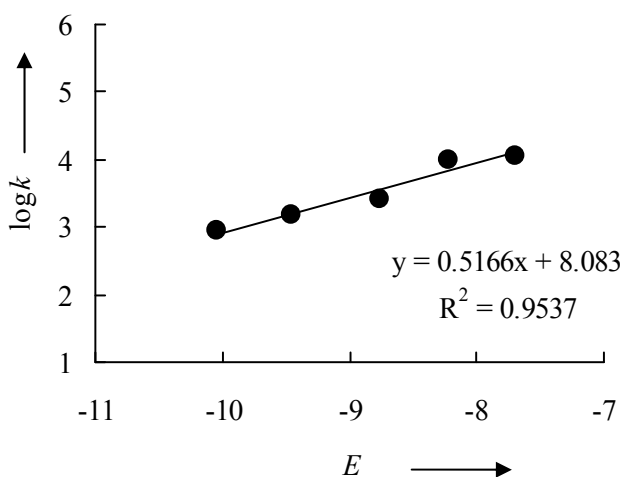
[ <b>4g</b> ] / mol L <sup>-1</sup>	[ <b>1e</b> ] / mol L <sup>-1</sup>	$k_{\text{obs}}$ / s <sup>-1</sup>
$1.68 \times 10^{-5}$	$2.43 \times 10^{-4}$	0.255
	$2.83 \times 10^{-4}$	0.278
	$3.23 \times 10^{-4}$	0.322
	$4.45 \times 10^{-4}$	0.425



$$k = 8.61 \times 10^2 \text{ L mol}^{-1} \text{ s}^{-1}$$

**Table 22:** Determination of the parameters  $N$  and  $s_N$  for **1e** in THF.

Electrophiles	$E$	$k$ (M <sup>-1</sup> s <sup>-1</sup> )
<b>4c</b>	-7.69	$1.16 \times 10^4$
<b>4d</b>	-8.22	$9.85 \times 10^3$
<b>4e</b>	-8.76	$2.67 \times 10^3$
<b>4f</b>	-9.45	$1.52 \times 10^3$
<b>4g</b>	-10.04	$8.61 \times 10^2$



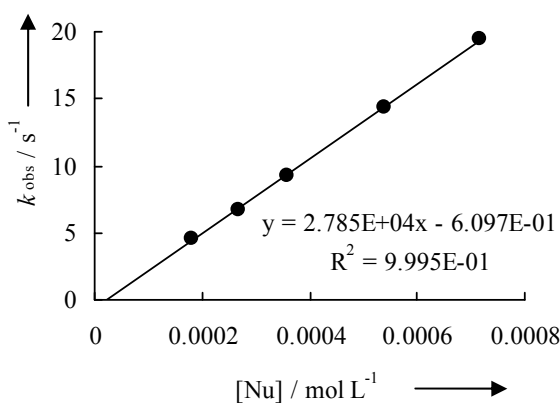
$$N = 15.65$$

$$s_N = 0.52$$

#### 4.8.5 Kinetics of the reactions of the **6** with the reference electrophiles **4**.

**Table 23:** Kinetics of the reaction of **6** with **4c** at 20 °C in THF (stopped-flow,  $\lambda = 625$  nm).

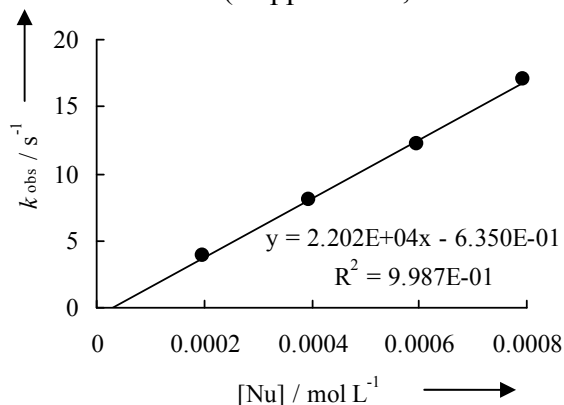
[ <b>4c</b> ] / mol L <sup>-1</sup>	[ <b>6</b> ] / mol L <sup>-1</sup>	$k_{\text{obs}}$ / s <sup>-1</sup>
$1.53 \times 10^{-5}$	$1.79 \times 10^{-4}$	4.57
	$2.69 \times 10^{-4}$	6.72
	$3.59 \times 10^{-4}$	9.28
	$5.38 \times 10^{-4}$	14.4
	$7.17 \times 10^{-4}$	19.4



$$k = 2.79 \times 10^4 \text{ L mol}^{-1} \text{ s}^{-1}$$

**Table 24:** Kinetics of the reaction of **6** with **4d** at 20 °C in THF (stopped-flow,  $\lambda = 625$  nm).

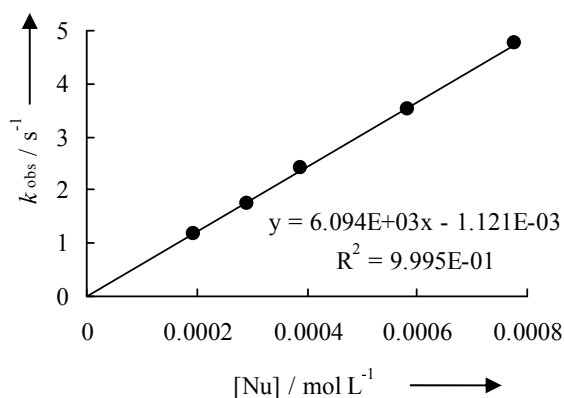
[ <b>4d</b> ] / mol L <sup>-1</sup>	[ <b>6</b> ] / mol L <sup>-1</sup>	$k_{\text{obs}} / \text{s}^{-1}$
$1.42 \times 10^{-5}$	$1.98 \times 10^{-4}$	3.86
	$3.96 \times 10^{-4}$	8.01
	$5.94 \times 10^{-4}$	12.2
	$7.92 \times 10^{-4}$	17.0



$$k = 2.20 \times 10^4 \text{ L mol}^{-1} \text{ s}^{-1}$$

**Table 25:** Kinetics of the reaction of **6** with **4e** at 20 °C in THF (stopped-flow,  $\lambda = 625$  nm).

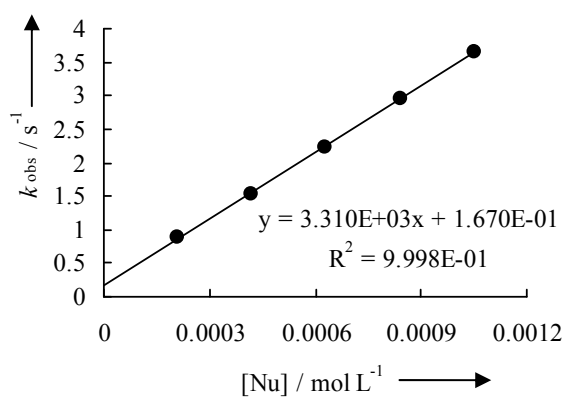
[ <b>4e</b> ] / mol L <sup>-1</sup>	[ <b>6</b> ] / mol L <sup>-1</sup>	$k_{\text{obs}} / \text{s}^{-1}$
$1.65 \times 10^{-5}$	$1.94 \times 10^{-4}$	1.18
	$2.91 \times 10^{-4}$	1.76
	$3.89 \times 10^{-4}$	2.41
	$5.83 \times 10^{-4}$	3.51
	$7.77 \times 10^{-4}$	4.75



$$k = 6.09 \times 10^3 \text{ L mol}^{-1} \text{ s}^{-1}$$

**Table 26:** Kinetics of the reaction of **6** with **4f** at 20 °C in THF (stopped-flow,  $\lambda = 636$  nm).

[ <b>4f</b> ] / mol L <sup>-1</sup>	[ <b>6</b> ] / mol L <sup>-1</sup>	$k_{\text{obs}} / \text{s}^{-1}$
$1.70 \times 10^{-5}$	$2.10 \times 10^{-4}$	0.880
	$4.20 \times 10^{-4}$	1.54
	$6.30 \times 10^{-4}$	2.24
	$8.40 \times 10^{-4}$	2.95
	$1.05 \times 10^{-3}$	3.65



$$k = 3.31 \times 10^3 \text{ L mol}^{-1} \text{ s}^{-1}$$

**Table 27:** Determination of the parameters  $N$  and  $s_N$  for **1e** in THF.

Electrophiles	$E$	$k$ ( $M^{-1} s^{-1}$ )
<b>4c</b>	-7.69	$2.79 \times 10^4$
<b>4d</b>	-8.22	$2.20 \times 10^4$
<b>4e</b>	-8.76	$6.09 \times 10^3$
<b>4f</b>	-9.45	$3.31 \times 10^3$

$N = 15.58$   
 $s_N = 0.57$

#### 4.9 Determination of the Equilibrium constants

**Table 28.** Equilibrium constant for the reaction of **1b** with **4b** in THF (20 °C, 611 nm).

Entry	$A_t$	$(A_0 - A_t)$	$[4b]_t$	$[1b]_t$	$K$ ( $M^{-1}$ )
0			$1.32 \times 10^{-5}$	0	
1	0.486	0.479	$6.66 \times 10^{-6}$	$3.16 \times 10^{-4}$	$3.18 \times 10^3$
2	0.380	0.585	$5.20 \times 10^{-6}$	$4.75 \times 10^{-4}$	$3.31 \times 10^3$
3	0.294	0.671	$4.03 \times 10^{-6}$	$6.33 \times 10^{-4}$	$3.66 \times 10^3$
4	0.232	0.732	$3.18 \times 10^{-6}$	$7.91 \times 10^{-4}$	$4.04 \times 10^3$
5	0.187	0.778	$2.56 \times 10^{-6}$	$9.49 \times 10^{-4}$	$4.43 \times 10^3$

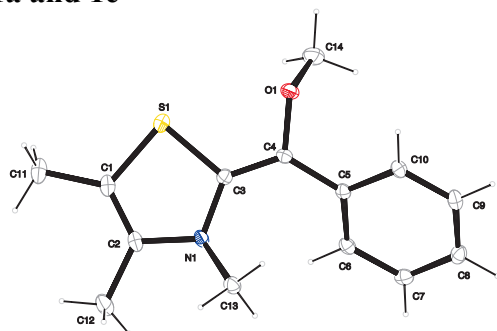
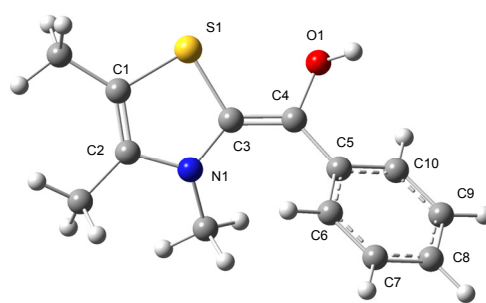
$$K = (3-5) \times 10^3 M^{-1}$$

**Table 29.** Equilibrium constant for the reaction of **1b** with **4c** in THF (20 °C, 618 nm).

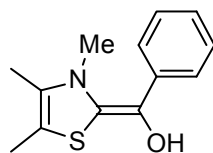
Entry	$A_t$	$(A_0 - A_t)$	$[4c]_t$	$[1b]_t$	$K$ ( $M^{-1}$ )
0			$1.37 \times 10^{-5}$	0	
1	0.821	0.129	$1.18 \times 10^{-5}$	$1.31 \times 10^{-3}$	$1.20 \times 10^2$
2	0.694	0.256	$9.99 \times 10^{-6}$	$1.96 \times 10^{-3}$	$1.89 \times 10^2$
3	0.479	0.471	$6.89 \times 10^{-6}$	$2.61 \times 10^{-3}$	$3.78 \times 10^2$
4	0.394	0.556	$5.47 \times 10^{-6}$	$3.27 \times 10^{-3}$	$4.33 \times 10^2$

$$K = (1-5) \times 10^2 M^{-1}$$

## 4.10 Comparison of the calculated structures of 1a-OH and 1e-OH with the crystal structures of 1a and 1e

Crystal structure of **1a**Calculated structure of **1a-OH**  
B3LYP/6-31+g(2d,p)<sup>[S7]</sup>

C3-C4	134.9	136.2
C3-S1	176.5	177.6
C3-N1	141.9	139.4
C1-S1	176.1	177.4
C1-C2	133.0	134.9
C2-N1	141.9	141.2
C4-O1	140.0	139.9
C4-C5	146.4	146.1
S1-O1	285.0	286.9
S1-C3-C4	120.6	120.8
C3-C4-O1	114.1	113.9
S1-C3-C4-O1	13.4	-14.1
N1-C3-C4-C5	14.8	-18.5
C3-C4-C5-C6	28.4	-32.3

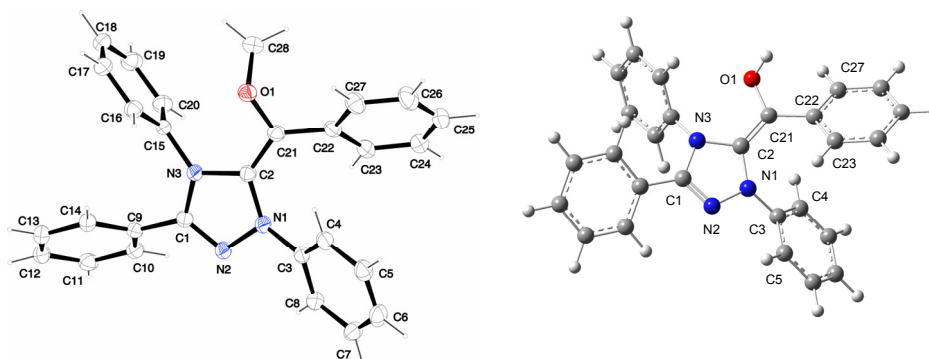
**1a-OH**

```

1|1|UNPC-HAFNIUM|FOpt|RB3LYP|6-31+G(2d,p)|C13H15N1O1S1|MBICH|28-May-20
12|0|# opt b3lyp/6-31+g(2d,p) geom=connectivity|[No Title]|0,1|C,-1
.9521926274,2.4264965775,0.1401053808|C,-2.1601641389,1.0938514743,0.1
718956926|N,-1.0115944667,0.3204727375,-0.1038921869|C,0.1452608835,1.
0822741916,-0.2650140913|S,-0.2653661513,2.8103325122,-0.2535535311|C,
1.4305837121,0.6717875568,-0.4522369256|C,3.1557967107,-1.0578392845,-
0.9308845747|C,-1.114142319,-1.0152886827,-0.6814071105|C,-2.904099469
2,3.5539568057,0.3872750602|C,-3.4463570037,0.3903443197,0.4878158982|
O,2.2809034356,1.6739783095,-0.9307284893|C,2.0350132101,-0.6314179918
,-0.1857053433|C,3.7911286965,-2.2636468418,-0.6468546537|C,3.33451491
48,-3.0798602465,0.3903783064|C,2.2380549702,-2.6641953151,1.149621926
|C,1.6019824927,-1.4572503924,0.8734858354|H,3.5100737687,-0.439046832
,-1.7486498663|H,-0.3967748357,-1.1046035912,-1.50168915|H,-0.89443561
72,-1.8061828206,0.0438678305|H,-2.1179462329,-1.1713552031,-1.0782442
041|H,-3.9171429423,3.1889632109,0.5728136806|H,-2.9491993083,4.226200
4771,-0.4788187028|H,-2.6015571568,4.1595556811,1.2506007777|H,-3.2934
019238,-0.3895046255,1.2428346935|H,-4.180477004,1.0955309963,0.879849

```

6022|H,-3.8925819432,-0.0882063172,-0.3924168379|H,3.0856461994,1.6842  
 319023,-0.395138311|H,4.6450030738,-2.5706051436,-1.2435960492|H,3.831  
 7363986,-4.0186371388,0.6113840269|H,1.8884142653,-3.2746807727,1.9770  
 721897|H,0.7860684082,-1.1244435529,1.5064291271||Version=IA32W-G09Rev  
 A.02|State=1-A|HF=-1032.6057928|RMSD=5.864e-009|RMSF=1.254e-005|Dipole  
 =-1.0181725,-0.5409048,0.3798458|Quadrupole=6.9665136,-2.3240871,-4.64  
 24264,-1.6739281,-1.1272436,1.1936696|PG=C01 [X(C13H15N1O1S1)]||@

Crystal structure of **1e**Calculated structure of **1a-OH**  
B3LYP/6-31+g(d,p)<sup>[7c]</sup>

C2-C21	135.8	136.3
N3-C2	141.0	143.3
N1-C2	140.0	140.9
C1-N3	138.3	140.4
C1-N2	129.6	129.5
N1-N2	140.9	139.5
C21-O1	139.9	139.6
C21-C22	146.1	146.6
N2-N1-C3	116.3	116.2
C2-N1-C3	129.1	129.4
N3-C2-C21-O1	18.7	-16.2
N1-C2-C21-C22	11.7	-6.2
C2-C21-C22-C23	37.1	-31.1

## 5 References

- [1] a) T. Ukai, R. Tanaka, T. Dokawa, *J. Pharm. Soc. Jpn.* **1943**, *63*, 296-300; b) For an excellent review of asymmetric benzoin condensations (from 1966 to 2003) see: D. Enders, T. Balensiefer, *Acc. Chem. Res.* **2004**, *37*, 534-541.
- [2] a) D. Seebach, *Angew. Chem. Int. Ed. Engl.* **1979**, *18*, 239-258; b) X. Bugaut, F. Glorius, *Chem. Soc. Rev.* **2012**, *41*, 3511-3522.
- [3] R. Breslow, *J. Am. Chem. Soc.* **1958**, *80*, 3719-3726.
- [4] a) First isolation: A. J. Arduengo III, R. L. Harlow, M. Kline, *J. Am. Chem. Soc.* **1991**, *113*, 361-363; b) For physicochemical data of NHCs see: T. Dröge, F. Glorius, *Angew. Chem. Int. Ed.* **2010**, *49*, 6940-6952; c) For studies on nucleophilicities and

- Lewis basicities of NHCs see: B. Maji, M. Breugst, H. Mayr, *Angew. Chem. Int. Ed.* **2011**, *50*, 6915–6919.
- [5] For reviews of NHC catalyzed reactions see: a) D. Enders, O. Niemeier, A. Henseler, *Chem. Rev.* **2007**, *107*, 5606–5655; b) N. Marion, S. Díez-González, S. P. Nolan, *Angew. Chem. Int. Ed.* **2007**, *46*, 2988–3000; c) P.-C. Chiang, J. W. Bode in *N-Heterocyclic Carbenes: From Laboratory Curiosities to Efficient Synthetic Tools* (Ed.: S. S. Díez-González), Royal Society of Chemistry: Cambridge, **2010**, pp. 399–435; d) K. Zeitler, *Angew. Chem. Int. Ed.* **2005**, *44*, 7506–7510; e) J. L. Moore, T. Rovis, *Top. Curr. Chem.* **2010**, *291*, 77; f) V. Nair, R. S. Menon, A. T. Biju, C. R. Sinu, R. R. Paul, A. Jose, V. Sreekumar, *Chem. Soc. Rev.* **2011**, *40*, 5336–5346; g) A. T. Biju, N. Kuhl, F. Glorius, *Acc. Chem. Res.* **2011**, *44*, 1182–1195.
- [6] For umpolung of Michael acceptors see: a) C. Fischer, S. W. Smith, D. A. Powell, G. C. Fu, *J. Am. Chem. Soc.* **2006**, *128*, 1472–1473; b) S. Matsuoka, Y. Ota, A. Washio, A. Katada, K. Ichioka, K. Takagi, M. Suzuki, *Org. Lett.* **2011**, *13*, 3722–3725; c) A. T. Biju, M. Padmanaban, N. E. Wurcz, F. Glorius, *Angew. Chem.* **2011**, *23*, 8562–8565; *Angew. Chem. Int. Ed.* **2011**, *50*, 8412–8415; d) R. L. Atienza, H. S. Roth, K. A. Scheidt, *Chem. Sci.* **2011**, *2*, 1772–1776; e) Y. Zhang, E. Y. X. Chen, *Angew. Chem. Int. Ed.* **2012**, *51*, 2465–2469.
- [7] For selected examples see: a) T. Dudding, K. N. Houk, *Proc. Natl. Acad. Sci. U.S.A.* **2004**, *101*, 5570–5775; b) J. M. Um, D. A. DiRocco, E. L. Noey, T. Rovis, K. N. Houk, *J. Am. Chem. Soc.* **2011**, *133*, 11249–11254; c) A. Berkessel, S. Elfert, K. Etzenbach-Effers, J. H. Teles, *Angew. Chem. Int. Ed.* **2010**, *49*, 7120–7124; d) K. J. Hawkes, B. F. Yates, *Eur. J. Org. Chem.* **2008**, 5563–5570; e) P. Verma, P. A. Patni, R. B. Sunoj, *J. Org. Chem.* **2011**, *76*, 5606–5613; f) M. Schumacher, B. Goldfuss, *Tetrahedron*, **2008**, *64*, 1648–1653; g) L. R. Domingo, M. J. Aurell, M. Arnó, *Tetrahedron*, **2009**, *65*, 3432–3440.
- [8] a) A. E. Mattson, A. R. Bharadwaj, A. M. Zuhl, K. A. Scheidt, *J. Org. Chem.* **2006**, *71*, 5715–5724; b) L. Pignataro, T. Papalia, A. M. Z. Slawin, S. M. Goldup, *Org. Lett.* **2009**, *11*, 1643–1646; c) J. H. Teles, J.-P. Melder, K. Ebel, R. Schneider, E. Gehrler, W. Harder, S. Bode, D. Enders, K. Breuer, G. Raabe, *Helv. Chim. Acta* **1996**, *79*, 61–83; d) R. Breslow, R. Kim, *Tetrahedron Lett.* **1994**, *35*, 699–702.
- [9] a) F. Jordan, Z. H. Kudzin, C. B. Rios, *J. Am. Chem. Soc.* **1987**, *109*, 4415–4416; b) F. G. Bordwell, A. V. Satish, F. Jordan, C. B. Rios, A. C. Chung, *J. Am. Chem. Soc.* **1990**, *112*, 792–797.

- [10] D. A. DiRocco, K. M. Oberg, T. Rovis, *J. Am. Chem. Soc.* **2012**, *134*, 6143–6145.
- [11] Use of MeOTf is superior to the use of  $\text{Me}_3\text{O}^+\text{BF}_4^-$  which has previously been described: G. L. Barletta, A. C. Chung, C. B. Rios, F. Jordan, J. M. Schlegel, *J. Am. Chem. Soc.* **1990**, *112*, 8144–8145.
- [12] a) Single crystal X-ray structure of (*Z*)-**1a** (crystallized from *n*-pentane): B. Maji, H. Mayr, P. Mayer, *Acta Crystallogr., Sect. E: Struct. Rep. Online*, **2012**, *68*, o2644; b) single crystal X-ray structure of (*E*)-**1e** (crystallized from  $\text{CH}_3\text{CN}$ ); b) B. Maji, G. Berionni, H. Mayr, P. Mayer, *Acta Crystallogr., Sect. E: Struct. Rep. Online*, **2012**, accepted.
- [13] a) B. Maji, M. Horn, H. Mayr, *Angew. Chem. Int. Ed.* **2012**, *51*, 6231–6235; b) C. E. I. Knappke, J. M. Neudorfl, A. J. von Wangelin, *Org. Biomol. Chem.* **2010**, *8*, 1695–1705; c) C. E. I. Knappke, A. J. Arduengo, III, H. Jiao, J.-M. Neudörfl, A. J. von Wangelin, *Synthesis* **2011**, 3784–3795.
- [14] a) P. Franchetti, L. Cappellacci, M. Grifantini, A. Barzi, G. Nocentini, H. Yang, A. O'Connor, H. N. Jayaram, C. Carrell, B. M. Goldstein, *J. Med. Chem.* **1995**, *38*, 3829–3837; b) Y. Nagao, T. Hirata, S. Goto, S. Sano, A. Kakehi, K. Iizuka, M. Shiro, *J. Am. Chem. Soc.* **1998**, *120*, 3104–3110.
- [15] See Experimental Section 4.10 for the comparison of the calculated structures of **1a**-OH and **1e**-OH with the crystal structures of **1a** and **1e**.
- [16] a) H. Mayr, T. Bug, M. F. Gotta, N. Hering, B. Irrgang, B. Janker, B. Kempf, R. Loos, A. R. Ofial, G. Remennikov, H. Schimmel, *J. Am. Chem. Soc.* **2001**, *123*, 9500–9512; b) R. Lucius, R. Loos, H. Mayr, *Angew. Chem. Int. Ed.* **2002**, *41*, 91–95; c) H. Mayr, B. Kempf, A. R. Ofial, *Acc. Chem. Res.* **2003**, *36*, 66–77; d) H. Mayr, A. R. Ofial, *Pure Appl. Chem.* **2005**, *77*, 1807–1821; e) H. Mayr, *Angew. Chem. Int. Ed.* **2011**, *50*, 3612–3618; f) For a comprehensive listing of nucleophilicity parameters *N* and electrophilicity parameters *E*, see <http://www.cup.uni-muenchen.de/oc/mayr/DBintro.html>.
- [17] For thiazolium ylidene catalyzed cross-coupling of aromatic aldehydes with activated alkyl halides see: M. Padmanaban, A. T. Biju, F. Glorius, *Org. Lett.* **2011**, *13*, 98–101.
- [18] Compound **6** was synthesized by deprotonation of the corresponding azolium triflate (See Experimental Section 4.6).
- [19] H. Mayr, A. R. Ofial, *Angew. Chem. Int. Ed.* **2006**, *45*, 1844–1854.
- [20] a) L. Hintermann, *Beilstein J. Org. Chem.* **2007**, *3* (22), doi:10.1186/1860-5397-3-22;

- b) L. Jafarpour, E. D. Stevens, S. P. Nolan, *J. Organomet. Chem.* **2000**, 606, 49–54; c) D. Enders, K. Breuer, U. Kallfass, T. Balensiefer, *Synthesis*, **2003**, 1292–1295.
- [21] a) S. Florio, V. Capriati, G. Colli, *Tetrahedron* **1997**, 53, 5839–5846; b) S. Rudrawar, A. Kondaskar, A. K. Chakraborti, *Synthesis* **2005**, 2521–2526.
- [22] Calculated using Gaussian 09 program package. M. J. Frisch, G. W. Trucks, H. B. Schlegel, G. E. Scuseria, M. A. Robb, J. R. Cheeseman, G. Scalmani, V. Barone, B. Mennucci, G. A. Petersson, H. Nakatsuji, M. Caricato, X. Li, H. P. Hratchian, A. F. Izmaylov, J. Bloino, G. Zheng, J. L. Sonnenberg, M. Hada, M. Ehara, K. Toyota, R. Fukuda, J. Hasegawa, M. Ishida, T. Nakajima, Y. Honda, O. Kitao, H. Nakai, T. Vreven, J. A. Montgomery, Jr., J. E. Peralta, F. Ogliaro, M. Bearpark, J. J. Heyd, E. Brothers, K. N. Kudin, V. N. Staroverov, R. Kobayashi, J. Normand, K. Raghavachari, A. Rendell, J. C. Burant, S. S. Iyengar, J. Tomasi, M. Cossi, N. Rega, J. M. Millam, M. Klene, J. E. Knox, J. B. Cross, V. Bakken, C. Adamo, J. Jaramillo, R. Gomperts, R. E. Stratmann, O. Yazyev, A. J. Austin, R. Cammi, C. Pomelli, J. W. Ochterski, R. L. Martin, K. Morokuma, V. G. Zakrzewski, G. A. Voth, P. Salvador, J. J. Dannenberg, S. Dapprich, A. D. Daniels, O. Farkas, J. B. Foresman, J. V. Ortiz, J. Cioslowski, and D. J. Fox, Gaussian, Inc., Wallingford CT, **2009**.

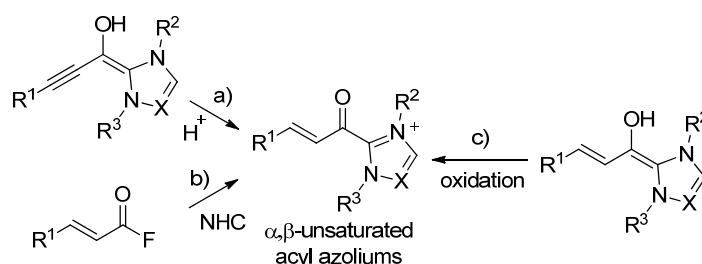
## Chapter 8

# Nucleophilic Addition of Enols and Enamines to $\alpha,\beta$ -Unsaturated Acyl Azoliums: Mechanistic Studies

R. C. Samanta, B. Maji, S. De Sarkar, K. Bergander, R. Fröhlich, C. Mück-Lichtenfeld, H. Mayr, A. Studer, *Angew. Chem. Int. Ed.* **2012**, *51*, 5234–5238.

## 1 Introduction

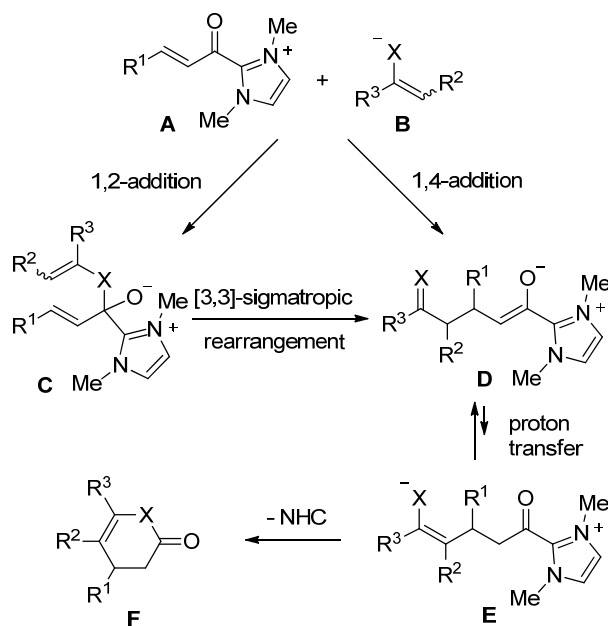
N-Heterocyclic carbenes (NHCs) have been successfully used as catalysts in various C-C bond forming reactions.<sup>[1]</sup> Along this line, the chemistry of  $\alpha,\beta$ -unsaturated acyl azoliums has recently gained great attention. These reactive intermediates can be generated via three different routes: a) Protonation of the Breslow intermediate formed in the reaction of an ynal with an NHC;<sup>[2,3]</sup> b) reaction of an  $\alpha,\beta$ -unsaturated acyl fluoride with an NHC<sup>[4]</sup> and c) oxidation of the Breslow intermediate formed in the reaction of an enal with an NHC (Scheme 1).<sup>[5]</sup>



**Scheme 1.** Different routes for generation of acyl azoliums.

$\alpha,\beta$ -Unsaturated acyl azoliums turned out to be reactive and synthetically highly useful electrophiles in intermolecular reactions with  $\alpha$ -ketoenols,<sup>[6]</sup>  $\beta$ -diketones,<sup>[7]</sup> and enamines<sup>[8]</sup> for the preparation of dihydropyranones and dihydropyridinones. Two different mechanisms have been suggested for such transformations (Scheme 2). The deprotonated enol (enamine) **B** can react with **A** via a Michael-type 1,4-addition to give enolate **D**.<sup>[7]</sup> Alternatively, the

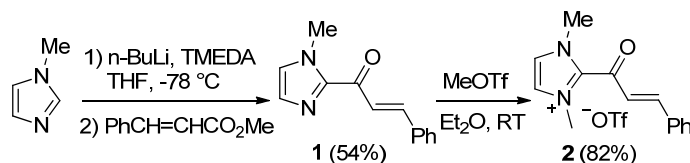
same intermediate **D** can be generated via 1,2-addition to generate **C** which further reacts in a [3,3]-sigmatropic rearrangement to **D**.<sup>[6,8]</sup> Proton transfer provides **E** and intramolecular acylation eventually leads to dihydropyranones or dihydropyridinones **F**. In the present communication we give experimental and theoretical support for an isolated acylazolium salt to react with various nucleophiles via the 1,4-addition reaction pathway. Moreover, we present the first X-ray structure of an  $\alpha,\beta$ -unsaturated acyl azolium **A**.<sup>[9]</sup>



**Scheme 2.** Possible mechanisms for reaction of enols or enamines with acyl azoliums **A** (NHC = N,N'-dimethylimidazoline, X = O, NH).

## 2 Result and discussions

To properly investigate the reactivity of acyl azoliums, we decided to prepare and fully characterize such an intermediate **A** and to study its reactivity towards different nucleophiles. The synthesis of **A** ( $R^1 = \text{Ph}$ ) turned out to be surprisingly straightforward. *N*-Methylimidazole was deprotonated with *n*-BuLi in THF at  $-78\text{ }^\circ\text{C}$  in the presence of TMEDA. Subsequent addition of methyl cinnamate at that temperature afforded ketone **1** in 54% isolated yield (Scheme 3).<sup>[10]</sup> Reaction of **1** with MeOTf in Et<sub>2</sub>O at room temperature and purification by recrystallization provided acyl azolium salt **2** in 82% yield.



**Scheme 3.** Synthesis of acyl azolium **2**.

X-ray analysis (Figure 1)<sup>[11]</sup> showed that the C=C double bond and the carbonyl group are nearly perfectly in plane (torsion angle =  $6.2(9)^\circ$ ). In this conformation, the carbonyl moiety ideally activates the olefin for a 1,4-addition reaction. The plane of the 5-membered ring is twisted with respect to the carbonyl group (torsion angle around  $35.5^\circ$ ).

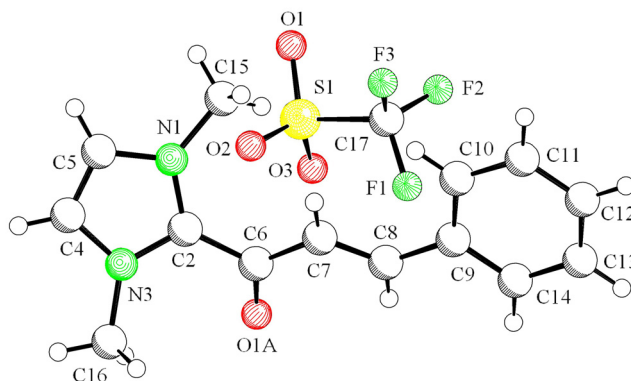
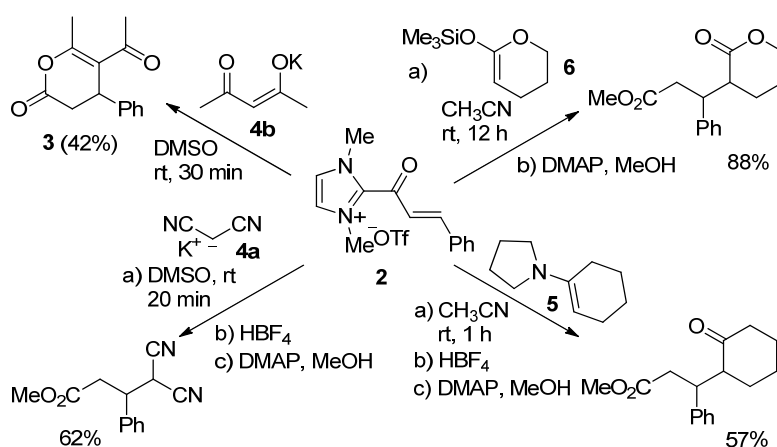


**Figure 1.** Molecular structure of **2** representing an example of a compound of type **A**.

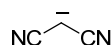
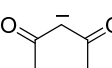
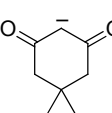
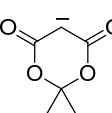
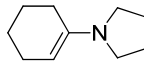
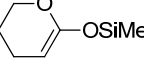
We first studied reaction of the acyl azolium salt **2** with various nucleophiles in  $\text{CH}_3\text{CN}$  or DMSO at room temperature (rt).  $\beta$ -Diketones and  $\beta$ -ketoesters are well known to react with acceptors **A** to afford compounds of type **F**. Indeed, reaction of **2** with deprotonated acetylacetone delivered **3** (Scheme 4). In the reactions with deprotonated malonodinitrile **4a**, enamine **5** and ketene acetal **6** the corresponding product acyl azolium salts were difficult to isolate. The intermediate azoliums obtained after nucleophilic addition were therefore first treated with 1 equiv  $\text{HBF}_4$  (for **4a** and **5** for enolate protonation) followed by MeOH and *N,N*-dimethylaminopyridine (DMAP, 2 equiv) to provide the corresponding methyl esters in moderate to good yields (57-88%).



**Scheme 4.** Reactions of **2** with various kinds of nucleophiles.

The kinetics of the addition reaction of **4–6** to **2** were followed by photometric monitoring of the decay of the absorbance of **2** at 20 °C in dry DMSO or in dry CH<sub>3</sub>CN at  $\lambda_{\text{max}} = 333$  nm (in DMSO) or at  $\lambda_{\text{max}} = 326$  nm (in CH<sub>3</sub>CN) using the previously described equipment.<sup>[12]</sup> All kinetic experiments were performed under pseudo-first-order conditions using an excess of nucleophiles. From the exponential decay of the UV-Vis absorbance of **2**, the pseudo-first-order rate constants  $k_{\text{obs}}$  (s<sup>-1</sup>) were obtained. Plots of  $k_{\text{obs}}$  versus the concentrations of the nucleophiles were linear with negligible intercepts (Tables 2–8). The slopes of these linear plots gave the second-order rate constants  $k$  (M<sup>-1</sup> s<sup>-1</sup>) which are listed in Table 1. We found that the counteranion in **2** by switching from OTf to I<sup>-</sup> did not influence the  $k$ -value for the reaction with acac<sup>-</sup> to a large extent. Addition of acac<sup>-</sup> to the iodide salt at 20 °C in DMSO occurred with a rate constant of  $6.14 \times 10^4$  M<sup>-1</sup>s<sup>-1</sup> (Table S8) which compares well with the value measured for **2** ( $5.84 \times 10^4$  M<sup>-1</sup>s<sup>-1</sup>).

**Table 1.** Second-order rate constants for the reactions of **2** with the nucleophiles **4**, **5** and **6** at 20 °C.

Nucleophile	$N / s_N$ <sup>[a]</sup>	$k / \text{M}^{-1} \text{s}^{-1}$
 <b>4a</b>	19.36 / 0.67	$2.29 \times 10^5$ <sup>[b]</sup>
 <b>4b</b>	17.64 / 0.73	$5.84 \times 10^4$ <sup>[b]</sup>
 <b>4c</b>	16.27 / 0.77	$9.03 \times 10^3$ <sup>[b]</sup>
 <b>4d</b>	13.91 / 0.86	$2.75 \times 10^2$ <sup>[b]</sup>
 <b>5</b>	16.42 / 0.70	$4.96 \times 10^2$ <sup>[c]</sup>
 <b>6</b>	10.52 / 0.78	$6.19 \times 10^{-2}$ <sup>[c]</sup>

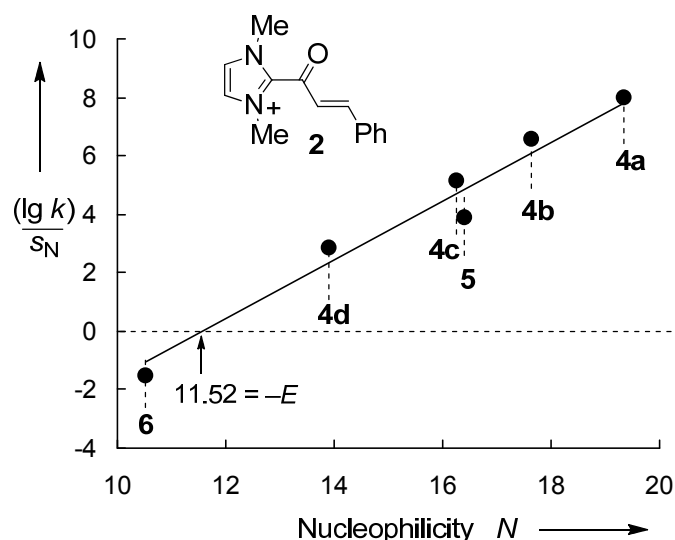
[a] Nucleophile-specific parameters  $N$  and  $s_N$  from ref. [13]. [b] Solvent DMSO. [c] Solvent CH<sub>3</sub>CN.

Figure 2 shows that  $(\lg k)/s_N$  correlates linearly with  $N$  as required by equation (1),<sup>[12]</sup> which calculates second-order rate constants from the electrophile-specific parameter  $E$  and two solvent-dependent nucleophile-specific parameters  $N$  and  $s_N$ . One can, therefore, conclude that the rate-determining step of the reactions of **2** with **4–6** is mechanistically analogous to the reactions of **4–6** with benzydrylium ions which react via C-C bond formation (see reactions

on section 4.3 in the Experimental Section). These adduct formations have previously been used to derive the  $N$  and  $s_N$  parameters listed in Table 1.

$$\lg k_{20^\circ\text{C}} = s_N(E + N) \quad (1)$$

The kinetic experiments do not exclude attack of these nucleophiles at the carbonyl group of **2** in a rapid preequilibrium step, which is kinetically irrelevant. Since initial carbonyl attack followed by [3,3]-sigmatropic rearrangement cannot be formulated for all nucleophiles of Table 1, however, one would have to postulate that this stepwise process can only lead to the observed products if it proceeds with the same rate as the direct attack of these nucleophiles at the conjugate position of **2**, a rather unlikely construction.



**Figure 2.** Plot of  $(\lg k)/s_N$  versus  $N$  for the reactions of **2** with the nucleophiles **4**, **5** and **6** (solvents are specified in Table 1). Slope of the correlation line is fixed to 1.0 as required by Eq. (1).

According to equation (1), the negative intercept on the abscissa of Figure 2 yields  $E = -11.52$  for **2** (by minimization of  $\Delta^2 = \Sigma[\lg k - s_N(N + E)]^2$ ), which is compared with other electrophiles in Figure 3. This Figure shows that due to the strong electron withdrawing nature of the imidazolium ring, **2** is 7 orders of magnitude more electrophilic than a structurally analogous chalcone, comparable to highly electron-deficient neutral Michael acceptors such as benzylidene malononitriles, and 2-benzylidene indan-1,3-diones.<sup>[13]</sup> However, its electrophilicity is 1000 times lower than that of the structurally related iminium ion derived from *Hayashi-Jorgensen* and  $10^4$  to  $10^6$  lower than those derived from *MacMillan's* imidazolidinones.<sup>[13]</sup>

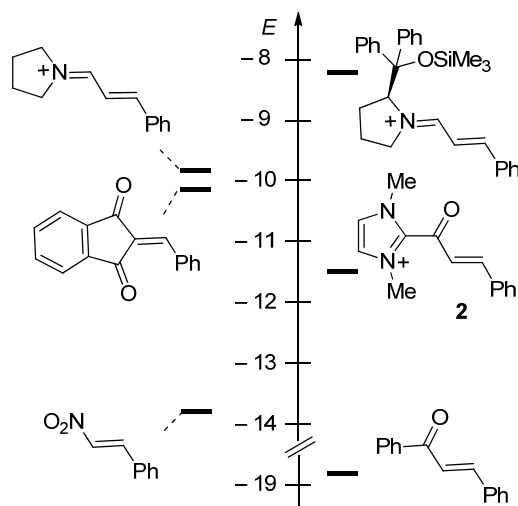


**Figure 3.** Comparison of electrophilicity  $E$  of **2** with other types of electrophiles.  $E$  parameters from ref. [13].

To get further information on the reaction, we followed the transformation of **2** with acetylacetone in presence of base by low temperature  $^1\text{H}$  NMR spectroscopy. We found that acetylacetone did not react with **2** at room temperature in  $[\text{D}_8]\text{-THF}$  in the absence of base. The NMR sample was then cooled to  $-78\text{ }^\circ\text{C}$  and DBU (1,8-diazabicyclo[5.4.0]undec-7-ene, 1.5 equiv) was added. The NMR tube was quickly transferred into the NMR probe which was precooled to  $-40\text{ }^\circ\text{C}$ . The resonances of the acyl azolium **2** fully disappeared and novel broad signals appeared. In agreement with the kinetic experiment using **4b**, this NMR study revealed that reaction of **2** with deprotonated acetylacetone is very fast at low temperature ( $< 30$  sec, time necessary for mixing and transfer to the NMR probe). An intermediate of type **C** derived from 1,2-addition was not detectable, either because it was not formed or because the sigmatropic rearrangement was very fast. We noted that upon warming the probe to  $-20\text{ }^\circ\text{C}$  the NMR signals remained unchanged. However, further warming to room temperature led to formation of **3** (see Scheme 4) which represents a compound of the general structure **F**. Hence, this NMR experiment showed that intramolecular acylation from **E** to **F** under liberation of the carbene needs temperatures above  $-20\text{ }^\circ\text{C}$ . We performed additional NMR experiments with deprotonated malonodinitrile and 3-aminocrotononitrile as nucleophiles and unambiguously identified the corresponding 1,4-addition products. No indication for formation of an intermediate derived from a 1,2-addition reaction was obtained (3-aminocrotononitrile could react in a 1,2-addition by C-N bond formation). In all NMR experiments we could identify intermediates of type **D** (for  $\text{acac}^-$  after O-silylation) but not

the corresponding proton transfer intermediates of type **E**. Obviously the proton transfer from **D** to **E** is reversible with **D** dominating in the equilibrium.

Since both kinetic and NMR experiments did not allow us to exclude a rapid preequilibrium step in the reaction of **2** with deprotonated acetylacetone, we finally decided to study that particular transformation using high level DFT calculations. We investigated the addition of deprotonated acetylacetone to **2** with a meta GGA functional (TPSS) including a correction for dispersion interactions using a triple zeta quality basis set (TPSS-D3(BJ)/def2-TZVP).<sup>[14]</sup> Furthermore, a continuum solvation model (COSMO)<sup>[15]</sup> was used in all calculations, simulating the THF ( $\epsilon = 7.58$ ) solvent properties.

The formation of a close ion pair (**2**/acac<sup>-</sup>) in THF was found to be exothermic by  $-23.5$  kcal/mol (Scheme 2,  $R^1 = \text{Ph}$ ,  $R^2 = \text{COCH}_3$ ,  $R^3 = \text{CH}_3$ ,  $X = \text{O}$ ). Attempts to calculate the energy of the corresponding intermediate **C** were unsuccessful, because it was not a local minimum in the solvent, but relaxed to the ion pair **2**/acac<sup>-</sup> showing that **C** cannot be an intermediate. On the other hand, 1,4-addition leads to the intermediate of type **D**, that has a relative energy of  $-25.8$  kcal/mol with respect to the isolated reactants. We have located a transition structure for the C-C bond formation in the addition step (Figure 4). This structure also reveals that the 1,4-addition leads to the *cis*-enolate, in agreement with the NMR studies. The relative energy of this structure is  $-17.9$  kcal/mol. The very low barrier ( $\Delta E^\ddagger = 5.6$  kcal/mol, without ZPE correction) allows a facile and fast 1,4-addition even at low temperatures, as observed in the NMR experiment.

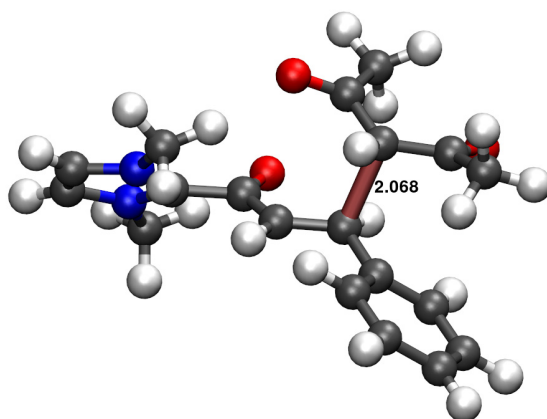


**Figure 4.** DFT-D3(BJ)+COSMO optimized transition structure of the 1,4-addition of deprotonated acac to acyl azolium **2**. The C-C distance is given in Å.

In order to address solvent effects we also calculated the relative energy  $\Delta E$  between the ion pair (**2**/acac<sup>-</sup>) and the 1,4-adduct and the 1,4 addition barrier  $\Delta E^\ddagger$  in DMSO ( $\epsilon = 46.7$ ) and

CH<sub>3</sub>CN ( $\epsilon = 37.5$ ). We obtained very similar values indicating that solvent effects are weak for this reaction (DMSO:  $\Delta E^\ddagger = 6.3$  kcal/mol,  $\Delta E = -1.4$  kcal/mol; CH<sub>3</sub>CN:  $\Delta E^\ddagger = 6.2$  kcal/mol,  $\Delta E = -1.5$  kcal/mol). The calculated barrier fits very well with the activation enthalpy  $\Delta H^\ddagger = 4.9$  kcal/mol calculated from  $\Delta G^\ddagger = 10.7$  kcal/mol derived from the kinetic experiment (see Table 1) assuming  $\Delta S^\ddagger = -20$  e.u.

Since many NHC catalyzed reactions have been conducted with triazole-derived carbenes, we conducted additional calculations for the reaction of *acac*<sup>-</sup> with the triazole congener of **2** (see Scheme 1, R<sup>1</sup> = Ph, R<sup>2</sup> = R<sup>3</sup> = Me, X = N) and found the addition reaction starting with the ion pair to be slightly more exothermic (THF:  $\Delta E = -4.7$  kcal/mol,  $\Delta E^\ddagger = 4.0$  kcal/mol; CH<sub>3</sub>CN:  $\Delta E = -4.2$  kcal/mol,  $\Delta E^\ddagger = 4.4$  kcal/mol). Consequently, reaction barrier was even lower. Interestingly, for the triazole system we found an intermediate of type **C** for the 1,2-addition pathway. However, the relative energy with respect to the ion pair was +13.3 kcal/mol (THF) and therefore the 1,2-addition pathway at least with deprotonated acetylacetone can also be excluded for the triazole derivative.

### 3 Conclusion

In conclusion, we reported the synthesis and full characterization of the acyl azolium **2**. High level DFT-calculations and kinetic experiments clearly revealed that acetylacetone, malonodinitrile, enamine **5**, and silylenol ether **6** react with the  $\alpha,\beta$ -unsaturated acyl azolium **2** via a 1,4-Michael type addition reaction. Based on the kinetic experiments and on the calculations the two step mechanism via 1,2-addition followed by [3,3]-sigmatropic rearrangement for the key C-C-bond formation can be excluded.

### 4 Experimental Section

In order to identify my contributions to this multiauthor publication, only the experiments, which were performed by me, are described in sections 4.2, 4.4 and 4.5 of this Experimental Section.

#### 4.1 General

##### *Chemicals.*

All reactions involving air or moisture sensitive reagents or intermediates were carried out in dried glassware under an argon atmosphere. THF was distilled from potassium under argon.

Diethyl ether was distilled from sodium or potassium under argon. All other solvents and reagents were purified according to standard procedures or were used directly from *Sigma Aldrich*, *Acros Organics*, *ABCR*, *Alfa Aesar* or *Fluka* as received.

*Analitics.*

NMR spectroscopy: *Bruker DPX 300* (at 300 K), *Bruker AV400*, *Varian* NMR-systems (300 MHz, 400 MHz), *Varian Unity plus 600*, *Varian Inova 500*. Chemical shifts,  $\delta$  (in ppm), are reported relative to TMS ( $\delta(^1\text{H})$  0.0 ppm,  $\delta(^{13}\text{C})$  0.0 ppm) which was used as the inner reference. Otherwise the solvents residual proton resonance and carbon resonance (THF,  $\delta(^1\text{H})$  3.58 ppm and 1.73 ppm,  $\delta(^{13}\text{C})$  67.5 ppm and 25.3 ppm; were used for calibration). NMR signal assignments are based on additional 1D and 2D (COSY, NOESY, HSQC and HMBC) NMR experiments. TLC: *Merck* silica gel 60 F 254 plates; detection with UV light or by dipping into a solution of  $\text{KMnO}_4$  (1.5 g in 400 mL  $\text{H}_2\text{O}$ , 5 g  $\text{NaHCO}_3$ ) or a solution of  $\text{Ce}(\text{SO}_4)_2 \times \text{H}_2\text{O}$  (10 g), phosphormolybdic acid hydrate (25 g), and conc.  $\text{H}_2\text{SO}_4$  (60 mL) in  $\text{H}_2\text{O}$  (940 mL), followed by heating. Flash column chromatography (FC): *Merck* or *Fluka* silica gel 60 (40–63  $\mu\text{m}$ ) at approximately 0.4 bar. Infrared spectra were recorded on a *Varian Associates* FT-IR 3100 Excalibur and *Shimadzu* FTIR 8400S and reported as wavenumber ( $\text{cm}^{-1}$ ). Mass spectra were recorded on a *Finnigan MAT 4200S*, a *Bruker Daltonics MicroTof*, a *Waters Micromass Quatro LCZ* (ESI), a *Finnigan MAT 95* (EI), a *Thermo Finnigan LTQ FT* (ESI) mass spectrometer.

*Kinetics.*

The rates of all investigated reactions were determined photometrically. The temperature of the solutions during all kinetic studies was kept constant ( $20.0 \pm 0.1^\circ\text{C}$ ) by using a circulating bath thermostat. The kinetic experiments were carried out with freshly prepared stock solutions of **2**, **4**, **5**, and **6** in dry DMSO or  $\text{CH}_3\text{CN}$ . First-order kinetics were achieved by employing excess of the nucleophiles. For the evaluation of fast kinetics ( $\tau_{1/2} < 15\text{--}20$  s) the spectrophotometer system Applied Photophysics SX.18MV-R stopped-flow reaction analyser was used.

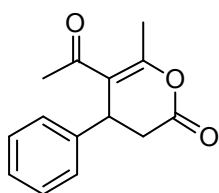
The rates of slow reactions ( $\tau_{1/2} > 15\text{--}20$  s) were determined by using a J&M TIDAS diode array spectrophotometer controlled by Labcontrol Spectacle software and connected to a Hellma 661.502-QX quartz Suprasil immersion probe (5 mm light path) via fiber optic cables and standard SMA connectors.

Rate constants  $k_{\text{obs}}$  ( $\text{s}^{-1}$ ) were obtained by fitting the single exponential  $A_t = A_0 \exp(-k_{\text{obs}}t) + C$  (exponential decrease) to the observed time-dependent absorbance (averaged from at least 5 kinetic runs for each nucleophile concentration in case of stopped-flow methodology).

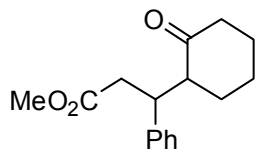
#### 4.2 Reaction products for the reactions of **2** with nucleophiles **4a**, **5** and **6**

*Methyl 4,4-dicyano-3-phenylbutanoate*: To a stirred DMSO (1 mL) solution of **2** (188 mg, 0.500 mmol) a DMSO (2 mL) solution of potassium dicyanomethanide (**4a**) (104 mg, 0.998 mmol) was added under nitrogen atmosphere. The mixture was allowed to stir for 20 min, followed by the addition of 100  $\mu\text{L}$  of 50-55% ethereal  $\text{HBF}_4$  (44 mg, 0.50 mmol). After stirring for 10 min, a MeOH solution (2 mL) of DMAP (122 mg, 0.100 mmol) was added and the mixture was allowed to stir for another 30 min. The reaction was quenched with brine solution and the organic compounds were extracted with  $\text{CH}_2\text{Cl}_2$ . The combined organic layers were dried over  $\text{Na}_2\text{SO}_4$  and concentrated in vacuum. The crude product was purified by flash silica gel chromatography using EtOAc/*n*-pentane (15: 85) as eluent to obtain the title compound as colorless oil (71 mg, 0.31 mmol, 62%). IR (ATR)  $\tilde{\nu}$  ( $\text{cm}^{-1}$ ): 3355, 2957, 2918, 2359, 2343, 2233, 2217, 1731, 1639, 1605, 1456, 1438, 1378, 1266, 1206, 1169, 1003, 761, 702, 667.  $^1\text{H}$  NMR ( $\text{CDCl}_3$ , 300 MHz)  $\delta$  = 2.92-3.12 (m, 2 H), 3.70 (s, 3 H), 3.72-3.76 (m, 1 H), 4.49 (d,  $J$  = 5.8 Hz, 1 H), 7.34-7.43 (m, 5 H) ppm.  $^{13}\text{C}$  NMR ( $\text{CDCl}_3$ , 75 MHz)  $\delta$  = 29.0 (d), 36.2 (t), 42.4 (d), 52.6 (t), 111.7 (s, CN), 128.0 (d), 129.5 (d), 129.6 (d), 126.0 (s), 171.0 (s, CO) ppm. HRMS (EI)  $[\text{M}]^+$ : calculated for  $[\text{C}_{13}\text{H}_{12}\text{O}_2\text{N}_2]^+$  is 228.0893; found 228.0887.

*5-acetyl-6-methyl-4-phenyl-3,4-dihydro-2H-pyran-2-one (3)*: To a stirred DMSO (1 mL) solution of **2** (75.2 mg, 0.200 mmol) a DMSO (1 mL) solution of potassium (*Z*)-4-oxopent-2-en-2-olate (**4b**) (41.6 mg, 0.301 mmol) was added under nitrogen atmosphere. The mixture was allowed to stir for 30 min at room temperature. The reaction was quenched with brine solution and the organic compounds were extracted with  $\text{CH}_2\text{Cl}_2$ . The combined organic layers were dried over  $\text{Na}_2\text{SO}_4$  and concentrated in vacuum. The crude product was purified by flash silica gel chromatography using MTBE/*n*-pentane (1: 2) as eluent to obtain the title compound as white solid (19 mg, 0.083 mmol, 42%). All the analytics are in agreement with those reported in literature<sup>[7a]</sup>.



*Methyl 3-(2-oxocyclohexyl)-3-phenylpropanoate*: To a stirred  $\text{CH}_3\text{CN}$  (1 mL) solution of **2** (188 mg, 0.500 mmol) a  $\text{CH}_3\text{CN}$  (2 mL) solution of **5** (151 mg, 0.998 mmol) was added under nitrogen atmosphere. The mixture was allowed

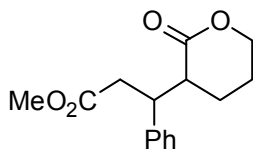


to stir for 1 h, followed by the addition of 100  $\mu\text{L}$  of 50-55% ethereal  $\text{HBF}_4$  (44 mg, 0.50 mmol). After stirring for 10 min, a MeOH solution (2 mL) of DMAP (122 mg, 0.100 mmol) was added and the reaction mixture was allowed to stir for another 30 min. 2 mL of 5% AcOH solution was added into the reaction mixture and the resulting solution was stirred for another 20 min. Excess of acid was neutralized by adding saturated  $\text{NaHCO}_3$  solution and the organic compounds were extracted with  $\text{CH}_2\text{Cl}_2$ . The combined organic layers were washed with brine solution, dried over  $\text{Na}_2\text{SO}_4$  and concentrated in vacuum. The crude product was purified by flash silica gel chromatography using EtOAc/*n*-pentane (1:4) as eluent to obtain a white powder (74 mg, 0.28 mmol, 57%, mixture of diastereomers; d.r.  $\approx$  3:1). Upon cooling down a dichloromethane/*n*-pentane solution of the mixture the major diastereomer could be separated by partial precipitation.

*Major diastereomer*: IR (ATR)  $\tilde{\nu}$  ( $\text{cm}^{-1}$ ): 2938, 2859, 2360, 2341, 1732, 1703, 1495, 1448, 1436, 1365, 1248, 1215, 1157, 1127, 1021, 768, 748, 701.  $^1\text{H}$  NMR ( $\text{CDCl}_3$ , 400 MHz)  $\delta$  = 1.17-1.26 (m, 1 H), 1.51-1.78 (m, 4 H), 1.94-2.05 (m, 1 H), 2.33-2.40 (m, 1 H), 2.44-2.50 (m, 1 H), 2.55-2.66 (m, 2 H), 2.85 (dd,  $J$  = 4.7, 15.5 Hz, 1 H), 3.48-3.52 (m + s, 1 H + 3 H), 7.17-7.31 (m, 5 H) ppm.  $^{13}\text{C}$  NMR ( $\text{CDCl}_3$ , 100 MHz)  $\delta$  = 24.5 (t), 28.8 (t), 32.7 (t), 39.8 (t), 41.6 (d), 42.6 (d), 51.6 (q), 55.5 (d), 126.9 (d), 128.4 (d), 128.7 (d), 141.8 (s), 172.7 (s,  $\text{COCH}_3$ ), 213.2 (s, CO) ppm. HRMS (ESI)  $[\text{M} + \text{Na}]^+$ : calculated for  $[\text{C}_{16}\text{H}_{20}\text{O}_3\text{Na}]^+$  is 283.1310; found 283.1309.

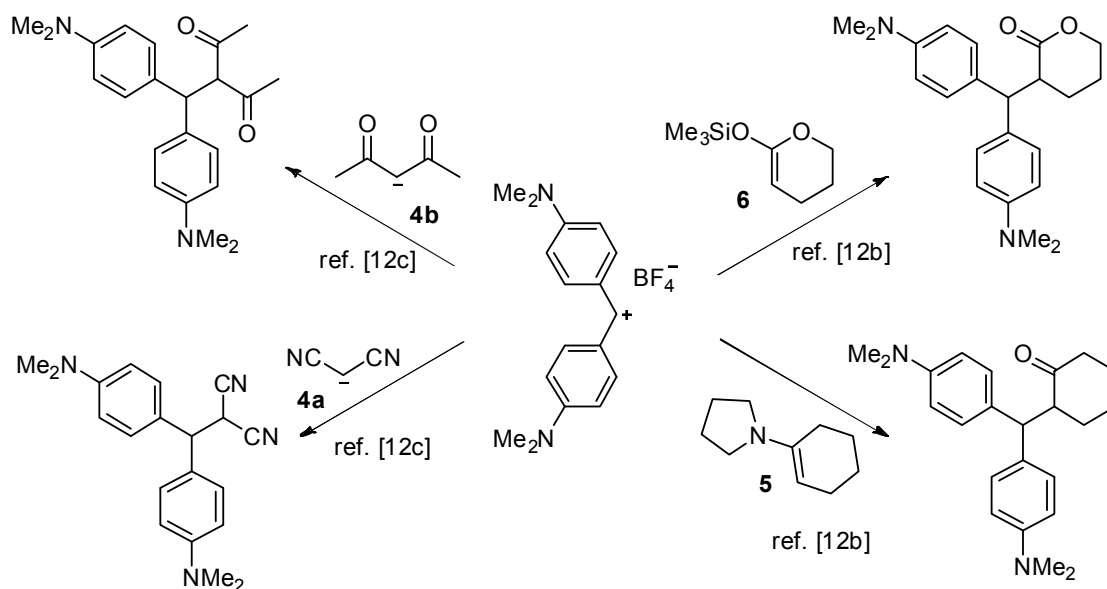
*Minor diastereomer*:  $^1\text{H}$  NMR ( $\text{CDCl}_3$ , 300 MHz)  $\delta$  = 1.17-1.28 (m, 1 H), 1.50-1.80 (m, 4 H), 1.88-2.07 (m, 1 H), 2.17-2.73 (m, 4 H), 2.73-2.89 (m, 1 H), 3.54 (s, 3 H), 3.72-3.81 (m, 1 H), 7.16-7.31 (m, 5 H) ppm.  $^{13}\text{C}$  NMR ( $\text{CDCl}_3$ , 75 MHz)  $\delta$  = 25.0, 27.8, 29.5, 29.9, 36.0, 40.4, 51.7, 55.9, 126.7, 128.3, 128.5, 142.7, 173.0, 211.4 ppm.  $^1\text{H}$  and  $^{13}\text{C}$  NMR spectra for the minor diastereomer were obtained by comparing the spectra of the mixture and that of pure major diastereomer.

*Methyl 3-(2-oxotetrahydro-2H-pyran-3-yl)-3-phenylpropanoate*: To a stirred  $\text{CH}_3\text{CN}$  (1 mL) solution of **2** (188 mg, 0.500 mmol) a  $\text{CH}_3\text{CN}$  (2 mL) solution of **6** (215 mg, 1.25 mmol) was added under nitrogen atmosphere and the mixture was allowed to stir for 12 h. Then a MeOH solution (2 mL) of DMAP

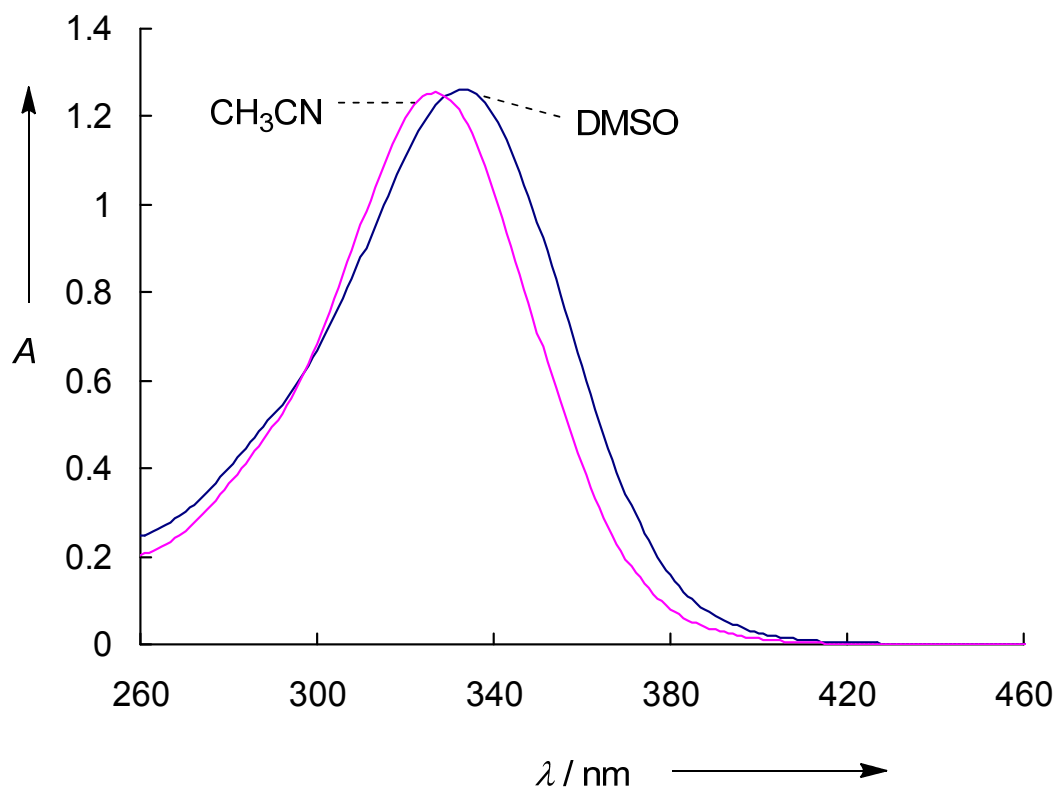


(122 mg, 0.100 mmol) was added and the reaction mixture was allowed to stir for another 30 min. The reaction was quenched with brine solution and the organic compounds were extracted with  $\text{CH}_2\text{Cl}_2$ . The combined organic layers were dried over  $\text{Na}_2\text{SO}_4$  and concentrated in vacuum. The crude product was purified by flash silica gel chromatography using EtOAc/*n*-pentane (1:4) as eluent to obtain the title compound as colorless oil (115 mg, 0.438 mmol, 88%, mixture of diastereomers; d.r.  $\approx$  1: 0.85). IR (ATR)  $\tilde{\nu}$  ( $\text{cm}^{-1}$ ): 2952, 2360, 2341, 1727, 1603, 1453, 1436, 1259, 1146, 1076, 953, 758, 702.  $^1\text{H}$  NMR ( $\text{CDCl}_3$ , 300 MHz)  $\delta$  = 1.61-1.95 (m, 4  $\text{H}^{\text{A}}$  + 4  $\text{H}^{\text{B}}$ ), 2.71-2.92 (m, 2  $\text{H}^{\text{A}}$  + 2  $\text{H}^{\text{B}}$ ), 3.02-3.13 (m, 1  $\text{H}^{\text{A}}$  + 1  $\text{H}^{\text{B}}$ ), 3.55 (s, 3  $\text{H}^{\text{A}}$ ), 3.58 (s, 3  $\text{H}^{\text{B}}$ ), 3.69-3.82 (m, 1  $\text{H}^{\text{A}}$  + 1  $\text{H}^{\text{B}}$ ), 3.99-4.29 (m, 2  $\text{H}^{\text{A}}$  + 2  $\text{H}^{\text{B}}$ ), 7.20-7.34 (m, 5  $\text{H}^{\text{A}}$  + 5  $\text{H}^{\text{B}}$ ) ppm.  $^{13}\text{C}$  NMR ( $\text{CDCl}_3$ , 75 MHz)  $\delta$  = 21.7 (t), 22.2 (t), 22.6 (t), 22.7 (t), 36.1 (d), 38.9 (d), 42.4 (d), 42.8 (d), 44.1 (t), 45.3 (t), 51.7 (q), 51.8 (q), 68.2 (t), 67.0 (t), 127.24 (d), 127.25 (d), 128.40 (d), 128.44 (d), 128.70 (d), 128.73 (d), 140.7 (s), 141.1 (s), 172.36 (s, CO), 172.42 (s, CO), 172.8 (s, CO), 173.4 (s, CO) ppm. HRMS (ESI)  $[\text{M} + \text{Na}]$ : calculated for  $[\text{C}_{16}\text{H}_{18}\text{O}_4\text{Na}]^+$  is 285.1103; found 285.1103.

#### 4.3 Reaction products for the reactions of bis(4 (dimethylamino)phenyl)methylium tetrafluoroborates with nucleophiles 4a,b, 5 and 6.



#### 4.4 UV-Vis spectra of the acyl azolium salt



#### 4.5 Kinetics

##### 4.5.1 Determinations of the rate constants for the reactions of **2** with **4**, **5**, and **6**.

The rates of the reactions of **2** with nucleophiles **4** (isolated potassium salts), **5**, and **6** were measured photometrically under pseudo-first-order conditions (excess of nucleophile), at the absorption maximum of **2** by using UV-Vis spectrometers (conventional diode array or stopped-flow) as described previously<sup>[12b]</sup> at 20 °C in dry DMSO or CH<sub>3</sub>CN. First-order rate constants  $k_{\text{obs}}$  (s<sup>-1</sup>) were obtained by least-squares fitting of the absorbances to the mono-exponential curve  $A_t = A_0 \exp(-k_{\text{obs}}t) + C$ . Since  $k_{\text{obs}} = k[\text{Nu}]$ , the second-order rate constants  $k$  (L mol<sup>-1</sup> s<sup>-1</sup>) were derived from the slopes of the linear plots of  $k_{\text{obs}}$  (s<sup>-1</sup>) vs. [Nu].

**Table 2:** Kinetics of the reaction of **2** with **4a** at 20 °C in DMSO (stopped-flow,  $\lambda = 333$  nm).

[2] / mol L <sup>-1</sup>	[4a] / mol L <sup>-1</sup>	$k_{\text{obs}} / \text{s}^{-1}$
$8.62 \times 10^{-5}$	$2.17 \times 10^{-4}$	51.9
$8.62 \times 10^{-5}$	$4.35 \times 10^{-4}$	104
$8.62 \times 10^{-5}$	$6.52 \times 10^{-4}$	151
$8.62 \times 10^{-5}$	$8.70 \times 10^{-4}$	206
$8.62 \times 10^{-5}$	$1.09 \times 10^{-3}$	250

The end absorption does not go to zero because of the overlap with product absorption.

$$k = 2.29 \times 10^5 \text{ L mol}^{-1} \text{ s}^{-1}$$

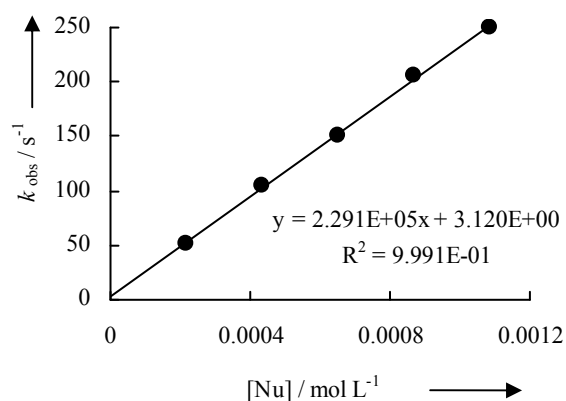


**Table 3:** Kinetics of the reaction of **2** with **4b** at 20 °C in DMSO (stopped-flow,  $\lambda = 333$  nm).

[2] / mol L <sup>-1</sup>	[4b] / mol L <sup>-1</sup>	$k_{\text{obs}} / \text{s}^{-1}$
$8.62 \times 10^{-5}$	$4.28 \times 10^{-4}$	30.4
$8.62 \times 10^{-5}$	$8.55 \times 10^{-4}$	56.5
$8.62 \times 10^{-5}$	$1.28 \times 10^{-3}$	82.1
$8.62 \times 10^{-5}$	$1.71 \times 10^{-3}$	103
$8.62 \times 10^{-5}$	$2.14 \times 10^{-3}$	132

The end absorption does not go to zero because of the overlap with product absorption.

$$k = 5.84 \times 10^4 \text{ L mol}^{-1} \text{ s}^{-1}$$

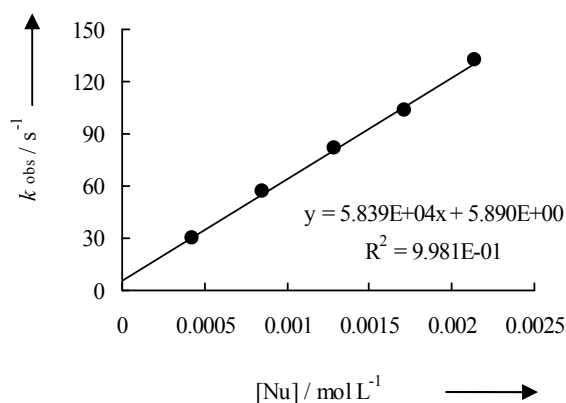


**Table 4:** Kinetics of the reaction of **2** with **4c** at 20 °C in DMSO (stopped-flow,  $\lambda = 333$  nm).

[2] / mol L <sup>-1</sup>	[4c] / mol L <sup>-1</sup>	$k_{\text{obs}} / \text{s}^{-1}$
$9.43 \times 10^{-5}$	$1.96 \times 10^{-3}$	19.3
$9.43 \times 10^{-5}$	$2.45 \times 10^{-3}$	23.5
$9.43 \times 10^{-5}$	$2.94 \times 10^{-3}$	28.3
$9.43 \times 10^{-5}$	$3.44 \times 10^{-3}$	32.4
$9.43 \times 10^{-5}$	$3.93 \times 10^{-3}$	37.1

The end absorption does not go to zero because of the overlap with product absorption.

$$k = 9.03 \times 10^3 \text{ L mol}^{-1} \text{ s}^{-1}$$

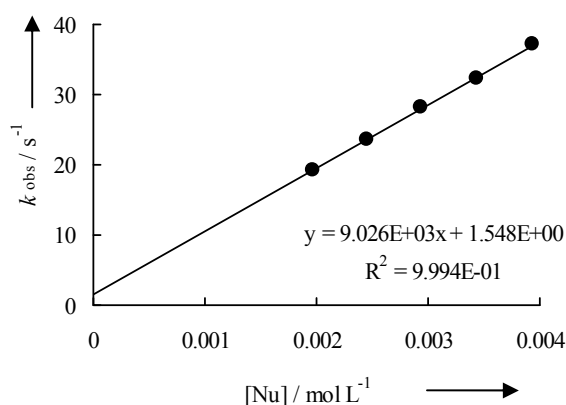


**Table 5:** Kinetics of the reaction of **2** with **4d** at 20 °C in DMSO (stopped-flow,  $\lambda = 333$  nm).

[ <b>2</b> ] / mol L <sup>-1</sup>	[ <b>4c</b> ] / mol L <sup>-1</sup>	$k_{\text{obs}}$ / s <sup>-1</sup>
$9.43 \times 10^{-5}$	$1.19 \times 10^{-3}$	$3.58 \times 10^{-1}$
$9.43 \times 10^{-5}$	$1.49 \times 10^{-3}$	$4.37 \times 10^{-1}$
$9.43 \times 10^{-5}$	$1.78 \times 10^{-3}$	$5.20 \times 10^{-1}$
$9.43 \times 10^{-5}$	$2.38 \times 10^{-3}$	$6.90 \times 10^{-1}$
$9.43 \times 10^{-5}$	$2.97 \times 10^{-3}$	$8.46 \times 10^{-1}$

The end absorption does not go to zero because of the overlap with product absorption.

$$k = 2.75 \times 10^2 \text{ L mol}^{-1} \text{ s}^{-1}$$

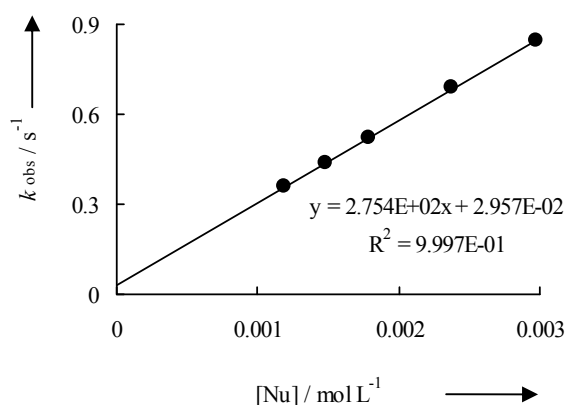


**Table 6:** Kinetics of the reaction of **2** with **5** at 20 °C in CH<sub>3</sub>CN (stopped-flow,  $\lambda = 326$  nm).

[ <b>2</b> ] / mol L <sup>-1</sup>	[ <b>5</b> ] / mol L <sup>-1</sup>	$k_{\text{obs}}$ / s <sup>-1</sup>
$8.76 \times 10^{-5}$	$9.18 \times 10^{-4}$	$4.52 \times 10^{-1}$
$8.76 \times 10^{-5}$	$1.38 \times 10^{-3}$	$6.79 \times 10^{-1}$
$8.76 \times 10^{-5}$	$1.84 \times 10^{-3}$	$8.98 \times 10^{-1}$
$8.76 \times 10^{-5}$	$2.29 \times 10^{-3}$	1.13
$8.76 \times 10^{-5}$	$2.75 \times 10^{-3}$	1.36

The end absorption does not go to zero because of the overlap with product absorption.

$$k = 4.96 \times 10^2 \text{ L mol}^{-1} \text{ s}^{-1}$$

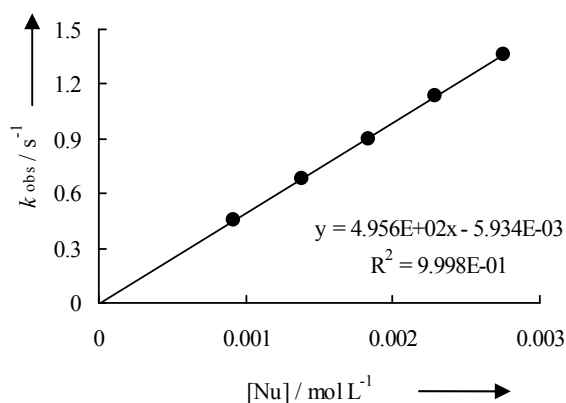


**Table 7:** Kinetics of the reaction of **2** with **6** at 20 °C in CH<sub>3</sub>CN (diode array,  $\lambda = 326$  nm).

[ <b>2</b> ] / mol L <sup>-1</sup>	[ <b>6</b> ] / mol L <sup>-1</sup>	$k_{\text{obs}}$ / s <sup>-1</sup>
$9.27 \times 10^{-5}$	$1.93 \times 10^{-3}$	$1.11 \times 10^{-4}$
$7.97 \times 10^{-5}$	$2.49 \times 10^{-3}$	$1.48 \times 10^{-4}$
$7.74 \times 10^{-5}$	$4.02 \times 10^{-3}$	$2.33 \times 10^{-4}$
$9.90 \times 10^{-5}$	$6.89 \times 10^{-3}$	$4.19 \times 10^{-4}$

$$k = 6.19 \times 10^{-2} \text{ L mol}^{-1} \text{ s}^{-1}$$

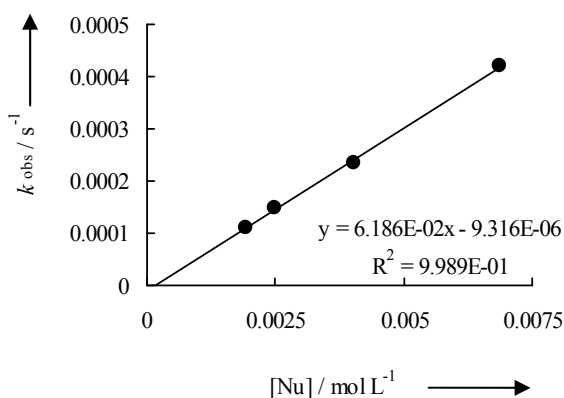
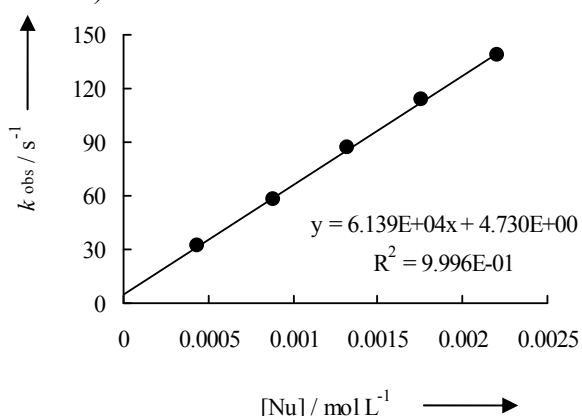


**Table 8:** Kinetics of the reaction of 2-Cinnamoyl-1,3-dimethyl-1*H*-imidazol-3-ium iodide with **4b** at 20 °C in DMSO (stopped-flow,  $\lambda = 333$  nm).

[ <b>2</b> ] / mol L <sup>-1</sup>	[ <b>4b</b> ] / mol L <sup>-1</sup>	$k_{\text{obs}}$ / s <sup>-1</sup>
$7.34 \times 10^{-5}$	$4.41 \times 10^{-4}$	31.6
$7.34 \times 10^{-5}$	$8.81 \times 10^{-4}$	58.3
$7.34 \times 10^{-5}$	$1.32 \times 10^{-3}$	86.5
$7.34 \times 10^{-5}$	$1.76 \times 10^{-3}$	114
$7.34 \times 10^{-5}$	$2.20 \times 10^{-3}$	139

The end absorption does not go to zero because of the overlap with product absorption.



$$k = 6.14 \times 10^4 \text{ L mol}^{-1} \text{ s}^{-1}$$

## 5 References

- [1] Recent reviews on NHC catalyzed transformations: a) D. Enders, O. Niemeier, A. Henseler, *Chem. Rev.* **2007**, *107*, 5606–5655; b) N. Marion, S. Díez-González, S. P. Nolan, *Angew. Chem. Int. Ed.* **2007**, *46*, 2988–3000; c) V. Nair, S. Vellalath, B. P. Babu, *Chem Soc. Rev.* **2008**, *37*, 2691–2698; d) J. L. Moore, T. Rovis, *Top. Curr. Chem.* **2010**, *291*, 77; e) V. Nair, R. S. Menon, A. T. Biju, C. R. Sinu, R. R. Paul, A. Jose, V. Sreekumar, *Chem. Soc. Rev.* **2011**, *40*, 5336–5346.
- [2] Pioneering studies on homoenolate chemistry using NHC catalysis, see: a) C. Burstein, F. Glorius, *Angew. Chem. Int. Ed.* **2004**, *43*, 6205–6208; b) S. S. Sohn, E. L. Rosen, J. W. Bode, *J. Am. Chem. Soc.* **2004**, *126*, 14370–14371.
- [3] K. Zeitler, *Org. Lett.* **2006**, *8*, 637–640. See also refs 6 and 7b,c. Initial report on protonation of a homoenolate generated by NHC catalysis: A. Chan, K. A. Scheidt, *Org. Lett.* **2005**, *7*, 905–908. See also: S. S. Sohn, J. W. Bode, *Org. Lett.* **2005**, *7*, 3873–3876.
- [4] a) S. J. Ryan, L. Candish, D. W. Lupton, *J. Am. Chem. Soc.* **2009**, *131*, 14176–14177; b) L. Candish, D. W. Lupton, *Org. Lett.* **2010**, *12*, 4836–4839; c) S. J. Ryan, L. Candish, D. W. Lupton, *J. Am. Chem. Soc.* **2011**, *133*, 4694–4697; d) S. Ryan, L. Candish, D. W. Lupton, *Synlett* **2011**, 2275–2278; e) S. J. Ryan, A. Stasch, M. N. Paddon-Row, D. W. Lupton, *J. Org. Chem.* **2012**, *77*, 1113–1124.
- [5] Acyl azoliums via oxidation using external oxidants, some recent examples: a) B. E. Maki, A. Chan, E. M. Phillips, K. A. Scheidt, *Org. Lett.* **2007**, *9*, 371–374; b) B. E.

- Maki, K. A. Scheidt, *Org. Lett.* **2008**, *10*, 4331–4334; c) C. Noonan, L. Baragwanath, S. J. Connon, *Tetrahedron Lett.* **2008**, *49*, 4003–4006; d) J. Guin, S. De Sarkar, S. Grimme, A. Studer, *Angew. Chem. Int. Ed.* **2008**, *47*, 8727–8730; e) S. De Sarkar, S. Grimme, A. Studer, *J. Am. Chem. Soc.* **2010**, *132*, 1190–1191; f) S. De Sarkar, A. Studer, *Org. Lett.* **2010**, *12*, 1992–1995; g) C. A. Rose, K. Zeitler, *Org. Lett.* **2010**, *12*, 4552–4555; h) Y.-C. Xin, S.-H. Shi, D.-D. Xie, X.-P. Hui, P.-F. Xu, *Eur. J. Org. Chem.* **2011**, 6527–6531; i) S. Iwahana, H. Iida, E. Yashima, *Chem. Eur. J.* **2011**, *17*, 8009–8013; j) B. Maji, S. Vedachalan, X. Ge, S. Cai, X.-W. Liu, *J. Org. Chem.* **2011**, *76*, 3016–3023; k) S. De Sarkar, A. Biswas, C. H. Song, A. Studer, *Synthesis* **2011**, 1974–1983; l) R. S. Reddy, J. N. Rosa, L. F. Veiros, S. Caddick, P. M. P. Gois, *Org. Biomol. Chem.* **2011**, *9*, 3126–3129.
- [6] a) J. Kaeobamrung, J. Mahatthananchai, P. Zheng, J. W. Bode, *J. Am. Chem. Soc.* **2010**, *132*, 8810–8812; b) J. Mahatthananchai, P. Zheng, J. W. Bode, *Angew. Chem. Int. Ed.* **2011**, *50*, 1673–1677.
- [7] a) S. De Sarkar, A. Studer, *Angew. Chem. Int. Ed.* **2010**, *49*, 9266–9269; b) Z.-Q. Zhu, J.-C. Xiao, *Adv. Synth. Catal.* **2010**, *352*, 2455–2458; c) Z.-Q. Zhu, X.-L. Zheng, N.-F. Jiang, X. Wan, J.-C. Xiao, *Chem. Commun.* **2011**, *47*, 8670–8672; d) Z.-Q. Rong, M.-Q. Jia, S.-L. You, *Org. Lett.* **2011**, *13*, 4080–4083.
- [8] B. Wanner, J. Mahatthananchai, J. W. Bode, *Org. Lett.* **2011**, *13*, 5378–5381.
- [9] For an X-ray structure of a benzoylazolium salt, see: N. Kuhn, M. Steimann, M. Walker, *Z. Naturforsch.* **2001**, *56 b*, 129.
- [10] a) A. Miyashita, A. Kurachi, Y. Matsuoka, N. Tanabe, Y. Suzuki, K.-i. Iwamoto, T. Higashino, *Heterocycles* **1997**, *44*, 417–426; b) L. M. Ferreira, A. M. Lobo, S. Prabhakar, A. C. Teixeira, *Tetrahedron* **1999**, *55*, 3541–3452.
- [11] CCDC 857879 contains the supplementary crystallographic data for this paper. These data can be obtained free of charge at [www.ccdc.cam.ac.uk/conts/retrieving.html](http://www.ccdc.cam.ac.uk/conts/retrieving.html) [or from the Cambridge Crystallographic Data Centre, E-mail: [deposit@ccdc.cam.ac.uk](mailto:deposit@ccdc.cam.ac.uk)].
- [12] a) H. Mayr, M. Patz, *Angew. Chem. Int. Ed. Engl.* **1994**, *33*, 938–957; b) H. Mayr, T. Bug, M. F. Gotta, N. Hering, B. Irrgang, B. Jancker, B. Kempf, R. Loos, A. R. Ofial, G. Remennikov, H. Schimmel, *J. Am. Chem. Soc.* **2001**, *123*, 9500–9512; c) R. Lucius, R. Loos, H. Mayr, *Angew. Chem. Int. Ed.* **2002**, *41*, 91–95; d) H. Mayr, B. Kempf, A. R. Ofial, *Acc. Chem. Res.* **2003**, *36*, 66–77; e) H. Mayr, A. R. Ofial, *Pure Appl. Chem.* **2005**, *77*, 1807–1821; f) H. Mayr, *Angew. Chem. Int. Ed.* **2011**, *50*, 3612–3518.

- [13] For a comprehensive listing of nucleophilicity parameters  $N$  and electrophilicity parameters  $E$ , see <http://www.cup.uni-muenchen.de/oc/mayr/DBintro.html>.
- [14] a) J. Tao, J. P. Perdew, V. N. Staroverov and G. E. Scuseria, *Phys. Rev. Lett.* **2003**, *91*, 146401–146401-4; b) S. Grimme, J. Antony, S. Ehrlich, H. Krieg, *J. Chem. Phys.* **2010**, *132*, 154104-19; c) S. Grimme, S. Ehrlich, L. Goerigk, *J. Comput. Chem.* **2011**, *32*, 1456–1465; d) F. Weigend, R. Ahlrichs *Phys. Chem. Chem. Phys.* **2005**, *7*, 3297–3305.
- [15] A. Klamt, G. Schüürmann, *J. Chem. Soc. Perkin Trans. 2* **1993**, 799–805.

## Chapter 9

# Nucleophilicity Parameters of Enamides and their Implications for Organocatalytic Transformations

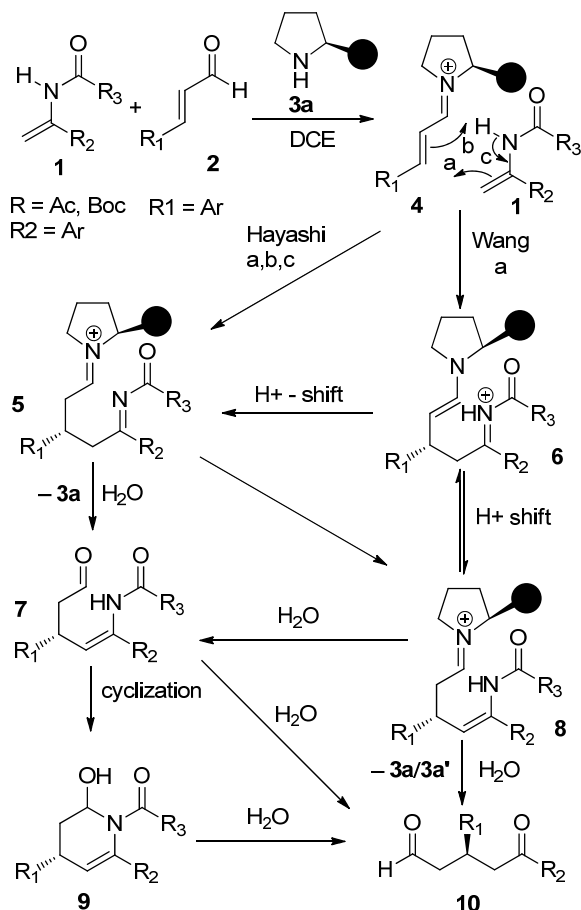
B. Maji, S. Lakhdar, H. Mayr, *Chem. Eur. J.* **2012**, *18*, 5732–5740.

### 1 Introduction

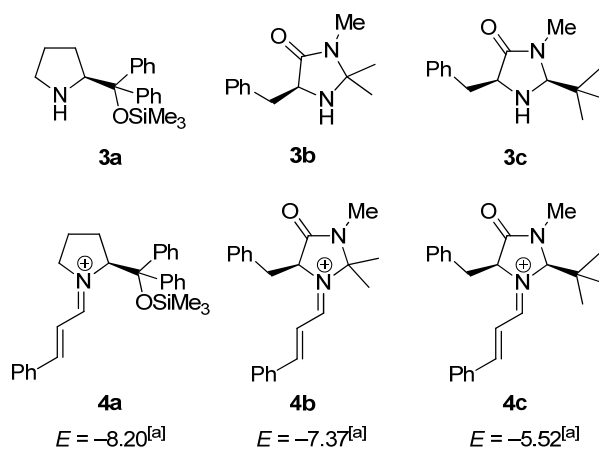
Enamides and enecarbamates (**1**)<sup>[1]</sup> endowed with a fine balance of stability and reactivity, may be considered as “tunable enamines”.<sup>[1b]</sup> Their facile synthetic accessibility and stability in air makes them attractive reagents in organic synthesis. They have frequently been used as nucleophiles in a manifold of organic reactions, including metal- and organo-catalyzed asymmetric transformations. Although reactions of electrophiles with enamides and enecarbamates have been known for two decades,<sup>[1c]</sup> their use in asymmetric synthesis has only recently been pioneered by Kobayashi and coworkers,<sup>[1a,2]</sup> who achieved enantioselective Cu(II)-ligand-catalyzed additions of **1** to imines, aldehydes, azodicarboxylates, and Michael acceptors.<sup>[1a,2]</sup> Enantioselective ene reactions of *N*-acylimines and glyoxylates with **1** have been developed by Terada et al. using chiral phosphoric acid derivatives as catalysts.<sup>[3]</sup> Recently, Zhong et al. used chiral Brønsted acids to catalyze  $\alpha$ -aminooxylations of enamides.<sup>[4]</sup>

The use of enamides as nucleophilic substrates in iminium-activated enantioselective reactions<sup>[5]</sup> has been investigated independently by Hayashi and Wang,<sup>[6]</sup> who reported enantioselective formations of tetrahydropyridines **9** via diarylprolinol silyl ether **3a** catalyzed reactions of **1** with  $\alpha,\beta$ -unsaturated aldehydes **2** (Scheme 1).<sup>[6]</sup> While Hayashi proposed a concerted ene reaction of the intermediate iminium ion **4** with **1** to give **5** (a, b, c in Scheme 1), Wang suggested a stepwise mechanism with initial nucleophilic attack of the enamide **1** at the iminium ion **4** to yield the Michael adduct **6** (a in Scheme 1) which tautomerizes to give **8**. Both mechanistic suggestions agree that a series of proton shifts and

partial hydrolysis yield **7** which may cyclize with formation of **9**. Hydrolysis of **5**, **6**, **7**, or **8** may yield the diketone **10**, which was observed by Hayashi as a side product and obtained by Wang through hydrolysis of **9**.<sup>[6]</sup>



**Scheme 1.** Mechanisms for the diarylprolinol ether **3a** catalyzed formation of tetrahydropyridines **9** from α,β-unsaturated aldehydes **2** and enamides **1**; DCE = 1,2-dichloroethane.



**Scheme 2.** Chiral amine catalysts **3** and corresponding iminium ions **4** formed from cinnamaldehyde. <sup>[a]</sup> Empirical electrophilicity parameters *E* from refs. [8a,d].

Iminium ions derived from chiral amines **3** (Scheme 2) have previously been isolated and characterized by NMR and X-ray analysis.<sup>[7,8a]</sup> Since we had studied their reactivity with different nucleophiles and found that iminium ions derived from MacMillan's second generation catalyst **3c** are  $10^2$  times more reactive than those derived from **3a** (Scheme 2),<sup>[8d]</sup> we were puzzled by Wang's report that in contrast to **3a**, **3c** was unable to catalyze the reactions of  $\alpha,\beta$ -unsaturated aldehydes with enamides.<sup>[6b]</sup> We, therefore, employed the kinetic methods developed in our laboratory to elucidate the mechanism of iminium-activated reactions of enamides.<sup>[8,9]</sup>

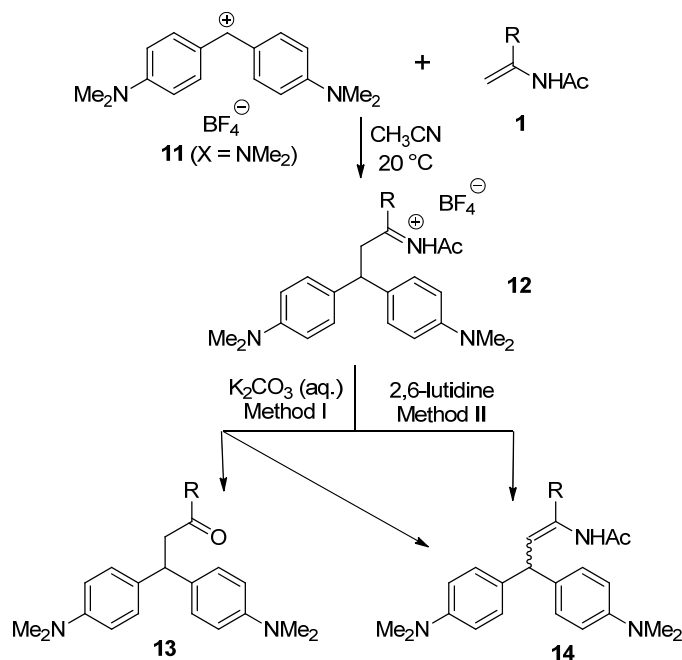
Qualitative studies had shown that enamides are generally less nucleophilic than enamines and enolate anions.<sup>[1a]</sup> In order to include enamides in our quantitative nucleophilicity scale<sup>[9]</sup> we have studied the kinetics of their reactions with benzhydrylium ions, and we will then demonstrate the implications of these results for elucidating the mechanism of iminium-activated Michael additions of enamides.<sup>[6]</sup>

## 2 Results and Discussion

### 2.1 Reactions of enamides with benzhydrylium ions

The reactions of **1** with the dimethylamino-substituted benzhydrylium tetrafluoroborate  $(\text{dma})_2\text{CH}^+\text{BF}_4^-$  gave the acyl-iminium salts **12** which were converted into mixtures of the ketones **13** and the benzhydryl substituted enamides **14** (as a mixture of *E/Z* isomers) by hydrolysis with aqueous potassium carbonate (method I) (Table 1). Compounds **14** were obtained exclusively when the addition products **12** were treated with 2,6-lutidine (method II). However, the reaction of  $(\text{dma})_2\text{CH}^+\text{BF}_4^-$  with the enamide **1h** yielded an imine (entry 8), and the reactions of **1i** and **1j** with  $(\text{dma})_2\text{CH}^+\text{BF}_4^-$  gave enamides in which the position of the double bond has been shifted (entries 9 and 10).

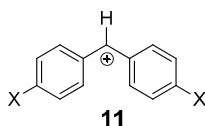
**Table 1.** Products of the reactions of several enamides **1** with the dimethylamino-substituted benzhydrylium tetrafluoroborate  $(\text{dma})_2\text{CH}^+\text{BF}_4^-$  in  $\text{CH}_3\text{CN}$  at  $20\text{ }^\circ\text{C}$ .<sup>[a]</sup>



Entry	Enamide	Method	Yield [%] <sup>[d]</sup>	
			<b>13</b>	<b>14</b>
1		I <sup>[b]</sup>	22	62
2		II <sup>[c]</sup>	-	89
3		I <sup>[b]</sup>	29	52
4		II <sup>[c]</sup>	-	95
5		I <sup>[b]</sup>	30	64
6		II <sup>[c]</sup>	-	90
7		II <sup>[c]</sup>	-	89
8		II <sup>[c]</sup>	-	
9		II <sup>[c]</sup>	-	
10		II <sup>[c]</sup>	-	

<sup>[a]</sup> For reaction conditions see the Experimental Section 4.2.1. <sup>[b]</sup> Method I: work-up with aqueous K<sub>2</sub>CO<sub>3</sub>. <sup>[c]</sup> Method II: work-up with 2,6-lutidine. <sup>[d]</sup> Isolated yield after column chromatography. dma = *p*-Me<sub>2</sub>NC<sub>6</sub>H<sub>4</sub>.

**Table 2.** Abbreviations and electrophilicity parameters  $E$  for the benzhydrylium ions **11** used as reference electrophiles in this work.



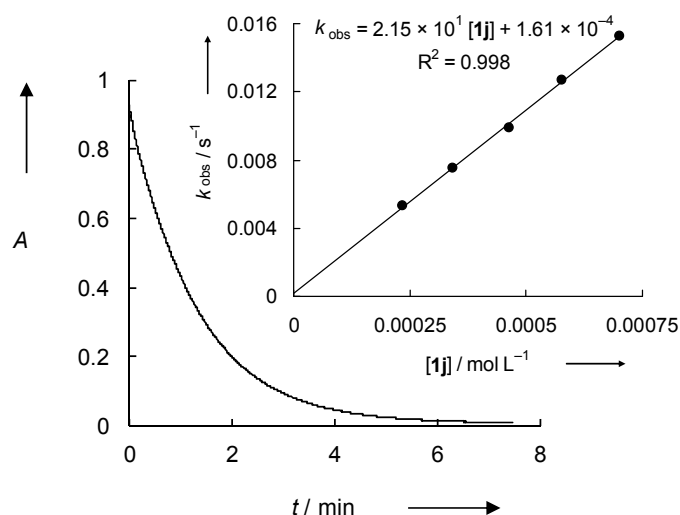
X	Abbreviations	$E^{[a]}$
N(Ph)CH <sub>2</sub> CF <sub>3</sub>	(pfa) <sub>2</sub> CH <sup>+</sup>	-3.14
N(CH <sub>3</sub> )CH <sub>2</sub> CF <sub>3</sub>	(mfa) <sub>2</sub> CH <sup>+</sup>	-3.85
N(CH <sub>2</sub> CH <sub>2</sub> ) <sub>2</sub> O	(mor) <sub>2</sub> CH <sup>+</sup>	-5.53
N(Ph)CH <sub>3</sub>	(mpa) <sub>2</sub> CH <sup>+</sup>	-5.89
N(CH <sub>3</sub> ) <sub>2</sub>	(dma) <sub>2</sub> CH <sup>+</sup>	-7.02

<sup>[a]</sup> Electrophilicity parameters  $E$  for benzhydrylium ions from ref. [9b].

The rates of the reactions of **1** with the benzhydrylium ions **11** (Table 2) were determined photometrically in CH<sub>3</sub>CN at 20 °C by monitoring the decrease of the absorbances of the benzhydrylium ions using conventional or stopped-flow UV-Vis spectrometers as described before.<sup>[9]</sup> An excess of the nucleophiles **1** over **11** was used to achieve pseudo-first-order conditions, and the pseudo-first-order rate constants  $k_{\text{obs}}$  (s<sup>-1</sup>) were obtained by least squares fits of the mono-exponential decays of the absorbances of **11** to the function  $A = A_0 e^{-k_{\text{obs}}t}$ . The plots of  $k_{\text{obs}}$  against the concentrations of **1** were linear with negligible intercepts (Figure 1) indicating a second-order rate law [Eq. (1)].

$$-d[\mathbf{11}]/dt = k_2[\mathbf{1}][\mathbf{11}] \quad (1)$$

The slopes of these correlation lines yielded the second-order rate constants  $k_2$  (M<sup>-1</sup> s<sup>-1</sup>) listed in Table 3.

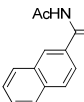


**Figure 1.** Exponential decay of the absorbance  $A$  at 612 nm during the reaction of  $\mathbf{1j}$  ( $5.76 \times 10^{-4}$  M) with  $(\text{mor})_2\text{CH}^+\text{BF}_4^-$  ( $2.05 \times 10^{-5}$  M) in  $\text{CH}_3\text{CN}$  at  $20^\circ\text{C}$  ( $k_{\text{obs}} = 1.27 \times 10^{-2} \text{ s}^{-1}$ ). Insert: Determination of the second-order rate constant  $k_2 = 2.15 \times 10^1 \text{ M}^{-1}\text{s}^{-1}$  from the dependence of  $k_{\text{obs}}$  on the concentration of  $\mathbf{1j}$ .

**Table 3.** Second-order rate constants for the reactions of the benzhydrylium ions  $\mathbf{11}$  with the enamides  $\mathbf{1}$  in acetonitrile at  $20^\circ\text{C}$ .

Enamide	$N, s_N^{[a]}$	$(\text{Ar})_2\text{CH}^+$	$k_2 / \text{M}^{-1}\text{s}^{-1}$
 <b>1a</b>	5.73, 0.97	$(\text{pfa})_2\text{CH}^+$	$4.73 \times 10^2$
		$(\text{mfa})_2\text{CH}^+$	$4.20 \times 10^1$
		$(\text{mor})_2\text{CH}^+$	$1.82 \times 10^0$
 <b>1b</b>	6.57, 0.91	$(\text{pfa})_2\text{CH}^+$	$1.29 \times 10^3$
		$(\text{mor})_2\text{CH}^+$	$6.01 \times 10^0$
		$(\text{mpa})_2\text{CH}^+$	$6.35 \times 10^0$
		$(\text{dma})_2\text{CH}^+$	$3.61 \times 10^{-1}$
 <b>1c</b>	7.06, 0.85	$(\text{pfa})_2\text{CH}^+$	$2.40 \times 10^3$
		$(\text{mfa})_2\text{CH}^+$	$4.37 \times 10^2$
		$(\text{mor})_2\text{CH}^+$	$2.12 \times 10^1$
		$(\text{dma})_2\text{CH}^+$	$1.08 \times 10^0$
 <b>1d</b>	5.60, 1.00	$(\text{pfa})_2\text{CH}^+$	$2.94 \times 10^2$
		$(\text{mor})_2\text{CH}^+$	$1.19 \times 10^0$

Table 3 continued

Enamide	$N, s_N$ <sup>[a]</sup>	(Ar) <sub>2</sub> CH <sup>+</sup>	$k_2 / \text{M}^{-1}\text{s}^{-1}$
 1e	6.21, 0.87	(pfa) <sub>2</sub> CH <sup>+</sup>	$4.53 \times 10^2$
		(mor) <sub>2</sub> CH <sup>+</sup>	$2.78 \times 10^0$
		(mpa) <sub>2</sub> CH <sup>+</sup>	$3.47 \times 10^0$
		(dma) <sub>2</sub> CH <sup>+</sup>	$1.59 \times 10^{-1}$
 1f	(5.44, 1.0) <sup>[b]</sup>	(mor) <sub>2</sub> CH <sup>+</sup>	$8.22 \times 10^{-1}$
 1g	6.28, 0.95	(pfa) <sub>2</sub> CH <sup>+</sup>	$1.50 \times 10^3$
		(mfa) <sub>2</sub> CH <sup>+</sup>	$1.05 \times 10^2$
		(mor) <sub>2</sub> CH <sup>+</sup>	$6.23 \times 10^0$
 1h	4.91, 0.87	(pfa) <sub>2</sub> CH <sup>+</sup>	$4.64 \times 10^1$
		(mfa) <sub>2</sub> CH <sup>+</sup>	$5.24 \times 10^0$
		(mor) <sub>2</sub> CH <sup>+</sup>	$3.28 \times 10^{-1}$
 1i	5.64, 0.79	(mfa) <sub>2</sub> CH <sup>+</sup>	$2.30 \times 10^1$
		(mor) <sub>2</sub> CH <sup>+</sup>	$1.62 \times 10^0$
		(dma) <sub>2</sub> CH <sup>+</sup>	$6.91 \times 10^{-2}$
 1j	7.06, 0.87	(pfa) <sub>2</sub> CH <sup>+</sup>	$3.39 \times 10^3$
		(mfa) <sub>2</sub> CH <sup>+</sup>	$4.16 \times 10^2$
		(mor) <sub>2</sub> CH <sup>+</sup>	$2.15 \times 10^1$
		(dma) <sub>2</sub> CH <sup>+</sup>	$1.16 \times 10^0$
 1k	4.61, 0.98	(pfa) <sub>2</sub> CH <sup>+</sup>	$3.6 \times 10^1$ <sup>[c]</sup>
		(mfa) <sub>2</sub> CH <sup>+</sup>	$3.8 \times 10^0$ <sup>[c]</sup>
		(mor) <sub>2</sub> CH <sup>+</sup>	$1.4 \times 10^{-1}$ <sup>[c]</sup>

<sup>[a]</sup> Nucleophilicity parameters  $N$  (and  $s_N$ ) derived by using Equation (2). <sup>[b]</sup>  $N$  calculated with the assumption  $s_N = 1.0$ . <sup>[c]</sup> Kinetics of lower quality; mono-exponential behavior was only observed during the first half-reaction time.

## 2.2 Relationships between structure and nucleophilicity of enamides

In previous publications, it has been shown that the rates of the reactions of carbocations and Michael acceptors with  $n$ ,  $\pi$ , and  $\sigma$ -nucleophiles can be described by the linear-free-energy relationship (2), where electrophiles are characterized by the electrophilicity parameter  $E$  and nucleophiles are characterized by the nucleophilicity parameter  $N$  and the nucleophile-specific sensitivity parameter  $s_N$  (previously termed  $s$ ).<sup>[9]</sup> On the basis of Equation (2) it was possible to develop the most comprehensive nucleophilicity scale presently available.<sup>[9]</sup>

$$\log k_2 (20\text{ }^\circ\text{C}) = s_N(N + E) \quad (2)$$

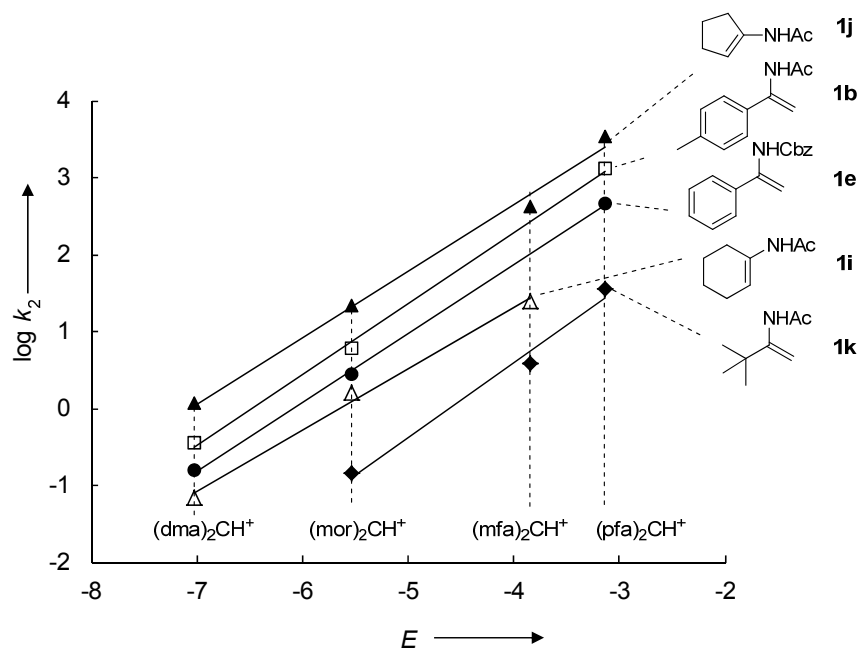


**Figure 2.** Plots of  $\log k_2$  for the reactions of the enamides **1** with the benzhydrylium ions **11** in  $\text{CH}_3\text{CN}$  at  $20\text{ }^\circ\text{C}$  versus the electrophilicity parameters  $E$ . For the sake of clarity, correlation lines are shown only for few nucleophiles (for others see the Experimental Section).

When the logarithms of the second-order rate constants (Table 3) for the reactions of the enamides **1** with benzhydrylium ions **11** were plotted against the electrophilicity parameters  $E$  for the benzhydrylium ions **11** (Table 2), linear correlations were obtained in accordance with Equation 2 (Figure 2). The slopes of the correlation lines yielded the nucleophile-specific sensitivity parameters  $s_N$ , and the intercepts on the abscissa gave the nucleophilicity parameters  $N$ , which are tabulated in Table 3.

The similar magnitudes of the slopes of these correlation lines ( $s_N \approx 1.0$ ) imply that the relative nucleophilicities of the enamides depend only slightly on the reactivities of the electrophiles.

Table 4 compares some enamides with structurally related compounds and shows that an acetamido group ( $\rightarrow$  **1a**) enhances the nucleophilicity of styrene by  $\sim 5$  orders of magnitude. While replacement of the acetamido group by the benzamido group ( $\rightarrow$  **1f**) slightly reduces the nucleophilicity (factor of 2 towards  $(\text{mor})_2\text{CH}^+$ ), the benzylcarbamate group ( $\rightarrow$  **1e**) has a small accelerating effect, the magnitude of which slightly depends on the electrophile (factor

1.7 toward  $(\text{mor})_2\text{CH}^+$ ). As the sensitivity parameters do not deviate significantly from  $s_N = 1$ , one can generalize, however, that enamides have similar nucleophilicities as analogously substituted enol ethers and are approximately 4 orders of magnitude less reactive than structurally analogous enamines.<sup>[9b,10]</sup>

**Table 4.** Comparison of the nucleophilicity parameters for enamides with those of structurally related  $\pi$ -systems.

$\pi$ -system		 <b>1a</b>	 <b>1f</b>	 <b>1e</b>		
$N$	0.78 <sup>[a]</sup>	5.73	5.44	6.21	6.22 <sup>[a]</sup>	9.96 <sup>[a]</sup>

<sup>[a]</sup>  $N$  parameters in  $\text{CH}_2\text{Cl}_2$  from refs. [9b] and [10].

As in the enamine series,<sup>[9f,10]</sup> the cyclopentanone derived enamide **1j** is significantly more nucleophilic than the cyclohexanone-derived enamide **1i** (Figure 2), and the pinacolone derived enamide **1k** is the least nucleophilic compound in this series.

The correlation of  $\log k_2$  for the reactions of 4-X-substituted 1-aryl enamides with the benzhydrylium ion  $(\text{mor})_2\text{CH}^+$  with Hammett's  $\sigma_p^+$  constants<sup>[11]</sup> of the aryl substituents X gives the reaction constant  $\rho = -1.40$  (Figure 3). The small magnitude of  $\rho$  indicates that in the transition state most of the developing charge is stabilized by the acetamido group and only a small amount of the positive charge requires stabilization by the aryl ring.

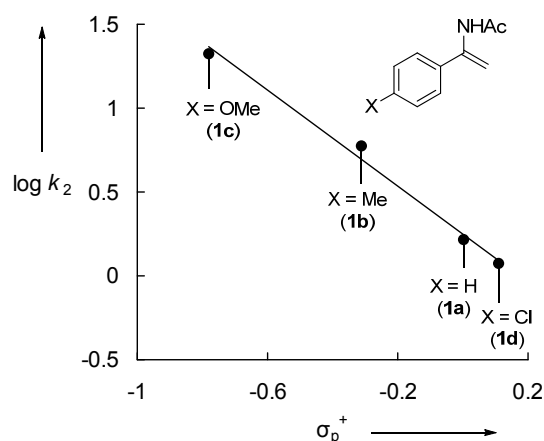


**Figure 3.** Correlation of  $\log k_2$  for the reactions of 4-X-substituted 1-aryl enamides with  $(\text{mor})_2\text{CH}^+\text{BF}_4^-$  with  $\sigma_p^+$  (from ref. [11]) ( $\log k_2 = -1.40\sigma_p^+ + 0.27$ ,  $r^2 = 0.9909$ ).

### 2.3 Reactions with Michael acceptors and chlorinating agents

To examine the applicability of the  $N$  and  $s_N$  parameters in Table 3 for reactions of enamides with other electrophiles, we have investigated the rates of the reactions of enamides with 5-benzylidene-2,2-dimethyl-1,3-dioxane-4,6-dione (**15**), which yield the Michael adducts **16** after hydrolysis (Table 5).

The rates of the reactions of **1** with **15** were measured by the same method as described before, following the decay of the absorbance of **15** at  $\lambda = 317$  nm. Table 5 shows that the experimental second-order rate constants agree within a factor of 1.7 with those calculated by Equation (2) using the  $N$  parameters in Table 3 and previously reported electrophilicity parameter ( $E = -9.15$ )<sup>[12]</sup> for **15**. This remarkable agreement supports a mechanism with rate limiting CC-bond formation,<sup>[2i]</sup> i.e., the type of electrophile-nucleophile combination for which Equation (2) has been parameterized.

**Table 5.** Yields, experimental ( $k_2^{\text{exp}}$ ) and calculated ( $k_2^{\text{calcd}}$ ) second order rate constants (in  $\text{M}^{-1} \text{s}^{-1}$ ) for the reactions of the enamides **1b,c** with **15**.

The reaction scheme shows an enamide (1b,c) reacting with a cyclic Michael acceptor (15) to form a Michael adduct (16). The enamide has an N-acetyl group and a substituent X on the phenyl ring. The Michael acceptor is a cyclic dione with a benzylidene group. The reaction conditions are CH<sub>3</sub>CN at 20 °C, followed by hydrolysis with concentrated HCl in THF.

Nucleophile	Yield [%] <sup>[a]</sup>	$k_2^{\text{exp}}$	$k_2^{\text{calcd}}$ [b]	$k_2^{\text{exp}} / k_2^{\text{calcd}}$
<b>1b</b>	45	$7.54 \times 10^{-3}$	$4.49 \times 10^{-3}$	1.7
<b>1c</b>	66	$2.64 \times 10^{-2}$	$1.67 \times 10^{-2}$	1.6

<sup>[a]</sup> Isolated yield after column chromatography. <sup>[b]</sup> Calculated by using Equation (2), the electrophilicity parameter  $E = -9.15$  (from ref. [12]), and  $N$ ,  $s_N$  values of **1b** and **1c** from Table 3.

Chlorinations and brominations of alkenes often proceed via bridged intermediates, i.e., simultaneous formation of two new bonds in the rate-limiting step, and therefore, do not follow Equation (2). We have reported, however, that in the reactions of 2,3,4,5,6,6-hexachlorocyclohexa-2,4-dienone **17** with enamines, enol ethers, pyrroles, and indoles, non-bridged intermediates are involved with the consequence that these reactions follow the correlation (2) and can be used to derive the electrophilicity parameter  $E$  for **17**.<sup>[13]</sup> Analogously, fair agreement between  $k_2^{\text{exp}}$  and  $k_2^{\text{calcd}}$  has also been found for the reactions of enamides with the chlorinating agent **17** (Table 6), which is quite remarkable because the  $N$

and  $s_N$  parameters of **1** (as those of most other nucleophiles) have been derived from the kinetics of their reactions with benzhydrylium ions.

**Table 6.** Yields, experimental ( $k_2^{\text{exp}}$ ) and calculated ( $k_2^{\text{calcd}}$ ) second-order rate constants (in  $\text{M}^{-1} \text{s}^{-1}$ ) for the reactions of nucleophiles **1** with **17**.

Nucleophile	Yield [%] <sup>[a]</sup>	$k_2^{\text{exp}}$	$k_2^{\text{calcd}}$ [b]	$k_2^{\text{calcd}}/k_2^{\text{exp}}$
<b>1a</b>	56	$3.20 \times 10^{-2}$	$1.02 \times 10^{-1}$	3.2
<b>1b</b>	44	$3.39 \times 10^{-2}$	$6.86 \times 10^{-1}$	20
<b>1c</b>		$1.59 \times 10^{-1}$	1.83	12
<b>1i</b>	52	$1.63 \times 10^{-1}$	$1.33 \times 10^{-1}$	0.82
<b>1j</b>		$7.94 \times 10^{-1}$	1.86	2.3

<sup>[a]</sup> Isolated yields after column chromatography; <sup>[b]</sup> Calculated by using Equation (2), the electrophilicity parameter  $E = -6.75$  (from ref. [13]), and  $N$ ,  $s_N$  values of **1** from Table 3.

## 2.4 Iminium activated reactions of enamides

When the iminium salts **4a**-OTf, **4b**-OTf, **4b**-PF<sub>6</sub>, or **4c**-PF<sub>6</sub> ( $\sim 5 \times 10^{-5} \text{ M}$ ), which were synthesized according to literature procedures,<sup>[7]</sup> were combined with  $\sim 25$  equivalents of **1b** or **1c** in CH<sub>2</sub>Cl<sub>2</sub> or CH<sub>3</sub>CN, no consumption of the iminium ions was observed. This observation was surprising for us since second-order rate constants of  $10^{-2}$  to  $10^1 \text{ M}^{-1} \text{ s}^{-1}$  can be calculated by using Equation (2),  $N$  and  $s_N$  of **1b,c** (Table 3), and  $E$  of the iminium ions **4a–c** (Scheme 2),<sup>[8a,d]</sup> suggesting readily occurring reactions at room temperature. On the other hand Wang reported that imidazolidinone **3c** did not catalyze the reaction of  $\alpha,\beta$ -unsaturated aldehydes with enamides,<sup>[6b]</sup> while Hayashi-Jørgensen's catalyst **3a**, precursor of the  $10^2$  times less electrophilic iminium ion **4a**, proved to be an effective catalyst for this conversion.<sup>[6]</sup>

A solution for this discrepancy came from Table 1 of reference [6b], which shows that the two catalysts were employed with different cocatalysts. While HOTs was used as a cocatalyst for the attempted reactions with MacMillan's catalyst **3c**, benzoic acid served as a co-catalyst for the efficient catalysis with the pyrrolidine **3a**.

Assuming that the failure of the iminium triflates and hexafluorophosphates to react with **1b,c** was due to unfavorable thermodynamics, we tried to investigate the kinetics of the reactions

of **1b** and **1c** with the iminium salts **4a**-OTf, **4b**-OTf, **4b**-PF<sub>6</sub>, or **4c**-PF<sub>6</sub> in the presence bases, using previously described methods (photometric monitoring of the decay of the absorbances of **4a–c** at  $\lambda = 367$  nm).<sup>[8]</sup> Additives of tetra-*n*-butylammonium benzoate and potassium trifluoroacetate turned out to be inefficient as the iminium ions **4a–c** underwent fast combinations with PhCO<sub>2</sub><sup>-</sup> and slowly decomposed in the presence of CF<sub>3</sub>CO<sub>2</sub><sup>-</sup>.<sup>[14]</sup> Addition of 3-chloropyridine did not promote the reaction, and pyridine led to incomplete reactions with the iminium salts **4a**-OTf, **4b**-PF<sub>6</sub>, and **4c**-PF<sub>6</sub>. Full conversion (Figure 4) of the iminium salts **4b**-PF<sub>6</sub> and **4c**-PF<sub>6</sub> was observed, however, when 2,6-lutidine or 2,4,6-collidine were added.<sup>[15]</sup>

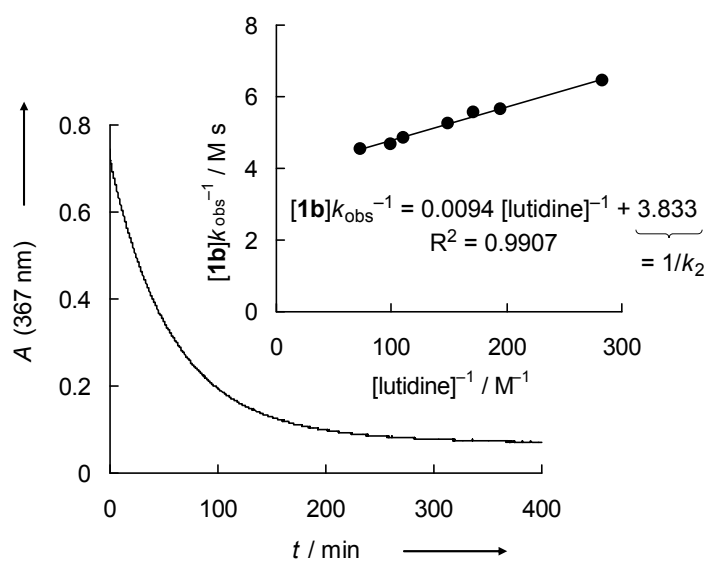
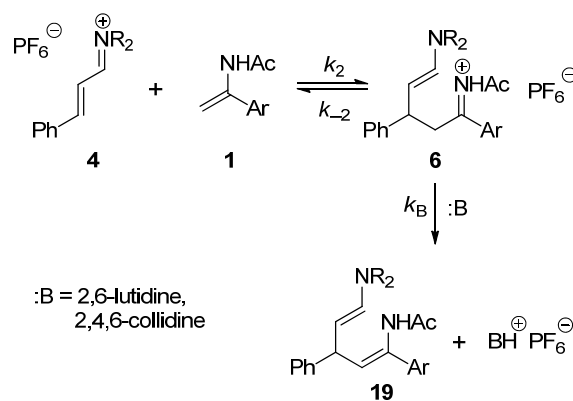


**Figure 4.** Exponential decay of the absorbance  $A$  (at 367 nm) of **4b**-PF<sub>6</sub> ( $3.94 \times 10^{-5}$  M) in the reaction with **1b** ( $1.82 \times 10^{-3}$  M) in the presence of 2,6-lutidine ( $3.53 \times 10^{-3}$  M) in CH<sub>2</sub>Cl<sub>2</sub> at 20 °C. Insert: Determination of second-order rate constant  $k_2 = (1/3.8) = 0.26$  (M<sup>-1</sup> s<sup>-1</sup>) from the plot  $[\mathbf{1b}]k_{\text{obs}}^{-1}$  vs.  $[\text{lutidine}]^{-1}$ ;  $[\mathbf{4b}] = 3.9 \times 10^{-5}$  M,  $[\mathbf{1b}] = 1.75 \times 10^{-3}$  M,  $3.53 \times 10^{-3}$  M  $< [\text{lutidine}] < 1.37 \times 10^{-2}$  M.

These observations can be rationalized by assuming that the reaction of **4** with **1** gives **6** in a small, not observable, equilibrium concentration (Scheme 3). In the presence of lutidine, deprotonation of **6** occurs, and the equilibrium is shifted toward the adduct **19**. Wang's proposal<sup>[6b]</sup> of a stepwise process (path a in Scheme 1) is thus supported, because the formation of **5** from **4** and **1** by a concerted ene reaction (path a, b, c in Scheme 1) would not require base catalysis.



**Scheme 3.** Proposed mechanism for the reactions of iminium ions **4** with enamides **1**.<sup>[16]</sup>

When the intermediate **6** is formed reversibly in a low equilibrium concentration, the observed rate constant  $k_{\text{obs}}$  for a pseudo-first order reaction with  $[\mathbf{1}]_0 \gg [\mathbf{4}]_0$  is given by Equation (3), where the second term reflects the ratio of forward ( $k_B[\text{B}]$ ) over the sum of backward ( $k_{-2}$ ) and forward reaction.

$$k_{\text{obs}} = k_2 [\mathbf{1}] \frac{k_B[\text{B}]}{k_{-2} + k_B[\text{B}]} \quad (3)$$

$$\frac{[\mathbf{1}]}{k_{\text{obs}}} = \frac{1}{k_2} + \frac{k_{-2}}{k_B k_2 [\text{B}]} \quad (4)$$

Rearrangement of Equation (3) yields Equation (4) which implies a linear plot of  $[\mathbf{1}]/k_{\text{obs}}$  vs  $[\text{B}]^{-1}$  as depicted in the insert of Figure 4.<sup>[17]</sup> The reciprocals of the intercepts of these plots give the second-order rate constants  $k_2$ , listed in Table 7.<sup>[18]</sup>

**Table 7.** Experimental and calculated rate constants  $k_2$  (in  $\text{M}^{-1} \text{s}^{-1}$ ) for the reactions of **4b** and **4c** with **1b** and **1c** in the presence of 2,6-lutidine in  $\text{CH}_2\text{Cl}_2$  at 20 °C.

Enamide	Iminium Ion	$k_2^{\text{exp}}$	$k_2^{\text{calcd [a]}}$	$k_2^{\text{exp}}/k_2^{\text{calcd}}$
<b>1b</b>	<b>4b</b>	0.26	0.19	1.4
<b>1c</b>	<b>4b</b>	0.73	0.55	1.3
<b>1b</b>	<b>4c</b>	3.3	9.0	0.36
<b>1c</b>	<b>4c</b>	7.1	20	0.35

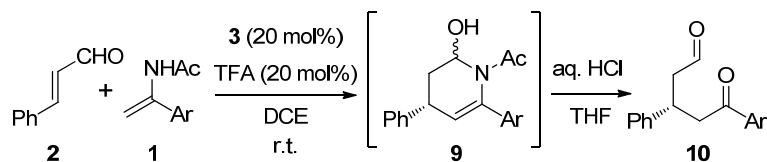
<sup>[a]</sup> Calculated by Equation (2) using  $N$  and  $s_N$  of **1** from Table 3 and  $E$  of **4** from Scheme 2.

The second-order rate constants for the reactions of the enamides **1b** and **1c** with **4b** and **4c** (Table 7) agree within a factor of 3 with those calculated by Equation (2) from the  $E$  parameters of **4b** and **4c** (Scheme 2) and the  $N$  and  $s_N$  parameters for the enamides **1b** and **1c** (Table 3) which were derived from the rates of their reactions with benzhydrylium ions (Table 2). The fair agreement between the experimental and the calculated rate constants is a

further argument for the stepwise mechanism of the reactions of the enamides **1** with the iminium ions **4**, where CC bond formation becomes rate determining in the presence of an appropriate base.

It appeared likely, therefore, that in contrast to statements in the literature,<sup>[6b]</sup> MacMillan's imidazolidinones **3b** and **3c** should be able to catalyze the reactions of enamides with  $\alpha,\beta$ -unsaturated aldehydes, if deprotonation of **6** by a base is warranted. In line with this conclusion, we found that **3b,c** (Table 8) do catalyze the reactions of cinnamaldehyde (**2**) with the enamides **1a–c** in 1,2-dichloroethane at room temperature, when CF<sub>3</sub>CO<sub>2</sub>H was used as cocatalyst because then CF<sub>3</sub>CO<sub>2</sub><sup>-</sup> may act as the base. According to Table 8, ketoaldehydes **10** are formed in moderate yields and enantioselectivities under these conditions.

**Table 8.** Reactions of the enamides **1a–c** with cinnamaldehyde (**2**) in the presence of the catalysts **3b,c** using CF<sub>3</sub>CO<sub>2</sub>H as co-catalyst.<sup>[a]</sup>



Enamide	Catalyst	Yield [%] <sup>[b]</sup>	ee [%] <sup>[c]</sup>
<b>1a</b>	<b>3b</b>	73	19
<b>1b</b>	<b>3b</b>	75	13
<b>1c</b>	<b>3b</b>	64	9
<b>1a</b>	<b>3c</b>	63	52
<b>1b</b>	<b>3c</b>	58	50
<b>1c</b>	<b>3c</b>	51	55

<sup>[a]</sup> For the reaction conditions see the Experimental Section 4.2.4. <sup>[b]</sup> Isolated yield of **10** after column chromatography. <sup>[c]</sup> Determined by chiral HPLC. TFA = trifluoroacetic acid, DCE = 1,2-dichloroethane.

The clean second-order kinetics observed for the reactions of benzhydrylium ions with **1** (see above) were surprising in view of the problems encountered in the kinetics of the reactions of the iminium ions **4** with **1b** and **1c**. In order to elucidate whether the adducts **12** (Table 1) are formed by reversible or irreversible reactions, the kinetics of the reaction of (dma)<sub>2</sub>CH<sup>+</sup>BF<sub>4</sub><sup>-</sup> with **1b** was also studied in the presence of variable concentrations of 2,6-lutidine. As the first-order rate constants  $k_{\text{obs}}$  were not affected by the concentration of 2,6-lutidine (Figure 5) and are the same as those observed in the absence of base we can conclude that the first step of the sequence depicted in the reaction scheme of Table 1 is irreversible.

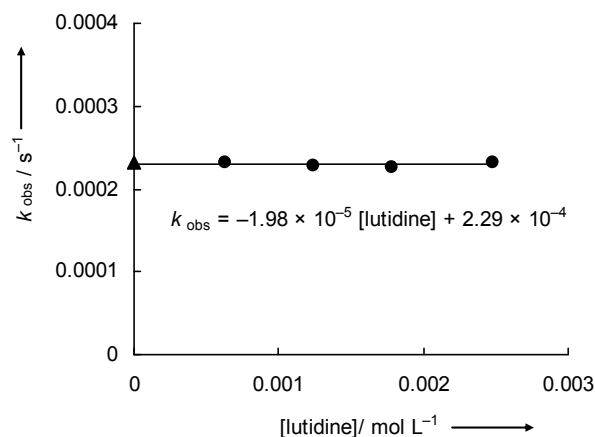


**Figure 5.** Plot of  $k_{\text{obs}}$  vs [lutidine] for the reaction of  $(\text{dma})_2\text{CH}^+\text{BF}_4^-$  ( $1.90 \times 10^{-5}$  M) with **1b** ( $7.41 \times 10^{-4}$  M) at variable concentrations of 2,6-lutidine in  $\text{CH}_3\text{CN}$  at  $20^\circ\text{C}$ . ( $\blacktriangle$ ) Extrapolated from Table 10.

Now, the question arises why benzhydrylium ions **11** react with enamides **1** without a base, while iminium ions **4** of similar electrophilicity (i. e., comparable  $k_2$ ) do not? Obviously, the reverse reactions ( $k_{-2}$ ) are much faster for iminium ions than for the corresponding benzhydrylium ions, with the result that the equilibrium constants  $K = k_2/k_{-2}$  are much smaller for iminium ions than for benzhydrylium ions of similar reactivity ( $k_2$ ). In other words, iminium ions **4** are weaker Lewis acids (i. e., smaller  $K$ ) than benzhydrylium ions of equal electrophilicity (i. e., equal  $k_2$ ).

Deviations from Bronsted correlations or, more general, from rate-equilibrium relationships ( $\log k$  vs  $\log K$ ) have been a topic of intensive research in recent decades. Bernasconi used the term “Nonperfect Synchronization” to account for deviations from nucleophilicity/Lewis basicity or from electrophilicity/Lewis acidity correlations,<sup>[19]</sup> while other authors prefer to discuss these phenomena in terms of Marcus theory,<sup>[20]</sup> which derives the activation free energy of a reaction from a combination of the reaction free energy  $\Delta G^0$  and the intrinsic barriers  $\Delta G_0^\ddagger$  [Equation (5)].

$$\Delta G^\ddagger = \Delta G_0^\ddagger + 0.5 \Delta G^0 + ((\Delta G^0)^2/16 \Delta G_0^\ddagger) \quad (5)$$

As recently discussed in detail,<sup>[21]</sup> the intrinsic barrier corresponds to the barrier of a reaction, from which the thermodynamic component has been eliminated. Since the quadratic term in Eq. (5) is generally negligible in group transfer reactions or electrophile-nucleophile combinations, one can conclude that reactions which proceed slower despite higher thermodynamic driving force (i. e., more negative  $\Delta G^0$ ) react via higher intrinsic barriers

$\Delta G_0^\ddagger$ . Thus, the lower nucleophilicity of DMAP compared with the less basic DABCO has been assigned to the higher intrinsic barriers for the reactions with DMAP.<sup>[22]</sup> A revision of the rationalization of ambident reactivity has recently been based on this concept.<sup>[21]</sup>

According to Marcus, the intrinsic barrier  $\Delta G_0^\ddagger$  is related to the reorganization energy  $\Delta$  ( $= 4\Delta G_0^\ddagger$ ). As less reorganization is required for the addition of a nucleophile to the  $\beta$ -carbon of an  $\alpha,\beta$ -unsaturated iminium ion than to the central carbon of benzhydrylium ions, we have recently explained why additions of azoles to iminium ions are more reversible than comparably fast additions of azoles to benzhydrylium ions.<sup>[23]</sup> The different behavior of benzhydrylium and iminium ions in this work can be explained analogously.

### 3 Conclusion

The reactions of the enamides **1** with benzhydrylium ions have been found to follow the linear-free energy relationship (2) which allowed us to determine nucleophilicity parameters  $4.6 < N < 7.1$  for the enamides **1** and to integrate them into our comprehensive nucleophilicity scale as shown in Figure 6.

Using the rule of thumb that electrophile-nucleophile combinations may take place at room temperature when  $E + N > -5$ <sup>[9c]</sup> one can rationalize that enamides **1** do not react with aldehydes, imines or simple Michael acceptors like benzylidenemalonates in the absence of catalysts.<sup>[24]</sup> Reactions with electrophiles in the presence of either Lewis<sup>[2]</sup> or Brønsted acid<sup>[3]</sup> have been reported, however.

Because of their low Lewis acidity, iminium ions react only with enamides when bases (e.g. 2,6-lutidine) are present, which deprotonate the initially generated acyliminium ions **6**. As bases are not involved in the pericyclic process (a,b,c) of Scheme 1, one can conclude that the amine-catalyzed reactions of enamides with  $\alpha,\beta$ -unsaturated aldehydes do not proceed via concerted ene reactions with the intermediate iminium ions to give **5** directly, but via a stepwise mechanism through the intermediate **6**. By clarifying the role of general base catalysis for the deprotonation of **6**, one can furthermore rationalize, why strong acids such as HOTs are not suitable cocatalysts for the organocatalytic reactions of enamides with  $\alpha,\beta$ -unsaturated aldehydes. The reported failure of MacMillan's 2<sup>nd</sup> generation catalyst **3c** to catalyze the reaction of enamides with  $\alpha,\beta$ -unsaturated aldehydes is, therefore, not due to the nature of **3c**, but can be accounted to the use of HOTs as cocatalyst in the reported experiment. In line with this interpretation, MacMillan's imidazolidines **3b** and **3c** were

found to catalyze the reactions of cinnamaldehyde with the enamides **1a–c** in the presence of  $\text{CF}_3\text{CO}_2\text{H}$  as cocatalyst, though with low enantioselectivity.

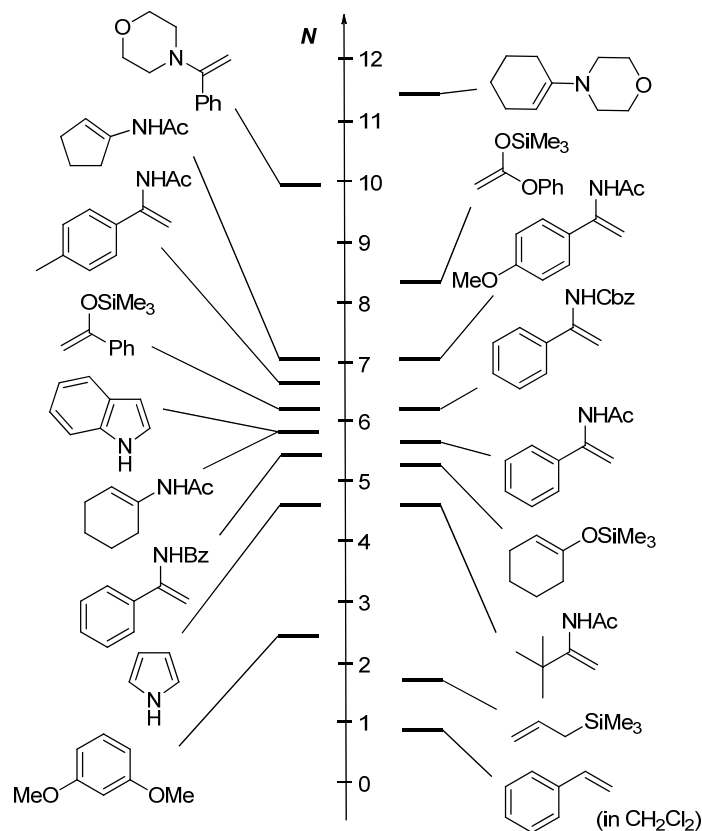


**Figure 6.** Comparison of the nucleophilicities of the enamides **1** with several other C nucleophiles (solvent is  $\text{CH}_3\text{CN}$  unless otherwise mentioned, *N* from ref. [9f]).

## 4 Experimental Section

### 4.1 General

#### Materials

Commercially available acetonitrile (VWR, Prolabo, HPLC-gradient grade and Acros, 99.9%, Extra Dry, AcroSeal) was used as received. Commercially available  $\text{CH}_2\text{Cl}_2$  (VWR) was freshly distilled over  $\text{CaH}_2$  before use.

The benzhydrylium tetrafluoroborates **11**- $\text{BF}_4$  were prepared as described before.<sup>[S1]</sup> Enamides **1** were synthesized by reductive acylation of oximes according to a literature procedure.<sup>[S2]</sup> Iminium salts **4** were generated according to published procedures.<sup>[S3]</sup>

### *Analytatics*

<sup>1</sup>H- and <sup>13</sup>C-NMR spectra were recorded on Varian NMR system (300, 400 or 600 MHz) in CDCl<sub>3</sub>, CD<sub>3</sub>CN, and d<sub>6</sub>-DMSO and the chemical shifts in ppm refer to the residual solvent signals in CDCl<sub>3</sub> ( $\delta_{\text{H}} = 7.24$ ,  $\delta_{\text{C}} = 77.2$ ), CD<sub>3</sub>CN ( $\delta_{\text{H}} = 1.94$ ,  $\delta_{\text{C}} = 1.4$ ), and d<sub>6</sub>-DMSO ( $\delta_{\text{H}} = 2.50$ ,  $\delta_{\text{C}} = 39.5$ ) as internal standard. The following abbreviations were used for chemical shift multiplicities: br s = broad singlet, s = singlet, d = doublet, t = triplet, q = quartet, m = multiplet. NMR signal assignments and assignment of (*E*)- and (*Z*)-configurations are based on additional 2D-NMR experiments (COSY, NOESY, HSQC, and HMBC).

### *Kinetics*

The rates of all investigated reactions were determined photometrically. The temperature of the solutions during all kinetic studies was kept constant ( $20.0 \pm 0.1^{\circ}\text{C}$ ) by using a circulating bath thermostat. The kinetic experiments with enamides **1** were carried out with freshly prepared stock solutions of the enamides in CH<sub>3</sub>CN or CH<sub>2</sub>Cl<sub>2</sub>. The electrophiles **11**, **4**, **15** and **17** (also prepared as stock solutions in CH<sub>3</sub>CN or in CH<sub>2</sub>Cl<sub>2</sub>) were always employed as minor component in the reactions with the nucleophiles, resulting in first-order kinetics.

The rates of slow reactions ( $\tau_{1/2} > 15\text{--}20$  s) were determined by using a J&M TIDAS diode array spectrophotometer controlled by Labcontrol Spectacle software and connected to a Hellma 661.502-QX quartz Suprasil immersion probe (5 mm light path) via fiber optic cables and standard SMA connectors.

For the evaluation of fast kinetics ( $\tau_{1/2} < 20$  s) the stopped-flow spectrophotometer systems Hi-Tech SF-61DX2 or Applied Photophysics SX.18MV-R stopped-flow reaction analyser were used.

Rate constants  $k_{\text{obs}}$  (s<sup>-1</sup>) were obtained by fitting the single exponential  $A_t = A_0 \exp(-k_{\text{obs}}t) + C$  (exponential decrease) to the observed time-dependent absorbance (averaged from at least 5 kinetic runs for each nucleophile concentration in case of stopped-flow methodology).

## **4.2 Reaction Products**

### **4.2.1 Reactions of Enamides **1** with the Benzhydrylium Ion (dma)<sub>2</sub>CH<sup>+</sup>BF<sub>4</sub><sup>-</sup>.**

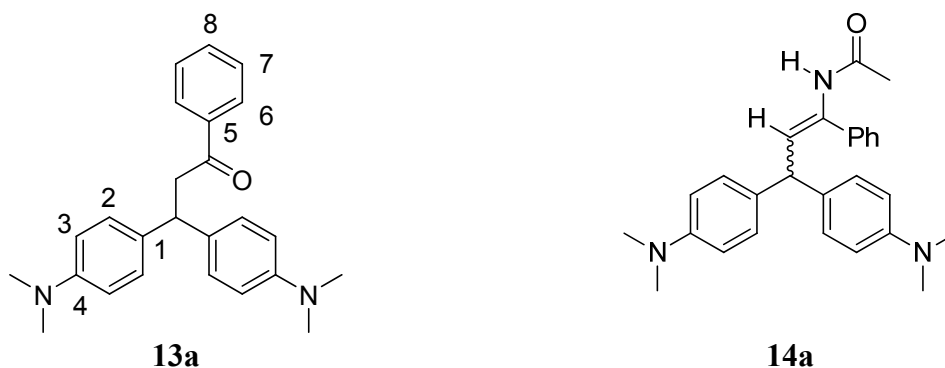
#### **4.2.1.1 General procedure (GP I)**

To a blue CH<sub>3</sub>CN solution of (dma)<sub>2</sub>CH<sup>+</sup>BF<sub>4</sub><sup>-</sup> (48.6 mg, 0.143 mmol) was added a solution of **1** in dry CH<sub>3</sub>CN under nitrogen at room temperature, and the reaction mixture was allowed to stir for 1 h. After adding aqueous K<sub>2</sub>CO<sub>3</sub> the solution was stirred for another hour. The

organic part was extracted with  $\text{CH}_2\text{Cl}_2$  and dried over anhydrous  $\text{Na}_2\text{SO}_4$ . Flash chromatographic separation using ethylacetate and *n*-pentane as eluent yielded **13** and **14**.

*Reaction of 1a with  $(\text{dma})_2\text{CH}^+\text{BF}_4^-$*

According to the GP I from **1a** (23.0 mg, 0.143 mmol) and  $(\text{dma})_2\text{CH}^+\text{BF}_4^-$  (48.6 mg, 0.143 mmol): **13a** (12 mg, 32  $\mu\text{mol}$ , 22 %) and **14a** (37 mg, 89  $\mu\text{mol}$ , 62%, *E:Z* = 4:1).

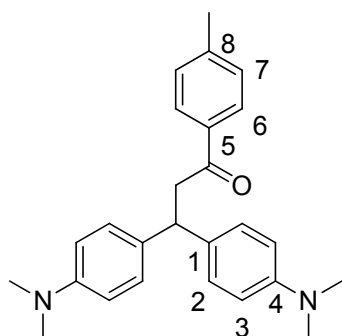


*3,3-Bis(4-(dimethylamino)phenyl)-1-phenylpropan-1-one (13a)*:  $^1\text{H-NMR}$  ( $\text{CDCl}_3$ , 400 MHz):  $\delta$  = 2.86 (s, 12 H,  $\text{N}(\text{CH}_3)_2$ ), 3.63 (d,  $J$  = 7.4 Hz, 2 H,  $\text{CH}_2$ ), 4.62 (t,  $J$  = 7.4 Hz, 1 H,  $\text{Ar}_2\text{CH}$ ), 6.63 (d,  $J$  = 8.7 Hz, 4 H, 3-H), 7.10 (d,  $J$  = 8.7 Hz, 4 H, 2-H), 7.39-7.43 (m, 2 H, 7-H), 7.49-7.53 (m, 1 H, 8-H), 7.90-7.92 (m, 2 H, 6-H) ppm.  $^{13}\text{C-NMR}$  ( $\text{CDCl}_3$ , 100 MHz):  $\delta$  = 41.0 (q,  $\text{N}(\text{CH}_3)_2$ ), 44.4 (t,  $\text{CH}_2$ ), 45.6 (d,  $\text{Ar}_2\text{CH}$ ), 113.1 (d, C-2), 128.3 (d, C-6), 128.5 (d, C-3), 128.7 (d, C-7), 133.0 (d, C-8), 133.3 (s, C-1), 137.6 (s, C-5), 149.3 (s, C-4), 199.0 (s, C=O) ppm. HRMS (ESI):  $[\text{M}+\text{H}]^+$  calculated for  $\text{C}_{25}\text{H}_{29}\text{N}_2\text{O}^+$ : 373.2274, found: 373.2275;  $[\text{M}+\text{Na}]^+$  calculated for  $\text{C}_{25}\text{H}_{28}\text{N}_2\text{ONa}^+$ : 395.2094, found: 395.2095.

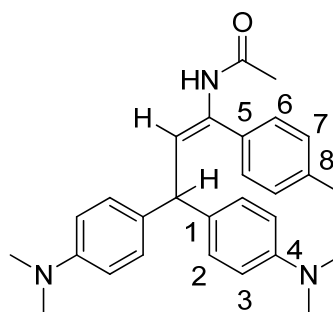
*N-(3,3-Bis(4-(dimethylamino)phenyl)-1-phenylprop-1-enyl)acetamide (14a)*:  $^1\text{H-NMR}$  ( $\text{DMSO-d}_6$ , 400 MHz):  $\delta$  = 1.91\* (s, 3 H,  $\text{CH}_3$ ), 2.01\*\* (s, 3 H,  $\text{CH}_3$ ), 2.83 (2s, 12 H + 12 H,  $\text{N}(\text{CH}_3)_2$ ), 4.38\* (d,  $J$  = 11.1 Hz, 1 H,  $(\text{Ar})_2\text{CH}$ ), 4.83\*\* (d,  $J$  = 10.2 Hz, 1 H,  $(\text{Ar})_2\text{CH}$ ), 6.31\*\* (d,  $J$  = 10.2 Hz, 1 H  $\text{CH}=\text{C-NH}$ ), 6.53\* (d,  $J$  = 11.1, 1 H  $\text{CH}=\text{C-NH}$ ), 6.54 (2d, 4 H + 4 H, Ar), 6.90\* (d,  $J$  = 8.7 Hz, 4 H, Ar), 7.06 (d,  $J$  = 8.7 Hz, 4 H, Ar), 7.22-7.23\* (m, 2 H, Ar), 7.32-7.41 (m, 3 H + 5 H, Ar), 9.20\* (s, 1 H, N-H), 9.23\*\* (s, 1 H, N-H) ppm.  $^{13}\text{C-NMR}$  ( $\text{DMSO-d}_6$ , 100 MHz):  $\delta$  = 22.7\*\* (q,  $\text{COCH}_3$ ), 23.6\* (q,  $\text{COCH}_3$ ), 40.30\* (q,  $\text{N}(\text{CH}_3)_2$ ), 40.35\*\* (q,  $\text{N}(\text{CH}_3)_2$ ), 46.4\*\* (d,  $(\text{Ar})_2\text{CH}$ ), 46.8\* (d,  $(\text{Ar})_2\text{CH}$ ), 112.56\*\* (d, Ar), 112.63\* (d, Ar), 121.4\* (d,  $\text{HC}=\text{CN}$ ), 125.2, 127.2, 127.8, 128.07, 128.13, 128.42, 128.48, 132.3, 132.7, 133.2, 133.4, 136.7, 138.5, 148.8, 148.9, 168.4\* (s, C=O), 168.5\*\* (s, C=O) ppm. HRMS (ESI):  $[\text{M}+\text{H}]^+$  calculated for  $\text{C}_{27}\text{H}_{32}\text{N}_3\text{O}^+$ : 414.2540, found: 414.2541;  $[\text{M}+\text{Na}]^+$  calculated for  $\text{C}_{27}\text{H}_{31}\text{N}_3\text{ONa}^+$ : 436.2359, found: 436.2360. \* Can be assigned to the major isomer, \*\* can be assigned to the minor isomer, and the rest could not be assigned.

Reaction of **1b** with  $(dma)_2CH^+BF_4^-$

According to the GP I from **1b** (26 mg, 0.15 mmol) and  $(dma)_2CH^+BF_4^-$  (48.6 mg, 0.143 mmol): **13b** (17 mg, 44  $\mu$ mol, 31%) and **14b** (32 mg, 75  $\mu$ mol, 52%, *E:Z*  $\approx$  3:1).



**13b**



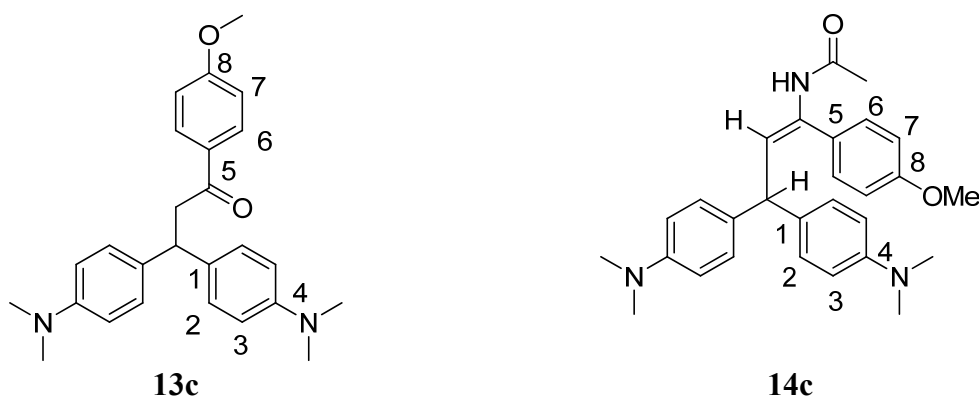
**14b**

*3,3-Bis(4-(dimethylamino)phenyl)-1-p-tolylpropan-1-one (13b)*:  $^1H$ -NMR ( $CD_3CN$ , 400 MHz):  $\delta$  = 2.38 (s, 3 H,  $CH_3$ ), 2.83 (s, 12 H,  $N(CH_3)_2$ ), 3.65 (d,  $J$  = 7.6 Hz, 2 H,  $CH_2$ ), 4.47 (t,  $J$  = 7.6 Hz, 1 H,  $Ar_2CH$ ), 6.64 (d,  $J$  = 8.7 Hz, 4 H, 3-H), 7.10 (d,  $J$  = 8.7 Hz, 4 H, 2-H), 7.28 (d, 8.4 Hz, 2 H, 6-H), 7.86 (d,  $J$  = 8.4 Hz, 2 H, 7-H) ppm.  $^{13}C$ -NMR ( $CD_3CN$ , 100 MHz):  $\delta$  = 21.7 (q,  $CH_3$ ), 41.0 (q,  $N(CH_3)_2$ ), 45.0 (t,  $CH_2$ ), 45.6 (d,  $Ar_2CH$ ), 113.8 (d, C-3), 129.1 (d, C-2), 129.2 (d, C-7), 130.3 (d, C-6), 134.5 (s, C-1), 135.9 (s, C-5), 145.0 (s, C-8), 150.4 (s, C-4), 199.3 (s, C=O) ppm. HRMS (ESI):  $[M+H]^+$  calculated for  $C_{26}H_{31}N_2O^+$ : 387.2431, found: 387.2430;  $[M+Na]^+$  calculated for  $C_{26}H_{30}N_2ONa^+$ : 409.2250, found: 409.2251.

*N-(3,3-Bis(4-(dimethylamino)phenyl)-1-p-tolylprop-1-enyl)acetamide (14b)*:  $^1H$ -NMR ( $CD_3CN$ , 400 MHz):  $\delta$  = 1.92\* (s, overlapped with solvent signal,  $COCH_3$ ), 2.00\*\* (s, 3 H,  $COCH_3$ ), 2.31\*\* (s, 3 H,  $C_6H_4-CH_3$ ), 2.35\* (s, 3 H,  $C_6H_4-CH_3$ ), 2.85, 2.86 (2 s, 12 H + 12 H,  $N(CH_3)_2$ ), 4.47\* (d,  $J$  = 11.0 Hz, 1 H,  $(Ar)_2CH$ ), 4.87\*\* (d,  $J$  = 9.9 Hz, 1 H,  $(Ar)_2CH$ ), 6.25\*\* (d,  $J$  = 9.9 Hz, 1 H,  $CH=C-N$ ), 6.58\* (d,  $J$  = 11.0 Hz, 1 H,  $CH=C-N$ ), 6.65-6.71 (m, 4 H + 4 H, 3-H), 6.96\* (d,  $J$  = 8.5 Hz, 4 H, 6-H), 7.07-7.20 (m, 10 H, Ar), 7.31 (d,  $J$  = 8.2 Hz, 2 H, 7-H), 7.57\* (brs, 1 H, NH), 7.61\*\* (brs, 1 H, NH) ppm.  $^{13}C$ -NMR ( $CD_3CN$ , 100 MHz):  $\delta$  = 21.2\*\* (q,  $C_6H_4-CH_3$ ), 21.4\* (q,  $C_6H_4-CH_3$ ), 23.3\*\* (q,  $COCH_3$ ), 24.2\* (q,  $COCH_3$ ), 41.1 (q,  $N(CH_3)_2$ ), 48.0\*\* (d,  $Ar_2CH$ ), 48.4\* (d,  $Ar_2CH$ ), 113.87\*\* (d, C-3), 113.88\* (d, C-3), 122.5\* (d,  $N-C=CH$ ), 126.5 (d, Ar), 128.6\*\* (d,  $N-C=CH$ ), 129.1 (d, Ar), 129.4\* (d, C-2), 129.6\*\* (d, C-2), 129.85 (d, Ar), 129.91 (d, Ar), 133.8 (s, 1-C), 134.5 (s), 134.71 (s), 134.76 (s), 135.0 (s), 136.9 (s, C-5), 138.4\*\* (s, C-8), 138.9\* (s, C-8), 150.4\* (s, C-4), 150.5\*\* (s, C-4), 169.8\* (s, C=O), 169.9\*\* (s, C=O) ppm. \* Can be assigned to the major isomer, \*\* can be assigned to the minor isomer, and the rest could not be assigned. HRMS (ESI): Calculated for  $C_{28}H_{34}N_3O^+$   $[M + H^+]$ : 428.2696, found: 428.2698.

Reaction of **1c** with  $(dma)_2CH^+BF_4^-$

According to the GP I from **1c** (29 mg, 0.15 mmol) and  $(dma)_2CH^+BF_4^-$  (48.6 mg, 0.143 mmol): **13c** (17 mg, 42  $\mu$ mol, 29%) and **14c** (41 mg, 92  $\mu$ mol, 64%, *E:Z*  $\approx$  1.1:1).



**13c**: *3,3-Bis(4-(dimethylamino)phenyl)-1-(4-methoxyphenyl)propan-1-one* (**13c**):  $^1H$ -NMR ( $CDCl_3$ , 400 MHz):  $\delta$  = 2.86 (s, 12 H,  $N(CH_3)_2$ ), 3.57 (d,  $J$  = 7.4 Hz, 2 H,  $CH_2$ ), 3.83 (s, 3 H,  $OCH_3$ ), 4.62 (t,  $J$  = 7.4 Hz, 1 H,  $Ar_2CH$ ), 6.63 (d,  $J$  = 8.7 Hz, 4 H, 3-H), 6.88 (d,  $J$  = 8.9 Hz, 2 H, 7-H), 7.09 (d,  $J$  = 8.7 Hz, 4 H, 2-H), 7.90 (d,  $J$  = 8.9 Hz, 2 H, 6-H) ppm.  $^{13}C$ -NMR ( $CDCl_3$ , 100 MHz):  $\delta$  = 41.0 (q,  $N(CH_3)_2$ ), 44.6 (d,  $Ar_2CH$ ), 45.2 (t,  $CH_2$ ), 55.6 (q,  $OCH_3$ ), 113.1 (d, C-3), 113.8 (d, C-7), 128.6 (d, C-2), 130.6 (d, C-6), 130.7 (s, C-5), 133.5 (s, C-1), 149.2 (s, C-4), 163.5 (s, C-8), 197.5 (s, C=O) ppm. HRMS (ESI):  $[M+H]^+$  calculated for  $C_{26}H_{31}N_2O_2^+$ : 403.2380, found: 403.2377.

**14c**: *N-(3,3-Bis(4-(dimethylamino)phenyl)-1-(4-methoxyphenyl)prop-1-enyl)acetamide* (**14c**):  $^1H$ -NMR ( $CD_3CN$ , 400 MHz):  $\delta$  = 1.92\* (s, 3 H,  $COCH_3$ ), 2.00\*\* (s, 3 H,  $COCH_3$ ), 2.85\*, 2.86\*\* (2s, 12 H + 12 H,  $N(CH_3)_2$ ), 3.77\*\* (s, 3H,  $OCH_3$ ), 3.79\* (s, 3H,  $OCH_3$ ), 4.47\* (d,  $J$  = 11.0 Hz, 1 H, ( $Ar$ ) $_2CH$ ), 4.85\*\* (d,  $J$  = 9.9 Hz, 1 H, ( $Ar$ ) $_2CH$ ), 6.20\*\* (d,  $J$  = 9.9 Hz, 1 H,  $CH=C-N$ ), 6.56\* (d,  $J$  = 11.0 Hz, 1 H,  $CH=C-N$ ), 6.65-6.71 (m, 4 H + 4 H, 3-H), 6.86\*\* (d,  $J$  = 8.9 Hz, 2 H, 6-H), 6.90\* (d,  $J$  = 8.9 Hz, 2 H, 6-H), 6.96\* (d,  $J$  = 8.5 Hz, 4 H, 2-H), 7.08\*\* (d,  $J$  = 8.6 Hz, 4 H, 2-H), 7.20\* (d,  $J$  = 8.9 Hz, 2 H, 7-H), 7.35\*\* (d,  $J$  = 8.9 Hz, 2 H, 7-H), 7.55\* (brs, 1 H,  $NH$ ), 7.59\*\* (brs, 1 H,  $NH$ ) ppm.  $^{13}C$ -NMR ( $CD_3CN$ , 100 MHz):  $\delta$  = 23.3 (q,  $COCH_3$ ), 24.2 (q,  $COCH_3$ ), 41.1 (q,  $N(CH_3)_2$ ), 48.0\*\* (d,  $Ar_2CH$ ), 48.5\* (d,  $Ar_2CH$ ), 56.01\*\* (q,  $OCH_3$ ), 56.03\* (q,  $OCH_3$ ), 113.86\*\* (d, C-3), 113.88\* (d, C-3), 114.5\* (d, C-6), 114.6\*\* (d, C-6), 122.3\* (d,  $N-C=CH$ ), 127.7\*\* (d, C-7), 127.8\*\* (d,  $N-C=CH$ ), 129.4\* (d, C-2), 129.6\*\* (d, C-2), 130.2\* (s, C-5), 131.0\* (d, C-7), 132.1\*\* (s, C-5), 133.9\* (s, C-1), 134.1 (s,  $N-C=CH$ ), 134.4 (s,  $N-C=CH$ ), 134.9\*\* (s, C-1), 150.4 (s, C-4), 150.5 (s, C-4), 160.4 (s, C-8), 160.5 (s, C-8), 169.7 (s, C=O), 169.9 (s, C=O) ppm. \* Can be assigned to the major

isomer, \*\* can be assigned to the minor isomer, and the rest could not be assigned. HRMS (EI):  $[M]^+$  Calculated for  $C_{28}H_{33}N_3O_2^+$  is 443.2567, found: 443.2567.

#### 4.2.1.2 General procedure (GP II)

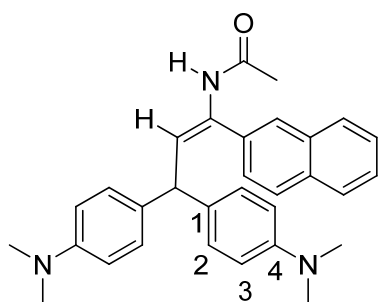
To a blue solution of  $(dma)_2CH^+BF_4^-$  (32 mg, 94  $\mu$ mol) in dry  $CH_3CN$  (1 mL) was added a solution of the enamide **1** in  $CH_3CN$  (1 mL) under nitrogen and the mixture was allowed to stir for approximately 1 h. Then 2,6-lutidine (20 mg, 0.19 mmol) was added, and the mixture was stirred for another 30 min before the solvent was removed by evaporation. The crude mixture was dissolved in  $CH_2Cl_2$ , washed with water, and dried over  $Na_2SO_4$ . The crude product was purified by flash chromatographic separation on silica gel using ethyl acetate and *n*-pentane as eluent to yield the products **14**.

*N*-(3,3-Bis(4-(dimethylamino)phenyl)-1-phenylprop-1-enyl)acetamide (**14a**): According to the GP II from **1a** (18 mg, 0.11 mmol) and  $(dma)_2CH^+BF_4^-$  (32 mg, 94  $\mu$ mol): 37 mg (89  $\mu$ mol, 95%) as a 3.5:1-mixture of *E/Z* isomers. Spectroscopic data are the same as above.

*N*-(3,3-Bis(4-(dimethylamino)phenyl)-1-*p*-tolylprop-1-enyl)acetamide (**14b**): According to the GP II from **1b** (20 mg, 0.11 mmol) and  $(dma)_2CH^+BF_4^-$  (34 mg, 0.10 mmol): 38 mg (89  $\mu$ mol, 89%) as a 3:1-mixture of *E/Z* isomers. Spectroscopic data are the same as above.

*N*-(3,3-Bis(4-(dimethylamino)phenyl)-1-(4-methoxyphenyl)prop-1-enyl)acetamide (**14c**): According to the GP II from **1c** (21 mg, 0.11 mmol) and  $(dma)_2CH^+BF_4^-$  (32 mg, 94  $\mu$ mol): 38 mg (85  $\mu$ mol, 90%) as a 1.1:1-mixture of *E/Z* isomers. Spectroscopic data are the same as above.

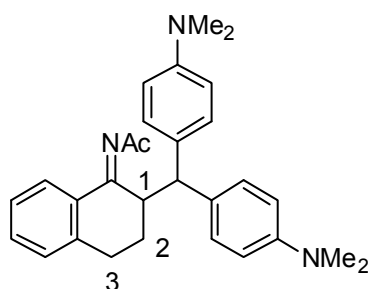
(*E*)-*N*-(3,3-Bis(4-(dimethylamino)phenyl)-1-(naphthalen-2-yl)prop-1-enyl)acetamide (**14g**):



According to the GP II from **1g** (24 mg, 0.11 mmol) and  $(dma)_2CH^+BF_4^-$  (32 mg, 94  $\mu$ mol): 39 mg (84  $\mu$ mol, 89%), pure (*E*)-isomer.  $^1H$ -NMR ( $d_6$ -DMSO, 400 MHz):  $\delta$  = 1.94 (s, 3 H, COCH<sub>3</sub>), 2.83 (s, 12 H, N(CH<sub>3</sub>)<sub>2</sub>), 4.46 (d,  $J$  = 11.1 Hz, 1 H, Ar<sub>2</sub>CH), 6.59 (d,  $J$  = 11.1 Hz, 1 H, CH=C-N), 6.65 (d,  $J$  = 8.8 Hz, 4 H, 3-H), 6.94 (d,  $J$  = 8.8 Hz, 4 H, 2-H), 7.36 (dd,  $J$  = 1.6 Hz, 8.4 Hz, 1 H, Ar), 7.52-7.54 (m, 2 H, Ar), 7.75 (s, 1 H, Ar), 7.84-7.87 (m, 1 H, Ar), 7.90-7.94 (m, 2 H, Ar), 9.35 (s, 1 H, NH) ppm.  $^{13}C$ -NMR ( $d_6$ -DMSO, 100 MHz):  $\delta$  =

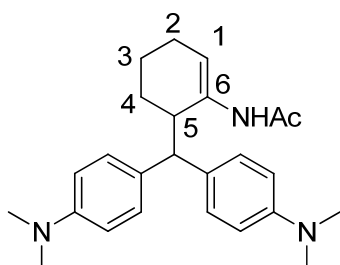
23.6 (q, COCH<sub>3</sub>), 40.3 (q, N(CH<sub>3</sub>)<sub>2</sub>), 46.9 (d, (Ar)<sub>2</sub>CH), 112.6 (d, C-3), 122.0 (d, NC=CH), 126.2 (d, Ar), 126.3 (d, Ar), 126.6 (d, Ar), 127.2 (d, Ar), 127.4 (d, Ar), 127.5 (d, Ar), 127.9 (d, Ar), 128.1 (d, C-2), 132.4 (s, Ar), 132.5 (s, Ar), 133.2 (s, Ar), 133.4 (s, C-1), 134.2 (s, NC=CH), 148.8 (s, C-4), 168.4 (s, C=O) ppm. HRMS (ESI): [M+H]<sup>+</sup> calculated for C<sub>31</sub>H<sub>34</sub>N<sub>3</sub>O<sup>+</sup>: 464.2696, found: 464.2695; [M+Na]<sup>+</sup> calculated for C<sub>31</sub>H<sub>34</sub>N<sub>3</sub>ONa<sup>+</sup>: 486.2516, found: 486.2516.

*N*-(2-(Bis(4-(dimethylamino)phenyl)methyl)-3,4-dihydronaphthalen-1(2H)-ylidene)acetamide (**14h**): According to the GP II from **1h** (21 mg, 0.11 mmol) and (dma)<sub>2</sub>CH<sup>+</sup>BF<sub>4</sub><sup>-</sup> (32 mg, 94



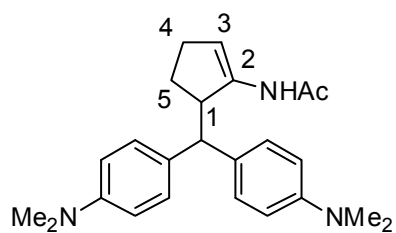
μmol): 32 mg (73 μmol, 78%). <sup>1</sup>H-NMR (CDCl<sub>3</sub>, 599 MHz): δ = 1.33 (s, 3 H, COCH<sub>3</sub>), 2.08-2.17 (m, 2 H, 3-H), 2.63-2.66 (m, 1 H, 2-H), 2.81 (s, 6 H, N(CH<sub>3</sub>)<sub>2</sub>), 2.91 (s, 6 H, N(CH<sub>3</sub>)<sub>2</sub>), 2.93-3.02 (m, 1 H, 2-H), 3.68 (dt, *J* = 3.2 Hz, 12.0 Hz, 1 H, 1-H), 3.92 (d, *J* = 12.0 Hz, 1 H, Ar<sub>2</sub>CH), 6.55 (d, *J* = 8.8 Hz, 2 H, Ar), 6.69 (d, *J* = 8.7 Hz, 2 H, Ar), 6.83 (d, *J* = 8.8 Hz, 2 H, Ar), 7.17 (d, *J* = 8.7 Hz, 2 H, Ar), 7.19 (d, *J* = 7.7 Hz, 1 H, Ar), 7.29 (t, *J* = 7.5 Hz, 1 H, Ar), 7.42 (td, *J* = 1.0 Hz, 7.5 Hz, 1 H, Ar), 7.88 (dd, *J* = 1.0 Hz, 7.8 Hz, 1 H, Ar) ppm. <sup>13</sup>C-NMR (CDCl<sub>3</sub>, 100 MHz): δ = 24.3 (q, COCH<sub>3</sub>), 24.5 (t, C-2), 26.6 (t, C-3), 40.8 (q, N(CH<sub>3</sub>)<sub>2</sub>), 41.0 (q, N(CH<sub>3</sub>)<sub>2</sub>), 44.7 (d, C-1), 49.1 (d, (Ar)<sub>2</sub>CH), 113.0 (d, Ar), 113.4 (d, Ar), 126.8 (d, Ar), 127.7 (d, Ar), 128.9 (d, Ar), 129.1 (d, Ar), 129.2 (d, Ar), 129.7 (s, Ar), 131.6 (d, Ar), 132.0 (s, Ar), 132.9 (s, Ar), 141.3 (s, Ar), 149.4 (s, Ar), 149.7 (s, Ar), 168.0 (s, C=NAc), 186.3 (s, C=O) ppm. HRMS (ESI): [M+H]<sup>+</sup> calculated for C<sub>29</sub>H<sub>34</sub>N<sub>3</sub>O<sup>+</sup>: 440.2696, found: 440.2702.

*N*-(6-(Bis(4-(dimethylamino)phenyl)methyl)cyclohex-1-enyl)acetamide (**14i**): According to



the GP II from **1i** (15 mg, 0.11 mmol) and (dma)<sub>2</sub>CH<sup>+</sup>BF<sub>4</sub><sup>-</sup> (32 mg, 94 μmol): 34 mg (87 μmol, 93%). <sup>1</sup>H-NMR (CDCl<sub>3</sub>, 300 MHz): δ = 1.41 (s, 3 H, COCH<sub>3</sub>), 1.53-1.67 (m, 4 H, 4-CH<sub>2</sub> and 2-CH<sub>2</sub>), 2.15 (m, 2 H, 3-CH<sub>2</sub>), 2.75 (m, 1 H, 5-CH), 2.86, 2.88 (2 s, 12 H, 2 × N(CH<sub>3</sub>)<sub>2</sub>), 3.81 (d, *J* = 11.0 Hz, 1 H, Ar<sub>2</sub>CH), 5.42 (s, 1H, N-H), 6.24 (t, *J* = 3.8 Hz, 1 H, 1-CH), 6.67 (m, 4 H, Ar), 7.15 (m, 4 H, Ar) ppm. <sup>13</sup>C-NMR (CDCl<sub>3</sub>, 75 MHz): δ = 17.9 (t, CH<sub>2</sub>), 24.3 (q, COCH<sub>3</sub>), 24.5 (t, C-3), 26.9 (t, CH<sub>2</sub>), 40.9 (q, N(CH<sub>3</sub>)<sub>2</sub>), 41.0 (q, N(CH<sub>3</sub>)<sub>2</sub>), 42.0 (d, C=CH), 54.6 (d, Ar<sub>2</sub>CH), 113.2 (d, Ar), 113.6 (d, Ar), 116.7 (s, NC=CH), 128.7 (d, Ar), 128.9 (s, Ar), 132.0 (s, Ar), 133.1 (s, Ar), 135.2 (s, Ar), 149.2 (s, Ar), 149.7 (s, Ar), 168.1 (s, C=O) ppm.

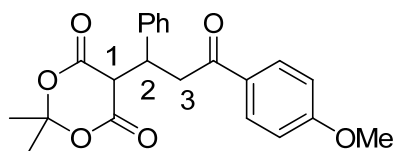
*N*-(5-(Bis(4-(dimethylamino)phenyl)methyl)cyclopent-1-en-1-yl)acetamide (**14j**):



to the GP II from **1j** (22 mg, 0.18 mmol) and (dma)<sub>2</sub>CH<sup>+</sup>BF<sub>4</sub><sup>-</sup> (34 mg, 0.10 mmol): 35 mg (93 μmol, 93%). <sup>1</sup>H-NMR (CD<sub>3</sub>CN, 400 MHz): δ = 1.54 (s, 3 H, COCH<sub>3</sub>), 1.56-1.60 (m, 1 H, 5-CH<sub>2</sub>), 1.89-1.96 (m, 1 H, 5-CH<sub>2</sub>), 2.08-2.13 (m, 2 H, 4-CH<sub>2</sub>), 2.85, 2.86 (2s, 12 H, 2 × N(CH<sub>3</sub>)<sub>2</sub>), 3.44 (m, 1 H, 1-H), 3.76 (d, *J* = 9.2 Hz, 1 H, Ar<sub>2</sub>CH), 5.93 (br s, 1 H, 3-H), 6.52 (br s, 1 H, N-H), 6.66 (d, *J* = 8.8 Hz, 2 H, Ar), 6.73 (d, *J* = 8.8 Hz, 2 H, Ar), 7.09 (d, *J* = 8.8 Hz, 2 H, Ar), 7.17 (d, *J* = 8.8 Hz, 2 H, Ar) ppm. <sup>13</sup>C-NMR (CD<sub>3</sub>CN, 100 MHz): δ = 24.0 (q, COCH<sub>3</sub>), 28.6 (t, C-5), 29.7 (t, C-4), 41.03, 41.05 (2 q, 2 × N(CH<sub>3</sub>)<sub>2</sub>), 50.1 (d, C-1), 54.4 (d, Ar<sub>2</sub>CH), 112.5 (d, C-3), 113.6 (d, Ar), 114.2 (d, Ar), 129.6 (d, Ar), 129.8 (d, Ar), 133.6 (s, Ar), 133.9 (s, Ar), 140.2 (s, C-2), 150.4 (s, Ar), 150.8 (s, Ar), 168.5 (s, C=O) ppm. HRMS (ESI): [M+H]<sup>+</sup> calculated for C<sub>24</sub>H<sub>32</sub>N<sub>3</sub>O<sup>+</sup>: 378.2540, found: 378.2539; [M+Na]<sup>+</sup> calculated for C<sub>24</sub>H<sub>31</sub>N<sub>3</sub>ONa<sup>+</sup>: 400.2359, found: 400.2360.

#### 4.2.2 Reactions of Enamides **1** with 5-Benzylidene-2,2-dimethyl-1,3-dioxane-4,6-dione (**15**)

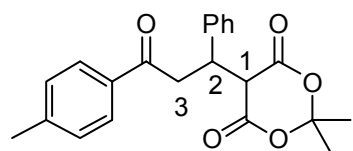
5-(3-(4-Methoxyphenyl)-3-oxo-1-phenylpropyl)-2,2-dimethyl-1,3-dioxane-4,6-dione. To a



CH<sub>3</sub>CN solution of **15** (42.3 mg, 0.182 mmol) was added a solution of the enamide **1c** (53.3 mg, 0.279 mmol) in CH<sub>3</sub>CN under nitrogen. The mixture was allowed to stir at room temperature. The course of the reaction was monitored by TLC on silica gel. After complete conversion of **15**, the solvent was evaporated. Then THF (2 mL) and conc. HCl (0.6 mL) were added to the residue, and the mixture was stirred for 10 min. The reaction was quenched with saturated aq. NaHCO<sub>3</sub>. The organic phase was extracted with dichloromethane, dried over Na<sub>2</sub>SO<sub>4</sub>, and concentrated in the vacuum. The crude product was purified by flash chromatographic separation on silica gel (ethyl acetate/*n*-pentane): 46 mg (0.12 mmol, 66%). <sup>1</sup>H-NMR (CDCl<sub>3</sub>, 600 MHz): δ = 1.33 (s, 3 H, CH<sub>3</sub>), 1.66 (s, 3 H, CH<sub>3</sub>), 3.51 (dd, *J* = 4.8 Hz, 18.2 Hz, 1 H, 3-H), 3.85 (s, 3 H, OCH<sub>3</sub>), 4.21 (dd, *J* = 10.4 Hz, 18.2 Hz, 1 H, 3-H), 4.34 (d, *J* = 3.3 Hz, 1 H, 1-H), 4.44-4.47 (m, 1 H, 2-H), 6.91 (d, *J* = 8.9 Hz, 2 H, Ar), 7.22-7.25 (m, 1 H, Ar), 7.28-7.30 (m, 2 H, Ar), 7.40 (d, *J* = 7.2 Hz, 2 H, Ar), 7.96 (d, *J* = 8.9 Hz, 2 H, Ar) ppm. <sup>13</sup>C-NMR (CDCl<sub>3</sub>, 150 MHz): δ = 28.1 (q, CH<sub>3</sub>), 28.4 (q, CH<sub>3</sub>), 40.3 (d, C-2), 40.5 (t, C-3), 49.6 (d, C-1), 55.7 (q, OCH<sub>3</sub>), 105.4 (s, C(CH<sub>3</sub>)<sub>2</sub>), 114.0 (d, Ar), 127.9 (d, Ar), 129.0 (d, Ar), 129.2 (d, Ar), 130.0 (s, Ar), 130.6 (d, Ar), 140.4 (s, Ar), 164.0 (s, Ar), 165.5 (s,

CH<sub>2</sub>COO), 165.7 (s, CH<sub>2</sub>COO), 197.8 (s, ArCOCH<sub>2</sub>) ppm. HRMS (ESI): [M+H]<sup>+</sup> calculated for C<sub>22</sub>H<sub>23</sub>O<sub>6</sub><sup>+</sup>: 383.1489, found: 383.1488; [M+Na]<sup>+</sup> calculated for C<sub>22</sub>H<sub>22</sub>O<sub>6</sub>Na<sup>+</sup>: 405.1309, found: 405.1308.

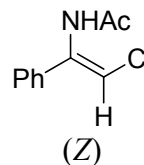
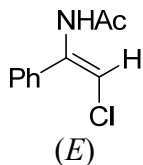
*2,2-Dimethyl-5-(3-oxo-1-phenyl-3-p-tolylpropyl)-1,3-dioxane-4,6-dione*. Obtained from **1b**



(48.9 mg, 0.279 mmol) and **15** (42.3 mg, 0.182 mmol) by following the procedure described above: 30 mg (82 μmol, 45%). <sup>1</sup>H-NMR (CDCl<sub>3</sub>, 400 MHz): δ = 1.35 (s, 3 H, CH<sub>3</sub>), 1.68 (s, 3 H, CH<sub>3</sub>), 2.41 (s, 3 H, CH<sub>3</sub>), 3.56 (dd, *J* = 4.8 Hz, 18.3 Hz, 1 H, 3-H), 4.26 (dd, *J* = 10.4 Hz, 18.3 Hz, 1 H, 3-H), 4.35 (d, *J* = 3.3 Hz, 1 H, 1-H), 4.47-4.50 (m, 1 H, 2-H), 7.25-7.27 (m, 3 H, Ar), 7.30-7.31 (m, 2 H, Ar), 7.42 (d, *J* = 7.3 Hz, 2 H, Ar), 7.90 (d, *J* = 8.3 Hz, 2 H, Ar) ppm. <sup>13</sup>C-NMR (CDCl<sub>3</sub>, 100 MHz): δ = 21.9 (q, CH<sub>3</sub>), 28.1 (q, CH<sub>3</sub>), 28.4 (q, CH<sub>3</sub>), 40.2 (d, C-2), 40.8 (t, C-3), 49.6 (d, C-1), 105.4 (s, C(CH<sub>3</sub>)<sub>2</sub>), 128.0 (d, Ar), 128.4 (d, Ar), 129.0 (d, Ar), 129.2 (d, Ar), 129.5 (d, Ar), 134.4 (s, Ar), 140.3 (s, Ar), 144.5 (s, Ar), 165.5 (s, CH<sub>2</sub>COO), 165.7 (s, CH<sub>2</sub>COO), 198.9 (s, ArCOCH<sub>2</sub>) ppm.

#### 4.2.3 Reactions of Enamides **1** with 2,3,4,5,6,6-Hexachlorocyclohexa-2,4-dienone (**17**)

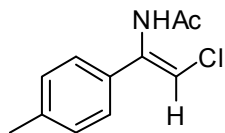
*N*-(2-Chloro-1-phenylvinyl)acetamide. To a CH<sub>3</sub>CN solution of 2,3,4,5,6,6-hexachlorocyclohexa-2,4-dienone (**17**) (75 mg, 0.25 mmol) was added a solution of **1a** (47.9 mg, 0.297 mmol) under nitrogen. The mixture was allowed to stir at room temperature for 40 min. After addition of 0.05 M hydrochloric acid (1 mL) the reaction mixture was stirred for another 10 min. The organic layer was then extracted with dichloromethane, dried (Na<sub>2</sub>SO<sub>4</sub>), and concentrated in the vacuum. The crude product mixture was separated by flash chromatography on neutral alumina (activity IV): 27 mg (12 mg of the (*E*)- + 15 mg of the (*Z*)-isomer, *E*:*Z* = 4:5, 0.14 mmol, 56 %).



(*E*)-Isomer: <sup>1</sup>H-NMR (CD<sub>3</sub>CN, 400 MHz): δ = 1.97 (s, 3 H, COCH<sub>3</sub>), 7.15 (s, 1 H, NC=CHCl), 7.40-7.45 (m, 5 H, Ar), 7.77 (br s, 1 H, N-H) ppm. <sup>13</sup>C-NMR (CD<sub>3</sub>CN, 100 MHz): δ = 23.9 (q, COCH<sub>3</sub>), 108.0 (d, NC=CHCl), 129.4 (d, Ar), 129.95 (d, Ar), 130.04 (d, Ar), 135.7 (s, NC=CHCl), 138.6 (s, Ar), 170.2 (s, C=O) ppm. HRMS (EI): [M]<sup>+</sup> calculated for C<sub>10</sub>H<sub>10</sub>NO<sup>35</sup>Cl<sup>+</sup>: 195.0445, found: 195.0455.

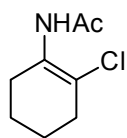
(*Z*)-Isomer:  $^1\text{H-NMR}$  ( $\text{CD}_3\text{CN}$ , 400 MHz):  $\delta = 2.06$  (s, 3 H,  $\text{COCH}_3$ ), 6.30 (s, 1 H,  $\text{NC}=\text{CHCl}$ ), 7.34-7.38 (m, 5 H, Ar), 7.87 (br s, 1 H, N-H) ppm.  $^{13}\text{C-NMR}$  ( $\text{CD}_3\text{CN}$ , 100 MHz):  $\delta = 23.4$  (q,  $\text{COCH}_3$ ), 111.2 (d,  $\text{NC}=\text{CHCl}$ ), 126.9 (d, Ar), 129.5 (d, Ar), 129.6 (d, Ar), 136.8 (s,  $\text{NC}=\text{CHCl}$ ), 139.2 (s, Ar), 169.5 (s,  $\text{C}=\text{O}$ ) ppm.

(*Z*)-*N*-(2-Chloro-1-*p*-tolylvinyl)acetamide. Obtained from **1b** (53 mg, 0.30 mmol) and **17** (75 mg, 0.25 mmol) by following the procedure described above: 23 mg (0.11 mmol, 44%), only (*Z*)-isomer was isolated. Decomposition of the title compound was observed in the NMR tube.

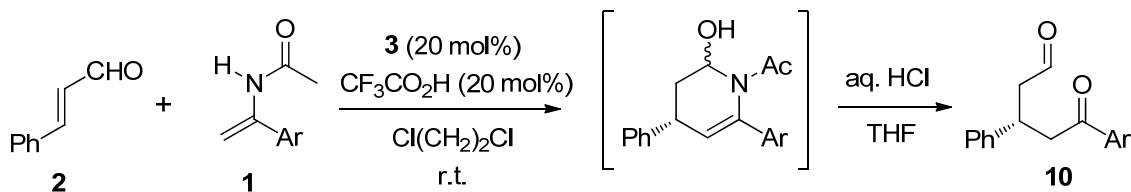


$^1\text{H-NMR}$  ( $\text{CD}_3\text{CN}$ , 400 MHz):  $\delta = 1.97$  (s, 3 H,  $\text{COCH}_3$ ), 2.37 (s, 3 H,  $\text{CH}_3$ ), 7.11 (s, 1 H,  $\text{NC}=\text{CHCl}$ ), 7.24-7.26 (m, 2 H, Ar), 7.34 (d,  $J = 8.1$  Hz, 2 H, Ar), 7.73 (br s, 1 H, N-H) ppm.  $^{13}\text{C-NMR}$  ( $\text{CD}_3\text{CN}$ , 100 MHz):  $\delta = 21.4$  (q,  $\text{CH}_3$ ), 24.0 (q,  $\text{COCH}_3$ ), 107.8 (d,  $\text{NC}=\text{CHCl}$ ), 126.9 (d, Ar), 130.0 (d, Ar), 132.8 (s), 138.5 (s), 140.0 (s), 170.2 (s,  $\text{C}=\text{O}$ ) ppm.

*N*-(2-Chlorocyclohex-1-enyl)acetamide. Obtained from **1b** (42 mg, 0.30 mmol) and **17** (75 mg, 0.25 mmol) by following the procedure described above: 23 mg (0.13 mmol, 52%) as a colorless solid.  $^1\text{H-NMR}$  ( $\text{CDCl}_3$ , 300 MHz):  $\delta = 1.64$ -1.70 (m, 4 H,  $\text{CH}_2$ ), 2.04 (s, 3H,  $\text{COCH}_3$ ), 2.34-2.37 (m, 2 H,  $\text{CH}_2$ ), 2.69 (br s, 2 H,  $\text{CH}_2$ ), 7.03 (br s, 1 H, N-H) ppm.  $^{13}\text{C-NMR}$  ( $\text{CDCl}_3$ , 75 MHz):  $\delta = 22.5$  (t,  $\text{CH}_2$ ), 23.5 (t,  $\text{CH}_2$ ), 24.6 (q,  $\text{COCH}_3$ ), 28.2 (t,  $\text{CH}_2$ ), 32.5 (t,  $\text{CH}_2$ ), 109.0 (s), 131.5 (s), 168.2 (s,  $\text{C}=\text{O}$ ) ppm. HRMS (EI):  $[\text{M}]^+$  calculated for  $\text{C}_8\text{H}_{12}\text{NO}^{35}\text{Cl}^+$ : 173.0602, found: 173.0603.



#### 4.2.4 Organocatalytic Reactions of Enamides **1** with Cinnamaldehyde (**2**)

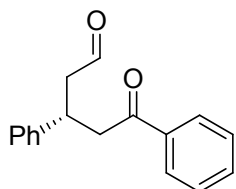


##### General Procedure:

To a 1,2-dichloroethane solution (0.5 mL) of **3**· $\text{CF}_3\text{COOH}$  (0.039 mmol) and **2** (25  $\mu\text{L}$ , 26 mg, 0.20 mmol), a 1,2-dichloroethane solution (0.7 mL) of enamide **1** (0.30 mmol) was added at room temperature under nitrogen, and the reaction mixture was allowed to stir at room temperature. The reaction was monitored by TLC and after complete conversion of the aldehyde **2** (~70 h) the solvent was evaporated. THF (1 mL) and 2 M HCl (0.5 mL) were added to the crude mixture and stirred overnight. The solution was neutralized with saturated

aqueous NaHCO<sub>3</sub>, and the organic part was extracted with ethylacetate and dried over Na<sub>2</sub>SO<sub>4</sub>. Chromatographic separation on silica gel using EtOAc/*n*-pentane as eluant gave the ketoaldehydes **10**. The absolute configurations of **10** were determined by comparing the HPLC chromatogram to those reported in reference [6b,25].

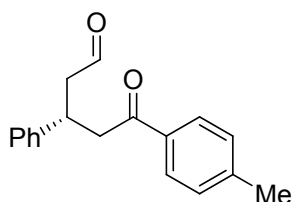
Using catalyst **3b**



*5-Oxo-3,5-diphenylpentanal*: 37 mg (0.15 mmol, 73 %), colorless solid.

Spectroscopic data are in agreement with the literature.<sup>[25]</sup>

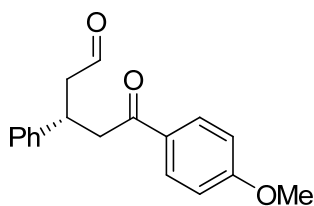
19% *ee*. HPLC condition: Chiralcel AS-H column, isopropanol/hexane 10:90, flow rate 0.95 mL/min, UV detection at 254 nm,  $t_{\text{minor}} = 24.3$  min,  $t_{\text{major}} = 27.0$  min.



*5-Oxo-3-phenyl-5-p-tolylpentanal*: 40 mg (0.15 mmol, 75%), colorless solid.

Spectroscopic data are in agreement with the literature.<sup>[25]</sup>

13% *ee*. HPLC condition: Chiralcel AS-H column, isopropanol/hexane 20:80, flow rate 0.3 mL/min, UV detection at 254 nm,  $t_{\text{minor}} = 50.8$  min,  $t_{\text{major}} = 53.4$  min.

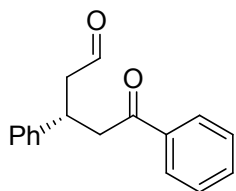


*5-(4-Methoxyphenyl)-5-oxo-3-phenylpentanal*: 36 mg (0.13 mmol, 64%), colorless solid.

Spectroscopic data are in agreement with the literature.<sup>[25]</sup>

10% *ee*. HPLC condition: Chiralcel AS-H column, isopropanol/hexane 20:80, flow rate 0.8 mL/min, UV detection at 254 nm,  $t_{\text{minor}} = 35.4$  min,  $t_{\text{major}} = 38.0$  min.

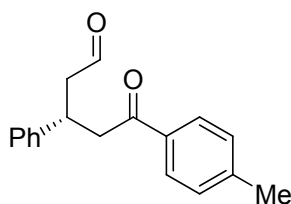
Using catalyst **3c**:



*5-Oxo-3,5-diphenylpentanal*: 32 mg (0.13 mmol, 63 %), colorless solid.

Spectroscopic data are in agreement with the literature.<sup>[25]</sup>

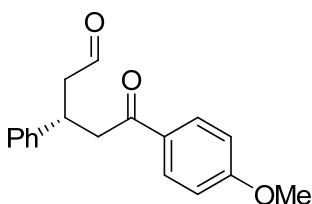
52% *ee*. HPLC condition: Chiralcel AS-H column, isopropanol/hexane 10:90, flow rate 0.95 mL/min, UV detection at 215 nm,  $t_{\text{minor}} = 24.7$  min,  $t_{\text{major}} = 27.4$  min.



*5-Oxo-3-phenyl-5-p-tolylpentanal*: 31 mg (0.12 mmol, 58%), colorless solid.

Spectroscopic data are in agreement with the literature.<sup>[25]</sup>

50% *ee*. HPLC condition: Chiralcel AS-H column, isopropanol/hexane 20:80, flow rate 0.3 mL/min, UV detection at 254 nm,  $t_{\text{minor}} = 51.0$  min,  $t_{\text{major}} = 53.5$  min.



*5-(4-Methoxyphenyl)-5-oxo-3-phenylpentanal*: 29 mg (0.10 mmol, 51%), colorless solid.

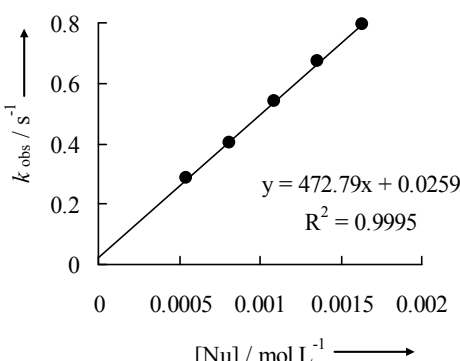
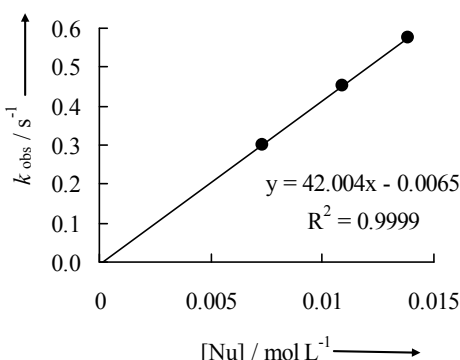
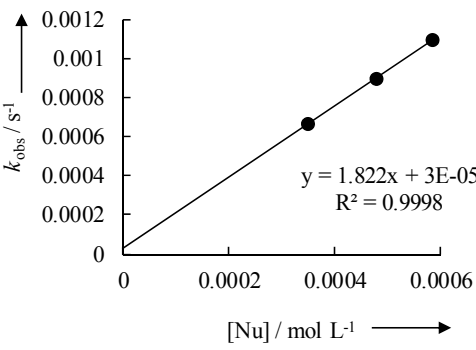
Spectroscopic data are in agreement with the literature.<sup>[25]</sup>

55% *ee*. HPLC condition: Chiralcel AS-H column, isopropanol/hexane 20:80, flow rate 0.8 mL/min, UV detection at 254 nm,  $t_{\text{minor}} = 35.5$  min,  $t_{\text{major}} = 37.8$  min.

### 4.3 Kinetics

#### 4.3.1 Kinetics of the reactions of the enamides **1** with benzhydrylium ions (Ar<sub>2</sub>CH<sup>+</sup>) **11**

**Table 9.** Kinetics of the reactions of *N*-(1-phenylvinyl)acetamide (**1a**) with (Ar)<sub>2</sub>CH<sup>+</sup> in CH<sub>3</sub>CN at 20°C.

[(pfa) <sub>2</sub> CH <sup>+</sup> ] (mol L <sup>-1</sup> )	[Nu] (mol L <sup>-1</sup> )	<i>k</i> <sub>obs</sub> (s <sup>-1</sup> )	λ = 592 nm (Stopped-flow)	<i>k</i> <sub>2</sub> (M <sup>-1</sup> s <sup>-1</sup> )
2.00 × 10 <sup>-5</sup>	5.43 × 10 <sup>-4</sup>	0.285		4.73 × 10 <sup>2</sup>
	8.15 × 10 <sup>-4</sup>	0.404		
	1.09 × 10 <sup>-3</sup>	0.543		
	1.36 × 10 <sup>-3</sup>	0.672		
	1.63 × 10 <sup>-3</sup>	0.794		
[(mfa) <sub>2</sub> CH <sup>+</sup> ] (mol L <sup>-1</sup> )	[Nu] (mol L <sup>-1</sup> )	<i>k</i> <sub>obs</sub> (s <sup>-1</sup> )	λ = 586 nm (Stopped-flow)	<i>k</i> <sub>2</sub> (M <sup>-1</sup> s <sup>-1</sup> )
1.03 × 10 <sup>-5</sup>	7.30 × 10 <sup>-3</sup>	0.301		4.20 × 10 <sup>1</sup>
	1.09 × 10 <sup>-3</sup>	0.452		
	1.39 × 10 <sup>-2</sup>	0.577		
[(mor) <sub>2</sub> CH <sup>+</sup> ] (mol L <sup>-1</sup> )	[Nu] (mol L <sup>-1</sup> )	<i>k</i> <sub>obs</sub> (s <sup>-1</sup> )	λ = 613 nm (diode array)	<i>k</i> <sub>2</sub> (M <sup>-1</sup> s <sup>-1</sup> )
1.57 × 10 <sup>-5</sup>	3.48 × 10 <sup>-4</sup>	6.62 × 10 <sup>-4</sup>		1.82
1.62 × 10 <sup>-5</sup>	4.79 × 10 <sup>-4</sup>	8.95 × 10 <sup>-4</sup>		
1.58 × 10 <sup>-5</sup>	5.85 × 10 <sup>-4</sup>	1.09 × 10 <sup>-3</sup>		

Chapter 9: Nucleophilicity Parameters of Enamides and their Implications for Organocatalytic Transformations

**Table 9** Continued.

Reactivity parameters for *N*-(1-phenylvinyl)acetamide (**1a**) in CH<sub>3</sub>CN

Ar <sub>2</sub> CH <sup>+</sup>	<i>E</i>	<i>k</i> <sub>2</sub> (M <sup>-1</sup> s <sup>-1</sup> )
(pfa) <sub>2</sub> CH <sup>+</sup>	-3.14	4.73 × 10 <sup>2</sup>
(mfa) <sub>2</sub> CH <sup>+</sup>	-3.85	4.20 × 10 <sup>1</sup>
(mor) <sub>2</sub> CH <sup>+</sup>	-5.53	1.82

**Table 10.** Kinetics of the reactions of *N*-(1-*p*-tolylvinyl)acetamide (**1b**) with (Ar)<sub>2</sub>CH<sup>+</sup> in CH<sub>3</sub>CN at 20°C.

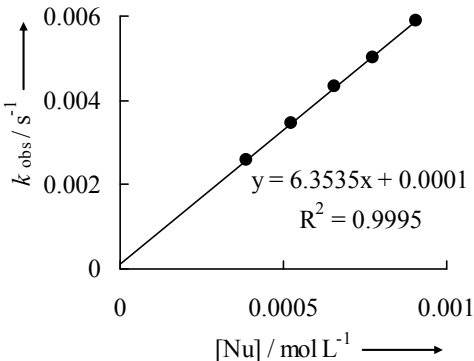
[(pfa) <sub>2</sub> CH <sup>+</sup> ] (mol L <sup>-1</sup> )	[Nu] (mol L <sup>-1</sup> )	<i>k</i> <sub>obs</sub> (s <sup>-1</sup> )	λ = 592 nm (Stopped-flow)	<i>k</i> <sub>2</sub> (M <sup>-1</sup> s <sup>-1</sup> )
1.60 × 10 <sup>-5</sup>	3.23 × 10 <sup>-4</sup>	0.509		1.29 × 10 <sup>3</sup>
	4.85 × 10 <sup>-4</sup>	0.701		
	6.46 × 10 <sup>-4</sup>	0.898		
	8.08 × 10 <sup>-4</sup>	1.118		
	9.69 × 10 <sup>-4</sup>	1.343		

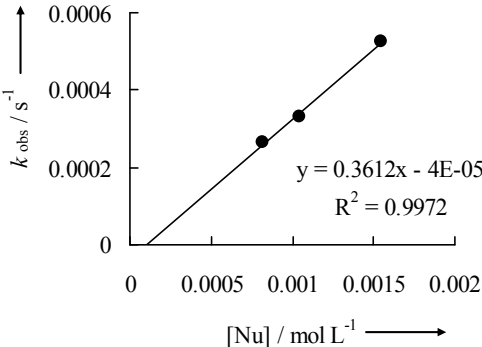
  

[(mor) <sub>2</sub> CH <sup>+</sup> ] (mol L <sup>-1</sup> )	[Nu] (mol L <sup>-1</sup> )	<i>k</i> <sub>obs</sub> (s <sup>-1</sup> )	λ = 613 nm (diode array)	<i>k</i> <sub>2</sub> (M <sup>-1</sup> s <sup>-1</sup> )
2.17 × 10 <sup>-5</sup>	2.92 × 10 <sup>-4</sup>	1.57 × 10 <sup>-3</sup>		6.01
1.94 × 10 <sup>-5</sup>	3.61 × 10 <sup>-4</sup>	2.05 × 10 <sup>-3</sup>		
1.94 × 10 <sup>-5</sup>	4.35 × 10 <sup>-4</sup>	2.46 × 10 <sup>-3</sup>		
1.92 × 10 <sup>-5</sup>	5.74 × 10 <sup>-4</sup>	3.30 × 10 <sup>-3</sup>		
1.92 × 10 <sup>-5</sup>	7.14 × 10 <sup>-4</sup>	4.13 × 10 <sup>-3</sup>		

Chapter 9: Nucleophilicity Parameters of Enamides and their Implications for Organocatalytic Transformations

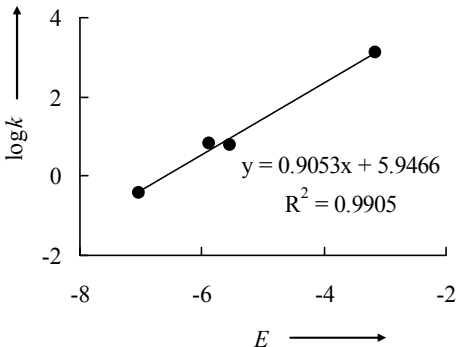
Table 10 Continued.

$[(\text{mpa})_2\text{CH}^+]$ (mol L <sup>-1</sup> )	[Nu] (mol L <sup>-1</sup> )	$k_{\text{obs}}$ (s <sup>-1</sup> )	$\lambda = 613 \text{ nm}$ (diode array)	$k_2$ (M <sup>-1</sup> s <sup>-1</sup> )
$2.26 \times 10^{-5}$	$3.88 \times 10^{-4}$	$2.57 \times 10^{-3}$		6.35
$2.30 \times 10^{-5}$	$5.26 \times 10^{-4}$	$3.45 \times 10^{-3}$		
$2.29 \times 10^{-5}$	$6.56 \times 10^{-4}$	$4.33 \times 10^{-3}$		
$2.26 \times 10^{-5}$	$7.76 \times 10^{-4}$	$5.02 \times 10^{-3}$		
$2.27 \times 10^{-5}$	$9.09 \times 10^{-4}$	$5.88 \times 10^{-3}$		

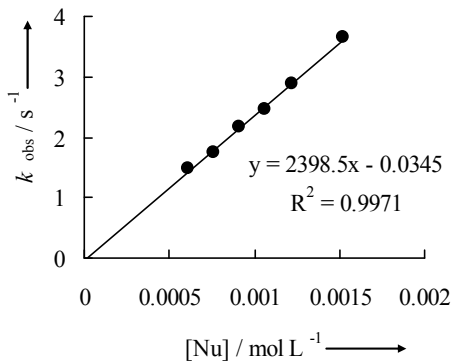
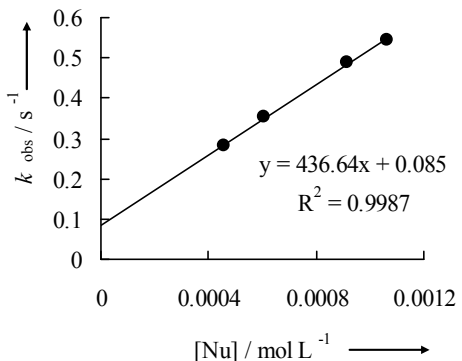
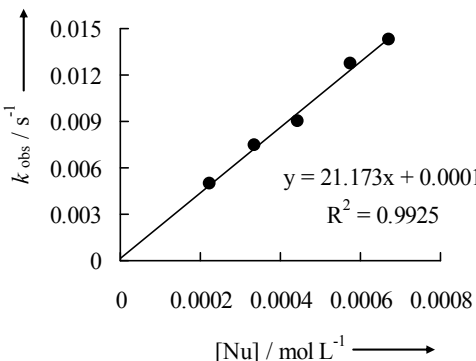
$[(\text{dma})_2\text{CH}^+]$ (mol L <sup>-1</sup> )	[Nu] (mol L <sup>-1</sup> )	$k_{\text{obs}}$ (s <sup>-1</sup> )	$\lambda = 613 \text{ nm}$ (diode array)	$k_2$ (M <sup>-1</sup> s <sup>-1</sup> )
$1.40 \times 10^{-5}$	$8.21 \times 10^{-4}$	$2.64 \times 10^{-4}$		$3.61 \times 10^{-1}$
$1.33 \times 10^{-5}$	$1.04 \times 10^{-3}$	$3.31 \times 10^{-4}$		
$1.32 \times 10^{-5}$	$1.55 \times 10^{-3}$	$5.25 \times 10^{-4}$		

Reactivity parameters for *N*-(1-*p*-tolylvinyl)acetamide (**1b**) in CH<sub>2</sub>Cl<sub>2</sub>

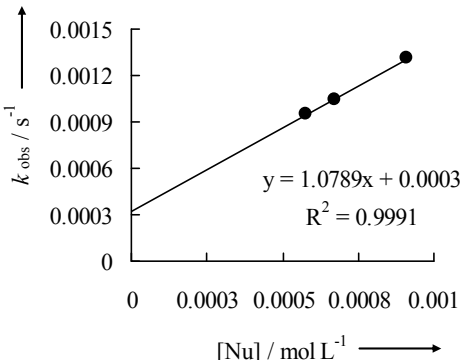
Ar <sub>2</sub> CH <sup>+</sup>	<i>E</i>	$k_2$ (M <sup>-1</sup> s <sup>-1</sup> )	$N = 6.57$ $s = 0.91$
(pfa) <sub>2</sub> CH <sup>+</sup>	-3.14	$1.29 \times 10^3$	
(mor) <sub>2</sub> CH <sup>+</sup>	-5.53	6.01	
(mpa) <sub>2</sub> CH <sup>+</sup>	-5.89	6.35	
(dma) <sub>2</sub> CH <sup>+</sup>	-7.02	$3.61 \times 10^{-1}$	

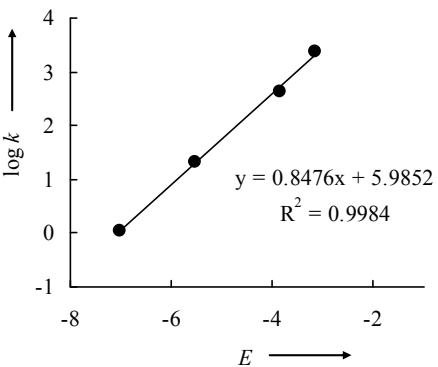
**Table 11.** Kinetics of the reactions of N-(1-(4-methoxyphenyl)vinyl)acetamide (**1c**) with (Ar)<sub>2</sub>CH<sup>+</sup> in CH<sub>3</sub>CN at 20°C.

[(pfa) <sub>2</sub> CH <sup>+</sup> ] (mol L <sup>-1</sup> )	[Nu] (mol L <sup>-1</sup> )	<i>k</i> <sub>obs</sub> (s <sup>-1</sup> )	λ = 592 nm (Stopped-flow)	<i>k</i> <sub>2</sub> (M <sup>-1</sup> s <sup>-1</sup> )
1.70 × 10 <sup>-5</sup>	6.09 × 10 <sup>-4</sup>	1.48		2.40 × 10 <sup>3</sup>
	7.61 × 10 <sup>-4</sup>	1.75		
	9.13 × 10 <sup>-4</sup>	2.18		
	1.07 × 10 <sup>-3</sup>	2.47		
	1.22 × 10 <sup>-3</sup>	2.88		
	1.52 × 10 <sup>-3</sup>	3.65		
[(mfa) <sub>2</sub> CH <sup>+</sup> ] (mol L <sup>-1</sup> )	[Nu] (mol L <sup>-1</sup> )	<i>k</i> <sub>obs</sub> (s <sup>-1</sup> )	λ = 586 nm (Stopped-flow)	<i>k</i> <sub>2</sub> (M <sup>-1</sup> s <sup>-1</sup> )
1.51 × 10 <sup>-5</sup>	4.57 × 10 <sup>-4</sup>	0.282		4.37 × 10 <sup>2</sup>
	6.09 × 10 <sup>-4</sup>	0.352		
	9.13 × 10 <sup>-4</sup>	0.489		
	1.07 × 10 <sup>-3</sup>	0.546		
[(mor) <sub>2</sub> CH <sup>+</sup> ] (mol L <sup>-1</sup> )	[Nu] (mol L <sup>-1</sup> )	<i>k</i> <sub>obs</sub> (s <sup>-1</sup> )	λ = 613 nm (diode array)	<i>k</i> <sub>2</sub> (M <sup>-1</sup> s <sup>-1</sup> )
1.38 × 10 <sup>-5</sup>	4.45 × 10 <sup>-4</sup>	9.04 × 10 <sup>-3</sup>		2.12 × 10 <sup>1</sup>
2.00 × 10 <sup>-5</sup>	3.38 × 10 <sup>-4</sup>	7.42 × 10 <sup>-3</sup>		
2.00 × 10 <sup>-5</sup>	2.26 × 10 <sup>-4</sup>	4.98 × 10 <sup>-3</sup>		
2.05 × 10 <sup>-5</sup>	5.78 × 10 <sup>-4</sup>	1.27 × 10 <sup>-3</sup>		
1.98 × 10 <sup>-5</sup>	6.71 × 10 <sup>-4</sup>	1.42 × 10 <sup>-3</sup>		

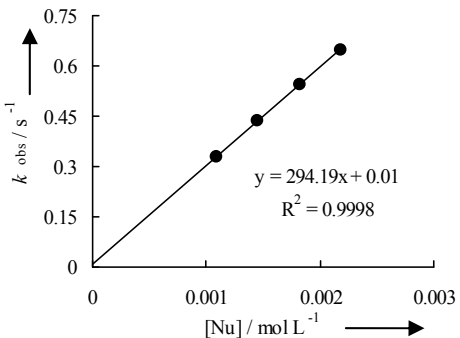
**Table 11** continued

$[(\text{dma})_2\text{CH}^+]$ (mol L <sup>-1</sup> )	$[\text{Nu}]$ (mol L <sup>-1</sup> )	$k_{\text{obs}}$ (s <sup>-1</sup> )	$\lambda = 606 \text{ nm}$ (diode array)	$k_2$ (M <sup>-1</sup> s <sup>-1</sup> )
$1.03 \times 10^{-5}$	$5.74 \times 10^{-4}$	$9.50 \times 10^{-4}$		1.08
$1.21 \times 10^{-5}$	$6.73 \times 10^{-4}$	$1.05 \times 10^{-3}$		
$1.23 \times 10^{-5}$	$9.10 \times 10^{-4}$	$1.31 \times 10^{-3}$		

Reactivity parameters for N-(1-(4-methoxyphenyl)vinyl)acetamide (**1c**) in CH<sub>3</sub>CN

$\text{Ar}_2\text{CH}^+$	$E$	$k_2$ (M <sup>-1</sup> s <sup>-1</sup> )		
$(\text{pfa})_2\text{CH}^+$	-3.14	$2.40 \times 10^3$		<b><math>N = 7.06</math></b> <b><math>s = 0.85</math></b>
$(\text{mfa})_2\text{CH}^+$	-3.85	$4.37 \times 10^2$		
$(\text{mor})_2\text{CH}^+$	-5.53	$2.12 \times 10^1$		
$(\text{dma})_2\text{CH}^+$	-7.02	1.08		

**Table 12.** Kinetics of the reactions of N-(1-(4-chlorophenyl)vinyl)acetamide (**1d**) with  $(\text{Ar})_2\text{CH}^+$  in CH<sub>3</sub>CN at 20°C.

$[(\text{pfa})_2\text{CH}^+]$ (mol L <sup>-1</sup> )	<b>[1d]</b> (mol L <sup>-1</sup> )	$k_{\text{obs}}$ (s <sup>-1</sup> )	$\lambda = 613 \text{ nm}$ (stopped-flow)	$k_2$ (M <sup>-1</sup> s <sup>-1</sup> )
$1.75 \times 10^{-5}$	$1.09 \times 10^{-3}$	0.327		$2.94 \times 10^2$
	$1.46 \times 10^{-3}$	0.437		
	$1.82 \times 10^{-3}$	0.543		
	$2.18 \times 10^{-3}$	0.648		

**Table 12** continued

$[(\text{mor})_2\text{CH}^+]$ (mol L <sup>-1</sup> )	<b>[1d]</b> (mol L <sup>-1</sup> )	$k_{\text{obs}}$ (s <sup>-1</sup> )	$\lambda = 620 \text{ nm}$ (diode array)	$k_2$ (M <sup>-1</sup> s <sup>-1</sup> )
$1.85 \times 10^{-5}$	$5.66 \times 10^{-4}$	$7.57 \times 10^{-4}$		1.19
$1.90 \times 10^{-5}$	$8.71 \times 10^{-4}$	$1.12 \times 10^{-3}$		
$1.85 \times 10^{-5}$	$9.90 \times 10^{-4}$	$1.27 \times 10^{-3}$		
$1.85 \times 10^{-5}$	$1.41 \times 10^{-3}$	$1.76 \times 10^{-3}$		

Reactivity parameters for N-(1-(4-chlorophenyl)vinyl)acetamide (**1d**) in CH<sub>3</sub>CN

Ar <sub>2</sub> CH <sup>+</sup>	<i>E</i>	$k_2$ (M <sup>-1</sup> s <sup>-1</sup> )	<i>N</i> = 5.60 <i>s</i> = 1.00
(pfa) <sub>2</sub> CH <sup>+</sup>	-3.14	$3.04 \times 10^2$	
(mor) <sub>2</sub> CH <sup>+</sup>	-5.53	1.19	

**Table 13.** Kinetics of the reactions of benzyl 1-phenylvinylcarbamate (**1e**) with (Ar)<sub>2</sub>CH<sup>+</sup> in CH<sub>3</sub>CN at 20°C.

$[(\text{pfa})_2\text{CH}^+]$ (mol L <sup>-1</sup> )	[Nu] (mol L <sup>-1</sup> )	$k_{\text{obs}}$ (s <sup>-1</sup> )	$\lambda = 592 \text{ nm}$ (stopped-flow)	$k_2$ (M <sup>-1</sup> s <sup>-1</sup> )
$1.35 \times 10^{-5}$	$1.97 \times 10^{-4}$	$7.30 \times 10^{-2}$		$4.53 \times 10^2$
	$2.95 \times 10^{-4}$	0.130		
	$3.94 \times 10^{-4}$	0.149		
	$4.92 \times 10^{-4}$	0.218		
	$7.88 \times 10^{-4}$	0.347		
	$9.85 \times 10^{-4}$	0.429		

Chapter 9: Nucleophilicity Parameters of Enamides and their Implications for Organocatalytic Transformations

Table 13 Continued

$[(\text{mor})_2\text{CH}^+]$ (mol L <sup>-1</sup> )	[Nu] (mol L <sup>-1</sup> )	$k_{\text{obs}}$ (s <sup>-1</sup> )	$\lambda = 613$ nm (diode array)	$k_2$ (M <sup>-1</sup> s <sup>-1</sup> )
$1.46 \times 10^{-5}$	$7.61 \times 10^{-4}$	$2.79 \times 10^{-3}$		2.78
$1.44 \times 10^{-5}$	$8.02 \times 10^{-4}$	$2.88 \times 10^{-3}$		
$1.43 \times 10^{-5}$	$9.31 \times 10^{-4}$	$3.32 \times 10^{-3}$		
$1.48 \times 10^{-5}$	$1.28 \times 10^{-3}$	$4.23 \times 10^{-3}$		
$[(\text{mpa})_2\text{CH}^+]$ (mol L <sup>-1</sup> )	[Nu] (mol L <sup>-1</sup> )	$k_{\text{obs}}$ (s <sup>-1</sup> )	$\lambda = 642$ nm (diode array)	$k_2$ (M <sup>-1</sup> s <sup>-1</sup> )
$9.99 \times 10^{-6}$	$2.28 \times 10^{-4}$	$8.06 \times 10^{-4}$		3.47
$1.00 \times 10^{-5}$	$2.86 \times 10^{-4}$	$1.01 \times 10^{-3}$		
$9.94 \times 10^{-6}$	$3.40 \times 10^{-4}$	$1.19 \times 10^{-3}$		
$9.95 \times 10^{-6}$	$4.55 \times 10^{-4}$	$1.58 \times 10^{-3}$		
$9.91 \times 10^{-6}$	$5.65 \times 10^{-4}$	$1.98 \times 10^{-3}$		
$[(\text{dma})_2\text{CH}^+]$ (mol L <sup>-1</sup> )	[Nu] (mol L <sup>-1</sup> )	$k_{\text{obs}}$ (s <sup>-1</sup> )	$\lambda = 605$ nm (diode array)	$k_2$ (M <sup>-1</sup> s <sup>-1</sup> )
$1.20 \times 10^{-5}$	$4.16 \times 10^{-4}$	$6.64 \times 10^{-5}$		$1.59 \times 10^{-1}$
$1.23 \times 10^{-5}$	$5.69 \times 10^{-4}$	$9.21 \times 10^{-5}$		
$1.18 \times 10^{-5}$	$6.86 \times 10^{-4}$	$1.09 \times 10^{-4}$		

**Table 13** Continued

Reactivity parameters for benzyl 1-phenylvinylcarbamate (**1e**) in CH<sub>3</sub>CN

Ar <sub>2</sub> CH <sup>+</sup>	<i>E</i>	<i>k</i> <sub>2</sub> (M <sup>-1</sup> s <sup>-1</sup> )
(pfa) <sub>2</sub> CH <sup>+</sup>	-3.14	4.53 × 10 <sup>2</sup>
(mor) <sub>2</sub> CH <sup>+</sup>	-5.53	2.78
(mpa) <sub>2</sub> CH <sup>+</sup>	-5.89	3.47
(dma) <sub>2</sub> CH <sup>+</sup>	-7.02	1.59 × 10 <sup>-1</sup>

**Table 14.** Kinetics of the reactions of benzyl (1-phenylvinyl)carbamate (**1f**) with (Ar)<sub>2</sub>CH<sup>+</sup> in CH<sub>3</sub>CN at 20°C.

[(mor) <sub>2</sub> CH <sup>+</sup> ]	[Nu]	<i>k</i> <sub>obs</sub>	λ = 612 nm (diode array)	<i>k</i> <sub>2</sub>
(mol L <sup>-1</sup> )	(mol L <sup>-1</sup> )	(s <sup>-1</sup> )		(M <sup>-1</sup> s <sup>-1</sup> )
1.66 × 10 <sup>-5</sup>	5.11 × 10 <sup>-4</sup>	4.53 × 10 <sup>-4</sup>		8.22 × 10 <sup>-1</sup>
1.65 × 10 <sup>-5</sup>	6.32 × 10 <sup>-4</sup>	5.27 × 10 <sup>-4</sup>		
1.63 × 10 <sup>-5</sup>	7.50 × 10 <sup>-4</sup>	6.40 × 10 <sup>-4</sup>		
1.62 × 10 <sup>-5</sup>	8.71 × 10 <sup>-4</sup>	7.15 × 10 <sup>-4</sup>		
1.61 × 10 <sup>-5</sup>	1.11 × 10 <sup>-3</sup>	9.44 × 10 <sup>-4</sup>		

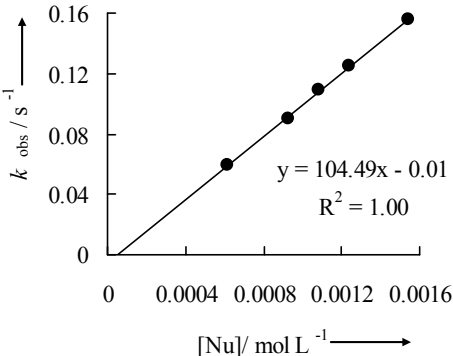
  

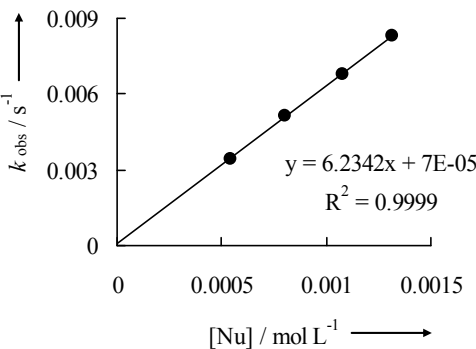
**Table 15.** Kinetics of the reactions of N-(1-(naphthalen-2-yl)vinyl)acetamide (**1g**) with (Ar)<sub>2</sub>CH<sup>+</sup> in CH<sub>3</sub>CN at 20°C.

[(pfa) <sub>2</sub> CH <sup>+</sup> ]	[Nu]	<i>k</i> <sub>obs</sub>	λ = 592 nm (stopped-flow)	<i>k</i> <sub>2</sub>
(mol L <sup>-1</sup> )	(mol L <sup>-1</sup> )	(s <sup>-1</sup> )		(M <sup>-1</sup> s <sup>-1</sup> )
2.00 × 10 <sup>-5</sup>	6.79 × 10 <sup>-4</sup>	1.10		1.50 × 10 <sup>3</sup>
	8.15 × 10 <sup>-4</sup>	1.34		
	9.51 × 10 <sup>-4</sup>	1.50		
	1.09 × 10 <sup>-3</sup>	1.72		

Chapter 9: Nucleophilicity Parameters of Enamides and their Implications for Organocatalytic Transformations

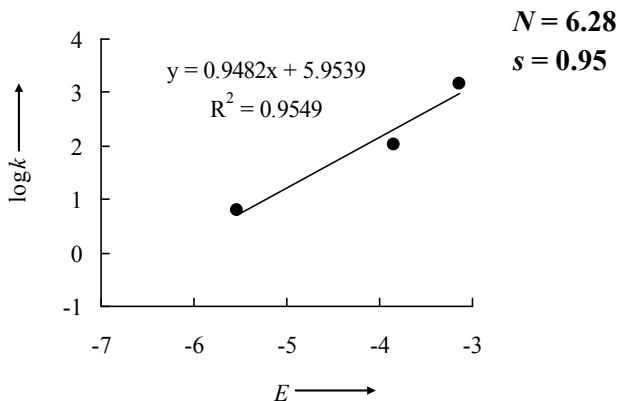
Table 15 Continued.

$[(\text{mfa})_2\text{CH}^+]$ (mol L <sup>-1</sup> )	$[\text{Nu}]$ (mol L <sup>-1</sup> )	$k_{\text{obs}}$ (s <sup>-1</sup> )	$\lambda = 587 \text{ nm}$ (stopped-flow)	$k_2$ (M <sup>-1</sup> s <sup>-1</sup> )
$2.66 \times 10^{-5}$	$6.18 \times 10^{-4}$	$5.97 \times 10^{-2}$		$1.05 \times 10^2$
	$9.27 \times 10^{-4}$	$9.01 \times 10^{-2}$		
	$1.08 \times 10^{-4}$	0.109		
	$1.24 \times 10^{-3}$	0.125		
	$1.54 \times 10^{-3}$	0.156		

$[(\text{mor})_2\text{CH}^+]$ (mol L <sup>-1</sup> )	$[\text{Nu}]$ (mol L <sup>-1</sup> )	$k_{\text{obs}}$ (s <sup>-1</sup> )	$\lambda = 613 \text{ nm}$ (diode array)	$k_2$ (M <sup>-1</sup> s <sup>-1</sup> )	
$1.60 \times 10^{-5}$	$5.42 \times 10^{-4}$	$3.43 \times 10^{-3}$		6.23	
	$1.58 \times 10^{-5}$	$8.03 \times 10^{-4}$			$5.11 \times 10^{-3}$
	$1.59 \times 10^{-5}$	$1.08 \times 10^{-3}$			$6.79 \times 10^{-3}$
	$1.56 \times 10^{-5}$	$1.32 \times 10^{-3}$			$8.29 \times 10^{-3}$

Reactivity parameters for N-(1-(naphthalen-2-yl)vinyl)acetamide (**1g**) in CH<sub>3</sub>CN

$\text{Ar}_2\text{CH}^+$	$E$	$k_2$ (M <sup>-1</sup> s <sup>-1</sup> )
$(\text{pfa})_2\text{CH}^+$	-3.14	$1.50 \times 10^3$
$(\text{mfa})_2\text{CH}^+$	-3.85	$1.05 \times 10^2$
$(\text{mor})_2\text{CH}^+$	-5.53	6.23

**Table 16.** Kinetics of the reactions of N-(3,4-dihydronaphthalen-1-yl)acetamide (**1h**) with (Ar)<sub>2</sub>CH<sup>+</sup> in CH<sub>3</sub>CN at 20°C

[(pfa) <sub>2</sub> CH <sup>+</sup> ] (mol L <sup>-1</sup> )	[Nu] (mol L <sup>-1</sup> )	<i>k</i> <sub>obs</sub> (s <sup>-1</sup> )	λ = 592 nm (stopped-flow)	<i>k</i> <sub>2</sub> (M <sup>-1</sup> s <sup>-1</sup> )
1.26 × 10 <sup>-5</sup>	5.16 × 10 <sup>-4</sup>	3.54 × 10 <sup>-2</sup>		4.64 × 10 <sup>1</sup>
	1.03 × 10 <sup>-3</sup>	5.96 × 10 <sup>-2</sup>		
	2.06 × 10 <sup>-3</sup>	0.108		
	2.58 × 10 <sup>-3</sup>	0.133		
	3.10 × 10 <sup>-3</sup>	0.154		
<b>Table 16 Continued.</b>				
[(mfa) <sub>2</sub> CH <sup>+</sup> ] (mol L <sup>-1</sup> )	[Nu] (mol L <sup>-1</sup> )	<i>k</i> <sub>obs</sub> (s <sup>-1</sup> )	λ = 586 nm (diode array)	<i>k</i> <sub>2</sub> (M <sup>-1</sup> s <sup>-1</sup> )
1.27 × 10 <sup>-5</sup>	5.01 × 10 <sup>-4</sup>	3.42 × 10 <sup>-3</sup>		5.24
	1.00 × 10 <sup>-3</sup>	6.27 × 10 <sup>-3</sup>		
	1.27 × 10 <sup>-3</sup>	7.48 × 10 <sup>-3</sup>		
	1.51 × 10 <sup>-3</sup>	8.73 × 10 <sup>-3</sup>		
1.54 × 10 <sup>-5</sup>	1.22 × 10 <sup>-3</sup>	4.77 × 10 <sup>-4</sup>		3.28 × 10 <sup>-1</sup>
	1.95 × 10 <sup>-3</sup>	7.32 × 10 <sup>-4</sup>		
	2.44 × 10 <sup>-3</sup>	8.72 × 10 <sup>-4</sup>		

Chapter 9: Nucleophilicity Parameters of Enamides and their Implications for Organocatalytic Transformations

**Table 16** Continued.

Reactivity parameters for N-(3,4-dihydronaphthalen-1-yl)acetamide (**1h**) in CH<sub>3</sub>CN

Ar <sub>2</sub> CH <sup>+</sup>	<i>E</i>	<i>k</i> <sub>2</sub> (M <sup>-1</sup> s <sup>-1</sup> )
(pfa) <sub>2</sub> CH <sup>+</sup>	-3.14	4.64 × 10 <sup>1</sup>
(mfa) <sub>2</sub> CH <sup>+</sup>	-3.85	5.24
(mor) <sub>2</sub> CH <sup>+</sup>	-5.53	3.28 × 10 <sup>-1</sup>

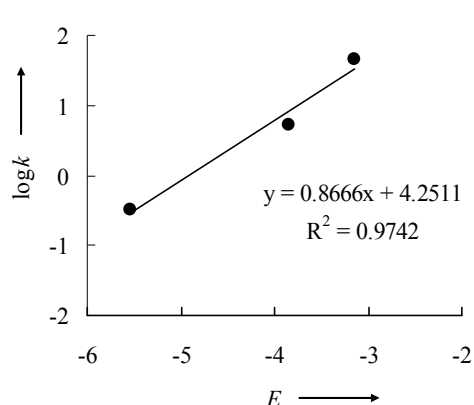
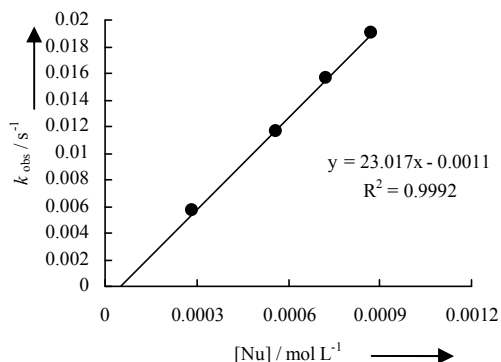


**Table 17.** Kinetics of the reactions of N-cyclohexenylacetamide (**1i**) with (Ar)<sub>2</sub>CH<sup>+</sup> in CH<sub>3</sub>CN at 20°C.

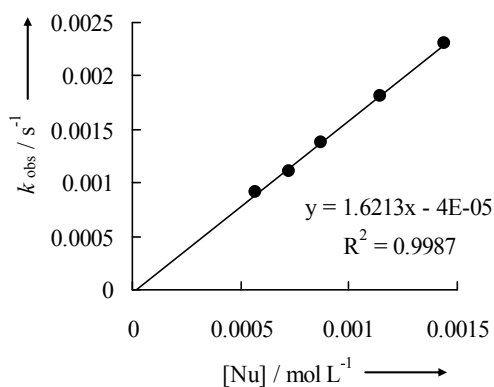
[(mfa) <sub>2</sub> CH <sup>+</sup> ] (mol L <sup>-1</sup> )	[Nu] (mol L <sup>-1</sup> )	<i>k</i> <sub>obs</sub> (s <sup>-1</sup> )	λ = 586 nm (diode array)	<i>k</i> <sub>2</sub> (M <sup>-1</sup> s <sup>-1</sup> )
---	--------------------------------	---	--------------------------	---

1.28 × 10 <sup>-5</sup>	2.87 × 10 <sup>-4</sup>	5.64 × 10 <sup>-3</sup>		2.30 × 10 <sup>1</sup>
1.28 × 10 <sup>-5</sup>	5.75 × 10 <sup>-4</sup>	1.16 × 10 <sup>-2</sup>		
1.29 × 10 <sup>-5</sup>	7.22 × 10 <sup>-4</sup>	1.56 × 10 <sup>-2</sup>		
1.30 × 10 <sup>-5</sup>	8.70 × 10 <sup>-4</sup>	1.90 × 10 <sup>-2</sup>		



[(mor) <sub>2</sub> CH <sup>+</sup> ] (mol L <sup>-1</sup> )	[Nu] (mol L <sup>-1</sup> )	<i>k</i> <sub>obs</sub> (s <sup>-1</sup> )	λ = 613 nm (diode array)	<i>k</i> <sub>2</sub> (M <sup>-1</sup> s <sup>-1</sup> )
---	--------------------------------	---	--------------------------	---

1.44 × 10 <sup>-5</sup>	5.70 × 10 <sup>-4</sup>	9.15 × 10 <sup>-4</sup>		1.62
1.47 × 10 <sup>-5</sup>	7.23 × 10 <sup>-4</sup>	1.11 × 10 <sup>-3</sup>		
1.47 × 10 <sup>-5</sup>	8.71 × 10 <sup>-4</sup>	1.37 × 10 <sup>-3</sup>		
1.45 × 10 <sup>-5</sup>	1.14 × 10 <sup>-3</sup>	1.80 × 10 <sup>-3</sup>		
1.46 × 10 <sup>-5</sup>	1.44 × 10 <sup>-3</sup>	2.31 × 10 <sup>-3</sup>		



Chapter 9: Nucleophilicity Parameters of Enamides and their Implications for Organocatalytic Transformations

Table 17 Continued.

$[(\text{dma})_2\text{CH}^+]$ (mol L <sup>-1</sup> )	[Nu] (mol L <sup>-1</sup> )	$k_{\text{obs}}$ (s <sup>-1</sup> )	$\lambda = 606 \text{ nm}$ (diode array)	$k_2$ (M <sup>-1</sup> s <sup>-1</sup> )
$1.46 \times 10^{-5}$	$8.57 \times 10^{-4}$	$7.53 \times 10^{-5}$		$6.91 \times 10^{-2}$
$1.21 \times 10^{-5}$	$1.94 \times 10^{-3}$	$1.46 \times 10^{-4}$		
$1.21 \times 10^{-5}$	$2.75 \times 10^{-3}$	$2.07 \times 10^{-4}$		

Reactivity parameters for N-cyclohexenylacetamide (**1i**) in CH<sub>3</sub>CN

Ar <sub>2</sub> CH <sup>+</sup>	<i>E</i>	$k_2$ (M <sup>-1</sup> s <sup>-1</sup> )		
(mf <sub>a</sub> ) <sub>2</sub> CH <sup>+</sup>	-3.85	$2.30 \times 10^1$		<i>N</i> = 5.64 <i>s</i> = 0.79
(mor) <sub>2</sub> CH <sup>+</sup>	-5.53	1.62		
(dma) <sub>2</sub> CH <sup>+</sup>	-7.02	$6.91 \times 10^{-2}$		

Table 18. Kinetics of the reactions of N-cyclopentenylacetamide (**1j**) with (Ar)<sub>2</sub>CH<sup>+</sup> in CH<sub>3</sub>CN at 20°C.

$[(\text{pfa})_2\text{CH}^+]$ (mol L <sup>-1</sup> )	[Nu] (mol L <sup>-1</sup> )	$k_{\text{obs}}$ (s <sup>-1</sup> )	$\lambda = 592 \text{ nm}$ (stopped-flow)	$k_2$ (M <sup>-1</sup> s <sup>-1</sup> )
$2.00 \times 10^{-5}$	$5.13 \times 10^{-4}$	1.74		$3.39 \times 10^3$
	$6.84 \times 10^{-4}$	2.32		
	$1.03 \times 10^{-3}$	3.48		
	$1.37 \times 10^{-3}$	4.61		
	$1.71 \times 10^{-3}$	5.81		

Chapter 9: Nucleophilicity Parameters of Enamides and their Implications for Organocatalytic Transformations

Table 18 Continued.

$[(\text{mfa})_2\text{CH}^+]$ (mol L <sup>-1</sup> )	[Nu] (mol L <sup>-1</sup> )	$k_{\text{obs}}$ (s <sup>-1</sup> )	$\lambda = 587 \text{ nm}$ (stopped-flow)	$k_2$ (M <sup>-1</sup> s <sup>-1</sup> )
$1.45 \times 10^{-5}$	$5.13 \times 10^{-4}$	0.179		$4.16 \times 10^2$
	$6.84 \times 10^{-4}$	0.245		
	$1.03 \times 10^{-3}$	0.380		
	$1.37 \times 10^{-3}$	0.524		
	$1.71 \times 10^{-3}$	0.677		
$[(\text{mor})_2\text{CH}^+]$ (mol L <sup>-1</sup> )	[Nu] (mol L <sup>-1</sup> )	$k_{\text{obs}}$ (s <sup>-1</sup> )	$\lambda = 612 \text{ nm}$ (diode array)	$k_2$ (M <sup>-1</sup> s <sup>-1</sup> )
$2.08 \times 10^{-5}$	$2.34 \times 10^{-4}$	$5.28 \times 10^{-3}$		$2.15 \times 10^1$
	$3.43 \times 10^{-4}$	$7.54 \times 10^{-3}$		
	$4.65 \times 10^{-4}$	$9.88 \times 10^{-3}$		
	$5.76 \times 10^{-4}$	$1.27 \times 10^{-2}$		
	$7.02 \times 10^{-4}$	$1.53 \times 10^{-2}$		
$[(\text{dma})_2\text{CH}^+]$ (mol L <sup>-1</sup> )	[Nu] (mol L <sup>-1</sup> )	$k_{\text{obs}}$ (s <sup>-1</sup> )	$\lambda = 606 \text{ nm}$ (diode array)	$k_2$ (M <sup>-1</sup> s <sup>-1</sup> )
$1.45 \times 10^{-5}$	$2.35 \times 10^{-4}$	$2.70 \times 10^{-4}$		1.16
	$4.77 \times 10^{-4}$	$5.90 \times 10^{-4}$		
	$6.99 \times 10^{-4}$	$8.81 \times 10^{-4}$		
	$1.63 \times 10^{-3}$	$1.91 \times 10^{-3}$		

Table 18 Continued.

Reactivity parameters for N-cyclopentenylnacetamide ( <b>1j</b> ) in CH <sub>3</sub> CN		
Ar <sub>2</sub> CH <sup>+</sup>	<i>E</i>	<i>k</i> <sub>2</sub> (M <sup>-1</sup> s <sup>-1</sup> )
(pfa) <sub>2</sub> CH <sup>+</sup>	-3.14	3.39 × 10 <sup>3</sup>
(mfa) <sub>2</sub> CH <sup>+</sup>	-3.85	4.16 × 10 <sup>2</sup>
(mor) <sub>2</sub> CH <sup>+</sup>	-5.53	2.15 × 10 <sup>1</sup>
(dma) <sub>2</sub> CH <sup>+</sup>	-7.02	1.16

Table 19. Kinetics of the reactions of N-(3,3-dimethylbut-1-en-2-yl)acetamide (**1k**) with (Ar)<sub>2</sub>CH<sup>+</sup> in CH<sub>3</sub>CN at 20°C.

[(pfa) <sub>2</sub> CH <sup>+</sup> ] (mol L <sup>-1</sup> )	[Nu] (mol L <sup>-1</sup> )	<i>k</i> <sub>obs</sub> (s <sup>-1</sup> )	λ = 592 nm (diode array)	<i>k</i> <sub>2</sub> (M <sup>-1</sup> s <sup>-1</sup> )
1.50 × 10 <sup>-5</sup>	5.68 × 10 <sup>-4</sup>	2.24 × 10 <sup>-2</sup>		3.57 × 10 <sup>1</sup>
1.50 × 10 <sup>-5</sup>	8.48 × 10 <sup>-4</sup>	3.08 × 10 <sup>-2</sup>		
1.49 × 10 <sup>-5</sup>	9.88 × 10 <sup>-4</sup>	3.79 × 10 <sup>-2</sup>		
1.49 × 10 <sup>-5</sup>	1.38 × 10 <sup>-3</sup>	5.11 × 10 <sup>-2</sup>		

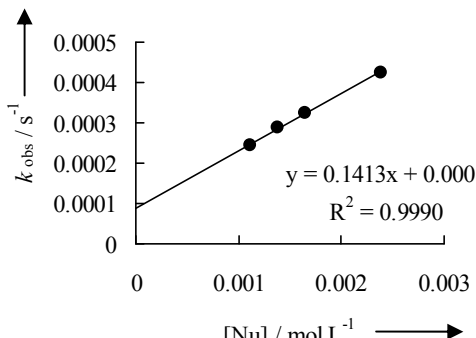
Because of the deviation from the mono-exponential kinetics only two half lives were used for the evaluation.

[(mfa) <sub>2</sub> CH <sup>+</sup> ] (mol L <sup>-1</sup> )	[Nu] (mol L <sup>-1</sup> )	<i>k</i> <sub>obs</sub> (s <sup>-1</sup> )	λ = 586 nm (diode array)	<i>k</i> <sub>2</sub> (M <sup>-1</sup> s <sup>-1</sup> )
1.85 × 10 <sup>-5</sup>	8.54 × 10 <sup>-4</sup>	3.49 × 10 <sup>-3</sup>		3.81
1.84 × 10 <sup>-5</sup>	1.13 × 10 <sup>-3</sup>	4.34 × 10 <sup>-3</sup>		
1.83 × 10 <sup>-5</sup>	1.40 × 10 <sup>-3</sup>	5.20 × 10 <sup>-3</sup>		
1.83 × 10 <sup>-5</sup>	1.97 × 10 <sup>-3</sup>	7.70 × 10 <sup>-3</sup>		

Because of the deviation from the mono-exponential kinetics only first half live was used for the evaluation.

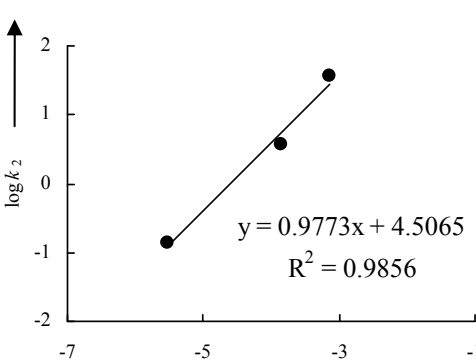
**Table 19** Continued.

$[(\text{mor})_2\text{CH}^+]$ (mol L <sup>-1</sup> )	$[\text{Nu}]$ (mol L <sup>-1</sup> )	$k_{\text{obs}}$ (s <sup>-1</sup> )	$\lambda = 612 \text{ nm}$ (diode array)	$k_2$ (M <sup>-1</sup> s <sup>-1</sup> )
$1.87 \times 10^{-5}$	$1.12 \times 10^{-3}$	$2.45 \times 10^{-4}$		$1.41 \times 10^{-1}$
$1.84 \times 10^{-5}$	$1.39 \times 10^{-3}$	$2.88 \times 10^{-4}$		
$1.77 \times 10^{-5}$	$1.65 \times 10^{-3}$	$3.26 \times 10^{-4}$		
$1.82 \times 10^{-5}$	$2.39 \times 10^{-3}$	$4.26 \times 10^{-4}$		

Because of the deviation from the mono-exponential kinetics only first half live was used for the evaluation.

Reactivity parameters for N-(3,3-dimethylbut-1-en-2-yl)acetamide (**1k**) in CH<sub>3</sub>CN

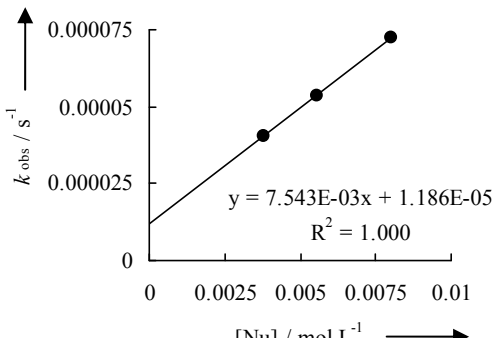
$\text{Ar}_2\text{CH}^+$	$E$	$k_2$ (M <sup>-1</sup> s <sup>-1</sup> )
$(\text{pfa})_2\text{CH}^+$	-3.14	$3.57 \times 10^1$
$(\text{mfa})_2\text{CH}^+$	-3.85	3.81
$(\text{mor})_2\text{CH}^+$	-5.53	$1.41 \times 10^{-1}$

$N = 4.61$   
 $s = 0.98$

### 4.3.2 Kinetics of the reactions of enamides with 5-benzylidene-2,2-dimethyl-1,3-dioxane-4,6-dione (**15**).

**Table 20.** Kinetics of the reactions of N-(1-*p*-tolylvinyl)acetamide (**1b**) with 5-benzylidene-2,2-dimethyl-1,3-dioxane-4,6-dione (**15**) in CH<sub>3</sub>CN at 20°C.

<b>[15]</b> (mol L <sup>-1</sup> )	$[\text{Nu}]$ (mol L <sup>-1</sup> )	$k_{\text{obs}}$ (s <sup>-1</sup> )	$\lambda = 317 \text{ nm}$	$k_2$ (M <sup>-1</sup> s <sup>-1</sup> )
$1.07 \times 10^{-4}$	$3.79 \times 10^{-3}$	$4.04 \times 10^{-5}$		$7.54 \times 10^{-3}$
$1.03 \times 10^{-4}$	$5.55 \times 10^{-3}$	$5.38 \times 10^{-5}$		
$1.04 \times 10^{-4}$	$8.00 \times 10^{-3}$	$7.22 \times 10^{-5}$		

**Table 21.** Kinetics of the reactions of *N*-(1-(4-methoxyphenyl)vinyl)acetamide (**1c**) with 5-benzylidene-2,2-dimethyl-1,3-dioxane-4,6-dione (**15**) in CH<sub>3</sub>CN at 20°C.

[ <b>15</b> ] (mol L <sup>-1</sup> )	[Nu] (mol L <sup>-1</sup> )	<i>k</i> <sub>obs</sub> (s <sup>-1</sup> )	λ = 325 nm	<i>k</i> <sub>2</sub> (M <sup>-1</sup> s <sup>-1</sup> )
1.09 × 10 <sup>-4</sup>	3.31 × 10 <sup>-3</sup>	1.08 × 10 <sup>-4</sup>		2.64 × 10 <sup>-2</sup>
1.06 × 10 <sup>-4</sup>	5.39 × 10 <sup>-3</sup>	1.63 × 10 <sup>-4</sup>		
1.06 × 10 <sup>-4</sup>	7.06 × 10 <sup>-3</sup>	2.11 × 10 <sup>-4</sup>		
1.04 × 10 <sup>-4</sup>	8.64 × 10 <sup>-3</sup>	2.48 × 10 <sup>-4</sup>		

#### 4.3.3 Kinetics of the reactions of the enamides with 2,3,4,5,6,6-hexachlorocyclohexa-2,4-dienone **17**.

**Table 22.** Kinetics of the reactions of *N*-(1-phenylvinyl)acetamide (**1a**) with 2,3,4,5,6,6-hexachlorocyclohexa-2,4-dienone in CH<sub>3</sub>CN at 20°C

[ <b>17</b> ] (mol L <sup>-1</sup> )	[Nu] (mol L <sup>-1</sup> )	<i>k</i> <sub>obs</sub> (s <sup>-1</sup> )	λ = 370 nm	<i>k</i> <sub>2</sub> (M <sup>-1</sup> s <sup>-1</sup> )
2.88 × 10 <sup>-4</sup>	2.99 × 10 <sup>-3</sup>	1.32 × 10 <sup>-4</sup>		3.20 × 10 <sup>-2</sup>
2.85 × 10 <sup>-4</sup>	5.93 × 10 <sup>-3</sup>	2.24 × 10 <sup>-4</sup>		
2.81 × 10 <sup>-4</sup>	1.75 × 10 <sup>-2</sup>	5.97 × 10 <sup>-4</sup>		

**Table 23.** Kinetics of the reactions of *N*-(1-*p*-tolylvinyl)acetamide (**1b**) with 2,3,4,5,6,6-hexachlorocyclohexa-2,4-dienone in CH<sub>3</sub>CN at 20°C .

[17] (mol L <sup>-1</sup> )	[Nu] (mol L <sup>-1</sup> )	<i>k</i> <sub>obs</sub> (s <sup>-1</sup> )	λ = 370 nm	<i>k</i> <sub>2</sub> (M <sup>-1</sup> s <sup>-1</sup> )
2.90 × 10 <sup>-4</sup>	4.51 × 10 <sup>-3</sup>	1.75 × 10 <sup>-4</sup>		3.39 × 10 <sup>-2</sup>
2.86 × 10 <sup>-4</sup>	6.66 × 10 <sup>-3</sup>	2.43 × 10 <sup>-4</sup>		
2.83 × 10 <sup>-4</sup>	8.80 × 10 <sup>-3</sup>	3.20 × 10 <sup>-4</sup>		

**Table 24.** Kinetics of the reactions of *N*-(1-(4-methoxyphenyl)vinyl)acetamide (**1c**) with 2,3,4,5,6,6-hexachlorocyclohexa-2,4-dienone in CH<sub>3</sub>CN at 20°C.

[17] (mol L <sup>-1</sup> )	[Nu] (mol L <sup>-1</sup> )	<i>k</i> <sub>obs</sub> (s <sup>-1</sup> )	λ = 370 nm	<i>k</i> <sub>2</sub> (M <sup>-1</sup> s <sup>-1</sup> )
1.88 × 10 <sup>-4</sup>	1.48 × 10 <sup>-3</sup>	1.78 × 10 <sup>-4</sup>		1.59 × 10 <sup>-1</sup>
1.91 × 10 <sup>-4</sup>	2.63 × 10 <sup>-3</sup>	3.74 × 10 <sup>-4</sup>		
1.89 × 10 <sup>-4</sup>	3.71 × 10 <sup>-3</sup>	5.30 × 10 <sup>-4</sup>		
2.28 × 10 <sup>-4</sup>	5.64 × 10 <sup>-3</sup>	8.45 × 10 <sup>-4</sup>		

**Table 25.** Kinetics of the reactions of *N*-cyclohexenylaetamide (**1i**) with 2,3,4,5,6,6-hexachlorocyclohexa-2,4-dienone in CH<sub>3</sub>CN at 20°C.

[17] (mol L <sup>-1</sup> )	[Nu] (mol L <sup>-1</sup> )	<i>k</i> <sub>obs</sub> (s <sup>-1</sup> )	λ = 370 nm	<i>k</i> <sub>2</sub> (M <sup>-1</sup> s <sup>-1</sup> )
2.23 × 10 <sup>-4</sup>	3.18 × 10 <sup>-3</sup>	5.11 × 10 <sup>-4</sup>		1.63 × 10 <sup>-1</sup>
2.22 × 10 <sup>-4</sup>	3.69 × 10 <sup>-3</sup>	5.79 × 10 <sup>-4</sup>		
2.29 × 10 <sup>-4</sup>	5.57 × 10 <sup>-3</sup>	8.84 × 10 <sup>-4</sup>		
2.30 × 10 <sup>-4</sup>	7.22 × 10 <sup>-3</sup>	1.16 × 10 <sup>-3</sup>		

**Table 26.** Kinetics of the reactions of *N*-cyclopentenylaetamide (**1j**) with 2,3,4,5,6,6-hexachlorocyclohexa-2,4-dienone in CH<sub>3</sub>CN at 20°C.

[17] (mol L <sup>-1</sup> )	[Nu] (mol L <sup>-1</sup> )	<i>k</i> <sub>obs</sub> (s <sup>-1</sup> )	λ = 370 nm	<i>k</i> <sub>2</sub> (M <sup>-1</sup> s <sup>-1</sup> )
2.39 × 10 <sup>-4</sup>	2.43 × 10 <sup>-3</sup>	1.79 × 10 <sup>-3</sup>		7.94 × 10 <sup>-1</sup>
2.45 × 10 <sup>-4</sup>	3.11 × 10 <sup>-3</sup>	2.38 × 10 <sup>-3</sup>		
2.35 × 10 <sup>-4</sup>	3.59 × 10 <sup>-3</sup>	2.71 × 10 <sup>-3</sup>		
2.34 × 10 <sup>-4</sup>	4.76 × 10 <sup>-3</sup>	3.73 × 10 <sup>-3</sup>		
2.31 × 10 <sup>-4</sup>	5.85 × 10 <sup>-3</sup>	4.49 × 10 <sup>-3</sup>		

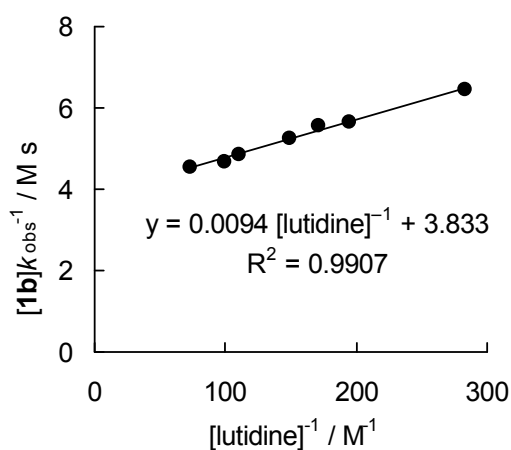
#### 4.3.4 Kinetics of the reactions of the enamides **1b,c** with α,β-unsaturated iminium ion **4b,c** in the presence of a base

The rates of the reactions between the enamides **1** with the α,β-unsaturated iminium ions **4b,c** were measured photometrically under pseudo-first-order condition (excess of enamide) with variable concentrations of a base (2,6-lutidine or 2,4,6-collidine) at the absorption maxima of iminium ions by using UV-Vis spectrometers (conventional diode array) at 20 °C in dry CH<sub>2</sub>Cl<sub>2</sub>. First-order rate constants *k*<sub>obs</sub> (s<sup>-1</sup>) were obtained by least-squares fitting of the

absorbances to the mono-exponential  $A_t = A_0 \exp(-k_{\text{obs}}t) + C$ . The second-order rate constants  $k_2$  ( $\text{M}^{-1} \text{s}^{-1}$ ) were derived from the intercept of the linear plots of  $[\mathbf{1}]k_{\text{obs}}^{-1}$  vs.  $[\text{base}]^{-1}$  [Eq. 4].

**Table 27.** Kinetics of the reactions of *N*-(1-*p*-tolylvinyl)acetamide **1b** with **4b**-PF<sub>6</sub> in the presence of 2,6-lutidine in CH<sub>2</sub>Cl<sub>2</sub> at 20 °C,  $\lambda = 367$  nm (variation of base concentration).

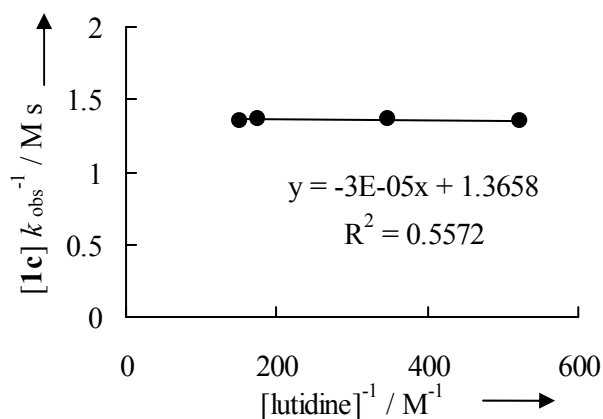
[ <b>4b</b> ] (M)	[ <b>1b</b> ] (M)	[lutidine] (M)	$k_{\text{obs}}$ ( $\text{s}^{-1}$ )	[lutidine] <sup>-1</sup> ( $\text{M}^{-1}$ )	[ <b>1b</b> ] $k_{\text{obs}}^{-1}$ (M s)
$3.94 \times 10^{-5}$	$1.82 \times 10^{-3}$	$3.53 \times 10^{-3}$	$2.82 \times 10^{-4}$	$2.83 \times 10^2$	6.46
$3.81 \times 10^{-5}$	$1.76 \times 10^{-3}$	$5.12 \times 10^{-3}$	$3.12 \times 10^{-4}$	$1.95 \times 10^2$	5.64
$3.92 \times 10^{-5}$	$1.81 \times 10^{-3}$	$5.83 \times 10^{-3}$	$3.25 \times 10^{-4}$	$1.72 \times 10^2$	5.56
$3.75 \times 10^{-5}$	$1.73 \times 10^{-3}$	$6.72 \times 10^{-3}$	$3.31 \times 10^{-4}$	$1.49 \times 10^2$	5.24
$3.90 \times 10^{-5}$	$1.80 \times 10^{-3}$	$9.02 \times 10^{-3}$	$3.71 \times 10^{-4}$	$1.11 \times 10^2$	4.85
$3.75 \times 10^{-5}$	$1.74 \times 10^{-3}$	$1.01 \times 10^{-2}$	$3.71 \times 10^{-4}$	99.2	4.68
$3.86 \times 10^{-5}$	$1.78 \times 10^{-3}$	$1.37 \times 10^{-2}$	$3.92 \times 10^{-4}$	72.8	4.55



Second-order rate constant  $k_2 = 1/\text{intercept} = 1/3.83 = 0.261 \text{ M}^{-1} \text{ s}^{-1}$ .

**Table 28.** Kinetics of the reactions of *N*-(1-(4-methoxyphenyl)vinyl)acetamide **1c** with **4b**-PF<sub>6</sub> in the presence of 2,6-lutidine in CH<sub>2</sub>Cl<sub>2</sub> at 20°C,  $\lambda = 367$  nm (variation of base concentration).

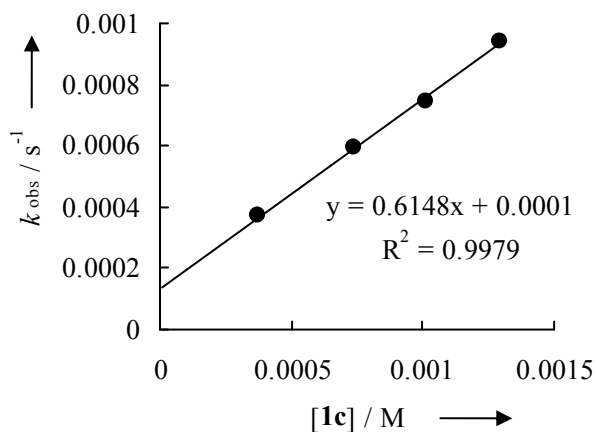
[ <b>4b</b> ] (M)	[ <b>1c</b> ] (M)	[lutidine] (M)	$k_{\text{obs}}$ ( $\text{s}^{-1}$ )	[lutidine] <sup>-1</sup> ( $\text{M}^{-1}$ )	[ <b>1c</b> ] $k_{\text{obs}}^{-1}$ (Ms)
$3.54 \times 10^{-5}$	$1.01 \times 10^{-3}$	$1.91 \times 10^{-3}$	$7.48 \times 10^{-4}$	$5.24 \times 10^2$	1.35
$3.51 \times 10^{-5}$	$1.01 \times 10^{-3}$	$2.88 \times 10^{-3}$	$7.43 \times 10^{-4}$	$3.48 \times 10^2$	1.36
$3.48 \times 10^{-5}$	$1.01 \times 10^{-3}$	$5.71 \times 10^{-3}$	$7.39 \times 10^{-4}$	$1.75 \times 10^2$	1.36
$3.45 \times 10^{-5}$	$9.96 \times 10^{-4}$	$6.60 \times 10^{-3}$	$7.33 \times 10^{-4}$	$1.52 \times 10^2$	1.36



Second-order rate constant  $k_2 = 0.732 \text{ M}^{-1} \text{ s}^{-1}$ .

**Table 29.** Kinetics of the reactions of *N*-(1-(4-methoxyphenyl)vinyl)acetamide **1c** with **4b**-PF<sub>6</sub> in the presence of 2,6-lutidine in CH<sub>2</sub>Cl<sub>2</sub> at 20°C,  $\lambda = 367 \text{ nm}$ , (variation of nucleophile concentration).

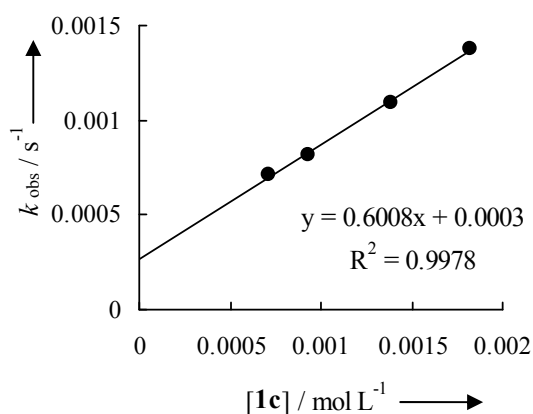
[ <b>9b</b> ] (M)	[ <b>1c</b> ] (M)	[lutidine] (M <sup>-1</sup> )	$k_{\text{obs}}$ (s <sup>-1</sup> )
$3.59 \times 10^{-5}$	$3.74 \times 10^{-4}$	$3.96 \times 10^{-3}$	$3.69 \times 10^{-4}$
$3.55 \times 10^{-5}$	$7.39 \times 10^{-4}$	$3.91 \times 10^{-3}$	$5.94 \times 10^{-4}$
$3.55 \times 10^{-5}$	$1.01 \times 10^{-3}$	$2.88 \times 10^{-3}$	$7.43 \times 10^{-4}$
$3.55 \times 10^{-5}$	$1.29 \times 10^{-3}$	$3.91 \times 10^{-3}$	$9.41 \times 10^{-4}$



Second-order rate constant  $k_2 = 0.615 \text{ M}^{-1} \text{ s}^{-1}$ .

**Table 30.** Kinetics of the reactions of *N*-(1-(4-methoxyphenyl)vinyl)acetamide **1c** with **4b**-PF<sub>6</sub> in the presence of 2,4,6-collidine in CH<sub>2</sub>Cl<sub>2</sub> at 20°C, λ = 370 nm (variation of nucleophile concentration).

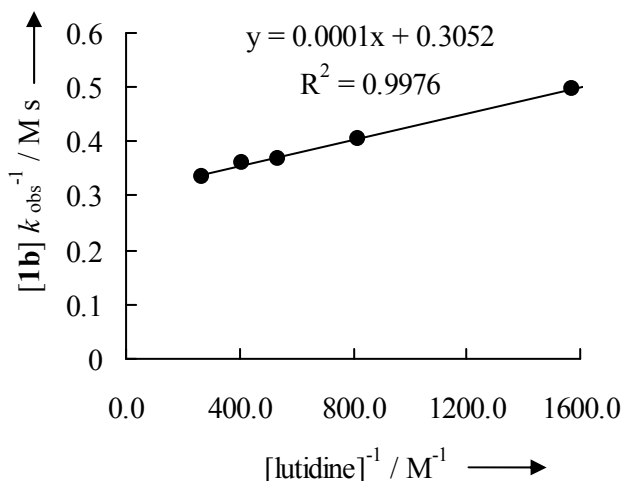
[ <b>9b</b> ] (M)	[ <b>1c</b> ] (M)	[collidine] (M <sup>-1</sup> )	<i>k</i> <sub>obs</sub> (s <sup>-1</sup> )
2.22 × 10 <sup>-5</sup>	7.13 × 10 <sup>-4</sup>	1.44 × 10 <sup>-3</sup>	7.11 × 10 <sup>-4</sup>
2.17 × 10 <sup>-5</sup>	9.29 × 10 <sup>-4</sup>	1.41 × 10 <sup>-3</sup>	8.17 × 10 <sup>-4</sup>
2.15 × 10 <sup>-5</sup>	1.39 × 10 <sup>-3</sup>	1.40 × 10 <sup>-3</sup>	1.09 × 10 <sup>-3</sup>
2.12 × 10 <sup>-5</sup>	1.82 × 10 <sup>-3</sup>	1.38 × 10 <sup>-3</sup>	1.37 × 10 <sup>-3</sup>



Second-order rate constant  $k_2 = 0.601 \text{ M}^{-1} \text{ s}^{-1}$ .

**Table 31.** Kinetics of the reactions of *N*-(1-p-tolylvinyl)acetamide **1b** with **4c**-PF<sub>6</sub> in the presence of 2,6-lutidine in CH<sub>2</sub>Cl<sub>2</sub> at 20°C, λ = 375 nm (variation of base concentration).

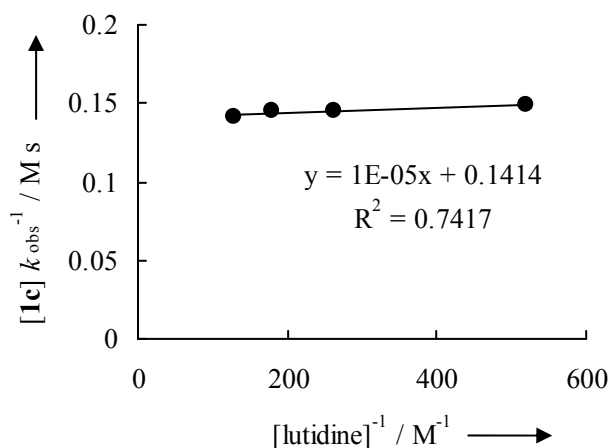
[ <b>4c</b> -PF <sub>6</sub> ] (M)	[ <b>1b</b> ] (M)	[lutidine] (M)	<i>k</i> <sub>obs</sub> (s <sup>-1</sup> )	[lutidine] <sup>-1</sup> (M <sup>-1</sup> )	[ <b>1b</b> ] <i>k</i> <sub>obs</sub> <sup>-1</sup> (M s)
3.46 × 10 <sup>-5</sup>	1.13 × 10 <sup>-3</sup>	6.36 × 10 <sup>-4</sup>	2.29 × 10 <sup>-3</sup>	1.57 × 10 <sup>3</sup>	0.496
3.33 × 10 <sup>-5</sup>	1.09 × 10 <sup>-3</sup>	1.22 × 10 <sup>-3</sup>	2.69 × 10 <sup>-3</sup>	8.17 × 10 <sup>2</sup>	0.406
3.37 × 10 <sup>-5</sup>	1.10 × 10 <sup>-3</sup>	1.86 × 10 <sup>-3</sup>	2.99 × 10 <sup>-3</sup>	5.39 × 10 <sup>2</sup>	0.370
3.35 × 10 <sup>-5</sup>	1.10 × 10 <sup>-3</sup>	2.46 × 10 <sup>-3</sup>	3.06 × 10 <sup>-3</sup>	4.06 × 10 <sup>2</sup>	0.359
3.40 × 10 <sup>-5</sup>	1.11 × 10 <sup>-3</sup>	3.74 × 10 <sup>-3</sup>	3.33 × 10 <sup>-3</sup>	2.67 × 10 <sup>2</sup>	0.334



Second-order rate constant  $k_2 = 3.28 M^{-1} s^{-1}$ .

**Table 32.** Kinetics of the reactions of *N*-(1-(4-methoxyphenyl)vinyl)acetamide **1c** with **4c**-OTf in the presence of 2,6-lutidine in  $CH_2Cl_2$  at  $20^\circ C$ ,  $\lambda = 375$  nm, (variation of base concentration).

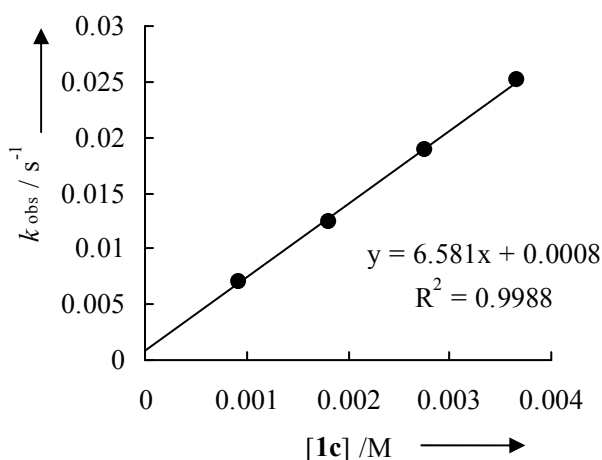
[4c] (M)	[1c] (M)	[lutidine] (M)	$k_{obs} (s^{-1})$	$[lutidine]^{-1} (M^{-1})$	$[1c] k_{obs}^{-1} (M s)$
$7.16 \times 10^{-5}$	$1.87 \times 10^{-3}$	$1.92 \times 10^{-3}$	$1.26 \times 10^{-2}$	$5.21 \times 10^2$	0.149
$7.12 \times 10^{-5}$	$1.86 \times 10^{-3}$	$3.82 \times 10^{-3}$	$1.28 \times 10^{-2}$	$2.62 \times 10^2$	0.145
$6.92 \times 10^{-5}$	$1.81 \times 10^{-3}$	$5.57 \times 10^{-3}$	$1.24 \times 10^{-2}$	$1.80 \times 10^2$	0.146
$7.19 \times 10^{-5}$	$1.88 \times 10^{-3}$	$7.71 \times 10^{-3}$	$1.33 \times 10^{-2}$	$1.30 \times 10^2$	0.142



Second order rate constant  $k_2 = 7.07 M^{-1} s^{-1}$ .

**Table 33.** Kinetics of the Reactions of *N*-(1-(4-methoxyphenyl)vinyl)acetamide **1c** with **4c**-PF<sub>6</sub> in the presence of 2,6-lutidine in CH<sub>2</sub>Cl<sub>2</sub> at 20°C, λ = 375 nm (variation of nucleophile concentration).

[ <b>4c</b> -PF <sub>6</sub> ] (M)	[ <b>1c</b> ] (M)	[lutidine] (M)	<i>k</i> <sub>obs</sub> (s <sup>-1</sup> )
7.07 × 10 <sup>-5</sup>	9.25 × 10 <sup>-4</sup>	5.69 × 10 <sup>-3</sup>	7.09 × 10 <sup>-3</sup>
6.92 × 10 <sup>-5</sup>	1.81 × 10 <sup>-3</sup>	5.57 × 10 <sup>-3</sup>	1.24 × 10 <sup>-2</sup>
7.06 × 10 <sup>-5</sup>	2.77 × 10 <sup>-3</sup>	5.68 × 10 <sup>-3</sup>	1.88 × 10 <sup>-2</sup>
7.02 × 10 <sup>-5</sup>	3.67 × 10 <sup>-3</sup>	5.65 × 10 <sup>-3</sup>	2.52 × 10 <sup>-2</sup>



Second-order rate constant  $k_2 = 6.58 \text{ M}^{-1} \text{ s}^{-1}$ .

**Table 34:** Results of the kinetic investigations for the reactions of **4b** and **4c** with **1b** and **1c** in the presence of a base. (Comparison of two different evaluation methods)

Enamide	Iminium ion	Base	<i>k</i> <sub>2</sub> <sup>exp.</sup> [M <sup>-1</sup> s <sup>-1</sup> ]	<i>k</i> <sub>2</sub> <sup>calcd.</sup> [c] [M <sup>-1</sup> s <sup>-1</sup> ]	<i>k</i> <sub>2</sub> <sup>exp.</sup> / <i>k</i> <sub>2</sub> <sup>calcd.</sup>
<b>1c</b>	<b>4b</b>	2,6-lutidine	0.732 <sup>[a]</sup>	0.545	1.3
<b>1c</b>	<b>4b</b>	2,6-lutidine	0.615 <sup>[b]</sup>	0.545	1.1
<b>1c</b>	<b>4b</b>	2,4,6-collidine	0.601 <sup>[b]</sup>	0.545	1.1
<b>1c</b>	<b>4c</b>	2,6-lutidine	7.07 <sup>[a]</sup>	20.4	0.35
<b>1c</b>	<b>4c</b>	2,6-lutidine	6.58 <sup>[b]</sup>	20.4	0.32

[a] From the intercept of  $[1]k_{\text{obs}}^{-1}$  vs  $[B]^{-1}$  plot at constant concentrations of **4** and **1**. [b] From the plot of  $k_{\text{obs}}$  vs  $[1]$  with constant concentrations of **4** and the base. [c]  $k_2$  calculated by equation (2) by using the *E* values of **4** (Scheme 2) and the *N*/*S<sub>N</sub>* values of **1c** (Table 3).

## 5 References

- [1] a) R. Matsubara, S. Kobayashi, *Acc. Chem. Res.* **2008**, *41*, 292–301; b) D. R. Carbery, *Org. Biomol. Chem.* **2008**, *6*, 3455–3460; c) K. Gopalaiah, H. B. Kagan, *Chem. Rev.* **2011**, *111*, 4599–4657; d) T. Shono, Y. Matsumura, K. Tsubata, Y. Sugihara, S. Yamane, T. Kanazawa, T. Aoki, *J. Am. Chem. Soc.* **1982**, *104*, 6697–6703.
- [2] a) R. Matsubara, Y. Nakamura, S. Kobayashi, *Angew. Chem. Int. Ed.* **2004**, *43*, 1679–1681; b) R. Matsubara, Y. Nakamura, S. Kobayashi, *Angew. Chem. Int. Ed.* **2004**, *43*, 3258–3260; c) R. Matsubara, P. Vital, Y. Nakamura, H. Kiyohara, S. Kobayashi, *Tetrahedron* **2004**, *60*, 9769–9784; d) R. Matsubara, N. Kawai, S. Kobayashi, *Angew. Chem. Int. Ed.* **2006**, *45*, 3814–3816; e) R. Matsubara, S. Kobayashi, *Angew. Chem. Int. Ed.* **2006**, *45*, 7993–7995; f) S. Kobayashi, T. Gustafsson, Y. Shimizu, H. Kiyohara, R. Matsubara, *Org. Lett.* **2006**, *8*, 4923–4925; g) J. S. Fossey, R. Matsubara, P. Vital, S. Kobayashi, *Org. Biomol. Chem.* **2005**, *3*, 2910–2913; h) H. Kiyohara, R. Matsubara, S. Kobayashi, *Org. Lett.* **2006**, *8*, 5333–5335; i) F. Berthiol, R. Matsubara, N. Kawai, S. Kobayashi, *Angew. Chem. Int. Ed.* **2007**, *46*, 7803–7805; j) For other examples of N,N'-dioxide-metal complex catalyzed reactions of enamides see: K. Zheng, X. Liu, J. Zhao, Y. Yang, L. Lin, X. Feng, *Chem. Commun.* **2010**, *46*, 3771–3773; k) L. Chang, Y. Kuang, B. Qin, X. Zhou, X. Liu, L. Lin, X. Feng, *Org. Lett.* **2010**, *12*, 2214–2217.
- [3] a) M. Terada, K. Machioka, K. Sorimachi, *Angew. Chem. Int. Ed.* **2006**, *45*, 2254–2257; b) M. Terada, K. Machioka, K. Sorimachi, *J. Am. Chem. Soc.* **2007**, *129*, 10336–10337; c) M. Terada, K. Soga, N. Momiyama, *Angew. Chem. Int. Ed.* **2008**, *47*, 4122–4125.
- [4] a) M. Lu, Y. Lu, D. Zhu, X. Zeng, X. Li, G. Zhong, *Angew. Chem. Int. Ed.* **2010**, *49*, 8588–8592; b) For other examples of chiral Brønsted acids catalyzed reactions of enamides see: H. Liu, G. Dagousset, G. Masson, P. Retailleau, J. Zhu, *J. Am. Chem. Soc.* **2009**, *131*, 4598–4599; c) G. Dagousset, J. Zhu, G. Masson, *J. Am. Chem. Soc.* **2011**, *133*, 14804–14813.
- [5] For reviews on asymmetric iminium catalysis, see: a) A. Berkessel, H. Gröger, *Asymmetric Organocatalysis*, Wiley-VCH, Weinheim, **2005**; b) J. Seayad, B. List, *Org. Biomol. Chem.* **2005**, *3*, 719–724; c) G. Lelais, D. W. C. MacMillan, *Aldrichimica Acta* **2006**, *39*, 79–87; d) *Enantioselective Organocatalysis* (Ed.: P. I.

- Dalko), Wiley-VCH, Weinheim, **2007**; e) A. Erkkilä, I. Majander, P. M. Pihko, *Chem. Rev.* **2007**, *107*, 5416–5470; f) D. W. C. MacMillan, *Nature*, **2008**, *455*, 304–308.
- [6] a) Y. Hayashi, H. Gotoh, R. Masui, H. Ishikawa, *Angew. Chem. Int. Ed.* **2008**, *47*, 4012–4015; b) L. Zu, H. Xie, H. Li, J. Wang, X. Yu, W. Wang, *Chem. Eur. J.* **2008**, *14*, 6333–6335.
- [7] a) D. Seebach, U. Grošelj, D. M. Badine, W. B. Schweizer, A. K. Beck, *Helv. Chim. Acta* **2008**, *91*, 1999–2034; b) G. Evans, T. J. K. Gibbs, R. L. Jenkins, S. J. Coles, M. B. Hursthouse, J. A. Platts, N. C. O. Tomkinson, *Angew. Chem. Int. Ed.* **2008**, *47*, 2820–2823; c) U. Grošelj, D. Seebach, D. M. Badine, W. B. Schweizer, A. K. Beck, I. Krossing, P. Klose, Y. Hayashi, T. Uchimaru *Helv. Chim. Acta* **2009**, *92*, 1225–1259; d) J. B. Brazier, G. Evans, T. J. K. Gibbs, S. J. Coles, M. B. Hursthouse, J. A. Platts, N. C. O. Tomkinson, *Org. Lett.* **2009**, *11*, 133–136.
- [8] a) S. Lakhdar, T. Tokuyasu, H. Mayr, *Angew. Chem. Int. Ed.*, **2008**, *47*, 8723–8726; b) S. Lakhdar, R. Appel, H. Mayr, *Angew. Chem. Int. Ed.* **2009**, *48*, 5034–5037; c) S. Lakhdar, H. Mayr, *Chem. Commun.* **2011**, *47*, 1866–1868; d) S. Lakhdar, J. Ammer, H. Mayr, *Angew. Chem. Int. Ed.* **2011**, *50*, 9953–9956.
- [9] a) H. Mayr, M. Patz, *Angew. Chem. Int. Ed. Engl.* **1994**, *33*, 938–957; b) H. Mayr, T. Bug, M. F. Gotta, N. Hering, B. Irrgang, B. Janker, B. Kempf, R. Loos, A. R. Ofial, G. Remennikov, H. Schimmel, *J. Am. Chem. Soc.* **2001**, *123*, 9500–9512; c) H. Mayr, B. Kempf, A. R. Ofial, *Acc. Chem. Res.* **2003**, *36*, 66–77; d) H. Mayr, A. R. Ofial, A. R. *Pure Appl. Chem.* **2005**, *77*, 1807–1821; e) H. Mayr, A. R. Ofial, *J. Phys. Org. Chem.* **2008**, *21*, 584–595; f) Database for  $N$ ,  $s_N$  and  $E$  parameters and references to original literature: <http://www.cup.uni-muenchen.de/oc/mayr/DBintro.html>.
- [10] B. Kempf, N. Hampel, A. R. Ofial, H. Mayr, *Chem. Eur. J.* **2003**, *9*, 2209–2218.
- [11] C. Hansch, A. Leo, R. W. Taft, *Chem. Rev.* **1991**, *91*, 165–195.
- [12] O. Kaumanns, H. Mayr, *J. Org. Chem.* **2008**, *73*, 2738–2745.
- [13] X.-H. Duan, H. Mayr, *Org. Lett.* **2010**, *12*, 2238–2241.
- [14] J. L. Hogg, W. P. Jencks, *J. Am. Chem. Soc.* **1976**, *98*, 5643–5645.
- [15] Decomposition of **4a**-OTf was observed at concentrations  $c > 0.02$  M of 2,6-lutidine.
- [16] The enamide/enamine structure **19** could not be isolated as a pure compound and unequivocally identified; its formation was indicated by *in situ*  $^1\text{H}$  NMR spectroscopy.

- [17] At very low concentration of base, a deviation from linearity was observed. For a similar observation, see: T. Kanzian, T. A. Nigst, A. Maier, S. Pichl, H. Mayr, *Eur. J. Org. Chem.* **2009**, 6379–6385.
- [18] In the reactions of **4b**-PF<sub>6</sub> and **4c**-PF<sub>6</sub> with the enamide **1c**,  $k_{\text{obs}}$  was independent of the concentrations of 2,6-lutidine (for  $1.9 \times 10^{-3} < c < 7 \times 10^{-3}$  M), i.e., the reverse reaction ( $k_{-2}$ ) was much slower than the deprotonation when a certain concentration of base was present, and Equation (4) simplifies to  $k_{\text{obs}} = k_2[\mathbf{1}]$ . The second-order rate constants  $k_2$  obtained from the slope of  $k_{\text{obs}}$  vs  $[\mathbf{1}]$  plots are in good agreement with those from the intercepts of the  $[\mathbf{1}]/k_{\text{obs}}$  vs.  $[\text{B}]^{-1}$  plots. See Table 34 for a comparison of the two methods of evaluation.
- [19] a) C. F. Bernasconi, *Acc. Chem. Res.* **1987**, *20*, 301–308; b) C. F. Bernasconi, *Adv. Phys. Org. Chem.* **1992**, *27*, 119–238; c) C. F. Bernasconi, *Acc. Chem. Res.* **1992**, *25*, 9–16; d) C. F. Bernasconi, *Adv. Phys. Org. Chem.* **2010**, *44*, 223–324.
- [20] a) R. A. Marcus, *J. Phys. Chem.* **1968**, *72*, 891–899; b) W. J. Albery, *Annu. Rev. Phys. Chem.* **1980**, *31*, 227–263.
- [21] H. Mayr, M. Breugst, A. R. Ofial, *Angew. Chem. Int. Ed.* **2011**, *50*, 6470–6505.
- [22] M. Baidya, S. Kobayashi, F. Brotzel, U. Schmidhammer, E. Riedle, H. Mayr, *Angew. Chem. Int. Ed.* **2007**, *46*, 6176–6179.
- [23] S. Lakhdar, M. Baidya, H. Mayr, *Chem. Commun.* **2012**, *48*, 4504–4506.
- [24] For  $E$  values see: a) R. Appel, H. Mayr, *J. Am. Chem. Soc.* **2011**, *133*, 8240–8251; b) O. Kaumanns, R. Lucius, H. Mayr, *Chem. Eur. J.* **2008**, *14*, 9675–9682.
- [25] W. Wang, H. Li, J. Wang, *Org. Lett.* **2005**, *7*, 1637–1639.

## Chapter 10

# Imidazolidinone-Derived Enamines: Nucleophiles with Low Reactivity

S. Lakhdar, B. Maji, H. Mayr, *Angew. Chem. Int. Ed.* **2012**, *51*, 5739–5742.

### 1 Introduction

During the last decade the concept of enamine activation has become a powerful tool in asymmetric synthesis. It uses chiral secondary amines as catalysts to activate saturated carbonyl compounds by conversion into enamines.<sup>[1]</sup> Among various catalysts tested, diarylprolinol silyl ether **1b** was found to be particularly useful for the stereoselective introduction of different functionalities into the  $\alpha$ -position of aldehydes.<sup>[2,3]</sup>

Imidazolidinones **1c–e** (Table 1), which have extensively been used in iminium catalysis,<sup>[4]</sup> were less effective in enamine-activated processes unless strong electrophiles were employed. Typical examples are enantioselective  $\alpha$ -halogenations<sup>[5]</sup> and  $\alpha$ -alkylations of aldehydes with stabilized carbocations which were generated by treatment of alcohols with acids.<sup>[6]</sup> Mechanistic investigations, focussing on the characterization and reactivities of the intermediate enamines, are rare.<sup>[7–9]</sup>

While the synthesis and the X-ray structure of the enamine **3b** have previously been described by Seebach et al.,<sup>[8]</sup> we are not aware of any X-ray structures of enamines derived from imidazolidinones. Gellman et al. used <sup>1</sup>H NMR spectroscopy to characterize the enamine generated from imidazolidinone **1c** and 3-phenylpropanal in DMSO solution and reported its reaction with methyl vinyl ketone catalyzed by 4-ethoxycarbonyl-catechol.<sup>[9]</sup>

In order to elucidate the relationships between structure and reactivities of enamines derived from **1a–e**, we have now synthesized the enamines **3a–e**, performed X-ray analyses of **3d** and **3e**, and measured the kinetics of their reactions with the stabilized benzhydrylium ions **4a–h** (Table 2).

## 2 Results and Discussion

Enamines **3c–e**, which have previously not been isolated, were obtained by refluxing phenylacetaldehyde **2** and the amines **1c–e** in the presence of 1 mol% of *p*-toluenesulfonic acid in toluene under argon using a Dean-Stark apparatus filled with molecular sieves (4 Å) to remove the generated water.<sup>[10]</sup> After evaporation of the solvent, **3e** was immediately obtained as a crystalline material in 87 % yield, while column chromatography was employed to separate the enamines **3c** and **3d** from the non-reacted imidazolidinones **1c** and **1d**, respectively.

**Table 1.** Amines **1a–e** and the corresponding phenylacetaldehyde-derived enamines **3a–e**.

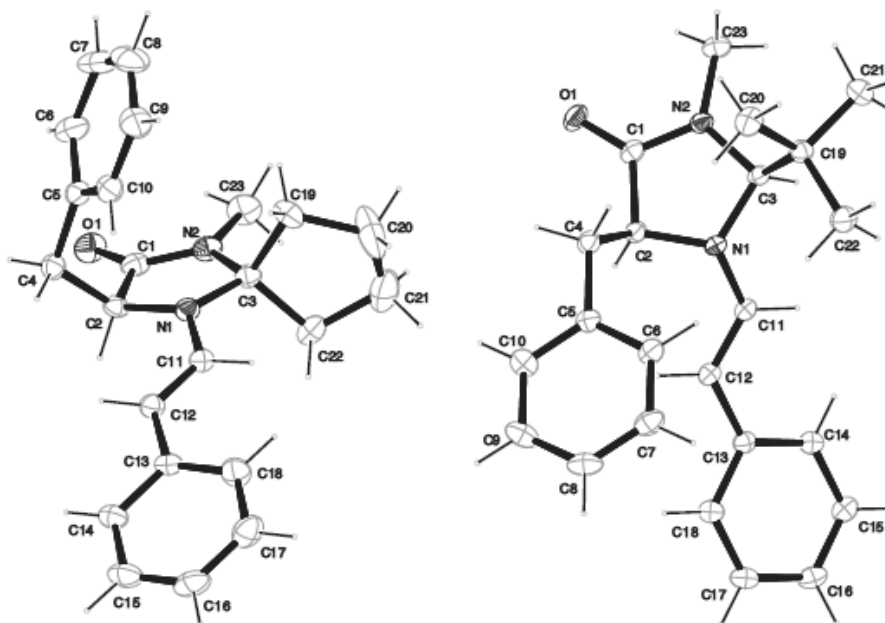
$\text{HNRR}'$ <b>1a–e</b>		$\text{O}=\text{CH}-\text{CH}_2-\text{Ph}$ <b>2</b>	$\xrightarrow[\text{toluene reflux}]{p\text{-TsOH (1\%)}}$	$\text{R}'-\text{N}(\text{R})-\text{CH}=\text{CH}-\text{Ph}$ <b>3a–e</b>	
Amine			Product		Yield / %
	<b>1a</b>			<b>3a</b>	86 <sup>[a]</sup>
	<b>1b</b>			<b>3b</b>	35 <sup>[b]</sup>
	<b>1c</b>			<b>3c</b>	44 <sup>[c]</sup>
	<b>1d</b>			<b>3d</b>	32 <sup>[c]</sup>
	<b>1e</b>			<b>3e</b>	87 <sup>[d]</sup>

[a] After distillation; [b] **3b** was prepared by refluxing **1b** and **2** in benzene following a procedure by Seebach (ref. [8]). After evaporation and crystallization in Et<sub>2</sub>O, **3b** was obtained as a pure material; [c] After column chromatography; [d] After crystallization.

Crystals of **3d** and **3e** suitable for X-ray analysis were grown by the vapor diffusion crystallization method in diethyl ether/*n*-pentane mixtures. As shown in Figure 1,<sup>[11]</sup> the C–N

bond between the heterocyclic ring and the (*E*)-configured CC double bond has *s*-trans conformation in both enamines **3d** and **3e**. Whereas the benzylic phenyl group is located over the imidazolidinone ring in **3d**, possibly because of stabilizing CH– $\pi$  interactions (London dispersion interaction between the phenyl ring and the cyclopentane ring),<sup>[12]</sup> benzyl is located over the CC-double bond in the enamine **3e** and thus directs electrophiles to the *Si*-face of the CC double bond.<sup>[5]</sup> NMR spectroscopy showed that the conformations of **3d** and **3e**, which were observed in the crystals, also dominate in CDCl<sub>3</sub> solution.

From the pyramidalization parameter  $\Delta$ , defined by Dunitz as the distance between the N atom and the plane marked by the three attached carbon atoms,<sup>[13]</sup> one can derive that the almost planar  $sp^2$ -hybridized nitrogen in **3b** ( $\Delta = 0.037 \text{ \AA}$ )<sup>[8]</sup> is adopting more and more  $sp^3$  character as one moves to **3d** ( $\Delta = 0.155 \text{ \AA}$ ) and eventually to **3e** ( $\Delta = 0.293 \text{ \AA}$ ).

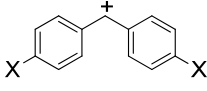
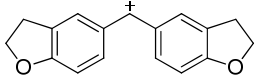
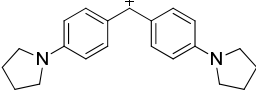
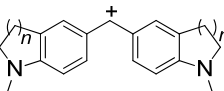
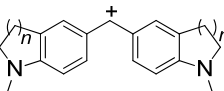


**Figure 1.** Crystal structures of the enamines **3d** (left) and **3e** (right).

In order to quantify the nucleophilic reactivities of **3a–e** we have studied the kinetics of their reactions with the benzhydrylium ions **4a–h** (Table 2), which have been used as reference electrophiles for the construction of comprehensive nucleophilicity scales on the basis of equation (1). Herein, nucleophiles are characterized by two parameters (nucleophilicity  $N$  and sensitivity parameter  $s_N$ ) and electrophiles by one parameter (electrophilicity  $E$ ).<sup>[14]</sup>

$$\lg k_2(20 \text{ }^\circ\text{C}) = s_N(N + E) \quad (1)$$

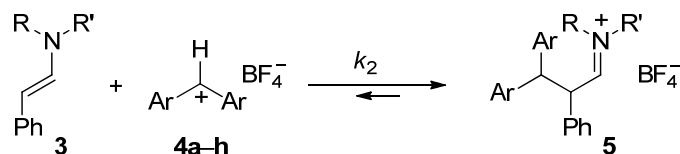
**Table 2.** Reference electrophiles **4a–h**.

		$E^{[a]}$
	<b>4a</b>	-1.36
X = N(Ph)CH <sub>2</sub> CF <sub>3</sub>	<b>4b</b>	-3.14
X = N(Me)CH <sub>2</sub> CF <sub>3</sub>	<b>4c</b>	-3.85
X = N(CH <sub>2</sub> CH <sub>2</sub> ) <sub>2</sub> O	<b>4d</b>	-5.53
X = NMe <sub>2</sub>	<b>4e</b>	-7.02
	<b>4f</b>	-7.69
	<b>4g</b> ( $n = 2$ )	-8.22
	<b>4h</b> ( $n = 1$ )	-8.76

[a] Electrophilicity parameters  $E$  from ref. [14b].

As described previously,<sup>[14b]</sup> the rates of the reactions of carbocations **4** with the enamines **3a–e** were measured photometrically by following the disappearance of the UV-vis absorbances of the diarylcarbenium ions **4** (Scheme 1), using conventional and stopped-flow instruments. All kinetic experiments were performed at 20 °C in acetonitrile with a high excess of the enamines **3a–e** in order to achieve first-order conditions.

The first-order rate constants  $k_{\text{obs}}$  were obtained by least-squares fitting of the function  $A_t = A_0 e^{-k_{\text{obs}} t} + C$  to the time-dependent absorbances of the electrophiles. Plots of  $k_{\text{obs}}$  versus the concentrations of the nucleophiles [**3**] were linear, as exemplified in Figure 2. The slopes of these plots gave the second-order rate constants  $k_2$  (in  $\text{M}^{-1} \text{s}^{-1}$ ), which are summarized in Table 3.



**Scheme 1.** Reactions of the enamines **3** with the carbocations **4** in acetonitrile at 20 °C.

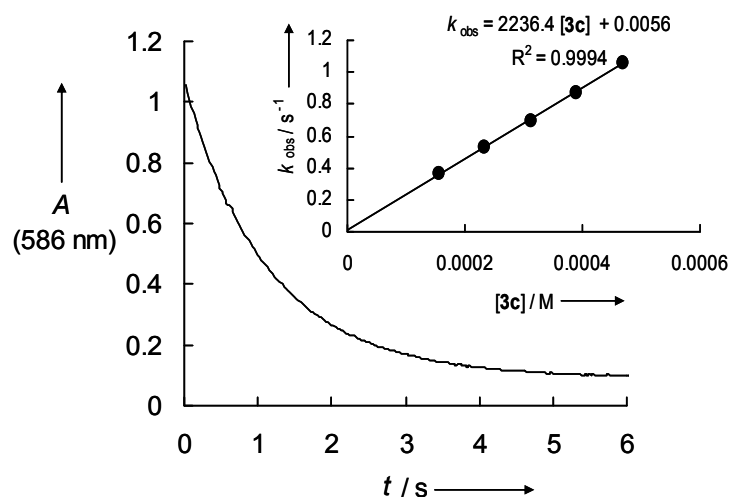


**Figure 2.** Exponential decay of the absorbance at 586 nm during the reaction of  $\mathbf{4c}\text{-BF}_4^-$  ( $1.60 \times 10^{-5}$  M) with  $\mathbf{3c}$  ( $3.90 \times 10^{-4}$  M). Inset: Plot of the rate constants  $k_{\text{obs}}$  versus  $[\mathbf{3c}]$  (20 °C in  $\text{CH}_3\text{CN}$ ).

**Table 3.** Second-order rate constants  $k_2$  for the reactions of the carbocations  $\mathbf{4a-h}$  with the enamines  $\mathbf{3a-e}$  (acetonitrile, 20 °C).

Enamine	$N, s_N^{[a]}$	$\text{R}^+$	$k_2 / \text{M}^{-1} \text{s}^{-1}$
<b>3a</b>	12.25, 0.99	<b>4e</b>	$1.38 \times 10^5$
		<b>4f</b>	$3.48 \times 10^4$
		<b>4g</b>	$9.94 \times 10^3$
		<b>4h</b>	$2.64 \times 10^3$
<b>3b</b>	10.56, 1.01	<b>4d</b>	$1.48 \times 10^5$
		<b>4e</b>	$2.33 \times 10^3$
		<b>4h</b>	$7.94 \times 10^1$
<b>3c</b>	7.20, 1.14	<b>4a</b>	$4.73 \times 10^6$
		<b>4b</b>	$7.80 \times 10^4$
		<b>4c</b>	$2.24 \times 10^3$
		<b>4d</b>	$1.15 \times 10^2$
<b>3d</b>	7.92, 1.07	<b>4b</b>	$2.77 \times 10^5$
		<b>4c</b>	$7.26 \times 10^3$
		<b>4d</b>	$4.93 \times 10^2$
<b>3e</b>	5.80, 0.87	<b>4b</b>	$3.46 \times 10^2$
		<b>4c</b>	$2.56 \times 10^1$
		<b>4d</b>	2.13

[a] Nucleophile-specific parameters as defined by equation (1).

Plots of  $\lg k_2$  versus the empirical electrophilicity parameters  $E$  are linear for all reactions studied in this investigation (Figure 3), indicating that equation (1) can be used to determine  $N$  and  $s_N$  parameters for the enamines **3a–e** (Table 3).

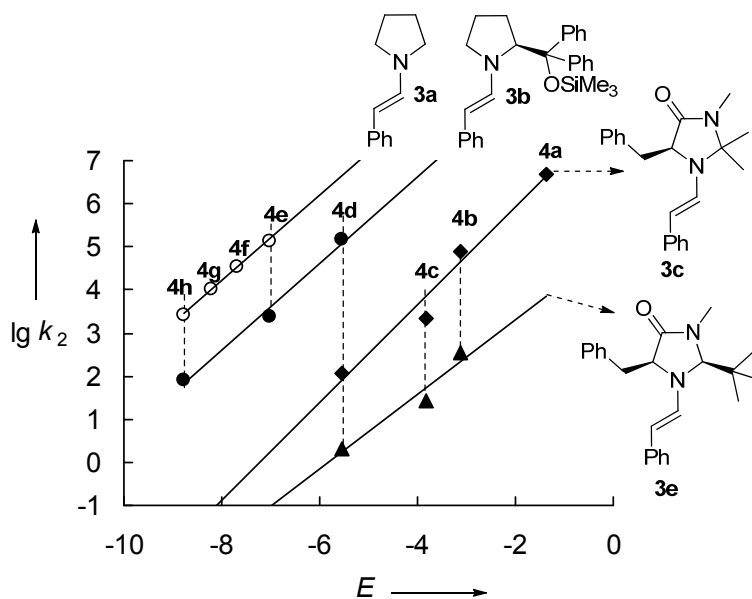


**Figure 3.** Plots of  $\lg k_2$  for the reactions of **3a–c**, and **3e** with the benzhydrylium ions **4** in  $\text{CH}_3\text{CN}$  at  $20^\circ\text{C}$  versus the corresponding electrophilicity parameters  $E$  (correlation for **3d** are omitted for the sake of clarity; it is shown in Figure 4).

One can see that the enamine **3b**, which is derived from the Hayashi-Jørgensen catalyst **1b**, is almost two orders of magnitude less reactive than **3a**, the parent compound of this series. As one of the diastereotopic faces of **3b** is completely open for electrophilic attack, the reduction of reactivity must predominantly be due to the electron-withdrawing inductive effect of the trimethylsilyloxybenzhydryl group in **3b**.

The inductive electron-withdrawing effect of the extra endocyclic amido group in the imidazolidinone derivatives **3c** and **3d**, the pyramidalization of the enamine nitrogen, and the steric shielding of both faces of the CC-double bond by the two alkyl groups at 2-position of the imidazolidinone ring reduce the nucleophilicities of these enamines by another 2 to 3 orders of magnitude compared with **3b**.

As the CC-double bond of **3e** has one open face, its  $10^2$ -times lower nucleophilicity compared with **3c** and **3d** must be due to the enhanced pyramidalization of the enamine nitrogen in **3e** (X-ray structure, Figure 1), which strongly reduces the electron density in the CC double bond.<sup>[15]</sup>

While the interpretation of the NMR chemical shifts of the  $\beta$ -protons in **3a–e** is problematic because of the anisotropy of the phenyl groups, the  $^{13}\text{C}$  NMR chemical shifts show the lower electron densities at the  $\beta$ -carbon of the imidazolidinone derived enamines **3c–e** (Table 4).

**Table 4.** NMR chemical shifts ( $\text{CDCl}_3$ ) of the enamines **3a–e**.

enamine	$\delta(\text{C}^\beta\text{-H}) / \text{ppm}$	$\delta(\text{C}^\beta) / \text{ppm}$
<b>3a</b>	5.18	97.4
<b>3b</b>	5.02 <sup>[a]</sup>	97.2 <sup>[a]</sup>
<b>3c</b>	5.47	101.9
<b>3d</b>	5.47	102.1
<b>3e</b>	4.76	102.9

<sup>[a]</sup> From ref. [8b].

The significantly higher nucleophilicity of **3b** compared with **3c–e** may explain why **1b** is a more suitable catalyst than **1c–e** for most enamine-activated reactions.

By using the  $N$  and  $s_N$  values of **3b** and the  $E$  values of Michael acceptors, equation (1) allows one to predict whether a reaction will take place at room temperature. Hayashi's observation that **1b** catalyzes Michael additions of aldehydes to  $\beta$ -nitrostyrenes<sup>[16]</sup> is in line with a calculated second-order rate constant ( $k_{\text{calcd}} = 4.8 \times 10^{-4} \text{ M}^{-1} \text{ s}^{-1}$ ) for the reaction of **3b** with  $\beta$ -nitrostyrene ( $E = -13.85$ ).<sup>[17]</sup> It has been shown, however, that the initially generated zwitterions from the enamines and nitrostyrene collapse with formation of cyclobutanes, the ring opening of which is the rate-determining step of the catalytic cycle.<sup>[7e,18]</sup> For that reason, a sufficiently fast reaction of the enamine with the Michael acceptor is only one of the criteria which have to be fulfilled for a catalytic cycle to proceed.

The more than 100 times higher nucleophilicity of **3b** compared with **3c,d** may also be responsible for the fact that **1b** and not **1c–e** are usually employed as catalysts for Mannich-type reactions of imines with aldehydes.<sup>[19]</sup> As a consequence of the low nucleophilicity of **3c–e**, the **3c**-catalyzed conjugate additions of aldehydes to enones require Brønsted acids as cocatalysts, which activate the enones in line with earlier suggestions by Gellman.<sup>[9]</sup>

### 3 Conclusion

In summary, we have documented the first X-ray structures of enamines derived from imidazolidinones. Nucleophilic reactivities of these enamines have been derived from the kinetics of their reactions with diarylcarbenium ions **4**, which showed that the enamine **3b**, derived from Hayashi-Jørgensen catalyst, is  $10^3$  to  $10^5$  times more nucleophilic than the enamines derived from the imidazolidinones **1c–e**.

### 4 Experimental Section

In order to identify my contributions to this multiauthor publication, only the experiments, which were performed by me, are described in section 4.1 of this Experimental Section.

#### 4.1 Kinetics

The kinetics of the reactions of the nucleophiles **3a–e** with the carbocations **4** were followed by UV-Vis spectroscopy at 20 °C.

The rates of slow reactions ( $t_{1/2} > 15\text{--}20$  s) were determined by using a J&M TIDAS diode array spectrophotometer controlled by Labcontrol Spectacle software and connected to Hellma 661.502-QX quartz Suprasil immersion probe (5 mm light path) via fiber optic cables and standard SMA connectors.

For the reactions with  $10^{-1} < k_2 < 10^6 \text{ M}^{-1} \text{ s}^{-1}$ , a stopped-flow spectrophotometer system (Applied Photophysics SX.18MV-R) was used. The kinetic runs were initiated by mixing equal volumes of acetonitrile solutions of the electrophiles and nucleophiles.

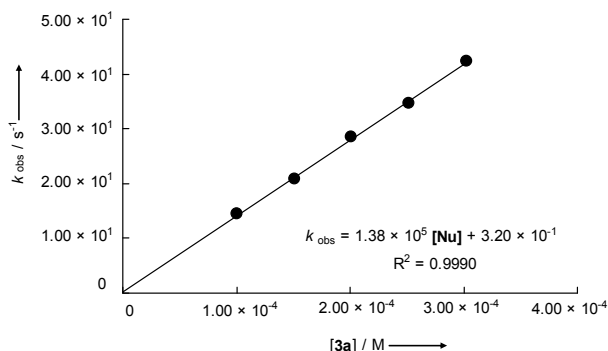
From the exponential decays of the absorbances at  $\lambda_{\text{max}}$  of the electrophiles **4**, the first-order rate constants  $k_{\text{obs}}$  ( $\text{s}^{-1}$ ) were obtained. The temperature of the solutions during the kinetic studies was kept constant at  $20 \pm 0.1$  °C by using a circulating bath cryostat and monitored with thermo-couple probes that were inserted into the reaction mixture.

The rate constants  $k_{\text{obs}}$  ( $\text{s}^{-1}$ ), which were obtained by least-squares fitting to the single exponential curve  $A_t = A_0 e^{-k_{\text{obs}} t} + C$ , depended linearly on the nucleophile concentrations. The second-order rate constants  $k_2$  ( $\text{M}^{-1} \text{ s}^{-1}$ ) for the combination reactions with nucleophiles were derived from the slopes of plots of  $k_{\text{obs}}$  for each nucleophile concentration versus the nucleophile concentrations.

**Table 5.** Rate constants for the reaction of **3a** with **4e** in acetonitrile (stopped-flow method, 20 °C,  $\lambda = 606$  nm).

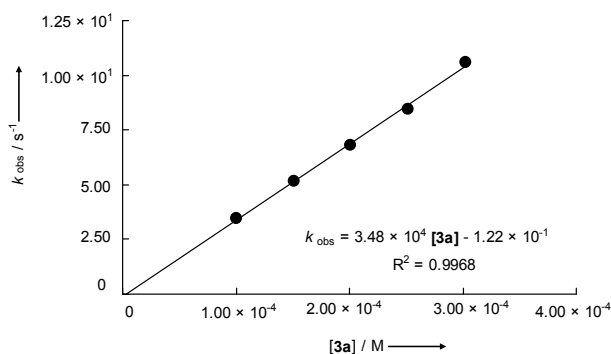
[ <b>4e</b> ] / M	[ <b>3a</b> ] / M	$k_{\text{obs}} / \text{s}^{-1}$
$1.29 \times 10^{-5}$	$1.01 \times 10^{-4}$	$1.44 \times 10^1$
$1.29 \times 10^{-5}$	$1.51 \times 10^{-4}$	$2.09 \times 10^1$
$1.29 \times 10^{-5}$	$2.01 \times 10^{-4}$	$2.84 \times 10^1$
$1.29 \times 10^{-5}$	$2.52 \times 10^{-4}$	$3.46 \times 10^1$
$1.29 \times 10^{-5}$	$3.02 \times 10^{-4}$	$4.23 \times 10^1$

$k_2 = 1.38 \times 10^5 \text{ M}^{-1} \text{ s}^{-1}$

**Table 6.** Rate constants for the reaction of **3a** with **4f** in acetonitrile (stopped-flow method, 20 °C,  $\lambda = 616$  nm).

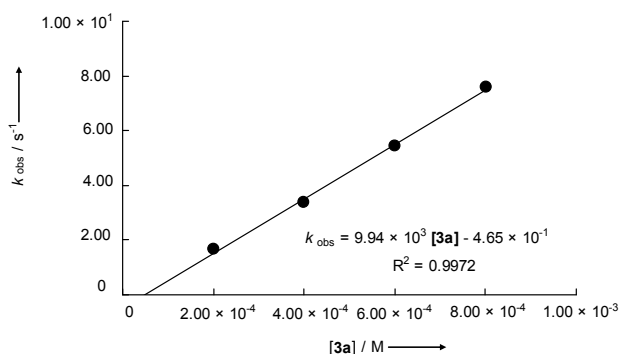
[ <b>4f</b> ] / M	[ <b>3a</b> ] / M	$k_{\text{obs}} / \text{s}^{-1}$
$1.53 \times 10^{-5}$	$1.01 \times 10^{-4}$	3.48
$1.53 \times 10^{-5}$	$1.51 \times 10^{-4}$	5.14
$1.53 \times 10^{-5}$	$2.01 \times 10^{-4}$	6.81
$1.53 \times 10^{-5}$	$2.52 \times 10^{-4}$	8.40
$1.53 \times 10^{-5}$	$3.02 \times 10^{-4}$	10.6

$k_2 = 3.48 \times 10^4 \text{ M}^{-1} \text{ s}^{-1}$

**Table 7.** Rate constants for the reaction of **3a** with **4g** in acetonitrile (stopped-flow method, 20 °C,  $\lambda = 616$  nm).

[ <b>4g</b> ] / M	[ <b>3a</b> ] / M	$k_{\text{obs}} / \text{s}^{-1}$
$1.53 \times 10^{-5}$	$2.00 \times 10^{-4}$	1.65
$1.53 \times 10^{-5}$	$4.01 \times 10^{-4}$	3.37
$1.53 \times 10^{-5}$	$6.01 \times 10^{-4}$	5.42
$1.53 \times 10^{-5}$	$8.01 \times 10^{-4}$	7.60

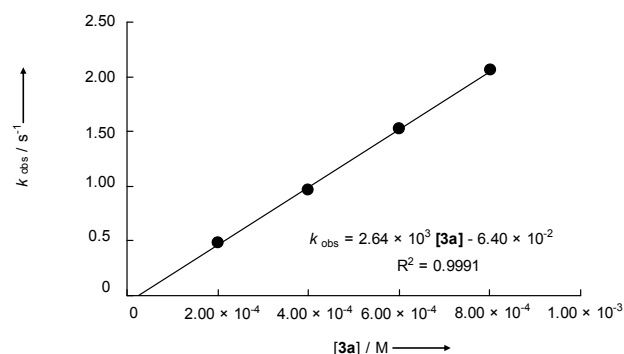
$k_2 = 9.94 \times 10^3 \text{ M}^{-1} \text{ s}^{-1}$



**Table 8.** Rate constants for the reaction of **3a** with **4h** in acetonitrile (stopped-flow method, 20 °C,  $\lambda = 616$  nm).

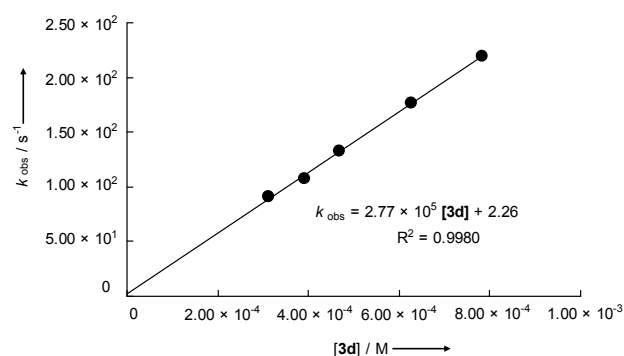
[ <b>4h</b> ] / M	[ <b>3a</b> ] / M	$k_{\text{obs}} / \text{s}^{-1}$
$1.44 \times 10^{-5}$	$2.00 \times 10^{-4}$	$4.84 \times 10^{-1}$
$1.44 \times 10^{-5}$	$4.01 \times 10^{-4}$	$9.64 \times 10^{-1}$
$1.44 \times 10^{-5}$	$6.01 \times 10^{-4}$	1.52
$1.44 \times 10^{-5}$	$8.01 \times 10^{-4}$	2.06

$$k_2 = 2.64 \times 10^3 \text{ M}^{-1} \text{ s}^{-1}$$

**Table 9.** Rate constants for the reaction of **3d** with **4b** in acetonitrile (stopped-flow method, 20 °C,  $\lambda = 591$  nm).

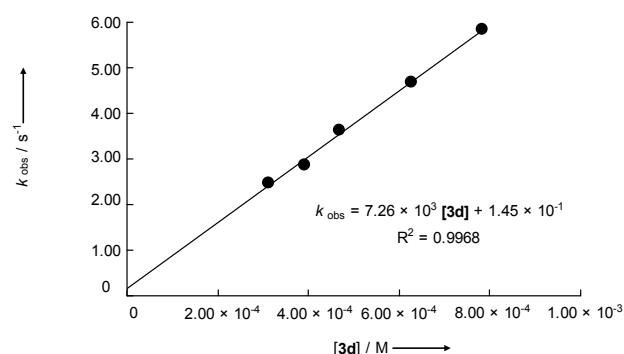
[ <b>4b</b> ] / M	[ <b>3d</b> ] / M	$k_{\text{obs}} / \text{s}^{-1}$
$1.60 \times 10^{-5}$	$3.13 \times 10^{-4}$	$9.15 \times 10^1$
$1.60 \times 10^{-5}$	$3.91 \times 10^{-4}$	$1.07 \times 10^2$
$1.60 \times 10^{-5}$	$4.69 \times 10^{-4}$	$1.33 \times 10^2$
$1.60 \times 10^{-5}$	$6.26 \times 10^{-4}$	$1.77 \times 10^2$
$1.60 \times 10^{-5}$	$7.82 \times 10^{-4}$	$2.19 \times 10^2$

$$k_2 = 2.77 \times 10^5 \text{ M}^{-1} \text{ s}^{-1}$$

**Table 10.** Rate constants for the reaction of **3d** with **4c** in acetonitrile (stopped-flow method, 20 °C,  $\lambda = 586$  nm).

[ <b>4c</b> ] / M	[ <b>3d</b> ] / M	$k_{\text{obs}} / \text{s}^{-1}$
$1.76 \times 10^{-5}$	$3.13 \times 10^{-4}$	2.48
$1.76 \times 10^{-5}$	$3.91 \times 10^{-4}$	2.86
$1.76 \times 10^{-5}$	$4.69 \times 10^{-4}$	3.62
$1.76 \times 10^{-5}$	$6.26 \times 10^{-4}$	4.68
$1.76 \times 10^{-5}$	$7.82 \times 10^{-4}$	5.83

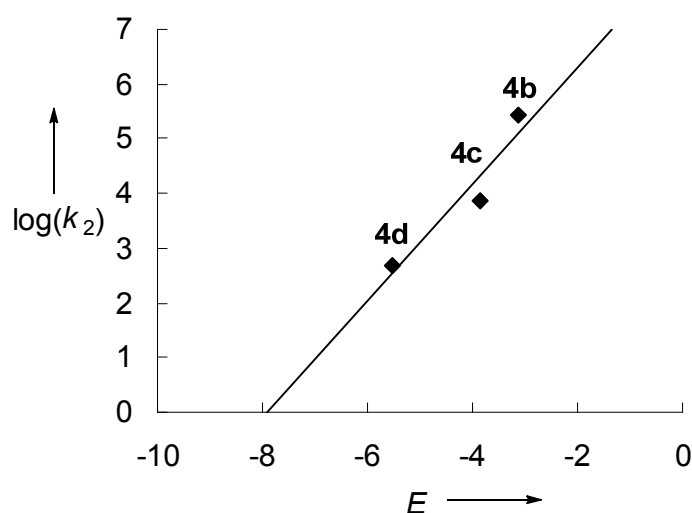
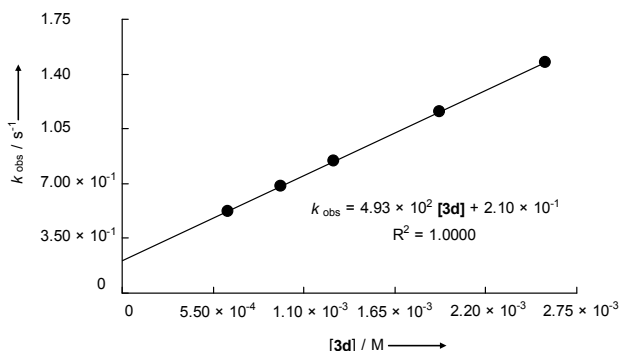
$$k_2 = 7.26 \times 10^3 \text{ M}^{-1} \text{ s}^{-1}$$



**Table 11.** Rate constants for the reaction of **3d** with **4d** in acetonitrile (stopped-flow method, 20 °C,  $\lambda = 611$  nm).

[ <b>4d</b> ] / M	[ <b>3d</b> ] / M	$k_{\text{obs}} / \text{s}^{-1}$
$3.20 \times 10^{-5}$	$6.41 \times 10^{-4}$	$5.24 \times 10^{-1}$
$3.20 \times 10^{-5}$	$9.61 \times 10^{-4}$	$6.82 \times 10^{-1}$
$3.20 \times 10^{-5}$	$1.28 \times 10^{-3}$	$8.44 \times 10^{-1}$
$3.20 \times 10^{-5}$	$1.92 \times 10^{-3}$	1.16
$3.20 \times 10^{-5}$	$2.56 \times 10^{-3}$	1.47

$k_2 = 4.93 \times 10^2 \text{ M}^{-1} \text{ s}^{-1}$

**Figure 4.** Plots of  $\lg k_2$  for the reactions of **3d** with benzhydrylium ions **4** in MeCN at 20 °C versus the corresponding electrophilicity parameters  $E$ .

## 5 References

- [1] a) B. List, *Acc. Chem. Res.* **2004**, *37*, 548–557; b) W. Notz, F. Tanaka, C. F. Barbas III, *Acc. Chem. Res.* **2004**, *37*, 580–591; c) S. Mukherjee, J. W. Yang, S. Hoffmann, B. List, *Chem. Rev.* **2007**, *107*, 5471–5569; d) C. F. Barbas III, *Angew. Chem. Int. Ed.* **2008**, *47*, 42–47; e) A. Dondoni, A. Massi, *Angew. Chem. Int. Ed.* **2008**, *47*, 4638–4660; f) P. Melchiorre, M. Marigo, A. Carlone, G. Bartoli, *Angew. Chem. Int. Ed.* **2008**, *47*, 6138–6171; g) S. Bertelsen, K. A. Jørgensen, *Chem. Soc. Rev.* **2009**, *38*, 2178–2189; h) M. Nielsen, D. Worgull, T. Zweifel, B. Gschwend, S. Bertelsen, K. A. Jørgensen, *Chem. Commun.* **2011**, *47*, 632–649.

- [2] a) A. Mieglo, C. Palomo, *Chem. Asian J.* **2008**, *3*, 922–948; b) C. Palomo, A. Mielgo, *Angew. Chem. Int. Ed.* **2006**, *45*, 7876–7880.
- [3] For a recent review on the impact of diaryl prolinol ethers in organocatalysis, see: K. L. Jensen, G. Dickmeiss, H. Jiang, L. Albrecht, K. A. Jørgensen *Acc. Chem. Res.* **2012**, *45*, 248–264.
- [4] a) G. Lelais, D. W. C. MacMillan, *Aldrichimica Acta.* **2006**, *39*, 79–87; b) A. Erkkilä, I. Majander, P. M. Pihko, *Chem. Rev.* **2007**, *107*, 5416–5470.
- [5] a) M. P. Brochu, S. P. Brown, D. W. C. MacMillan, *J. Am. Chem. Soc.* **2004**, *126*, 4108–4109; b) D. D. Steiner, N. Mase, C. F. Barbas III, *Angew. Chem. Int. Ed.* **2005**, *44*, 3706–3710; c) T. D. Beeson, D. W. C. MacMillan, *J. Am. Chem. Soc.* **2005**, *127*, 8826–8828.
- [6] For asymmetric S<sub>N</sub>1-type  $\alpha$ -alkylations of aldehydes with carbocations, see: a) R. R. Shaik, A. Mazzanti, M. Petrini, G. Bartoli, P. Melchiorre, *Angew. Chem. Int. Ed.* **2008**, *47*, 8707–8710; b) P. G. Cozzi, F. Benfatti and L. Zoli, *Angew. Chem. Int. Ed.* **2009**, *48*, 1313–1316; c) F. Benfatti, M. G. Capdevila, L. Zoli, E. Benedetto, P. G. Cozzi, *Chem. Commun.* **2009**, 5919–5921; d) F. Benfatti, E. Benedetto, P. G. Cozzi, *Chem. Asian J.* **2010**, *5*, 2047–2052; e) M. G. Capdevila, F. Benfatti, L. Zoli, M. Stenta, P. G. Cozzi, *Chem. Eur. J.* **2010**, *16*, 11237–11241; f) B. Zhang, S.-K. Xiang, L.-H. Zhang, Y. Cui, N. Jiao, *Org. Lett.* **2011**, *13*, 5212–5215; g) A. Gualandi, E. Emer, M. G. Capdevila, P. G. Cozzi, *Angew. Chem. Int. Ed.* **2011**, *50*, 7842–7846; h) L. Tak-Tak, H. Dhimane, P. I. Dalko, *Angew. Chem. Int. Ed.* **2011**, *50*, 12146–12147.
- [7] a) M. B. Schmid, K. Zeitler, R. M. Gschwind, *Angew. Chem. Int. Ed.* **2010**, *49*, 4997–5003; b) M. Wiesner, G. Upert, G. Angelici, H. Wennemers, *J. Am. Chem. Soc.* **2010**, *132*, 6–7; c) M. B. Schmid, K. Zeitler, R. M. Gschwind, *J. Org. Chem.* **2011**, *76*, 3005–3015; d) M. B. Schmid, K. Zeitler, R. M. Gschwind, *J. Am. Chem. Soc.* **2011**, *133*, 7065–7074; e) K. Patora-Komisarska, M. Benohoud, H. Ishikawa, D. Seebach, Y. Hayashi, *Helv. Chim. Acta* **2011**, *94*, 719–745; f) M. B. Schmid, K. Zeitler, R. M. Gschwind, *Chem. Sci.* **2011**, *2*, 1793–1803.
- [8] a) D. Seebach, U. Grošelj, D. M. Badine, W. B. Schweizer, A. K. Beck, *Helv. Chim. Acta* **2008**, *91*, 1999–2034; b) U. Grošelj, D. Seebach, D. M. Badine, W. B. Schweizer, A. K. Beck, I. Krossing, P. Klose, Y. Hayashi, T. Uchimaru, *Helv. Chim. Acta* **2009**, *92*, 1225–1259.
- [9] T. J. Peelen, Y. Chi, S. H. Gellman, *J. Am. Chem. Soc.* **2005**, *127*, 11598–11599.

- [10] This procedure is a modification of the method described in: K. L. Brown, L. Damm, J. D. Dunitz, A. Eschenmoser, R. Hobi, C. Kratky, *Helv. Chim. Acta* **1978**, *61*, 3108–3135.
- [11] CCDC 877482 (**3d**) and 877481 (**3e**) contain the supplementary crystallographic data for this paper. These data can be obtained free of charge from The Cambridge Crystallographic Data Centre via [www.ccdc.cam.ac.uk/data\\_request/cif](http://www.ccdc.cam.ac.uk/data_request/cif).
- [12] For a detailed analysis of the dispersion interactions in  $\alpha,\beta$ -unsaturated iminium ions derived from imidazolidinones, see: D. Seebach, U. Grošelj, W. B. Schweizer, S. Grimme, C. Mück-Lichtenfeld, *Helv. Chim. Acta* **2010**, *93*, 1–16
- [13] Reviews on pyramidalization indices: a) F. K. Winkler, J. D. Dunitz, *J. Mol. Biol.* **1971**, *59*, 169–182; b) J. D. Dunitz, *X-Ray Analysis and Structure of Organic Molecules*, Cornell University Press, London, **1979**.
- [14] a) H. Mayr, M. Patz, *Angew. Chem. Int. Ed. Engl.* **1994**, *33*, 938–957; b) H. Mayr, T. Bug, M. F. Gotta, N. Hering, B. Irrgang, B. Janker, B. Kempf, R. Loos, A. R. Ofial, G. Remennikov, H. Schimmel, *J. Am. Chem. Soc.* **2001**, *123*, 9500–9512; c) H. Mayr, B. Kempf, A. R. Ofial, *Acc. Chem. Res.* **2003**, *36*, 66–77; d) H. Mayr, A. R. Ofial, *Pure Appl. Chem.* **2005**, *77*, 1807–1821; e) H. Mayr, A. R. Ofial, *J. Phys. Org. Chem.* **2008**, *21*, 584–595; f) Data base for  $N$ ,  $s_N$ , and  $E$  parameters and references to their origin: <http://www.cup.uni-muenchen.de/oc/mayr/DBintro.html>.
- [15] a) G. Deslongchamps, P. Deslongchamps, *Org. Biomol. Chem.* **2011**, *9*, 5321–5333; b) see also discussion in ref. [10].
- [16] Y. Hayashi, H. Gotoh, T. Hayashi, M. Shoji, *Angew. Chem. Int. Ed.* **2005**, *44*, 4212–4215.
- [17] I. Zenz, H. Mayr, *J. Org. Chem.* **2011**, *76*, 9370–9378.
- [18] J. Bures, A. Armstrong, D. G. Blackmond, *J. Am. Chem. Soc.* **2011**, *133*, 8822–8825.
- [19] I. Ibrahim, A. Córdova, *Chem. Commun.* **2006**, 1760–1762.
-



# LEBENS LAUF

## Persönliche Daten

Name: Biplab Maji  
Date of birth: 26.01.1987  
Place of Birth: Howrah, India  
Family status: Single  
Nationality: Indian

## Schulbildung

1992-1996 Pantihal Nanimakham Vidyapith, Howrah, India  
1996-2002 Bargachia Union Priyanath Pathsala, Howrah, India  
2002-2004 Makardah Bamasunduri Institution, Howrah, India

## Studium

2004-2007 Bachelor of Science (Chemistry Honors), Ramakrishna Mission  
Vidyamandir, University of Calcutta, Kolkata, India  
2007-2009 Master of Science, Department of Chemistry,  
Indian Institute of Technology Kanpur (I.I.T.K), India.

## Dissertation

2009-2012 Ph.D. (Organische Chemie), Department Chemie,  
Ludwig-Maximilians-Universität München, Germany.  
Betreuer: Prof. Dr. Herbert Mayr

## Honors

2007-2009 MCM-scholarship from I.I.T. Kanpur, India.